DISSERTATION

STUDIES ON THE BIOSYNTHESIS OF PRENYLATED INDOLE SECONDARY

METABOLITES FROM *ASPERGILLUS VERSICOLOR* AND *ASPERGILLUS SP.*;

AND

A NOVEL APPROACH TO TUMOR SPECIFIC DRUG DELIVERY: USE OF A

NAPHTHYRIDINE DRUG LINKER WITH A DNA HAIRPIN

Submitted by

Jennifer M. Finefield

Department of Chemistry

In partial fulfillment of the requirements

for the Degree of Doctor of Philosophy

Colorado State University

Fort Collins, Colorado

Summer 2011

Doctoral Committee:

    Advisor: Robert M. Williams

    Tomislav Rovis
    Alan Kennan
    Mike Elliott
    Doug Thamm

ABSTRACT

STUDIES ON THE BIOSYNTHESIS OF PRENYLATED INDOLE ALKALOIDS

FROM *ASPERGILLUS VERSICOLOR* AND *ASPERGILLUS SP.*; AND

A NOVEL APPROACH TO TUMOR SPECIFIC DRUG DELIVERY: USE OF A

NAPHTHYRIDINE DRUG LINKER WITH A DNA HAIRPIN

Herein are documented our efforts in two projects, beginning with studies toward elucidating the biosynthesis of prenylated indole alkaloids from two different *Aspergillus* species. Marine-derived *Aspergillus* sp. and terrestrial-derived *Aspergillus versicolor* were found to produce antipodal metabolites, in which we have developed several putative biosynthetic pathways to determine the enantio-diverging point of these fungal cultures. Through the synthesis of several potential intermediates, both with and without isotopic labeling, as well as through bioinformatics analysis of both the (–)- and (+)-notoamide biosynthetic gene clusters, significant progress has been made toward identifying a single biosynthetic precursor that serves as an intermediate to the postulated enantio-diverging event, the intramolecular hetero Diels-Alder cycloaddition.

In the second project discussed, through collaboration with Dr. James Berenson at the University of California, Los Angeles, we have developed a novel tumor specific drug delivery system. Two naphthyridine-drug derivatives were synthesized and conjugated to a modified DNA oligonucleotide specifically targeted for multiple

myeloma cells.   The oligonucleotide-drug conjugate was successfully delivered and activated specifically within RMI8226 multiple myeloma cells.

ACKNOWLEDGEMENT

"Success builds character, failure reveals it"

The path I have traveled leading to this Ph.D. dissertation has been paved with success and failure. Thankfully, I have been blessed with the support and encouragement from so many wonderful people during the ups and downs of graduate school. Below is just a partial listing of the people I would like to thank.

Professor Robert M. Williams—For giving me the opportunity to succeed and fail and for all of your support and guidance along the way.

Professor Tomislav Rovis, Professor Alan Kennan, Professor Mike Elliott, and Dr. Doug Thamm—For pushing me to realize my potential, strength, and true character.

Professor Shawn "Doc" Hitchcock at Illinois State University for introducing me to organic chemistry and showing me the joy and wonder of research. Dr. Paul Humphries and Ranjan Rajapakse at Pfizer, Inc. for giving me the opportunity to experience the industrial world of organic chemistry. I am forever grateful for the advice and knowledge the three of you have shared with me.

Altorfer—For all the years of friendship and fun. I am so blessed to have such a wonderful support system, and I never could have made it to where I am today without you. Finally, Dustin Folger—For your seemingly limitless supply of patience and encouragement.

Last but not least, a huge thank you to my parents, Tim and Jean, and my sister, Erin— For always pushing me to do my best and for always being there to help me along the way.

TABLE OF CONTENTS

ABBREVIATIONS

Ac$_2$O	Acetic anhydride
AcOH	Acetic acid
Bn	Benzyl
Boc	*tert*-Butoxycarbonyl
Boc$_2$O	Di-*tert*-butyl dicarbonate
BOP reagent	benzotriazol-1-yloxytris(dimethylamino) phosphonium hexafluorophosphate
Bz	Benzoyl
BuLi	Butyllithium
Cbz	Benzyloxycarbonyl
CoA	Co-enzyme A
Collidine	2,4,6-trimethylpyridine
18-crown-6	1,4,7,10,13,16-hexaoxacyclooctadecane
DABCO	1,4-Diazabicyclo[2.2.2]octane
DCM	Dichloromethane
DDQ	2,3-dichloro-5,6-dicyano-1,4-benzoquinone
DEAD	Diethyl azocarboxylate
DIBAL	Diisobutylaluminum hydride
DIPEA	Diisopropylethylamine

DKP	Diketopiperazine
DMAP	4-(Dimethylamino)pyridine
DMAPP	Dimethylallyl pyrophosphate
DMF	Dimethylformamide
DMS	Dimethylsulfide
DMSO	Dimethylsulfoxide
EDCI (or EDC)	*N*-(3-dimethylaminopropyl)-*N*'-ethylcarbodiimide
Et	Ethyl
EtOAc	Ethyl acetate
Et$_2$O	Diethyl ether
EtOH	Ethanol
Fmoc	Fluorenylmethyloxycarbonyl
HATU	*O*-(7-Azabenzotriazol-1-yl)-*N,N,N',N'*-tetramethyluronium hexafluorophosphate
imid.	Imidazole
IPP	Isoprenylpyrophosphate
KHMDS	Potassium (bis)trimethylsilyl amide
LDA	Lithium diisopropylamine
LHMDS (or LiHMDS)	Lithium (bis)trimethylsilyl amide
2,6-lutidine	2,6-dimethylpyridine
*m*CPBA	*meta*-Chloroperbenzoic acid
Me	Methyl
MeI	Methyl iodide

MeOH	Methanol
Ms	Methanesulfonyl (mesylate)
MsCl	Methanesulfonyl chloride
NHMDS (or NaHMDS)	Sodium (bis)trimethylsilyl amide
NMM	*N*-methyl morpholine
PMB	*p*-Methoxybenzyl
PTLC	Preparative thin layer chromatography
i-Pr	Isopropyl
Py. or Pyr	Pyridine
TBAF	Tetrabutylammonium fluoride
TBDPS	*tert*-Butyldiphenylsilyl
TBS	*tert*-Butyldimethylsilyl
TBSCl	*tert*-Butyldimethylsilyl chloride
t-BuOK	Potassium *tert*-butoxide
TFA	Trifluoroacetic acid
TFAA	Trifluoroacetic anhydride
THF	Tetrahydrofuran
TLC	Thin layer chromatography
TMS	Trimethylsilyl
TMSCl	Trimethylsilyl chloride

CHAPTER 1

Introduction and Overview

1.1 Reverse Prenylated Indole Secondary Metabolites

1.1.1 Introduction

The brevianamides,[1-5] paraherquamides,[6-14] stephacidins,[15-18] and notoamides[19-25] are secondary metabolites produced by various genera of fungi, which include (among others) *Aspergillus* and *Penicillium* species (Figure 1). These reverse prenylated indole alkaloids exhibit a range of interesting structural features, such as a core bicyclo[2.2.2]diazaoctane ring system and a complex amino acid skeleton. A variety of bioactivities are also present in these families, including insecticidal, antitumor, anthelmintic, and antibacterial properties. Structurally, these natural products are comprised of tryptophan, a cyclic amino acid, and one or two isoprene units. The synthesis and biosynthesis of these natural products have been extensively investigated;[26-29] however, a detailed understanding of the assembly and modification of the advanced metabolites is still relatively unknown.
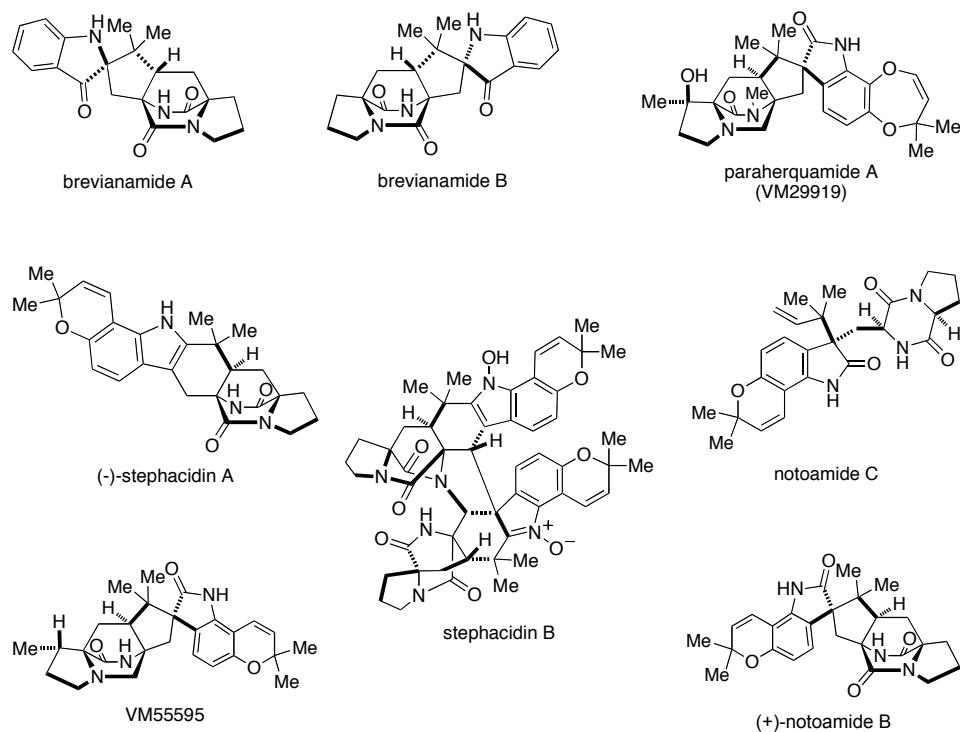
Figure 1. Structures of several members of the brevianamide, paraherquamide, stephacidin, and notoamide families of reverse prenylated indole alkaloids.

The biosynthesis of the paraherquamides has been deeply investigated over the past 15 years by Williams et al.;[26-27,30-32] however, several late-stage biosynthetic transformations are still unknown. Chapters 2 and 3 detail the groundwork that has been previously established for the biosynthesis of paraherquamide A via *Penicillium fellutanum* and asperparaline A via *Aspergillus japonicus*, as well as some of the recent advances that have been made toward determining their biosynthetic precursors. One specific area of focus addressed in Chapter 3 is the biosynthetic timing for the installation of the dioxepin ring found in many of the paraherquamides, along with the synthesis of two potential dioxepin intermediates: 6- and 7-hydroxypreparaherquamide. In addition, effort has been put forth toward determining whether the biosynthetic intermediate,

2

preparaherquamide, also serves as the precursor to asperparaline A in cultures of *Aspergillus japonicus*, which can be achieved through the synthesis of ^{13}C-labeled preparaherquamide and subsequent isotope incorporation studies.

Over the past several years, the number of new prenylated indole alkaloids isolated from fungi of both marine and terrestrial origin has greatly increased. Recently, Gloer and co-workers reported the isolation of (+)-versicolamide B, (−)-stephacidin A, and (+)-notoamide B from a terrestrial-derived fungus, *Aspergillus versicolor*.[25] In separate work, Tsukamoto and co-workers reported the isolation of the same prenylated indole alkaloids from a closely related, albeit, marine-derived *Aspergillus* sp. MF297-2[19,23] Surprisingly, the marine-derived fungus and the terrestrial-derived fungus were found to produce, in parallel, enantiomeric counterparts of versicolamide B, stephacidin A, and notoamide B (Figure 2). This raised the question as to whether these two fungal strains follow similar, if not identical, biosynthetic pathways.
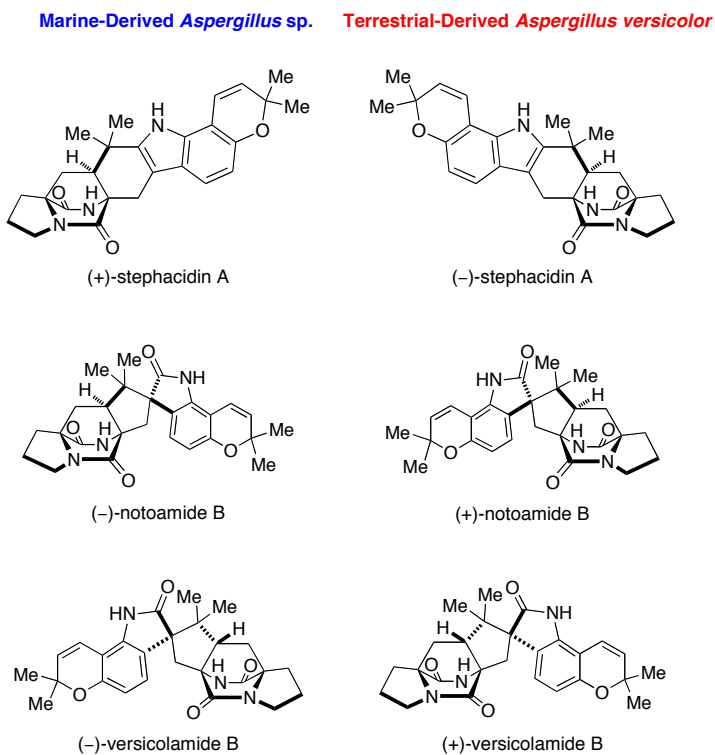
Figure 2. Structures of antipodal natural metabolites isolated from marine-derived *Aspergillus* sp. MF297-2 and terrestrial-derived *Aspergillus versicolor*.

As outlined in Chapters 4 and 5, extensive effort has been put forth to elucidate the enantio-divergent biosynthetic pathways of marine-derived *Aspergillus* sp. MF297-2 and terrestrial-derived *Aspergillus versicolor*. Several potential biosynthetic pathways that account for the formation of antipodal metabolites have been proposed. Isotopic incorporation studies and the synthesis of potential biosynthetic intermediates have enabled these pathways to be substantially explored. Recent advancements in the area of genomics have allowed for the mining of desired gene clusters from fungal species. This technique has been utilized for the isolation and characterization of the notoamide (*not*) gene sequence from both *Aspergillus* sp. MF297-2 and *Aspergillus versicolor*, which has

provided a more in-depth understanding of the biosynthetic pathway of these two fungal species.[33]

1.1.2 Overview of Results

Considerable effort has been put forth toward the synthesis of ^{13}C-labeled preparaherquamide, as delineated in Chapter 3. Completion of the synthesis of isotopically labeled preparaherquamide requires five steps, and once assembled, the isotope incorporation experiment of $[^{13}C]_2$-preparaherquamide with *Aspergillus japonicus* can commence. While the synthesis of the 6-hydroxytryptophan derivative has been achieved, completion of the 7-hydroxytryptophan derivative requires further screening of reaction conditions in order to synthesize the C-2 reverse prenylated moiety.

Three potential pathways for the biosynthesis of the notoamides and stephacidins have been proposed and studied. Both unlabeled and labeled potential precursors have been synthesized, and their presence and/or incorporation in the biosynthetic pathway of *Aspergillus* sp. MF297-2 are discussed in Chapter 4. With a promising biosynthesis of the notoamides and stephacidins established via sequencing of the *Aspergillus* sp. MF297-2 and *Aspergillus versicolor* genome (Chapters 4 and 5), attention was directed toward determining whether these antipodal metabolites shared a similar, if not identical, biosynthetic pathway. Through isotope incorporation studies with *Aspergillus versicolor*, a common intermediate to the two enantiomeric pathways has been established and is explained in detail in Chapter 5.

1.2 Multiple Myeloma-Specific Targeted Drug Delivery

1.2.1 Introduction

Multiple myeloma (MM) is a plasma cell malignancy, characterized by the accumulation of plasma cells predominantly in the bone marrow, leading to pathologic fractures, anemia, hypercalcemia, renal failure, and recurrent bacterial infections.[34,35] MM accounts for 13.4% of all hematologic malignancies diagnosed, 19% of all deaths resulting from hematologic malignancies, and 2% of all cancer deaths.[36] Epidemiological studies have shown that MM is associated with older age, and found to occur more often in men than in women.[37]

Currently, MM is incurable with a five year survival rate, and treatment focuses on the reduction in tumor growth and management of symptoms.[38] Until recently, autologous peripheral blood stem cell transplant, cytotoxic drugs, and steroids have formed the mainstay of MM treatment. Traditionally, either a melphalan-prednisone regimen or a single high-dose of melphalan is administered to MM patients. Recent advances in targeted therapy have lead to the development of several new MM treatment options, such as bortezomib, and the immunomodulatory agents thalidomide and lenalidomide.

Since MM is a malignancy of clonal antibody-secreting plasma cells, the mutated cells often contain a specific rearrangement of DNA, which is transcribed into a unique mRNA sequence.[39,40] Translation of the mRNA sequence results in the formation of a tumor specific monoclonal antibody, which is abundant in all of the malignant cells. From this tumor specific transcript, a unique complementary determining region (CDR) gene sequence can be identified.[41] Recently, Berenson and coworkers were able to

demonstrate that a tumor specific oligonucleotide could specifically recognize the MM tumor cell population.[42]   As shown in Figure 3, using a quenched fluorescein-labeled oligonucleotide probe (designated as MB8226) displaying a sequence complementary to the CDR3 gene sequence from the MM cell line RPMI8226, they were able to establish that MB8226 could not only recognize the specific cell line, but also differentiate the RPMI8226 cell line from other MM cell lines.   This provided additional support that MB8226 selectively enters and reacts with cells expressing this explicit mRNA sequence; and since the targeted mRNA sequence is found in a specific type of cancer cells, it was postulated that MB8226 could be used as a method of drug delivery for patients with MM.

A. MB8226 with quenched fluorophore

B. Binding of MB8226 to mRNA of the MM cell line RPMI8226 CDR3 gene sequence with fluorescence

Probe sequence = CDR[1]

GCATG

C—G
A—T
G—C
C—G
G—C

Q F

Complementary sequence of mRNA

CGTAC

GCGAC GCATG GTCGC

CDR

Q

F

Q F = quenched fluorophore

Q = quencher
F = fluorophore

F = fluorescence

[1] CDR = complementary determining region
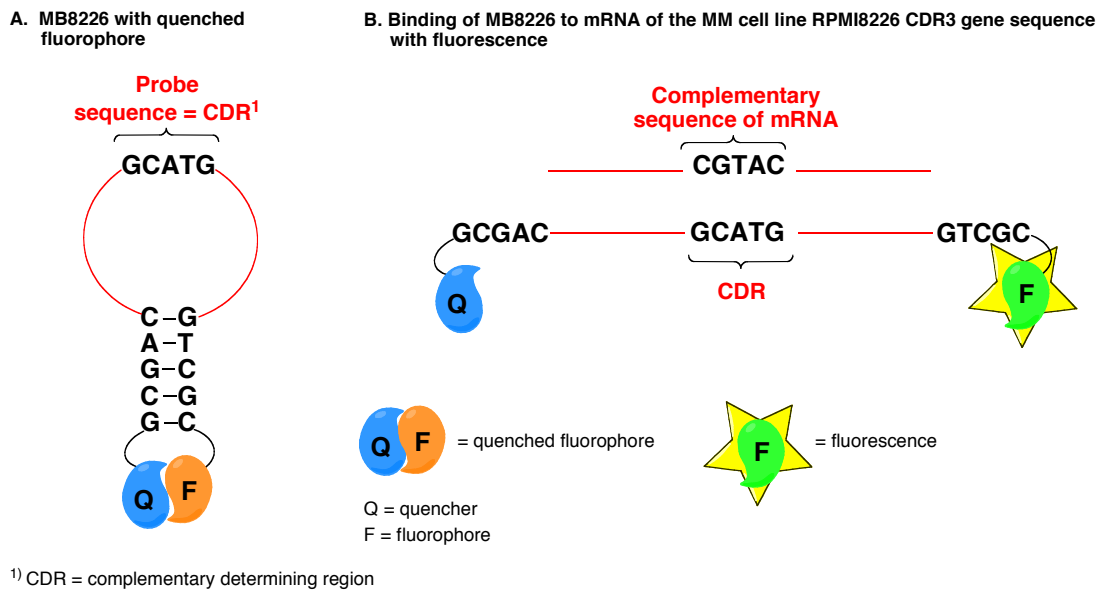
Figure 3. A) Closed/quenched molecular beacon (MB8226). **B)** Open/fluorescent molecular beacon upon binding to mRNA of the CDR3 gene sequence from the MM cell line RPMI8226.

1.2.2 Overview of Results

To convert MB8226 into a drug delivery agent, the first necessary modification was the addition of an extra guanine base to the stem of the oligonucleotide.[43] By adding a naphthyridine ligand to the desired drug, an oligonucleotide-naphthyridine drug conjugate can be used for drug delivery. As shown in Figure 4, the addition of an extra guanine to the stem of MB8226 could allow for the desired "Trojan Horse" method of drug delivery.   By coupling the desired cancer drug to a naphthyridine moiety, the naphthyridine-drug complex could be inserted into the G-bulge of the closed MB8226 and held in place by hydrogen bonding. Since MB8226 only reacts with the RPMI8226 cell line, the MM drug would only be released within cancer cells upon the binding of MB8226 to the complementary sequence and the subsequent unzipping of the stem.

A. Modified-MB8226 with drug conjugate

GCATG

G–C
T–A
C–G
G▰
C–G
A–T

▮ = cytotoxic agent + naphthyridine conjugate

B. Modified-MB8226 binding to mRNA of the MM cell line RPMI8226 CDR3 gene sequence

CGTAC

ACGCTG———GCATG———CAG GT
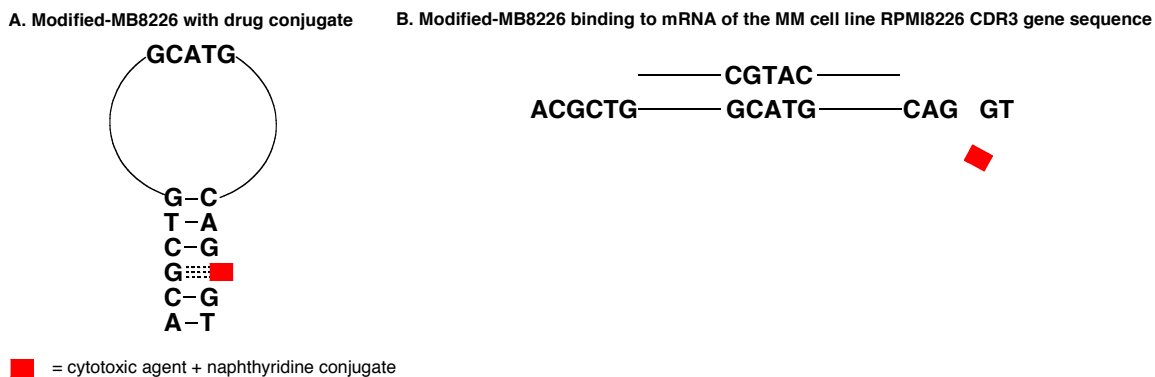
Figure 4. "Trojan Horse" design **A)** Closed conformation of MB8226 with the cytotoxic agent contained in the stem at the G-bulge. **B)** Open conformation of MB8226 and release of the drug.

The two drugs selected for use in this experiment were vorinostat and melphalan. Vorinostat is an FDA-approved histone deacetylase inhibitor that is used for the treatment

of cutaneous T-cell lymphoma, and in 2008 a vorinostat-velcade (vorinostat-bortezomib)

combination drug entered phase I clinical trials for the treatment of MM.[44] As mentioned

previously, melphalan is the mainstay treatment of MM, and is a nitrogen mustard

alkylating agent.[41] In order for either of these two drugs to be used in the therapeutic

application of MB8226, they had to be converted to the respective naphthyridine-

modified (N) drug derivatives (Scheme 1), the syntheses of which are discussed in detail

in Chapter 6.
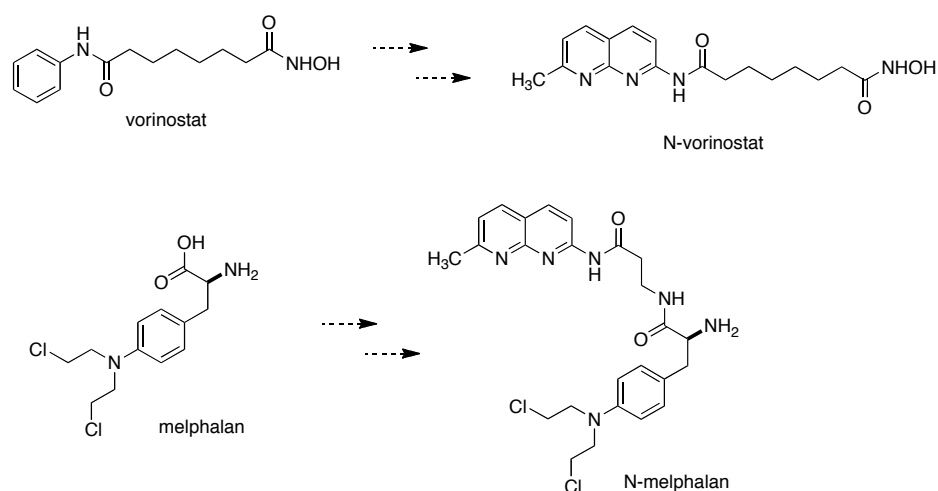
Scheme 1. Structures of two MM drugs (vorinostat and melphalan) and their

naphthyridine derivatives (N-vorinostat and N-melphalan).

CHAPTER 2

Reverse Prenylated Indole Secondary Metabolites

2.1 Isolation, Structure, and Pharmacology

2.1.1 The Brevianamides

Between 1969 and 1972, Birch and co-workers isolated six novel secondary metabolites, brevianamides A-F (**1-6**, Figure 5), from a fungal culture of *Penicillium brevicompactum*.[1-3] Radiolabeled precursor incorporation studies carried out by Birch demonstrated that these fungal alkaloids are biogenetically derived from tryptophan, proline, and mevalonic acid. The isolation and biosynthetic elucidation of these natural products exemplify a new class of fungal natural products that contain a unique bicyclo[2.2.2]diazaoctane core, a now known feature of various families of prenylated indole alkaloids.[26] Structurally, brevianamides A and B are stereoisomers, while brevianamides C and D are artifacts of isolation due to light irradiation.[3] During this time, Steyn and co-workers reported the isolation of deoxybrevianamide E (**7**) from *Aspergillus ustus*.[4] This simple metabolite, along with brevianamide F, have been established as biosynthetic precursors to numerous prenylated indole alkaloids.[33] As shown in Table 1, the brevianamides have been isolated from various *Penicillium* and *Aspergillus* fungal cultures.
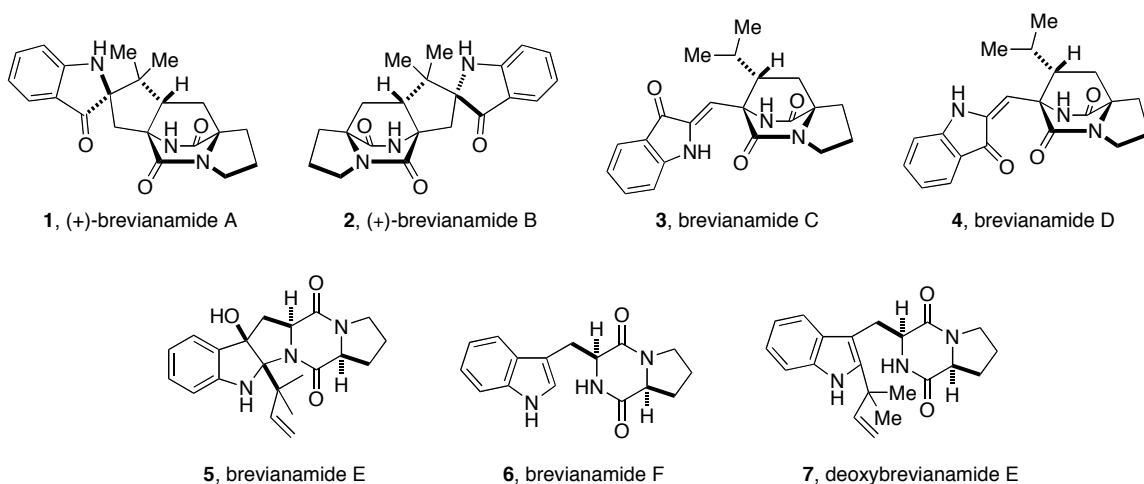
Figure 5. Structures of brevianamides and related metabolites.

Table 1. Fungal origin of the brevianamides.

Compound	Fungal Species	Reference
brevianamide A (**1**)	*Penicillium brevicompactum*	1-3
	Penicillium ochraceum	5
	Penicillium viridicatum	45
brevianamide B (**2**)	*Penicillium brevicompactum*	1-3
brevianamide C (**3**)	*Penicillium brevicompactum*	1-3
brevianamide D (**4**)	*Penicillium brevicompactum*	1-3
brevianamide E (**5**)	*Penicillium brevicompactum*	1-3
brevianamide F (**6**)	*Aspergillus fumigatus*	46
	Aspergillus versicolor	25
	Penicillium brevicompactum	1-3
	Pseudallescheria species	47
deoxybrevianamide E (**7**)	*Aspergillus* species	19
	Aspergillus ustus	4

The brevianamides represent a unique structural class of fungal alkaloids. Besides containing the bicyclo[2.2.2]diazaoctane ring system, the *anti*-relationship (**8**) of the bicyclic core is distinct to the brevianamides, as opposed to the more common *syn*-relationship (**9**) found in the paraherquamides. The *anti* and *syn* relationship is determined by the position of the C-H proton (or C-19, brevianamide numbering) at the bridgehead of the bicyclic core in relation to the bridging secondary lactam (Figure 6).[48]

Additionally, brevianamides A and B display a *spiro*-indoxyl moiety, while brevianamides E and F both contain a diketopiperazine moiety. Another structural characteristic is that all of the brevianamides contain an unsubstituted proline ring.

8, *anti*-diastereomer   **9**, *syn*-diastereomer
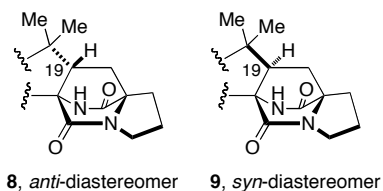
Figure 6. *Anti*- and *syn*- relationship of the bicyclo[2.2.2]diazaoctane core.

The brevianamides are a class of mycotoxins that display modest biological activities. Brevianamide A has been shown to possess antifeedant and insecticidal effects,[49] and brevianamide F exhibited mild antibacterial activity against *Staphylococcus aureus*, methicillin-resistant *S. aureus*, and multidrug-resistant *S. aureus*.[47]

2.1.2 The Paraherquamides

Ten years after Birch isolated the first family of prenylated indole alkaloids, the second group of similar fungal metabolites, the paraherquamides, was isolated. Paraherquamide A (**10**, Figure 7) was the first member of this family to be isolated by Yamazaki et al. from *Penicillium paraherquei*.[6] A decade later, paraherquamide A was isolated from *Penicillium charlesii* (*P. fellutanum*) along with six structurally related novel analogues, paraherquamides B-G (**11-16**).[7] In the following years the paraherquamide family of prenylated indole alkaloids continued to expand with the isolation of paraherquamides H (**17**) and I (**18**) and several related compounds, including VM55595 (**19**), VM55596 (**20**), VM55597 (**21**), VM55599 (**22**), SB200437 (**23**), and

SB203105 (**24**).[8-10]   The paraherquamides and related metabolites have been isolated

from various *Penicillium* and *Aspergillus* species, as illustrated in Table 2.   More

recently, Sherman and co-workers reported the existence of pre-paraherquamide (**25**) in

cultures of paraherquamide A producing *Penicillium fellutanum,* as well as in the

asperparaline A producing fungus, *Aspergillus japonicus.*[14]   Furthermore, they were able

to demonstrate that paraherquamides A and B were also produced by *Aspergillus*

japonicus. The existence of pre-paraherquamide in both *Penicillium* and *Aspergillus* sp.

MF297-2 provides evidence that **25** is a biosynthetic precursor to the paraherquamides

and the asperparalines (See Section 2.2 and Chapter 3 for more information).

10, (–)-paraherquamide A, R_1 = OH, R_2 = Me, R_3 = H_2, X = N
11, (–)-paraherquamide B, R_1 = H, R_2 = H, R_3 = H_2, X = N
12, (–)-paraherquamide C, R_1 = R_2 = CH_2, R_3 = H_2, X = N
13, (–)-paraherquamide D, R_1 = O, R_2 = CH_2, R_3 = H_2, X = N
17, paraherquamide H, R_1 = H, R_2 = Me, R_3 = O, X = N
20, VM55596, R_1 = OH, R_2 = Me, R_3 = H_2, X = N^+-O^-
21, VM55597, R_1 = OH, R_2 = Me, R_3 = O, X = N

14, paraherquamide E, R_1 = Me, R_2 = H
23, SB200437, R_1 = H, R_2 = H
24, SB203105, R_1 = Me, R_2 = OH

18, paraherquamide I

15, paraherquamide F, R_1 = H, R_2 = Me, R_3 = Me
16, paraherquamide G, R_1 = OH, R_2 = Me, R_3 = Me
19, VM55595, R_1 = H, R_2 = Me, R_3 = H

22, VM55599

25, pre-paraherquamide

Figure 7. Structures of the paraherquamides and related compounds.

Table 2. Fungal origin of the paraherquamides.

Compound	Fungal Species	Reference
paraherquamide A (**10**)	*Penicillium charlesii (fellutanum)*	7
	Penicillium cluniae	8
	Penicillium paraherquei	6
	Penicillium species IMI 332995	9
	Penicillium species (isolated from soil in Kemer, Turkey)	11

13

paraherquamide B (**11**)	*Penicillium charlesii (fellutanum)*	7, 12
	Penicillium cluniae	8
paraherquamide C (**12**)	*Penicillium charlesii (fellutanum)*	7, 12
paraherquamide D (**13**)	*Penicillium charlesii (fellutanum)*	7, 12
paraherquamide E (**14**)	*Aspergillus* species IMI 337664	10
	Penicillium charlesii (fellutanum)	7, 12
	Penicillium cluniae	8
	Penicillium species IMI 332995	9
	Penicillium species (isolated from soil in Kemer, Turkey)	11
paraherquamide F (**15**)	*Penicillium charlesii (fellutanum)*	7, 12
	Penicillium species IMI 332995	9
	Penicillium species (isolated from soil in Kemer, Turkey)	11
paraherquamide G (**16**)	*Penicillium charlesii (fellutanum)*	7, 12
	Penicillium species IMI 332995	9
	Penicillium species (isolated from soil in Kemer, Turkey)	11
paraherquamide H (**17**)	*Penicillium cluniae*	8
paraherquamide I (**18**)	*Penicillium cluniae*	8
VM55595 (**19**)	*Penicillium* species IMI 332995	9
VM55596 (**20**)	*Penicillium cluniae*	8
VM55597 (**21**)	*Penicillium cluniae*	8
	Penicillium species IMI 332995	9
VM55599 (**22**)	*Penicillium paneum*	13
	Penicillium species IMI 332995	9
SB200437 (**23**)	*Aspergillus* species IMI 337664	10
SB203105 (**24**)	*Aspergillus* species IMI 337664	10
pre-paraherquamide (**25**)	*Aspergillus japonicus*	14
	Penicillium charlesii (fellutanum)	14

Structurally, all of the paraherquamides contain the bicyclo[2.2.2]diazaoctane core with the *syn*-configuration; however, the paraherquamide family displays a plethora of skeletal diversity. For example, the paraherquamides display varying substitution and oxygenation on the proline ring and the *spiro*-oxindole moiety. Several of the paraherquamides contain a unique dioxepin ring, while others contain a pyran moiety. Within this family of secondary metabolites, VM55599 and pre-paraherquamide are the

only two compounds that do not contain either a *spiro*-oxindole functionality or an oxygenated ring system on the indole ring.

The paraherquamides have attracted considerable interest due to their potent anthelmintic activity. Parasitic nematodes cause severe health problems in humans and domestic animals, and the severity of this problem is increasing due to the development of drug resistant strains of parasites.[50] Initial anthelmintic activity was detected in *Trichostrongylus colubriformis*[51] and subsequent investigations showed that paraherquamide A is effective against strains of parasites that are resistant to broad-spectrum anthelmintics.[52] Unfortunately, the toxicity of paraherquamide A was determined to be too great for it to be used as a broad-spectrum anthelmintic.[53] To decrease the toxicity, but maintain the potency, several paraherquamide derivatives have been synthesized and tested for anthelmintic activity.[50] Of these derivatives, 2-deoxy-paraherquamide A (**26**, Figure 8), later named PNU-141962, displayed excellent activity in models of *Haemonchus contortus*, *Trichostrongylus colubriformis*, and *Ostertagia ostertagi*, while maintaining a safe level of toxicity, which makes it an attractive potential candidate for commercialization.[54]
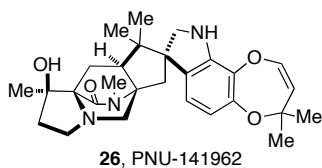
26, PNU-141962

Figure 8. Structure of 2-deoxyparaherquamide A (PNU-141962).

2.1.3 The Stephacidins and Notoamides

Following the isolation of numerous paraherquamide type compounds isolated in the 1990s, the 2000s saw the emersion of another family of closely related prenylated

indole alkaloids, the stephacidins and notoamides. The first member of the stephacidins and notoamides, sclerotiamide (**27**, Figure 9), was first isolated in 1996 from *Aspergillus sclerotiorum*, and was actually classified as a paraherquamide type compound.[15] Structurally similar to the paraherquamides, sclerotiamide contains the core bicyclo[2.2.2]diazaoctane moiety, a *spiro*-oxindole ring system with a pyran group, and an unsubstituted proline ring. However, unlike the paraherquamides, sclerotiamide retains an unreduced diketopiperazine unit and also contains a unique C-10 hydroxyl group. At the time, the rare structural skeleton of sclerotiamide made it a possible biosynthetic precursor to the paraherquamides. It was not until 1999 that other structurally related prenylated indole alkaloids were isolated, including (+)-stephacidin A (**28**), stephacidin B (**29**) and avrainvillamide (**30**). Stephacidins A and B were both isolated from terrestrial-derived *Aspergillus ochraceus* by a group at Bristol-Myers Squibb,[16] while avrainvillamide was independently isolated from marine-derived *Aspergillus* sp. MF297-2 CNC358 by Fenical.[17] Two years later, Sugie and coworkers reported the isolation of avrainvillamide, under the name of CJ-17,665, from *Aspergillus ochraceus*.[18]
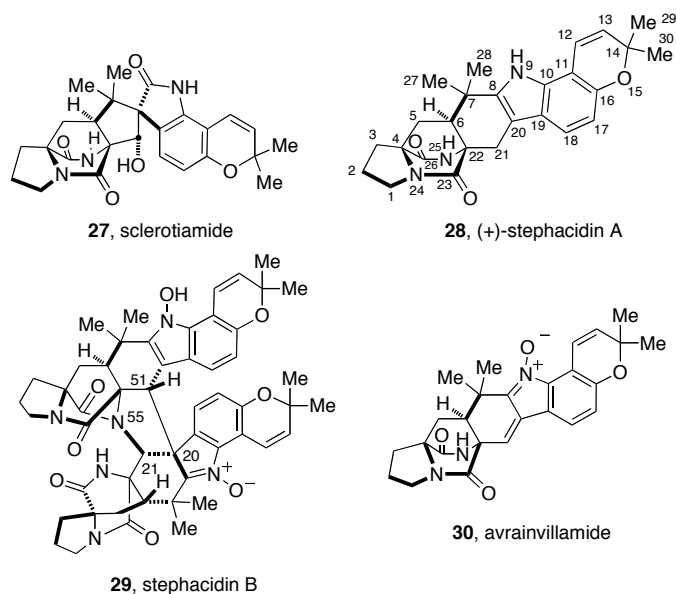
Figure 9. Structures of the stephacidins and related compounds.

Upon closer inspection, stephacidin A, stephacidin B, and avrainvillamide appeared to be structurally and biogenetically related to each other. All three compounds contain the core bridging bicycle with an unreduced diketopiperazine, similar to sclerotiamide; however, they also display an unoxidized indole moiety resembling pre-paraherquamide and VM55599. Biogenetically, it was proposed that stephacidin A could be oxidized to afford avrainvillamide, an imine oxide with C-8–N-9 and C-20–C-21 double bonds (Figure 10).[16b] Stephacidin B could then result from the dimerization of avrainvillamide. To test these theories, Myers and co-workers were the first to synthesize avrainvillamide and effect the dimerization to afford stephacidin B under mild basic conditions.[55] Baran and Williams have separately carried out the biomimetic conversion of stephacidin A to avrainvillamide to stephacidin B.[56,57]
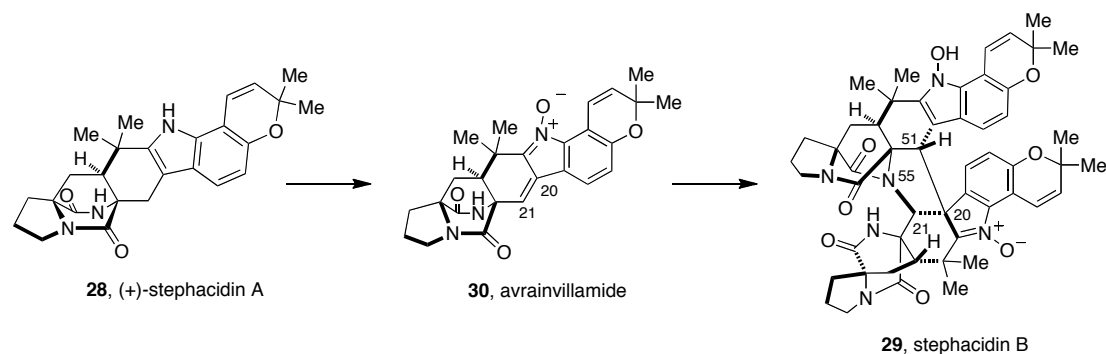
Figure 10. Proposed biosynthetic pathway from stephacidin A to stephacidin B.

In 2007, Tsukamoto and co-workers reported the isolation of notoamides A-D (**31**-**34**, Figure 11) from a marine-derived *Aspergillus* sp. MF297-2 found growing on the mussel, *Mytilus edulis*, collected off the Noto Peninsula in the Sea of Japan.[19] Along with the notoamides, the known compounds, sclerotiamide, (+)-stephacidin A, and deoxybrevianamide E (**7**), were also isolated. Notoamides A-D contain the pyranoindole ring system common in the stephacidins and some of the paraherquamides. Notoamides A and B both contain the core bridging bicycle with C-12 oxidation, as well as the *spiro*-oxindole ring system. In 2005, a group of structurally similar indole alkaloids, named the norgeamides (**34**, **35**-**37**) were isolated by the Hans-Knöll institute from a cold water *Aspergillus* sp. MF297-2[20] Norgeamides A (**35**), B (**36**), and D (**37**) appear to be closely related in their biogenesis to notoamides C (**33**) and D (**34**, also named norgeamide D), and are potential metabolites along the pathway to the more complex prenylated indoles (+)-stephacidin A (**28**) and notoamides A (**31**) and B (**32**). Minor metabolites of the notoamides continue to be isolated from marine-derived *Aspergillus* sp. MF297-2; notoamides E-R (**38**-**51**) are known natural products while notoamides S and T (**52** and **53**) are potential biosynthetic intermediates that have yet to be isolated.[21-24,58-59]
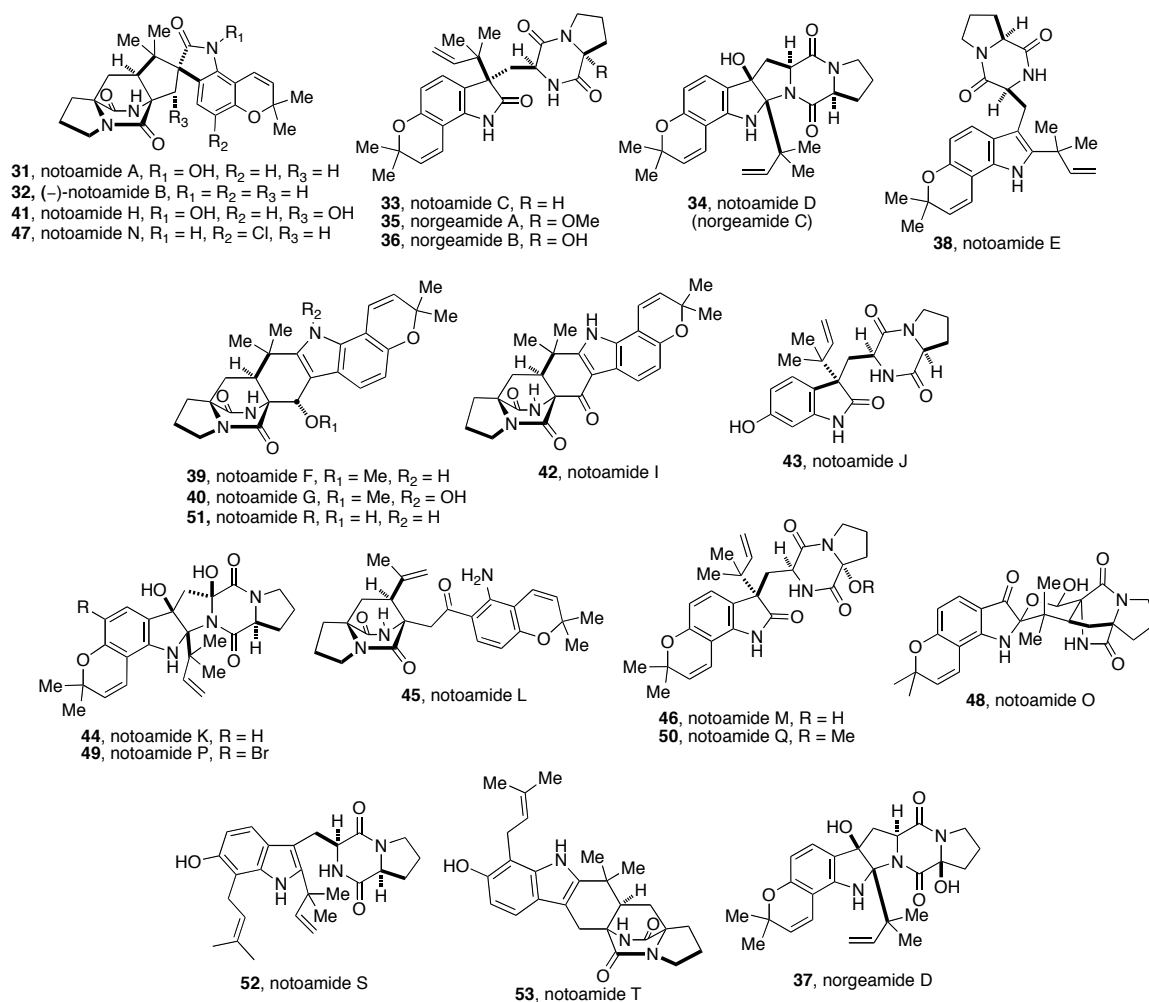
Figure 11. Structures of the notoamides and related compounds.

Stephacidin A and notoamide B were also recently isolated from terrestrial-derived *Aspergillus versicolor*, along with a new fungal metabolite, versicolamide B (**54**).[25] This new secondary metabolite displays a structural feature unique to the stephacidins and notoamides. Versicolamide B represents the first member outside of the brevianamide family to contain the *anti*-relative configuration at C-19 in the bicyclo[2.2.2]diazaoctane ring system. Following the isolation of versicolamide B from *Aspergillus versicolor*, it was found that this metabolite is also produced by marine-

derived *Aspergillus* sp. MF297-2.[23] Further investigation of the metabolites isolated from *Aspergillus versicolor* and *Aspergillus* sp. MF297-2 led to the discovery of another unique trait within this family. (−)-Stephacidin A (**55**), (+)-notoamide B (**56**), and (+)-versicolamide B (**54**) from *Aspergillus versicolor* are antipodal to (+)-stephacidin A (**28**), (−)-notoamide B (**32**), and (−)-versicolamide B (**1.57**) produced by marine-derived *Aspergillus* sp. MF297-2 (Figure 12). Additionally, (−)-stephacidin A is the antipode to (+)-stephacidin A isolated from *Aspergillus ochraceus*.   The discovery of these enantiomeric metabolites produced by two different *Aspergillus* species represents the first known occurrence of reverse prenylated antipodal natural products.
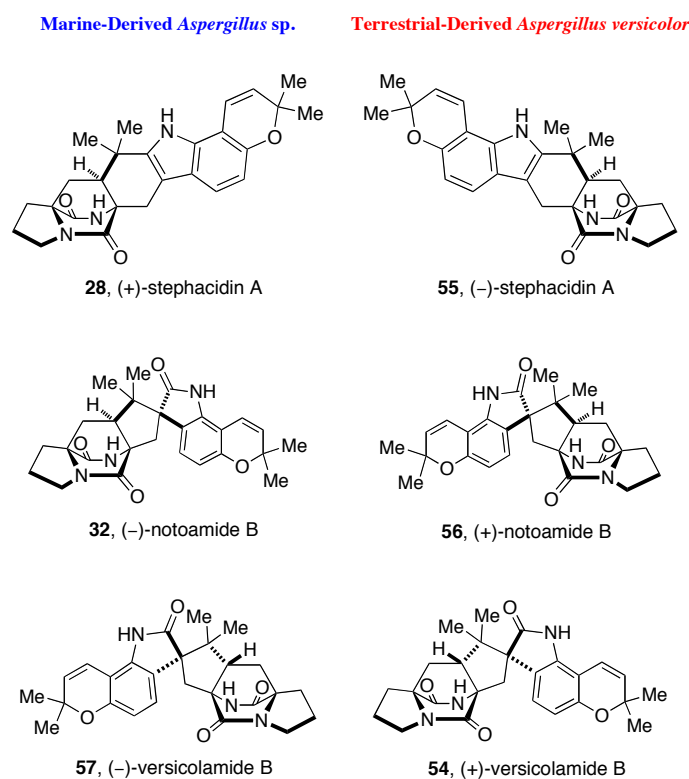
Figure 1.7. Structures of the antipodal metabolites produced by *Aspergillus* sp. MF297-2 and *Aspergillus versicolor*.

As shown in Table 3, numerous prenylated indole alkaloids belonging to the stephacidin and notoamide family have been isolated from varying *Aspergillus* fungal cultures. The structural diversity of the notoamides isolated from *Aspergillus* sp. MF297-2 represents one of the most extensive co-metabolite profiles within the numerous families of prenylated indole alkaloids. This profile suggests that there exists a possible biosynthetic relationship between members of the stephacidin and notoamide family of secondary metabolites, which will be discussed further in Chapter 4.[19]

Table 3. Fungal origin of the stephacidins and notoamides.

Compound	Fungal Species	Reference
sclerotiamide (**27**)	*Aspergillus sclerotiorum*	15
	Aspergillus sp. MF297-2	19
(+)-stephacidin A (**28**)	*Aspergillus ochraceus* WC76466	16
	Aspergillus sp. MF297-2	19
(−)-stephacidin A (**55**)	*Aspergillus versicolor*	25
stephacidin B (**29**)	*Aspergillus ochraceus* WC76466	16
avrainvillamide (**30**)	*Aspergillus ochraceus* CL41582	18
	Aspergillus species CNC358	17
notoamide A (**31**)	*Aspergillus* sp. MF297-2	19
(−)-notoamide B (**32**)	*Aspergillus* sp. MF297-2	19
(+)-notoamide B (**56**)	*Aspergillus versicolor*	25
notoamide C (**33**)	*Aspergillus* sp. MF297	19
notoamide D (**34**)	*Aspergillus* sp. MF297	19
(norgeamide C)	*Aspergillus* sp. MF297	20
notoamide E (**38**)	*Aspergillus* sp. MF297	21
notoamide F (**39**)	*Aspergillus* sp. MF297	22
notoamide G (**40**)	*Aspergillus* sp. MF297	22
notoamide H (**41**)	*Aspergillus* sp. MF297	22
notoamide I (**42**)	*Aspergillus* sp. MF297	22
notoamide J (**43**)	*Aspergillus* sp. MF297	22
notoamide K (**44**)	*Aspergillus* sp. MF297	22
notoamide L (**45**)	*Aspergillus* sp. MF297	23
notoamide M (**46**)	*Aspergillus* sp. MF297	23
notoamide N (**47**)	*Aspergillus* sp. MF297	23
notoamide O (**48**)	*Aspergillus* sp. MF297	24
notoamide P (**49**)	*Aspergillus* sp. MF297	24

notoamide Q (**50**)	*Aspergillus* sp. MF297	24
notoamide R (**51**)	*Aspergillus* sp. MF297	24
(−)-versicolamide B (**57**)	*Aspergillus* sp. MF297	23
(+)-versicolamide B (**54**)	*Aspergillus versicolor*	25
norgeamide A (**35**)	*Aspergillus* sp. MF297	20
norgeamide B (**36**)	*Aspergillus* sp. MF297	20
norgeamide D (**37**)	*Aspergillus* sp. MF297	20
	Aspergillus versicolor	25

Fungi have proven to be a good source of bioactive natural products. While the notoamides appear to have moderate and limited biological activity, the structurally related norgeamides have all been shown to inhibit the growth of a variety of cancer cell lines with varying efficacies.[1.38] Preliminary biological assays reveal that norgeamide A is the most cytotoxic against several carcinoma cell lines. However, sclerotiamide, avrainvillamide, and stephacidins A and B appear to be the most bioactive of the stephacidins and notoamides. These secondary metabolites display anti-insecticidal, antibacterial, and antitumor properties.[16b,15,18]

Sclerotiamide has been shown to exhibit potent activity against first instar larvae of the corn earworm *Helicoverpa zea*.[15] When incorporated into standard test diets of 200 ppm, sclerotiamide resulted in a 46% mortality rate of *H. zea*. There was also a 98% reduction in growth rate, relative to controls, among the survivors. Several physiological effects, such as shriveling and blackening, were also observed in the larvae. In a feeding assay against adults and larvae of the fungivorous beetle *Carpophilus hemipterus*, at a 100-ppm dietary level, sclerotiamide reduced feeding rates by 44% and 40%, respectively.

Avrainvillamide is an antibiotic that inhibits the growth of multi-drug resistant *Staphylococcus aureus*, *Streptococcus pyogenes*, and *Enterococcus faecalis* with MICs of

12.5, 12.5, and 25 μg/ml, respectively.[18]   When tested against *Escherichia coli*, at 100 μg/ml it showed no antibacterial activity.   Avrainvillamide also displays antitumor activity against a variety of tumor cell lines, including human colon HCT116 cells, melanoma MALME-3M cells, and two breast cancer cells, βT-549 and T-47D.[17]

Stephacidins A and B both demonstrate in vitro cytotoxicity against various human tumor cell lines (Table 4).   Stephacidin B exhibited more potent and selective antitumor activities, especially in the testosterone-dependent LNCaP cells.[16]   The effects of stephacidins A and B indicate a novel mode of action since they are not mediated by p53, mdr, or bc12, and they are not tubulin- or topoisomerase II-mediated.

Table 4. In vitro cytotoxicity (μM) of (+)-stephacidin A (**28**) and stephacidin B (**29**).[16]

Cell Line	Histotype	Characteristic	28 (IC_{50})	29 (IC_{50})
PC3	prostate	testosterone-independent	2.10	0.37
LNCaP	prostate	testosterone-sensitive	1.00	0.06
A2780	ovarian	parental	4.00	0.33
A2780/DDP	ovarian	mutp53/bc12+	6.80	0.43
A2780/Tax	ovarian	taxol-resistant	3.60	0.26
HCT116	colon	parental	2.10	0.46
HCT116/mdr+	colon	overexpress mdr+	6.70	0.46
HCT116/topo	colon	resistant to etoposide	13.10	0.42
MCF-7	breast	estradiol-sensitive	4.20	0.27
SKBR3	breast	estradiol-independent	2.15	0.32
LX-1	lung	sensitive	4.22	0.38

2.1.4 The Asperparalines

Asperparaline A (**58**, Figure 13) is an indole alkaloid that was first isolated in 1997 by Hayashi and coworkers from the fungus *Aspergillus japonicus* JV-23 in Sakai, Japan.[60]   In 2000, the same group reported the isolation of two new related indole alkaloids, asperparalines B (**59**) and C (**60**), from the same fungal strain.[61]   In separate

work, Everett et al. reported the isolation of asperparaline A, named aspergillimide, from *Aspergillus* sp. MF297-2 IMI 337664.[62] From the same fungal culture, the 16-keto derivative of asperparaline A was isolated and named SB202327 (**61**).

58, asperparaline A   **59**, asperparaline B

60, asperparaline C   **61**, SB202327
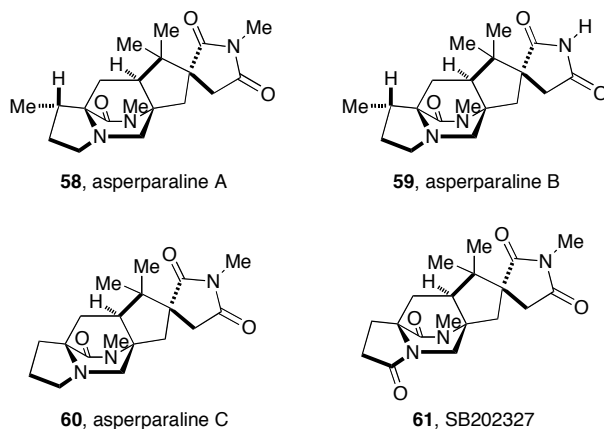
Figure 13. Structures of the asperparalines.

Similar to many of the prenylated indole alkaloids, the asperparalines possess a core bicyclo[2.2.2]diazaoctane ring system. Asperparalines A and B both contain a β-methyl proline ring, whereas asperparaline C is the C-3–desmethyl analog. The asperparalines also contain a unique 3-*spiro*-succinimide ring system in place of the *spiro*-oxindole ring system commonly observed in the paraherquamides, stephacidins and notoamides, and brevianamides.[63]

All members of the asperparaline family have exhibited some form of biological activity. Asperparaline A exhibited paralysis against silkworms at a dose of 10 µg/g of diet within one hour and lasted for 7 to 10 hours upon oral administration.[60] Asperparalines B and C displayed almost the same effect on silkworms.[61] Separately, asperparaline A and SB202327 were tested for anthelmintic activity against adult *Trichostrongylus colubriformis* infections in gerbils.[62] Results from this experiment

showed that asperparaline A displayed a 44% and 98% reduction in faecal egg count when dosed with 10 mg/kg and 20 mg/kg, respectively. SB202327 exhibited in vitro activity against *Haemonchus contortus* L$_3$ larvae, but did not display in vivo activity against *T. colubriformis* in gerbils.

2.1.5 Related Secondary Metabolites

The structural diversity of reverse prenylated indole alkaloids isolated from fungal sources is vast. The austamides (**62-65**, Figure 14), malbrancheamide (**66**), and the marcfortines (**67-70**) all contain unique structural features, different from those discussed earlier. Similar to the previously mentioned fungal metabolites, many of these related indole alkaloids also exhibit biological activity. As displayed in Table 5, these related prenylated indole alkaloids are isolated from various *Penicillium* and *Aspergillus* species.
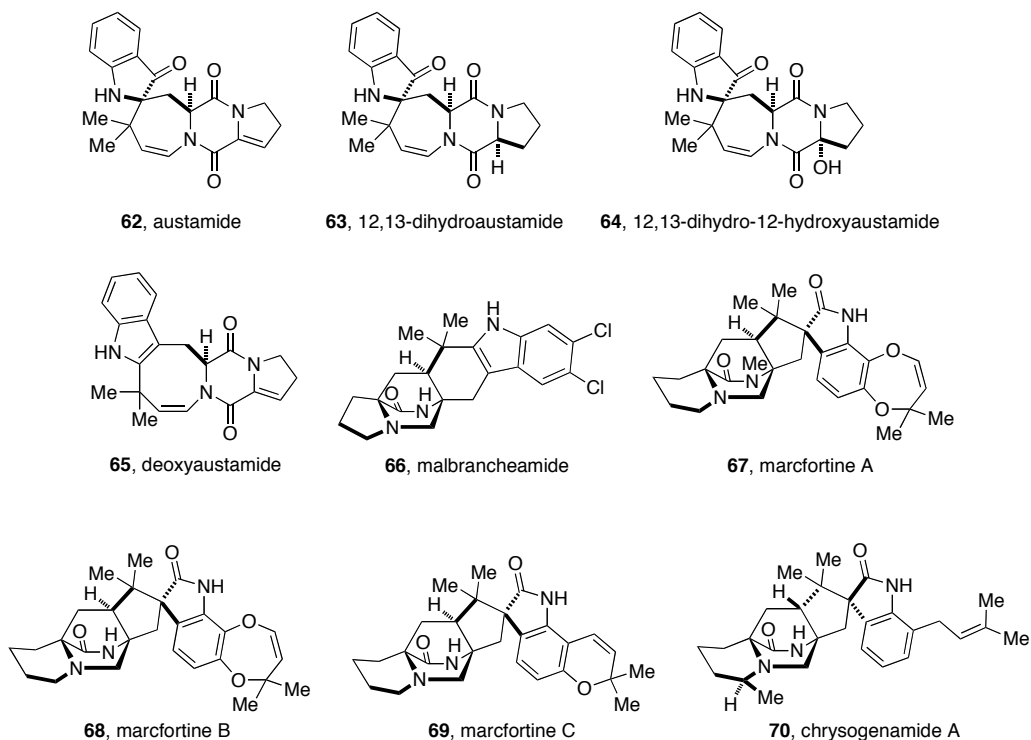
Figure 14. Structures of related secondary metabolites.

Table 5. Fungal origin of several related secondary metabolites.

Compound	Fungal Species	Reference
austamide (**62**)	*Aspergillus ustus*	4, 64
12,13-dihydroaustamide (**63**)	*Aspergillus ustus*	64a
12,13-dihydro-12-hydroxyaustamide (**64**)	*Aspergillus ustus*	64b
deoxyaustamide (**65**)	*Aspergillus ustus*	64a
malbrancheamide (**66**)	*Malbranchea aurantiaca*	65
marcfortine A (**67**)	*Aspergillus carneus*	66
	Penicillium paneum	67
	Penicillium roqueforti	68a
marcfortine B (**68**)	*Penicillium paneum*	67
	Penicillium roqueforti	68
marcfortine C (**69**)	*Penicillium paneum*	67
	Penicillium roqueforti	68
chrysogenamide A (**70**)	*Penicillium chrysogenum*	69

Austamide (**62**), 12,13-dihydroaustamide (**63**), and 12,13-dihydro-12-hydroxyaustamide (**64**) all contain a *spiro*-indoxyl group similar to the brevianamides, however these metabolites also contain a unique seven-membered spiro-indoxyl ring.[4,64] Another metabolite isolated from *Aspergillus ustus* is deoxyaustamide (**65**), which displays an eight membered ring between the indole and diketopiperazine ring, making it a potential metabolic precursor to the austamides.

More recently, Mata and co-workers reported the isolation of malbrancheamide (**66**) from *Malbranchea aurantiaca*.[65] This metabolite is closely related to the paraherquamides and stephacidins and contains the core bicyclo[2.2.2]diazaoctane ring system; however, malbrancheamide is chlorinated at the C-5 and C-6 positions of the indole ring. Malbrancheamide also possesses moderate inhibition of growth of *Amaranthus hypochondriacus* and inhibits the activation of the calmodulin-dependent enzyme PDE1.

The marcfortine family of secondary metabolites also contains the bridging bicycle, a *spiro*-oxindole ring, and substitution on the aromatic ring of the tryptophan moiety. Marcfortines A and B (**67** and **68**) both display the seven-membered dioxepin moiety, while marcfortine C (**69**) exhibits the six-membered pyran ring.[68] Unique to the marcfortines, as well as all other prenylated indole alkaloids, is the presence of the C-7 prenyl group in chrysogenamide A (**70**).[69] Unlike the prenylated indole alkaloids previously discussed, the marcfortines posses a pipecolic acid moiety instead of a proline residue, and with the exception of chrysogenamide A, the six-membered pipecolic acid ring is unsubstituted. Of the marcfortine metabolites, only chrysogenamide A has reported bioactivity; specifically it exhibits a neurocyte protection effect against oxidative stress-induced cell death in SH-SY5Y human neuroblastoma cells.[69]

2.2 Precursor Incorporation Studies in Relation to Biosynthesis

2.2.1 Amino Acid Precursors

As previously stated, early radiolabeling and feeding experiments carried out by Birch demonstrated that the brevianamides are biogenetically derived from tryptophan, proline, and mevalonic acid (Scheme 2).[2,3] In 1970, Birch hypothesized that brevianamide F and deoxybrevianamide E were biosynthetic precursors to brevianamide A, which was later supported by Birch and Williams, respectively.[70,71]
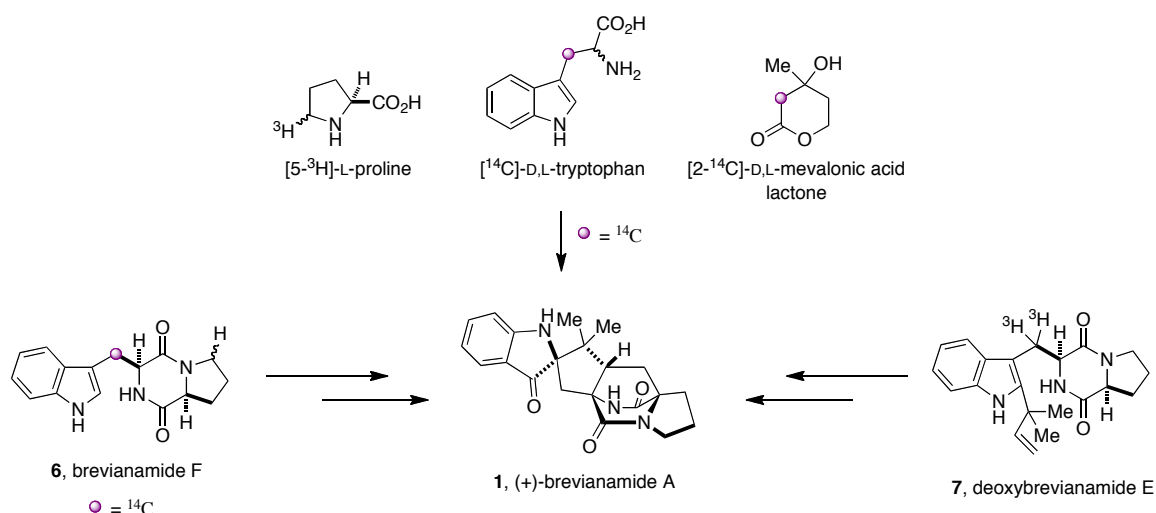
Scheme 2. Biosynthetic study of brevianamide A.[72]

Based on the results obtained from the precursor incorporation studies of the brevianamides, Williams and co-workers postulated that the structurally similar paraherquamides follow a comparable biosynthetic pathway. To determine which amino acid residues are incorporated into paraherquamide A, feeding experiments were performed on *Penicillium fellutanum* using [1-^{13}C]-L-tryptophan, [*methyl*-^{13}C]-L-methionine, [1-^{13}C]-L-proline, and [1-^{13}C]-L-isoleucine (Scheme 3).[27] Through ^{13}C-NMR spectroscopy and electrospray mass spectrometry, the position and percentage of ^{13}C incorporation was analyzed. As expected, [1-^{13}C]-L-tryptophan incorporated at the C-12 position of the oxindole ring with 2.5% incorporation, while only a small amount (0.6%) of [*methyl*-^{13}C]-L-methionine was found to incorporate at the nitrogen methyl of the monoketopiperazine ring. With regard to the β–methyl-β-hydroxyproline ring, precedence established by Arigoni and co-workers for the biosynthesis of bottromycin in *Streptomyces bottropenis* revealed incorporation of [*methyl*-^{13}C]-L-methionine into bottromycin at the 3(*R*)-methyl group of the β–methyl proline ring of bottromycin.[27b]

Unfortunately, results from the precursor incorporation study with *Penicillium fellustanum* showed that neither [*methyl*-^{13}C]-L-methionine nor [1-^{13}C]-L-proline incorporated into paraherquamide A. It was later found that [1-^{13}C]-L-isoleucine exhibited incorporation to the extent of 3.3-3.7%, with the label at the C-18 position. To establish a potential mechanism of incorporation of isoleucine into paraherquamide A, [^{13}C]-[^{2}H]$_3$-L-isoleucine was synthesized and fed to cultures of *Penicillium fellutanum*. Results showed that only one deuterium label was retained, thus confirming a 4-electron oxidative cyclization pathway to form β–methyl-L-proline (Scheme 3B). This possibility was supported by an additional ^{13}C-labeling study, which revealed a higher percentage of ^{13}C incorporation in the monoketopiperazine ring when L-isoleucine underwent oxidative cyclization to form the β–methyl-L-proline prior to the precursor incorporation study with *P. fellutanum*. An incorporation of 14.6% was observed in this case, compared to the previously observed 3.7% incorporation of L-isoleucine.
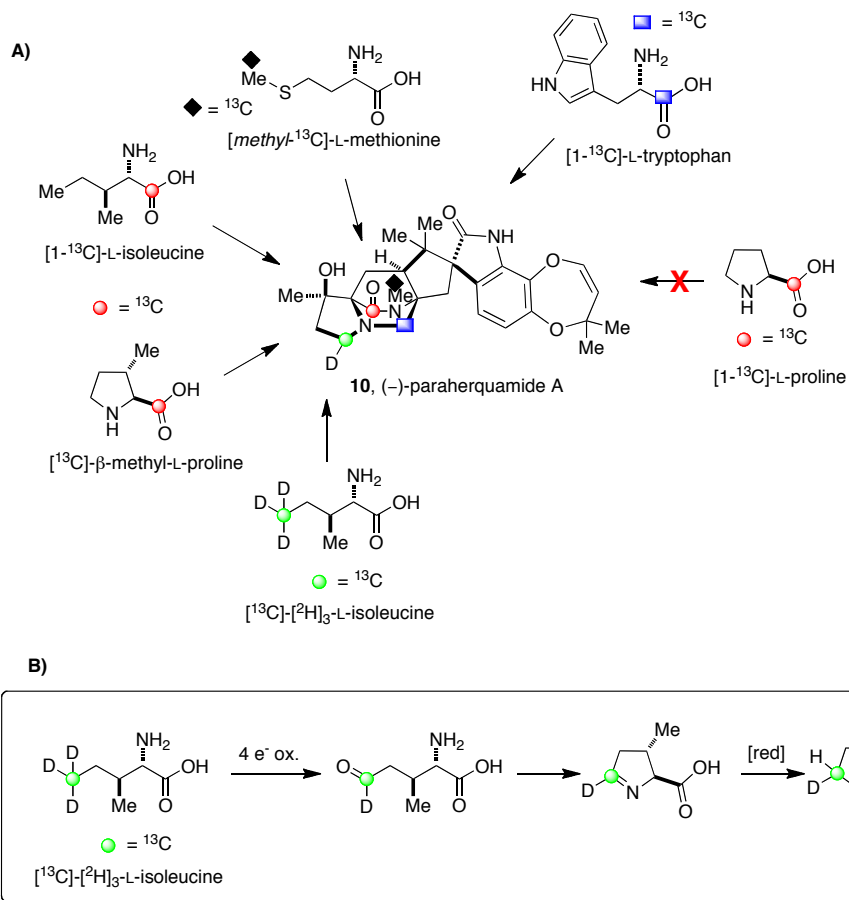
Scheme 3. (A) ^{13}C-labeled amino acid incorporation into paraherquamide A in *Penicillium fellutanum*. (B) Proposed biosynthetic pathway for the conversion of L-isoleucine to 3(*S*)-methyl-L-proline.[27]

2.2.2 Advanced Intermediate

As shown in Scheme 4, the most advanced ^{13}C-labeled intermediate to be synthesized and incorporated into paraherquamide A was doubly ^{13}C-labeled pre-paraherquamide (**25**), with an incorporation of 0.72%. When fed to *P. fellutanum*, this material was incorporated with the double label intact, suggesting that pre-paraherquamide is in fact a precursor in the paraherquamide biosynthesis. This

information also indicates that oxidation of the indole ring to form the dioxepin ring and the *spiro*-oxindole moiety occurs after the formation of this intermediate.[30]
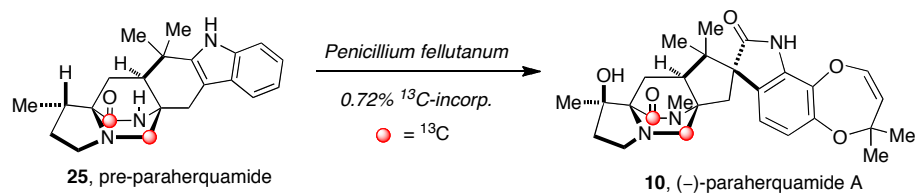
Scheme 4. Incorporation of ^{13}C-labeled pre-paraherquamide into paraherquamide A in *P. fellutanum*.

2.2.3 Isoprene Units

Initial characterization of the paraherquamides, notoamides, and stephacidins led to the conclusion that two isoprene units are present in these alkaloid families (Figure 15). One of the two isoprene units is involved in the formation of the bicyclo[2.2.2] nucleus (shown in red), while the other isoprene unit contributes to the formation of the dioxepin ring and the pyran ring (highlighted in blue).[31]
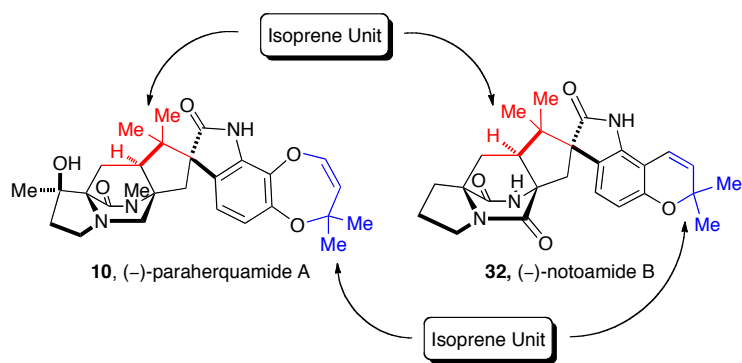
Figure 15. Location of the isoprene units in prenylated indole alkaloids.

To determine the biosynthetic pathway from which the isoprene units originate [13C_2]-acetate was fed to *P. fellutanum* (Scheme 5). Specific incorporation of intact C_2

31

units, combined with the ^{13}C coupling patterns observed by ^{13}C-NMR spectroscopy demonstrated that the isoprene units in paraherquamide A arise from dimethylallylpyrophosphate (DMAPP), a product of the mevalonic acid pathway.[31,32]
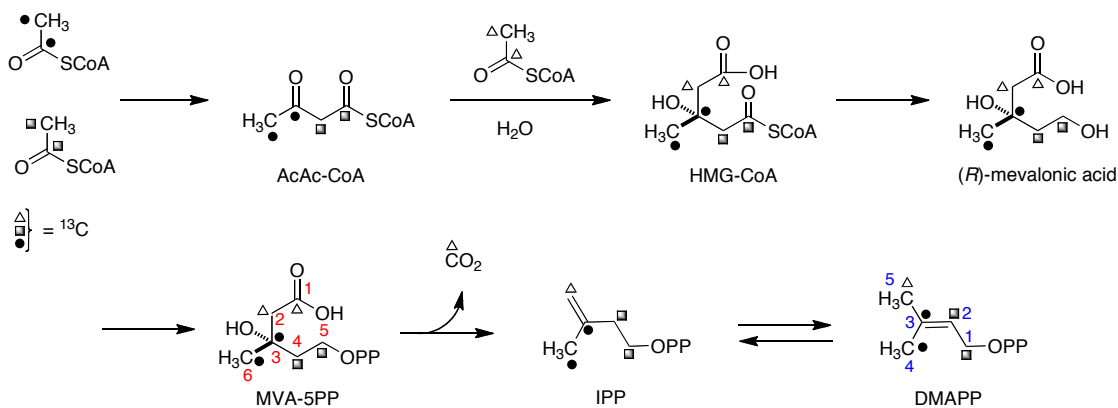
Scheme 5. The classical mevalonic acid pathway showing the labeling pattern via 1,2-doubly labeled acetate (note the change in carbon numbering).

Biosynthetic research has also shown that the addition of $[^{13}C_2]$-acetate into the above pathway presents distinct coupling patterns. In this instance, coupling was observed between C-1 and C-2, and between C-3 and C-4 of DMAPP; however, no coupling was observed between C-3 and C-5 since it has been demonstrated that C-5 of DMAPP is derived from C-2 of mevalonic acid (Figure 16).[31]
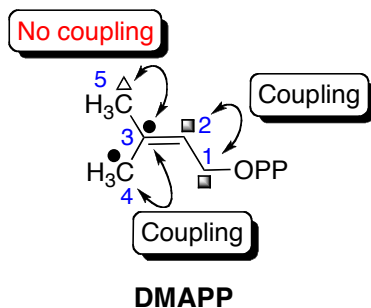
DMAPP

Figure 16. Observed coupling pattern in DMAPP.

32

When [13C$_2$]-acetate was fed to *P. fellutanum*, it was demonstrated that the isoprene units in paraherquamide A were introduced in two distinct manners (Figure 17).[31] Through 13C-NMR spectroscopy, the coupling of intact C$_2$ units revealed that in the C$_5$ fragment formed by C19 to C23, C19 was coupled to C-20, while C-21 was coupled to C-22 and C-23, but not to both simultaneously. For the second C$_5$ unit in paraherquamide A, C-24 to C-28, the coupling constants showed that C-24 was coupled to C-25, while C-26 was coupled to C-27, but not to C-28.[31] Through the observed coupling patterns, it was concluded that the introduction of the C-24 to C-28 isoprene unit must proceed through a direct prenyl transferase in which nucleophilic displacement at the pyrophosphate-bearing methylene carbon occurs while the hydrophobic tail of DMAPP is buried in the enzyme active site.

10, (–)-paraherquamide A
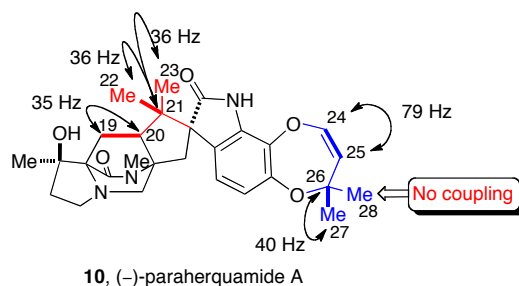
Figure 17. Relevant coupling patterns observed in the 13C NMR spectrum of paraherquamide A. Thick lines represent intact acetate units.

The mechanistic formation of the C-19 to C-23 fragment was further complicated by the observed scrambling of the 13C labels of the geminal methyl groups at C-22 and C-23, thus indicating a loss of stereochemical integrity during the biosynthetic construction of the quaternary center.[31,32] These unexpected results pointed to a reverse prenyl transferase. In this case, the olefinic π system of DMAPP is presented in such a manner

that both faces are susceptible to attack by the 2-position of the indole moiety. As shown in Scheme 6, one possible explanation is that the pyrophosphate group is anchored in the enzyme active site with the hydrophobic isopropenyl moiety being presented in a conformationally flexible disposition (A⇌B).
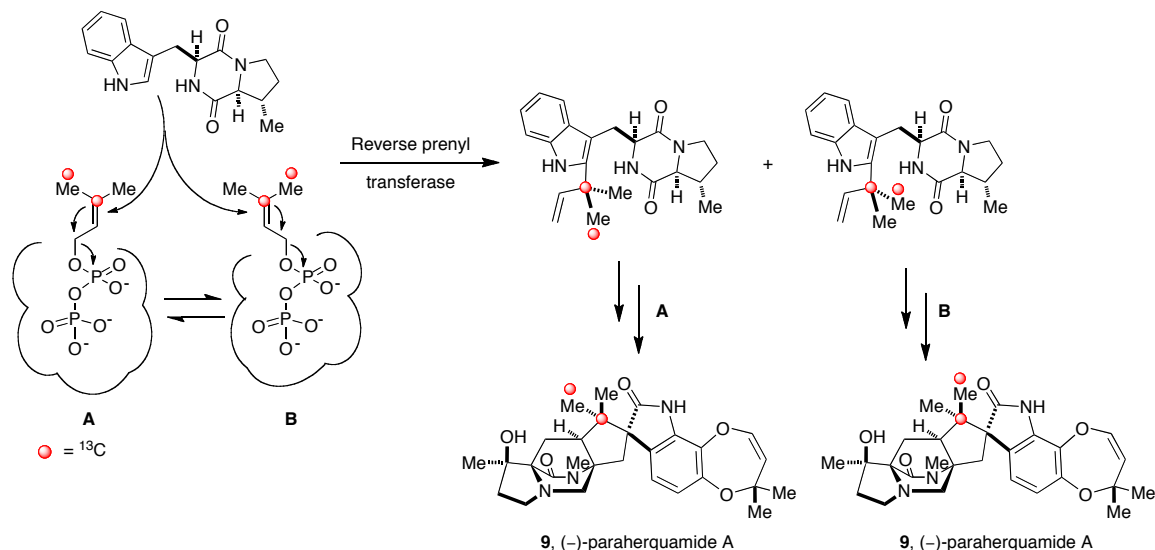
Scheme 6: A possible biosynthetic sequence that may explain the scrambling of the geminal methyl ^{13}C labels.

2.2.4 Additional Studies

Following the informative results obtained on the biosynthesis of the paraherquamides, similar biosynthetic studies were performed on *Aspergillus japonicus*. To determine the primary amino acid building blocks of asperparaline A [1,2-^{13}C$_2$]-acetate, [*methyl*-^{13}C]-L-methionine, [1-^{13}C]- L-isoleucine, [1-^{13}C]- L-tryptophan, and [*indole*-2-^{13}C]- L-tryptophan were employed in precursor incorporation studies.[73] The position of the ^{13}C enrichment in asperparaline A was determined by ^{13}C-NMR and the percentage of labeled amino acid enrichment was determined by ^{13}C-NMR and electrospray mass spectrometry. Results showed that [1,2-^{13}C$_2$]-acetate incorporates into

asperparaline A in an analogous manner to that of paraherquamide A, indicating that the isoprene units in asperparaline A also arise from the mevalonic acid pathway. A significant amount of incorporation from [*methyl*-^{13}C]-L-methionine was observed at the C-29 (25.2%) and C-30 (26.9%) positions of asperparaline A, but no incorporation was observed in any part of the β-methyl proline ring. However, as expected, [1-^{13}C]- L-isoleucine exhibited a 5.8% incorporation at the C-18 position of the β-methyl proline ring. While the asperparalines appear at first glance to be the only prenylated indole alkaloids not derived from tryptophan, the precursor incorporation studies show otherwise. Both [1-^{13}C]- L-tryptophan and [*indole*-2-^{13}C]- L-tryptophan showed incorporation at the C-12 (6.4-7.2%) and C-2 (12.2%) positions of asperparaline A, respectively. This indicates that tryptophan is responsible for the construction of the *spiro*-succinimide ring found in the asperparalines. Furthermore, these results suggest that asperparaline A and paraherquamide A share a common biosynthetic pathway.

Further establishing a unified biosynthetic pathway between the families of prenylated indole alkaloids, Kuo and co-workers have demonstrated that marcfortine A is biogenetically derived from tryptophan, methionine, lysine, and two isoprene units.[74] Precursor incorporation studies revealed that lysine, via α-ketoglutarate, is responsible for the formation of the pipecolic acid moiety present in the marcfortines. This study also showed that methionine is the precursor to the C-29 N-methyl group and that both isoprene units are derived via the mevalonate pathway.

2.3 Formation of the Bicyclo[2.2.2]diazaoctane Ring

A majority of the prenylated indole alkaloids contain the unique core bicyclo[2.2.2]diazaoctane ring, and as such, the synthetic formation of this ring system has become a vastly studied area. Two important synthetic approaches that have been developed are the biomimetic Diels-Alder cycloaddition and the intramolecular S_N2' cyclization. These two synthetic strategies, largely utilized by Williams and co-workers, have resulted in the total synthesis of brevianamide B, paraherquamide B, stephacidin A, avrainvillamide, stephacidin B, VM55599, marcfortine C, malbrancheamide B, and (+)- and (−)-versicolamide B.[75] Select synthetic examples of these two approaches are discussed below.

2.3.1 Biomimetic Diels-Alder Cycloaddition

Shortly following the isolation of the brevianamides, Porter and Sammes proposed that the core bicyclo[2.2.2]diazaoctane moiety was the result of an intramolecular hetero Diels-Alder cycloaddition (IMDA) of a 5-hydroxy-pyrazine-2(1*H*)-one (Scheme 7).[76] Since then, extensive research has been carried out to synthetically support a biosynthetic Diels-Alder reaction via biomimetic routes. Concurrently, considerable effort has been put forth to isolate and characterize the putative Diels-Alderase enzyme responsible for this biosynthetic transformation, but to date, no such enzyme has been isolated.
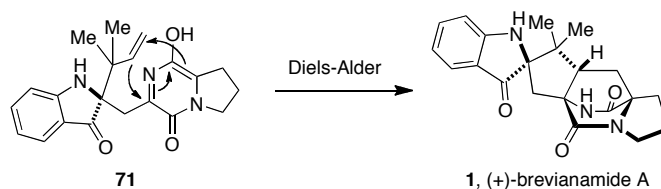
Scheme 7. Proposed biosynthetic Diels-Alder reaction.

The first application of the biomimetic Diels-Alder reaction for the formation of the bicyclo[2.2.2]diazaoctane ring system in the prenylated indole alkaloids was in the biomimetic total synthesis of brevianamide B (Scheme 8).[77] Starting with *epi*-deoxybrevianamide E (**72**), formation of the lactim ether **73** with methyl Meerwein's salt was followed by oxidation to give the Diels-Alder precursor **74**. Tautomerization (**75**) was achieved upon treatment with aqueous KOH, which subsequently underwent an intramolecular Diels-Alder reaction to afford a 2:1 mixture of *syn*- and *anti*-diastereomers (**76** and **77**). The minor *anti*-diastereomer (**77**) underwent oxidation, pinacol, and deprotection of the lactim ether to provide racemic brevianamide B (**2**).
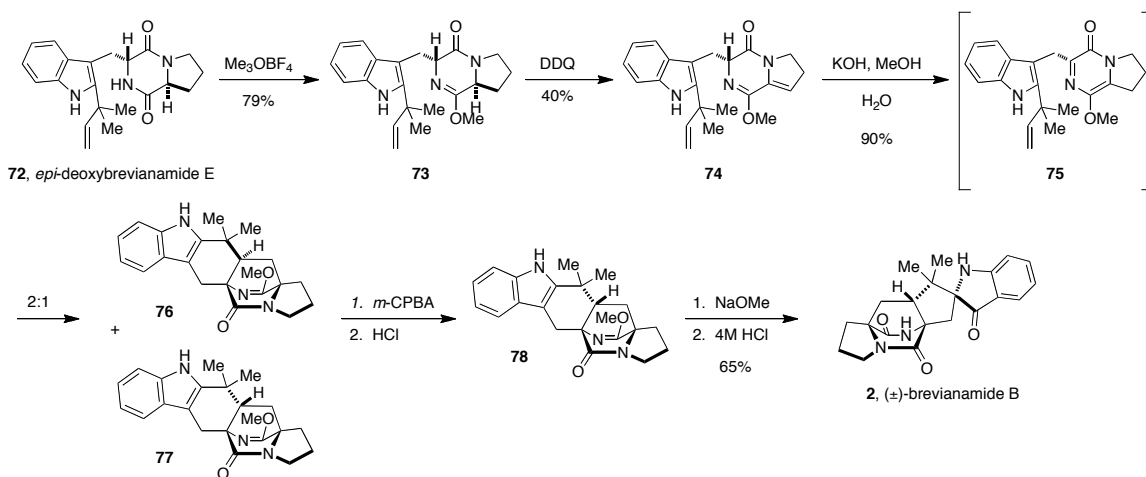
Scheme 8. Biomimetic Diels-Alder formation of racemic brevianamide B.

Williams et al. recently developed two different biomimetic Diels-Alder strategies for the total synthesis of stephacidin A. The first route (Scheme 9) relies on the formation of the lactim ether version of the key azadiene precursor, similar to that of the total synthesis of racemic brevianamide B.[78] The reverse prenylated tryptophan derivative **79** was first coupled to *cis*-3-hydroxyproline ethyl ester hydrochloride **80** to afford the amide **81**, which was subsequently deprotected and cyclized to provide dioxopiperazine **82**. A Mitsunobu-type elimination yielded the enamide, which was further converted to the desired lactim ether **83**. The bicyclo[2.2.2]diazaoctane ring was formed following tautomerization of **83** to the intermediate azadiene **84**, which underwent a spontaneous intramolecular Diels-Alder reaction to afford the cycloadducts **85** and **86**. The predominant *syn*-isomer (**85**) was deprotected under acidic conditions to afford racemic stephacidin A.
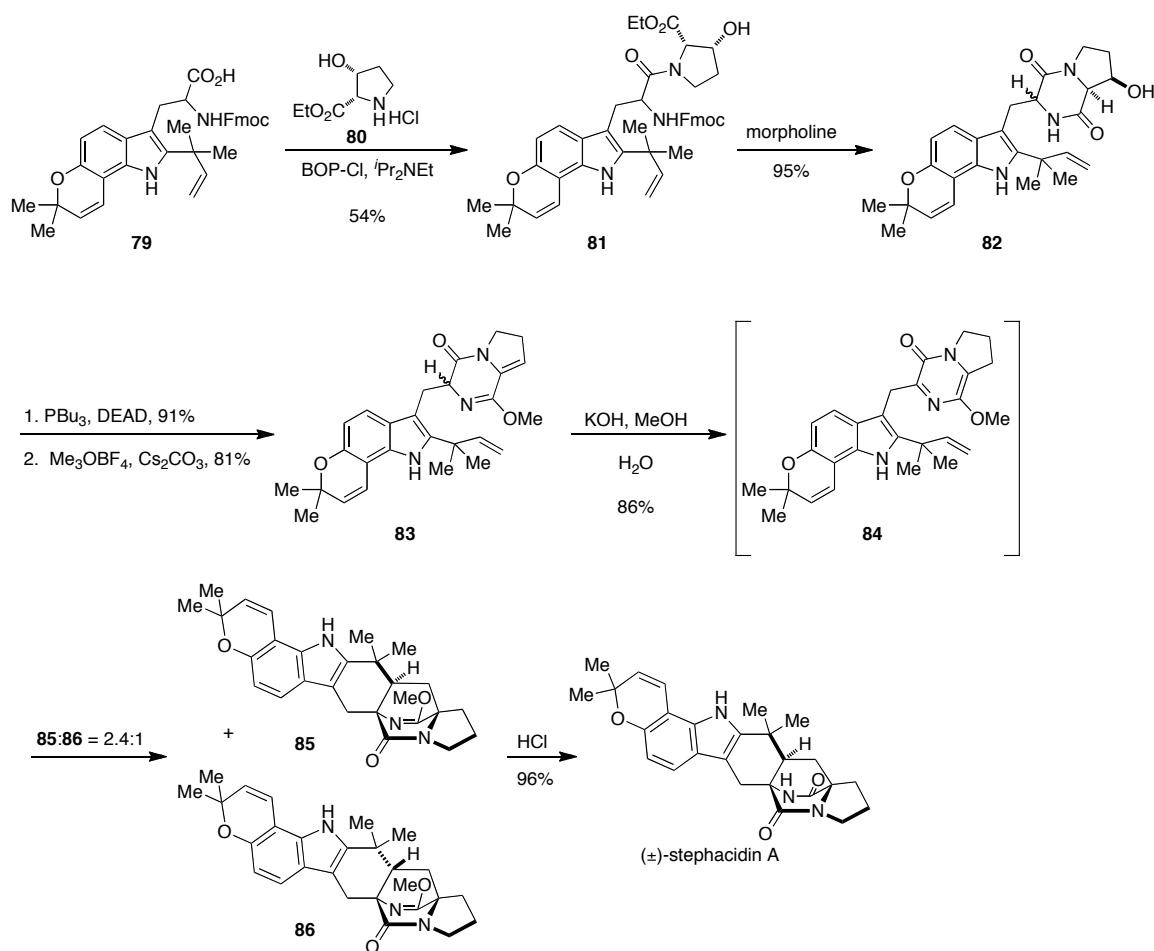
Scheme 9. Biomimetic total synthesis of stephacidin A utilizing the lactim ether.

The second approach by Williams utilizes the originally proposed biosynthetic precursor, 5-hydroxy-pyrazine-2(1H)-one (**71**) as the intermediate to the Diels-Alder reaction (Scheme 10).[79] From diketopiperazine **82**, treatment with PBu$_3$ and DEAD in CH$_2$Cl$_2$ at 40 °C for 20 hours directly afforded stephacidin A, along with the *anti*-isomer in a 2.4:1 ratio, respectively. This biomimetic route to stephacidin A represents the first successful example wherein the putative biosynthetic 5-hydroxy-pyrazine-2(1H)-one intermediate serves as the substrate for the Diels-Alder cycloaddition,[80] thus providing

further support for the possible intermediacy of this species within the biosynthetic pathway.
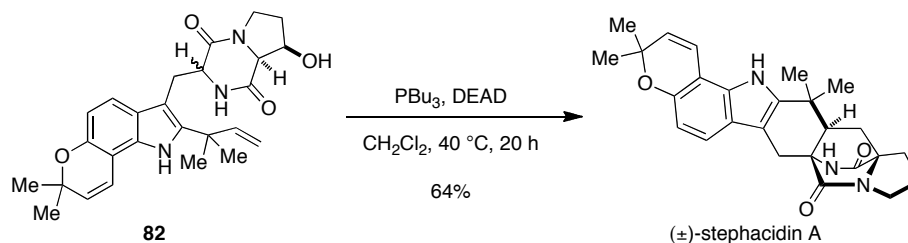
Scheme 10. Improved biomimetic total synthesis of stephacidin A.

Following the isolation of both antipodes of versicolamide B, interest was sparked in developing a biomimetic total synthesis of both (+)- and (−)-versicolamide B utilizing the IMDA approach (Scheme 11).[81] Starting from the *cis*-diastereomer of **82**, the same intermediate used in the stephacidin synthesis, oxidative rearrangement using the Davis oxaziridine reagent (**87**) gave a 3:1 mixture of oxindoles **88** and **89**. Each oxindole underwent Mitsunobu conditions to afford the corresponding enamides **90** and **91** (only the pathway leading from enamide **90** to (+)-versicolamide is shown in Scheme 11). (+)-Versicolamide B (**54**) and a minor diastereomer **92** were formed exclusively as the *anti*-cycloadducts via the IMDA under basic conditions. *Ab initio* calculations reveal that the lack of formation of the *syn*-isomer is explained by the particularly stable transition state leading to the *anti*-cycloadduct when an oxindolic azadiene is used.[82] When an indolic azadiene is present, such as in the synthesis of stephacidin A, both *syn*- and *anti*-transition states are roughly equally stable resulting in the formation of both isomers.
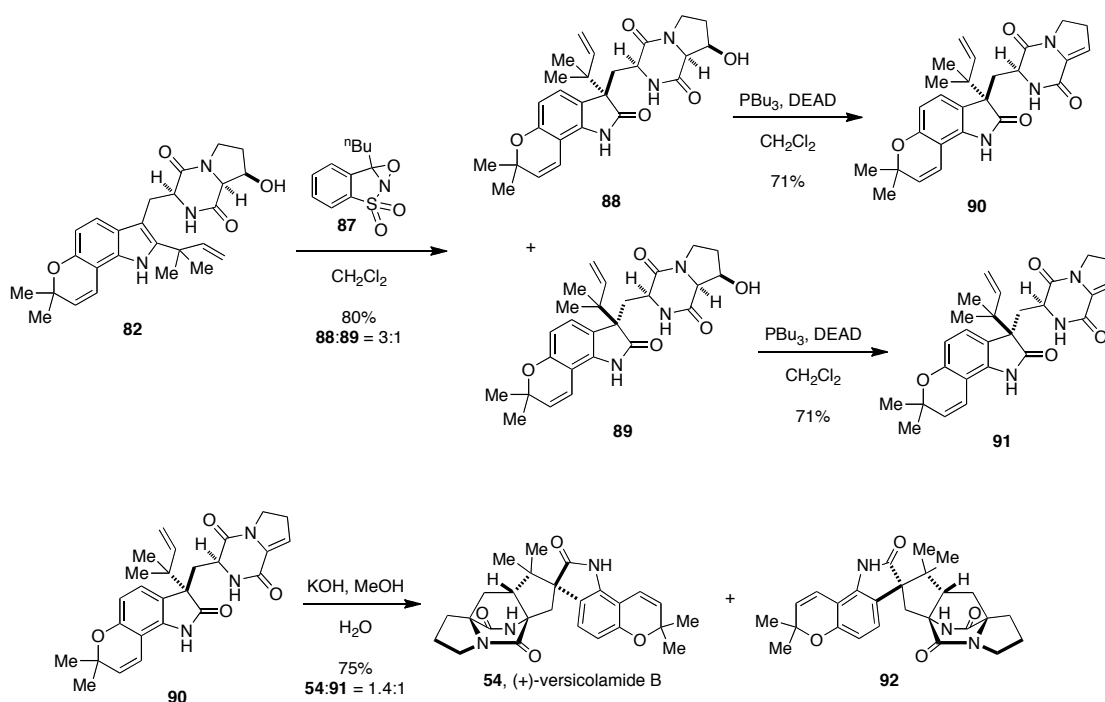
Scheme 11. Biomimetic total synthesis of (+)-versicolamide B.

2.3.2 Intramolecular S$_N$2´ Cyclization

Another synthetic strategy for the formation of the core bicyclo[2.2.2]diazaoctane ring system developed by the Williams research group is the intramolecular S$_N$2´ cyclization reaction. This method was first employed in 1988 in the total synthesis of brevianamide B (Scheme 12).[83] Starting with the known prenylated proline derivative **93**, nucleophilic ring opening provided the PMB-protected amide **94**. Following acylation and cyclization of **94** to form the diketopiperazine **95**, ozonolysis afforded the aldehyde, which underwent a Wittig olefination and reduction to afford **96**. The primary alcohol was subsequently protected as the silyl ether and deprotonation of the diketopiperazine, followed by quenching with methyl chloroformate, provided the methyl ester intermediate **97**. A Somei-Kamatani coupling of **97** with gramine **98** afforded **99**,

which then underwent removal of the methyl ester and conversion of the TBS-protected primary alcohol to the primary chloride **100**, the key intermediate in the S_N2' cyclization. Treatment of **100** with NaH and 18-crown-6 provided the core bicyclo[2.2.2]diazaoctane ring system (**101**) predominantly as the *anti*-isomer, which was followed by deprotection of the indole and olefin-cation cyclization to yield the hexacyclic indole substrate **102**. Formation of the *spiro*-indoxyl **103** and removal of the PMB-protecting group provided brevianamide B.
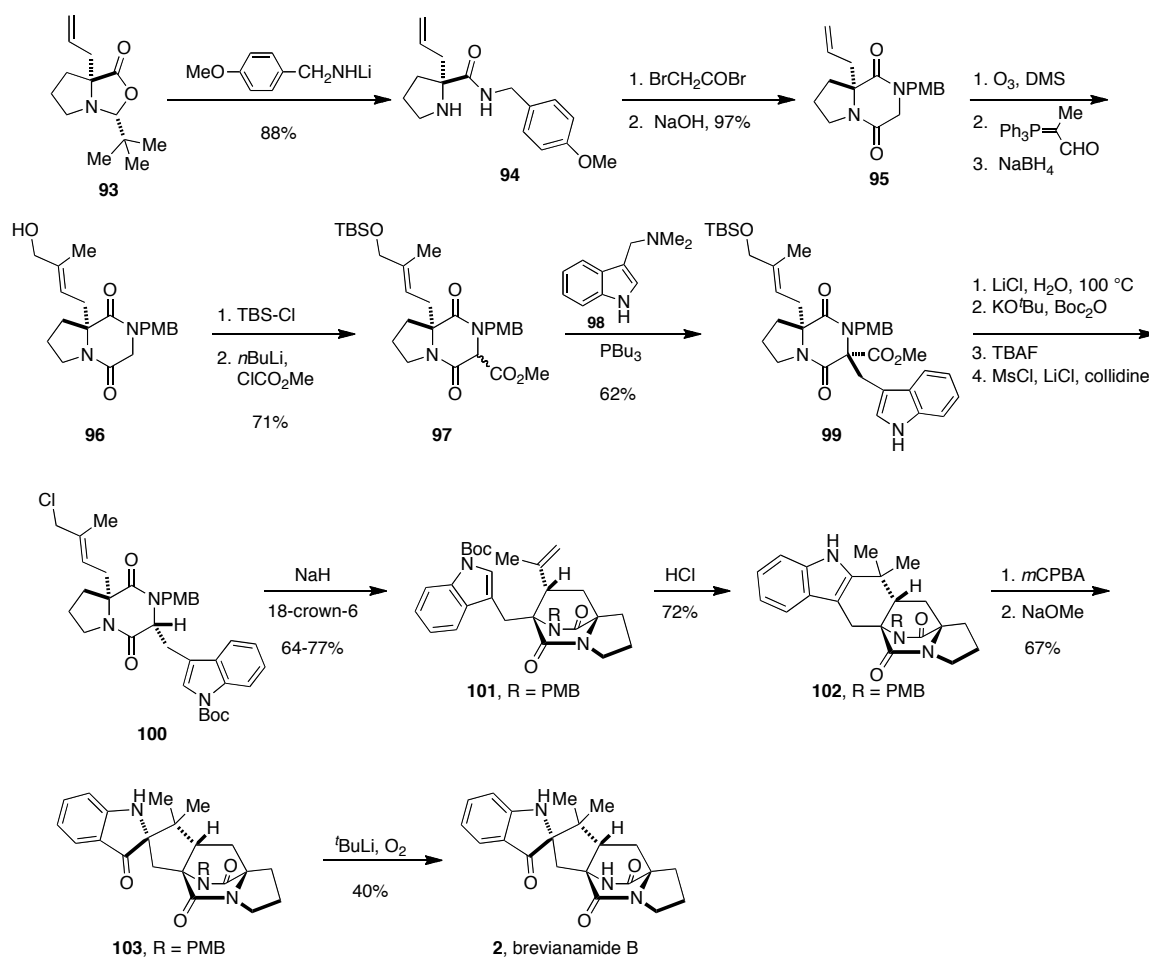
Scheme 12. Total synthesis of brevianamide B utilizing an intramolecular S_N2' cyclization.

Williams and co-workers later utilized the intramolecular S_N2' cyclization strategy for the total synthesis of stephacidin A (Scheme 13); however, unlike the above synthesis of brevianamide B, the installation of the allylic chloride came about via a cross-metathesis reaction.[57] To start, tryptophan derivative **104** underwent a traditional coupling reaction with allyl proline **105**, followed by microwave heating to afford the dioxopiperazine **106**. Lactim ether formation and protection of the indole as the Boc-carbamate provided the key precursor (**107**) for the cross-metathesis. Utilizing methacrolein and 5 mol% of the Hoveyda-Grubbs 2nd generation catalyst with **107**, the desired aldehyde **108** was obtained. Reduction of the aldehyde and conversion to the allylic chloride afforded **109**, which underwent a *syn*-selective intramolecular S_N2' cyclization to give the core bridging bicycle **110**. Palladium-mediated cyclization of **111** followed by thermal removal of the Boc-protecting group on the indole afforded stephacidin A.
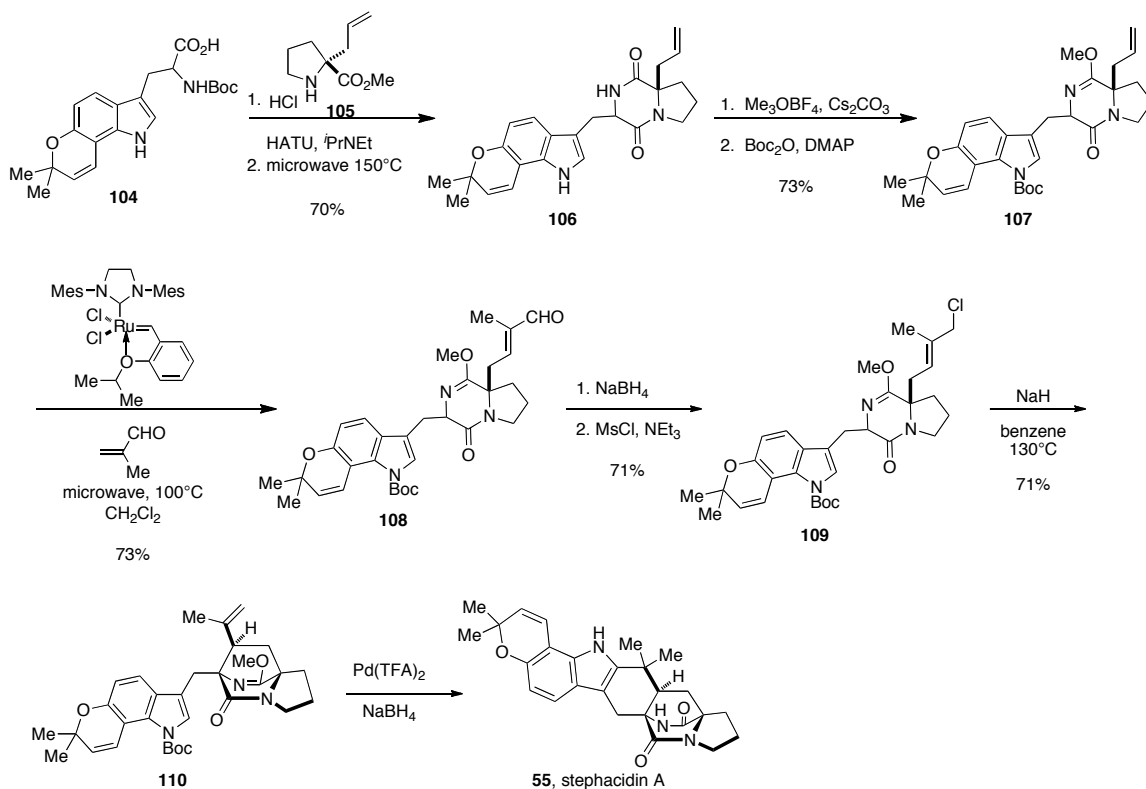
Scheme 13. Intramolecular S_N2' cyclization approach to the total synthesis of stephacidin A.

The contrast in selectivity of the intramolecular S_N2' cyclization between the brevianamides and stephacidins is believed to be a result of an open versus closed transition state, respectively.[83] The *anti*-diastereoselectivity observed in the brevianamide synthesis could be the result of 18-crown-6 weakly coordinating to the enolate counterion, resulting in an open transition state where cyclization occurs from the alternate rotamer of the allylic halide. Alternatively, the use of benzene allows for a tight, intramolecular contact ion pair-driven closed transition state model, resulting in the *syn*-isomer.

2.4 Research Objectives

The original intent of my research was to further explore the biosynthetic pathway of the paraherquamides and asperparalines (Chapter 3). During this time, Tsukamoto and co-workers reported the isolation of the notoamides, which resulted in my focus being shifted toward determining the biosynthetic pathway of the stephacidins and notoamides in marine-derived *Aspergillus* sp. MF297-2 (Chapter 4) and terrestrial-derived *Aspergillus versicolor* (Chapter 5).

CHAPTER 3

Efforts to Further Elucidate the Biosynthesis of Paraherquamide A and

Asperparaline A

3.1 Pre-paraherquamide as a Biosynthetic Precursor

In 1993, Everett and co-workers isolated eight secondary metabolites from *Penicillium* sp. IMI 332995 (Figure 18). Along with (−)-paraherquamides A (**10**), E (**14**), F (**15**), and G (**16**), four novel secondary metabolites were also isolated (**19-22**). More importantly, the isolation of VM55599 (**22**) represented the first documented example of the hexacyclic indole species that had long been proposed as a potential precursor within the biosynthetic pathway of the brevianamides and paraherquamides.[9]
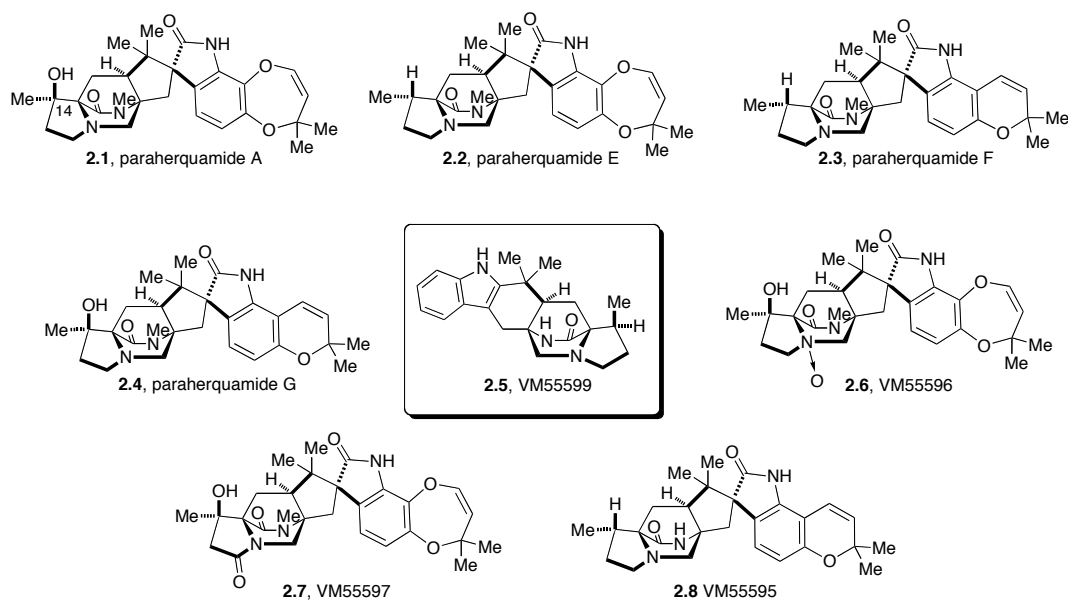
Figure 18. Secondary metabolites isolated from *Penicillium* sp. IMI 332995.

With the isolation of VM55599, it was thought that this metabolite could be a biosynthetic intermediate to paraherquamide A; however, one disadvantage to VM55599 serving as a precursor to any of these metabolites is the stereochemistry of the methyl group of the β-methyl proline ring. In the case of VM55599, the methyl group is disposed *syn* to the bridging isoprene residue, whereas in each of the other metabolites, the methyl group is *anti* to the bridged bicycle. In order for VM55599 to be a precursor to paraherquamide A, oxidation of the β-methyl proline ring would have to occur with inversion of stereochemistry at the C-14 position. To determine whether VM55599 serves a precursor to paraherquamide A, the Williams group synthesized doubly ^{13}C-labeled VM55599.[30] Through a series of feeding experiments with *P. fellutanum* it was determined that VM55599 did not incorporate into paraherquamide A, which suggests that VM55599 is not a precursor within the biosynthetic pathway.

As mentioned in Chapter 1, ^{13}C-labeled pre-paraherquamide (**25**), which displays the correct stereochemistry at C-14, was synthesized by the Williams group and fed to *Penicillium fellutanum*.[33] Results from the precursor incorporation study showed significant incorporation of pre-paraherquamide into paraherquamide A, establishing that **25** is a biosynthetic precursor to paraherquamide A. Given that the core skeletal arrangement found in pre-paraherquamide is displayed in several of the reverse prenylated indole metabolites, pre-paraherquamide could serve as a precursor to numerous indole natural products. If this is the case, pre-paraherquamide may have, at best, a fleeting existence, making its isolation a daunting and difficult task. However, Sherman and co-workers recently obtained evidence for the existence of pre-paraherquamide in cultures of *Penicillium fellutanum* and *Aspergillus japonicus* by

matching the MS/MS fragmentation patterns of synthetic pre-paraherquamide to natural pre-paraherquamide.[14]

The above work done by Sherman establishes the presence of pre-paraherquamide in cultures of *Aspergillus japonicus*, as well as the presence of paraherquamide A and paraherquamide B. These results provide indirect support that: (a) pre-paraherquamide is a precursor to asperparaline A; and (b) paraherquamide A and asperparaline A share a unified biosynthetic scheme. To address both of these hypotheses a unified biogenetic pathway starting from pre-paraherquamide has been proposed. As illustrated in Scheme 14, the biosynthesis of paraherquamide A could arise via oxidation of the aromatic ring of pre-paraherquamide to the catechol derivative (**111**), followed by prenylation, dioxepin formation, and oxidation to the *spiro*-oxindole (**10**). Along this same pathway, formation of the *spiro*-succinimide ring of asperparaline A (**58**), would occur via interruption of the paraherquamide A biosynthesis just before the prenylation step of the catechol derivative. This would provide a branching point for the oxidative cleavage of four carbons of the aromatic ring.[14,32,73]

Scheme 14. Proposed unified biosynthetic pathway of the paraherquamides and asperparalines.

Unfortunately, substantial evidence is still lacking to definitively confirm either hypothesis. The incorporation of ^{13}C-labeled pre-paraherquamide into asperparaline A through a feeding study with *Aspergillus japonicus* would not only show that pre-paraherquamide is an intermediate, but also provide additional support for a unified biosynthetic pathway.

3.1.1 Progress Toward the Synthesis of Pre-paraherquamide

Before synthesizing ^{13}C-labeled pre-paraherquamide for feeding experiments, the synthesis was first carried out on unlabeled material through the Diels-Alder pathway described in Scheme 15.[84] First, the reverse prenylated indole **112** can be converted to the tryptophan derivative **113**, which could be subsequently coupled with β-methyl-β-hydroxyproline (**114**) and cyclized to yield the diketopiperazine **115**. Formation of the azadiene **116** followed by tautomerization **117** sets the stage for the Diels-Alder

cycloaddition. Pre-paraherquamide (**25**) is provided following cleavage of the lactim ether and selective reduction.
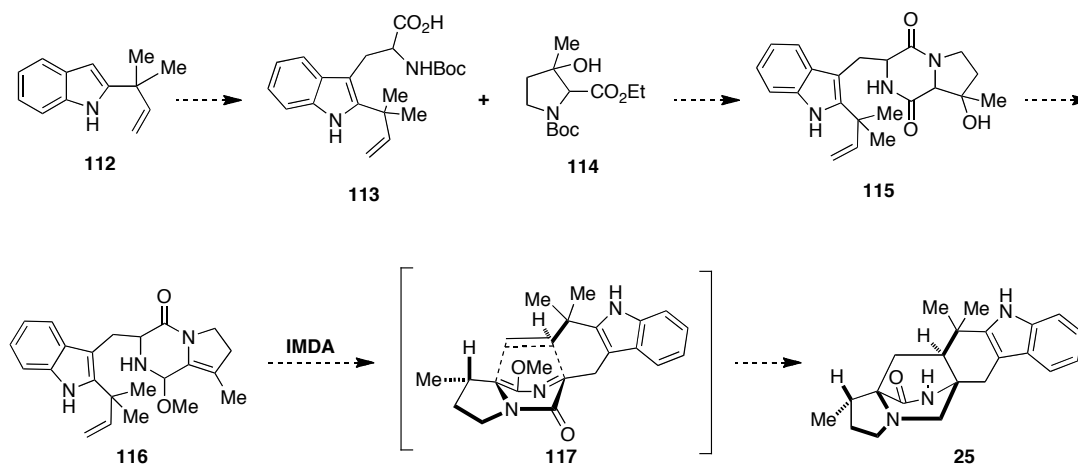
Scheme 15. Key steps towards pre-paraherquamide using the Diels-Alder approach.

Formation of the reverse prenylated indole **112** followed the excellent procedure established by Danishefsky and co-workers,[85] which began by reacting commercially available indole **118** with N-chlorosuccinimide to yield C-3 chloro-indole **119** (Scheme 16). Treatment of **119** with prenyl-9-BBN and allene **120** furnished the C-2 reverse prenylated indole **112**.
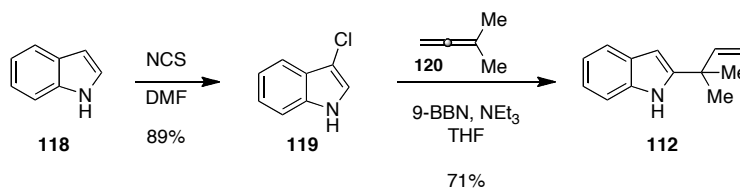
Scheme 16. Synthesis of the reverse prenylated indole.

With the reverse prenylated indole in hand, gramine **121** was obtained from **112**, and subsequently coupled with **122** in a microwave assisted Somei-Kametani[86] coupling to afford **123** in high yield (Scheme 17). As shown in Scheme 18, **122** was synthesized from commercially available benzophenone imine **124** and glycine ethyl ester **125** in high

yield. At this point, instead of proceeding with the originally planned deprotection-reprotection, saponification of the ethyl ester was attempted. Product formation was observed, albeit in poor yield. For this reason, the originally planned synthesis was continued from **123**. Deprotection of the benzophenone imine was followed by Boc protection of the resulting amine and saponification of the ethyl ester **128** gave the N-Boc acid **113**.
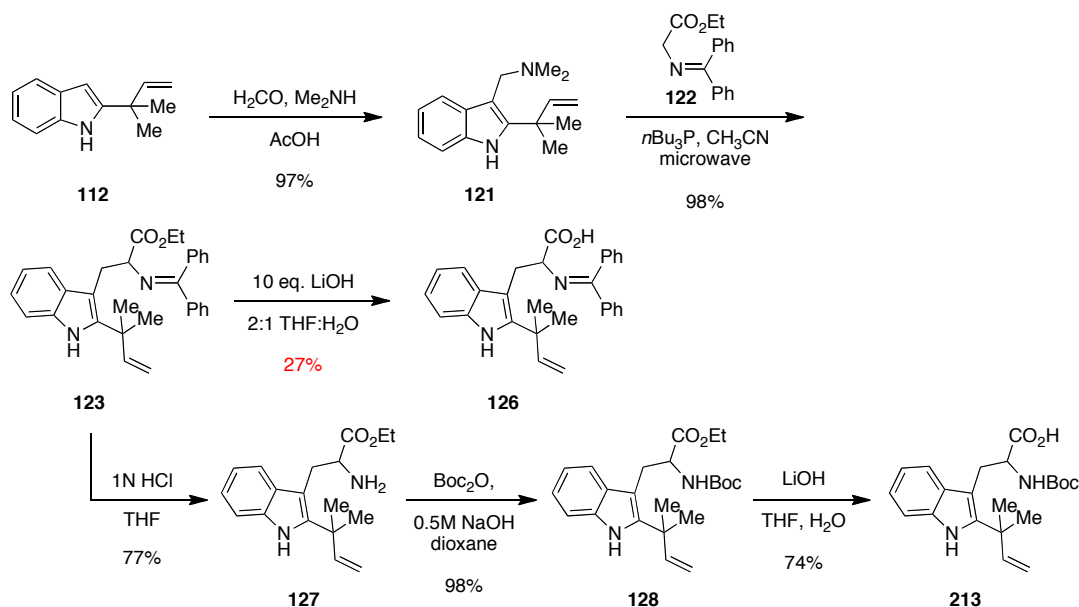
Scheme 17. Formation of the reverse prenyl tryptophan derivative.
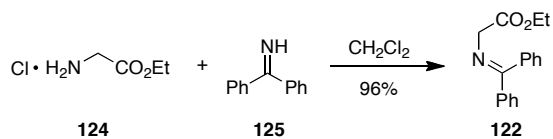
Scheme 18. Synthesis of benzophenone imine of glycine ethyl ester.

The formation of the β-methyl-β-hydroxyproline (Scheme 19) started by first reacting glycine ethyl ester (**124**) with ethyl acrylate (**129**) to yield the secondary amine **130**. This was followed by N-Boc protection of the amine and a subsequent cyclization

of **131** with LiHMDS to afford the β-ketoproline **132**. Conversion of **132** to **114** was accomplished in one step with AlMe$_3$. This reaction proceeded in 63% conversion with 20% recovered starting material.[87]
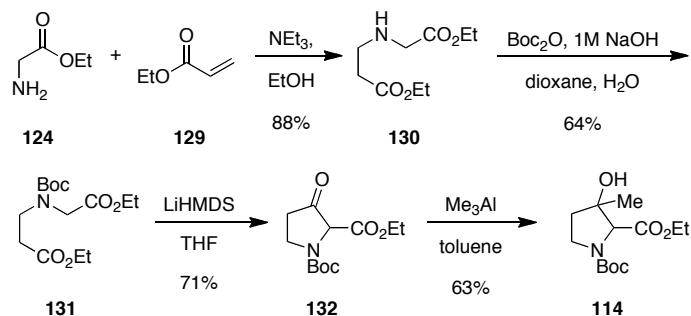
Scheme 19. Formation of the β-methyl-β-hydroxyproline.

With **113** and **114** in hand, first deprotection of **114** with TFA provided the free amine **133**, which was subsequently coupled with **113** using HATU and diisopropylethylamine to afford **134** in excellent yield (Scheme 20).[84] TFA provided the free amine **135**, which was subsequently cyclized to furnish **115**. Treatment of **115** with SOCl$_2$ and pyridine, yielded the unsaturated compound **136**. Treatment of the enamide with methyl Meerwein's salt afforded the lactim ether **116**, which was subsequently reacted with aqueous KOH in methanol to effect tautomerization and the consequent IMDA cycloaddition to furnish the diastereomers **137-140**. Based on previous calculation, the mixture of *syn-* and *anti-* diastereomers should form in a 2.4:1 ratio, in favor of the *syn*-isomer. Likewise, the stereochemistry of the methyl group in the β-methyl proline ring greatly should favor *syn* formation in respect to the bridging isoprene unit.
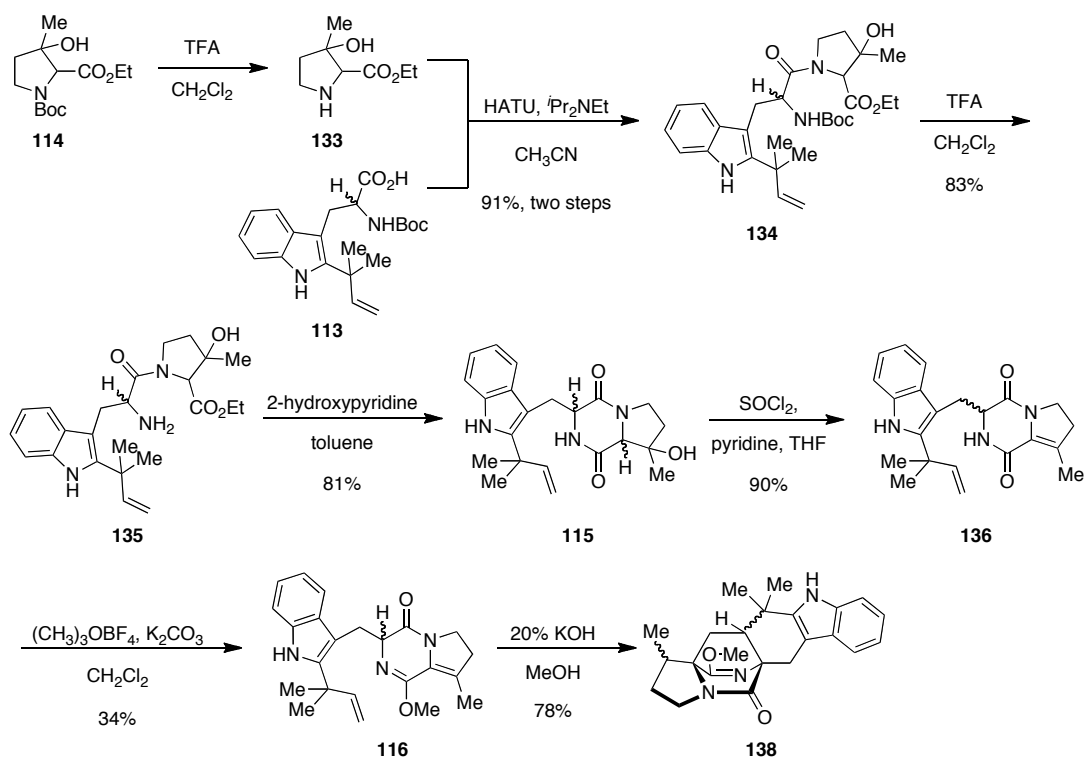
Scheme 20. Formation of the Diels-Alder cycloadduct.

3.1.2 Progress Toward the Synthesis of ^{13}C-Pre-paraherquamide

With the reaction conditions leading to the synthesis of **137** laid out, ^{13}C-labeled material was taken through the synthesis. As shown in Scheme 21, the labeled protected glycine **138** was synthesized from benzophenone imine **125** and ^{13}C-labeled glycine ethyl ester **139**. Coupling **138** with gramine **112** formed the tryptophan derivative **140**. Removal of the benzophenone imine protecting group afforded the free amine, which was subsequently Boc protected to furnish **141**. Saponification yielded the acid **142**, which was coupled with the ^{13}C-labeled β-methyl-β-hydroxyproline **143**. The Boc protecting group was removed and the crude free amine **145** was cyclized to provide the diketopiperazine **146** in 77% yield.
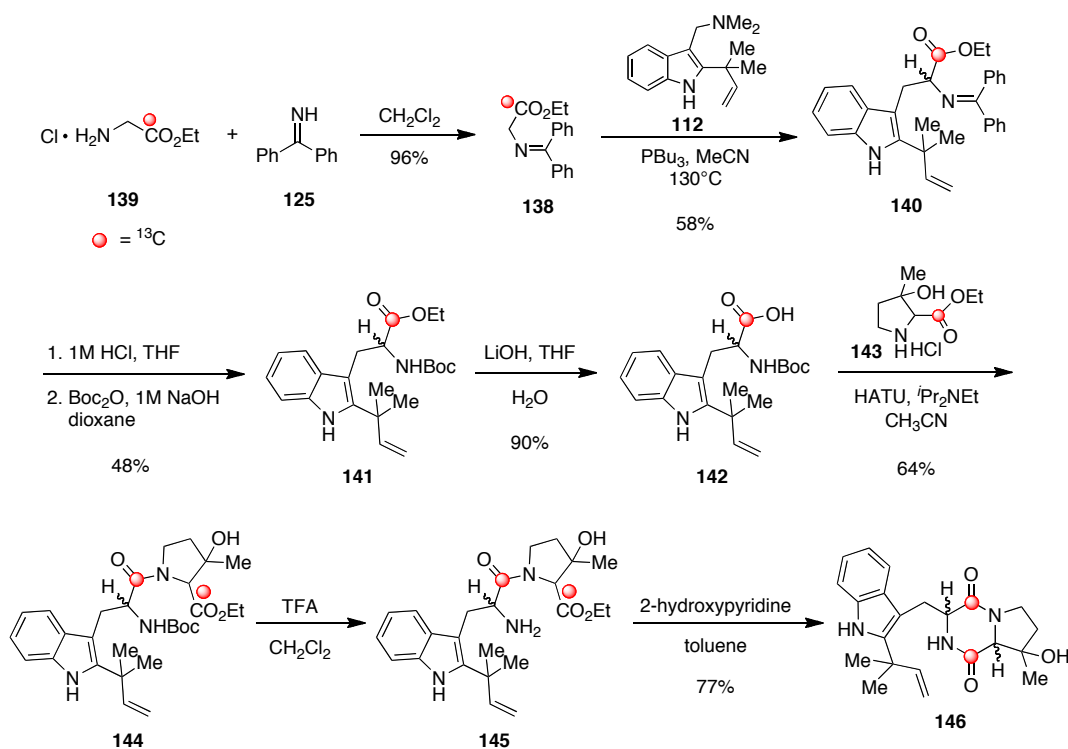
Scheme 21. Formation of double ^{13}C-labeled diketopiperazine **146**.

3.1.3 Future Directions

Doubly ^{13}C-labeled pre-paraherquamide can be easily accessed from **146** in five steps (Scheme 22). Once the final steps have been optimized on unlabeled material, the doubly ^{13}C-labeled substrate will be converted to pre-paraherquamide following the same route. From **146**, the Diels-Alder cycloadduct **149** can be obtained in three steps. Removal of the lactim ether followed by selective reduction of **150** will yield pre-paraherquamide. Once **25** is obtained, it will be fed to *Aspergillus japonicus* to check for the incorporation of intact double ^{13}C-labels into asperparaline A.
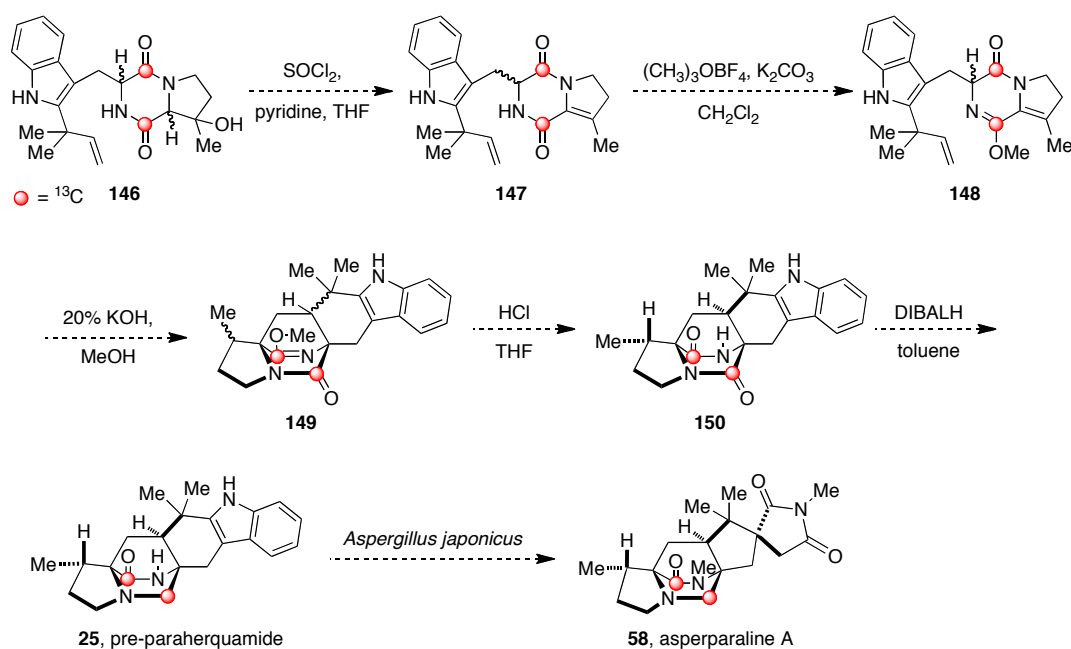
Scheme 22. Future work towards the synthesis of pre-paraherquamide.

3.2 Biosynthetic Formation of the Dioxepin Ring System

The dioxepin ring system, commonly found in the paraherquamides, is a seven-membered oxygenated heterocycle located at the C-6 and C-7 positions of the trytophyl moiety. Precursor incorporation studies previously established that dimethylallyl pyrophosphate (DMAPP) was responsible for the biosynthetic formation of the C_5 fragment, and specifically demonstrated in paraherquamide A, the introduction of the C-24 to C-28 isoprene unit to form the dioxepin ring proceeds through a direct prenyl transferase.[31] Additionally, the incorporation of ^{13}C-labeled pre-paraherquamide into paraherquamide A provides support that formation of the dioxepin ring occurs after the IMDA cycloaddition.

While the exact biosynthetic mechanism for the formation of the dioxepin moiety from pre-paraherquamide is largely unknown, a potential biosynthesis has been proposed (Scheme 23).[32] Starting from the biosynthetic intermediate pre-paraherquamide (**25**),

oxidation at the C-6 and C-7 positions affords the hypothetical intermediate **11**. The bishydroxyindole (**111**) is then alkylated with DMAPP to form **151**. From this intermediate, one of two routes is possible for the formation of the dioxepin ring. A face-selective epoxidation of olefin **151** followed by a completely stereospecific ring-opening of epoxide **152**, and subsequent dehydration would yield the final dioxepin ring of the paraherquamides (**10**). Alternatively, face-selective complexation of a transition metallo-protein to the olefinic π system of **151** affording **154**, followed by stereospecific intramolecular nucleophilic addition and β hydride elimination of **155** to the enol ether would also furnish **10**. Of these two pathways, the face-selective epoxidation is the most widely accepted hypothesis.
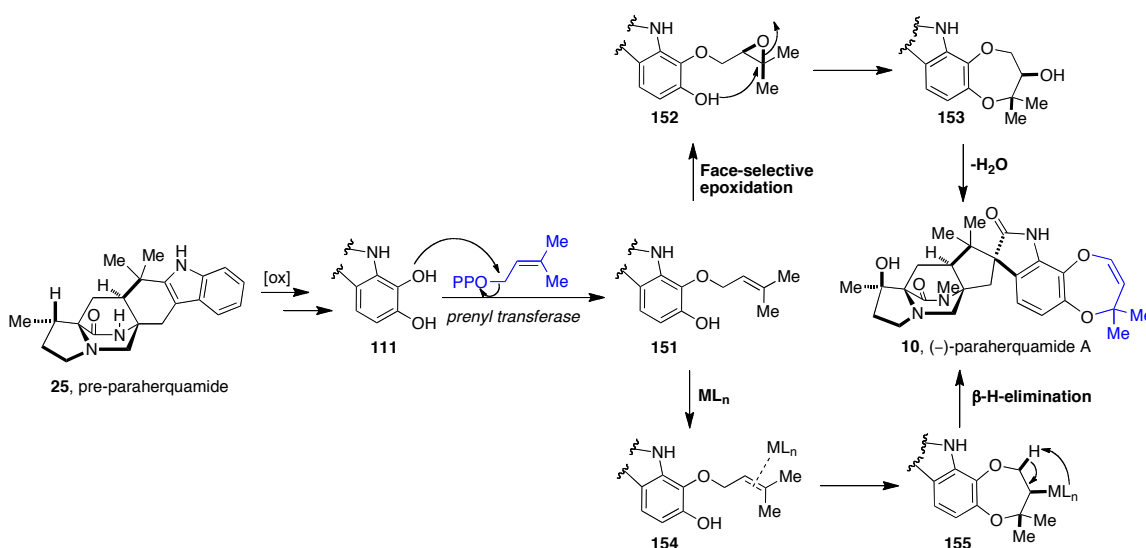
Scheme 23. Proposed biosynthetic formation of the dioxepin ring.

As previously stated, pre-paraherquamide incorporates into paraherquamide A when fed to *P. fellutanum*; therefore, catechol derivative **111** should also incorporate during a feeding experiment. Incorporation of **111** would also provide another advanced precursor along the biosynthetic pathway to paraherquamide A; however, when **111** was

synthesized in the laboratory, it underwent oxidation to form the more stable quinone (**156**), which cannot be further alkylated by DMAPP (Scheme 24).[88]
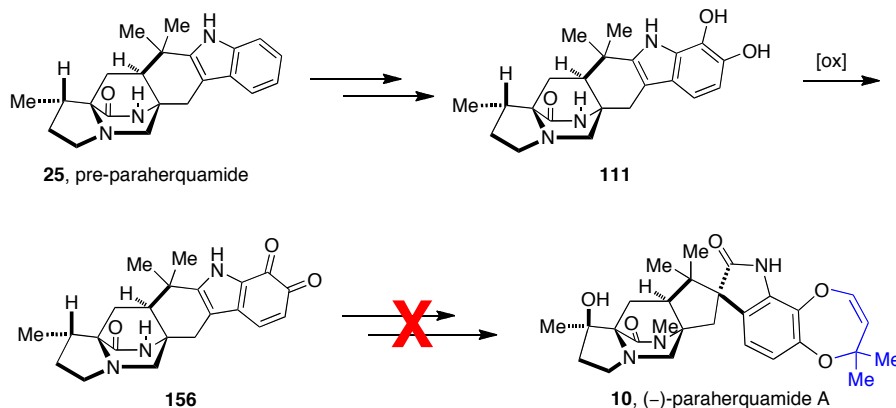
Scheme 24. Quinone formation from the catechol derivative of pre-paraherquamide.

Since the bishydroxyindole cannot be synthesized and tested as an intermediate along the biosynthetic pathway, two alternate approaches have been developed (Scheme 25). Based on the coupling patterns observed from the dioxepin ring, it is known that addition of this isoprene unit occurs via direct prenylation; therefore, one possibility is that the 7-position of the tryptophan core is first oxidized to **157**, followed by prenylation to provide **158** and subsequent oxidation at the 6-position to yield **151**. From the originally proposed intermediate **151**, one of the two possibilities previously discussed may occur to afford the dioxepin ring.
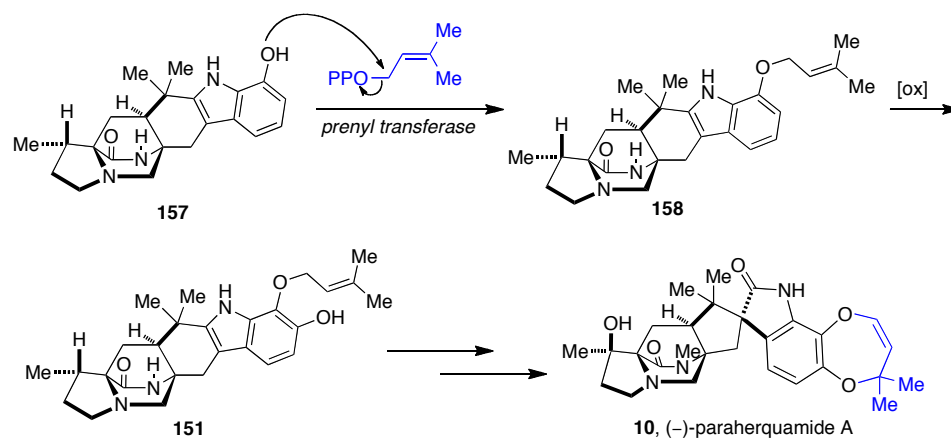
Scheme 25. Possible biosynthetic route for formation of the dioxepin ring.

Since **111** is not a synthetic option, another viable approach involves the synthesis of the 6-hydroxy tryptophan core **159**, which could undergo oxidation in vivo to furnish the catechol intermediate **111** (Scheme 26). From here, the bishydroxyindole could undergo prenylation **151** and subsequent ring closure to afford paraherquamide A.
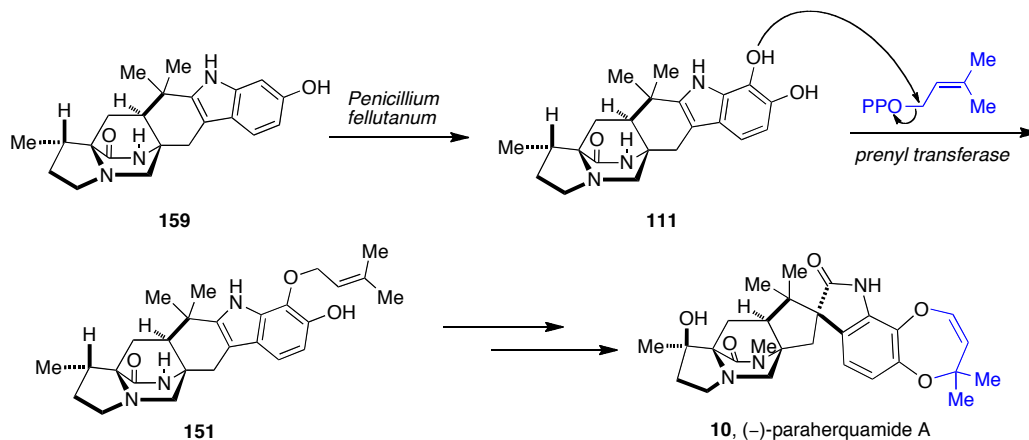
Scheme 26. Possible biosynthetic route for formation of the dioxepin ring.

3.2.1 Efforts Toward the Synthesis of Potential Precursors via S$_N$2´ cyclization

In order to determine if **157** or **159** are potential precursors to paraherquamide A, plans were constructed to synthesize both compounds with double ^{13}C-labels, and through precursor incorporation studies with *Penicillium fellutanum*, check for their incorporation into the known secondary metabolite, paraherquamide A. Both **157** and **159** can be synthesized along a common route, with **157** originating from 7-benzyloxyindole (**160**) and **159** originating from 6-benzyloxyindole (**161**). One currently established strategy for the synthesis of **157** and **159** centers around the intramolecular S$_N$2´ approach for the preparation of the core bicyclic ring system.[57] As shown in Scheme 27, **161** and **161** are converted to the corresponding tryptophan derivatives **162** and **163**, subsequently coupled to the proline **164**, and cyclized to furnish **165** and **166**, respectively. Upon conversion of the terminal olefin to the allylic chloride **2.68** and **2.69**, the bridged bicycle is accessible through an S$_N$2´ reaction. The final two compounds are obtained following closure of the cyclohexyl ring and removal of the benzyl protecting groups to afford the hydroxylated compounds **157** and **159**, respectively.
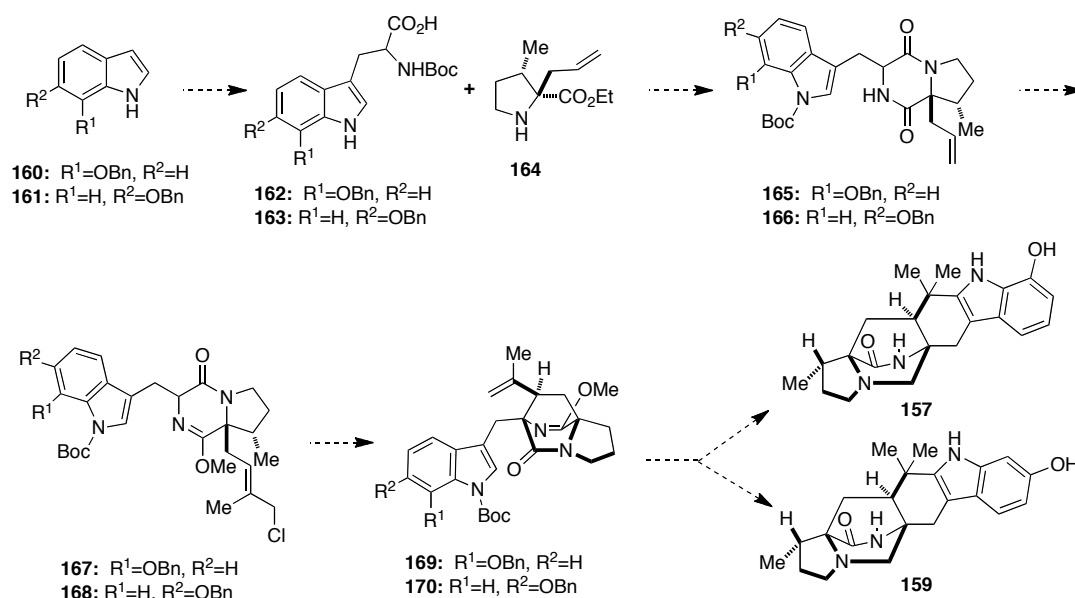
Scheme 27. Key steps towards **157** and **159** using an S$_N$2' approach.

The synthesis of the 6- and 7-benzyloxy tryptophan derivatives, as shown in Scheme 28, was attained from the respective commercially available 7- and 6-benzyloxyindole (**160** and **161**). Conversion of **160** and **161** to the gramine **171** and **172** was achieved with formaldehyde and dimethylamine in glacial acetic acid in high yield. Gramines **171** and **172** then underwent a microwave assisted Somei-Kametani reaction with **122**. Subsequent treatment with acid afforded the crude amines **175** and **176**, which were Boc protected to furnish **177** and **178**. The crude N-Boc protected amines were saponified with LiOH in THF/H$_2$O to form the final respective tryptophan derivatives **162** and **163** in high yield (87-89%).
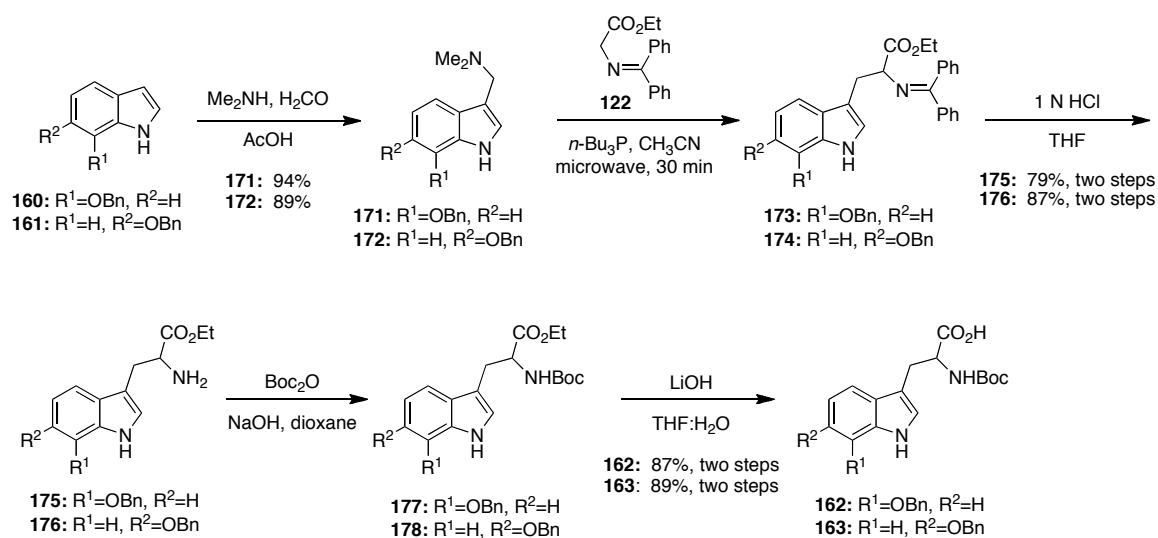
Scheme 2.15. Synthesis of 6- and 7-benzyloxy tryptophan derivatives.

The synthesis of the β–methyl proline derivative (Scheme 29) started from commercially available (*R*)-α-methyl benzyl amine **179**, which was alkylated with 4-bromo-1-butene **180** to give the corresponding secondary amine **181**.[89] Subsequent alkylation with ethyl bromoacetate afforded **182** in 58% yield. Formation of the N-protected-β–methyl proline derivative **183** was accomplished via deprotonation of **182** with LDA. The lithium enolate was then transmetalated with a 1M solution of ZnBr$_2$ in diethyl ether. Work up with an aqueous solution of ammonium chloride afforded **183**.[90] In a protecting group swap, hydrogenation of **183** was followed by Boc protection to yield **185**. The first attempt at the allylation of **185** with allyl bromide and NaHMDS in THF afforded **186** in 5% yield. Further optimization was attempted (Table 6); however, when using allyl bromide, only starting material was recovered. The yield was increased to 25% with allyl iodide.
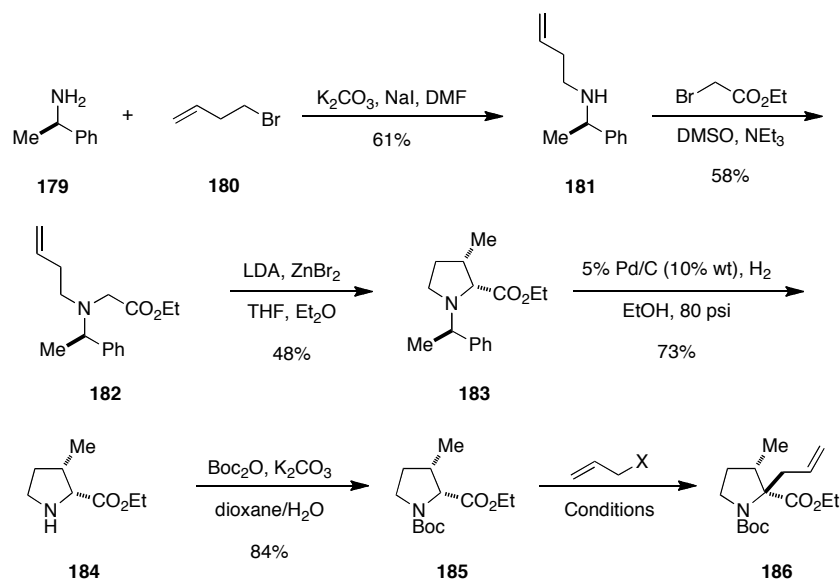
Scheme 29. Synthesis of proline derivative **186**.

Table 6. Select reaction condition for the formation of **186**.

Entry	X	Conditions	Results
a	Br	NaHMDS, THF, -78°C →RT, 24 h	5%
b	Br	LiHMDS, THF, -78°C →RT, 3 d	NR
c	Br	LDA, THF, -78°C →RT, 24 h	NR
d	Br	NaH, TBAI, THF, 0°C →40°C, 24 h	NR
e	Br	KHMDS, TBAI, THF, 0°C→RT, 24 h	NR
f	I	KHMDS, THF, -78°C →RT, 24 h	NR
g	I	NaHMDS, THF, -78°C →RT, 24 h	25%
h	I	NaHMDS, DMF, 0°C →RT, 24 h	18%

Along this route, there are several low yielding steps. The allylation and cyclization (**181** to **183**) both provide less than 50% product, while the first two steps each yield roughly 60%. These difficulties so early on in the synthesis prompted reconsideration of this approach to **157** and **159**.

3.2.2 Progress Toward the Synthesis of the 6-Hydroxy and 7-Hydroxy Precursors (Diels-Alder Route)

Another well-established route utilizes a biomimetic intramolecular Diels-Alder reaction to form the core bridged bicycle ring system (Scheme 30).[78,79] To start, the 6- and 7-hydroxy indoles (**187** and **188**) are first protected and converted to the corresponding tryptophan derivative (**189** and **190**) with the reverse prenyl group located at the C-2 position of the indole. The reverse prenylated indole is then coupled to β-methyl-β-hydroxyproline **114** to form the respective diketopiperazine **191** and **192**. The enamide is formed from the diketopiperazine, followed by conversion to the lactim ether **193** and **194**. The Diels-Alder cycloadduct is accessible from a base-induced tautomerization to form the azadiene followed by a [4+2] cycloaddition to furnish **157** and **159**, respectively.

187: R^1=OH, R^2=H
188: R^1=H, R^2=OH

189: R^1=OBoc, R^2=H
190: R^1=H, R^2=OBoc

114

191: R^1=OBoc, R^2=H
192: R^1=H, R^2=OBoc

193: R^1=OBoc, R^2=H
194: R^1=H, R^2=OBoc

195: R^1=OBoc, R^2=H
196: R^1=H, R^2=OBoc

157

159
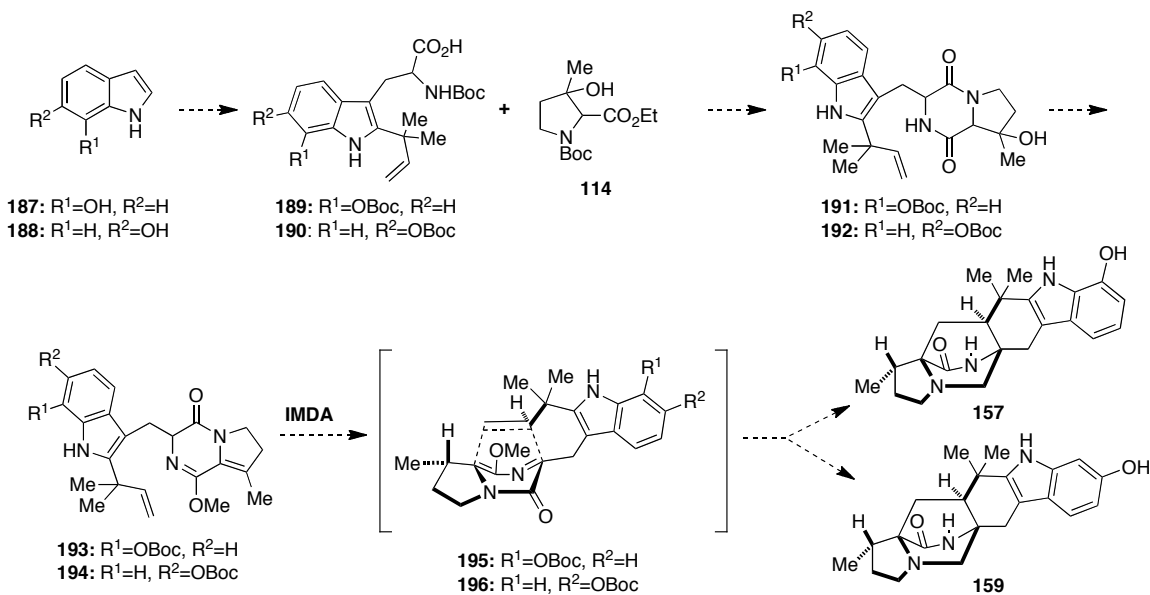
Scheme 30. Key steps towards **157** and **159** using the Diels-Alder approach.

Several approaches were attempted toward the synthesis of the 6-hydroxyindole **188**, with each route derived from the known Leimgruber-Batcho indole synthesis.[91] For the synthesis of the 6-hydroxyindole (Scheme 31), commercially available nitrophenol **197** was protected as either the Boc- or benzyl-oxynitrotoluene (**198** and **199**). Conversion of **198** and **199** to enamines **200** and **201** with DMF-DMA and pyrrolidine were successful, however the Boc-protected nitrotoluene was low yielding. Unfortunately, a one step cyclization and deprotection of **200** proved unsuccessful. Several cyclization reactions were attempted on **201**. The use of catalytic Rh/C, H_2, and Fe(OAc)$_2$ resulted in decomposition, however, trace amounts of product were detected when using dry Rh/C and H_2 without Fe(OAc)$_2$.[92] Reacting **201** with Zn and AcOH yielded **202** albeit in low yield. The desired product was obtained in good yield by reacting **201** with hydrazine monohydrate and Ni$_2$B (prepared from Ni(OAc)$_2$) in ethanol.[93] Formation of the desired unprotected 6-hydroxyindole **188** was formed in a one pot hydrogenation using 10% Pd/C and THF in quantitative yield.
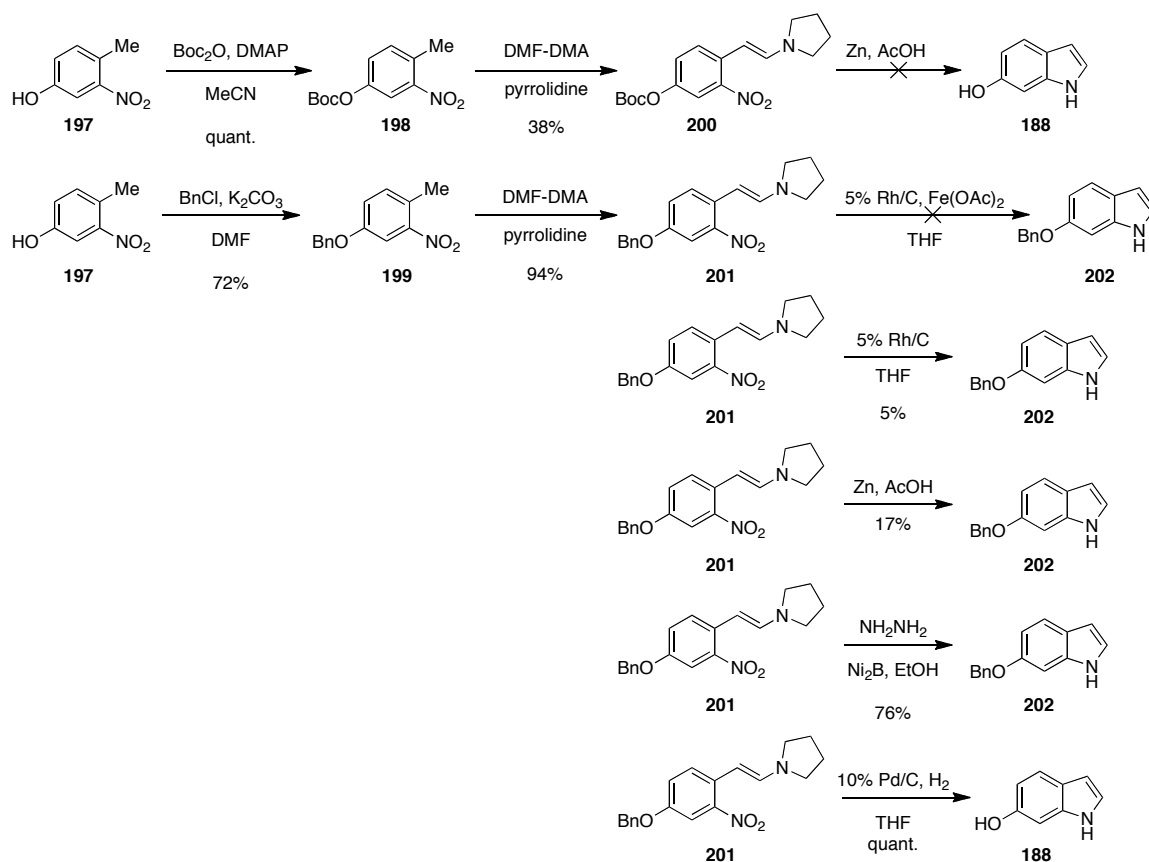
Scheme 31. Synthesis of the 6-benzyloxyindole **202**.

With the 6-benzyloxyindole in hand, completion of the reverse prenylated indole was underway (Scheme 32). First, **202** was deprotected and reprotected to afford the 6-OBoc indole **203**, which was followed by formation of the C-2 reverse prenylated indole using the excellent procedure established by Danishefsky and co-workers.[85] The C-3 indole position of **203** was chlorinated using NCS in DMF to afford **204**, which was treated with prenyl-9-BBN in the presence of NEt$_3$ to yield the reverse prenylated indole **205**. With the reverse prenylated indole in hand, the gramine **206** was formed in good yield, which was subsequently reacted with the **122** in a Somei-Kamatani microwave reaction. Imine hydrolysis afforded the tryptophan derivative **207**, which was readily

converted to the corresponding N-Boc carbamate **208**. Following standard saponification conditions, the N-Boc acid **190** was achieved in good yield.
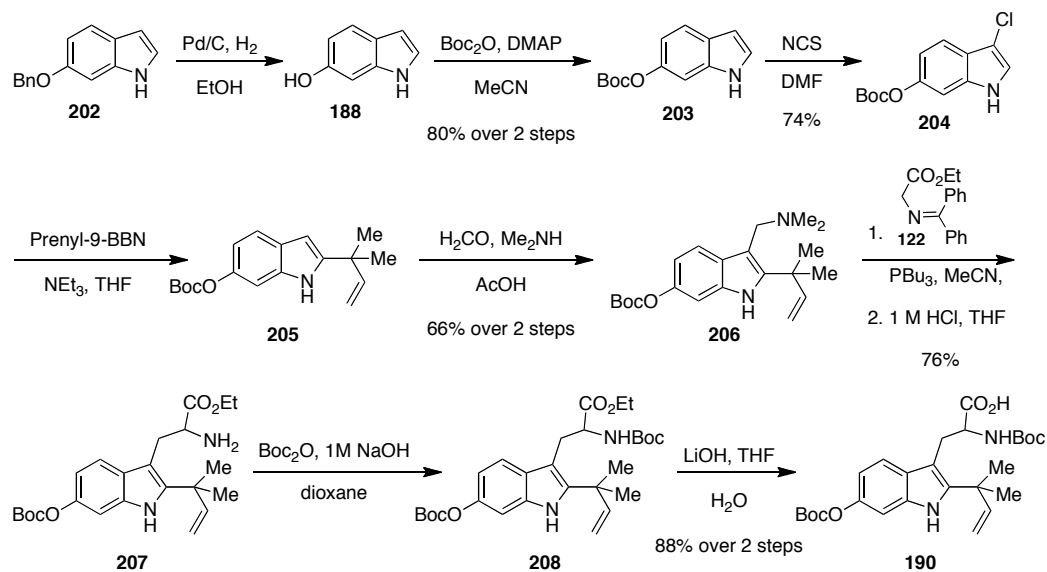
Scheme 32. Formation of the reverse prenylated 6-benzyloxyindole.

To form the 7-hydroxyindole, two different protecting groups of the hydroxy group were attempted while employing Leimgruber-Batcho indole synthesis. The first approach was to form the Boc-protected nitrotoluene **210** and subsequent formation of the enamine derivative **211** (Scheme 33). The synthesis of **210** proved to be successful, however after several attempts, enamine **211** could not be achieved.
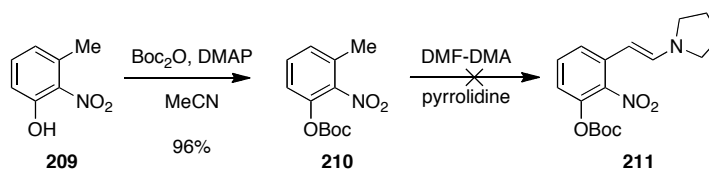
Scheme 33. First synthetic approach to form 7-hydroxyindole.

The second strategy (Scheme 34) began by benzyl protecting commercially available nitrophenol **209**. The enamine was formed by reacting the nitrotoluene **212** with DMF-DMA and pyrrolidine, which was subsequently converted to the semicarbazide **213** in decent yield.[94] The 7-hydroxyindole was formed in a hydrogenation reaction in which the benzyl-protecting group was also removed. The alcohol was immediately Boc protected to afford the desired 7-OBoc indole **214**. Chlorination of **214** with NCS in methanol afforded the C-3 chloro-indole **215**, which was then reacted with prenyl-9-BBN. Unfortunately after numerous attempts, only starting material was recovered.
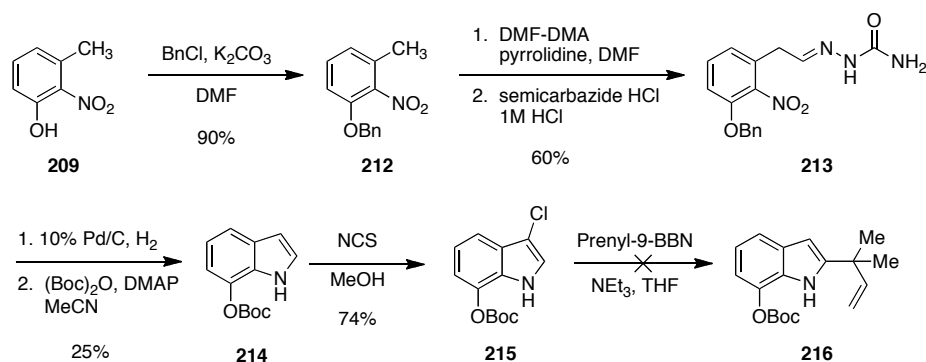
Scheme 34. Attempt to form the 7-OBoc reverse prenylated indole **216**.

3.2.3 Future Directions

Completion of the 6-hydroxy derivative **159** requires coupling of the tryptophan derivative with β-methyl-β-hydroxyproline and subsequent formation of the diketopiperazine. The Diels-Alder cycloadduct can be attained from the lactim ether, and following several functional group manipulations the desired 6-hydroxy precursor can be obtained. Once the reaction conditions have been optimized on unlabeled material, the

synthesis of doubly ^{13}C-labeled **159** can begin. Synthesis of the 7-hydroxy precursor will require screening of reaction conditions to form the reverse prenylated compound.

CHAPTER 4

The Biosynthesis of the Stephacidins and Notoamides in Cultures of Marine-Derived *Aspergillus* sp. MF297-2

4.1 Marine-Derived *Aspergillus* sp. MF297-2

4.1.1 Isolation of Secondary Metabolites

In 2007, Tsukamoto and coworkers reported the isolation of four new secondary metabolites, notoamides A-D (**31-34**, Figure 19) from a marine-derived fungus *Aspergillus* sp. MF297-2. The fungus was found growing on the mussel *Mytilus edulis*, which was collected off the Noto Peninsula in the Sea of Japan.[19] In addition to notoamides A-D, three known prenylated indole metabolites; sclerotiamide (**27**), (+)-stephacidin A (**28**), and deoxybrevianamide E (**7**), were also isolated from the fungal culture.
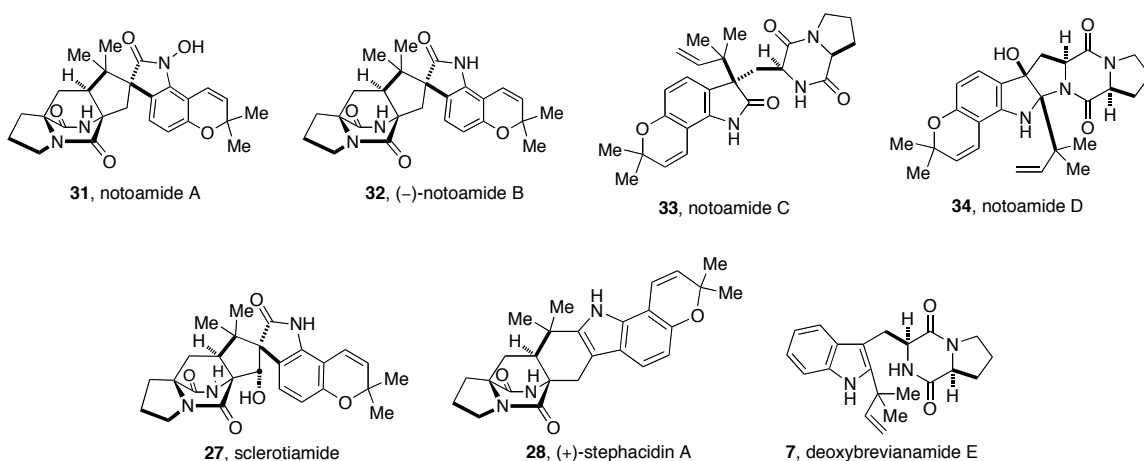
Figure 19. Structures of metabolites isolated from marine-derived *Aspergillus* sp. MF297-2.

Similar to other known prenylated indole metabolites, each of these compounds are derived from tryptophan, a cyclic amino acid, and one or two mevalonate-derived isoprene units.[26] Structural analysis revealed that notoamides A-D all contain the pyranoindole ring system common in the stephacidins, and that notoamides A and B contain the core bicyclo[2.2.2]diazaoctane ring system as well as a *spiro*-oxindole moiety. Notoamides C and D were found to display the diketopiperazine moiety in place of the bridging bicycle. Additionally, notoamide C contains an oxindole moiety, whereas notoamide D is a hexacyclic metabolite with a carbon skeleton closely related to brevianamide E.[19]

Shortly after the isolation of notoamides A-D from marine-derived *Aspergillus* sp. MF297-2, Tsukamoto reported the isolation of a fleeting potential precursor, notoamide E (**38**). As observed in many of the stephacidins and notoamides, notoamide E is a 2,3-disubstituted indole alkaloid that contains a pyranoindole and a diketopiperazine ring system (Figure 20). Through isolation experiments, it was established that notoamide E only exists in the fungal culture on day 5 of incubation, and that by day 6 the metabolite

has been completely converted to other downstream metabolites. These results clearly indicate that notoamide E is produced by the fungus as an early biosynthetic intermediate leading to more advanced prenylated indole metabolites.[21]
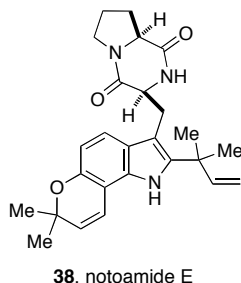
38, notoamide E

Figure 20. Structure of notoamide E.

Between 2008 and 2010, notoamides F-R (**39-51**) and (–)-versicolamide B (**57**) were also isolated by Tsukamoto from marine-derived *Aspergillus* sp. MF297-2.[22-24] These metabolites vary greatly in their structural arrangement, as shown in Figure 21. With the exception of notoamide J, all of these natural products contain a pyranoindole ring system. A small number of these metabolites contain the core bicyclo[2.2.2]diazaoctane ring, while others either possess an oxindole moiety or the hexacyclic skeleton. A structurally unprecedented prenylated indole metabolite in this grouping is notoamide O, which contains a hitherto unknown hemiacetal/hemiaminal ether functionality.[21] This family of secondary metabolites includes versicolamide B, which displays the unique *anti*-relative configuration common to the brevianamides.[23] The isolation of these new notoamide metabolites shows the vast variety of prenylated indole natural products produced by this fungal culture and provides further insight into the biosynthetic pathway of the notoamides and stephacidins.

71

41, notoamide H, R₁ = OH, R₂ = H, R₃ = OH
47, notoamide N, R₁ = H, R₂ = Cl, R₃ = H

39, notoamide F, R₁ = Me, R₂ = H
40, notoamide G, R₁ = Me, R₂ = OH
51, notoamide R, R₁ = H, R₂ = H

42, notoamide I

43, notoamide J

44, notoamide K, R = H
49, notoamide P, R = Br

45, notoamide L

46, notoamide M, R = H
50, notoamide Q, R = Me

48, notoamide O
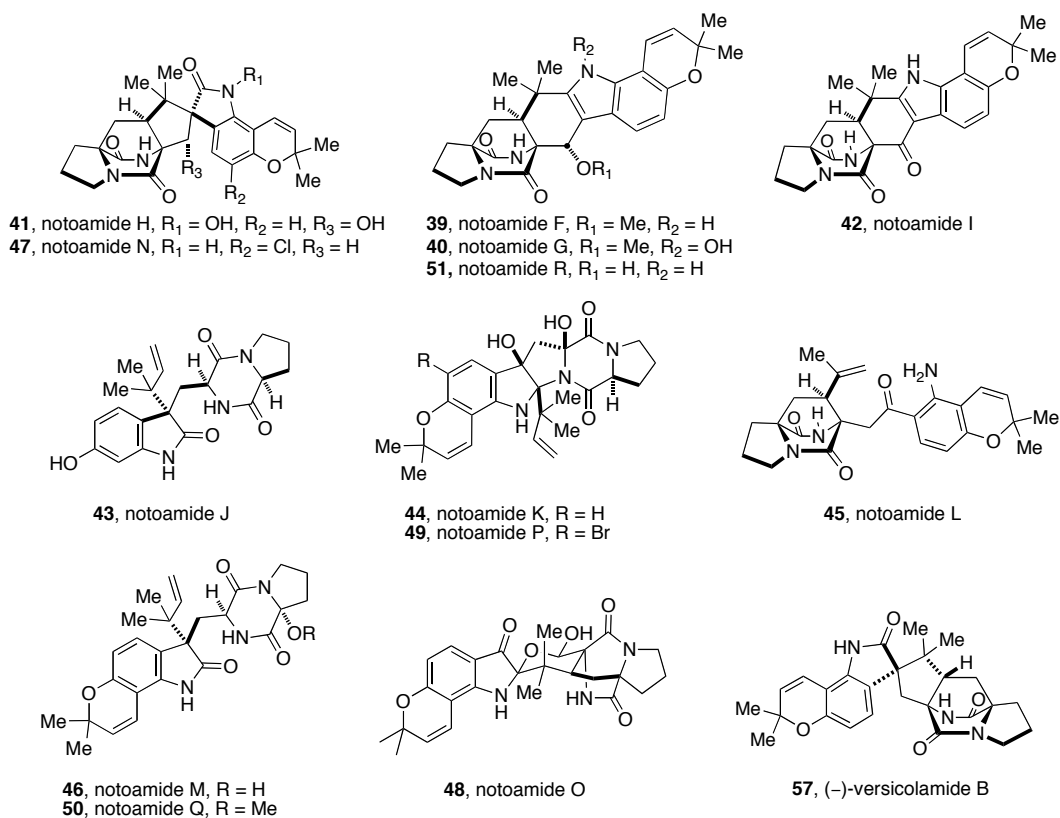
57, (–)-versicolamide B

Figure 21. Structures of notoamides F-R and versicolamide B.

4.1.2 Total Synthesis of Marine-Derived Metabolite Notoamide J[95]

With the aim to elucidate the entire notoamide/stephacidin biosynthetic pathway, a synthesis of notoamide J that was readily amenable to the incorporation of stable isotopes from which probe substrates could be interrogated was desired. Herein is the first total synthesis of notoamide J, which also serves to corroborate the structural assignment published by Tsukamoto and co-workers.[95]

As Scheme 35 shows, the synthesis of notoamide J (**43**) commenced with the coupling of tryptophan derivative **190** with proline-ethyl ester **217** using HATU and *i*Pr₂NEt. Peptide **218** was globally deprotected with TFA, and subsequently cyclized with 2-hydroxypyridine to furnish a 1:1 mixture of 6-hydroxydeoxybrevianamide E **220** and

diastereomer **221**. Treatment of **220** with Davis oxaziridine afforded the known natural

product, notoamide J (**43**) and *R*-diastereomer **222** in a 2:1 ratio.
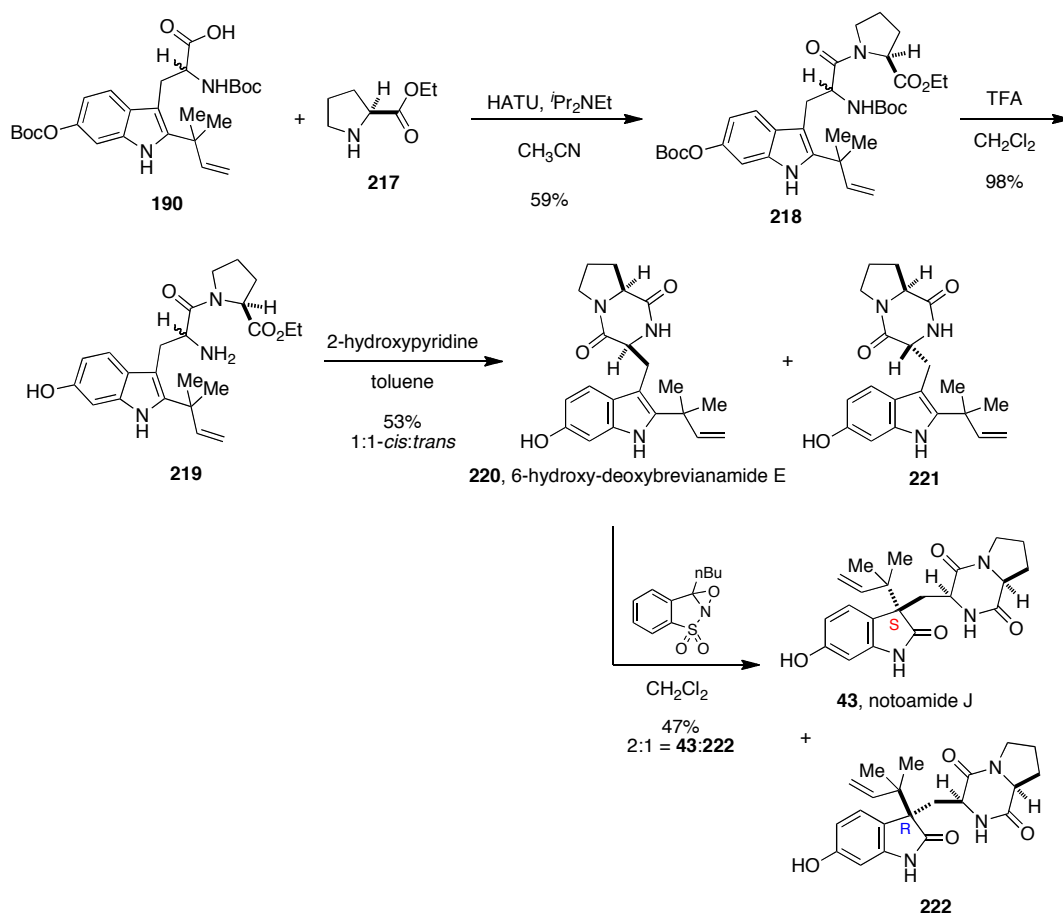
Scheme 4.13. Synthesis of 6-hydroxy-deoxybrevianamide E and notoamide J.

As desired, the total synthesis of notoamide J allows for easy access to
isotopomers of notoamide J, as described in detail in Section 4.3.1. Through isotopic
labeling of notoamide J, investigation of this species as a potential biosynthetic precursor
to more complex natural congeners is feasible and is discussed further in Section 4.3.2.
Additionally, this route provides a potential biosynthetic intermediate, 6-
hydroxydeoxybrevianamide E, which may act as a precursor not only to notoamide J, but
to other secondary metabolites as well.

4.2 Stereochemical Comparison to Metabolites Produced by *Aspergillus versicolor*:

Biosynthetic Implications

As mentioned in Chapter 2 (Section 2.1.3), metabolites displaying the opposite absolute stereochemistry to those isolated from *Aspergillus* sp. MF297-2 were isolated by Gloer and co-workers from terrestrial-derived *Aspergillus versicolor*. (For extended discussion on metabolites from *Aspergillus versicolor*, please refer to Chapter 5). As shown in Figure 4.4, (+)-stephacidin A (**28**), (−)-notoamide B (**32**), and (−)-versicolamide B (**57**) were isolated from *Aspergillus* sp. MF297-2, while (−)-stephacidin A (**55**), (+)-notoamide B (**56**), and (+)-versicolamide B (**55**) were produced by *Aspergillus versicolor*.[23,25] These enantiomeric natural metabolites represent the first set of known antipodal metabolites isolated from the notoamide, paraherquamide, and stephacidin families. This information sparked further interest in elucidating the biosynthetic pathway for the formation of the bicyclo[2.2.2]diazaoctane ring system, which has been strongly implicated as being responsible for the enantio-diverging event.[96] Focus was immediately placed on identifying a single species that could serve as a biosynthetic precursor to both sets of antipodal secondary metabolites.

28, (+)-stephacidin A   **55**, (−)-stephacidin A

32, (−)-notoamide B   **56**, (+)-notoamide B

57, (−)-versicolamide B   **54**, (+)-versicolamide B
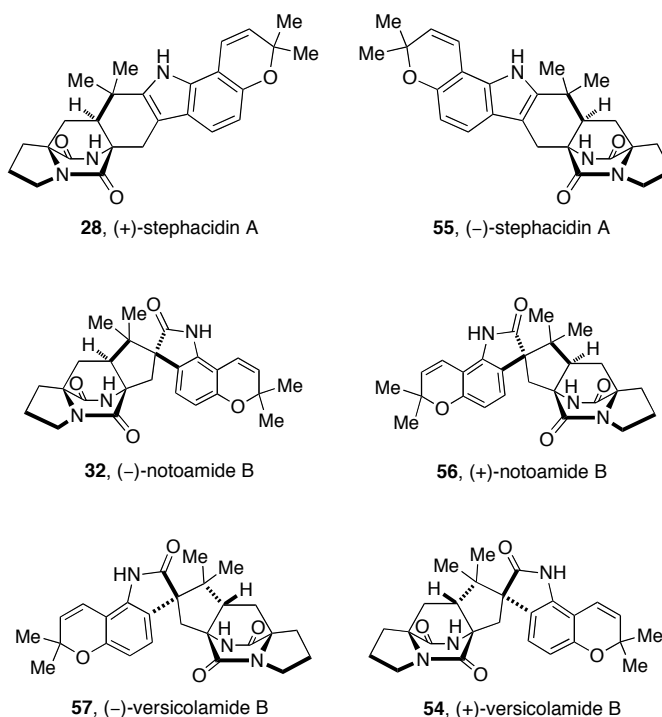
Figure 22. Structures of antipodal natural metabolites isolated from marine-derived *Aspergillus* sp. MF297-2 and terrestrial-derived *Aspergillus versicolor*.

4.3 First Generation Biosynthetic Pathway—Williams et al.

4.3.1 Notoamide E as the Diels-Alder Precursor

The extensive co-metabolite profile produced by *Aspergillus* sp. MF297-2 suggest a possible biosynthetic sequence of deoxybrevianamide E (**7**) leading to stephacidin A (**28**), and preceding to notoamide B (**32**), after which the pathway would branch to give either notoamide A (**31**) or sclerotiamide (**27**).[19] However, following the isolation of notoamide E from marine-derived *Aspergillus* sp. MF297-2, it was postulated by Williams and coworkers that notoamide E could serve as the biosynthetic precursor to the intramolecular Diels-Alder reaction (IMDA).[21] As shown in Scheme 36, notoamide E

(**38**) could arise from deoxybrevianamide E (**7**) following pyran formation. Subsequent oxidation and tautomerization of the diketopiperazine to form achiral azadiene **223** could then undergo a [4+2] cycloaddition. This sequence would give two stereoisomers per fungal strain: (+)-stephacidin A (**28**) and the C6-*epi*-stephacidin A (**224**) in *Aspergillus* sp. MF297-2 and the corresponding enantiomers (**55** and **225**) in *Aspergillus versicolor*. As shown in Scheme 36A, oxidation of the 2,3–disubstituted indole of (+)-stephacidin A to the corresponding *spiro*-oxindole would furnish (−)-notoamide B (**32**), while oxidation of C6-*epi*-stephacidin A (**224**) would give (−)-versicolamide B (**57**). Likewise, notoamide E could serve as a biosynthetic precursor to antipodal metabolites **54-56** and **225** isolated from *Aspergillus versicolor* (Scheme 36B).[4.7]
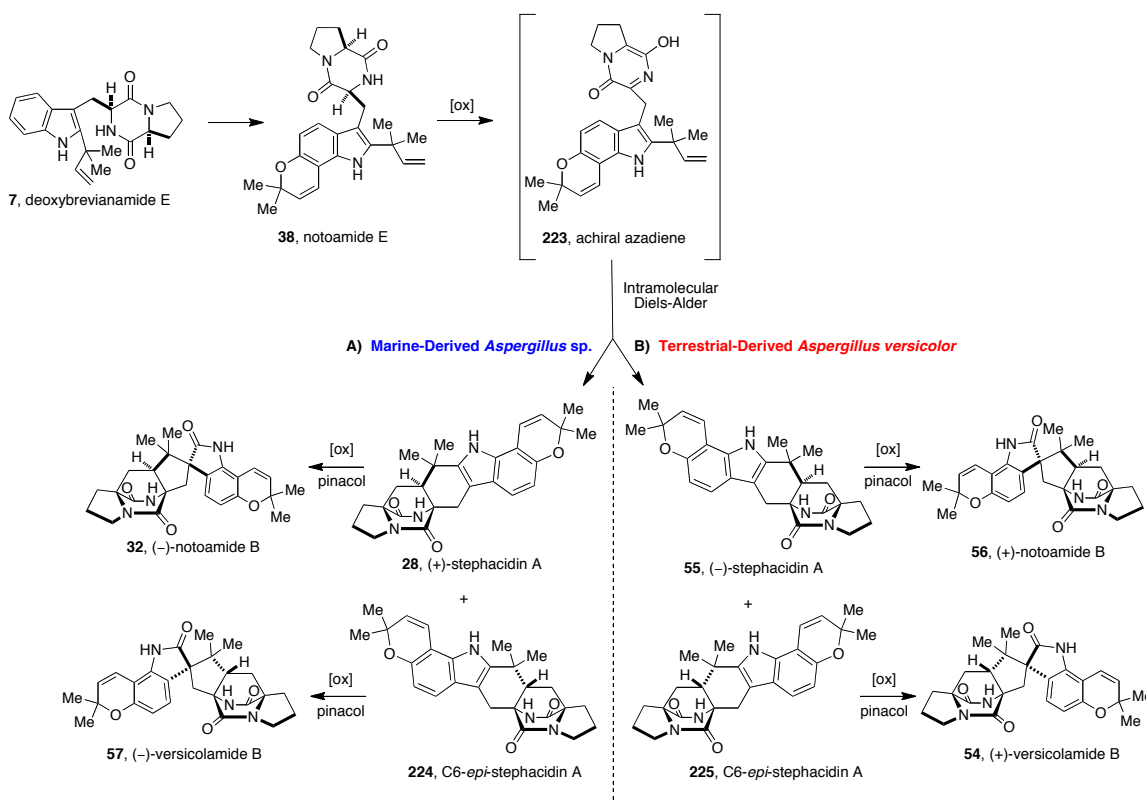
Scheme 36. A) Proposed biosynthetic pathway of notoamide E to (−)-notoamide B in *Aspergillus* sp. MF297-2. B) Similar pathway of notoamide E to (+)-notoamide B.

4.3.2 ^{13}C-Notoamide E Incorporation Study

To establish the role notoamide E plays in the biosynthetic pathway of these prenylated indole metabolites, ^{13}C-labeled notoamide E (**229**) was synthesized and fed to cultures of marine-derived *Aspergillus* sp. MF297-2 As shown in Scheme 37, readily accessible ^{13}C-labeled tryptophan derivative **226**, was first coupled to ^{13}C-proline ethyl ester **227** under standard coupling conditions to yield peptide **228**.[21] Subjecting **228** to morpholine in THF removed the Fmoc protecting group and afforded cyclization to give a 1:1 ratio of *cis*:*trans* diketopiperazines (notoamide E (**229**) and **230**).
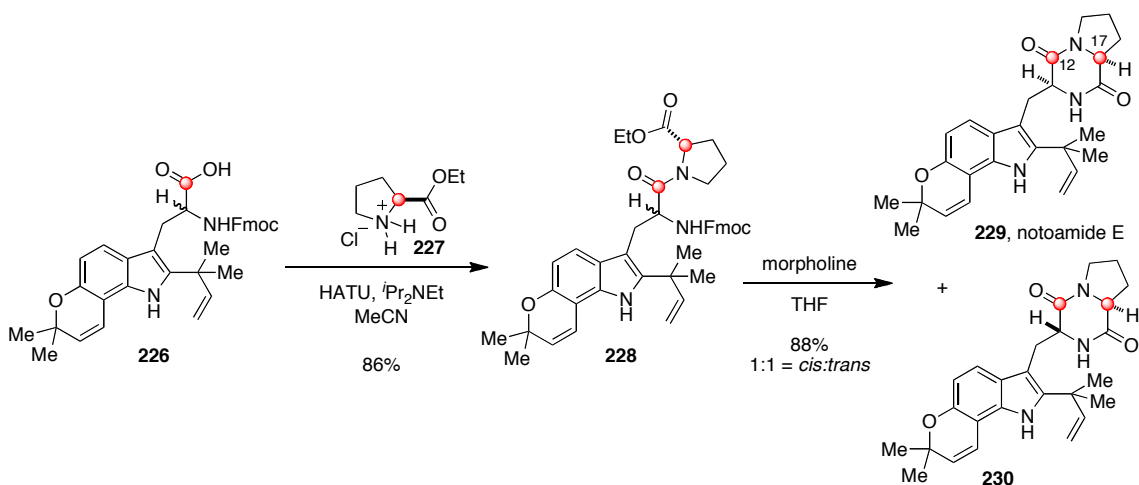
Scheme 37. Synthesis of [^{13}C]$_2$-notoamide E.[21]

The labeled potential precursor **229** was introduced to marine-derived *Aspergillus* sp. MF297-2 in an incorporation feeding study performed by Tsukamoto.[21] It was anticipated that the conversion of [^{13}C]$_2$-notoamide E into labeled (+)-stephacidin A, (–)-notoamide B, and (–)-versicolamide B would occur. While notoamide C (**33**) and D (**34**) were isolated and shown to display ^{13}C-enrichment at the expected C-12 and C-17 positions, **28**, **32**, **57**, and all other bridged bicyclo[2.2.2]diazaoctane-containing metabolites were absent. This is particularly notable as these are typically the major

metabolites produced by Aspergillus sp. MF297-2 (Scheme 38). Additionally, 3-*epi*-notoamide C (**231**), a diastereomer to **33** that is not produced by the culture under normal growth conditions, was isolated in nearly four times the yield of the natural diastereomer **33**. Three new structurally unique minor metabolites displaying ^{13}C-enrichment were also isolated. The new alkaloids, notoamides E2 (**232**), E3 (**233**), and E4 (**234**) are not present in the normal culture of *Aspergillus* sp. MF297-2 when cultivated on the standard nutrient-rich medium.[21,96]
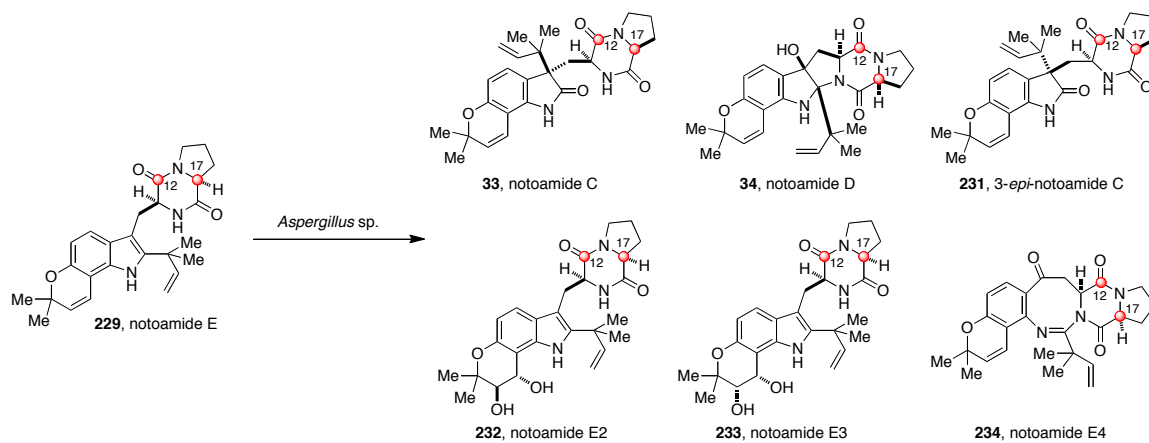
Scheme 38. Results of the [^{13}C]$_2$-notoamide E incorporation study.

The absence of (+)-stephacidin A, (−)-notoamide B, and (−)-versicolamide B in conjunction with the formation of "unnatural" metabolites **231**-**234**, suggest that the presence of excess notoamide E in the growth medium alters the metabolite profile of this fungal culture. Additionally, the conversion of [^{13}C]$_2$-notoamide E into notoamides C and D suggests the possibility of a branching biosynthetic pathway, albeit one that does not include notoamide E as a biosynthetic precursor to the Diels-Alder cycloaddition.[96]

4.4 Second Generation Biosynthetic Pathway—Tsukamoto et al.

Since the bicyclo[2.2.2]diazaoctane ring system is not biosynthetically derived from notoamide E, a second potential pathway was postulated by Tsukamoto and co-workers. This proposal also provides for the biosynthesis of both sets of antipodal metabolites. In regard to the generation of the antipodal stereoisomers of notoamide B and versicolamide B from *Aspergillus* sp. MF297-2 and *Aspergillus versicolor*, the enantio-divergence could arise as a consequence of an *R*- or *S*-selective indole oxidase, instead of the opposite facial selectivity of the IMDA reaction.[23] Starting from the same precursor proposed in the previously discussed biosynthetic pathway, deoxybrevianamide E could first undergo an oxidative rearrangement to furnish two oxindole diastereomers, with the *R*-oxindole leading to metabolites produced by marine-derived *Aspergillus* sp. MF297-2 In this biogenetic pathway, the *S*-selective indole oxidase would provide the correct stereochemistry necessary to furnish (+)-notoamide B and (+)-versicolamide B in terrestrial-derived *Aspergillus versicolor*. As illustrated in Scheme 39, deoxybrevianamide E (**7**) could undergo oxidation and pinacol-type rearrangement to yield **235** and **236**. Oxidation and tautomerization of **235** would provide azadiene intermediate **237**, which would subsequently undergo a [4+2] cycloaddition to furnish four potential stereoisomers (two are shown). Oxidation and prenylation of **238** and **239** would construct the pyran ring, leading to the desired products **32** and **57**, respectively. Following the same biogenesis, (+)-notoamide B and (+)-versicolamide B could arise from intermediate **236** in fungal cultures of terrestrial-derived *Aspergillus versicolor*.
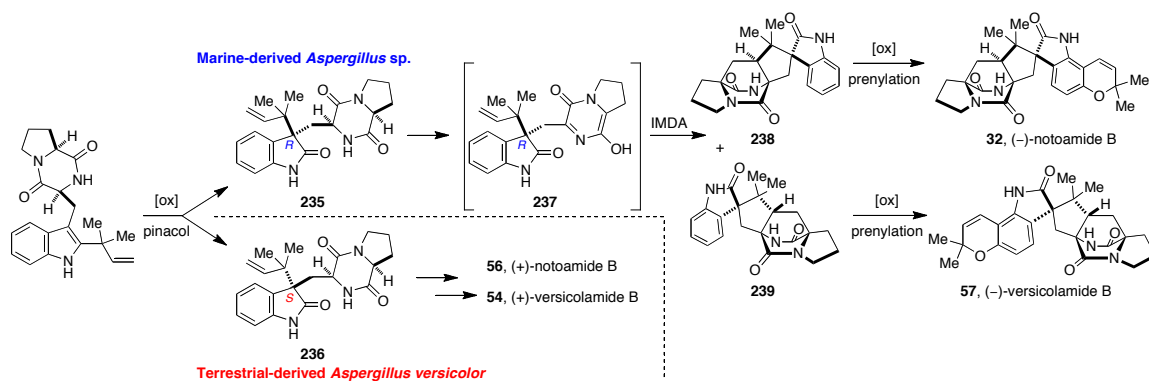
Scheme 39. Second generation biosynthesis of *spiro*-oxindole containing compounds notoamide B and versicolamide B. Shortened biosynthetic pathway leading to the *Aspergillus versicolor* metabolites is also shown.

An additional modification to the second generation biosynthesis of antipodal notoamide B and versicolamide B is the possibility that the C-6 position of **7** is first hydroxylated, thereby resulting in 6-hydroxydeoxybrevianamide E (**220**). This would then serve as the biogenetic precursor to the enantio-divergence point of the two biosyntheses (Scheme 40). 6-Hydroxydeoxybrevianamide E could undergo oxidative rearrangement to form **222** and the known natural product notoamide J. Cycloaddition of **222** via azadiene **240** would give **241** and **242**, in which prenylation and ring closure gives the pyranoindole ring and the desired natural products.
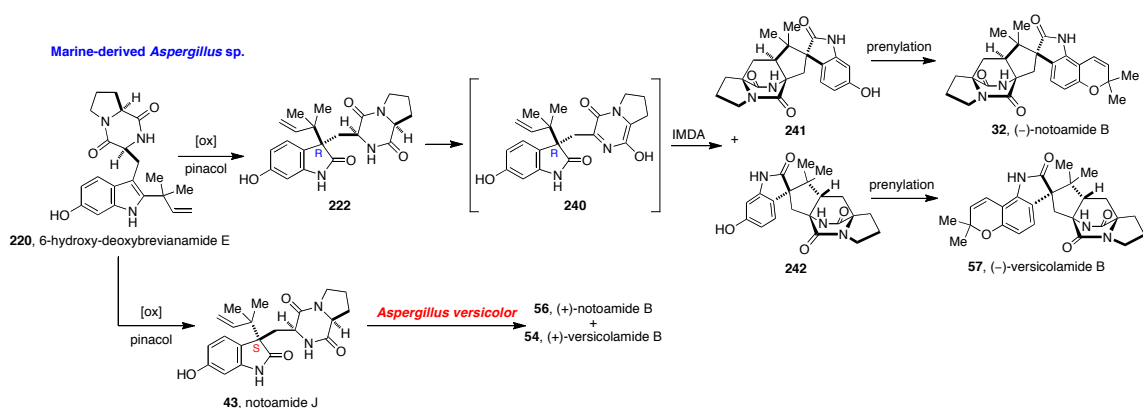
Scheme 40. Alternative biosynthetic pathway for the formation of *spiro*-oxindole compounds.

Additional support for this pathway is provided by the isolation of notoamide J, as well as the biomimetic conversion of 6-hydroxydeoxybrevianamide E to notoamide J. In marine-derived *Aspergillus* sp. MF297-2, notoamide J may be an artifact of the oxidative rearrangement of 6-hydroxydeoxybrevianamide E to the *R*-stereoisomer **222**, which could serve as a precursor to other downstream metabolites. This potential pathway would therefore render notoamide J a shunt metabolite in *Aspergillus* sp. MF297-2, but a precursor to notoamide B and versicolamide B in terrestrial-derived *Aspergillus versicolor*.

4.4.1 Synthesis of Potential Biosynthetic Intermediates

In order to determine the validity of both second generation biosynthetic pathways, unlabeled and isotopically labeled intermediates were synthesized. The unlabeled intermediates were used to detect the presence of these compounds in the normal culture of *Aspergillus* sp. MF297-2, while the isotopically labeled compounds were used in feeding studies with the marine fungal culture to check for incorporation

into advanced metabolites. Deoxybrevianamide E (**7**), 6-hydroxy-deoxybrevianamide E (**220**), and *epi*-notoamide J (**222**) were synthesized with and without isotopic labels, while oxindoles **235** and **236**, as well as the advanced metabolites **238** and **239**, were synthesized without any isotopic labeling.

As shown in Scheme 41, the synthesis of unlabeled deoxybrevianamide E started with the coupling of tryptophan derivative **113** to proline-ethyl ester **217** under standard conditions to afford peptide **243**. Removal of the Boc protecting group using TFA furnished free amine **244**, which was subsequently cyclized to give the diketopiperazine in a 1:1 ratio of the target molecule **7** and diastereomer **245**. Formation of *R*- and *S*-oxindole compounds **235** and **236** in a 1:2 ratio was obtained upon treatment of **7** with Davis oxaziridine.
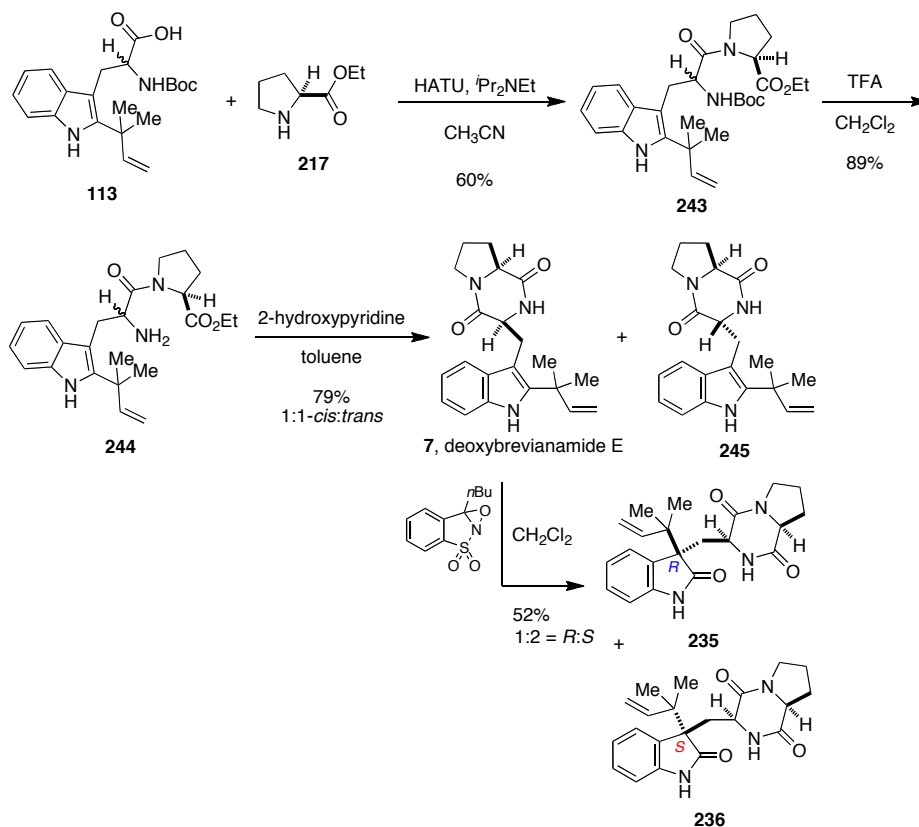
Scheme 41. Synthesis of deoxybrevianamide E and oxindoles **235** and **236**.

The synthesis of $[^{13}C]_2$-$[^{15}N]$-deoxybrevianamide E **246** started by coupling $[^{13}C]$-tryptophan derivative **142** with $[^{13}C]$-$[^{15}N]$-proline-ethyl-ester **247** in the presence of HATU, $^iPr_2NEt$, and acetonitrile to afford triply-labeled peptide **248** (Scheme 42). Removal of the Boc group and cyclization afforded a 1:1 ratio of $[^{13}C]_2$-$[^{15}N]$-deoxybrevianamide E **246** and diastereomer **250**, which were readily separated via column chromatography.
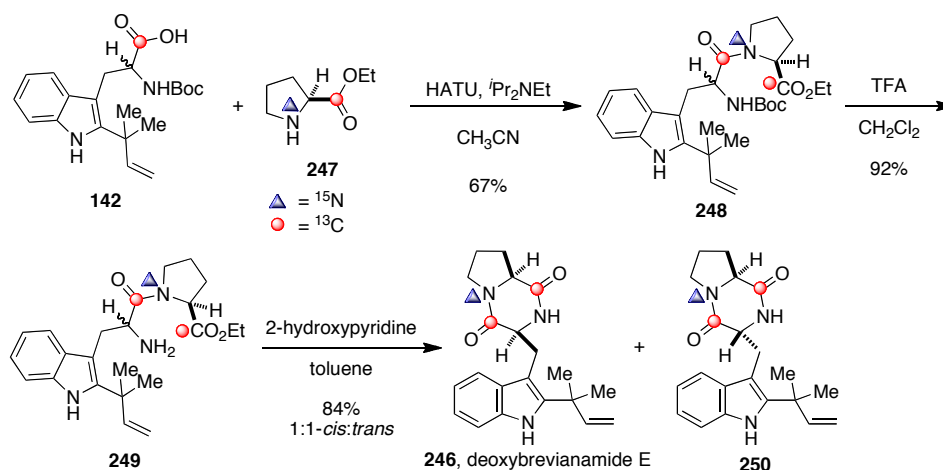
Scheme 42. Synthesis of $[^{13}C]_2$-$[^{15}N]$-deoxybrevianamide E.

Due to the difference in stereochemistry at the C-19 position of (−)-notoamide B and (−)-versicolamide B, two different routes were initially employed in the synthesis of the Diels-Alder cycloadducts **238** and **239**. As described in the biomimetic total synthesis of stephacidin A (Chapter 2), the desired *syn*- stereochemistry is preferentially formed in a 2.4:1 ratio when the C-2 reverse prenylated indole moiety is subjected to the IMDA reaction. Therefore, the synthesis of **238** was proposed following a similar route. For the synthesis of **239**, the *anti*-diastereomer is exclusively formed when the oxindole derivative undergoes a Diels-Alder cycloaddition reaction, as demonstrated in the

biomimetic synthesis of (+)- and (−)-versicolamide B (Chapter 2). Therefore, the most efficient synthesis of **239** would involve forming the oxindole moiety first.

Both syntheses began by Boc protecting *cis*-β-hydroxyproline **80** using standard conditions (Scheme 43). The *N*-Boc-*cis*-β-hydroxyproline **251** was then coupled to tryptophan derivative **252** to yield peptide **253**. Deprotection and cyclization furnished the desired diketopiperazine as a mixture of diastereomers (**254**). From this intermediate, the syntheses diverge.
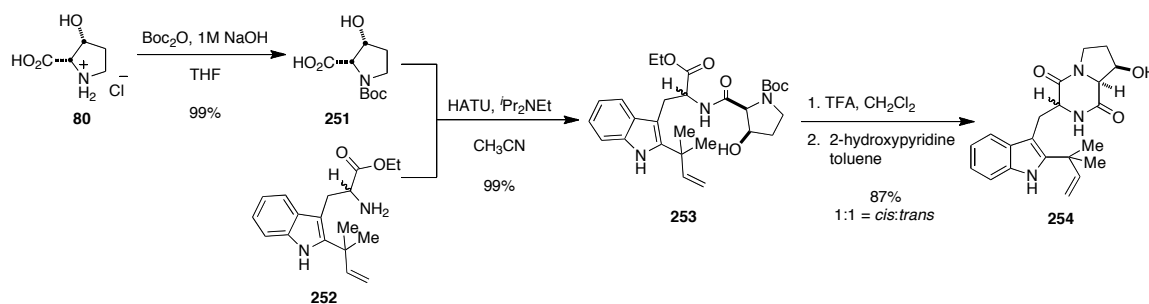
Scheme 43. Synthesis of diketopiperazine intermediate **253**.

For the synthesis of **238**, alcohol **254** was converted to enamide **255** using Mitsunobu conditions. The enamide was then treated with 20% aqueous KOH in MeOH to give a 2.4:1 ratio of *syn* (**257**):*anti* (**258**) Diels-Alder cycloadducts (Scheme 44). Treatment of **257** with Davis oxaziridine gave a 1:1 mixture of the desired *spiro*-oxindole **238** and the undesired diastereomer **259**. Stereochemical conformation of the desired *spiro*-oxindole was achieved through comparison of NOE data to known literature values.
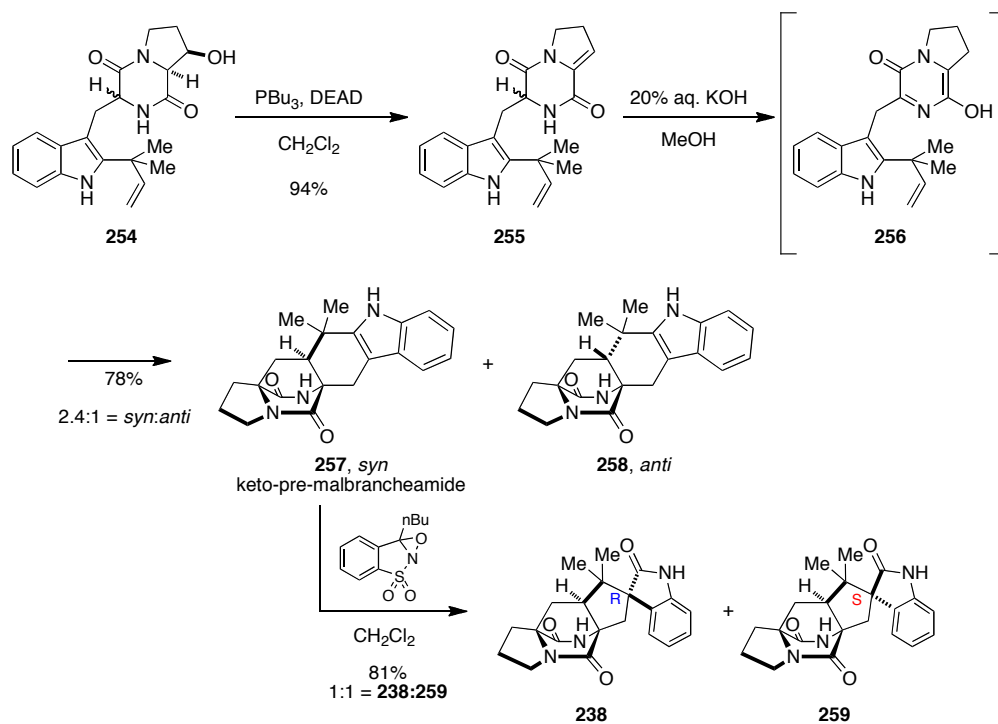
Scheme 44. Formation of *spiro*-oxindole **238**.

Synthesis of the *anti*-diastereomer followed the route established for the synthesis of (+)- and (–)-versicolamide B. Diketopiperazine **254** was converted to a 2:1 diastereomeric mixture of oxindoles **260** and **261** using Davis oxaziridine (Scheme 45). Elimination of the alcohol under Mitsunobu conditions provided **262**, which was subsequently treated to 20% KOH in MeOH to effect tautomerization and Diels-Alder cycloaddition. Unfortunately, after numerous attempts with both the *R*- and *S*-oxindole moieties, formation of the cycloadduct could not be achieved due to a competing retro-Michael reaction.
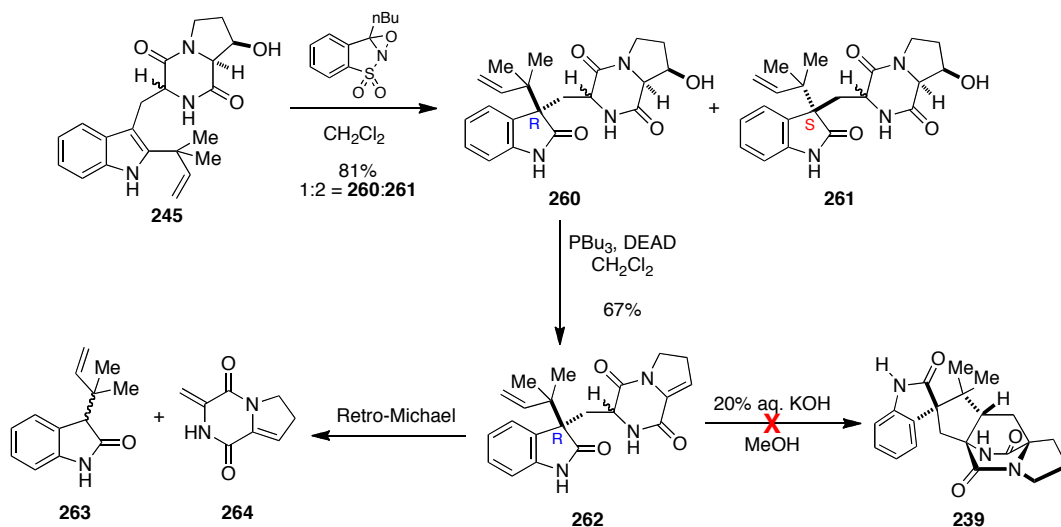
Scheme 45. Primary attempt to form (−)-versicolamide B precursor **239**.

Since **239** could not be synthesized as originally planned, an alternative synthesis was proposed. Following the same procedure established for the synthesis of **238**, the *anti*-diastereomer (**258**) underwent oxidation and a pinacol-type rearrangement using Davis oxaziridine to furnish **239** and **265** in a 1:1 ratio (Scheme 46). Unfortunately, one bottleneck in this route is the low yield of the *anti*-diastereomer formed from the IMDA reaction.
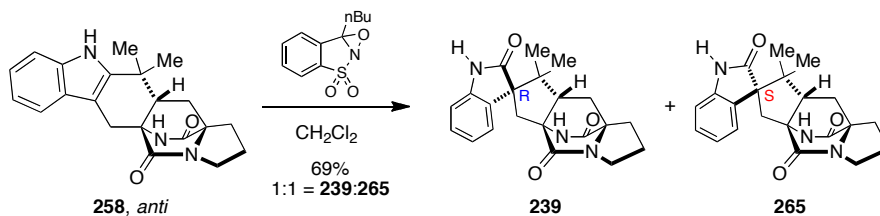
Scheme 46. Second attempt to synthesize **239**.

The unlabeled synthesis of 6-hydroxydeoxybrevianamide E and notoamide J is shown in detail in Section 4.1.2. Isotopically labeled 6-hydroxydeoxybrevianamide E

266 was readily synthesized from ^{13}C-labeled tryptophan derivative **267** (Scheme 47). Coupling of **267** with labeled [13]C-^{15}N-Boc-*L*-proline (**268**) in the presence of HATU and *i*Pr$_2$NEt provided **269**. Double Boc deprotection with TFA, followed by cyclization with 2-hydroxypyridine in refluxing toluene gave a 1:1 mixture of triply labeled diketopiperazines **266** and **271**. Conversion of **266** to labeled *epi*-notoamide J (**272**) was achieved in one step using Davis oxaziridine.
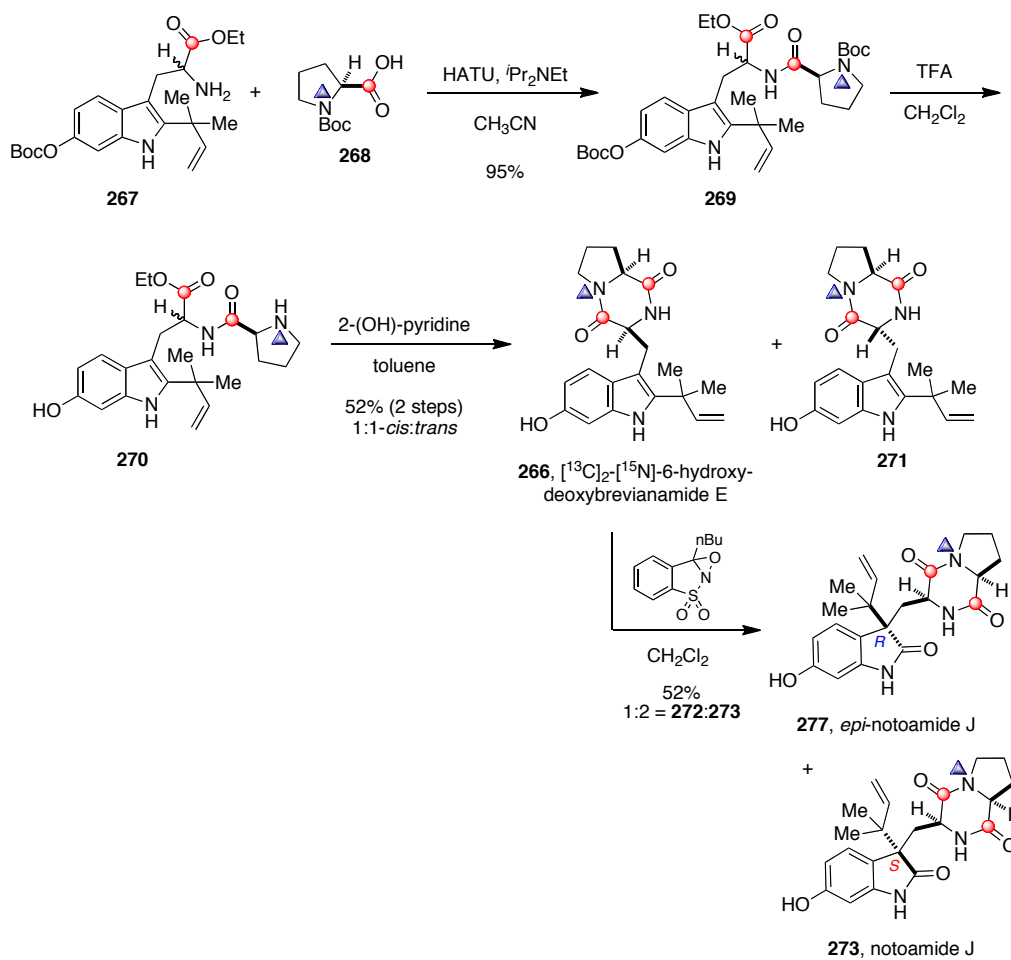
Scheme 47. Synthesis of [13]C$_2$-^{15}N-6-hydroxydeoxybrevianamide E and **277**.

4.4.2 Biosynthetic Results with *Aspergillus* sp. MF297-2

Through collaboration with Tsukamoto, a series of experiments were performed with the proposed biosynthetic intermediates to determine whether the proposed second generation biogenetic pathway is correct. Tsukamoto and coworkers compared the unlabeled potential precursors (**7**, **235**, **238**, **239**, and **220**; Figure 23) to metabolites isolated from the normal culture of marine-derived *Aspergillus* sp. MF297-2 via HPLC. The $[^{13}C]_2$-$[^{15}N]$-labeled precursors (**246**, **272**, **266**) were utilized in precursor incorporation feeding studies with Tsukamoto's *Aspergillus* sp. MF297-2

7, deoxybrevianamide E

246, $[^{13}C]_2$-$[^{15}N]$-deoxybrevianamide E

220, 6-hydroxydeoxybrevianamide E

266, $[^{13}C]_2$-$[^{15}N]$-6-hydroxy-deoxybrevianamide E

272, $[^{13}C]_2$-$[^{15}N]$-*epi*-notoamide J

235

238, (–)-notoamide B precursor

239, (–)-versicolamide B precursor
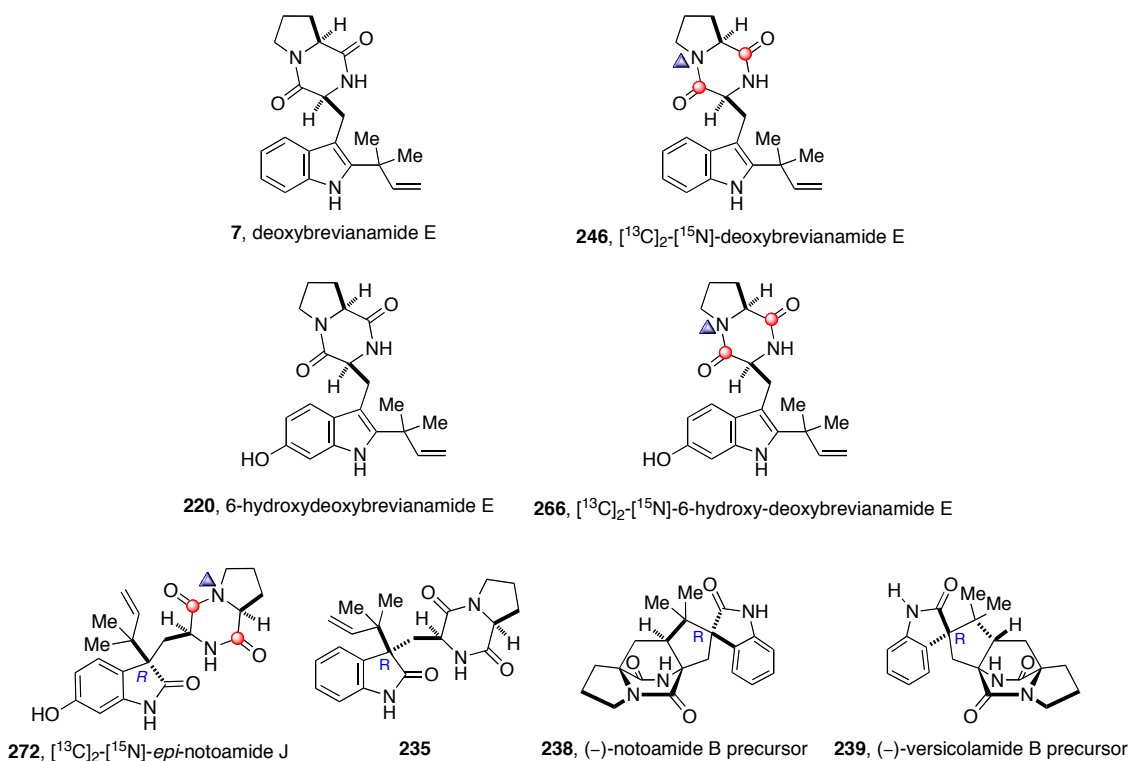
Figure 23. Potential biosynthetic precursors to metabolites isolated from marine-derived *Aspergillus* sp. MF297-2

Results from the precursor incorporation studies in *Aspergillus* sp. MF297-2 are illustrated in Scheme 48. It was determined that not only is deoxybrevianamide E a secondary metabolite produced by marine-derived *Aspergillus* sp. MF297-2, but also an intermediate along the biosynthetic pathway. Feeding experiments with $[^{13}C]_2$-$[^{15}N]$-deoxybrevianamide E showed incorporation of **246** into a 1:1 ratio of (+)- and (−)-notoamide B precursors (**274** and **275**), of which **274** matches the unlabeled metabolite **235**. Although it was clear from ^{1}H-NMR and ^{13}C-NMR analysis that the metabolites isolated from feeding studies with **272** did not contain the core bicyclo[2.2.2]diazaoctane ring system, further information was unavailable as the metabolites were produced only in trace amounts. Additionally, a majority of the precursor was recovered from this experiment. Currently, the feeding study with **266** is in progress by Tsukamoto and co-workers.
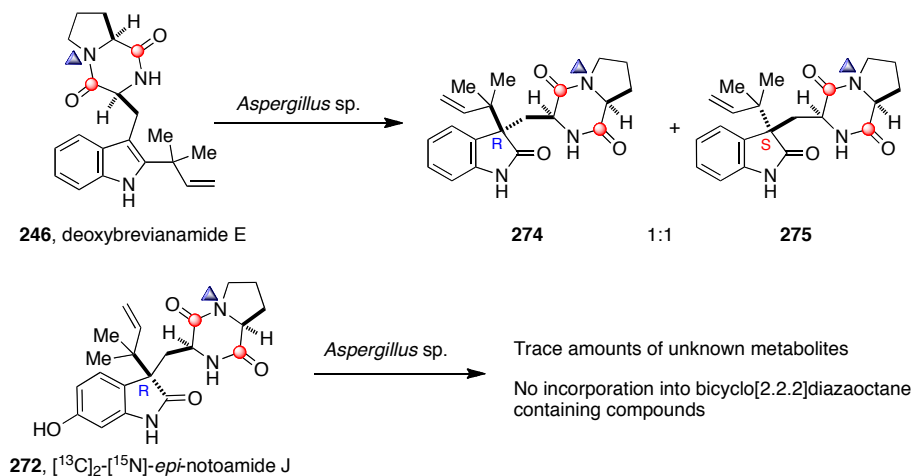
Scheme 48. Results of the *Aspergillus* sp. MF297-2 feeding experiment with $[^{13}C]_2$-$[^{15}N]$-deoxybrevianamide E.

Results from the comparison study of isolated metabolites with synthetic unlabeled metabolites demonstrated that 6-hydroxydeoxybrevianamide E was not

detected in the mature fungal culture; however, if this metabolite serves as a precursor to the advanced notoamide metabolites, detection of **220** would probably occur prior to day 5. Since **220** is a possible precursor to notoamide E, which is only detected on day 5, it is likely that **220** would only be present in the fungal culture prior to day 5. Likewise, the *spiro*-oxindole intermediates were not detected in the mature fungal culture. Therefore, this second generation biosynthetic proposal is unlikely to be the pathway used by the fungus.

4.5 Third Generation Biosynthetic Pathway—Sherman et al.

In a separate collaboration with Professor David Sherman at the University of Michigan, a third biosynthetic pathway was recently proposed that focuses on determining the early stage biosynthetic intermediates.[33] It is widely known that these prenylated indole metabolites are comprised of L-tryptophan and a second cyclic amino acid, such as L-proline. The condensation of these two amino acids leads to a known metabolite *cyclo*-L-tryptophan-L-proline more commonly known as brevianamide F (**6**). As shown in Scheme 49, there are two possibilities to form the proposed intermediate 6-hydroxydeoxybrevianamide E (**220**) from **6**: (1) brevianamide F could undergo hydroxylation at the C-6 position to yield 6-hydroxybrevianamide F (**276**), followed by reverse prenylation at the C-2 position to furnish 6-hydroxydeoxybrevianamide E (**220**); or (2) C-2 reverse prenylation to give deoxybrevianamide E (**7**) and subsequent C-6 hydroxylation to afford 6-hydroxydeoxybrevianamide E.
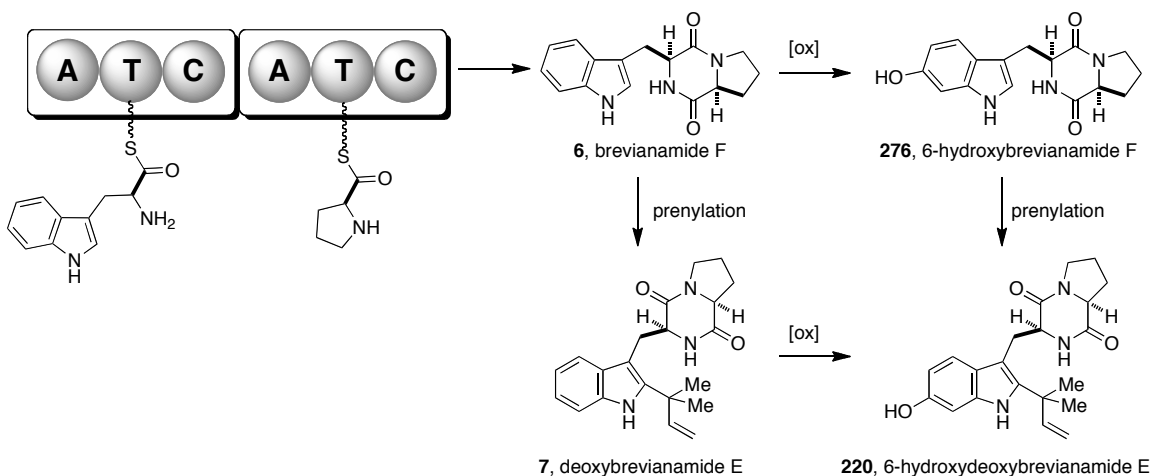
Scheme 49. Possible biogenesis of 6-hydroxydeoxybrevianamide E.

From **220**, C-7 prenylation would afford the proposed intermediate notoamide S (**52**), which could undergo cyclization to form the pyran ring to provide notoamide E (Scheme 50). Since notoamide E is not the Diels-Alder precursor, one of the three other C-2 reverse prenylated substrates must lend itself to the IMDA cycloaddition to ultimately produce (+)-stephacidin A in cultures of *Aspergillus* sp. MF297-2. The possibility of a stereoselective [4+2] cycloaddition of any of the three C-2 reverse prenylated indole alkaloids could account for the formation of the opposite enantiomers observed in terrestrial-derived *Aspergillus versicolor* (not shown in Scheme 50).
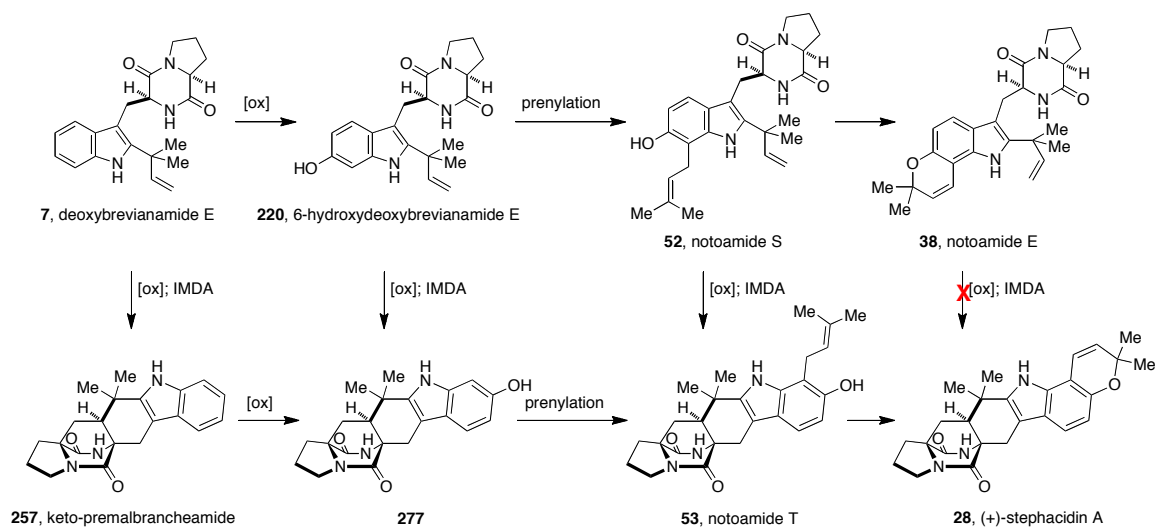
Scheme 50. Possible biosynthesis of the bicyclo[2.2.2]diazaoctane ring system found in *Aspergillus* sp. MF297-2 (*Aspergillus versicolor* not shown).

Continuing with the third generation biogenetic pathway, notoamide A and B could be derived biosynthetically from stephacidin A (Scheme 51). Depending on the fungal culture, formation of (+)- and (–)-notoamide B could arise from the face-selective oxidation of either (–)- or (+)-stephacidin A, respectively, followed by pinacol-type rearrangement. Notoamide A could then arise from *N*-oxidation of antipodal notoamide B.
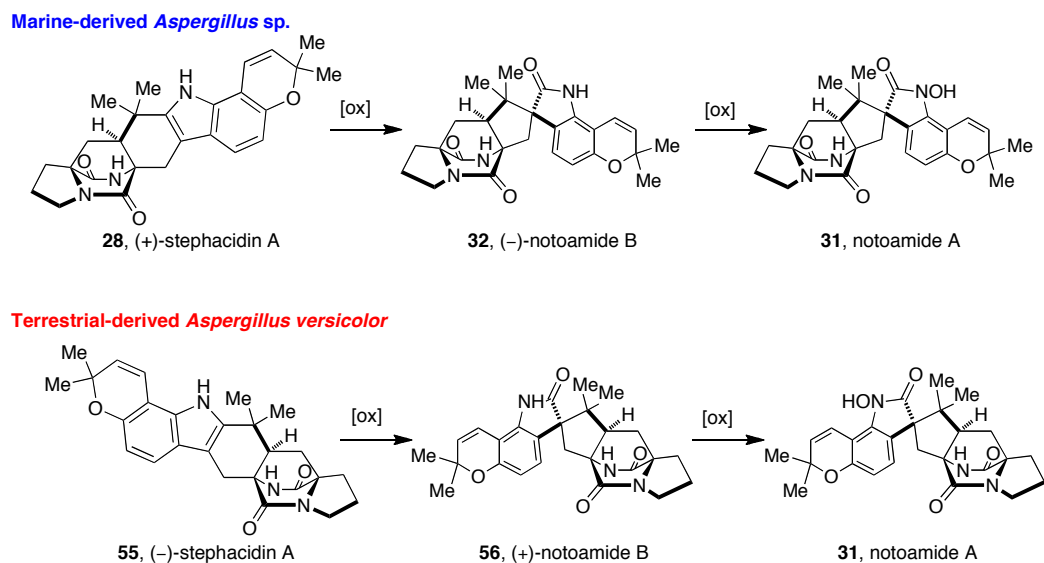
Scheme 51. Possible biosynthetic conversion of antipodal stephacidin A to the corresponding enantiomers, notoamide B and A.

4.5.1 (−)-Notoamide Biosynthetic Gene Cluster

In 2006, a bimodular nonribosomal peptide synthetase (NRPS) gene (*ftmA*) was mined from an *Aspergillus fumigatus* genome sequence, and its heterologous expression led to the accumulation of brevianamide F.[33,97] It was reasoned that an NRPS with a function coincident with FtmA would be present in the notoamide biosynthetic pathway, leading to the biosynthesis of brevianamide F in *Aspergillus* sp. MF297-2. Thus, using *ftmA* to probe for homologous genes, Sherman and coworkers identified an open reading frame (*orf*) named *notE* that shares 47% amino acid sequence identity with FtmA. In addition to *notE*, eighteen other genes were identified in a 42456-bp region of the chromosomes (Figure 24).
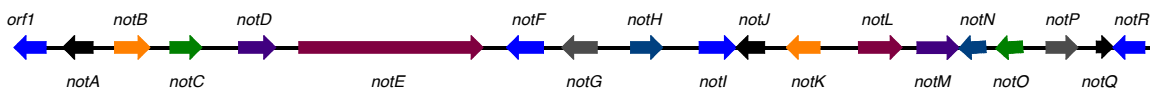
Figure 24. The notoamide (*not*) biosynthetic gene cluster derived from complete sequencing and bioinformatics mining of *Aspergillus* sp. MF297-2 genome.[33]

Additional bioinformatics analysis revealed that NotB and NotI showed high similarity to FAD-dependent monooxygenases, while NotD is a presumed flavin-dependent oxidoreductase. Furthermore, NotN is predicted to function as a dehydrogenase, while NotO could be a short-chain dehydrogenase/reductase. The *notK* gene encodes a putative efflux pump, which might specify excretion of alkaloid products from the cell. NotL and NotR both share a sequence identity to the AflJ aflatoxin pathway, while NotA is a predicted biosynthetic pathway transcriptional repressor.[33, 98,99]

Both NotG and NotH show a high sequence similarity to fungal CYP450s, which implicates either one in the formation of the isoprene-derived pyran ring. Upon closer comparison to the fumitremorgin biosynthetic gene cluster from *Aspergillus fumigatus*, NotG shows a high similarity to FtmC, which is responsible for C-6 hydroxylation of tryprostatin B in the biosynthetic formation of tryprostatin A (Scheme 52).[33,100] Based on the only other published pathway for isoprenylated alkaloids, it is proposed that in marine-derived *Aspergillus* sp. MF297-2, brevianamide F undergoes C-2 reverse-prenylation, followed by C-6 hydroxylation via NotG to form the proposed intermediate, 6-hydroxy-deoxybrevianamide E.
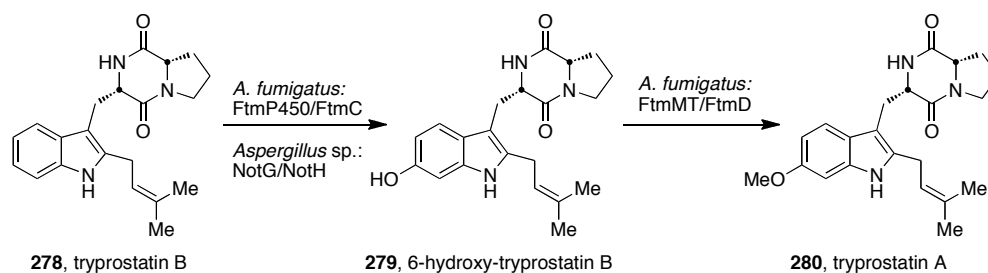
Scheme 52. Biogenetic conversion of tryprostatin B to tryprostatin A via *Aspergillus fumigatus*; proposed conversion of tryprostatin B to 6-hydroxytryprostatin B via the *not* genes from *Aspergillus* sp. MF297-2.

In addition to the regulators that were identified, two other proteins were noted as potential aromatic prenyltransferases. NotC and NotF are presumed to catalyze the two key prenylation reactions, with one protein acting as a reverse prenyltransferase and the other as a normal prenyltransferase. Upon closer analysis, NotC showed a 50% sequence identity to FtmH in *Aspergillus fumigatus*, while NotF shows a 40% identity to a putative dimethylallyl tryptophan synthase in *Coccidioides posadasii*.[101] However, the putative functions of products encoded by *notJ, notM, notP, and notQ* remain unknown based on bioinformatics analysis.[33]

4.5.2 Synthesis of Potential Early Stage Biosynthetic Precursors

To piece together the biosynthetic pathway of the stephacidin and notoamide metabolites, proposed biosynthetic intermediates from the third generation biogenetic pathway were synthesized and reacted with specific Not enzymes. Focus was initially placed on determining the correct biosynthetic pathway from brevianamide F to 6-hydroxydeoxybrevianamide E. Thus, the synthesis of 6-hydroxydeoxybrevianamide F

(**276**) commenced by subjecting **281** to a Mannich reaction to form gramine **282**, which was subsequently reacted with **122** in a Somei-Kamatani coupling reaction to furnish **283** (Scheme 53). Hydrolysis of **283** gave the free amine, which was then Boc protected to yield **284**. Treatment of **284** under standard saponification conditions afforded the *N*-Boc acid, which was coupled to proline-ethyl ester **217** to provide peptide **285**. Global Boc deprotection using TFA and cyclization in the presence of NEt$_3$ yielded the desired 6-hydroxybrevianamide F and the corresponding *trans*-diastereomer (not shown) in a 1:1 ratio.
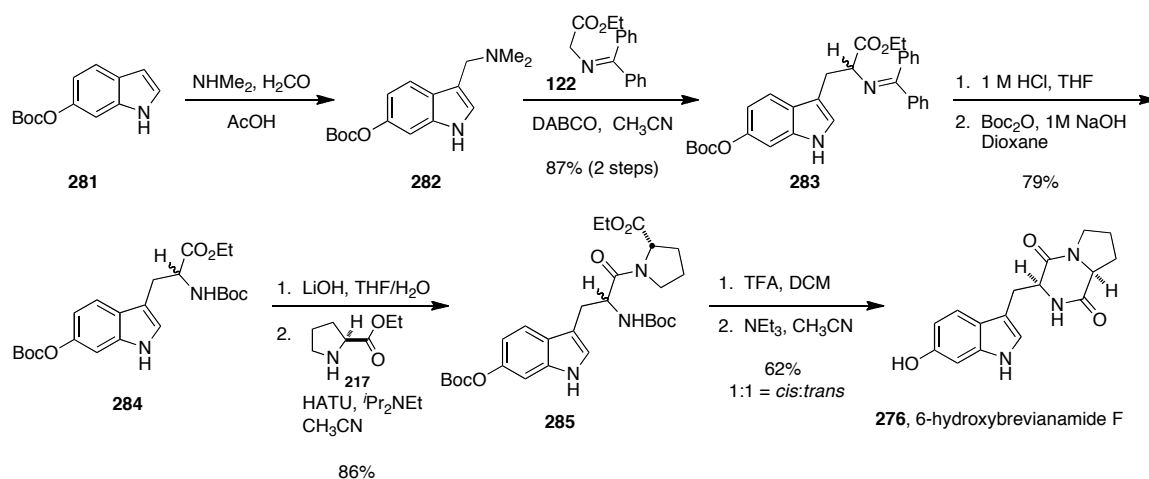
Scheme 53. Synthesis of potential biosynthetic precursor, 6-hydroxybrevianamide F.

Next, deoxybrevianamide E (**7**) was synthesized as an authentic standard of the reverse prenyltransferase reaction. Additionally, 6-hydroxydeoxybrevianamide E (**220**) and keto-premalbrancheamide (**257**) were synthesized to test as substrates for the normal prenyltransferase. As shown in Scheme 54 and previously discussed in Section 4.3.1, deoxybrevianamide E was synthesized from the standard coupling of **113** with **217**, to give **243**, which was converted to **7** in two further steps. 6-Hydroxydeoxybrevianamide E (**220**) was synthesized by coupling tryptophan derivative **190** with proline **217**.

Following a two-step conversion, **220** was obtained. The synthesis of keto-premalbrancheamide (**257**) was accomplished in five steps from tryptophan derivative **252** and proline **251**, and is discussed in Section 4.3.1.
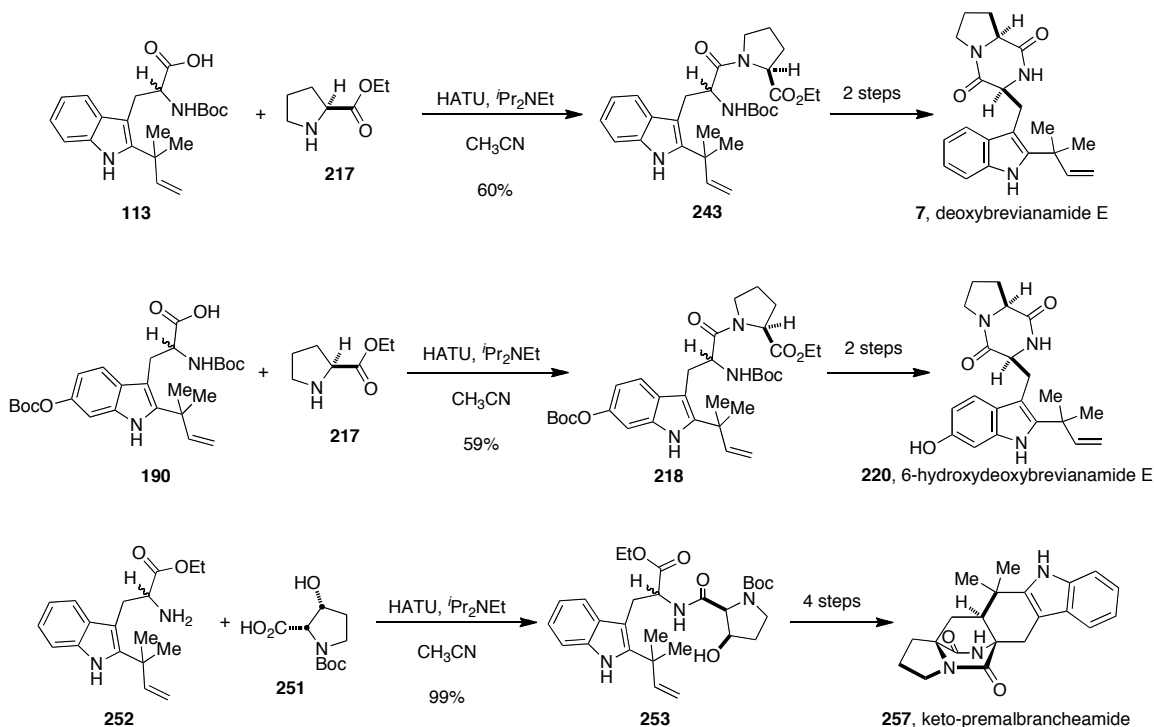
Scheme 54. Abbreviated syntheses of **7**, **220**, and **257**.

In addition to potential notoamide biosynthetic precursors, the known natural product tryprostatin B (**278**) was synthesized in order to determine whether NotG is responsible for C-6 hydroxylation of the indole moiety. Following a route similar to the synthesis of deoxybrevianamide E, the synthesis of tryprostatin B began by first forming C-2 prenylated indole **287** from **118** (Scheme 55). The indole nitrogen of **118** was first tosyl-protected, and then treated with *n*-BuLi and prenyl bromide to afford **286**. Removal of the tosyl-protecting group gave **287**, which was readily converted to gramine **288**. Somei-Kamatani coupling of **288** with **122** afforded imine **289**, and acid hydrolysis

provided the free amine, which underwent standard coupling with N-Boc-proline (**290**) to yield peptide **291**. Subsequent treatment with TFA cleaved the Boc-protecting group, and formation of the diketopiperazine was achieved upon treatment of the free amine with 2-hydroxypyridine to give tryprostatin B (**278**) and the *trans*-diastereomer (not shown) in a 1:1 ratio.
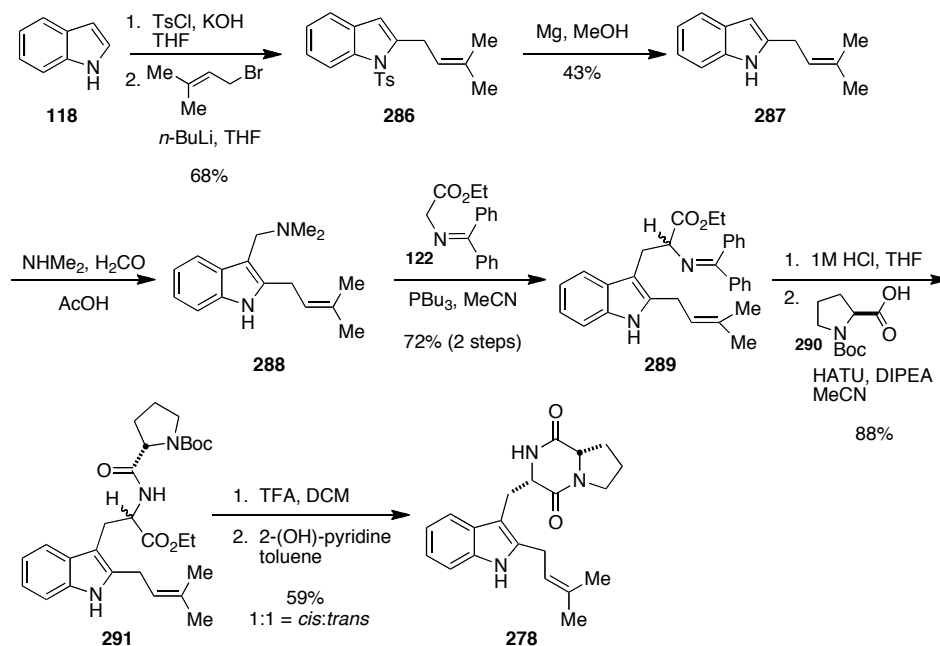
Scheme 55. Synthesis of tryprostatin B.

4.5.3 Results from Biogenetic Testing to Determine the Biosynthetic Pathway in *Aspergillus* sp. MF297-2

By over-expressing the isolated *not* genes from marine-derived *Aspergillus* sp. MF297-2, the synthesized substrates could be reacted with specific genes to check for their conversion into downstream metabolites. NotF was first tested with brevianamide F in the presence of dimethylallyl pyrophosphate (DMAPP), and the product exhibited the same retention time on HPLC as authentic deoxybrevianamide E (Scheme 56).[33] In

addition, NotF was tested with unnatural substrates, and no prenylated products were detected. These results demonstrate that NotF is the deoxybrevianamide E synthase and catalyzes the key reverse prenylation at C-2 of the indole ring leading to the bicyclo[2.2.2]diazaoctane core. Strong evidence was also provided for the early timing and high selectivity of the NotF-catalyzed reaction. However, since NotF has not yet been tested with 6-hydroxybrevianamide F, the order of hydroxylation and prenylation to form 6-hydroxydeoxybrevianamide E is still obscure.

6, brevianamide F

NotF
DMAPP

7, deoxybrevianamide E
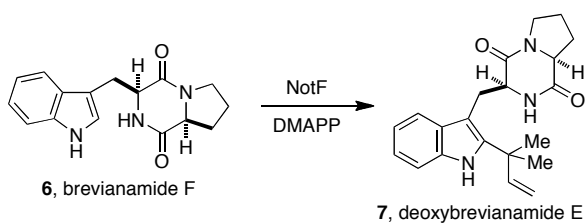
Scheme 56. Biogenetic conversion of brevianamide F to deoxybrevianamide E via the deoxybrevianamide E prenyltransferase from *Aspergillus* sp. MF297-2

The role of NotC, the second predicted prenyltransferase, was also investigated. There are several different possible substrates that could undergo C-7 normal prenylation on the indole ring, and each of these substrates could potentially appear on the pathway from deoxybrevianamide E to stephacidin A.[33] As Scheme 57 shows, the activity of NotC was tested on four structurally related putative substrates, deoxybrevianamide E (**7**), 6-hydroxydeoxybrevianamide E (**220**), keto-premalbracheamide (**257**), and 6-hydroxy-keto-premalbrancheamide (**277**). Results demonstrated that NotC showed high selectivity toward 6-hydroxydeoxybrevianamide E while the three other substrates failed to be converted. The NotC product was determined to be 6-hydroxy-7-prenyl-deoxybrevianamide E, later named notoamide S; thus, it was determined that NotC

catalyzes a normal prenyltransfer reaction at C-7 of the indole aromatic ring system in 6-hydroxydeoxybrevianamide E. These results also suggest that deoxybrevianamide E is first hydroxylated at C-6 of the indole ring, and the product **220** is subsequently prenylated at C-7 by NotC to generate notoamide S. However, the exact pathway leading from brevianamide F to notoamide S requires further investigation.
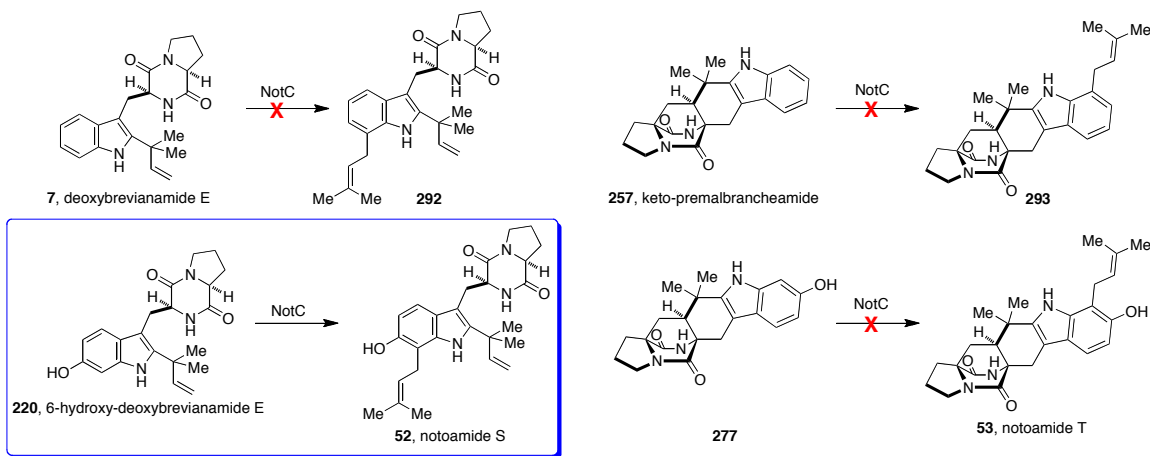
Scheme 57. Normal prenylation of **220** to notoamide S via NotC from *Aspergillus* sp. MF297-2

Using NADPH as cofactor, it was determined that NotB converts notoamide E (**38**) into notoamide D (**34**) and either notoamide C (**33**) or *epi*-notoamide C (**231**). Results from this study posed an interesting conundrum. When the products produced by the reaction of NotB with notoamide E were compared to synthetic standards, 3-*epi*-notoamide C was produced instead of the predicted natural metabolite notoamide C. The production of 3-*epi*-notoamide C from notoamide E in the presence of NotB could arise from a competing mechanistic pathway illustrated in Scheme 58. Following epoxidation of the β-face of notoamide E, the electrons from the indole nitrogen could open the epoxide, allowing for nucleophilic attack of the diketopiperazine on the imine and

forming notoamide D. On the other hand, a pinacol-type rearrangement of the β-face epoxide would yield 3-*epi*-notoamide C. In order for notoamide C to arise from notoamide E, epoxidation of the α-face of notoamide E is required, which did not occur via NotB. Therefore, it is proposed that the competing mechanistic pathway must not naturally occur in *Aspergillus* sp. MF297-2 as evident from the lack of formation of 3-*epi*-notoamide C in the natural fungal culture. The natural formation of notoamide C must either arise from a currently unknown enzyme, or perhaps the original structural assignment of notoamide C was incorrect. The crystallographic study of these metabolites is ongoing.
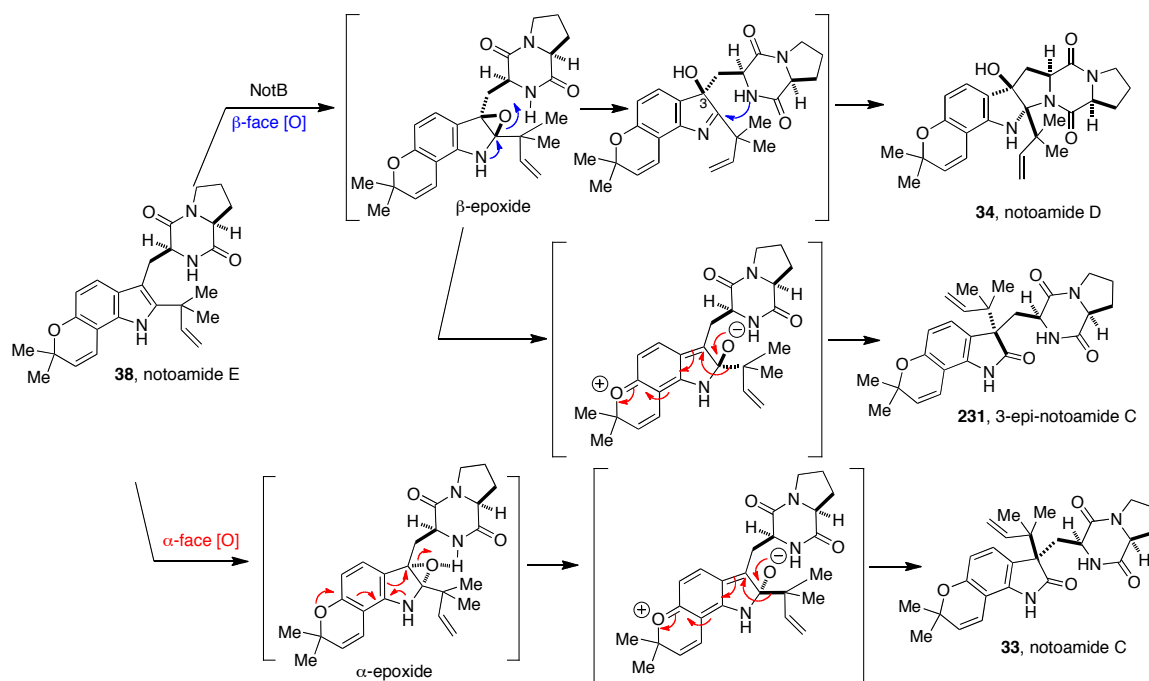
Scheme 58. Proposed mechanistic formation of notoamide D, notoamide C and 3-*epi*-notoamide C from notoamide E.

Based on the results from the biogenetic analysis of the *not* gene cluster isolated from marine-derived *Aspergillus* sp. MF297-2, as well as results from the notoamide E

incorporation study, a proposed biosynthetic pathway has been assembled (Scheme 59). It is widely known that brevianamide F (**6**) is biosynthetically constructed from tryptophan and proline, which is proposed to arise via NotE.[1-3,26] Brevianamide F could then undergo reverse prenylation at C-2 of the indole moiety via NotF in the presence of DMAPP to afford deoxybrevianamide E. Most likely, C-6 hydroxylation of **7** via NotG could result in formation of 6-hydroxydeoxybrevianamide E. NotC then affects prenylation in the normal fashion of **220** to provide notoamide S, which is believed to act as the branching point between the biosynthetic formation of notoamide E and stephacidin A. To form the desired bicyclo[2.2.2]diazaoctane ring system, oxidation and tautomerization of notoamide S (**52**) would provide the IMDA precursor, which would undergo a [4+2] cycloaddition to afford the potential biosynthetic intermediate notoamide T (**53**). Cyclization to form the pyran ring on the indole moiety would give stephacidin A (**28**). As previously discussed, pyranoindole formation of notoamide S would yield notoamide E, which is readily converted to notoamide D and either notoamide C or 3-*epi*-notoamide C via NotB.
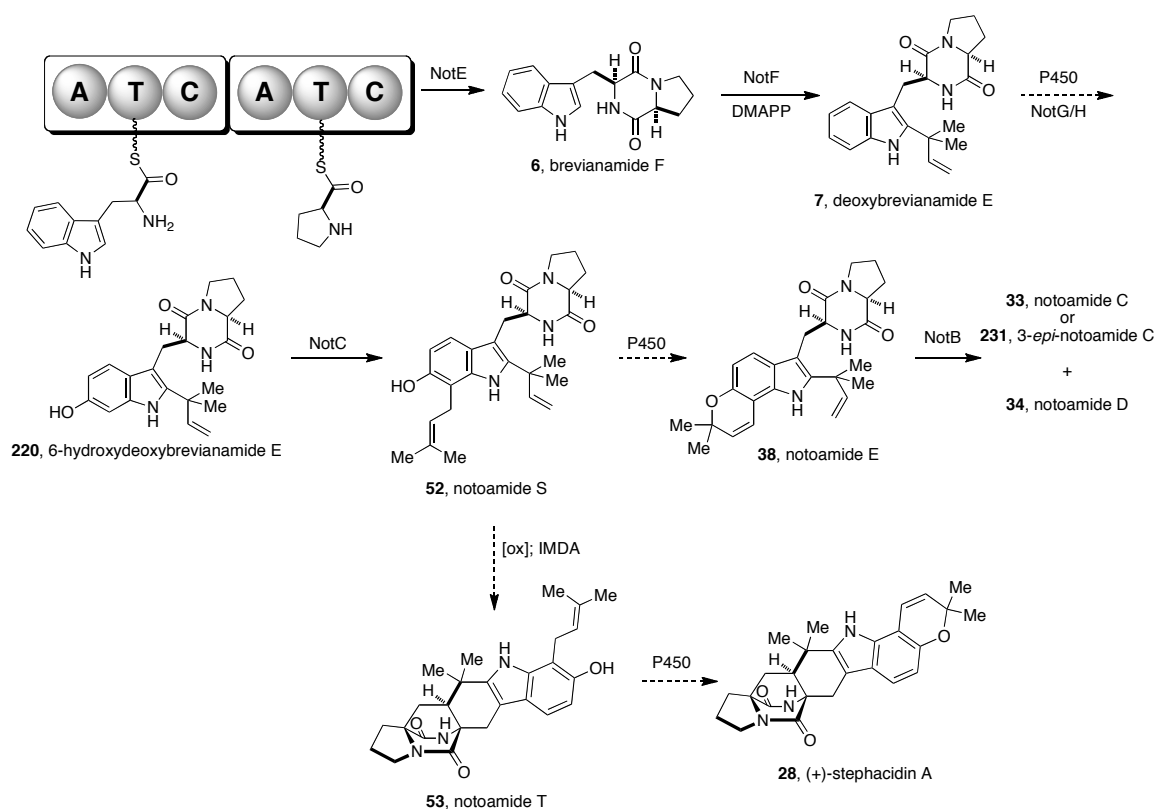
Scheme 59. Updated third generation biosynthetic pathway of *Aspergillus* sp. MF297-2

4.6 Future Directions

With the third generation biosynthetic pathway showing promise as the biogenetic route used by marine-derived *Aspergillus* sp. MF297-2 to synthesize the core bridging bicycle, further investigation of this pathway is necessary. Additional feeding experiments using isotopically labeled proposed intermediates, such as notoamide S and/or notoamide T would provide substantial support for this biogenetic pathway. Extra testing of the *not* genes on putative substrates could also unveil additional information about the biosynthetic substrates, as well as the presence of branching pathways used in the biosynthesis of other minor metabolites.

CHAPTER 5

Terrestrial-Derived *Aspergillus versicolor*: Elucidation of the Stephacidin and Notoamide Biosynthesis

5.1 Terrestrial-derived *Aspergillus versicolor*

5.1.1 Isolation of Metabolites

In 2008, Gloer and coworkers isolated five known prenylated indole metabolites from terrestrial-derived *Aspergillus versicolor* NRRL 35600.[25] The isolate of *Aspergillus versicolor* was obtained from a basidioma of *Gandoderma australe* collected in a Hawaiian forest. From this extract, brevianamide F (**6**), (−)-stephacidin A (**55**), norgeamide D (**37**), (+)-notoamide B (**56**), and (+)-versicolamide B (**54**) were obtained (Figure 25). Structural determination was obtained through comparison with NMR and MS data from literature. Additionally, through circular dichroism (CD) spectroscopy, both versicolamide B and notoamide B were found to display a 3*S* configuration of the *spiro*-oxindole stereogenic center. Additionally, versicolamide B (**54**) represents the first member outside of the brevianamide family to possess the rare *anti* relative configuration within the bicyclo[2.2.2]diazaoctane ring system (See Chapter 2 for a more in-depth explanation of *syn* and *anti*).
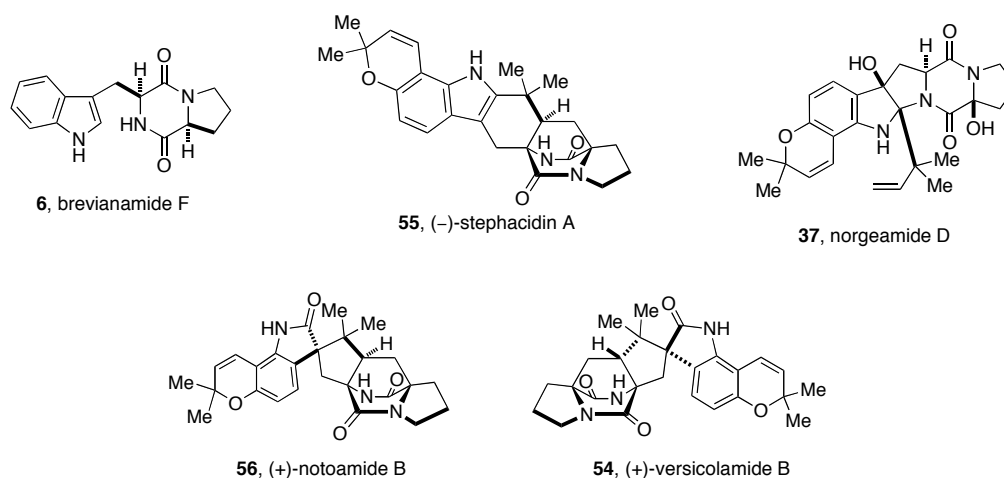
Figure 25. Secondary metabolites isolated from *Aspergillus versicolor* NRRL 35600.

5.1.2 Identification of Antipodal Metabolites

These five secondary metabolites were nearly identical to metabolites isolated from Tsukamoto's marine-derived *Aspergillus* sp. MF297-2 Upon further analysis of the *Aspergillus versicolor* metabolites, it was determined that stephacidin A, notoamide B, and versicolamide B possess the opposite absolute configurations to the known stephacidin A producer *Aspergillus ochraceus* WC76466 and metabolites previously isolated from and marine-derived *Aspergillus* sp. MF297-2 (Figure 26).[25] The assignment of (–)-stephacidin A (**55**), (+)-notoamide B (**56**), and (+)-versicolamide B (**54**) were determined based on examination and comparison of the CD spectra and optical rotation values of both sets of natural metabolites.

28, (+)-stephacidin A   **55**, (−)-stephacidin A

32, (−)-notoamide B   **56**, (+)-notoamide B

57, (−)-versicolamide B   **54**, (+)-versicolamide B
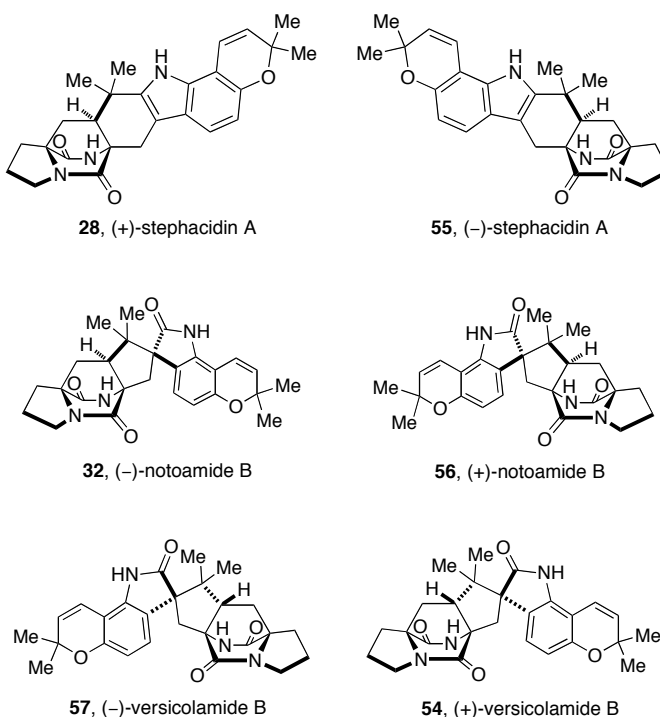
Figure 26. Structures of antipodal natural metabolites isolated from marine-derived *Aspergillus* sp. MF297-2 and terrestrial-derived *Aspergillus versicolor*.

5.2 Enantio-Divergent Biosynthetic Pathways

The isolation of these enantiomeric natural metabolites represents the first set of antipodal metabolites within the notoamide, paraherquamide, and stephacidin families. This sparked further interest in elucidating the biosynthetic pathway for the formation of the bicyclo[2.2.2]diazaoctane ring system in *Aspergillus* sp. MF297-2 and *Aspergillus versicolor*. It has been strongly implicated that the IMDA reaction forms the core bridging bicycle, which is also responsible for the enantio-divergence between the two *Aspergillus* species.[96] Devised from the proposed biosynthetic pathway established for the biosynthesis of the metabolites isolated from marine-derived *Aspergillus* sp. MF297-

2, it is postulated that the biosynthesis of metabolites from *Aspergillus versicolor* follow a similar, if not identical, biosynthetic pathway resulting in the formation of antipodal metabolites between the two *Aspergillus* species.

As shown in Scheme 60, starting from the common biosynthetic intermediate, notoamide S (**52**), the formation of achiral azadiene **278** allows for a stereospecific [4+2] cycloaddition reaction in *Aspergillus* sp. MF297-2 and *Aspergillus versicolor*, resulting in the formation of the proposed stephacidin A precursor notoamide T (**53** and **279**). Formation of the pyran ring affords either (+)- or (−)-stephacidin A (**28** or **55**), respectively. Likewise, a stereoselective oxidation and pinacol-type rearrangement of antipodal stephacidin A could account for the formation of (−)-notoamide B in *Aspergillus* sp. MF297-2, and (+)-notoamide B in cultures of *Aspergillus versicolor* (Scheme 61).
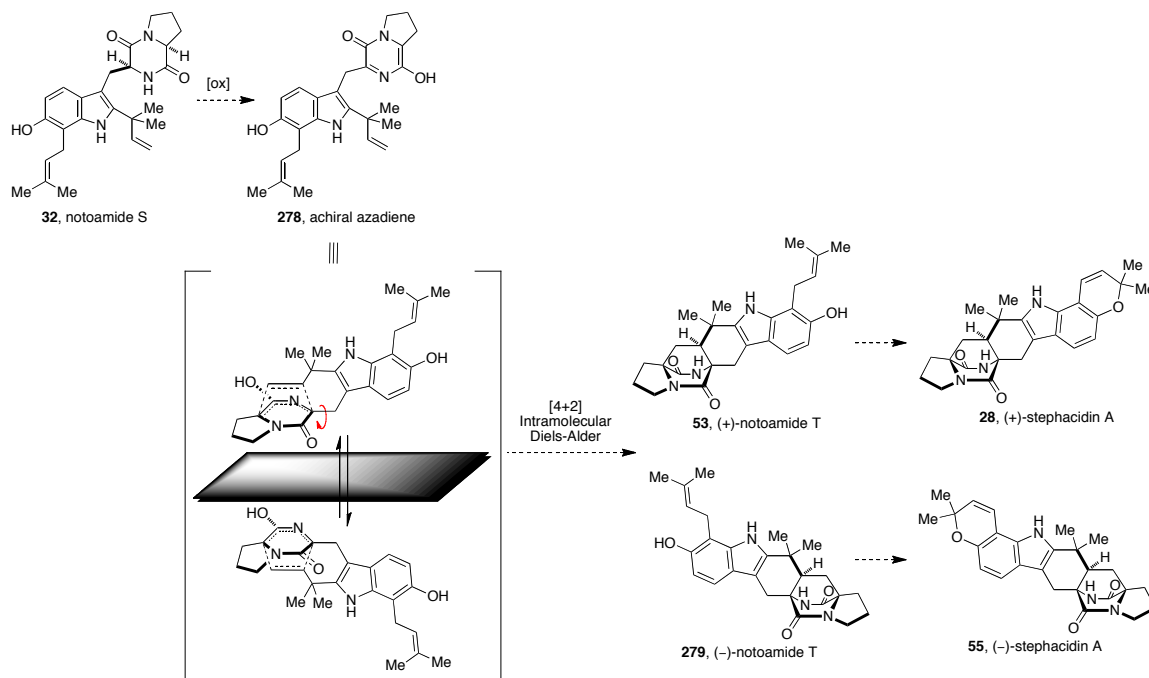
Scheme 60. Enantio-divergent pathway leading from notoamide S to (+)- and (−)-stephacidin A.
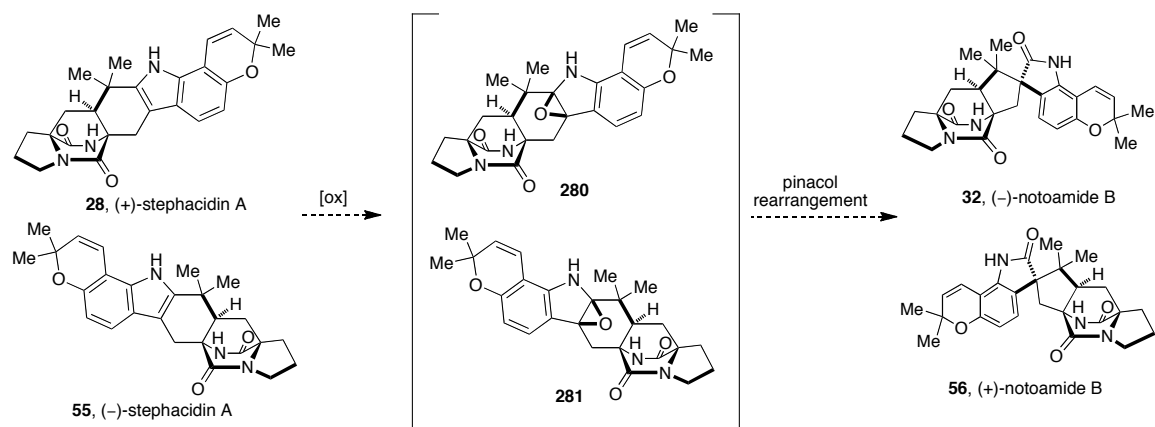
Scheme 61. Stereoselective formation of (+)- and (−)-notoamide B.

Another disparity in the biosynthesis of the notoamides and stephacidins not understood is the formation of (−)- and (+)-versicolamide B in *Aspergillus* sp. MF297-2 and *Aspergillus versicolor*, respectively. Since versicolamide B displays an *anti*-configuration within the bicyclo[2.2.2]diazaoctane ring system, two potential biosynthetic pathways have been proposed.[25] First, (+)- and (−)-versicolamide B could arise biosynthetically from the C-6 *epi*-diastereomer of stephacidin A, or secondly, from the oxindole of notoamide S (Scheme 62). At this time, neither proposed precursor has been isolated from the normal culture of *Aspergillus* sp. MF297-2 or *Aspergillus versicolor*.
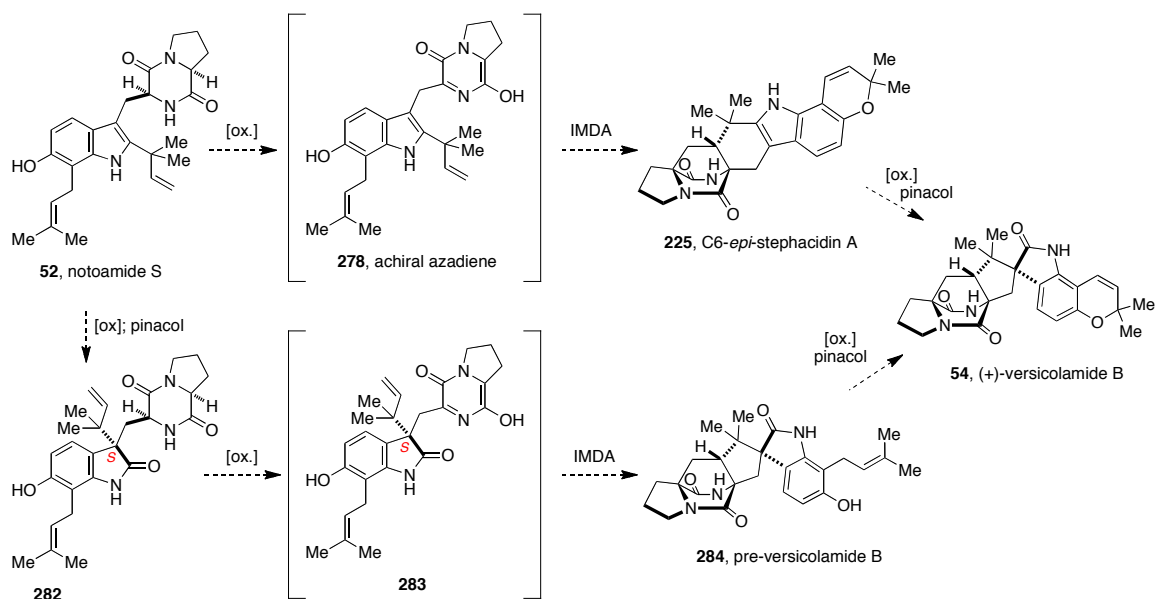
Scheme 62. Potential Biosynthetic Formation of (+)-Versicolamide B in *Aspergillus versicolor* (*Aspergillus* sp. MF297-2 not shown).

5.3 Isotope Incorporation Studies and Outcomes

To determine if the two sets of antipodal metabolites were biosynthesized along a similar, if not identical, biosynthetic pathway, four different isotope incorporation studies were performed with terrestrial-derived *Aspergillus versicolor* (Figure 27). With a potential biosynthetic pathway being set forth by Sherman and co-workers, it seems reasonable that *Aspergillus versicolor* would follow the same biosynthetic formation of prenylated indole metabolites. First, to determine similarities between the two pathways, an isotope incorporation experiment was carried out with $[^{13}C]_2$-notoamide E. Next, there exists two different species that could possibly lead to the formation of the bridged bicycle, and to determine which one is the pivotal intermediate along the biosynthetic pathway, $[^{13}C]_2$-$[^{15}N]$-6-hydroxydeoxybrevianamide E and $[^{13}C]_2$-$[^{15}N]_2$-notoamide S were provided to *Aspergillus versicolor*. Finally, the isolation of stephacidin A in the

presence of notoamide B within both fungal cultures raised the question as to whether stephacidin A is the biosynthetic precursor to notoamide B and if this conversion is stereoselective. Thus, $[^{13}C]_2$-(±)-stephacidin A was introduced to *Aspergillus versicolor* in an isotope incorporation study.

229, notoamide E

266, $[^{13}C]_2$-$[^{15}N]$-6-hydroxy-deoxybrevianamide E

285, notoamide S

286, (±)-stephacidin A
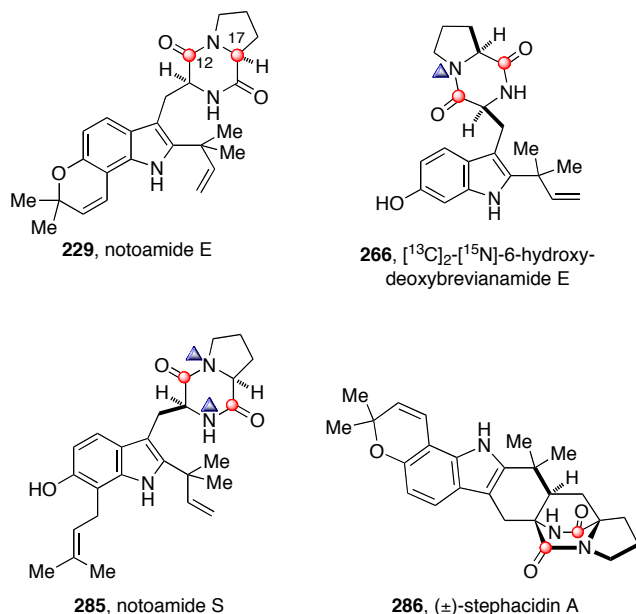
Figure 27. Four isotopically enriched compounds utilized in feeding experiments with terrestrial-derived *Aspergillus versicolor*.

5.3.1 Notoamide E

Although notoamide E has not yet been isolated from the natural *Aspergillus versicolor* culture, it was reasoned that if the biosynthetic pathways were substantially the same in both *Aspergillus* sp. MF297-2 and *Aspergillus versicolor*, then labeled notoamide E would incorporate into notoamide C, notoamide D, and 3-*epi*-notoamide C in the terrestrial-derived fungal culture. Furthermore, based on Tsukamoto's results,[25] it was expected that notoamide E would not incorporate into any compounds containing the bridged bicyclo[2.2.2]diazaoctane core, such as (–)-stephacidin A and (+)-notoamide B.

[^{13}C]$_2$-Notoamide E was introduced to *Aspergillus versicolor* in a precursor incorporation study, in which significant ^{13}C incorporation was observed by ^{13}C NMR spectroscopy at C-12 and C-17 of notoamides C and D (Scheme 63). From analysis of the electrospray mass spectra, incorporation of intact doubly ^{13}C-labeled notoamide E into notoamide C was determined to be 6.2%, while incorporation into notoamide D was 6.0%.[102,103] Interestingly, upon closer inspection, trace amounts of doubly ^{13}C-labeled 3-*epi*-notoamide C (**231**), unlabeled (−)-stephacidin A (**55**), and unlabeled (+)-notoamide B (**56**) were also detected by LC-MS (Table 7). In contrast to the metabolite profile observed by Tsukamoto and co-workers, only trace amounts of 3-*epi*-notoamide C (**231**) were detected and therefore the calculation of the percent of intact incorporation is unreliable. As mentioned previously, Tsukamoto observed a complete lack of production of any compounds containing the bicyclo[2.2.2]diazaoctane core, and while (−)-stephacidin A and (+)-notoamide B are usually the major metabolites in the normal medium of *Aspergillus versicolor*, only trace amounts of these unlabeled compounds were isolated.[25,96]
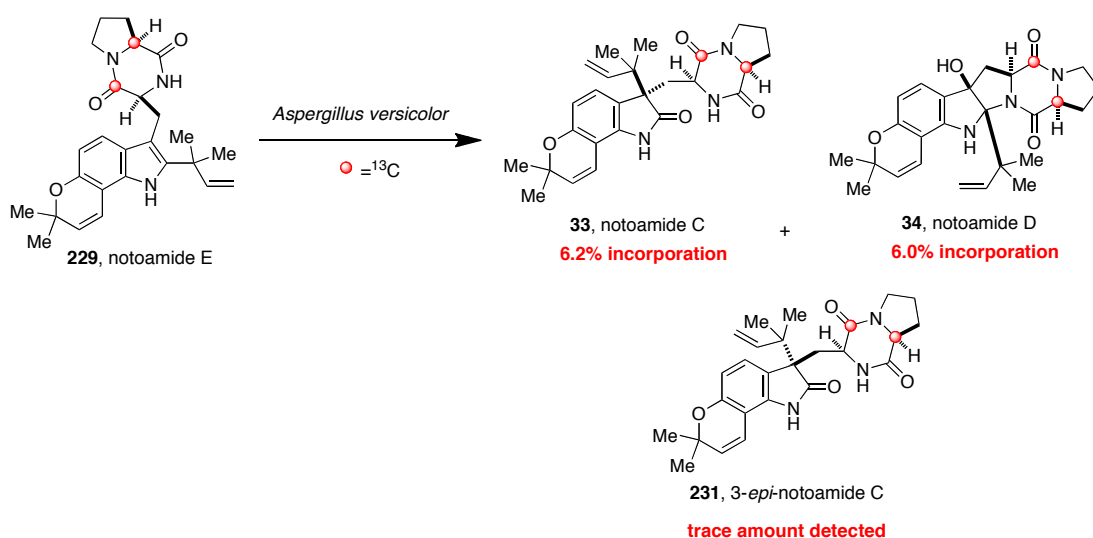
Scheme 63. Incorporation of [^{13}C]$_2$-notoamide E into notoamide C and D.

Table 7. Intact incorporation of double ^{13}C-labeled Notoamide E (**229**) into isolated metabolites.

Metabolite	% specific incorporation	Notes
notoamide C	6.2%	8.1 mg
3-*epi*-notoamide C	ND[a]	trace isolated
notoamide D	6.0%	11.2 mg
stephacidin A	0%	trace isolated
notoamide B	0%	trace isolated

a) Not enough material to adequately calculate the % incorporation

5.3.2 6-Hydroxydeoxybrevianamide E

Based on results obtained by Sherman et al. during the isolation and characterization of the *not* gene sequence, it was expected that an incorporation study of [13]C$_2$-[^{15}N]-6-hydroxydeoxybrevianamide E in cultures of *Aspergillus versicolor* would likely furnish labeled notoamide S, as well as labeled bridged bicycle-containing compounds. However, based on results obtained from the notoamide E feeding study, there was also the possibility that labeled notoamide J could result from the same incorporation experiment. As scheme 64 shows, 6-hydroxydeoxybreviamide E could undergo oxidation and pinacol-type rearrangement to afford notoamide J; or in contrast to this proposed route, 6-hydroxydeoxybrevianamide E could react with the NotC enzyme, yielding notoamide S. Either way, both notoamide J and notoamide S could serve as viable substrates for the biosynthetic IMDA reaction furnishing (+)-versicolamide B and (+)-notoamide B in *Aspergillus versicolor*. In order to determine which of the two possible routes is utilized in biosynthesis, a feeding experiment with 6-hydroxydeoxybrevianamide E was conducted.
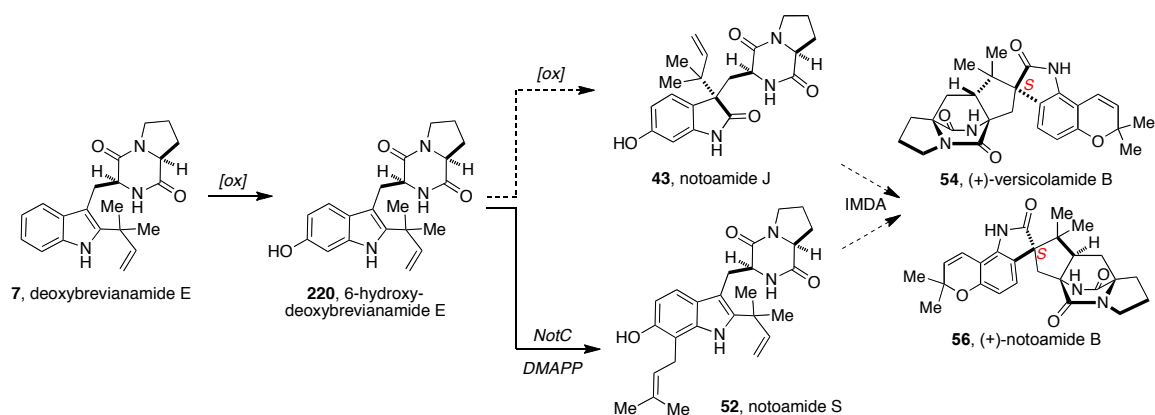
Scheme 64. Two possible biosynthetic pathway for the formation of (+)-versicolamide B and (+)-notoamide B from **7**.

$[^{13}C]_2$-$[^{15}N]$-6-Hydroxydeoxybrevianamide E (**266**) was synthesized as outlined in Chapter 4, Scheme 47, and introduced to terrestrial-derived *Aspergillus versicolor* in an incorporation study. Fungal extracts from the precursor incorporation experiment were analyzed by ^{13}C-NMR spectroscopy, in which significant ^{13}C-enrichment was detected at the C-12 and C-18 positions of notoamide J (**43**, Scheme 65). Analysis of the electrospray mass spectrum showed 8.4% incorporation of intact triply labeled 6-hydroxydeoxybrevianamide E (**266**) into **43**.[102,103] Further analysis of the fungal extract by LC-MS showed the production of several unlabeled advanced metabolites (Table 8), such as (−)-stephacidin A (**55**), (+)-notoamide B (**56**), and (+)-versicolamide B (**54**), as well as notoamides C and D (**33** and **34**). Unfortunately, only 32% of **266** incorporated into the biosynthetic pathway, based on recovered starting material.
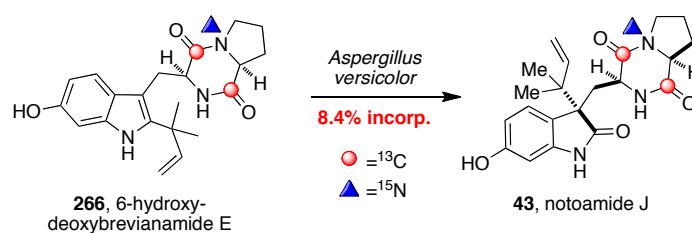
Scheme 65. Incorporation of $[^{13}C]_2$-$[^{15}N]$-6-Hydroxydeoxybrevianamide E into notoamide J in terrestrial-derived *Aspergillus versicolor*.

Table 8. Isolated metabolites from *Aspergillus versicolor* feeding study with **266** and percentage of intact incorporation.

Metabolite	% ^{13}C-incorporation	Amount
notoamide J	8.4%	1.4 mg
notoamide C	0%	0.6 mg
notoamide D	0%	0.9 mg
(−)-stephacidin A	0%	1.1 mg
(+)-notoamide B	0%	1.2 mg
(+)-versicolamide B	0%	1.5 mg

5.3.3 Notoamide S

The last logical possibility for a single species that could be produced by both *Aspergillus* sp. MF297-2 and *Aspergillus versicolor* and lead to the formation of antipodal bicyclo[2.2.2]diazaoctane-containing compounds is notoamide S. Sherman established support for the existence of notoamide S within *Aspergillus* sp. MF297-2 when the NotC enzyme was reacted with 6-hydroxydeoxybrevianamide E to yield notoamide S (**52**). To determine whether notoamide S is also a precursor within *Aspergillus versicolor*, $[^{13}C]_2$-$[^{15}N]_2$-notoamide S was synthesized and provided to terrestrial-derived *Aspergillus versicolor* in a precursor incorporation study.

Upon analysis of the fungal extracts of the $[^{13}C]_2$-$[^{15}N]_2$-notoamide S (**285**) feeding study, the following ^{13}C-incorporation was detected and calculated: 6.4% notoamide C, 6.2% notoamide D, 6.2% stephacidin A, 6.4% notoamide B, and 6.5% versicolamide B (Scheme 66). In addition to the above metabolites, through LC-MS ^{13}C incorporation was detected in notoamide A, notoamide I, notoamide M, notoamide K, and notoamide R, however, only trace amounts of these metabolites were detected, and as such the percentage of intact incorporation could not be calculated (Figure 28).
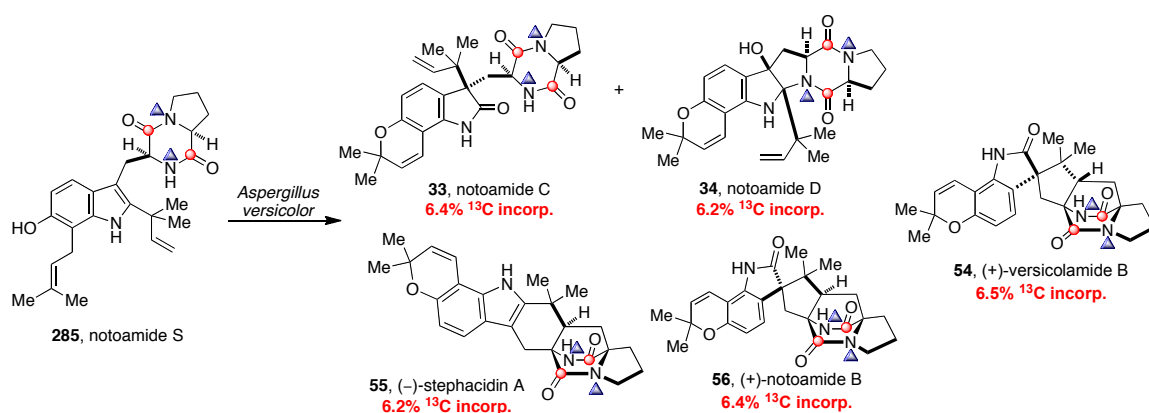
Scheme 66. Notoamide S incorporation in terrestrial-derived *Aspergillus versicolor*.
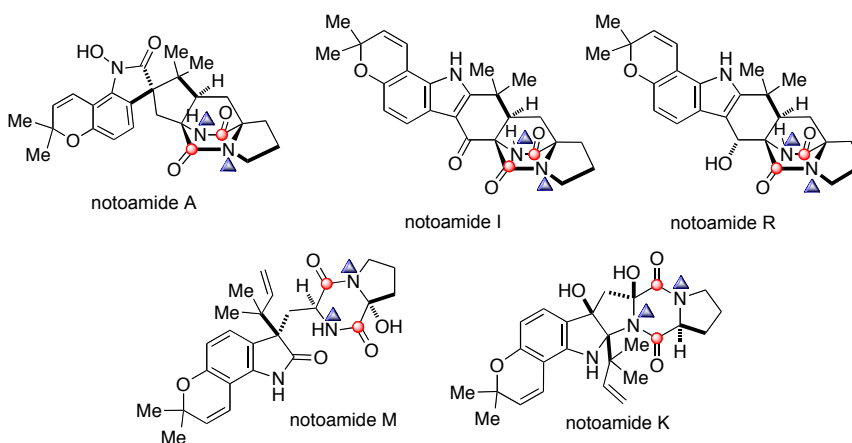
Figure 28. Possible metabolites formed from $[^{13}C]_2$-$[^{15}N]_2$-notoamide S.

5.3.4 Stephacidin A

With the isolation of stephacidin A in the presence of notoamide B, questions arose as to whether or not the stephacidins and notoamides share a common biogenesis, and if stephacidin A could be a direct precursor to notoamide B. Biosynthetically, face-selective oxidation of the 2,3-disubstituted indole of (−)- and (+)-stephacidin A would yield the corresponding *spiro*-oxindoles, (+)- and (−)-notoamide B, respectively. This conversion was recently supported synthetically through the efficient biomimetic oxidation of stephacidin A to notoamide B by deploying an oxaziridine, which further demonstrates that this chemically feasible oxidative transformation was indeed valid in Nature.[78,79] To specifically investigate the biosynthetic formation of notoamide B, a traditional isotopic substrate incorporation technique was employed in *Aspergillus versicolor* NRRL 35600 with $[^{13}C]_2$-(±)-stephacidin A (**286**).

As illustrated in Scheme 67, fungal extracts from the feeding study were analyzed by LC-MS and ^{13}C-NMR spectroscopy, and further analysis of the electrospray mass spectrum showed 2.7% intact incorporation of labeled (−)-**286** into (+)-**56**.[102,103] The unreacted stereoisomer (+)-**286** was also isolated from the fungal extract, which was anticipated since it possesses the opposite absolute configuration of the metabolite notoamide B produced by *A. versicolor*. The known minor metabolite versicolamide B (**54**) was also isolated from this precursor incorporation experiment; however, ^{13}C enrichment was not observed as expected, due to the diastereomeric relationship at C-19 between notoamide B and versicolamide B.
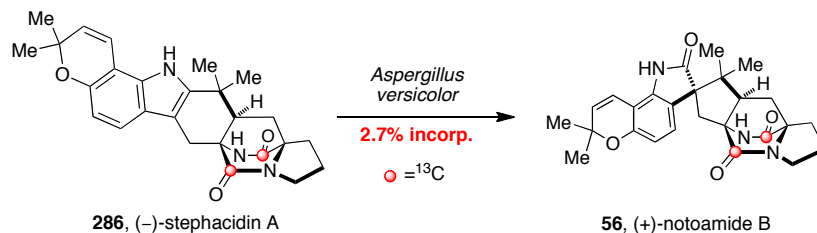
Scheme 67. Incorporation of $[^{13}C]_2$-(–)-stephacidin A into (+)-notoamide B in *Aspergillus versicolor*.

5.4 Analysis of Results from Feeding Studies

The results observed from the feeding experiments of double ^{13}C-labeled notoamide E with both the Tsukamoto marine-derived *Aspergillus* sp. MF297-2 and *Aspergillus versicolor* pose some interesting questions about the biosynthetic pathway of the major metabolites produced by these organisms. During the feeding experiment of notoamide E with *Aspergillus versicolor*, it was observed that 3-*epi*-notoamide C (**231**) was only produced in trace amounts, however, Tsukamoto's incorporation study with *Aspergillus* sp. MF297-2 showed increased yields of **231**. This could be a distinguishing difference between the two *Aspergillus* species. Furthermore, when labeled notoamide E was introduced to *Aspergillus versicolor* an inversion in the amounts of the major and minor metabolites occurred. When grown on normal media, notoamides C and D are produced in trace amounts by *Aspergillus versicolor*. In contrast, when labeled notoamide E was added to the culture media, these substances were isolated as the major metabolites. These results suggest that the addition of excess notoamide E does not abrogate the oxidative transformations of notoamide E into notoamides C, D and *epi*-notoamide C. On the other hand, the suppression of formation of stephacidin A and notoamide B observed in the presence of added notoamide E suggests that these

compounds inhibit or divert the enzymatic machinery responsible for the production of the bicyclo[2.2.2]diazaoctane-containing metabolites, especially stephacidin A and notoamide B. Furthermore, results from both sets of feeding studies establish that notoamide E is not a biosynthetic precursor to the proposed biological Diels-Alder cycloaddition, as evident by the lack of incorporation of notoamide E into any bicyclo[2.2.2]diazaoctane natural products. Alternatively, these findings suggest the presence of a branching biosynthetic pathway, wherein the biosynthesis of notoamide E results in the production of notoamides C and D.

The incorporation of $[^{13}C]_2$-$[^{15}N]$-6-hydroxydeoxybrevianamide E (**266**) into notoamide J only provides a small glimpse into the biosynthetic pathway of the notoamides and stephacidins. The lack of ^{13}C-incorporation into more advanced metabolites may implicate notoamide J as a shunt metabolite. One possibility for the biosynthetic formation of notoamide J is through a pinacol-type rearrangement via a promiscuous oxidase, the product of which cannot be further metabolized by the organism. The possibility of an enzyme that oxidizes 2,3-disubstituted indoles is also supported by results from the notoamide E incorporation study with *Aspergillus* sp. MF297-2 and *Aspergillus versicolor*.[21,96] The presence of a promiscuous oxidase also explains the lack of production of notoamide S by *A. versicolor*. Additionally, the recovery of **261** from the fungal extract shows that the starting material was taken up by the fungus, but did not fully incorporate into the biosynthetic pathway. Perhaps the timing at which **261** is fed and thus incorporated into the biosynthetic pathway is key to forming labeled advanced metabolites, such as (+)-notoamide B and (+)-versicolamide B.

The outcome of the notoamide S incorporation study provides great insight into the biosynthetic formation of the bicyclo[2.2.2]diazaoctane ring system. The results obtained from the $[^{13}C]_2$-$[^{15}N]_2$-notoamide S incorporation study with *Aspergillus versicolor* demonstrate that notoamide S serves as the pivotal precursor to the IMDA reaction, as well as the branching point for the formation of notoamide E, notoamide C, and notoamide D. Further insight about the putative Diels-Alderase has been provided; it is highly substrate specific and requires the presence of the 6-hydroxy-7-prenyl-indole moiety found on notoamide S, and cannot contain the pyran ring found on notoamide E.

The results obtained from the stephacidin A precursor incorporation study provide experimental validation for the hypothesis that a face-selective oxidative enzyme (presumed to be a flavo-enzyme) is present in *Aspergillus versicolor* NRRL 35600 and responsible for the biosynthetic conversion (–)-stephacidin A (**55**) into (+)-notoamide B (**56**). Additionally, this enzyme displays high substrate specificity, as evident by the conversion of only one enantiomer of stephacidin A.

5.5 (+)-Notoamide Biosynthetic Gene Cluster

In 2010, Sherman and co-workers sequenced the *Aspergillus versicolor* genome (Figure 29), and through bioinformatics mining identified similar *not* genes to those previously characterized from *Aspergillus* sp. MF297-2[104] The (+)-notoamide biosynthetic gene cluster was found to contain a 70.8% nucleotide identity with the (–)-notoamide biosynthetic gene cluster from Orf1 + NotA-NotJ. However, after NotJ, both protein similarity and gene organization are highly different from each other, suggesting the notoamide gene cluster might end at NotJ. Further characterization of NotA-NotI

revealed that these enzymes share a high amino acid identity/similarity between the two

gene clusters, and are responsible for the same function in both fungal strains (Table 9).
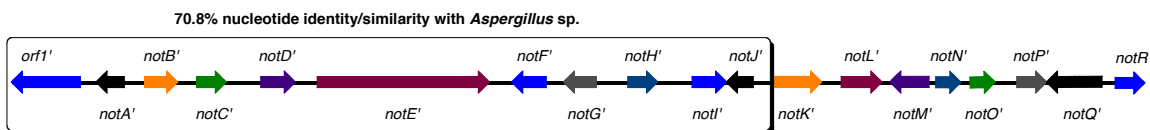
Figure 29. The notoamide (*not*) biosynthetic gene cluster from *A. versicolor*

Table 9. Comparison of (+)- and (−)-notoamide biosynthetic gene clusters.

Protein	Function	Protein	Function	Amino Acid Identity	Amino Acid Similarity
Orf1	Polysaccharide synthase	Orf1'	Polysaccharide synthase	ND[a]	ND
NotA	Negative regulator	NotA'	Negative regulator	70%	77%
NotB	FAD binding domain protein	NotB'	FAD binding domain protein	88%	94%
NotC	Prenyl-transferase	NotC'	Prenyl-transferase	87%	95%
NotD	Oxidoreductase	NotD'	Oxidoreductase	80%	86%
NotE	NRPS	NotE'	NRPS	79%	86%
NotF	Prenyl-transferase	NotF'	Prenyl-transferase	79%	85%
NotG	P450	NotG'	P450	87%	92%
NotH	P450	NotH'	P450	84%	92%
NotI	FAD binding domain protein	NotI'	FAD binding domain protein	85%	90%
NotJ	Unknown	NotJ'	Unknown	80%	84%
NotK	Efflux Pump	NotK'	Nucleoside transporter	14%	28%
NotL	Transcriptional activator	NotL'	Transcription factor	15%	22%
NotM	Unknown	NotM'	Unknown	-	-
NotN	Dehydrogenase	NotN'	Unknown	-	-
NotO	Short-chain dehydrogenase	NotO'	Unknown	-	-
NotP	Unknown	NotP'	Unknown	-	-
NotQ	Unknown	NotQ'	Transcription factor	12% (NotL)	21% (NotL)
NotR	Transcriptional co-activator	NotR'	Unknown	-	-

a) ND = Not Determined

120

5.6 Putative Biosynthesis of the Stephacidins and Notoamides

Based on the results obtained from the above precursor incorporation experiments, in conjunction with the (+)- and (–)-notoamide genome sequencing of both *Aspergillus* species, a new biosynthetic pathway for the formation of the stephacidins and notoamides is illustrated in Scheme 68. Starting with the formation of brevianamide F from the condensation of tryptophan and proline via NotE, subsequent reverse-prenylation with NotF furnishes deoxybrevianamide E. Hydroxylation at the C-6 position of the indole moiety via NotG gives 6-hydroxydeoxybrevianamide E, which undergoes C-7 normal-prenylation by NotC to afford the pivotal intermediate notoamide S. From this point, it is proposed that the pathway branches into at least two known directions. Formation of the pyranoindole to yield notoamide E results in the biosynthesis of notoamide C, 3-*epi*-notoamide C, and notoamide D via NotB. However, notoamide S could also undergo a 2-electron oxidation by either NotD or NotH to give the achiral azadiene, which acts as the enantio-diverging point in the biosynthesis. The achiral azadiene can undergo a stereoselective [4+2] cycloaddition to yield either (+)-notoamide T in *Aspergillus* sp. MF297-2 or (–)-notoamide T in *Aspergillus versicolor*. From these putative intermediates, cyclization to form the pyranoindole ring system furnishes antipodal stephacidin A. Face-selective oxidation of stephacidin A, followed by a pinacol-type rearrangement yields enantiomeric notoamide B, which upon additional oxidation could afford notoamide A.
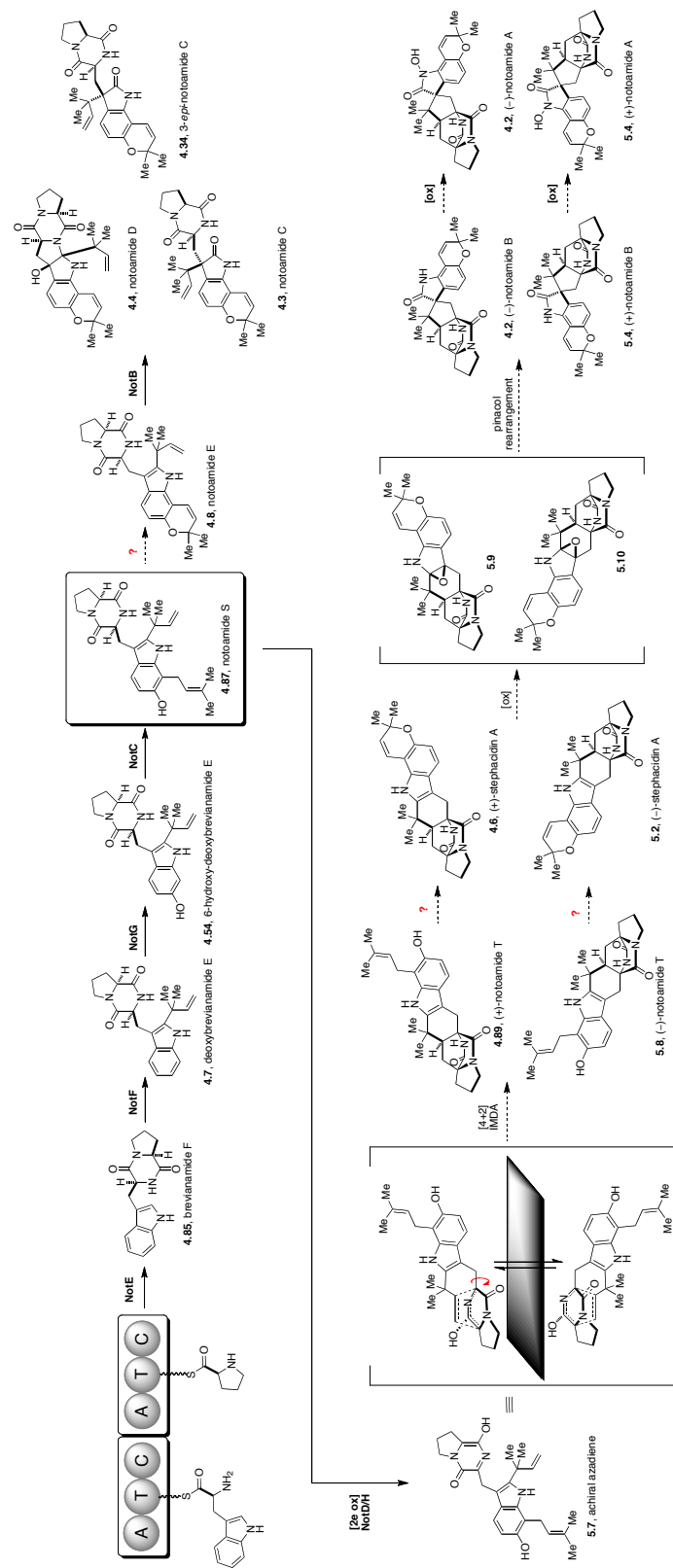
Scheme 68. Putative enantio-divergent biosynthesis of stephacidin A and the notoamides.

5.7 Future Directions

While the above results provide further insight into the biogenesis of the stephacidins and notoamides, several questions remain unanswered. In particular, mid-stage precursors between notoamide S and stephacidin A remain to be characterized. Future precursor incorporation studies with notoamide T could provide one of the final stephacidin A intermediates along this pathway. Additionally, the exact biosynthetic precursor to versicolamide B currently remains elusive, but through a feeding study with C6-*epi*-stephacidin A, insight into the biosynthesis of this rare metabolite could be obtained.

CHAPTER 6

Design and Synthesis of a Novel Drug Delivery Method Specifically Targeted to Multiple Myeloma Cells

6.1 Introduction—Part 2

6.1.1 Multiple Myeloma

Multiple myeloma (MM) is a plasma cell malignancy, characterized by the accumulation of plasma cells predominantly in the bone marrow, leading to pathologic fractures, anemia, hypercalcemia, renal failure, and recurrent bacterial infections.[34,35] MM accounts for 13.4% of all hematologic malignancies diagnosed, 19% of all deaths resulting from hematologic malignancies, and 2% of all cancer deaths.[36] Epidemiological studies have shown that MM is associated with older age and is found to occur more often in men than in women.[37]

The causes of MM remain unknown; however, recent scientific advancements have provided a greater understanding of the cellular events responsible for the development of MM.[34] Changes at a molecular level within the development of normal B-cells, adhesion molecules, cytokines, and/or bone marrow stromal cells can result in the preliminary stages of MM, such as monoclonal gammopathy of undetermined significance (MGSU) or smoldering MM (SMM).[36] MGUS is a premalignant stage to MM and is characterized by a limitation in the proliferation of monoclonal plasma cells

124

in the bone marrow and the absence of end-organ damage.[37] Unfortunately, MGUS is asymptomatic and treatment is limited to routine observation, without therapy. SMM is an asymptomatic intervening stage with a much higher risk of progression to MM than observed in patients with MGUS. Treatment of SMM is also limited to routine check-ups, but at a more frequent rate than patients with MGUS.[34] The risk of progression to MM or related disorders varies greatly between MGUS and SMM, about 1% per year compared to 10-20% per year, respectively.[36]

6.1.2 Current Treatment

Starting in 1962, the prescribed MM therapy of melphalan and a glucocorticoid, such as prednisone, became the traditional therapeutic regimen; however, complete remission was rare (< 5%), and median survival did not exceed 3 years.[39] The addition of other alkylating agents, anthracyclines, and vinca alkaloids to the standard melphalan-prednisone regimen did not improve patient survival. In 1983, it was documented that patients with high-risk myeloma had a high response rate when treated with a single high-dose of melphalan intravenously. In contrast with a single high-dose treatment, patients who were treated repeatedly with low-doses of melphalan suffered sublethal tumor cell damage and therefore ran the risk of procuring additional mutations by increasing genomic instability in tumor cells. Over the years, several other combination drug treatments have emerged, such as VMCP (vincristine, melphalan, cyclophosphamide, and prednisone) and VBAP (vincristine, BCNU, Adriamycin, and prednisone); however, these treatments have been found less effective than high-dose melphalan.

Until 1999 there were only two independently active compounds for treating MM on the market, and since then, thalidomide, revimid, and velcade have all shown efficacy against both advanced and refractory myeloma.[39] Of these agents, velcade is a proteasome inhibitor and represents an entirely new class of agents used in MM treatment. Velcade was FDA-approved for use in treating MM in 2003 and is currently under investigation for use in combination therapy with melphalan, vorinostat, and doxorubicin. Arsenic trioxide is a unique agent that works by targeting mitochondria, resulting in programmed cell death. This method, along with monoclonal antibodies to interleukin-6 (IL-6) and CD20, is currently under investigation as possible treatments for MM.[39]

6.1.3 Tumor Specific Immunoglobulin Gene Sequence

DNA hairpins have been found useful in a plethora of biological functions, such as the regulation of gene expression,[105] DNA recombination,[106] and facilitation of mutagenic events.[107] Hairpins arise when two regions of nucleotides in single-stranded (ss)DNA are palindromic, and thus able to base-pair to form a double helix. These hairpins also contain a loop of unpaired nucleotides. DNA hairpins exist in two different states and fluctuate between the open and closed conformations.[108] The closed-to-open transition requires enough energy to unzip the base-pairs located in the stem of the hairpin, whereas the open-to-closed transition requires a collision of the two arms of a hairpin, followed by the nucleation and the propagation of a base-paired stretch. One common way to determine the conformation of the hairpin in vivo is through the use of fluorescent DNA probes (molecular beacons), which are oligonucleotide probes capable

of identifying and reporting the presence of a specific nucleic acid sequence.[109] Molecular beacons (MB) contain a fluorophore (F) and a quencher (Q), usually located at the 5′ and 3′ positions. When the MB is in the closed conformation, the fluorophore is quenched and does not fluoresce, but upon binding of the MB to a target nucleic acid sequence, fluorescence is restored. This method is useful for the detection of specific sequences of nucleic acids and can be further applied to drug delivery by targeting a specific gene sequence unique to tumor cells.

Since MM is a malignancy of clonal antibody-secreting plasma cells, the mutated cells often contain a specific rearrangement of DNA, which is transcribed into a unique mRNA sequence.[39,110] Translation of the mRNA sequence results in the formation of a tumor specific monoclonal antibody, which is abundant in all of the malignant cells. From this tumor specific transcript, a unique complementary determining region (CDR) gene sequence can be identified.[111] Recently, Berenson and coworkers were able to demonstrate that a tumor specific oligonucleotide could specifically recognize the MM tumor cell population.[42] As shown in Figure 30, using a quenched fluorescein-labeled oligonucleotide probe (designated as MB8226) displaying a sequence complementary to the CDR3 gene from the MM cell line RPMI8226, Berenson was able to establish that MB8226 could not only recognize the specific cell line, but also differentiate the RPMI8226 cell line from other MM cell lines.[42] This provided additional support that MB8226 selectively enters and reacts with cells expressing this explicit mRNA sequence; and since the targeted mRNA sequence is found in a specific type of cancer cells, it was postulated that MB8226 could be used as a method of drug delivery for cancer patients.

A. MB8226 with quenched fluorophore

Probe sequence = CDR[1]

GCATG

C–G
A–T
G–C
C–G
G–C

Q F

B. Binding of MB8226 to mRNA of the MM cell line RPMI8226 CDR3 gene sequence with fluorescence

Complementary sequence of mRNA

CGTAC

GCGAC — GCATG — GTCGC

CDR

Q

F

Q F = quenched fluorophore

F = fluorescence

Q = quencher
F = fluorophore
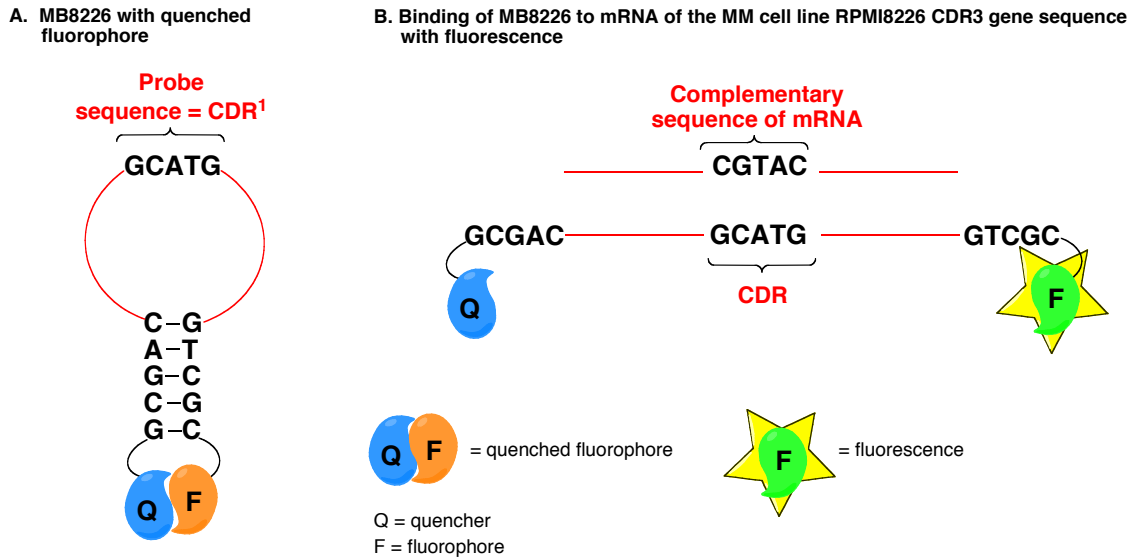
[1] CDR = complementary determining region

Figure 30. A) Closed/quenched molecular beacon (MB8226). **B)** Open/fluorescent molecular beacon upon binding to mRNA of the CDR3 gene sequence from the MM cell line RPMI8226.

6.1.4 Research Objectives—Part 2

In a collaborative effort with Dr. James Berenson at the UCLA David Geffen School of Medicine, I developed a novel targeted drug-delivery system utilizing a modified version of MB8226. This oligonucleotide hairpin is equipped with a naphthyridine-drug derivative that is only released upon the opening of the hairpin within multiple myeloma cells. This novel system minimizes exposure of healthy cells to the cytotoxic agent, while still delivering an effective dose of the drug to cancerous cells.

6.2 Development of a Drug-Oligonucleotide Conjugate

The challenge of converting MB8226 into a potential therapeutically active anti-MM agent centered upon the attachment of a current MM drug to MB8226 so as to only

allow release of the drug within the malignant cells, thereby minimizing exposure of healthy cells to the cytotoxic agent. One way to address this concern was through a "Trojan Horse" method. By slightly altering the matched base pairs in the stem of MB8226, the desired cytotoxic agent could be contained within the stem and transported into the cancerous cells. The design of the MB8226 altered stem was inspired by work from Nakatani and coworkers when they demonstrated that a naphthyridine ligand could bind to a guanine bulge in double helix DNA.[43] Since the naphthyridine ligand possesses hydrogen bonding groups fully complementary to the target bulged base, this allows for thermodynamic stabilization of the DNA.

As shown in Figure 31, the addition of an extra guanine to the stem of MB8226 could allow for the desired "Trojan Horse" method of drug delivery. By coupling the desired cancer drug to a naphthyridine moiety, the naphthyridine-drug complex could be inserted into the G-bulge of the closed MB8226 and held in place by hydrogen bonding. Since MB8226 only reacts with the RPMI8226 cell line, the MM drug would only be released within cancer cells upon binding of MB8226 to the complementary sequence and subsequent unzipping of the stem.

A. Modified-MB8226 with drug conjugate

B. Modified-MB8226 binding to mRNA of the MM cell line RPMI8226 CDR3 gene sequence

■ = cytotoxic agent + naphthyridine conjugate
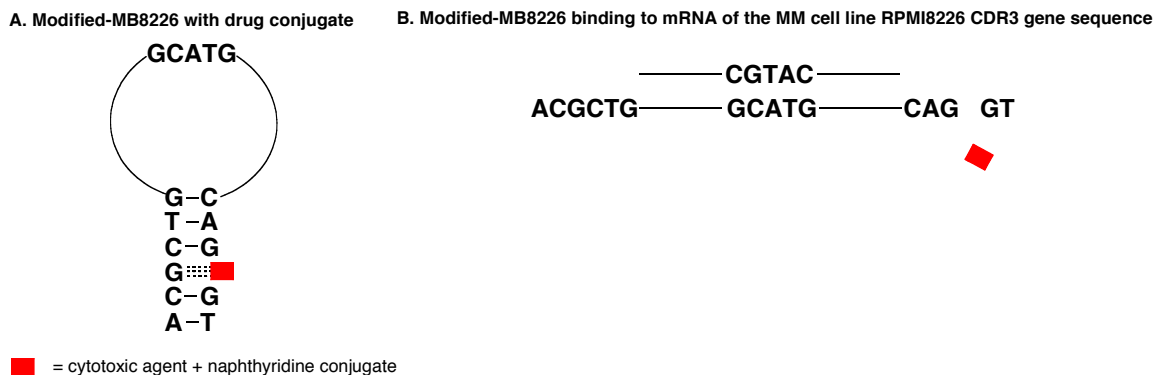
Figure 31. "Trojan Horse" design **A.** Closed conformation of MB8226 with the cytotoxic agent contained in the stem at the G-bulge. **B.** Open conformation of MB8226 and release of the drug.

The two drugs selected for use in this experiment were vorinostat (**287**) and melphalan (**288**). Vorinostat is an FDA-approved histone deacetylase inhibitor that is used for treating cutaneous T-cell lymphoma, and in 2008 a vorinostat-velcade (vorinostat-bortezomib) combination drug entered phase I clinical trials for the treatment of MM.[44] As mentioned previously, melphalan is the mainstay treatment of MM and is a nitrogen mustard alkylating agent.[38] In order for either of these two drugs to be used in the therapeutic application of MB8226, they had to be converted to the respective naphthyridine-modified (N) drug derivatives (**289** and **290**, Scheme 69).
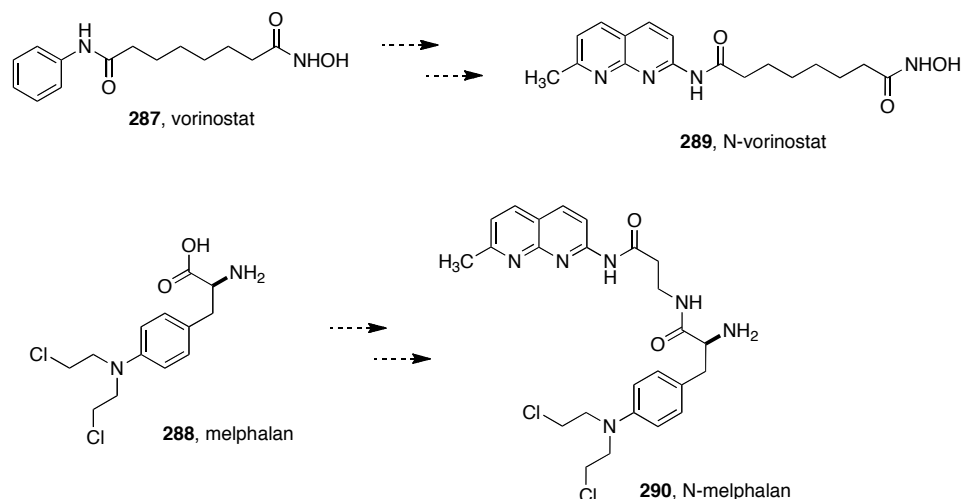
Scheme 6.1. Structures of two MM drugs (vorinostat and melphalan) and their naphthyridine derivatives.

6.2.1 Synthesis of Naphthyridine-Modified Vorinostat

The first proposed synthesis (Scheme 70) of the naphthyridine-vorinostat analogue (**289**) began by forming the naphthyridine core **293**.[43] Commercially available 2,6-diaminopyridine (**291**) was reacted with 3-ketobutanal dimethyl acetal (**292**) in concentrated H_3PO_4 to afford 2-methyl-7-amino-1,8-naphthyridine (**293**) in 89% yield.[112] The formation of the suberic acid methyl ester **296** was readily achieved from commercially available suberic acid (**294**). The bis-acid was converted to the dimethyl ester **295** in methanol and sulfuric acid, which was selectively saponified in methanol and potassium hydroxide to yield the suberic acid methyl ester **296**. Unfortunately, the coupling reaction of the **293** with **296** was unsuccessful.
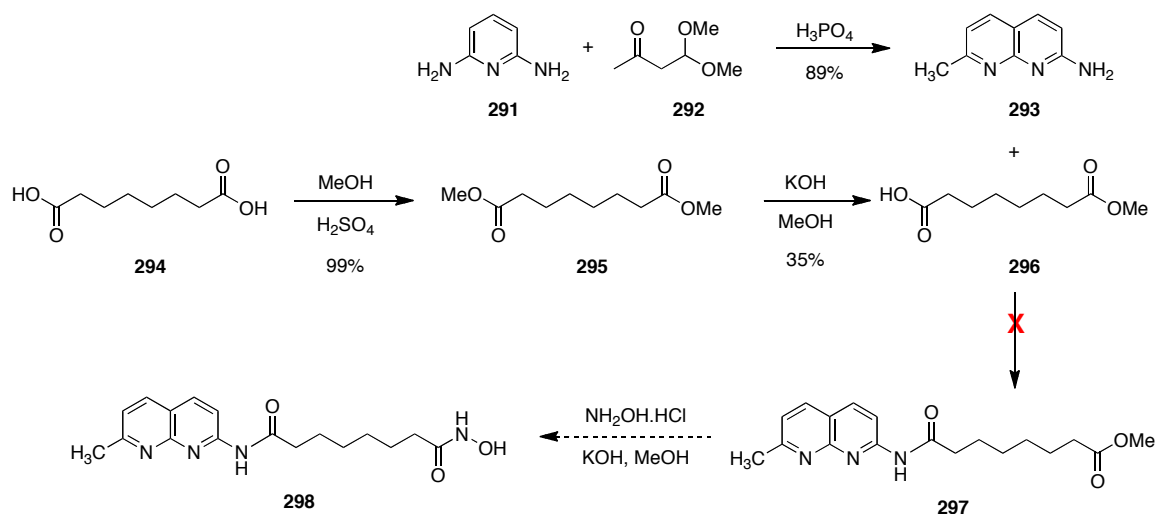
Scheme 70. First attempted synthesis of N-vorinostat.

The second proposed synthesis (Scheme 71) for **289** coupled **293** with the acid chloride of suberic acid monomethyl ester (**298**), which was formed from the reaction of **296** and oxalyl chloride in benzene and DMF. Acid chloride **298** was reacted with **293** to yield **297**. Several different reaction conditions were attempted to form the desired hydroxamic acid **289**. The reaction condition listed by Njar in the synthesis of SAHA was attempted;[113] however, only the naphthyridine core (**293**) was isolated. Several published variations of this reaction were attempted at various temperatures, all in which provided solely **193**.[114]
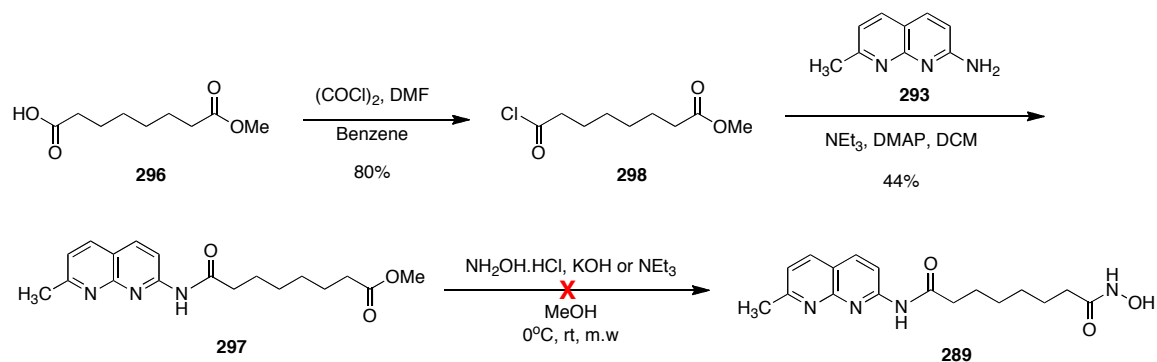
Scheme 71. Second attempted synthesis of **289**.

As outlined in Scheme 72, the third and successful synthesis of **289** started by reacting **293** with a preformed suberoyl anhydride (**299**). Suberic acid (**294**) was reacted with acetic anhydride to form **299**, which was subsequently treated with **293** to yield acid **300**. The acid intermediate was converted to the hydroxamic **289** in a two-step, one-pot sequence. The acid was first reacted with ethyl chloroformate in the presence of triethylamine in THF to form **301**, which was immediately treated with 50% hydroxylamine in water to afford the desired naphthyridine-SAHA analogue **289**.
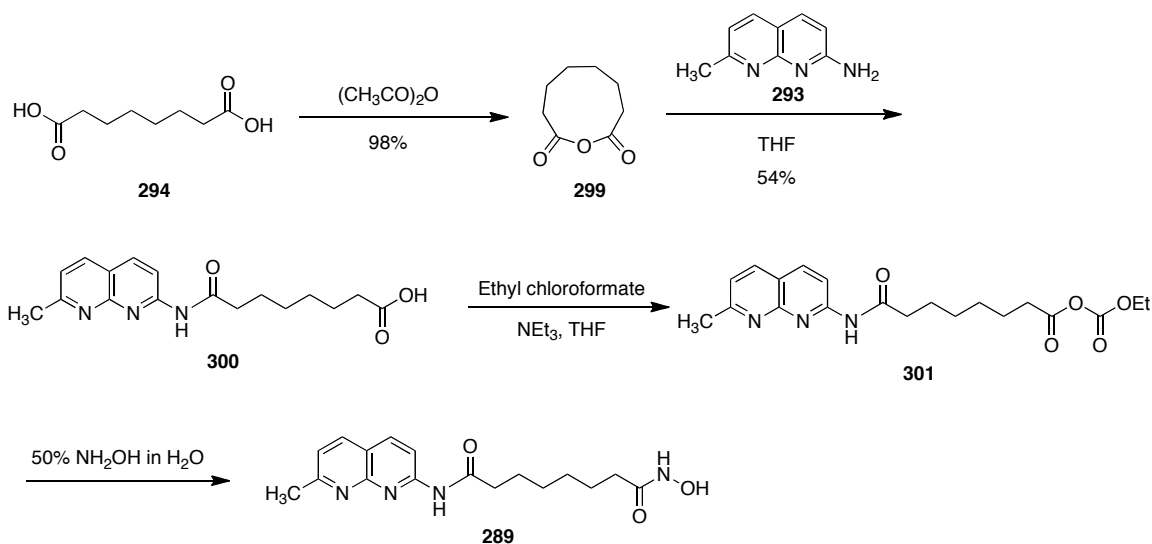
Scheme 72. Third attempted synthesis of **289**.

6.2.2 Synthesis of Naphthyridine-Modified Melphalan

With the core naphthyridine-suberic acid reaction conditions developed, the next step was the synthesis of the naphthyridine-melphalan derivative (Scheme 73). Starting with **300**, ethyl chloroformate was used to form the mixed anhydride **301**, which was subsequently reacted with melphalan **288**. Unfortunately, only trace amounts of the naphthyridine-melphalan (**302**) were isolated.
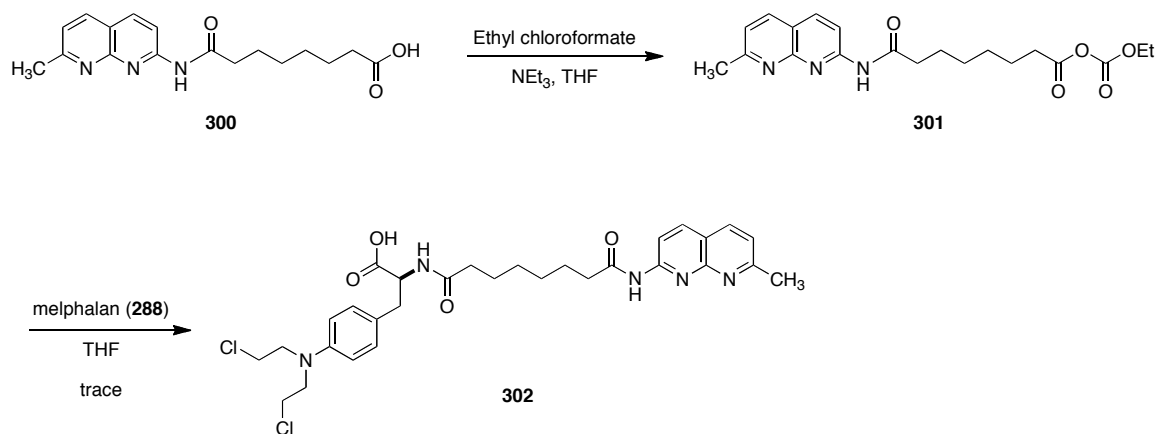
Scheme 73. First Attempted Synthesis of the Naphthyridine-Melphalan Derivative.

Since the first synthesis of N-melphalan resulted in only trace amounts of product, a new naphthyridine linker was designed. The original naphthyridine moiety used in the vorinostat derivative was designed specifically to contain the six carbon alkyl chain found in vorinostat, which was no longer necessary for the naphthyridine-melphalan derivative. The new naphthyridine derivative was based on the original G-bulge naphthyridine derivative synthesized by Nakatani and co-workers.[43] As outlined in Scheme 74, β-alanine (**303**) was first Boc protected (**304**), followed by conversion of the acid to activated ester **305**. The 2-amino-1,8-naphthyridine derivative **293** was reacted with **305** and subsequently deprotected to afford the desired naphthyridine derivative **307**. Next, N-Boc-melphalan (provided by Dr. Berensen) was coupled to **307** using EDCI and NMM to afford **308**. The desired N-melphalan derivative (**290**) was obtained following removal of the N-Boc group in 42% yield.
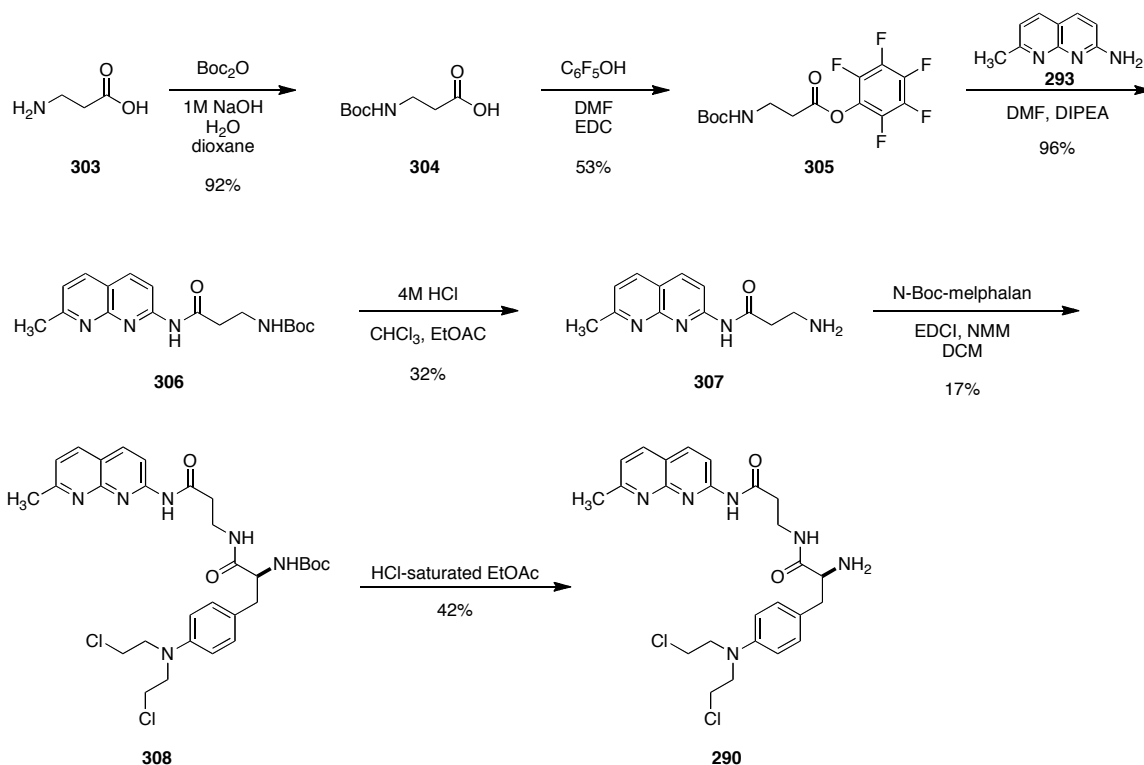
Scheme 74. Synthesis of N-melphalan (**290**).

6.3 Preliminary Test Results

Biological testing performed by Berensen and co-workers showed that the modification of vorinostat with naphthyridine did not change its function compared with the unmodified compound.[115] Moreover, using cell viability and apoptosis assays, there was no reduction in the cytotoxic effects of N-vorinostat or N-melphalan compared to the parent drugs (Figure 32).

(a)
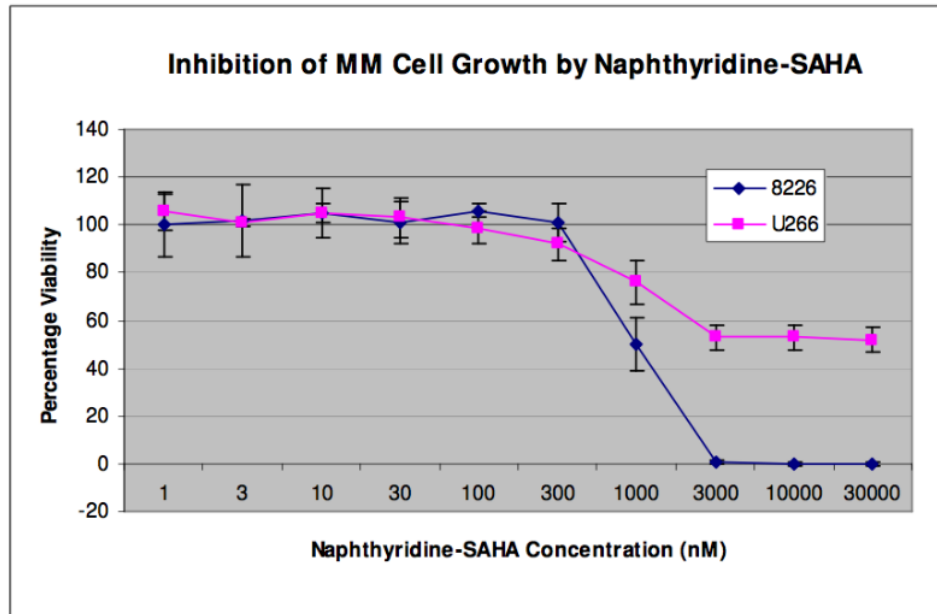
(b)
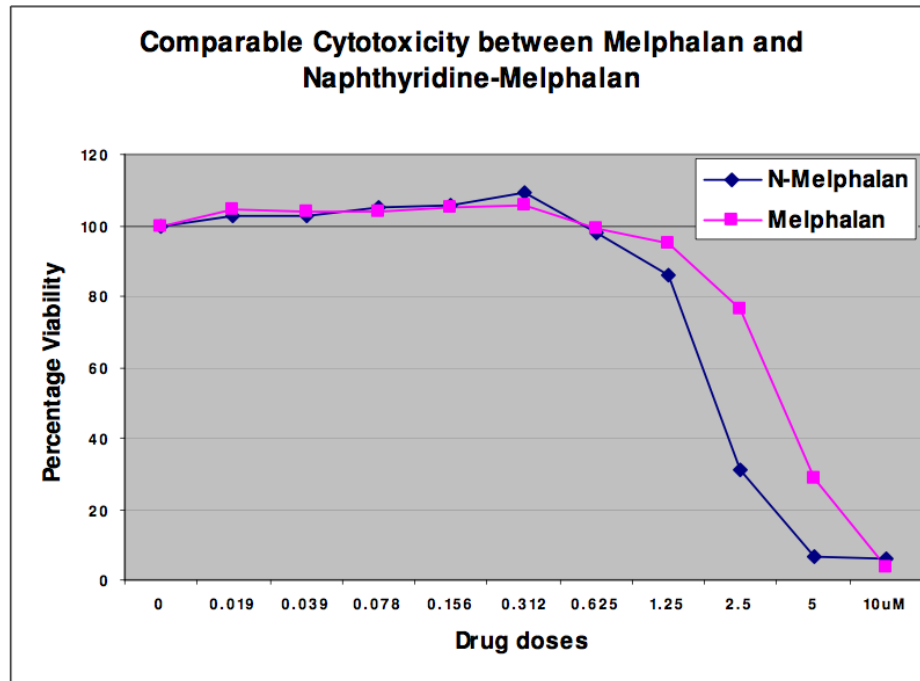
Figure 32. Cytotoxicity comparison between the parent drug and the naphthyridine conjugated drug (a) vorinostat (SAHA) and N-vorinostat; (b) melphalan and N-melphalan.

In addition, the modification of MB8226 allowed for the conjugation of N-vorinostat and N-melphalan, while retaining the ability to specifically react only with the RPMI8226 cell line.[115] Upon transfection with N-vorinostat conjugated MB8226, only RPMI8226 showed reactivity with the conjugated oligonucleotide-drug, while the U266 MM cell lines showed no cytotoxic effects from exposure to this tumor specific cytotoxic construct (Figure 33).

(a)

Apoptosis of 8226 cells treated with G-bulge-Naphthyridine-SAHA
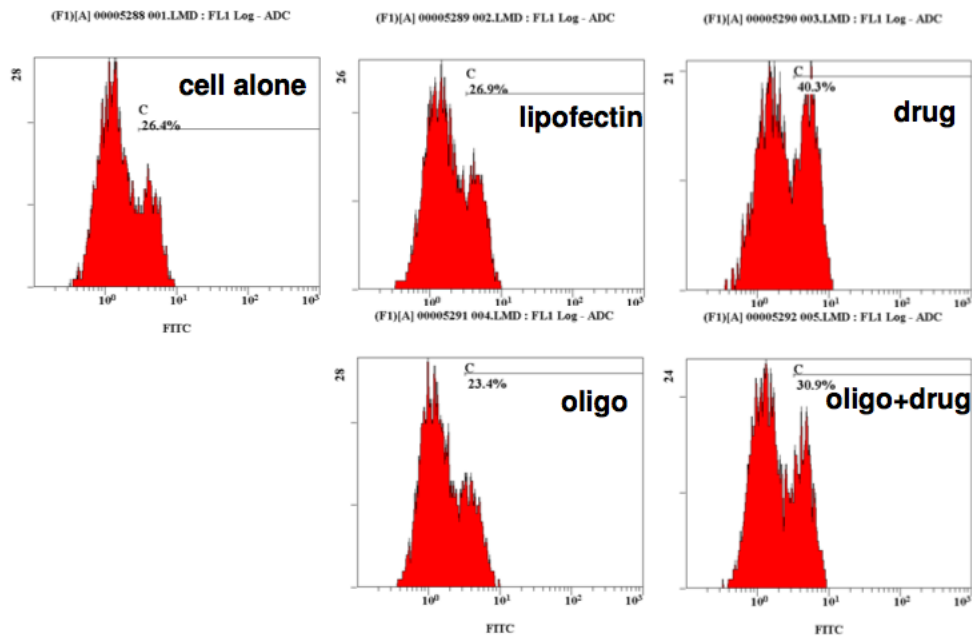
control, Lipofectin alone; drug, Naphthyridine-SAHA; oligo, G-bulge(8226)

(b)

Apoptosis of U266 cells treated with G-bulge-Naphthyridine-SAHA
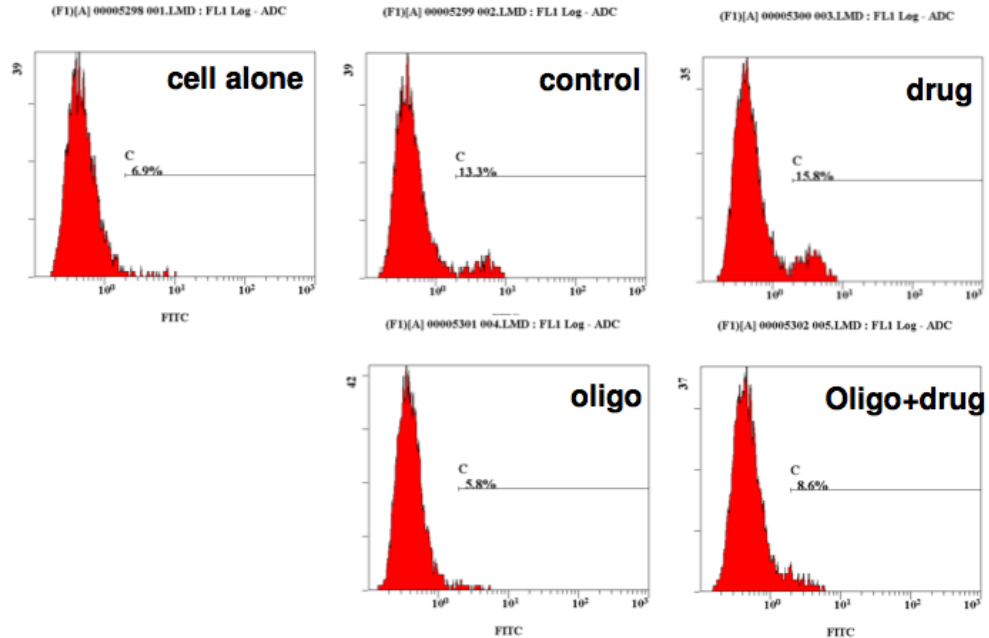
control, Lipofectin alone; drug, Naphthyridine-SAHA; oligo, G-bulge(8226)

Figure 33. Apoptosis of MM cells treated with oligonucleotide-N-vorinostat (SAHA) conjugate; (a) 8226 cells (matched oligonucleotide); (b) U266 cells (unmatched oligonucleotide).

This type of treatment should allow delivery of higher concentrations of drugs that will be active only within tumor cells, ultimately leading to more effective and better tolerated therapies for patients with MM. Further investigation would be necessary to explore the possibilities of this treatment. Unfortunately, funding limitation halted our research in this groundbreaking area of drug delivery.

CHAPTER 7

Experimental

7.1 General Synthetic Considerations

$[^{13}C]_2$-$[^{15}N]_2$-L-Proline and $[^{13}C]$- L-glycine were obtained from the NIH Stable Isotopes Resource at Los Alamos National Laboratory. All other reagents were commercial grade and used without further purification unless otherwise noted. Unless otherwise noted, all reactions were run under an argon atmosphere in flame or oven-dried glassware. Reactions were monitored by thin layer silica gel chromatography (TLC) using 0.25 mm silica gel 60F plates with fluorescent indicator (Merck). Products were purified via either flash column chromatography using silica gel grade 60 (230-400 mesh) purchased from Sorbent Technologies or preparative thin layer chromatography (1000 μm). Acetonitrile (CH$_3$CN), dichloromethane (CH$_2$Cl$_2$), diethyl ether (Et$_2$O), *N, N*-dimethylformamide (DMF), methanol (MeOH), tetrahydrofuran (THF), toluene (PhMe), and triethylamine (Et$_3$N) were all degassed with argon and passed through a solvent purification system containing alumina or molecular sieves. ^{1}H-NMR spectra and ^{13}C-NMR spectra were obtained on Varian 300, 400, 400 MR or 500 MHz NMR spectrometers. NMR spectra were taken in CDCl$_3$ (^{1}H, 7.26 ppm; ^{13}C, 77.0 ppm), CD$_3$OD (^{1}H, 3.31 ppm, 49.15 ppm), d$_6$-DMSO (^{1}H, 2.50 ppm, ^{13}C, 39.51 ppm) and D$_2$O (^{1}H, 4.79 ppm) obtained from Cambridge Isotope Labs. Mass spectra were obtained on Fisions VG Autospec using a high/low resolution magnetic sector.

7.2 Experimental Procedures

7.2.1 Chapter 3 Experimentals

3-chloro-1*H*-indole (119):
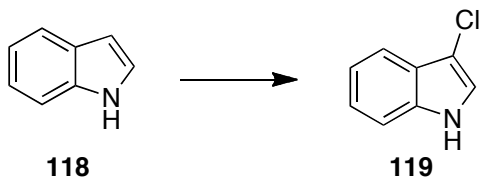
Indole **118** (4.0 g, 34.14 mmol) was dissolved in DMF (113 mL) and cooled to 0ºC. N-Chlorosuccinimide (4.56 g, 34.14 mmol) was added and the reaction stirred at room temperature for 20 hours. The mixture was quenched with 150 mL brine and extracted with diethyl ether (3 x 125 mL). The combined organic layer was washed 5 times with 100 mL water, dried over Na_2SO_4 and concentrated under vacuum. The crude material was purified via flash column chromatography with 4:1 hexanes-ethyl acetate. Yield: 4.61 g, 30.38 mmol, 89%

^{1}H NMR (300 MHz, $CDCl_3$) δ 8.05 (bs, 1H), 7.65 (d, *J* = 8.4 Hz, 1H), 7.37 (d, *J* = 8.7 Hz, 1H), 7.29-7.18 (m, 3H); ^{13}C NMR (75 MHz, $CDCl_3$) δ 135.1, 125.6, 123.3, 121.0, 120.7, 118.5, 11.7, 106.7; HRMS (ESI/APCI) calcd for C_8H_8N (M+H) 118.0651, found 118.0654. (jmf-02-665)

119
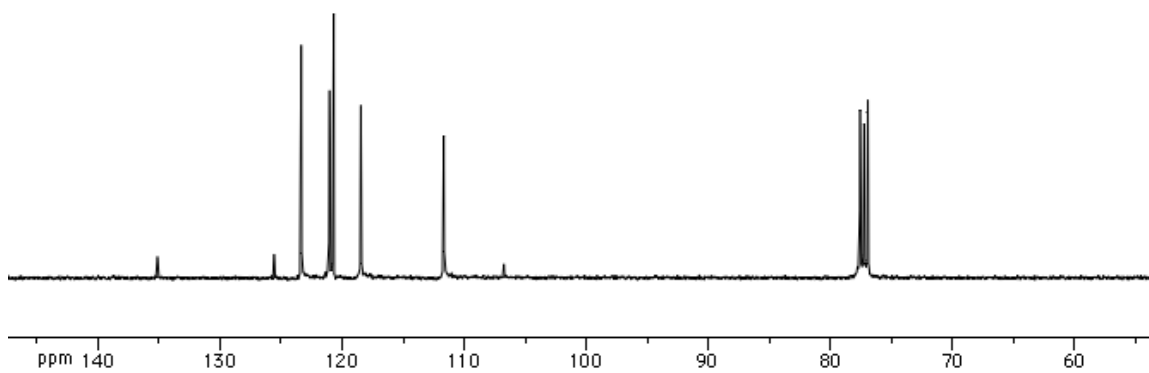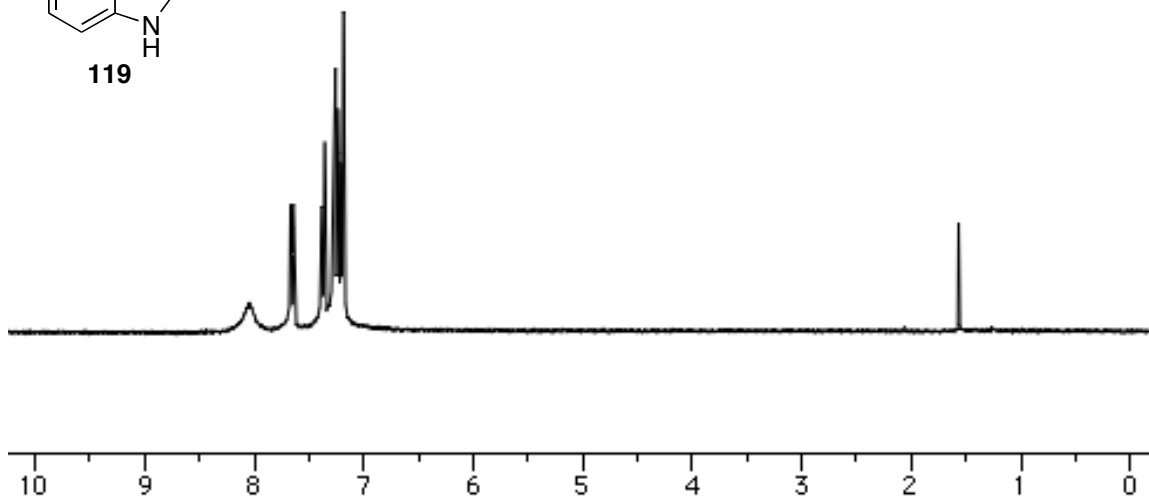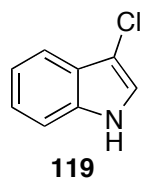
2-(2-methylbut-3-en-2-yl)-1*H*-indole (112):
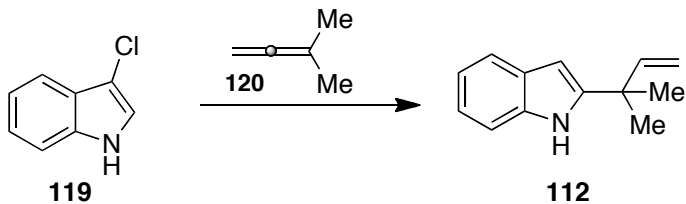
A 1.0 M solution of 9-BBN in THF (130 mL, 65.1 mmol) was cooled to 0°C. Allene **120** (7.53 mL, 76.0 mmol) was added to the solution and the reaction was capped with a yellow cap and wrapped in parafilm. The reaction stirred at room temperature for 15 hours. Indole **119** (3.29 g, 21.7 mmol) was dissolved in THF (72 mL) and NEt₃ (10.6 mL, 76.0 mmol) and the mixture stirred at room temperature for 20 minutes. The prenyl-9-BBN solution was added to the indole solution and the reaction stirred for 6 hours at room temperature. The reaction was concentrated and immediately purified via flash column chromatography 9:1 hexanes-ethyl acetate. Yield: 2.30 g, 12.4 mmol, 57%

^{1}H NMR (300 MHz, CDCl₃) δ 8.00 (bs, 1H), 7.77-7.74 (m, 1H), 7.44-7.41 (m, 1H), 7.34-7.27 (m, 2H), 6.50 (dd, *J* = 2.1, 0.9 Hz, 1H), 6.20 (dd, *J* = 17.7, 10.5 Hz, 1H), 5.30 (1/2ABq, *J* = 3.6 Hz, 1H), 5.25 (1/2ABq, *J* = 3.6 Hz, 1H), 1.64 (s, 6H); ^{13}C NMR (75 MHz, CDCl₃) δ 146.4, 236.3, 128.9, 121.7, 120.5, 120.0, 112.6, 110.9, 98.4, 38.6, 32.4, 27.8, 23.2, 22.7; HRMS (ESI/APCI) calcd for C₁₃H₁₆N (M+H) 186.1277, found 186.1282. (jmf-02-679)
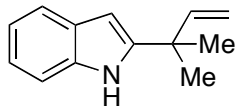
112
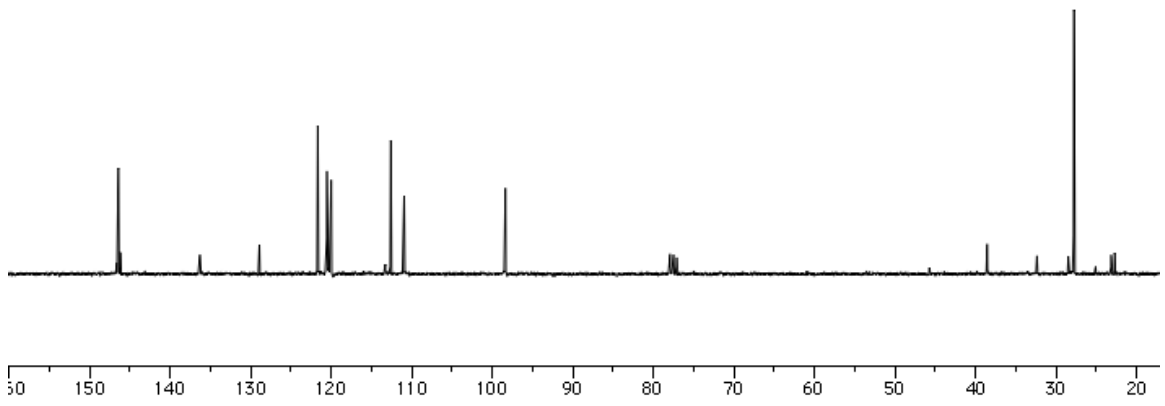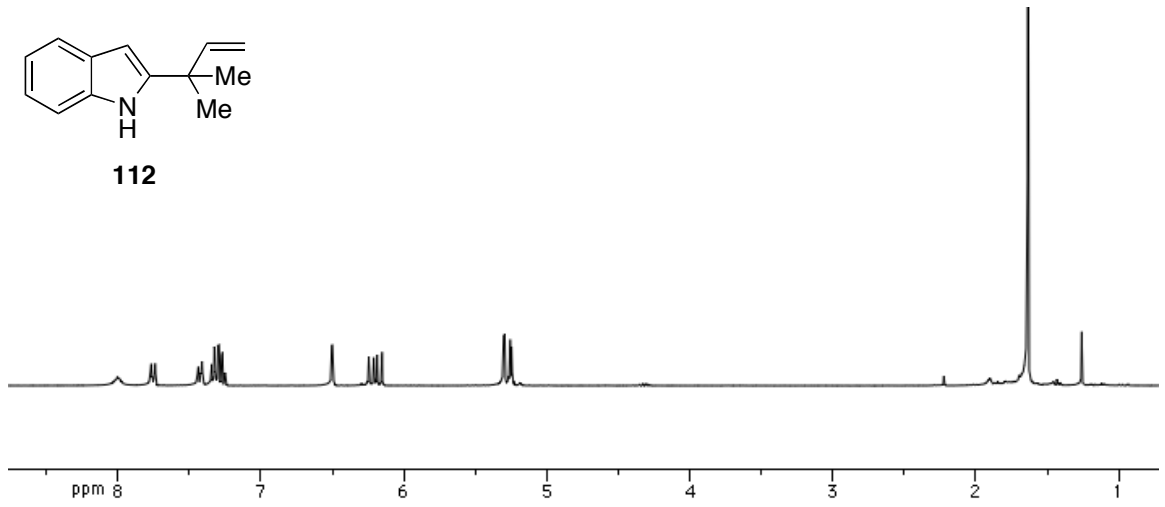
N,N-dimethyl-1-(2-(2-methylbut-3-en-2-yl)-1H-indol-3-yl)methanamine (121):

112   121
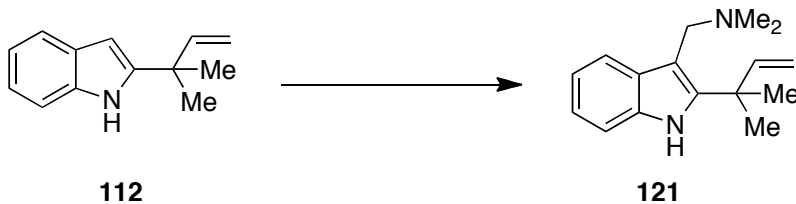
To a solution of glacial acetic acid (10 mL) in 37% aqueous formaldehyde (450 mL, 5.49 mmol), 40% aqueous dimethylamine (2.32 mL, 5.49 mmol) was added. A solution of reverse prenylated indole (900 mg, 4.86 mmol) in 5 mL of glacial acetic acid was slowly added. The reaction stirred at room temperature for 16 hours. The reaction mixture was diluted with 1N NaOH until pH>10. The aqueous layer was extracted with diethyl ether (3 x 30 mL) and the combined organic layers were dried over Na_2SO_4 and concentrated. Crude yield: 1.14 g, 4.72 mmol, 97%.

^{1}H NMR (300 MHz, CDCl$_3$) δ 8.29 (bs, 1H), 7.77-7.74 (m, 1H), 7.34-7.31 (m, 1H), 7.21-7.12 (m, 2H), 6.23 (dd, J = 17.7, 10.8 Hz, 1H), 5.24 (dd, J = 9.6, 1.2 Hz, 1H), 5.24 (q, J = 1.5, 1.2 Hz, 1H), 3.74 (s, 2H), 2.33 (s, 6H), 1.62 (s, 6H); ^{13}C NMR (75 MHz, CDCl$_3$) δ 146.5, 141.9, 134.3, 130.5, 121.5, 119.3, 112.2, 110.6, 108.1, 58.4, 53.9, 45.4, 39.6, 27.6. (jmf-02-683)

121
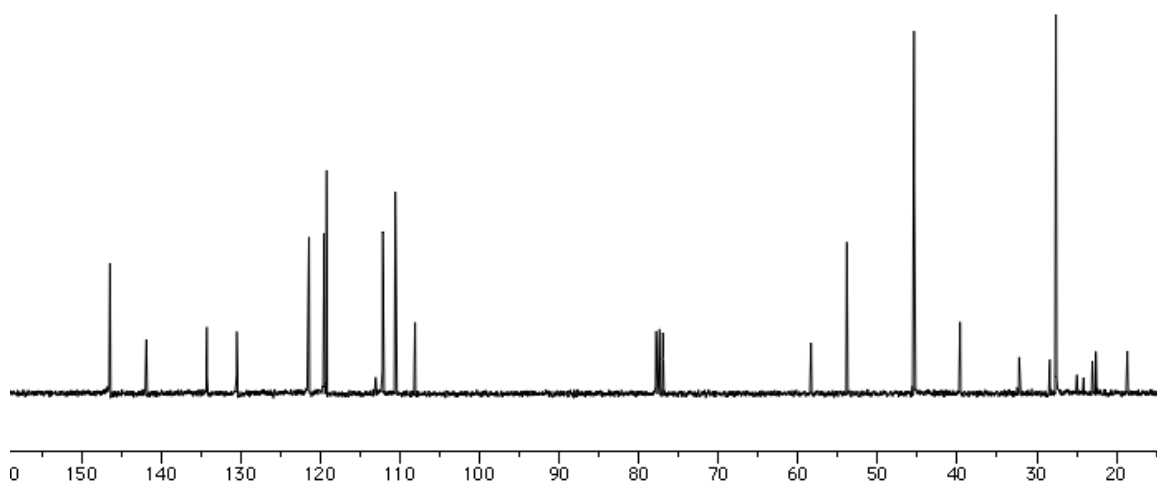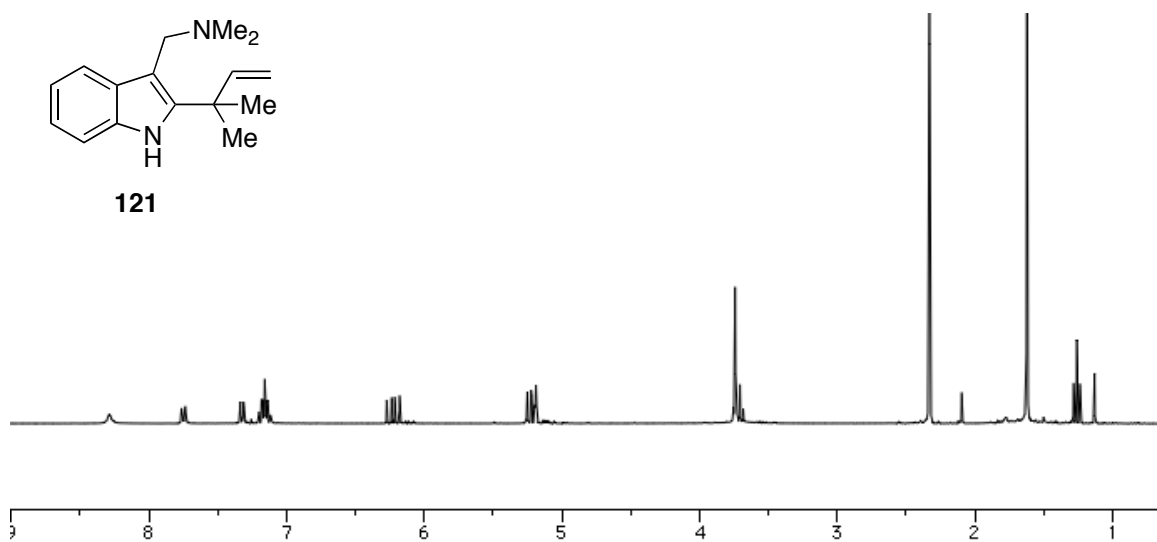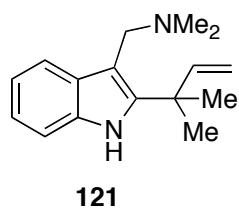
Ethyl 2-((diphenylmethylene)amino)acetate (122):
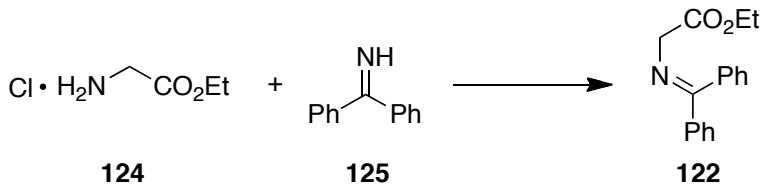
Glycine ethyl ester (770 mg, 5.52 mmol) and benzophenone imine (1.0 g, 5.52 mmol) were dissolved in 20 mL of DCM and stirred at room temperature for 24 hours. The reaction mixture was filtered through celite to remove NH_4Cl and the filtrate concentrated under vacuum. The residue was dissolved in 20 mL of diethyl ether and washed with H_2O (30 mL). The ether was dried over $MgSO_4$ and concentrated. The product was recrystallized in ethyl acetate and hexanes and collected as a white solid. Yield: 1.41 g, 5.30 mmol, 96%.

^{1}H NMR (300 MHz, CDCl$_3$) δ 7.68-7.65 (m, 2H), 7.29-7.29 (m, 6H), 7.19-7.16 (m, 2H), 4.21 (s, 2H), 4.20 (q, $J = 14.1, 7.2$ Hz, 2H), 1.26 (t, $J = 7.2$ Hz, 3H); ^{13}C NMR (75 MHz, CDCl$_3$) δ 172.0, 170.9, 139.5, 136.2, 130.7, 129.1, 129.0, 128.9, 128.3, 127.9, 61.1, 56.0, 14.5. (jmf-02-680)
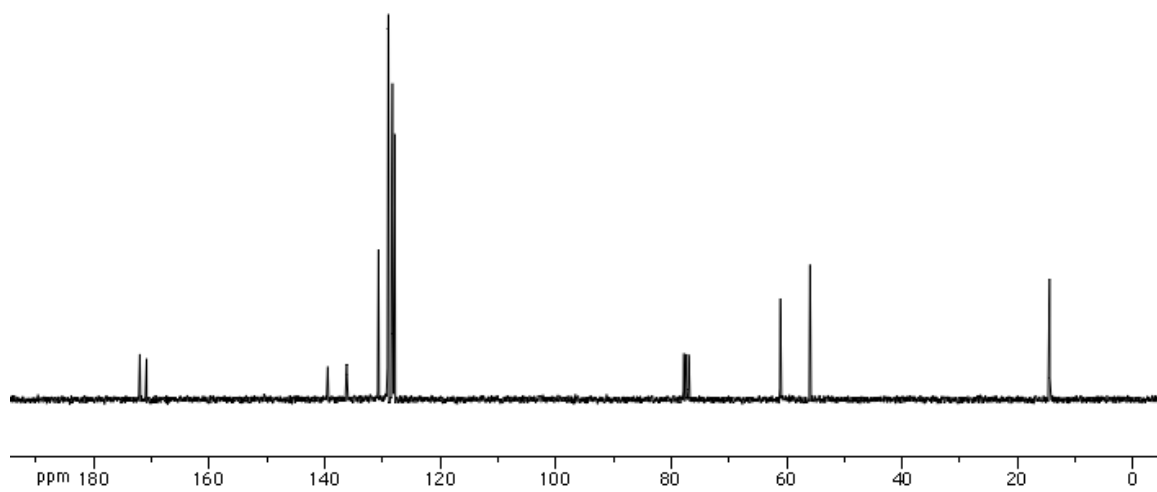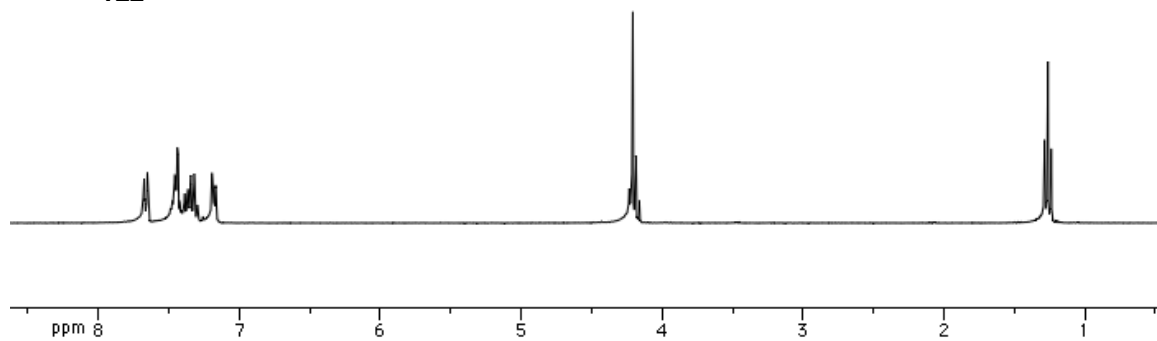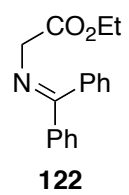
Ethyl 2-((diphenylmethylene)amino)-3-(2-(2-methylbut-3-en-2-yl)-1H-indol-3-yl)propanoate (123):
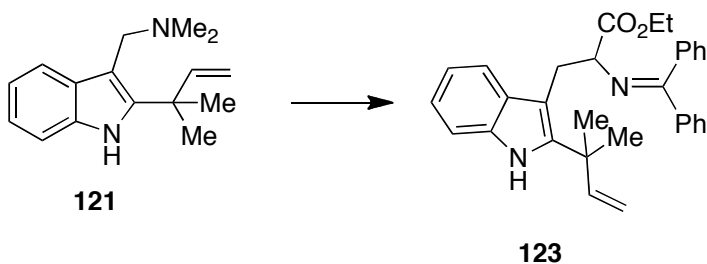
The gramine (1.14 g, 4.72 mmol), glycine benzophenone imine (1.15 g, 4.30 mmol) and $^nBu_3P$ (0.42 mL, 1.72 mmol) were dissolved in MeCN (21.5 mL) in a large microwave reaction flask. The mixture was heated to 130°C for 30 minutes. The reaction mixture was concentrated and purified via flash column chromatography in 9:1 hexanes:ethyl acetate to provide **123**. Yield: 1.96 g, 4.21 mmol, 98%.

^{1}H NMR (300 MHz, CDCl$_3$) δ 7.98 (bs, 1H), 7.89-7.85 (m, 1H), 7.65-7.62 (m, 2H), 7.54-7.46 (m, 2H), 7.37-7.23 (m, 5H), 7.14-7.05 (m, 3H), 6.93-6.87 (m, 1H), 6.38 (bs, 1H), 5.93 (dd, J = 17.4, 10.5 Hz, 1H), 5.13-5.03 (m, 2H), 4.55 (dd, J = 7.2, 6.0 Hz, 1H), 4.30-4.19 (m, 2H), 3.62 (d, J = 6.0 Hz, 2H), 1.43 (s, 3H), 1.40 (s, 3H), 1.30 (t, J = 7.2 Hz, 3H); ^{13}C NMR (75 MHz, CDCl$_3$) δ 172.8, 170.1, 146.4, 140.2, 139.5, 136.2, 134.2, 132.8, 130.4, 130.3, 129.1, 128.6, 128.1, 128.0, 127.4, 121.4, 119.7, 119.2, 111.9, 110.2, 107.5, 67.0, 61.1, 39.3, 29.1, 27.9, 14.5; IR (neat) 3405, 3057, 2972, 1621, 1575, 1462, 1185, 1029; HRMS (ESI/APCI) calcd for C$_{31}$H$_{33}$N$_2$O$_2$ (M+H) 465.2537, found 465.2543. (jmf-02-685)

123

Ethyl 2-amino-3-(2-(2-methylbut-3-en-2-yl)-1H-indol-3-yl)propanoate (127):
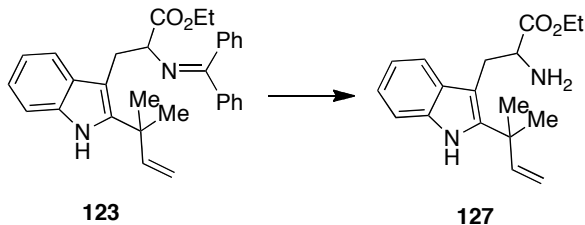
The imine (122 mg, 0.263 mmol) was dissolved in 2 mL of THF and 1N HCl (0.6 mL) and the reaction stirred for 30 minutes. The THF was removed under vacuum and the residue with rediluted with NaHCO$_3$ until basic. The aqueous layer was extracted with DCM and the combined organic layers were dried over Na$_2$SO$_4$ and concentrated. The crude material was purified via flash column chromatography in 3:1 hexanes:ethyl acetate and then flushed with 5% MeOH in DCM to obtain pure **127**. Yield: 55 mg, 0.183 mmol, 70%.

^{1}H NMR (300 MHz, CDCl$_3$) δ 8.87 (bs, 1H) 7.53 (d, J = 7.2 Hz, 1H), 7.27 (d, J = 7.2 Hz, 1H), 7.12-7.04 (m, 2H), 6.12 (dd, J = 17.4, 10.5 Hz, 1H), 5.14 (m, 9.3 Hz, 1H), 5.10 (d, J = 1.8 Hz, 1H), 4.16-4.06 (m, 2H), 3.84 (d, J = 9.6, 5.1 Hz, 1H), 3.31 (d, J = 5.1 Hz, 1H), 3.06 (dd, J = 14.4, 9.6 Hz, 1H), 1.53 (s, 3H), 1.525 (s, 3H), 1.15 (t, J = 7.2 Hz, 3H); ^{13}C NMR (75 MHz, CDCl$_3$) δ 175.6, 146.3, 141.1, 134.8, 129.8, 121.5, 119.4, 118.5, 112.0, 110.9, 106.4, 61.2, 56.0, 50.1, 39.4, 31.5, 28.1, 28.1, 14.2; IR (neat) 3399, 3243, 3081, 2973, 1733, 1638, 1580, 1462, 1195; HRMS (ESI/APCI) calcd for C$_{18}$H$_{25}$N$_2$O$_2$ (M+H) 301.1911, found 301.1914. (jmf-02-688)

127

ppm 9   8   7   6   5   4   3   2   1

180 160 140 120 100 80 60 40 20 0

151
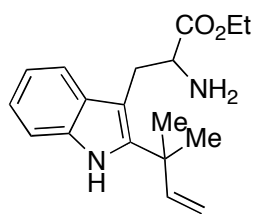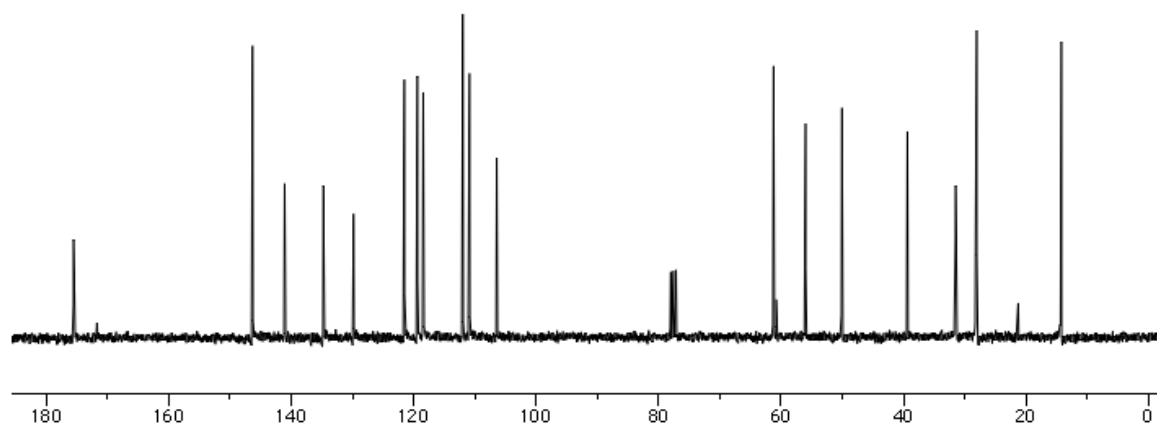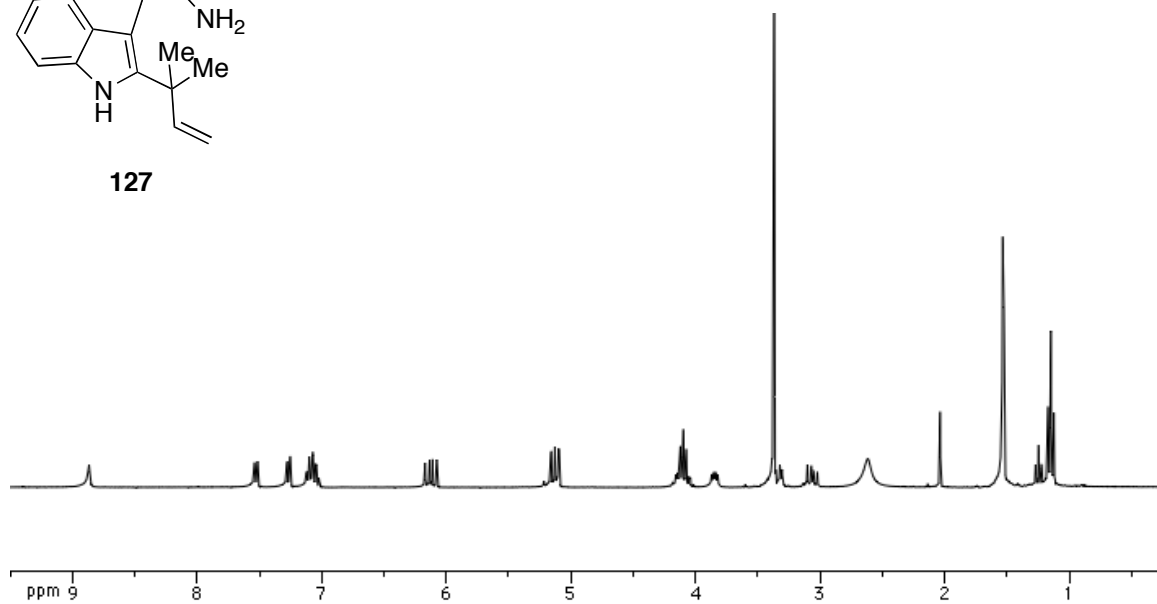
ethyl 2-((tert-butoxycarbonyl)amino)-3-(2-(2-methylbut-3-en-2-yl)-1H-indol-3-yl)propanoate (128):
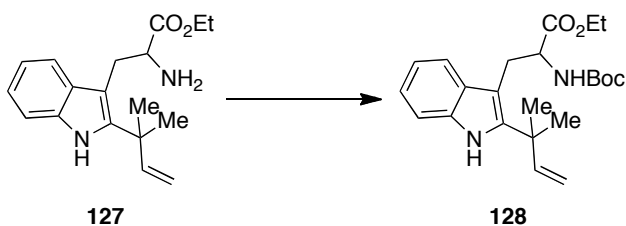
The amine (55 mg, 0.183 mmol) was dissolved in 1 mL of dioxane and cooled to 0°C. Di-*tert*-butyldicarbonate (43.9 mg, 0.201 mmol) and aqueous 0.5 M NaOH (36.6μL) were added to the solution. The reaction mixture was allowed to warm to room temperature while stirring for 2 hours. The solvent was removed in vacuo and the remaining residue was taken up in H_2O and acidified with 10% $KHSO_4$ to pH 2. The product was extracted with ethyl acetate (3 x 10 mL) and the combined organic layer was washed with brine, dried over Na_2SO_4 and concentrated. The residue was purified via flash column chromatography in 4:1 hexanes:ethyl acetate. Yield: 70 mg, 0.175 mmol, 96%.

^{1}H NMR (300 MHz, CDCl$_3$) δ 8.37 (bs, 1H) 7.52 (d, J = 7.2 Hz, 1H), 7.26 (d, J = 6.6 Hz, 1H), 7.14-7.05 (m, 2H), 6.15 (dd, J = 17.4, 10.5 Hz, 1H), 5.22-5.25 (m, 2H), 4.14-3.95 (m, 2H), 3.38-3.21 (m, 2H), 1.56 (s, 9H), 1.36 (s, 6H), 1.03 (t, J = 6.9 Hz, 3H); ^{13}C NMR (75 MHz, CDCl$_3$) δ 173.4, 155.4, 146.3, 140.8, 134.6, 129.9, 121.6, 119.5, 118.4, 112.3, 110.7, 105.9, 79.8, 67.3, 61.4, 55.0, 39.4, 28.7, 28.5, 28.1, 27.9, 27.6, 14.0; IR (neat) 3378, 3083, 3057, 2976, 1697, 1503, 1462, 1167; HRMS (ESI/APCI) calcd for $C_{23}H_{33}N_2O_4$ (M+H) 401.2435, found 401.2434. (jmf-02-689)
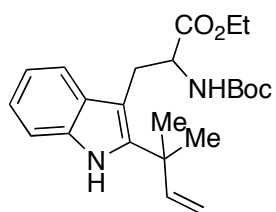
128
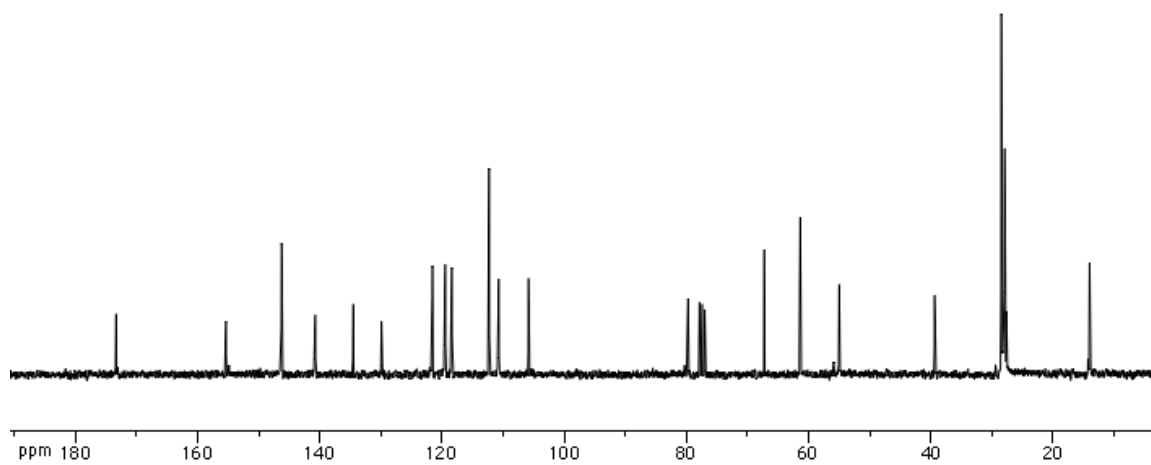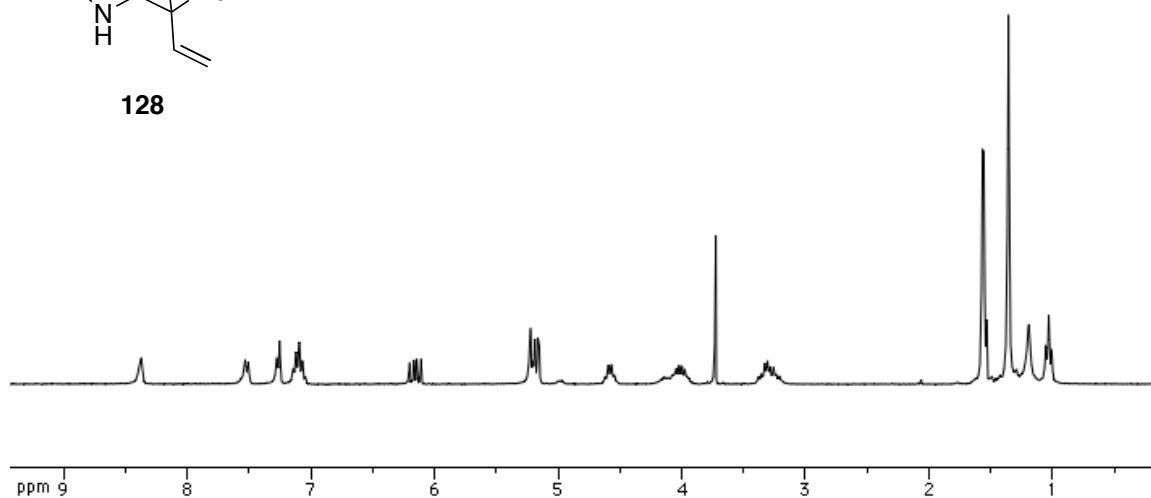
2-((tert-butoxycarbonyl)amino)-3-(2-(2-methylbut-3-en-2-yl)-1H-indol-3-yl)propanoic acid (113):
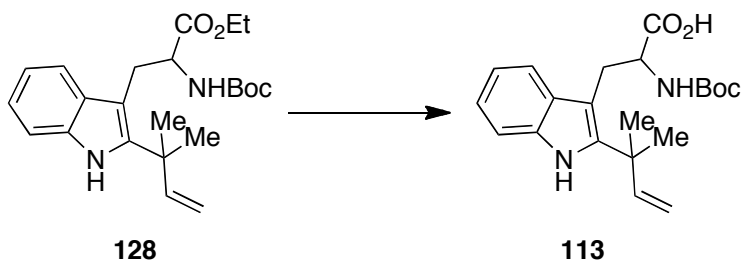
The ester (75 mg, 0.188 mmol) was dissolved in 1.2 mL of THF and 0.7 mL of H_2O. To the solution, LiOH (23 mg, 0.95 mmol) was added and the reaction stirred at room temperature for 18 hours. The solvent was removed under vacuum and the resulting slurry was acidified with 1M $KHSO_4$ to pH 2. The product was extracted with DCM (3 x 25 mL) and EtOAc (15 mL). The combined organic layers were dried over Na_2SO_4 and concentrated. Crude yield: 48.8 mg, 0.131 mmol, 70%.

^1H NMR (300 MHz, $CDCl_3$) δ 7.99-7.94 (m, 1H), 7.64-7.56 (m, 1H), 7.29-7.26 (m, 1H), 7.15-7.08 (m, 2H), 6.15 (dd, J = 17.4, 10.5 Hz, 1H), 5.22 (d, J = 8.1 Hz, 1H), 5.18 (s, 1H), 4.67-4.58 (m, 2H), 3.48-3.41 (m, 1H), 3.26-3.28 (m, 1H), 1.57 (s, 9H), 1.31 (s, 6H); ^{13}C NMR (100 MHz, 20:1 $CDCl_3/CD_3OD$) δ 175.2, 155.6, 146.3, 140.8, 134.4, 129.8, 121.4, 119.4, 118.5, 112.1, 110.5, 105.9, 79.8, 60.7, 54.7, 39.3, 28.3, 27.8, 21.1, 14.3; IR (neat) 3368, 3087, 3053, 2974, 1712, 1502, 1460, 1164; HRMS (ESI/APCI) calcd for $C_{21}H_{29}N_2O_4$ (M+H) 373.2122, found 373.2117. (jmf-02-690)
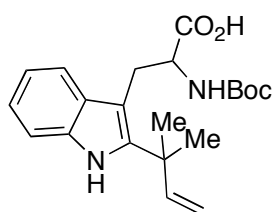
113
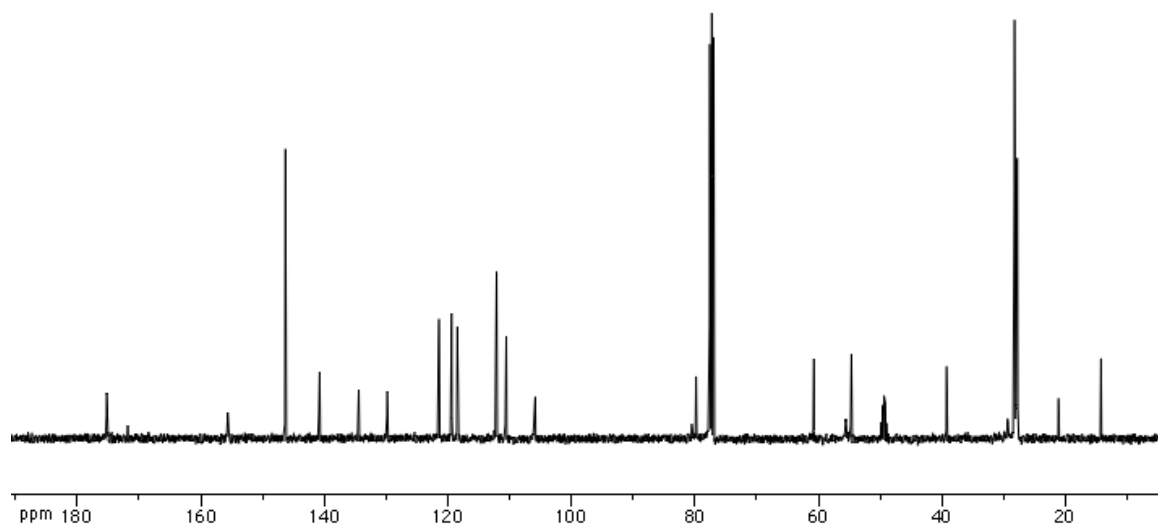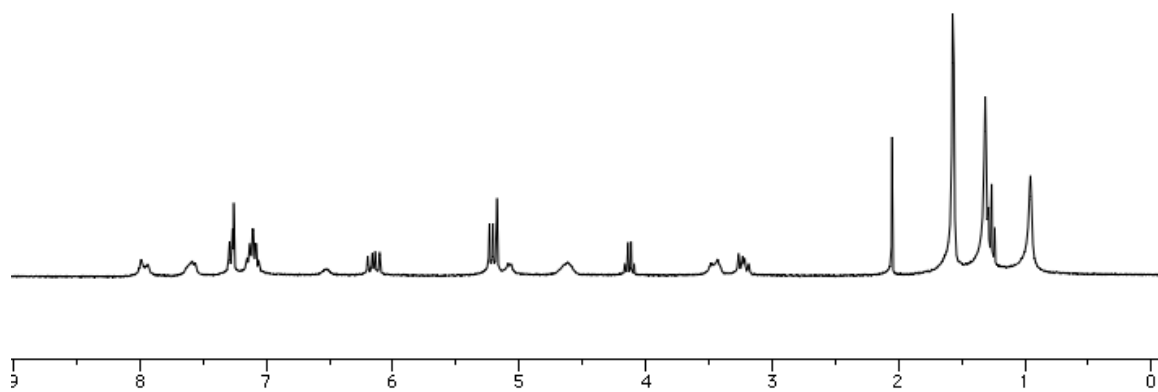
ethyl 3-((2-ethoxy-2-oxoethyl)amino)propanoate (130):

124   **129**   **130**
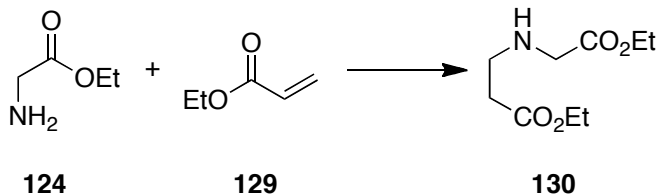
Glycine ethyl ester (20 g, 143.3 mmol) was dissolved in 286 mL of ethanol. Ethyl acrylate (17.0 mL, 157.6 mmol) and triethylamine (20.3 mL, 146.2 mmol) were added and the reaction stirred at room temperature for 48 hours. The solvent was removed in vacuo. Crude yield: 25.6 g, 126.1 mmol, 88%.

^{1}H NMR (300 MHz, CDCl$_3$) δ 4.22-4.07 (m, 4H), 3.41 (s, 1H), 2.89 (t, J = 6.6 Hz, 1H), 2.50 (t, J = 7.5 Hz), 2.03 (s, 1H), 1.29-1.21 (m, 6H). (jmf-01-123)
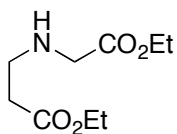
130
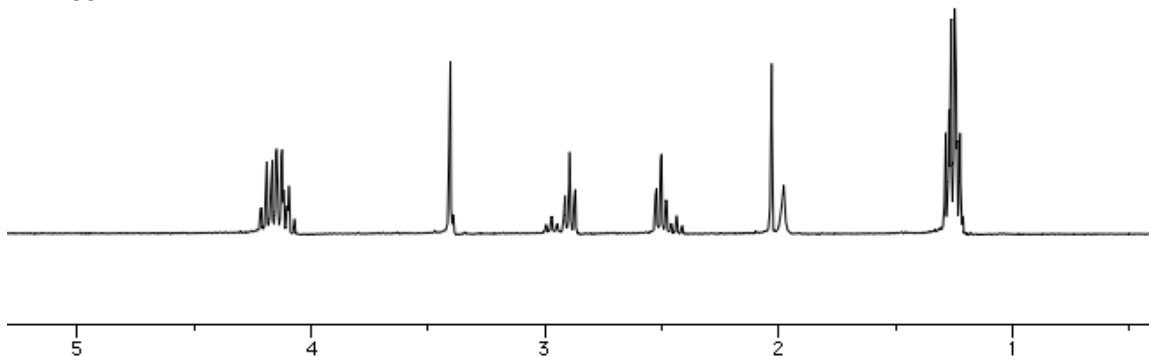
ethyl 3-(((*tert*-butoxycarbonyl)(2-ethoxy-2-oxoethyl)amino)propanoate (131):

130　　**131**
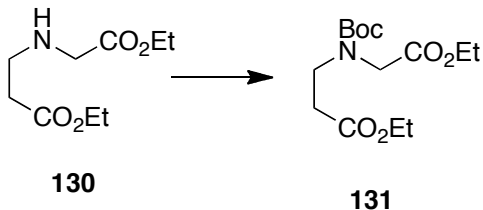
The amine (31.4 g, 155 mmol) was dissolved in 50 mL of dioxane and cooled to 0°C. Di-*tert*-butyldicarbonate (37.2 g, 170 mmol), 155 mL of 1M NaOH and 155 mL of water were added to the solution.　The reaction mixture stirred for 18 hours at room temperature.　Brine (100 mL) was added to the reaction and product was extracted with DCM (3 x 200 mL).　The combined organic layer was dried over Na_2SO_4 and concentrated in vacuo.　The crude material was purified by vacuum distillation and with the product distilling at 131°C.　Yield: 29.8 g, 98.2 mmol, 64%.

^{1}H NMR (300 MHz, CDCl$_3$) δ 4.19-4.09 (m, 4H), 3.97 (d, *J* = 19.8 Hz, 2H), 3.57-3.49 (m, 2H), 2.64-2.57 (m, 2H), 1.43 (d, *J* = 19.2 Hz, 9H), 1.28-1.21 (m, 6H). (jmf-01-123)

Boc
N CO₂Et
CO₂Et
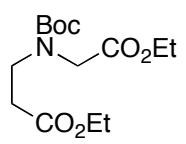
131
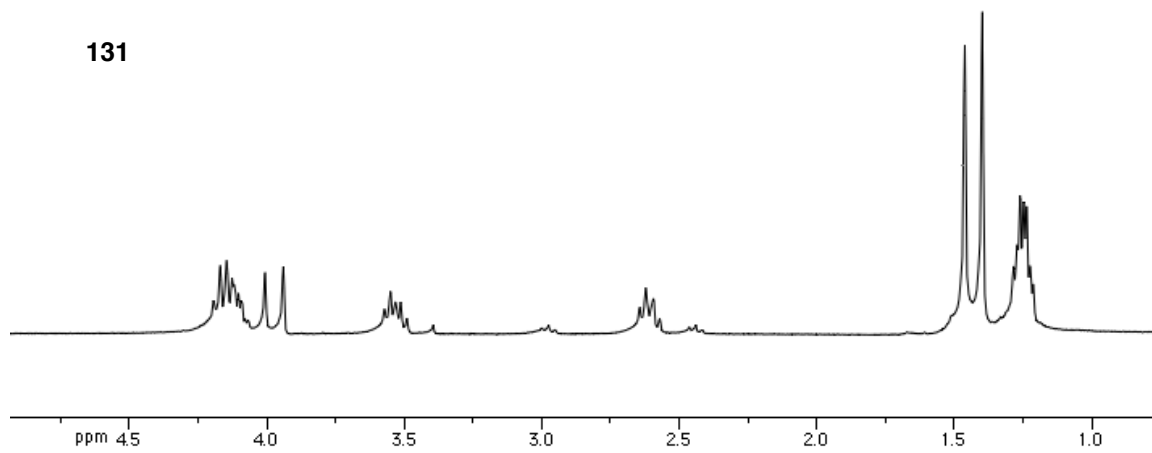
1-*tert*-butyl 2-ethyl 3-oxopyrrolidine-1,2-dicarboxylate (132):

131   **132**
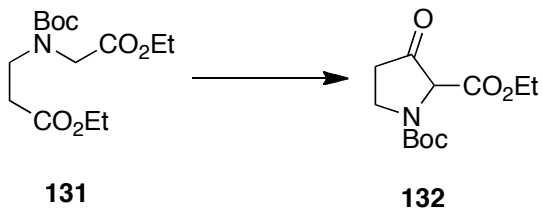
A 1M solution of lithium bis(trimethylsilyl)amide in THF (3.5 mL, 3.3 mmol) was cooled to -78°C and 10 mL of THF was added. The ester (500 mg, 1.65 mmol) was diluted with 5 mL of THF and the solution was added dropwise to the reaction mixture, which stirred for 4 hours at -78°C. The reaction was quenched with 1M HCl (20 mL) and the product was extracted with diethyl ether (3 x 25 mL). The combined organic layer was dried over Na_2SO_4, concentrated, and purified via flash column chromatography in 3:2 hexanes:ethyl acetate. Yield: 300 mg, 1.17 mmol, 71%.

^{1}H NMR (300 MHz, CDCl$_3$) δ 4.27-4.20 (m, 2H), 3.93-3.76 (m, 2H), 2.69 (t, J = 7.2 Hz, 2H), 1.58 (s, 1H), 1.43 (s, 9H), 1.30 (t, J = 7.2 Hz, 3H). (jmf-01-141)
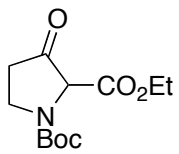
132
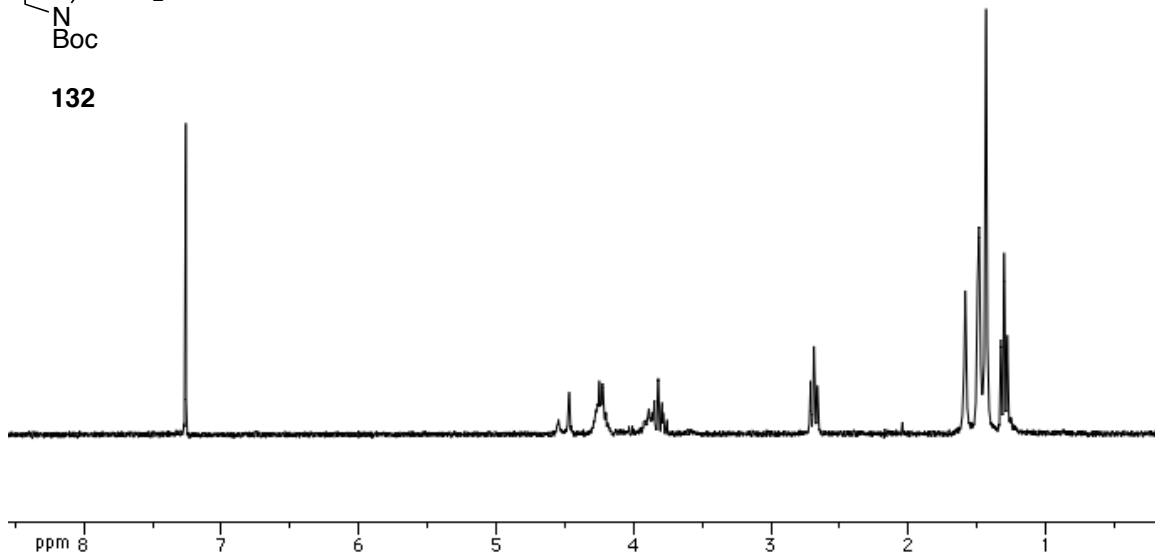
1-*tert*-butyl 2-ethyl 3-hydroxy-3-methylpyrrolidine-1,2-dicarboxylate (114):

132   **114**
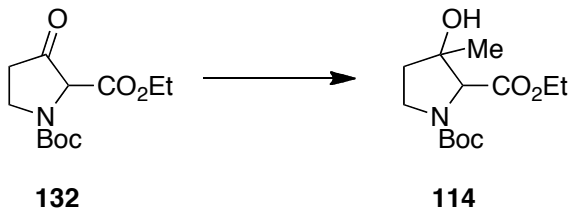
The ketoproline (300 mg, 1.17 mmol) was diluted with 6 mL of toluene and cooled to 0°C. A 2M solution of trimethylaluminum (1.17 mL, 2.34 mmol) was slowly added and the reaction mixture stirred at 0°C for 3 hours. The reaction was quenched with ice cold 10% aqueous KHSO$_4$ and extracted with diethyl ether (3 x 15 mL). The organic layer was dried over MgSO$_4$, concentrated, and purified via flash column chromatography in 3:2 hexanes/ethyl acetate. Yield: 200 mg, 0.732 mmol, 63%.

^{1}H NMR (300 MHz, CDCl$_3$) δ 4.17-4.19 (m, 2H), 4.05 (d, *J* = 22.2 Hz, 1H), 3.65-3.42 (m, 2H), 2.30 (d, *J* = 24.3 Hz, 1H), 2.12-2.02 (m, 1H), 1.92-1.83 (m, 1H), 1.48 (s, 3H), 1.40 (s, 9H), 1.32-1.26 (m, 3H). (jmf-01-142)

114
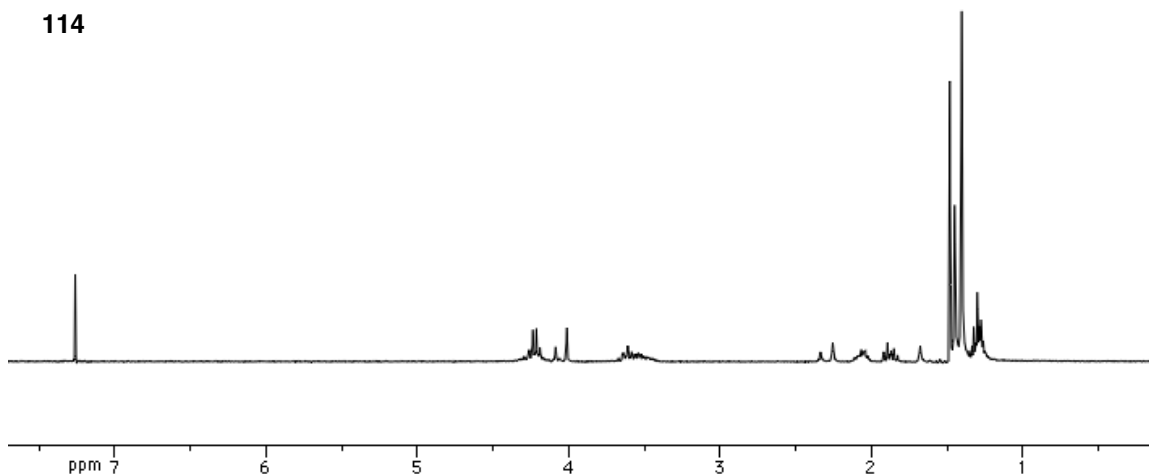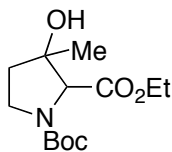
ethyl 3-hydroxy-3-methylpyrrolidine-2-carboxylate (133):
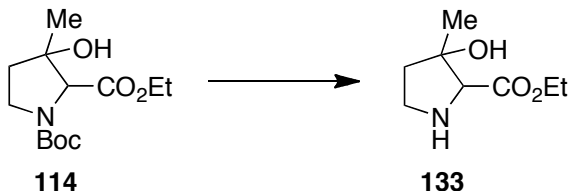
The proline (250 mg, 0.915 mmol) was stirred with TFA (1.5 mL) in 1.5 mL of DCM at 0°C. The reaction mixture warmed to room temperature and stirred for an additional 3 hours. The solvent was removed under vacuum and take on crude.

Ethyl 1-(2-(((*tert*-butoxycarbonyl)amino)-3-(2-(2-methylbut-3-en-2-yl)-1H-indol-3-yl)propanoyl)-3-hydroxy-3-methylpyrrolidine-2-carboxylate (2.35):
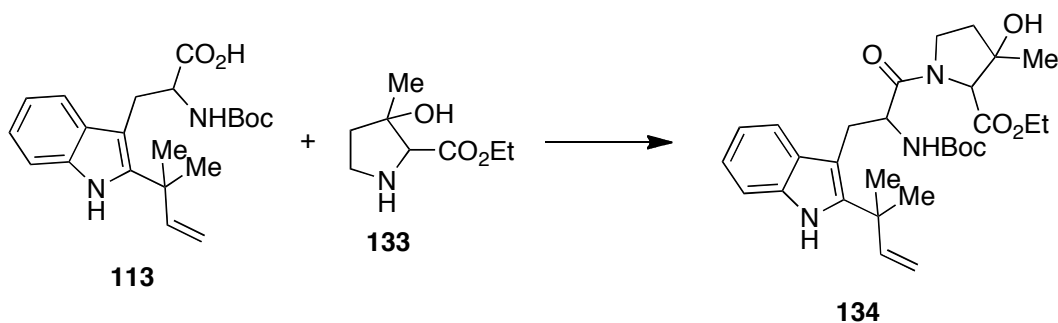
The indole (340 mg, 0.913 mmol) and crude proline **133** were dissolved in 10 mL of MeCN. HATU (521 mg, 1.37 mmol) and ^{i}Pr$_2$NEt (0.636 mL, 3.65 mmol) were added and the reaction stirred for 4 hours at room temperature. The reaction was quenched with 1M HCl (20 mL) and extracted with DCM (3 x 50 mL). The combined organic layer was dried over Na$_2$SO$_4$, concentrated and purified by flash column chromatography in 1:1 hexanes/ethyl acetate. Yield: 480 mg, 0.909 mmol, 99%

^{1}H NMR (300 MHz, CDCl$_3$) δ 7.95 (bs, 1H), 7.49 (dd, J = 21, 8.1 Hz, 1H), 7.36-7.22 (m, 1H), 7.15-7.05 (m, 2H), 6.13 (dd, J = 17.7, 10.8 Hz, 1H), 5.62-5.55 (m, 1H), 5.28-5.18 (m, 2H), 4.29-4.15 (m, 2H), 3.14-3.07 (m, 4H), 1.65-1.62 (m, 6H), 1.45 (s, 9H), 1.27 (t, J = 7.2 Hz, 3H). (jmf-01-091)
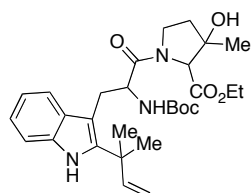
134
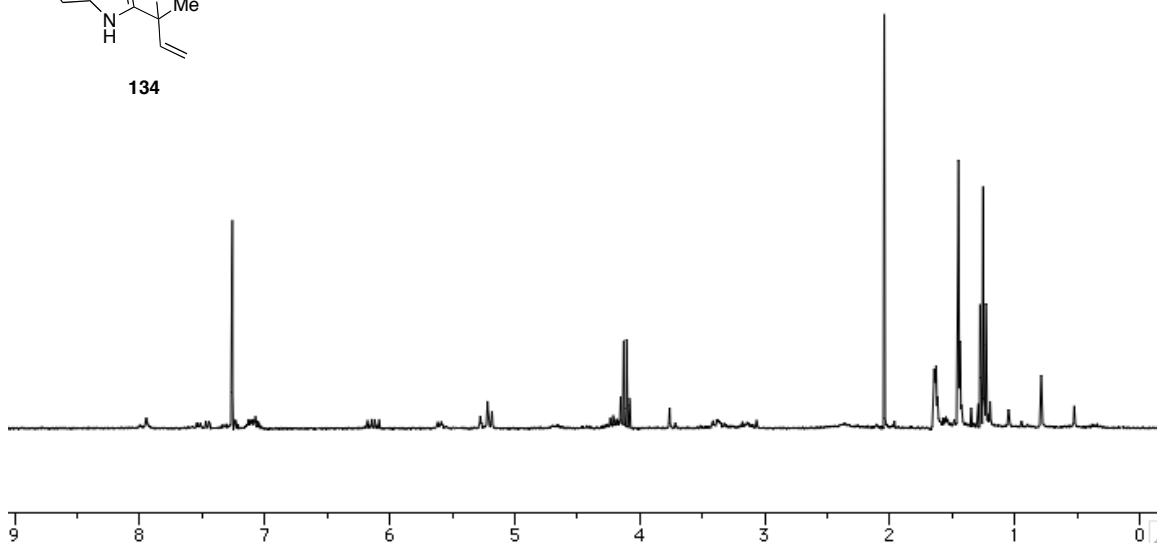
Diketopiperazine (115):

135   115
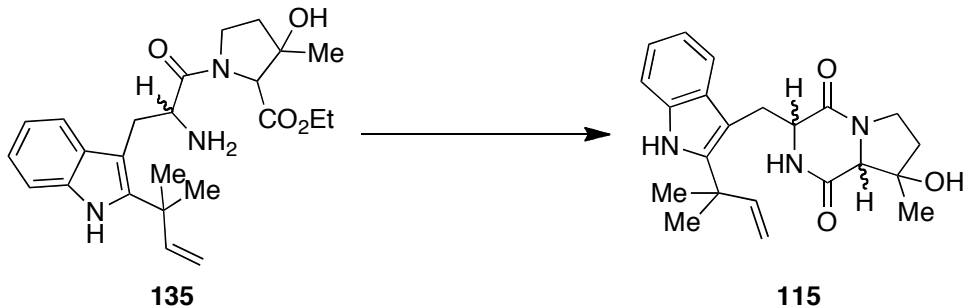
The peptide (480 mg, 0.909 mmol) was dissolved in 1.52 mL of DCM and cooled to 0°C. To the solution, TFA (1.52 mL) was slowly added and the reaction warmed to room temperature while stirring for 3 hours. The reaction was quenched with 5 mL of saturated aqueous $NaHCO_3$ and the organic layer was separated from the aqueous phase. The aqueous layer was extracted with ethyl acetate (3 x 20 mL). The combined organic layer was dried over Na_2SO_4 and concentrated. Crude yield: 320 mg, 0.748 mmol, 83%.

The crude free amine (320 mg, 0.748 mmol) was dissolved in 4 mL of toluene. To the solution, 2-hydroxypyridine (14.2 mg, 0.149 mmol) was added and the reaction mixture stirred at reflux for 16 hours. The reaction cooled to room temperature and the solvent was removed under vacuum. The residue was dissolved in DCM (20 mL) and washed with 1M HCl (2 x 20 mL). The organic layer was dried over Na_2SO_4 and concentrated. Crude yield: 233 mg, 0.611 mmol, 81%

^{1}H NMR (300 MHz, CDCl$_3$) δ 8.02 (bs, 1H), 7.54-7.47 (m, 1), 7.35-7.29 (m, 1H), 7.19-7.08 (m, 2H), 6.13 (dd, J = 17.4, 10.2 Hz, 1H), 6.06 (bs, 1H),5.23-5.15 (m, 1H), 4.31-4.23 (m, 1H), 3.79-3.68 (m, 2H), 3.57-3.50 (m, 2H), 3.31-3.13 (m, 2H), 2.21-1.86 (m, 3H), 1.57 (s, 3H), 1.54 (s, 3H), 1.53 (s, 3H); IR (neat) 3360, 3056, 2967, 1661, 1463 1138. (jmf-01-087).

115
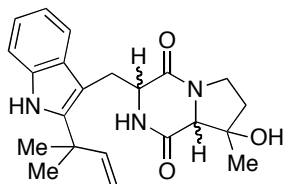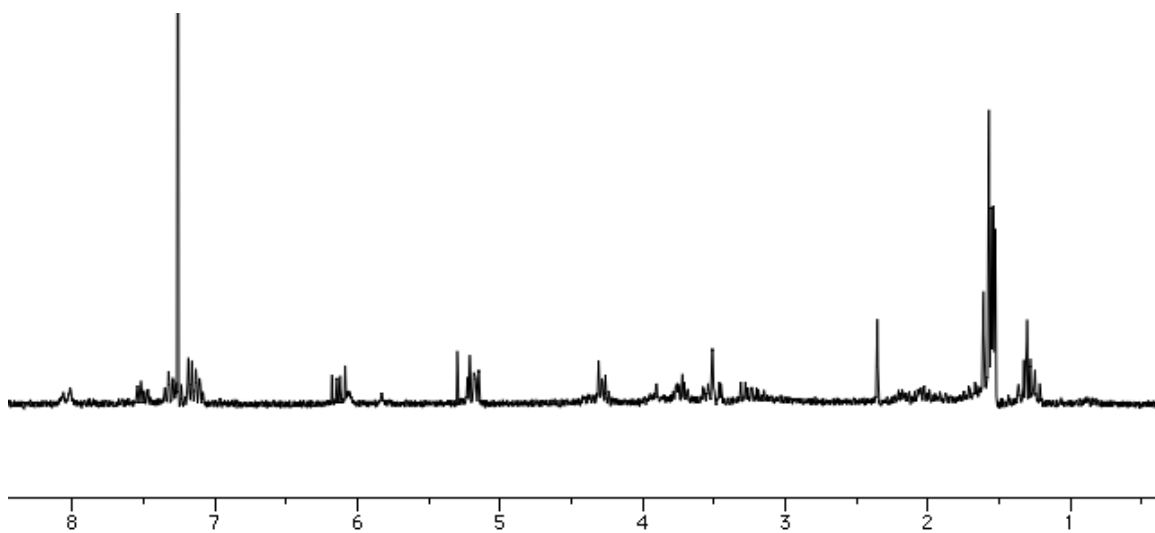
Enamide (136):

| 115 | 136 |
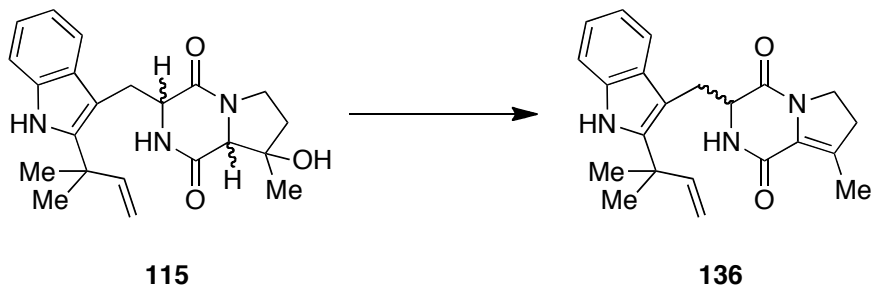
The alcohol (227 mg, 0.595 mmol) was dissolved in 2.5 mL of THF and cooled to 0°C.

Pyridine (96.2 μL, 1.19 mmol) was added and the solution stirred for 15 minutes.

Thionyl chloride (48 μL, 0.654 mmol) was added and the reaction stirred at room

temperature for 4 hours. Water (10 mL) was added to the reaction mixture and the

product was extracted with ethyl acetate (3 x 20 mL). The organic layer was dried over

Na_2SO_4, concentrated, and filtered through a silica plug with 5% MeOH in DCM. Yield:

195 mg, 0.534 mmol, 90%.

^{1}H NMR (300 MHz, CDCl$_3$) δ 8.03 (bs, 1H), 7.54 (d, J = 8.7 Hz, 1H), 7.34-7.31 (m, 1H),

7.19-7.09 (m, 2H), 6.12 (dd, J = 17.4, 10.8 Hz, 1H), 5.63-5.56 (m, 1H), 5.20-5.14 (m,

2H), 4.46 (d, J = 13.8 Hz, 1H), 3.90-3.89 (m, 2H), 3.71 (dd, J = 14.4, 3.3 Hz, 1H), 3.20

(dd, J = 15.0, 11.4 Hz, 1H), 2.72-2.65 (m, 2H), 2.19 (s, 3H), 1.55 (s, 6H); IR (neat) 3344,

3046, 2968, 1682, 1644, 1440, 1251, 1112. (jmf-01-119)
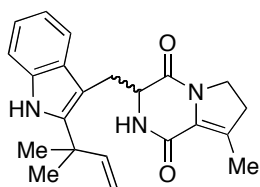
136
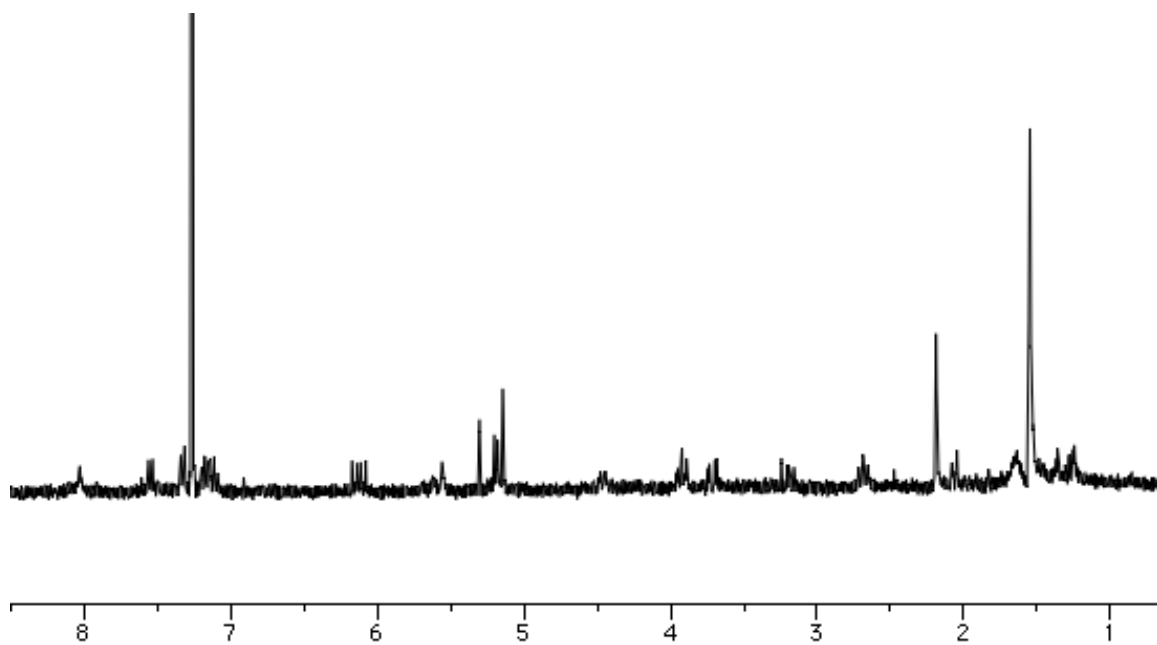
Lactim ether (116):

136   **116**
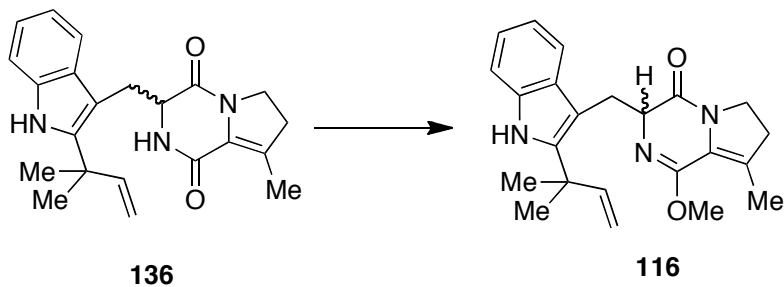
The enamide (195 mg, 0.534 mmol) was dissolved in 9 mL of DCM. Trimethyloxonium

tetrafluoroborate (236 mg, 1.60 mmol) and Cs_2CO_3 (3.48 g, 10.68 mmol) were added to

the solution and the reaction mixture stirred at room temperature for 24 hours. The

reaction was poured into ice water (20 mL) and extracted with DCM (3 x 35 mL). The

organic layer was washed with brine (50 mL), dried over Na_2SO_4 and concentrated. The

crude product was purified via flash column chromatography in 3:2 hexanes/ethyl

acetate. Yield: 68 mg, 0.180 mmol, 34%.

^{1}H NMR (300 MHz, CDCl$_3$) δ 7.86 (bs, 1H), 7.64 (d, J = 8.1 Hz, 1H), 7.24 (d, J = 8.1

Hz, 1H), 7.12-7.00 (m, 2H), 6.15 (dd, J = 17.7, 10.5 Hz, 1H), 5.17 (dd, J = 17.4, 1.2 Hz,

1H), 5.13 (dd, J = 10.5, 1.2 Hz, 1H), 4.57 (d, J = 12.0 Hz, 1H), 3.84-3.74 (m, 3H), 3.66

(m, 3H), 3.07 (dd, J = 14.4, 9.3 Hz, 1H), 2.56-2.50 (m, 2H), 1.98 (s, 3H), 1.61 (s, 3H),

1.60 (s, 3H); IR (neat) 3346, 2962, 1676, 1634, 1452, 1241. (jmf-01-121)
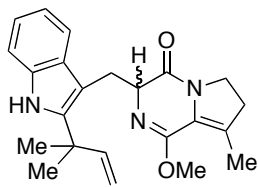
116
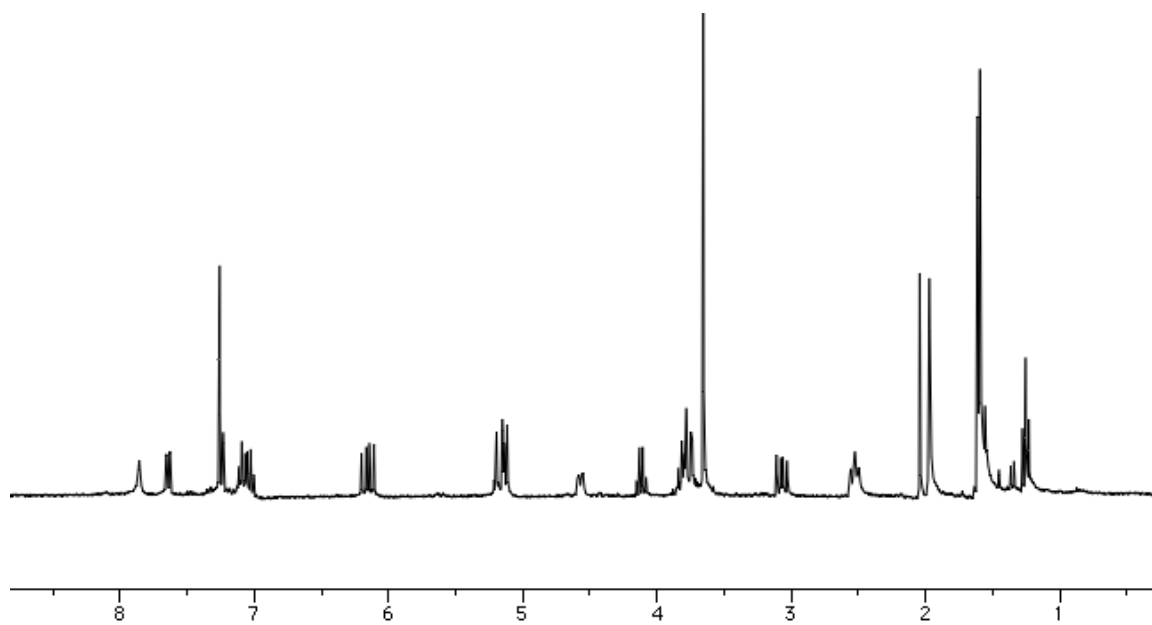
[¹³C]-Ethyl 2-((diphenylmethylene)amino)acetate (138):
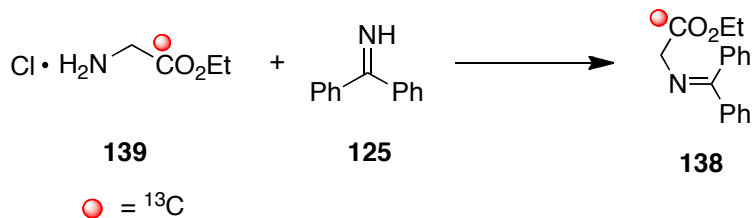
Glycine ethyl ester (3.87 g, 21.35 mmol) and benzophenone imine (3.0 g, 21.35 mmol) were dissolved in 71 mL of DCM and stirred at room temperature for 24 hours. The reaction mixture was filtered through celite to remove NH_4Cl and the filtrate concentrated under vacuum. The residue was dissolved in 100 mL of diethyl ether and washed with H_2O (100 mL). The ether was dried over $MgSO_4$ and concentrated. The product was recrystallized in ethyl acetate and hexanes and collected as a white solid. Yield: 5.49 g, 20.46 mmol, 96%.

¹H NMR (300 MHz, CDCl₃) δ 7.56-7.12 (m, 10H), 4.20-4.10 (m, 4H), 1.21 (t, *J* = 7.2 Hz, 3H); ¹³C NMR (75 MHz, CDCl₃) δ 170.7, 139.5, 136.2, 132.6, 130.7, 130.2, 129.04, 128.98, 128.91, 128.5, 128.3, 127.9, 61.0, 56.3, 55.5. ¹³C-enriched peak: 170.7 (jmf-02-798)
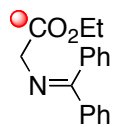
138
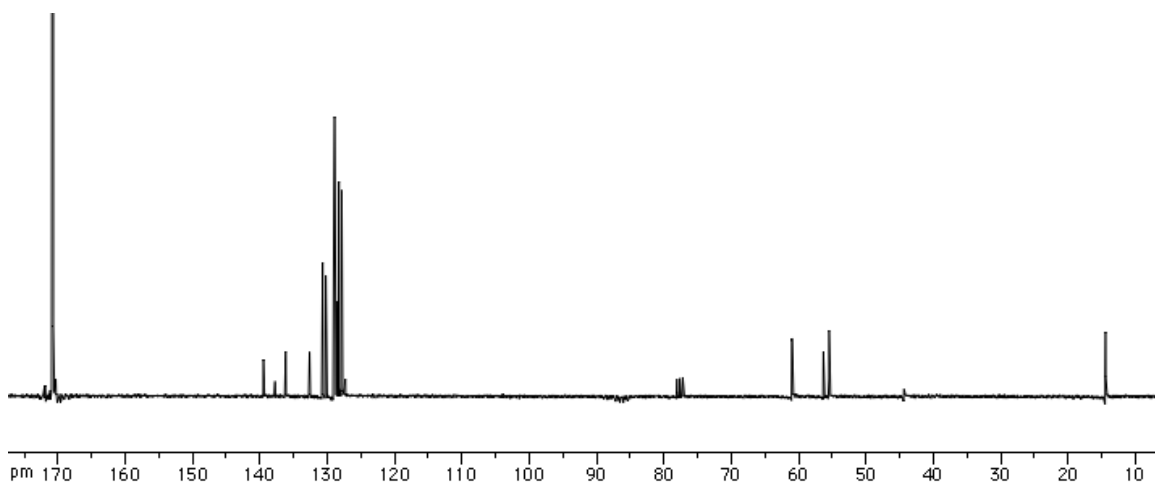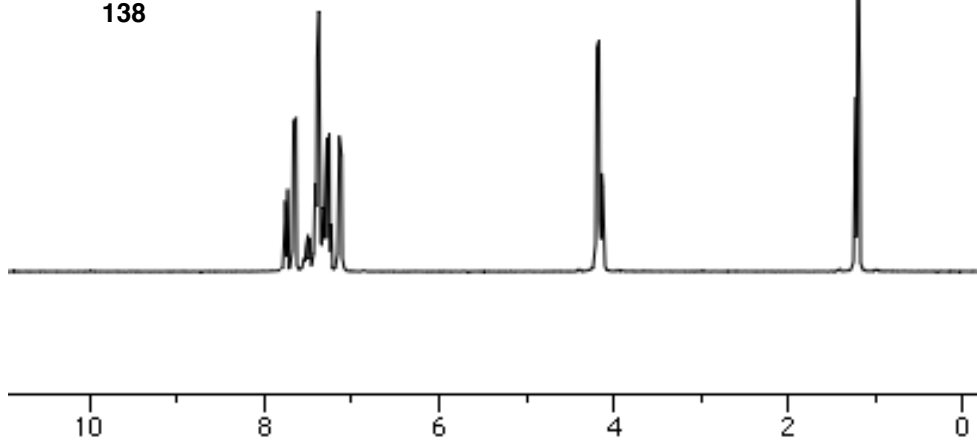
[^{13}C]-Ethyl 2-((diphenylmethylene)amino)-3-(2-(2-methylbut-3-en-2-yl)-1H-indol-3-yl)propanoate (140):
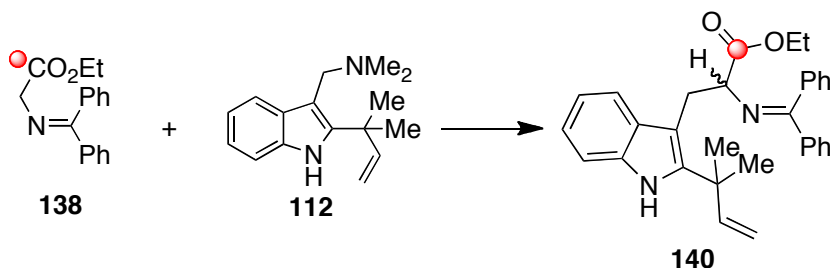
The gramine (1.65 g, 6.81 mmol), [^{13}C]-glycine benzophenone imine (1.66 g, 6.19 mmol) and ^{n}Bu$_3$P (0.61 mL, 2.48 mmol) were dissolved in MeCN (34.0 mL) and heated to reflux for 18 hours. The reaction mixture was concentrated and purified via flash column chromatography in 9:1 hexanes:ethyl acetate to provide **140**. Yield: 3.11 g, 6.68 mmol, 98%.

^{1}H NMR (300 MHz, CDCl$_3$) δ 7.89 (bs, 1H), 7.60-7.57 (m, 2H), 7.47-7.19 (m, 8H), 7.09-7.01 (m, 3H), 6.87-6.82 (m, 1H), 6.33 (bs, 1H), 5.89 (dd, J = 17.4, 10.5 Hz, 1H), 5.09-4.99 (m, 2H), 4.25-4.11 (m, 2H), 3.58 (d, J = 2.4 Hz, 1H), 3.55 (bs, 1H), 1.39 (s, 3H), 1.36 (s, 3H), 1.27 (t, J = 7.2 Hz, 3H); ^{13}C NMR (75 MHz, CDCl$_3$) δ 172.7, 170.9, 146.3, 140.1, 139.5, 136.2, 134.1, 130.2, 129.1, 128.0, 127.9, 127.8, 121.4, 119.6, 119.1, 111.8, 110.0, 107.6, 107.5, 67.3, 66.5, 61.0, 39.3, 31.8, 29.0, 18.4, 18.3, 17.9, 17.8, 24.8, 22.9, 14.4, 14.2; ^{13}C-enriched peak: 172.7. (jmf-01-480)

140
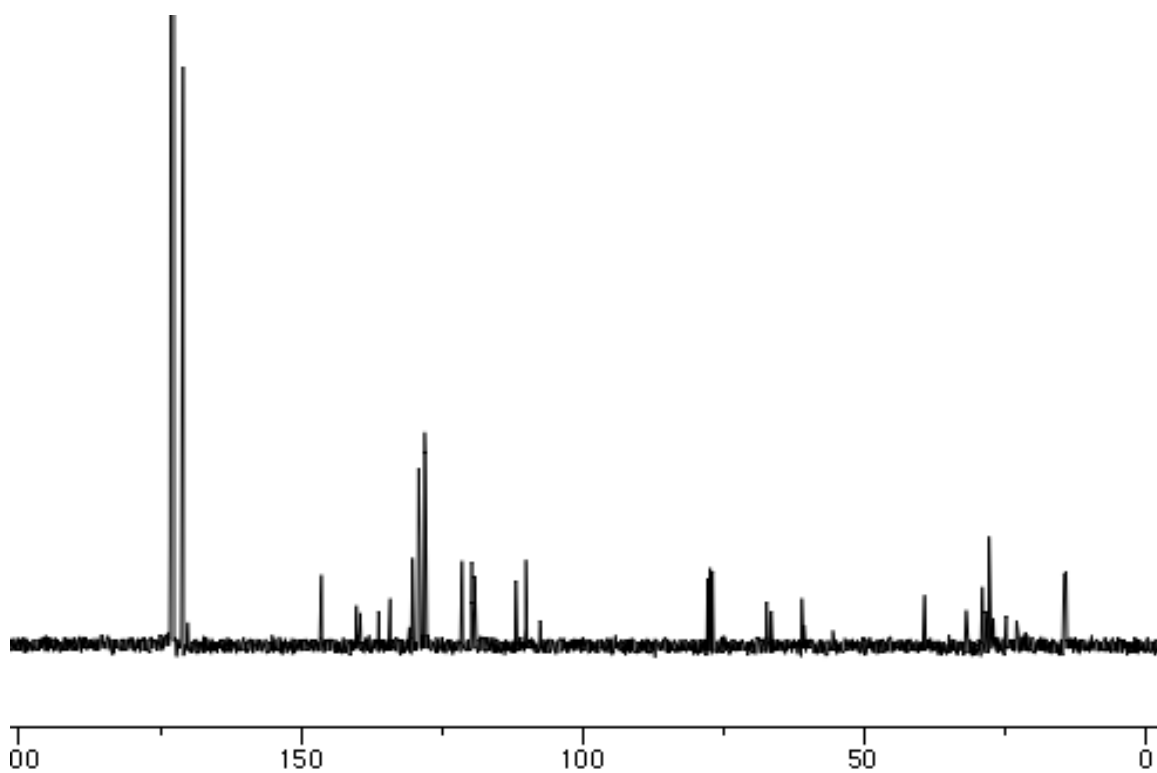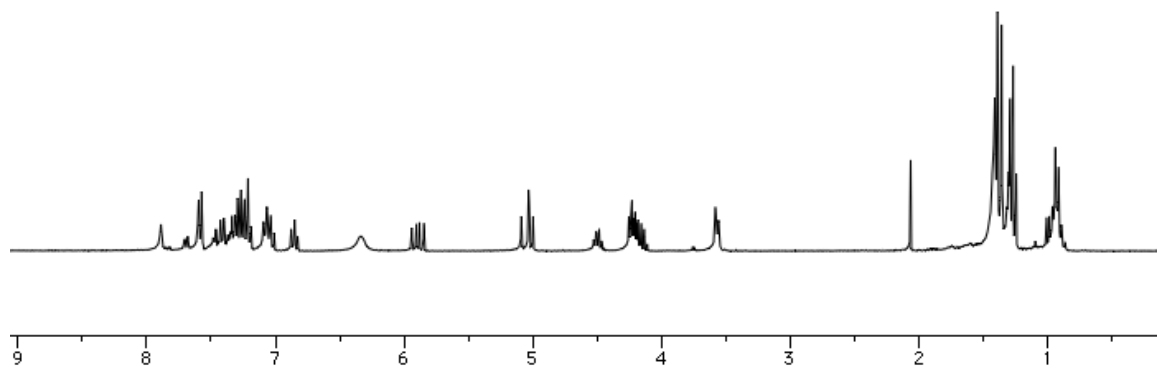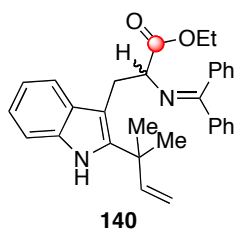
[¹³C]-Ethyl 2-((*tert*-butoxycarbonyl)amino)-3-(2-(2-methylbut-3-en-2-yl)-1H-indol-3-yl)propanoate (141):

140 → **141**
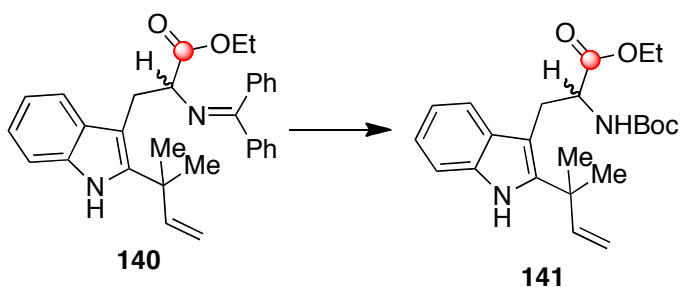
The [^{13}C]-imine (3.11 mg, 6.68 mmol) was dissolved in 50 mL of THF and 1N HCl (16.7 mL) and the reaction stirred for 30 minutes. The THF was removed under vacuum and the residue with diluted with NaHCO$_3$ until basic. The aqueous layer was extracted with DCM (2 x 100 mL) and the combined organic layers were dried over Na$_2$SO$_4$ and concentrated. The crude material was purified via flash column chromatography in 3:1 hexanes:ethyl acetate and then flushed with 5% MeOH in DCM. The [^{13}C]-amine (790 mg, 2.62 mmol) was dissolved in 13 mL of dioxane and cooled to 0°C. Di-*tert*-butyldicarbonate (600 mg, 2.75 mmol) and aqueous 0.5 M NaOH (2.6 mL) were added to the solution. The reaction mixture was allowed to warm to room temperature while stirring for 2 hours. The solvent was removed in vacuo and the remaining residue was taken up in H$_2$O and acidified with 10% KHSO$_4$to pH 2. The product was extracted with ethyl acetate (3 x 40 mL) and the combined organic layer was washed with brine, dried over Na$_2$SO$_4$ and concentrated. The residue was purified via flash column chromatography in 4:1 hexanes:ethyl acetate. Yield: 1.29 mg, 3.21 mmol, 48% (2 steps).

[¹³C]-2-((*tert*-butoxycarbonyl)amino)-3-(2-(2-methylbut-3-en-2-yl)-1H-indol-3-yl)propanoic acid (142):

141 → **142**
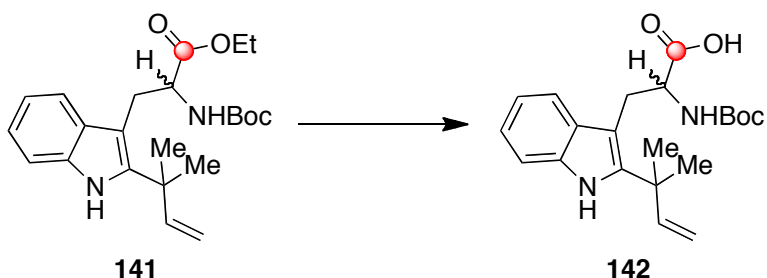
The [¹³C]-ester (1.05 g, 2.62 mmol) was dissolved in 8.73 mL of THF and 17.5 mL of H$_2$O. To the solution, LiOH (1.09 g, 26.2 mmol) was added and the reaction stirred at room temperature for 18 hours. The solvent was removed under vacuum and the resulting slurry was acidified with 1M KHSO$_4$ to pH 2. The product was extracted with DCM (3 x 40 mL) and EtOAc (40 mL). The combined organic layers were dried over Na$_2$SO$_4$ and concentrated. Crude yield: 780 mg, 2.09 mmol, 80%.

¹H NMR (300 MHz, CDCl$_3$) δ 7.95 (bs, 1H), 7.57 (d, *J* = 10.2 Hz, 1H), 7.29 (d, *J* = 8.4 Hz, 1H), 7.16-7.06 (m, 2H), 6.15 (dd, *J* = 17.1, 10.5 Hz, 1H), 5.22 (d, *J* = 7.2 Hz, 1H), 5.17 (s, 1H), 4.60 (bs, 1H), 3.46-3.39 (m, 1H), 3.27-3.15 (m, 1H), 1.57 (s, 3H), 1.56 (s, 3H), 1.32 (s, 9H) (jmf-01-497).
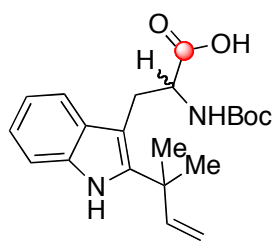
142
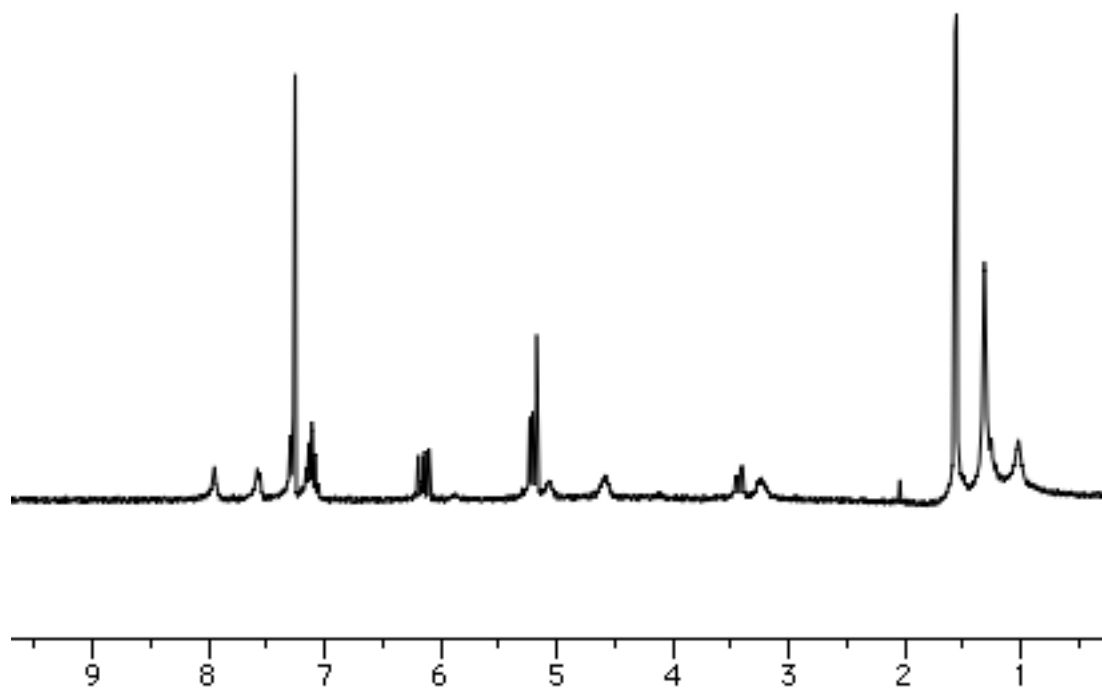
[¹³C₂]-Ethyl 1-(2-((*tert*-butoxycarbonyl)amino)-3-(2-(2-methylbut-3-en-2-yl)-1H-indol-3-yl)propanoyl)-3-hydroxy-3-methylpyrrolidine-2-carboxylate (144):
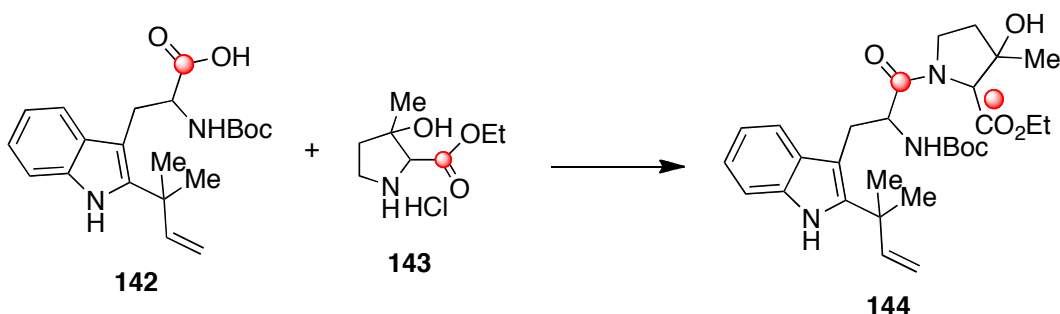
The [¹³C]-indole (600 mg, 1.61 mmol) and [¹³C]-proline (280 mg, 1.61 mmol) were dissolved in 16 mL of MeCN. HATU (916 mg, 2.41 mmol) and ^{i}Pr₂NEt (1.12 mL, 6.44 mmol) were added and the reaction stirred for 4 hours at room temperature. The reaction was quenched with 1M HCl (30 mL) and extracted with DCM (3 x 50 mL). The combined organic layer was dried over Na₂SO₄, concentrated and purified by flash column chromatography in 1:1 hexanes/ethyl acetate. Yield: 545 mg, 1.03 mmol, 64%.

¹H NMR (300 MHz, CDCl₃) δ 8.00 (bs, 1H), 7.59 (d, *J* = 9.0 Hz, 1H), 7.28 (d, *J* = 8.1 Hz, 1H), 7.15-7.04 (m, 2H), 6.14 (dd, *J* = 17.1, 10.5 Hz, 1H), 5.19 (d, *J* = 7.5 Hz, 2H), 5.14 (s, 1H), 4.17-4.05 (m, 2H), 3.85 (dd, *J* = 9.6, 4.8 Hz, 1H), 3.33 (dd, *J* = 14.1, 4.8 Hz, 2H), 3.06 (dd, *J* = 14.4, 9.6 Hz, 1H), 2.05 (s, 3H), 1.57 (s, 6H), 1.26 (t, *J* = 7.2 Hz, 3H). (jmf-01-106)

144
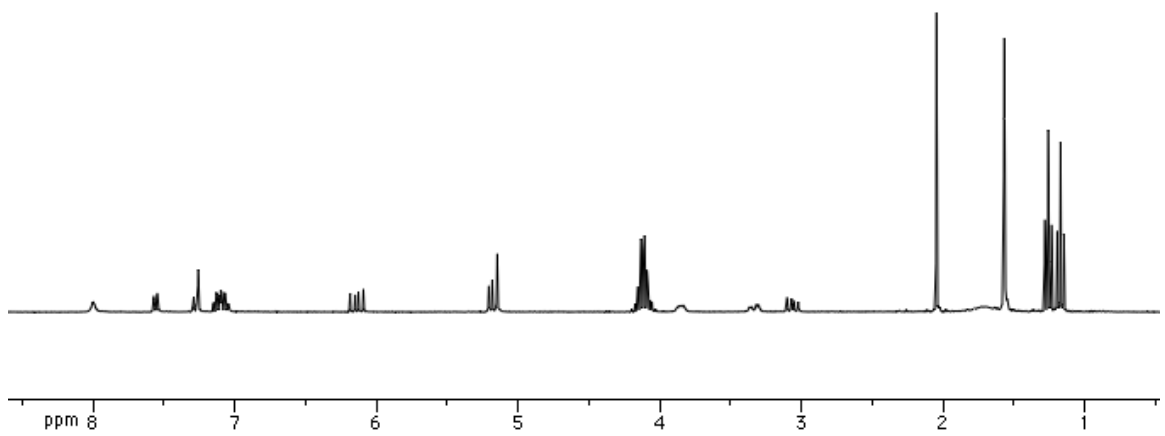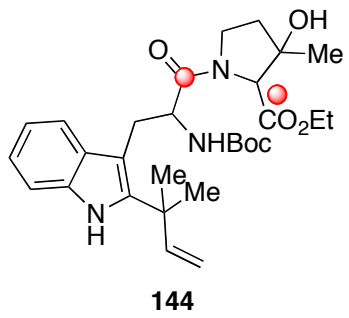
[$^{13}C_2$]-Diketopiperazine (146):

144 → **146**
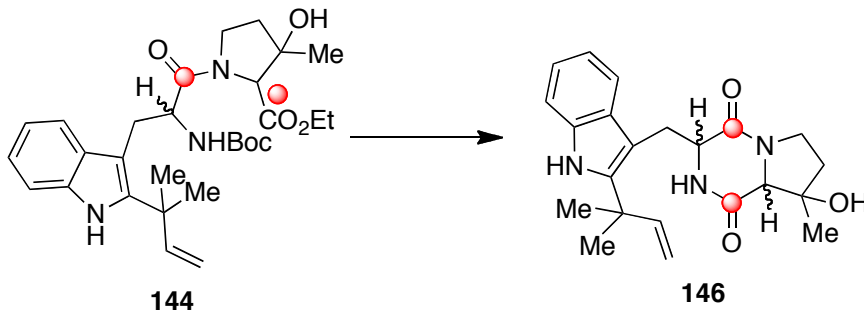
The [$^{13}C_2$]-peptide (900 mg, 1.69 mmol) was dissolved in 2.8 mL of DCM and cooled to 0°C. To the solution, TFA (2.8 mL) was slowly added and the reaction warmed to room temperature while stirring for 3 hours. The reaction was quenched with saturated aqueous NaHCO$_3$ to pH 9 and the organic layer was separated from the aqueous phase. The aqueous layer was extracted with ethyl acetate (3 x 60 mL). The combined organic layer was dried over Na$_2$SO$_4$ and concentrated. Crude yield: 730 mg, 1.69 mmol.

The crude [$^{13}C_2$]-free amine (790 mg, 1.69 mmol) was dissolved in 8.5 mL of toluene. To the solution, 2-hydroxypyridine (32 mg, 0.338 mmol) was added and the reaction mixture stirred at reflux for 16 hours. The reaction cooled to room temperature and the solvent was removed under vacuum. The residue was dissolved in DCM (40 mL) and washed with 1M HCl (2 x 40 mL). The organic layer was dried over Na$_2$SO$_4$ and concentrated. Crude yield: 498 mg, 1.3 mmol, 77%.

Mixture of diastereomers: ^{1}H NMR (300 MHz, CDCl$_3$) δ 8.02 (bs, 1H), 7.55-7.47 (m, 1H), 7.35-7.29 (m, 1H), 7.18-7.08 (m, 2H), 6.13 (dd, J = 17.1, 10.2 Hz, 1H), 5.23-5.15 (m, 2H), 4.31-4.23 (m, 1H), 3.78-3.70 (m, 1H), 3.58-3.44 (m, 2H), 3.30-3.13 (m, 1H), 1.57 (s, 3H), 1.56 (s, 3H), 1.53 (s, 3H). (jmf-01-111)
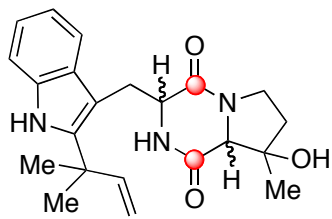
146
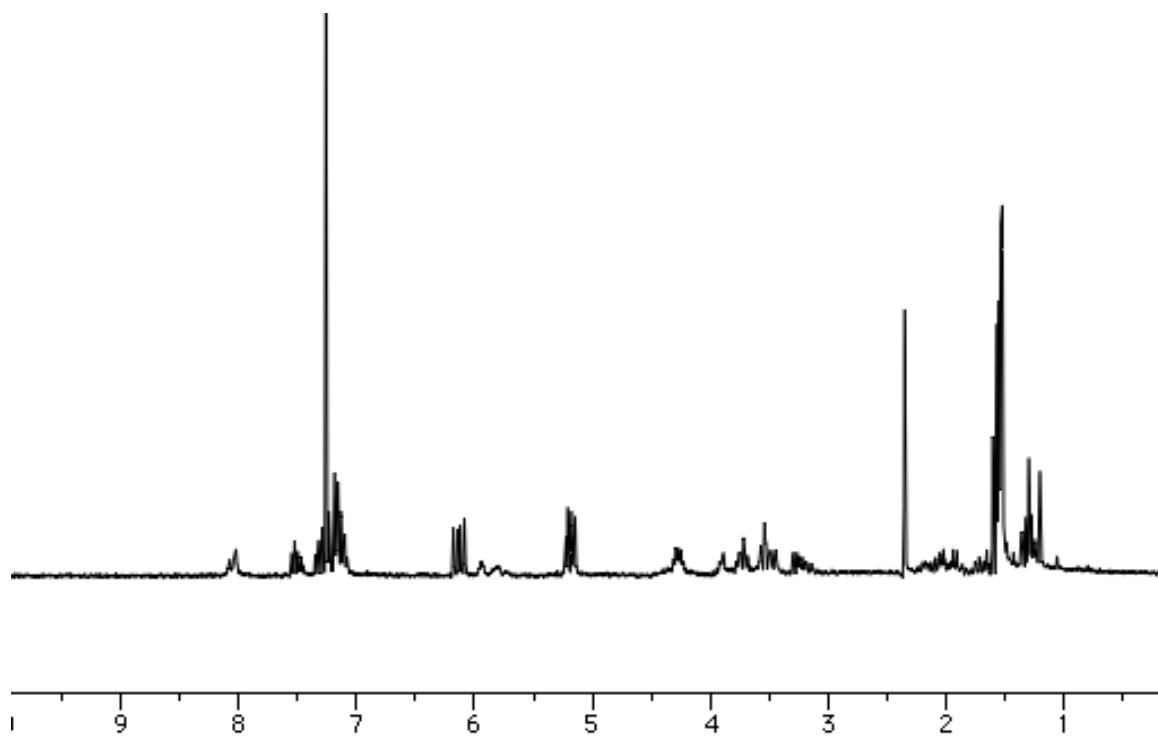
1-(7-(benzyloxy)-1H-indol-3-yl)-N,N-dimethylmethanamine (171):
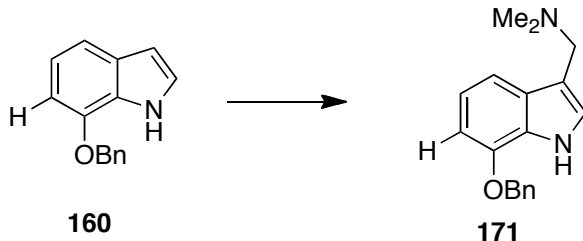
To a solution of glacial acetic acid (1.6 mL) in 37% aqueous formaldehyde (78.6 μL, 0.968 mmol), 40% aqueous dimethylamine (0.410 mL, 3.64 mmol) was added. A solution of 7-benzyloxyindole (200 mg, 0.857 mmol) in 1 mL of glacial acetic acid was slowly added. The reaction stirred at room temperature for 16 hours. The reaction mixture was diluted with 1N NaOH until pH>10. The aqueous layer was extracted with diethyl ether (3 x 30 mL) and the combined organic layers were dried over Na_2SO_4 and concentrated. Crude yield: 225 mg, 0.806 mmol, 94%.

^{1}H-NMR (300 MHz, CDCl$_3$) δ 8.39 (bs, 1H), 7.50-7.31 (m, 6H), 7.11 (d, J = 2.4 Hz, 1H), 7.03 (t, J = 7.8 Hz, 1H), 6.73 (d, J = 7.8 Hz, 1H), 5.20 (s, 2H), 3.61 (s, 2H), 2.27 (s, 6H). (jmf-01-048)

171
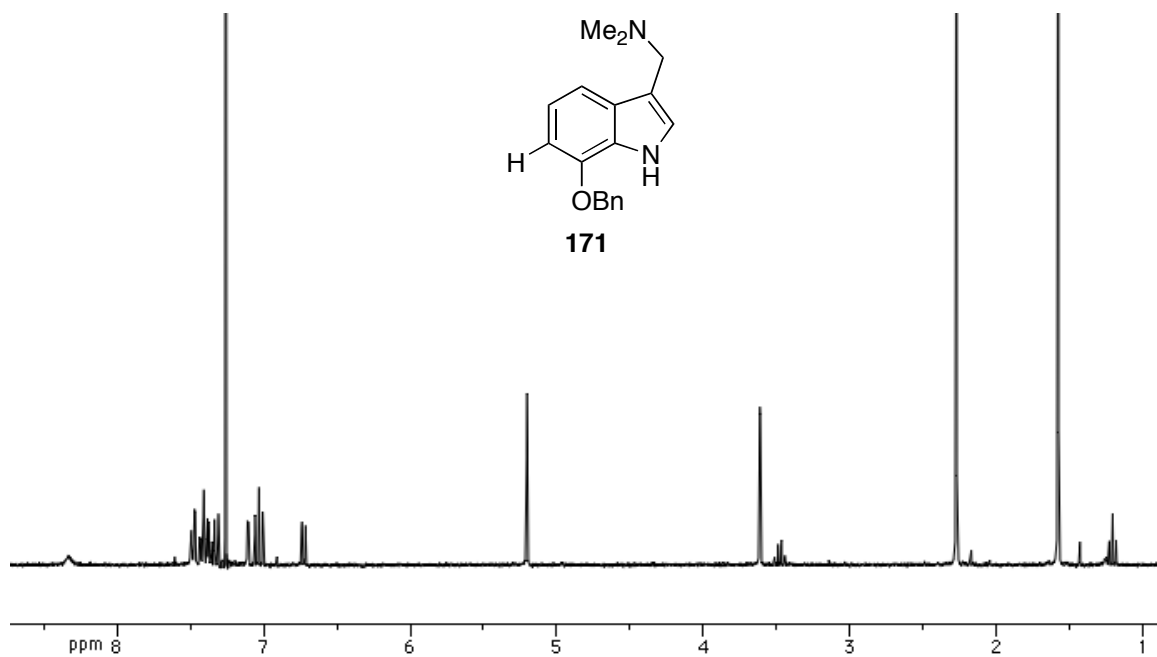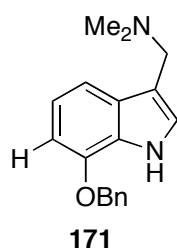
1-(6-(benzyloxy)-1*H*-indol-3-yl)-*N,N*-dimethylmethanamine (172):
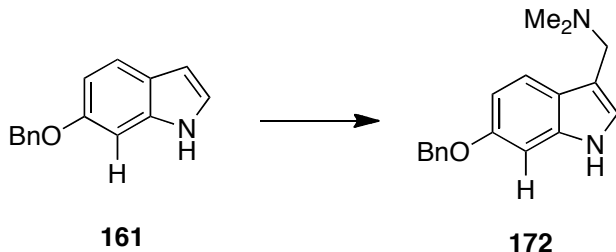
161   **172**

To a solution of glacial acetic acid (1.6 mL) in 37% aqueous formaldehyde (78.6 μL, 0.968 mmol), 40% aqueous dimethylamine (0.410 mL, 3.64 mmol) was added. A solution of 7-benzyloxyindole (200 mg, 0.857 mmol) in 1 mL of glacial acetic acid was slowly added. The reaction stirred at room temperature for 16 hours. The reaction mixture was diluted with 1N NaOH until pH>10. The aqueous layer was extracted with diethyl ether (3 x 30 mL) and the combined organic layers were dried over Na$_2$SO$_4$ and concentrated. Crude yield: 218 mg, 0.780 mmol, 91%.

^{1}H-NMR (300 MHz, CDCl$_3$) δ 7.96 (bs, 1H), 7.58 (d, *J* = 8.4 Hz, 1H), 7.48-7.31 (m, 5H), 7.01 (d, *J* = 2.4 Hz, 1H), 6.92-6.87 (m, 2H), 5.10 (s, 2H), 3.58 (2H), 2.27 (s, 6H). (jmf-01-049)

172
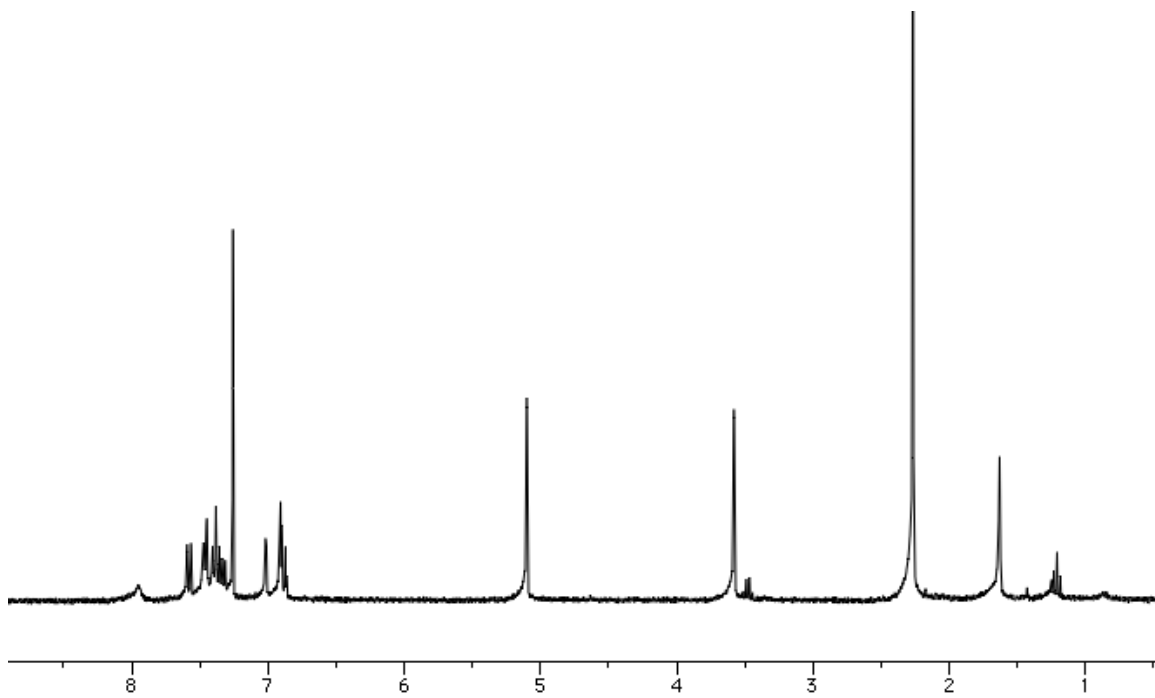
Ethyl 3-(7-(benzyloxy)-1H-indol-3-yl)-2-((diphenylmethylene)amino)propanoate (173):
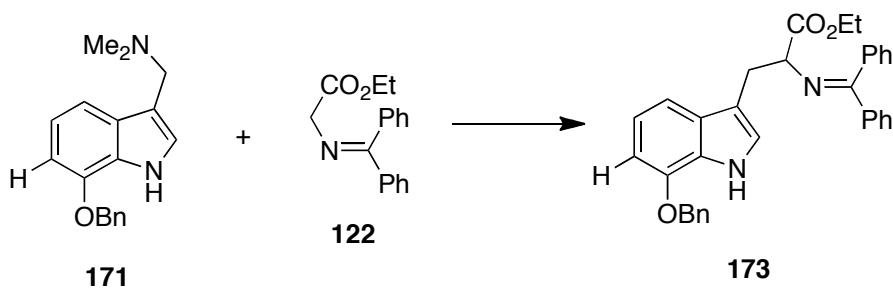
The gramine (115 mg, 0.411 mmol), glycine benzophenone imine (100 mg, 0.347 mmol) and ^{n}Bu$_3$P (37 μL, 0.15 mmol) were dissolved in MeCN (1.87 mL) in a large microwave reaction flask. The mixture was heated to 130°C for 30 minutes. The reaction mixture was concentrated and used without further purification. Crude yield: 206 mg, 0.411 mmol.

Ethyl 3-(6-(benzyloxy)-1H-indol-3-yl)-2-((diphenylmethylene)amino)propanoate (174):
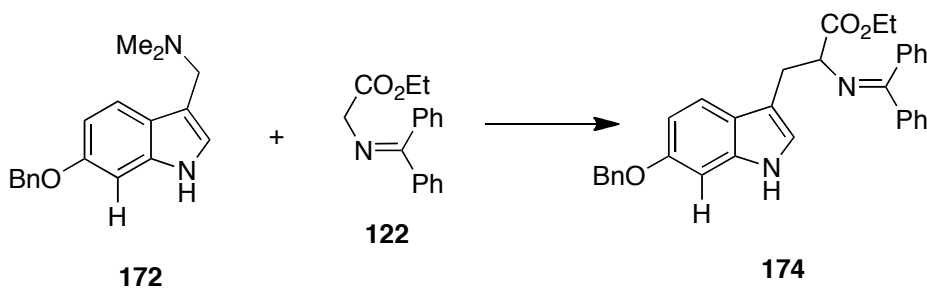
The gramine (115 mg, 0.411 mmol), glycine benzophenone imine (100 mg, 0.347 mmol) and ^{n}Bu$_3$P (37 μL, 0.15 mmol) were dissolved in MeCN (1.87 mL) in a large microwave reaction flask. The mixture was heated to 130°C for 30 minutes. The reaction mixture was concentrated and used without further purification. Crude yield: 206 mg, 0.411 mmol.

Ethyl 2-amino-3-(7-(benzyloxy)-1H-indol-3-yl)propanoate (175):
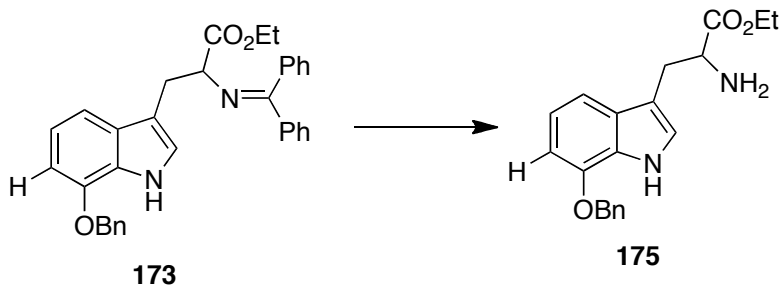
The imine (206 mg, 0.411 mmol) was dissolved in 3 mL of THF and 1N HCl (1 mL) and the reaction stirred for 30 minutes. The THF was removed under vacuum and the residue with diluted with NaHCO₃ until basic. The aqueous layer was extracted with DCM and the combined organic layers were dried over Na₂SO₄ and concentrated. The crude material was purified via flash column chromatography in 3:1 hexanes:ethyl acetate and then flushed with 5% MeOH in DCM to obtain pure **175**. Yield: 89.6 mg, 0.265 mmol, 76%.

^{1}H-NMR (300 MHz, CDCl₃) δ 8.40 (bs, 1H), 7.49-7.35 (m, 5H), 7.25 (d, J = 7.5 Hz, 1H), 7.02 (t, J = 7.8 Hz, 2H), 6.72 (d, J = 7.8 Hz, 1H), 5.19 (s, 2H), 4.16 (q, J = 7.2, 6.9 Hz, 2H), 3.81 (bs, 2H), 3.26 (dd, J = 14.4, 4.8 Hz, 1H), 3.02 (dd, J = 14.4, 7.8 Hz, 1H), 1.28-
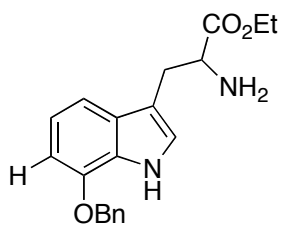
175
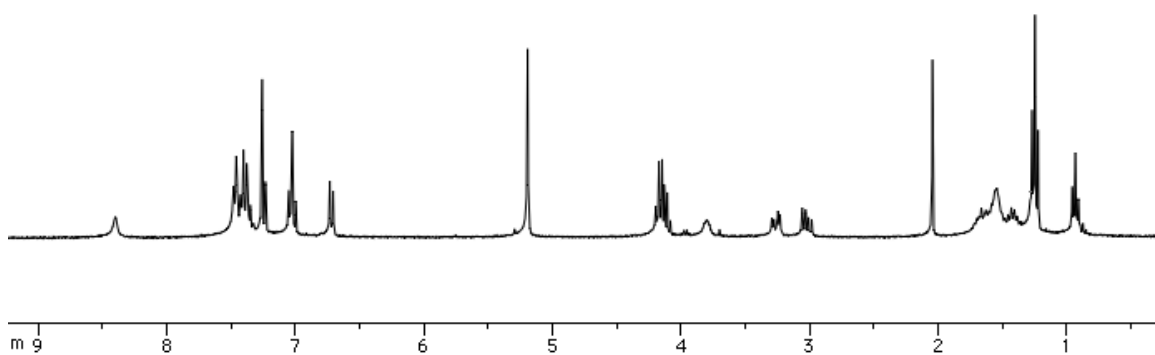
Ethyl 2-amino-3-(6-(benzyloxy)-1H-indol-3-yl)propanoate (176):
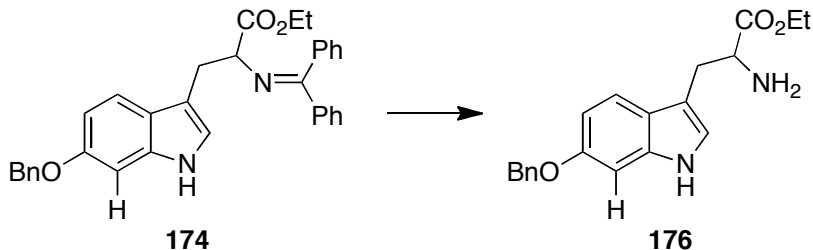
The imine (206 mg, 0.411 mmol) was dissolved in 3 mL of THF and 1N HCl (1 mL) and the reaction stirred for 30 minutes. The THF was removed under vacuum and the residue with diluted with NaHCO$_3$ until basic. The aqueous layer was extracted with DCM and the combined organic layers were dried over Na$_2$SO$_4$ and concentrated. The crude material was purified via flash column chromatography in 3:1 hexanes:ethyl acetate and then flushed with 5% MeOH in DCM to obtain pure **176**. Yield: 110 mg, 0.325 mmol, 93%.

^{1}H-NMR (300 MHz, CDCl$_3$) δ 8.02 (bs, 1H), 7.51-7.32 (m, 6H), 6.96-6.87 (m, 3H), 5.10 (s, 2H), 4.16 (q, J = 6.9, 7.2 Hz, 2H), 3.81-3.77 (m, 1H), 3.24 (dd, J = 14.4, 4.8 Hz, 1H), 3.00 (dd, J = 14.4, 7.8 Hz, 1H), 1.24 (t, J = 7.2 Hz, 3H). (jmf-01-052)

176
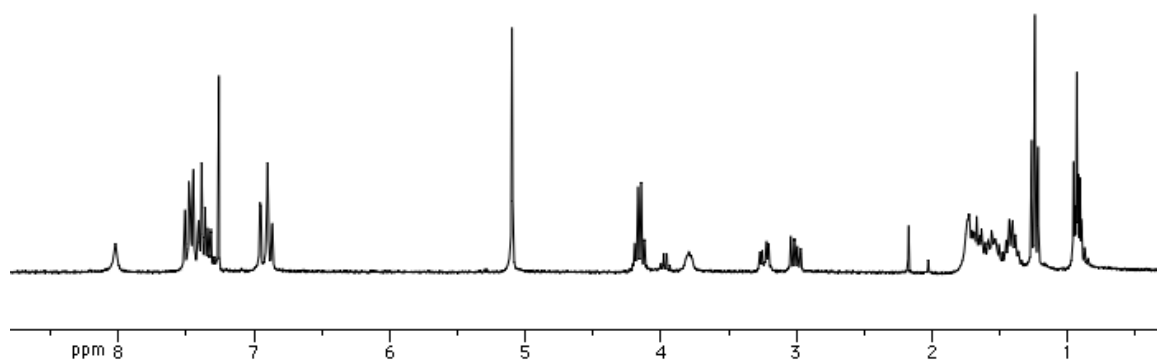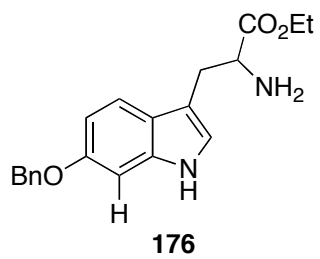
Ethyl   3-(7-(benzyloxy)-1H-indol-3-yl)-2-((tert-butoxycarbonyl)amino)propanoate (177):
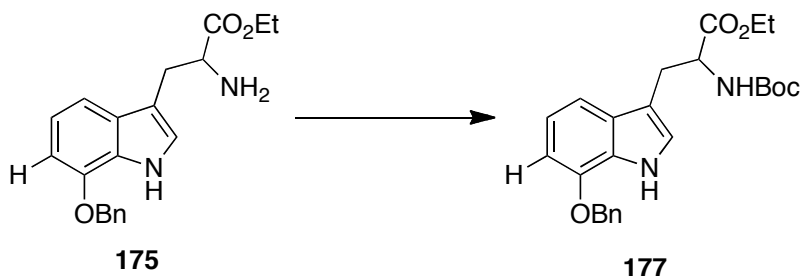
The amine (89.6 mg, 0.265 mmol) was dissolved in 1.33 mL of dioxane and cooled to 0°C. Di-*tert*-butyldicarbonate (63.7 mg, 0.292 mmol) and aqueous 0.5 M NaOH (53 μL) were added to the solution.   The reaction mixture was allowed to warm to room temperature while stirring for 2 hours.   The solvent was removed in vacuo and the remaining residue was taken up in H_2O and acidified with 10% $KHSO_4$ to pH 2.   The product was extracted with ethyl acetate (3 x 20 mL) and the combined organic layer was washed with brine, dried over Na_2SO_4 and concentrated.   The crude material was taken on without further purification. Crude yield: 100 mg, 0.228 mmol, 86%.

^{1}H-NMR (300 MHz, CDCl3) δ 8.42 (bs, 1H), 7.49-7.35 (m, 5H), 7.19 (d, *J* = 8.1 Hz, 1H), 7.02 (t, *J* = 8.1 Hz, 1H), 6.96 (m, 1H), 6.71 (d, *J* = 7.5 Hz, 1H), 5.19 (s, 2H), 5.10 (d, *J* = 8.1 Hz, 1H), 4.65-4.59 (m, 1H), 4.12 (q, *J* = 7.2, 6.9 Hz, 2H), 3.27 (d, *J* = 5.4 Hz, 2H), 1.43 (s, 9H), 1.20 (t, *J* = 7.2 Hz, 3H). (jmf-01-057)

177
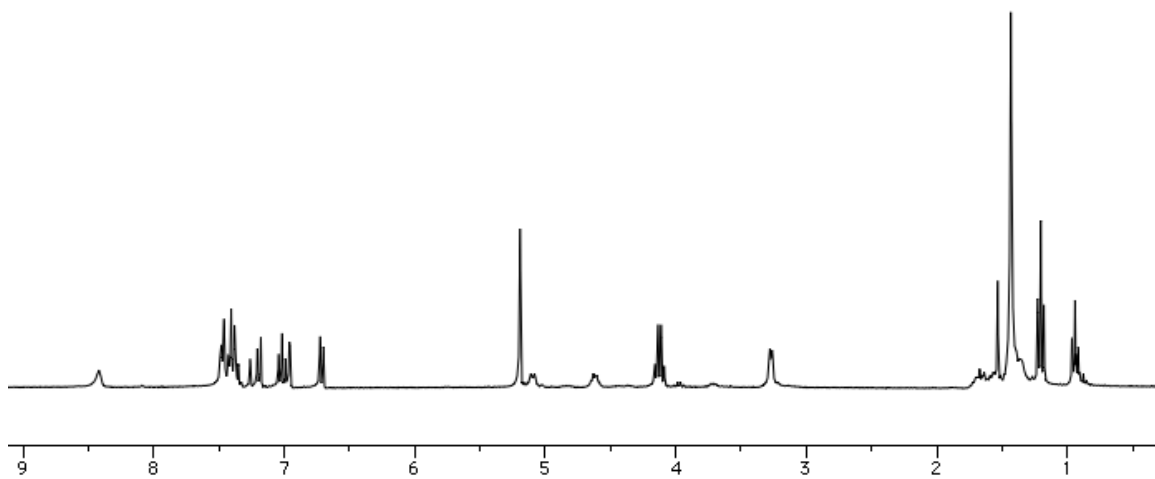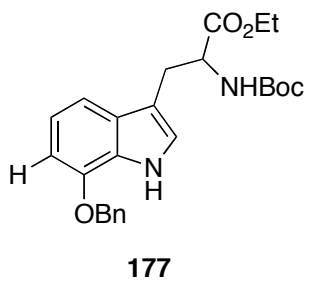
Ethyl 3-(6-(benzyloxy)-1H-indol-3-yl)-2-((tert-butoxycarbonyl)amino)propanoate (178):
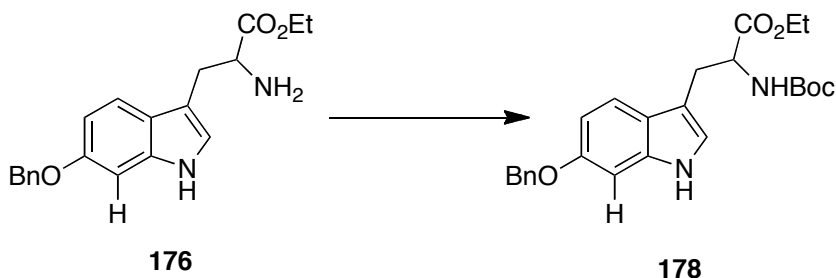
The amine (110 mg, 0.325 mmol) was dissolved in 1.63 mL of dioxane and cooled to 0°C. Di-*tert*-butyldicarbonate (78.1 mg, 0.358 mmol) and aqueous 0.5 M NaOH (65 μL) were added to the solution. The reaction mixture was allowed to warm to room temperature while stirring for 2 hours. The solvent was removed in vacuo and the remaining residue was taken up in H_2O and acidified with 10% $KHSO_4$ to pH 2. The product was extracted with ethyl acetate (3 x 20 mL) and the combined organic layer was washed with brine, dried over Na_2SO_4 and concentrated. Crude yield: 140 mg, 0.319 mmol, 98%.

^{1}H-NMR (300 MHz, CDCl$_3$) δ 7.96 (bs, 1H), 7.47-7.31 (m, 6H), 6.89-6.85 (m, 3H), 5.09 (s, 2H), 4.62-4.56 (m, 1H), 4.11 (q, $J = 7.2$, 7.2 Hz, 2H), 3.24 (d, $J = 5.4$ Hz, 2H), 1.42 (s, 9H), 1.19 (t, $J = 7.2$ Hz, 3H). (jmf-01-053)
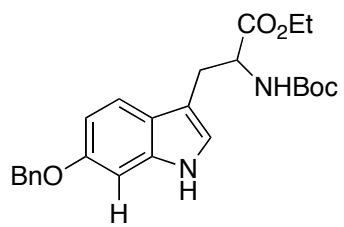
178
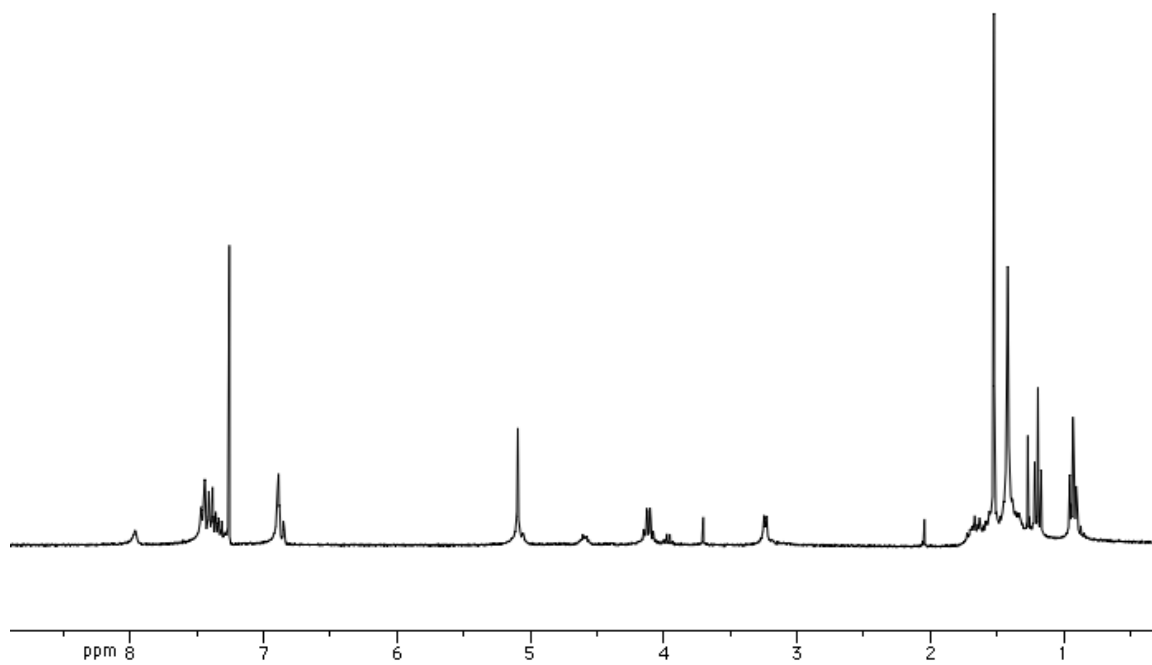
3-(7-(benzyloxy)-1H-indol-3-yl)-2-((tert-butoxycarbonyl)amino)propanoic   acid (162):
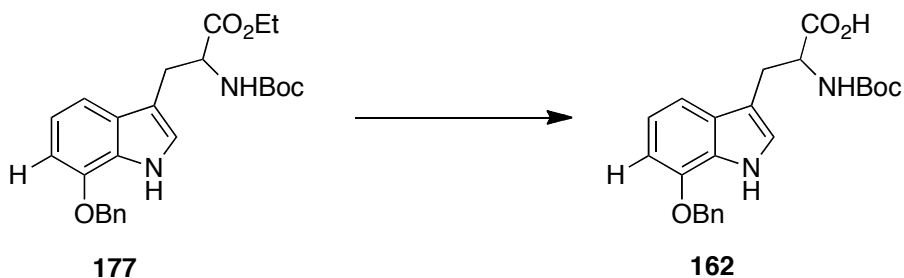
The ester (100 mg, 0.228 mmol) was dissolved in 6 mL of THF and 3 mL of H_2O. To the solution, LiOH (27 mg, 1.14 mmol) was added and the reaction stirred at room temperature for 18 hours. The solvent was removed under vacuum and the resulting slurry was acidified with 1M $KHSO_4$ to pH 2. The product was extracted with DCM (3 x 35 mL) and EtOAc (35 mL). The combined organic layers were dried over Na_2SO_4 and concentrated. Crude yield: 81 mg, 0.198 mmol, 87%.

^{1}H-NMR (300 MHz, CDCl$_3$) δ 11.18 (bs, 1H), 8.44 (bs, 1H), 7.46-7.37 (m, 5H), 7.24 (d, J = 10.5 Hz, 1H), 7.02-6.87 (m, 2H), 6.69 (d, J = 7.5 Hz, 1H), 5.16 (s, 2H), 4.66 (m, 1H), 3.39-3.23 (m, 2H), 1.43 (s, 9H). (jmf-01-058)

162
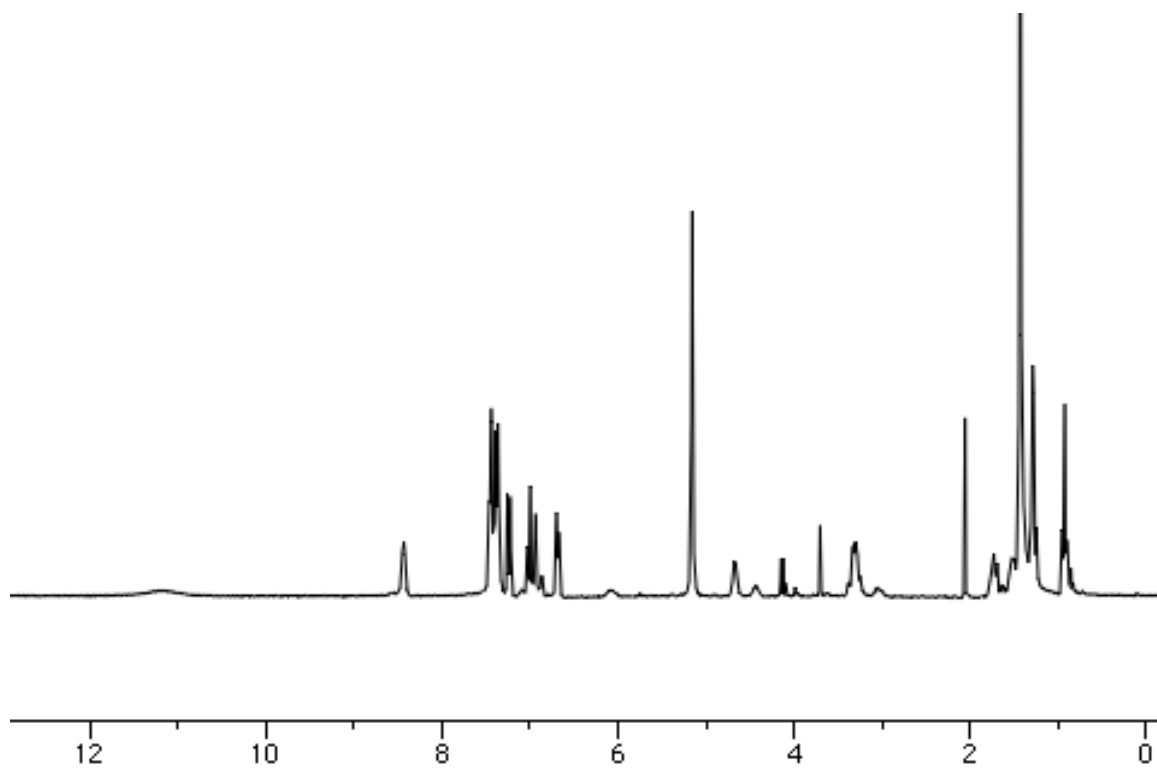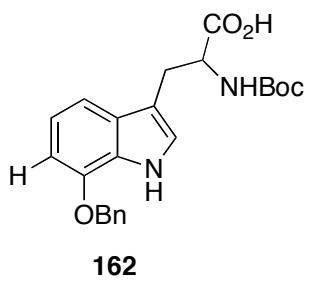
3-(6-(benzyloxy)-1H-indol-3-yl)-2-((tert-butoxycarbonyl)amino)propanoic   acid (163):
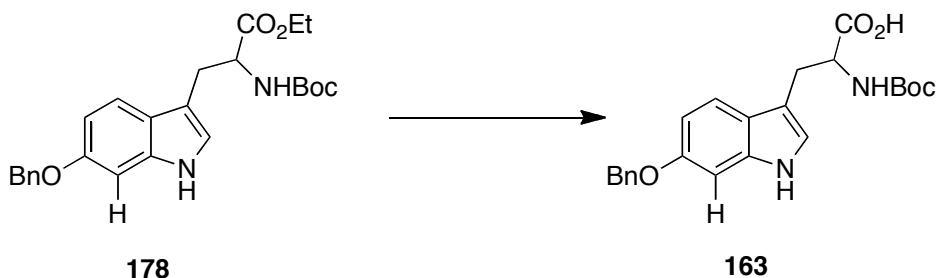
The ester (140 mg, 0.319 mmol) was dissolved in 8 mL of THF and 4 mL of H_2O. To the solution, LiOH (38 mg, 1.60 mmol) was added and the reaction stirred at room temperature for 18 hours. The solvent was removed under vacuum and the resulting slurry was acidified with 1M $KHSO_4$ to pH 2. The product was extracted with DCM (3 x 35 mL) and EtOAc (35 mL). The combined organic layers were dried over Na_2SO_4 and concentrated. Crude yield: 116 mg, 0.283 mmol, 89%.

^{1}H-NMR (300 MHz, CDCl$_3$) δ 10.18 (bs, 1H), 8.23 (bs, 1H), 7.48-7.26 (m, 6H), 6.83 (d, J = 9.0 Hz, 3H), 5.12 (d, J = 7.5 Hz, 1H), 5.04 (s, 2H), 4.65 (m, 1H), 4.3.34-3.19 (m, 1H), 1.42 (s, 9H). (jmf-01-054)

163
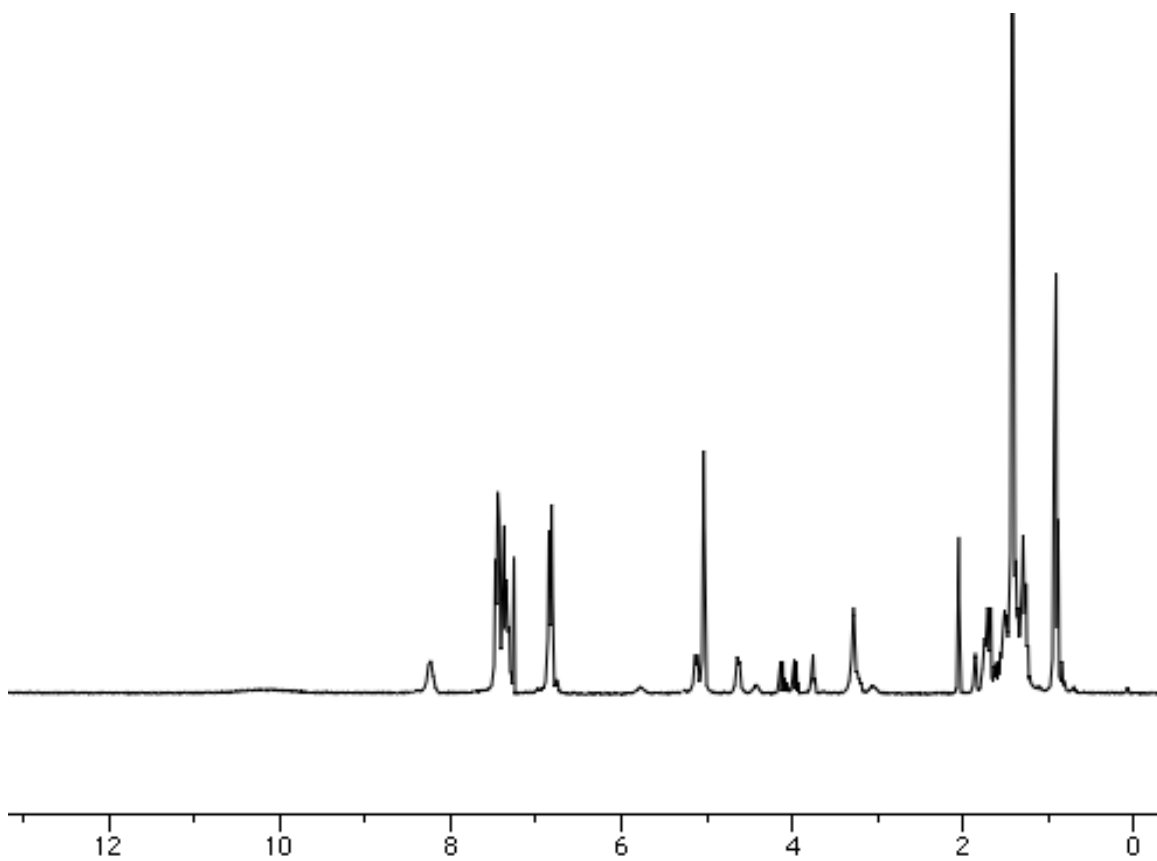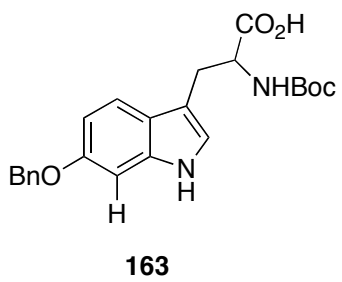
(*R*)-N-(1-phenylethyl)but-3-en-1-amine (181):
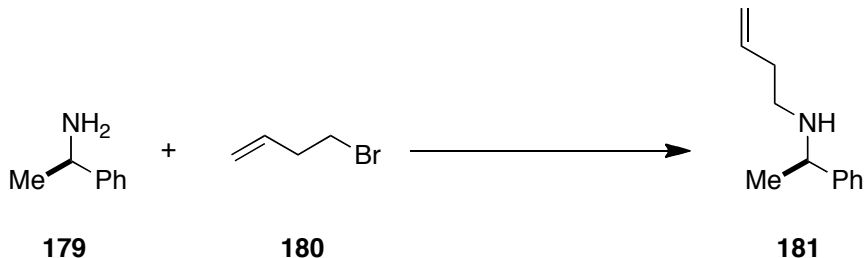
To a stirred solution of *R*-(+)-α-Methyl-benzylamine (5.00 g, 41.3 mmol) in dry DMF (50 mL) was added K$_2$CO$_3$ (18.8 g, 136 mmol) and NaI (20.4 g, 136 mmol) at room temperature under argon. To this solution, 4-bromo-1-butene (5.05 g, 37.6 mmol) was added and the reaction mixture stirred at 100°C for 22 hours. The reaction mixture was cooled to room temperature, diluted with diethyl ether (100 mL) and water (100 mL). The phases were separated and the aqueous layer was extracted twice with diethyl ether (50 mL) and once with methylene chloride (50 mL). The combined organic phases were dried over anhydrous Na$_2$SO$_4$ and concentrated. The crude oil was purified via flash column chromatography (hexane/diethyl ether: 90:10) to yield **181** as a clear yellow oil. Yield: 4.0 g, 22.8 mmol, 61%.

^{1}H-NMR (CDCl$_3$, 300 MHz) δ 1.37 (d, *J* = 6.6 Hz, 3H), 2.24 (m, 2H), 2.55 (m, 2H), 3.78 (q, *J* = 6.6 Hz, 1H), 5.03 (d, i = 10.3 Hz, 1H), 5.08 (d, *J* = 17.9, 1H), 5.76 (ddt, *J* = 6.6, 10.3, 17.2 Hz, 1H), 7.20-7.38 (m, 5H). (jmf-01-014)
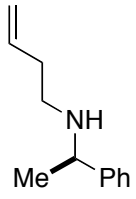
181
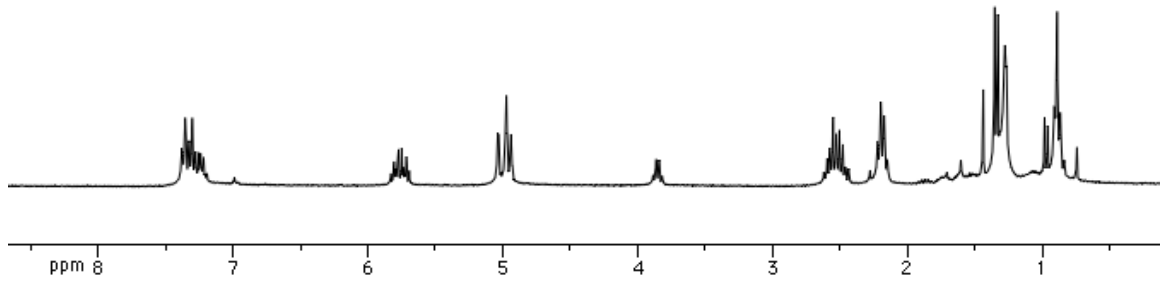
(*R*)-ethyl 2-(but-3-en-1-yl(1-phenylethyl)amino)acetate (182):
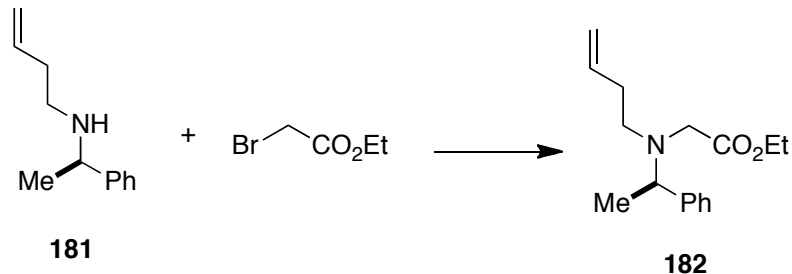
To a stirred solution of **181** (1.0 g, 5.70 mmol) in dry DMSO (6 mL) was slowly added

ethyl bromoacetate (0.351 mL, 3.17 mmol); after 30 minutes of stirring, dry NEt₃ (0.442

mL, 3.17 mmol) was slowly added followed by a new addition of ethyl bromoacetate

(0.351 mL, 3.17 mmol) and NEt₃ (0.442 mL, 3.17 mmol). The reaction mixture was

heated to 65°C for 46 hours, cooled to room temperature, and diluted with diethyl ether

(15 mL). Water (15 mL) was added and the separated organic phase was washed with

brine (15 mL). The organic phase was dried over anhydrous Na₂SO₄ and concentrated

under vacuum. To crude oil was purified by heating the reaction flask to 60°C while

under vacuum overnight, providing a clear yellow oil. Yield: 864 mg, 3.3 mmol, 58%.

¹H-NMR (CDCl₃, 300 MHz) δ 1.27 (t, *J* = 7.0 Hz, 3H), 1.36 (d, *J* = 6.6 Hz, 3H), 2.12-

2.30 (m, 2H), 2.60-2.78 (m, 2H), 3.30 (1/2ABq, *J* = 17.2 Hz, 1H) 3.45 (1/2ABq, i = 17.2

Hz, 1H), 4.06 (q, *J* = 7.0 Hz, 1H), 4.15 (q, *J* = 7.3 Hz, 2H), 4.97 (dq, *J* = 1.2, 10.5 Hz,

1H), 5.01 (dq, *J* = 1.8, 17.6 Hz, 1H), 5.76 (ddt, *J* = 6.6, 10.3, 17.2 Hz, 1H), 7.23 (t, *J* =

7.3 Hz, 1H), 7.31 (t, *J* = 7.7 Hz, 2H) 7.37 (t, *J* = 7.0 Hz, 2H). (jmf-01-021)
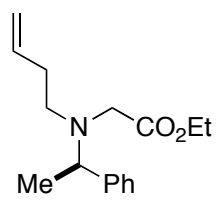
182
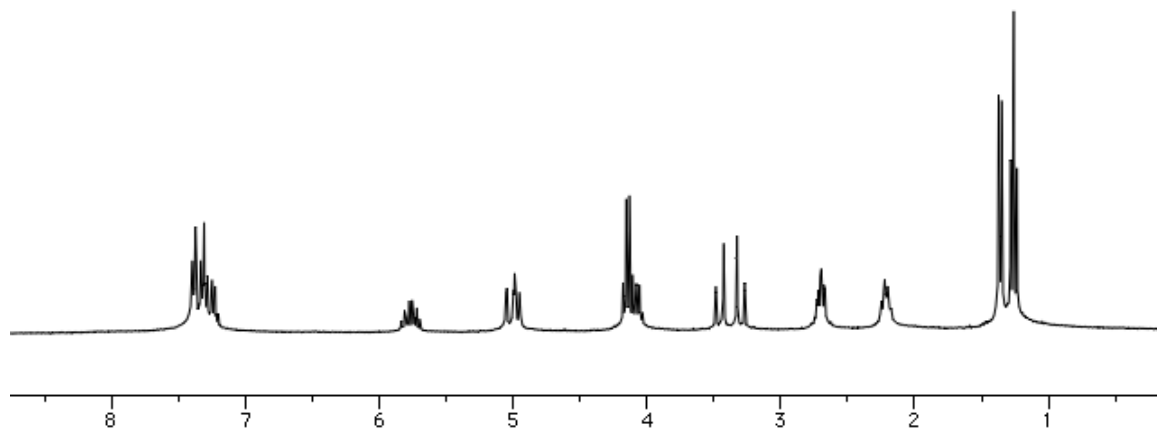
(2*R*,3*S*)-ethyl 3-methyl-1-((*R*)-1-phenylethyl)pyrrolidine-2-carboxylate (183):

182   **183**
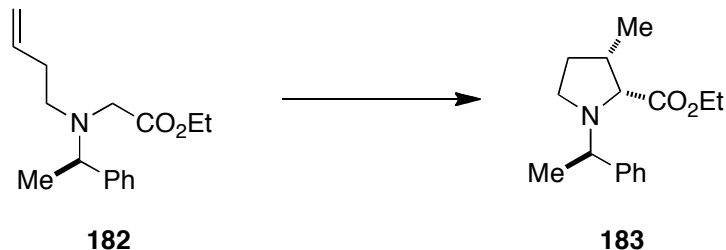
To a solution of **182** (400 mg, 1.54 mmol) in dry diethyl ether (6 mL) was added a solution of freshly prepared LDA (1.8 M) at -78°C. The temperature was raised to -20°C and then cooled back down to -78°C. Freshly prepared 1 M solution of anhydrous ZnBr$_2$ (1.21 g, 4.62 mmol) in 4 mL of dry diethyl ether was added dropwise. The reaction mixture was removed from the ice bath and warmed to room temperature overnight. The reaction mixture was quenched with saturated aqueous NH$_4$Cl (5 mL) and diluted with diethyl ether (5 mL). The phases were separated and the aqueous layer was extracted twice with diethyl ether (2 x 15 mL). The combined organic phases were dried over anhydrous Na$_2$SO$_4$ and concentrated under vacuum. The crude oil was purified via flash column chromatography (hexane/diethyl ether, 70:30) to yield **183** as a clear yellow oil. Yield: 193 mg, 0.740 mmol, 48%.

^{1}H-NMR (CDCl$_3$, 300 MHz) δ 0.92 (d, *J* = 7.0 Hz, 3H), 1.21 (t, *J* = 7.3 Hz, 3H), 1.35 (d, *J* = 6.9 Hz, 3H), 1.52-1.70 (m, 1H), 1.88-2.02 (m, 1H), 2.32-2.50 (m, 1H) 2.78-2.90 (m, 1H), 2.96-3.03 (m, 1H), 3.31 (d, *J* = 8.4 Hz, 1H), 3.62-3.76 (m, 1H), 4.09 (q, *J* = 7.0 Hz, 2H), 7.18-7.32 (m, 5H). (jmf-01-020)
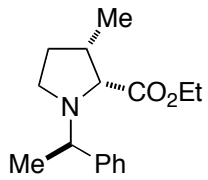
183
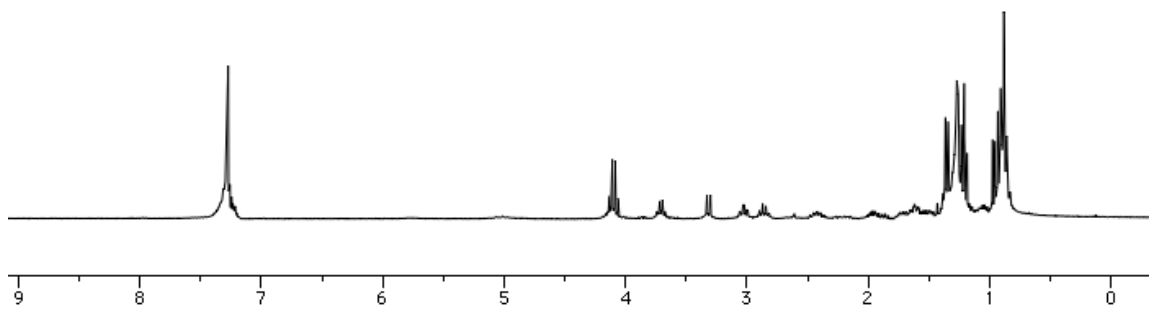
(2*R*,3*S*)-1-tert-butyl 2-ethyl 2-allyl-3-methylpyrrolidine-1,2-dicarboxylate (186):

185   **186**
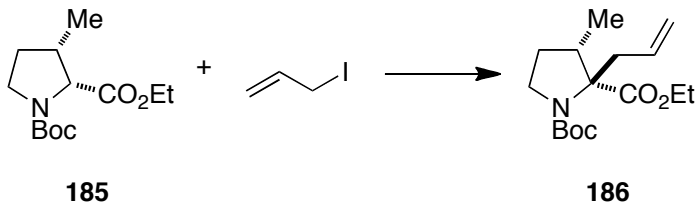
Proline (50 mg, 0.194 mmol) was dissolved in 2 mL of THF and the solution was cooled to -78°C. A 1M solution of sodium bis(trimethylsilyl)amide in THF (1.52 mL, 0.388 mmol) was added and the reaction stirred for 30 minutes. To the cooled solution, allyl iodide (35.5 μL, 0.388 mmol) was added and the mixture warmed to room temperature while stirring for 20 hours. The reaction was quenched with saturated aqueous NH$_4$Cl and extracted with ethyl acetate (3 x 15 mL). The combined organic layer was washed with brine, dried over Na$_2$SO$_4$ and concentrated. The crude product was purified via flash column chromatography (hexanes/ethyl acetate, 95:5). Yield: 14 mg, 0.049 mmol, 25%.

^{1}H-NMR (300 MHz, CDCl$_3$) δ 5.73-5.59 (m, 1H), 5.13-5.07 (m, 2H), 4.23-4.04 (m, 2H), 3.82-3.66 (m, 1H), 3.24-3.10 (m, 1H), 3.04-2.97 (m, 1H), 2.52-2.25 (m, 2H), 1.81-1.65 (m, 2H), 1.41 (s, 9H), 1.27 (t, *J* = 7.2 Hz, 3H), 0.92 (dd, *J* = 6.9, 1.5 Hz, 3H); (jmf-01-002)
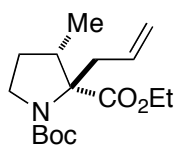
186
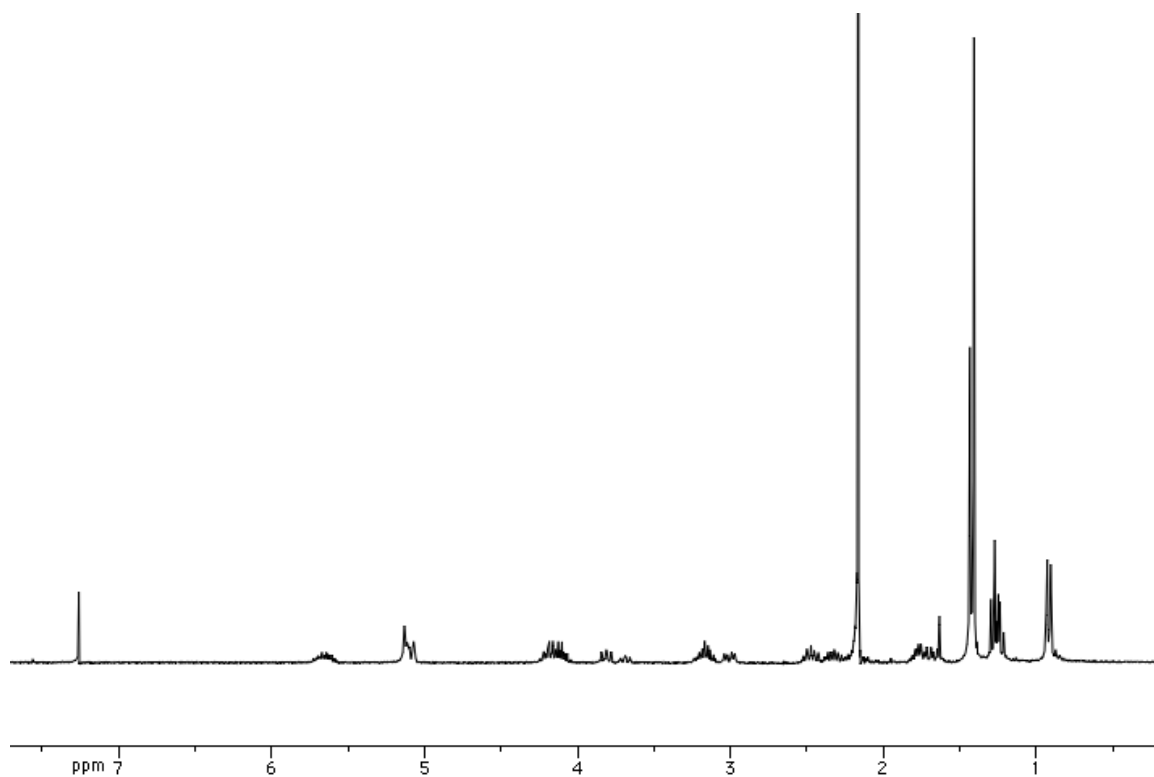
4-(benzyloxy)-1-methyl-2-nitrobenzene (199):
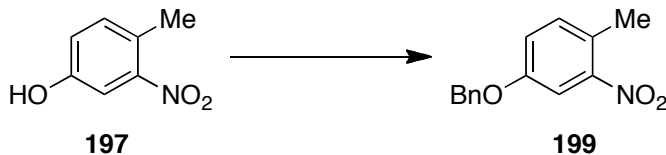
Commercially available nitrophenol (1.0 g, 6.53 mmol) was dissolved in 6.5 mL of DMF. Benzyl chloride (0.826 mL, 7.18 mmol) and potassium carbonate (0.903 mg, 6.53 mmol) were added and the reaction mixture stirred for 4 hours at 100°C. The reaction mixture cooled to room temperature and was poured into 15 ml of water and extracted with ethyl acetate (3 x 30 mL). The organic layer was washed with 30 mL of each 1M sodium hydroxide, water, and brine, then dried over Na_2SO_4 and concentrated under vacuum. The residue was recrystallized from ethyl acetate and hexanes to afford the pure desired product. Yield: 1.22 g, 5.03 mmol, 77%.

^{1}H-NMR (300 MHz, CDCl$_3$) δ 7.60 (d, J = 2.7 Hz, 1H), 7.44-7.33 (m, 5H), 7.23 (d, J = 8.4 Hz, 1H), 7.12 (dd, J = 8.7, 2.7 Hz, 1H), 5.10 (s, 2H), 2.53 (s, 3H); HRMS (ESI/APCI) calcd for (NH$_2$ not NO$_2$) $C_{14}H_{16}NO$ (M+H) 214.1226, found 214.1231. (jmf-01-197)
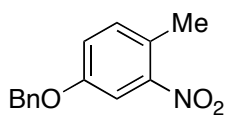
199
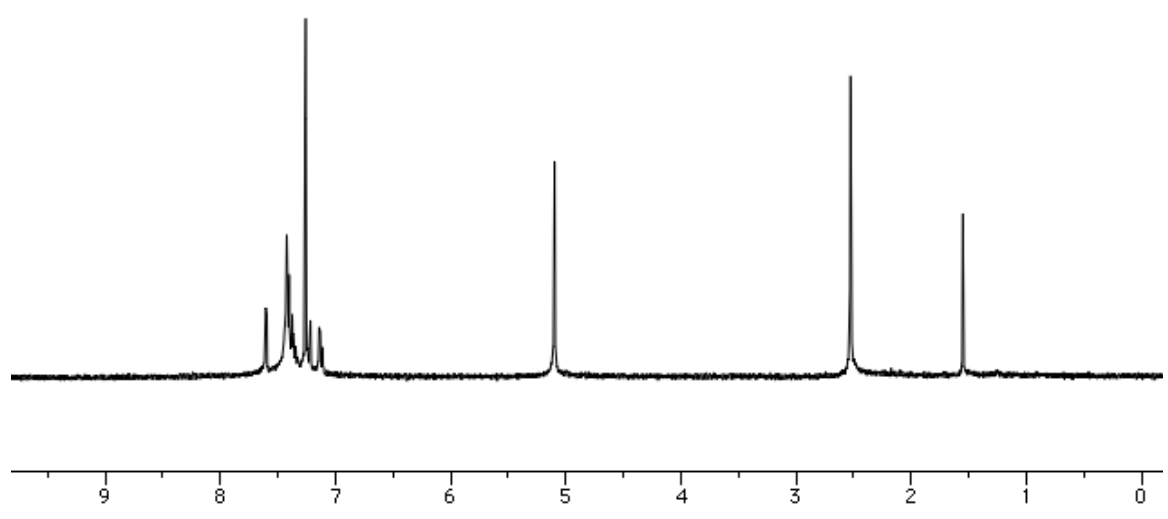
(*E*)-1-(4-(benzyloxy)-2-nitrostyryl)pyrrolidine (201):
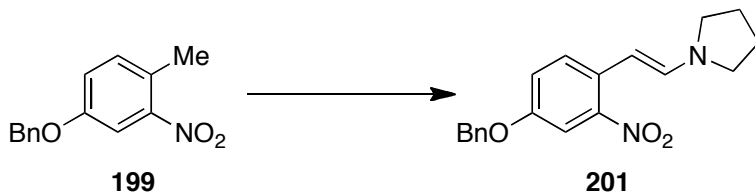
Compound **199** (1.06 g, 4.36 mmol) was dissolved in DMF-DMA (1.74 mL, 13.08 mmol) and pyrrolidine (1.09 mL, 13.08 mmol). The reaction mixture was heated to 110°C and stirred for 19 hours. The mixture was cooled to room temperature and ethanol was added. The solution was filtered to afford red/black/gold crystals. Yield: 1.33 g, 4.10 mmol, 94%.

^{1}H-NMR (300 MHz, CDCl$_3$) δ 7.50 (d, J = 2.7 Hz, 1H), 7.44-7.34 (m, 6H), 7.10 (d, J = 13.5 Hz, 1H), 7.06 (dd, J = 9.0, 2.7 Hz, 1H), 5.86 (d, J = 13.5 Hz, 1H), 5.04 (s, 2H), 3.31-3.27 (m, 4H), 1.95-1.91 (m, 4H); ^{13}C NMR (75 MHz, CDCl$_3$) δ 154.2, 144.4, 139.8, 136.5, 130.3, 128.9, 128.4, 127.9, 122.5, 109.6, 91.7, 70.7, 49.4, 25.5; HRMS (ESI/APCI) calcd for C$_{19}$H$_{21}$N$_2$O$_3$ (M+H) 325.1547, found 325.155. (jmf-02-699)

201
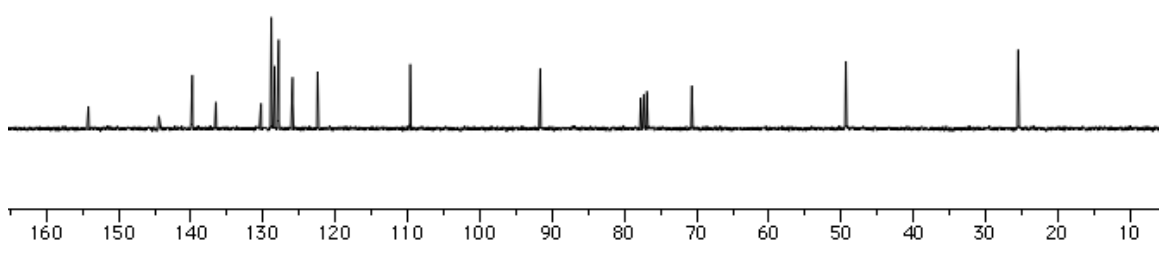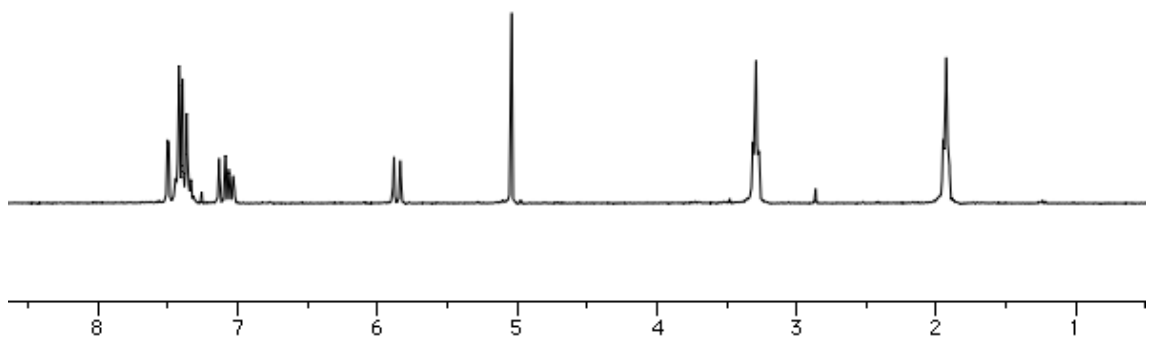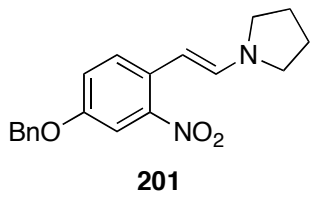
6-(benzyloxy)-1*H*-indole (202):

201 → **202**
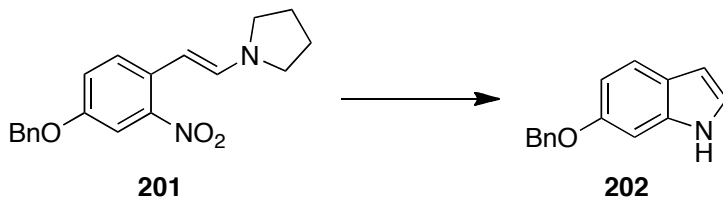
Formation of the Ni$_2$B: To a 0.5 M solution of ethanol (30 mL) and Ni(OAc)$_2$ (3.68 g, 14.8 mmol), NaBH$_4$ (1.12 g, 29.6 mmol) was slowly added portionwise. The reaction mixture stirred for one hour at room temperature.

The enamine (2.18 g, 6.72 mmol) was dissolved in 6.7 mL of ethanol and hydrazine monohydrate (1.43 mL, 29.6 mmol) was added to the solution. The reaction was heated to 80°C and stirred for 1 hour. The mixture was cooled to room temperature and slowly added to the freshly prepared solution of Ni$_2$B. The mixture was heated to 50°C and stirred for an additional hour, after which the reaction cooled to room temperature and was filtered through a pad of celite. The filtrate was concentrated under vacuum and the remaining residue was diluted with 100 mL of ethyl acetate. The organic layer was washed with 1M HCl (150 mL), saturated aqueous NaHCO$_3$ (150 mL), and brine (150 mL). The organic phase was dried over Na$_2$SO$_4$ and concentrated. Crude yield: 1.14 g, 5.11 mmol, 76%.

^{1}H-NMR (300 MHz, CDCl$_3$) δ 8.01 (bs, 1H), 7.54-7.32 (m, 6H), 7.10 (dd, *J* = 3.3, 2.4 Hz, 1H), 6.95 (m, 1H), 6.89 (dd, *J* = 8.7, 2.7 Hz, 1H), 6.50-6.48 (m, 1H), 5.11 (s, 2H); (jmf-01-338)

202
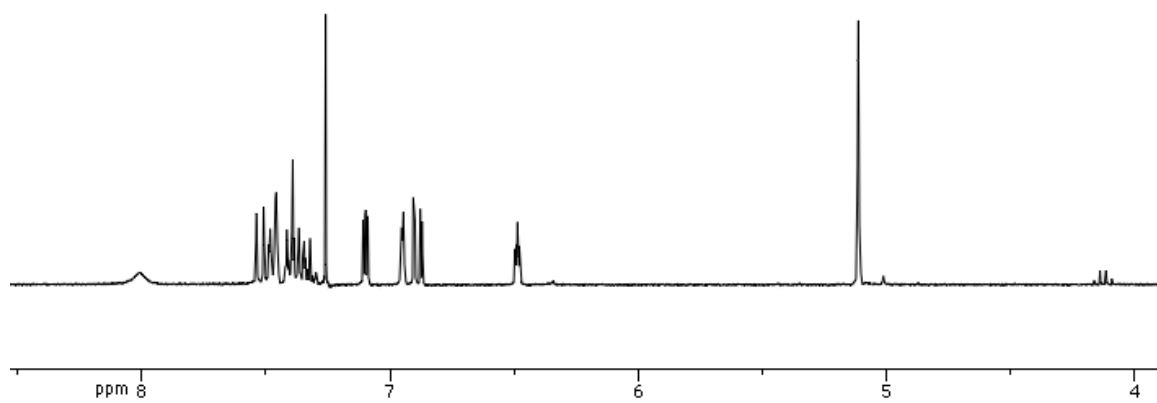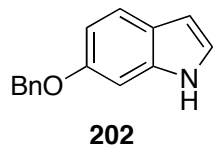
1*H*-indol-6-ol (188):
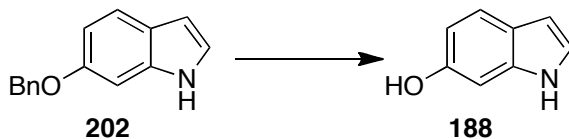
The 6-benzyloxyindole (1.14 g, 5.11 mmol) and 5% Pd/C (3 wt. %) were dissolved in 10 mL of ethanol in a purged hydrogenation vessel. To the reaction, 10 atm. of H_2 was added and the reaction stirred for 3 hours. The reaction mixture was purged with Ar and then filtered through a pad of celite, washing the catalyst with ethanol. The filtrate was concentrated and taken on immediately to the next reaction.

^{1}H-NMR (300 MHz, CDCl$_3$) δ 7.28 (d, J = 9.0 Hz, 1H), 6.92 (d, J = 3.3 Hz, 1H), 6.71 (m, 1H), 6.54 (dd, J = 8.4, 2.1 Hz, 1H), 6.26 (dd, J = 3.3, 0.9 Hz, 1H); ^{13}C NMR (75 MHz, CDCl$_3$) δ 152.8, 137.1, 131.0, 123.2, 121.1, 110.1, 101.9, 97.0; HRMS (ESI/APCI) calcd for C$_8$H$_6$NO (M–H) 132.0455, found 132.0455. (jmf-02-700)

188
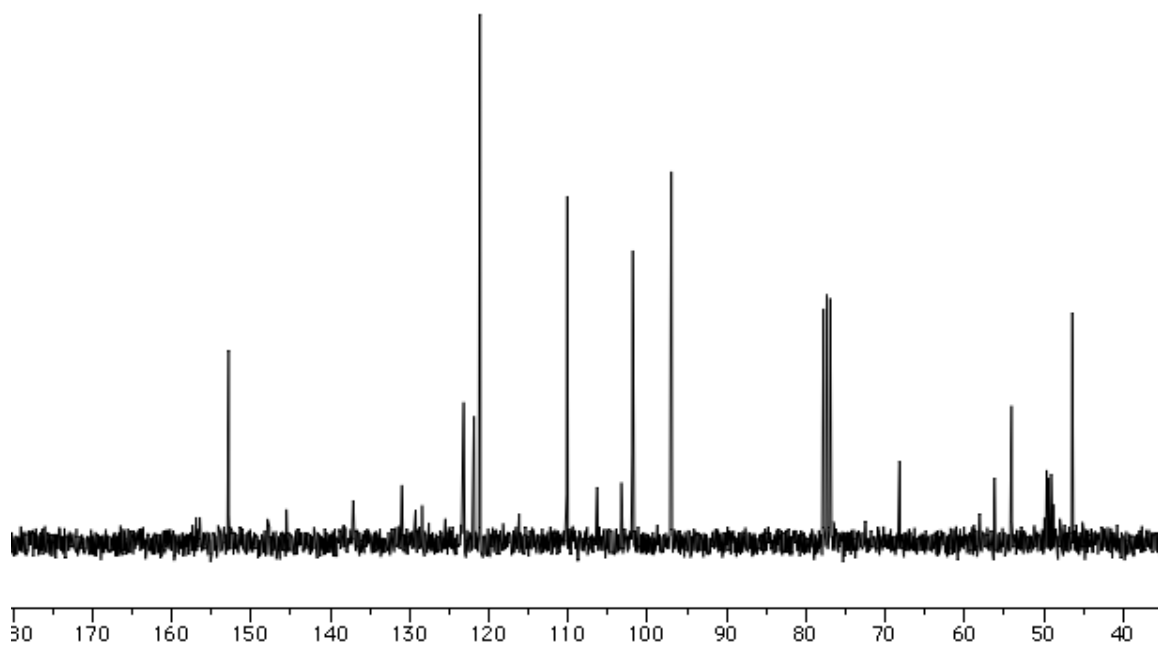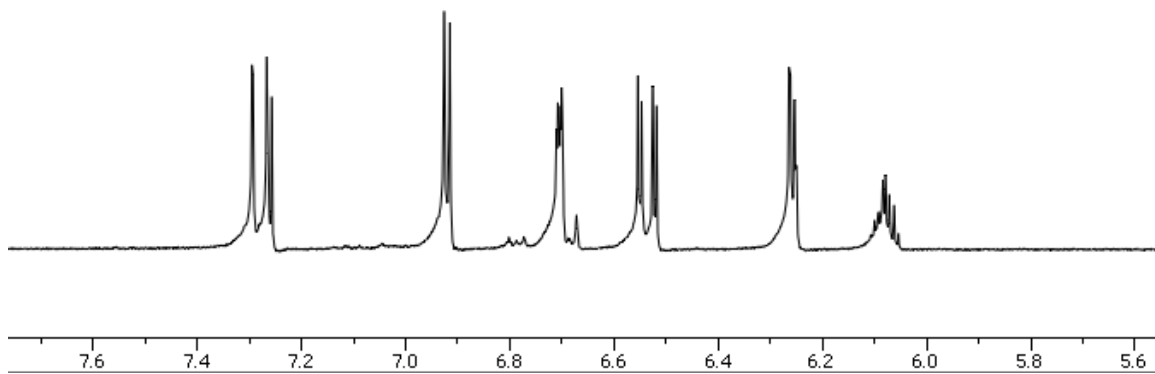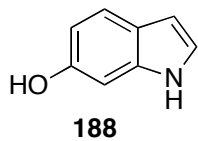
tert-butyl 1H-indol-6-yl carbonate (203):

188 → **203**

Crude 6-hydroxyindole (780 mg, 5.85 mmol) was taken up in acetonitrile (150 mL) and cooled to 0°C. Di-_tert_-butyl dicarbonate (895 mg, 4.09 mmol) and a catalytic amount of DMAP were added and the reaction mixture stirred for 16 hours at room temperature. The reaction was concentrated and purified via flash column chromatography in 95:5 hexanes/ethyl acetate. The product was collected as a white solid. Yield: 960 mg, 4.11 mmol, 70%.

White crystalline solid (mp 141-143ºC). ^{1}H-NMR (300 MHz, CDCl$_3$) δ 8.16 (bs, 1H), 7.60 (d, J = 8.4 Hz, 1H), 7.21 (m, 1H), 7.18 (t, J = 5.7 Hz, 1H) 6.93 (dd, J = 8.7, 2.1 1H), 6.52 (m, 1H), 1.58 (s, 9H); ^{13}C NMR (75 MHz, CDCl$_3$) δ 153.0, 147.0, 135.7, 126.0, 125.2, 121.2, 114.2, 104.0, 102.7, 83.5, 28.0; IR (neat) 3413, 2981, 1738, 1457, 1395, 883, 722 cm^{-1}; HRMS (ESI/APCI) calcd for C$_{13}$H$_{15}$NO$_3$Na (M+Na) 256.0944, found 256.0944. (jmf-02-597)

203
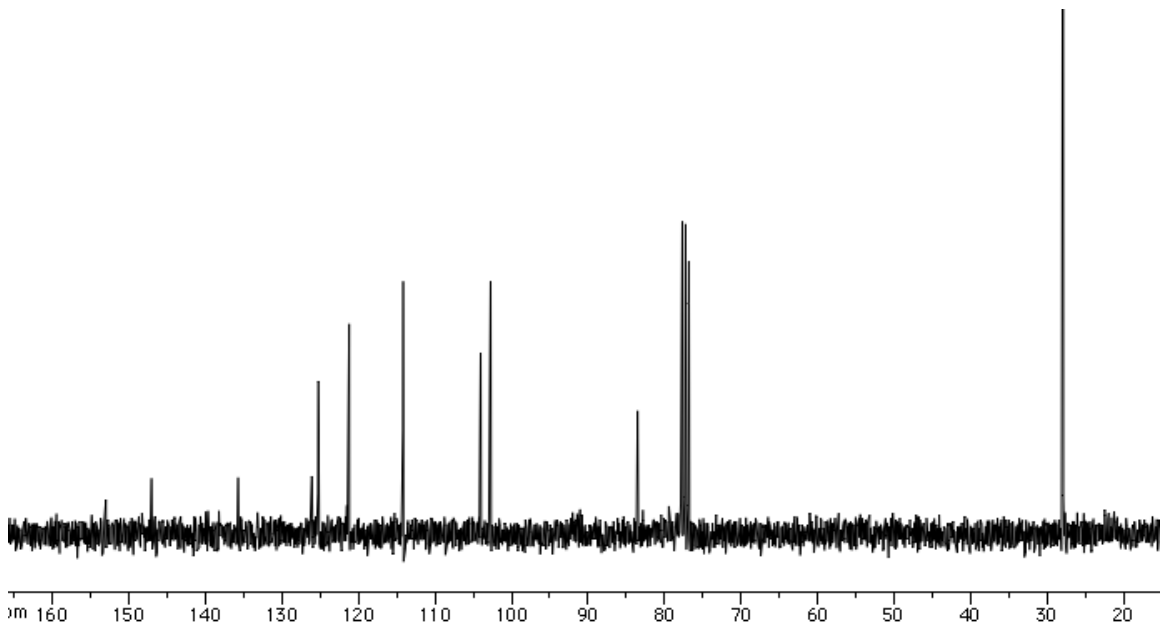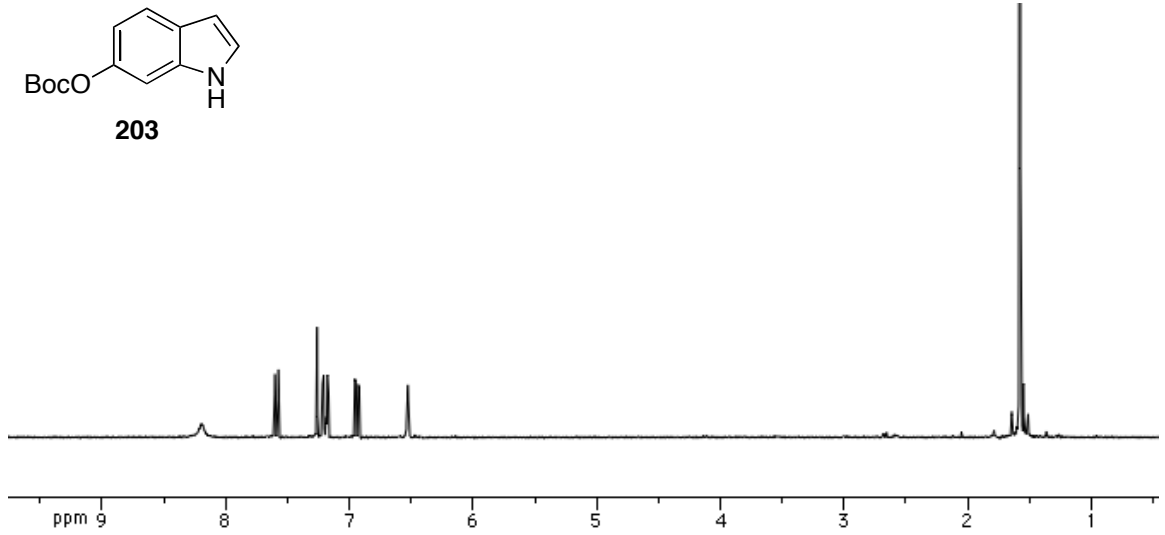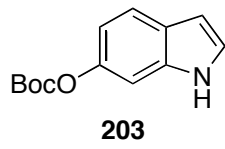
tert-butyl (3-chloro-1H-indol-6-yl) carbonate (204):
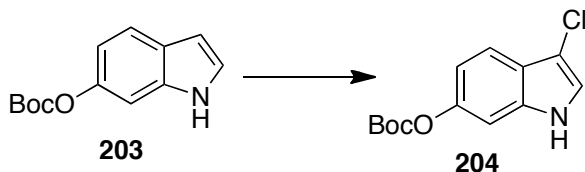
The 6-OBoc indole (7.26 g, 31.1 mmol) was dissolved in 100 mL of DMF and cooled to 0°C. *N*-Chlorosuccinimide (4.16 g, 31.1 mmol) was slowly added to the reaction mixture in portions. The solution stirred for 22 hours while warming to room temperature. The reaction was quenched with brine (20 mL) and extracted with diethyl ether (3 x 35 mL). The combined organic layer was washed 5 times with 35 mL of water, dried over Na_2SO_4, and concentrated. The crude oil was purified via flash column chromatography 85:15 hexanes/ethyl acetate to afford the 3-chloroindole as a white solid (mp 125-128°C). Yield: 6.91 g, 25.8 mmol, 83%.

^{1}H-NMR (300 MHz, CDCl$_3$) δ 8.18 (bs, 1 H), 7.55 (d, *J* = 8.7 Hz, 1H), 7.12 (d, *J* = 1.8 Hz, 1H), 7.04 (d, *J* = 2.4 Hz, 1H), 6.99 (dd, *J* = 8.1, 2.1 Hz, 1H) 1.58 (s, 9H); ^{13}C NMR (75 MHz, CDCl$_3$) δ 153.0, 147.7, 134.8, 123.6, 122.0, 119.0, 114.8, 106.5, 104.6, 84.0, 28.0; HRMS (ESI/APCI) calcd for $C_{13}H_{14}NO_3ClNa$ (M+Na) 290.0054, found 290.0562. (jmf-02-598)

204
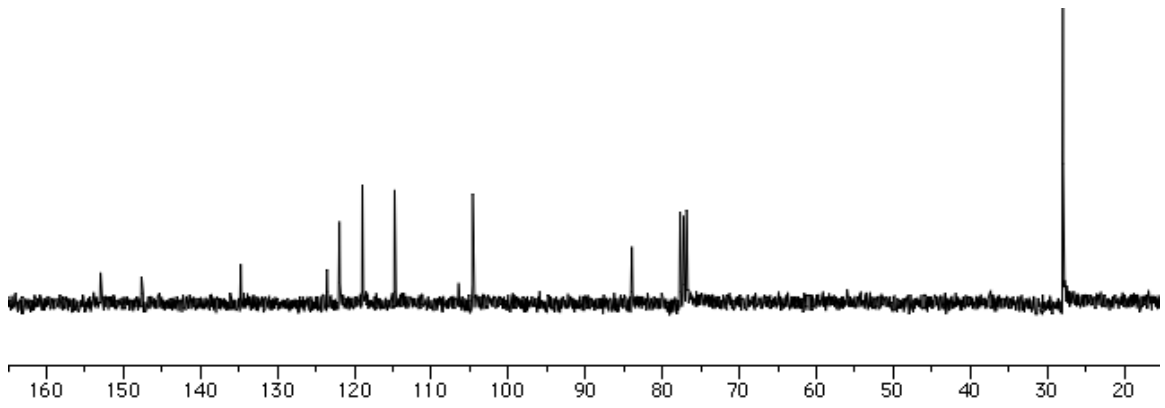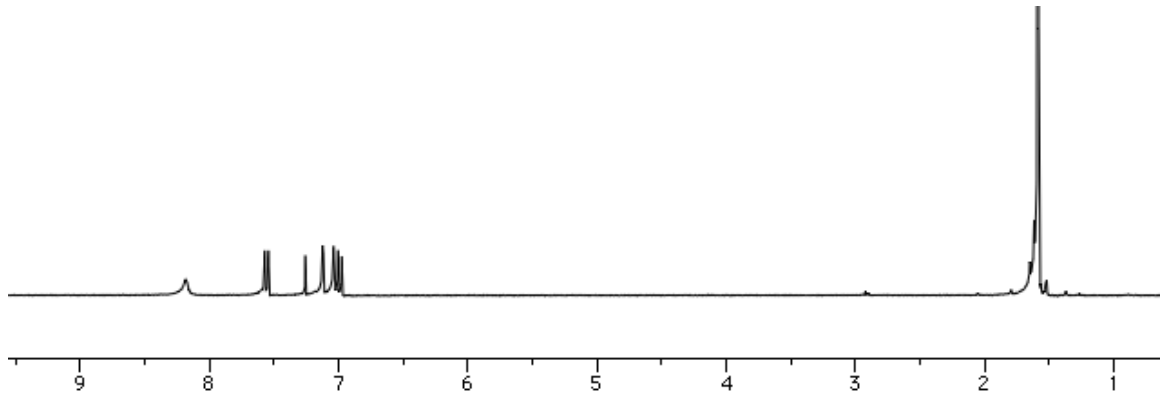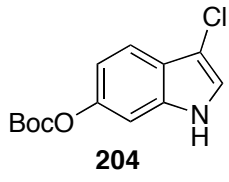
tert-Butyl 2-(2-mthylbut-3-en-2-yl)-1*H*-indol-6-yl carbonate (205):
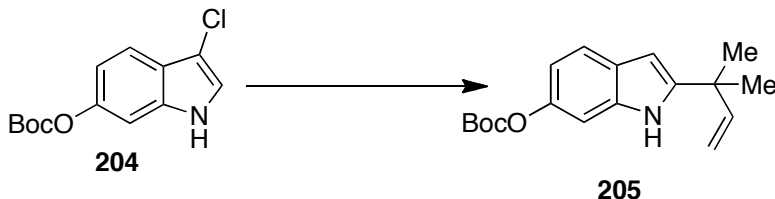
A 0.5M solution of 9-BBN in THF (171 mL, 85.5 mmol) was cooled to 0°C and allene[14] (9.89 mL, 99.8 mmol) was slowly added. The reaction mixture was capped with a yellow cap and wrapped in parafilm. The reaction stirred for 16 hours. Indole **103** (7.63 g, 28.5 mmol) was dissolved in THF (95 mL) and triethylamine (12.9 mL, 92.6 mmol). The reaction stirred for 20 minutes at room temperature and the solution of prenyl-9BBN was added via cannula. The reaction stirred for 4 hours, then concentrated and immediately purified via silica gel column chromatography (5% ethyl acetate in hexanes). The product was partitioned between hexanes and acetonitrile in order to remove the excess 9-BBN. The crude product was immediately taken on to the next step. Yield: 4.15 g, 12.8 mmol, 48%.

^{1}H-NMR (300 MHz, CDCl$_3$) δ 8.02 (bs, 1H), 7.46 (d, J = 8.7 Hz, 1H), 7.11 (d, J = 2.1 Hz, 1H), 6.87 (dd, J = 8.7, 2.1 Hz, 1H), 6.26 (m, 1H), 5.99 (dd, J = 27.9, 10.2 Hz, 1H), 5.10 (d, J = 0.6 Hz, 1H), 5.05 (dd, J = 5.7, 1.2 Hz, 1H), 1.56 (s, 9H), 1.44 (s, 6H). ^{13}C NMR (75 MHz, CDCl$_3$) δ 153.0, 146.8, 146.5, 146.1, 135.8, 126.7, 120.5, 113.8, 112.5, 103.5, 98.1, 83.4, 38.4, 28.0, 27.5. (jmf-02-599)
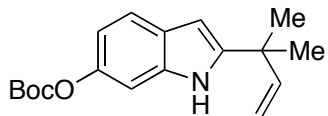
205
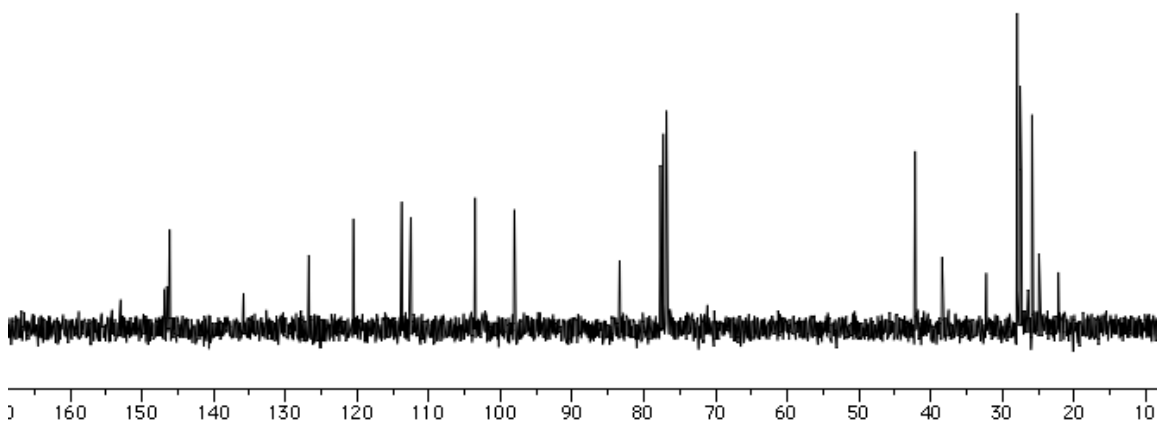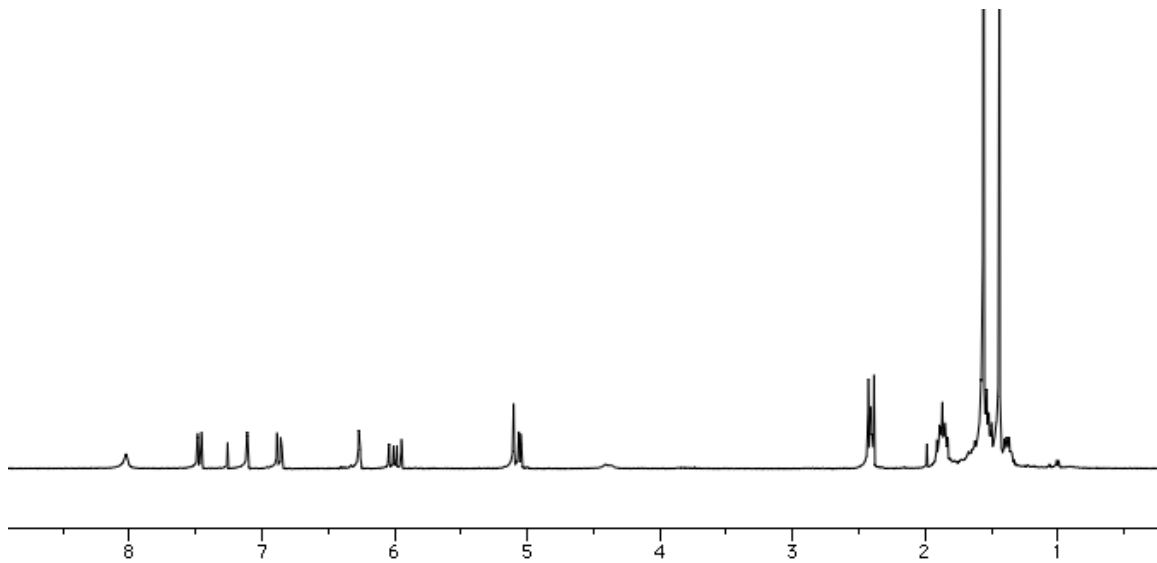
tert-Butyl-3-((dimethylamino)methyl)-2-(2-methylbut-3-en-2-yl)-1_H_-indol-6-yl carbonate (206):

Aqueous formaldehyde (1.26 mL, 15.5 mmol) was diluted with glacial acetic acid (35 mL). Aqueous dimethylamine (6.5 mL, 58.5 mmol) was added, followed by addition of indole **205** (4.15 g, 13.7 mmol) diluted in glacial acetic acid (10 mL). The reaction stirred at room temperature for 14 hours. The reaction mixture was diluted with 1M NaOH to a pH>10. The aqueous layer was extracted with diethyl ether (3 x 40 mL) and the combined organic layer was dried over Na_2SO_4 and concentrated to afford an amber oil that was taken on to the next reaction without further purification. Crude yield: 4.14 g, 13.02 mmol, 84%.

^{1}H-NMR (300 MHz, CDCl$_3$) δ 7.99 (bs, 1H), 7.62 (d, J = 8.7 Hz, 1H), 7.08 (d, J = 2.1 Hz, 1H), 6.87 (dd, J = 8.4, 2.1 Hz, 1H), 6.12 (dd, J = 17.7, 11.1 Hz, 1H), 5.16 (dd, J = 6.0, 0.9 Hz, 1H), 5.12 (d, J = 0.3 Hz, 1H), 3.55 (s, 2H), 2.19 (s, 6H), 1.56 (s, 9H), 1.53 (s, 6H); ^{13}C NMR (100 MHz, CDCl$_3$) δ 152.9, 146.5, 146.3, 142.0, 133.7, 128.6, 119.7, 113.4, 112.32, 109.0, 103.1, 83.3, 54.1, 45.5, 39.6, 28.0, 27.3; IR (neat) 3385, 2933, 1734, 1466, 1142, 1013, 886 cm^{-1}; HRMS (ESI/APCI) calcd for $C_{21}H_{31}N_2O_3$ (M+H) 359.2329, found 359.2324. (jmf-02-600)

206
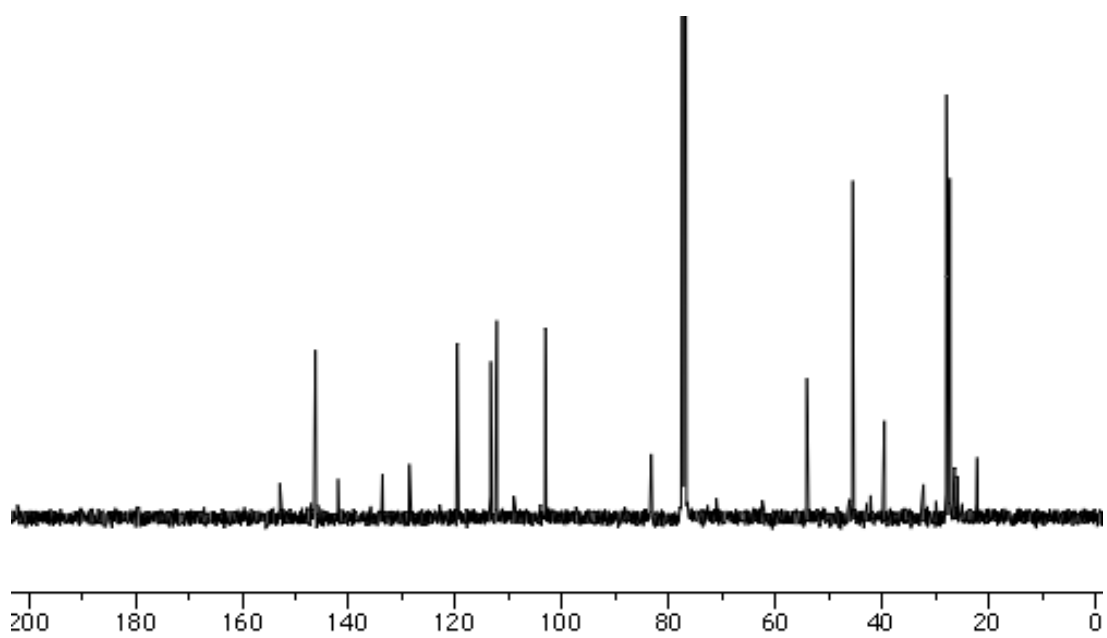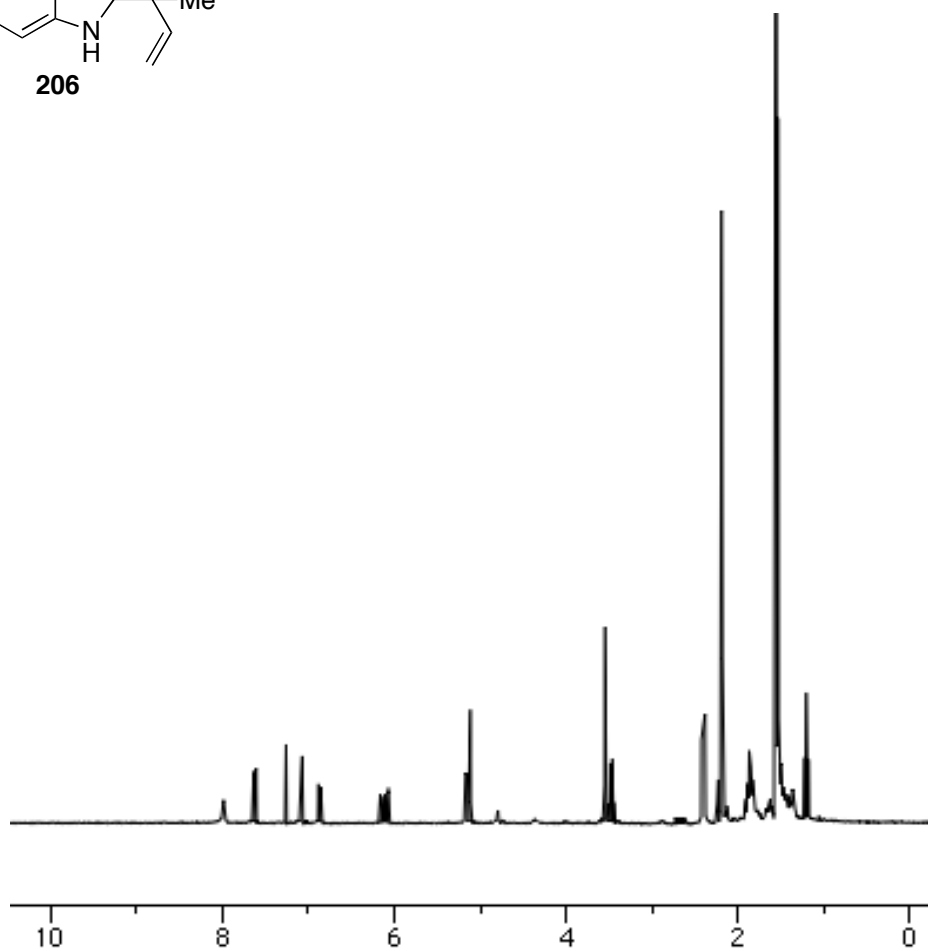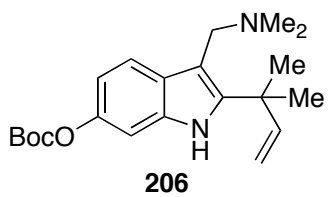
Ethyl 2-amino-3-(6-((tert-butoxycarbonyl)oxy)-2-(2-methylbut-3-en-2-yl)-1H-indol-3-yl)propanoate (207):
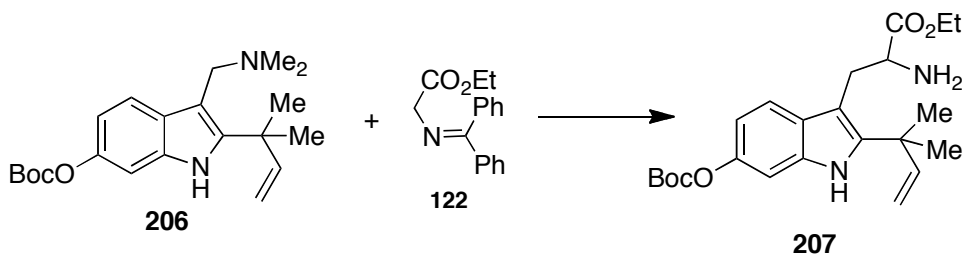
Gramine **206** (4.14 g, 11.5 mmol), **122** (2.80 g, 10.5 mmol), tributylphosphine (850 μL, 4.2 mmol) and MeCN (53 mL) were combined and stirred for 20 hours at reflux under Ar. The reaction was concentrated and purified via flash column chromatography in 10% ethyl acetate in hexanes to afford 2.76 g of a yellow amorphous solid, which was dissolved in THF (36 mL). 1M HCl (12.0 mL) was added and the reaction mixture stirred for 30 minutes at room temperature. The solvent was removed under reduced pressure and the residue was rediluted with saturated aqueous NaHCO$_3$ until basic. The mixture was extracted with CH$_2$Cl$_2$ (x2), dried over Na$_2$SO$_4$ and concentrated. The crude residue was purified by flash column chromatography (3:1 hexanes/ethyl acetate; 5:95 MeOH/CH$_2$Cl$_2$) to give **207** as a yellow oil. Yield: 1.51 g, 3.62 mmol, 76%.

^{1}H-NMR (300 MHz, CDCl$_3$) δ 8.44 (bs, 1H), 7.43 (d, J = 8.7 Hz, 1H), 7.05 (d, J = 1.8 Hz, 1H), 6.83 (dd, J = 8.7, 2.1 Hz, 1H), 6.00 (dd, J = 17.7, 10.2 Hz, 1H), 5.07-5.01 (m, 2H), 4.12-4.00 (m, 2H), 3.75 (dd, J = 9.6, 5.1 Hz, 1H), 3.22 (dd, J = 14.4, 4.8 Hz, 1H), 2.95 (dd, J = 14.4, 9.6 Hz, 1H), 1.53 (s, 9H), 1.42 (s, 6H), 1.12 (t, J = 6.9 Hz, 3H); ^{13}C NMR (75 MHz, CDCl$_3$) δ 175.6, 153.1, 146.5, 146.1, 141.6, 134.2, 127.9, 119.0, 113.3, 112.0, 106.8, 103.7, 83.4, 61.0, 56.1, 39.3, 31.3, 27.9, 27.8, 14.4, 14.2; IR (neat) 3389,

2977, 1734, 1465, 1243, 1143, 885 cm^{-1}; HRMS (ESI/APCI) calcd for C$_{23}$H$_{33}$N$_{2}$O$_{5}$ (M+H) 417.2384, found 417.2388. (jmf-02-602)
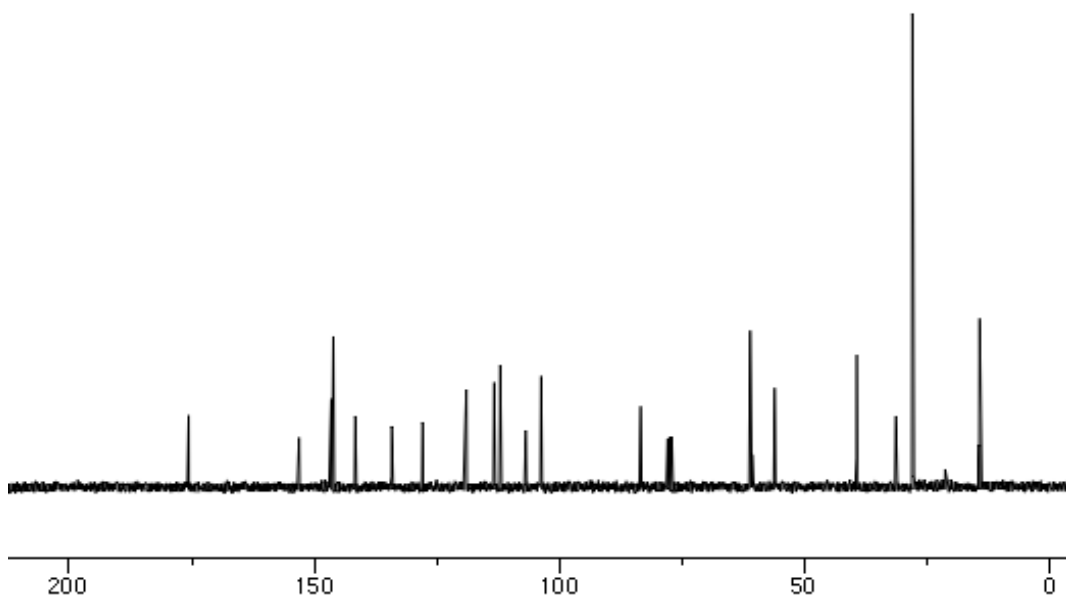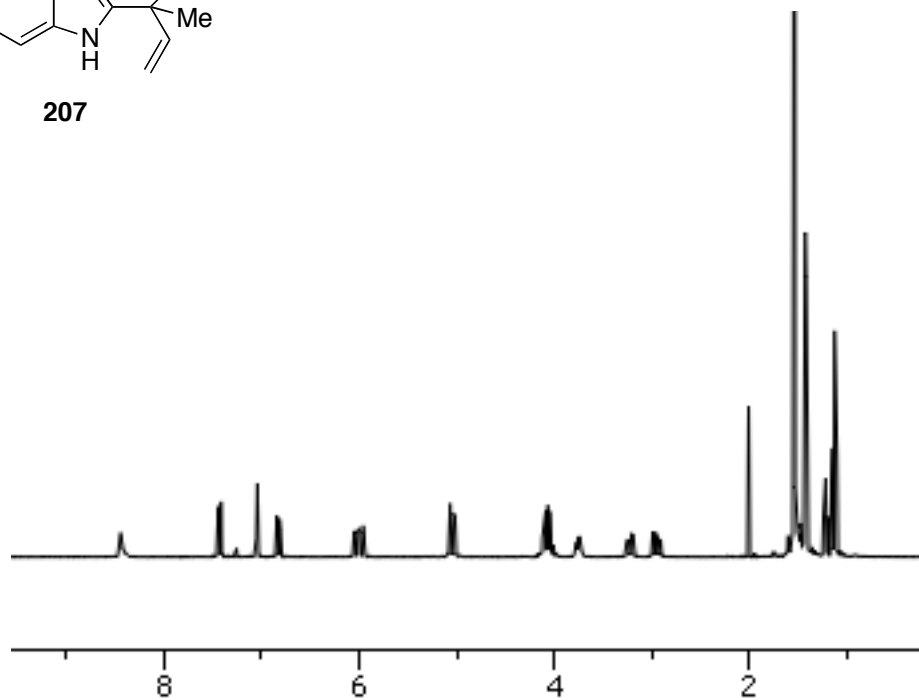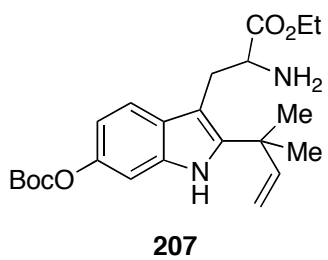
Ethyl 2-((tert-butoxycarbonyl)amino)-3-(6-((tert-butoxycarbonyl)oxy)-2-(2-methylbut-3-en-2-yl)-1H-indol-3-yl)propanoate (208).
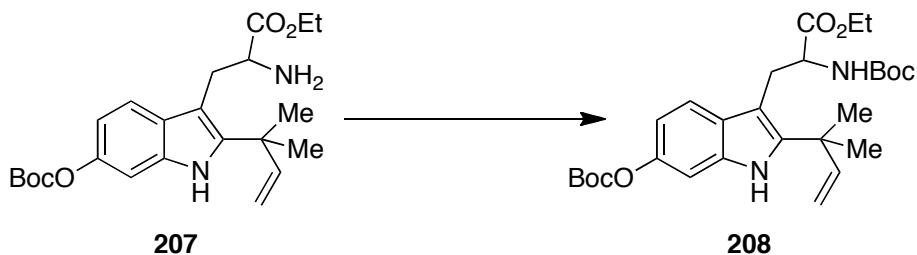
To a solution of amine **207** (1.50 g, 3.60 mmol) in dioxane (18 mL), di-*tert*-butyldicarbonate (824 mg, 3.78 mmol) and 1M NaOH (3.60 mL, 3.60 mmol) were added. The reaction mixture stirred at room temperature for 1 hour, and then concentrated under reduced pressure to remove the dioxane. The resulting slurry was taken up in H$_2$O, acidified to pH 2 with 1M KHSO$_4$, and extracted with EtOAc (3 x 50 mL). The combined organic layers were dried over Na$_2$SO$_4$ and concentrated under reduced pressure to afford **208** as a yellow amorphous solid that was used without further purification. Crude yield: 1.85 g, 3.58 mmol.

^{1}H-NMR (300 MHz, CDCl$_3$) δ 8.11 (bs, 1H), 7.42 (d, J = 8.7 Hz, 1H), 7.06 (s, 1H), 6.86 (d, J = 8.4 Hz, 1H), 6.07 (dd, J = 17.7, 10.5 Hz, 1H), 5.17-5.06 (m, 3H), 4.49 (m, 1H), 4.05-3.90 (m, 2H), 3.28-3.12 (m, 2H), 1.55 (s, 9H), 1.52 (s, 9H), 1.32 (s, 6H), 1.02 (t, J = 6.9 Hz, 3H); ^{13}C NMR (75 MHz, CDCl$_3$) δ 173.1, 152.8, 146.7, 146.0, 141.4, 134.0, 128.0, 119.0, 113.5, 112.4, 106.1, 103.4, 83.3, 79.8, 61.4, 54.8, 39.4, 28.4, 28.0, 27.8, 27.6, 14.4, 14.0; IR (neat) 3388, 2979, 1755, 1464, 1369, 1143 cm^{-1}; HRMS (ESI/APCI) calcd for C$_{28}$H$_{40}$N$_2$O$_7$Na (M+Na) 539.2728, found 539.2727. (jmf-02-603)
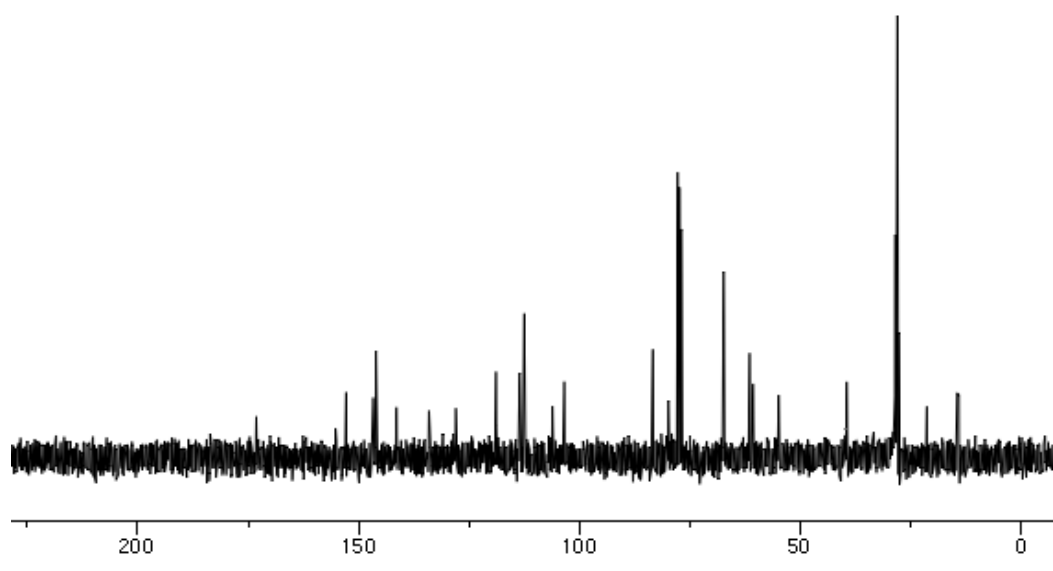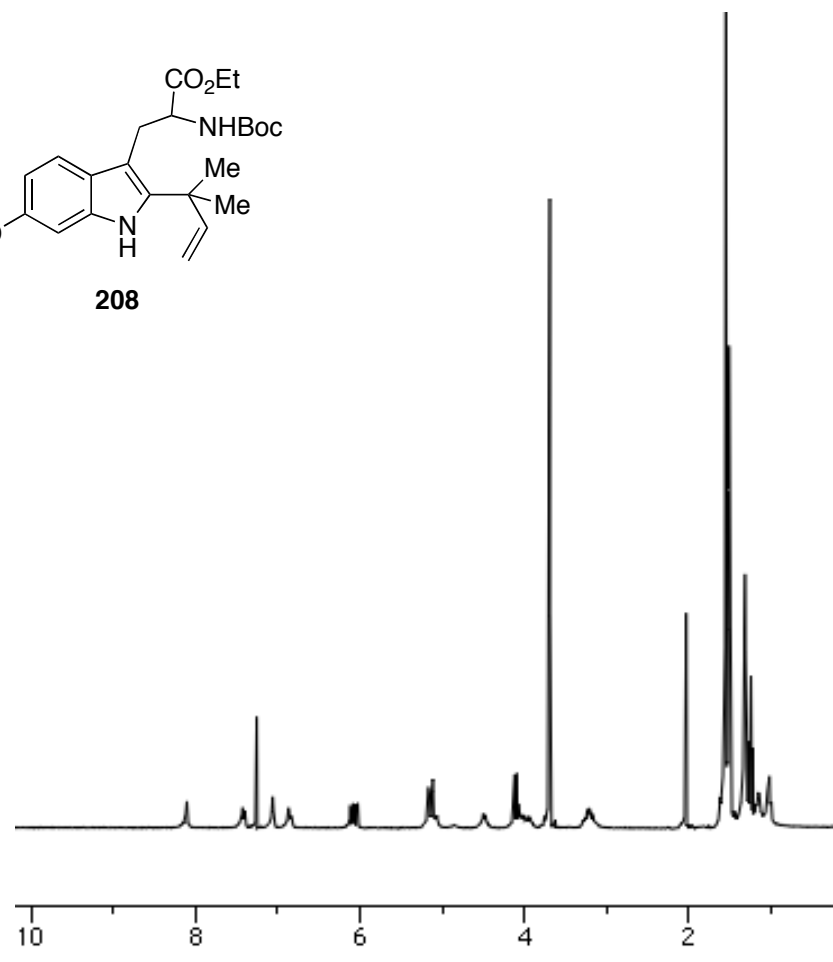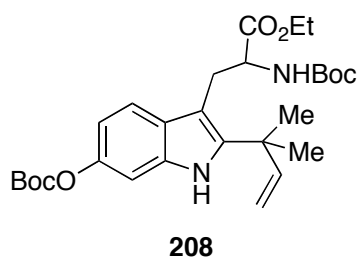
208

2-((tert-butoxycarbonyl)amino)-3-(6-((tert-butoxycarbonyl)oxy)-2-(2-methylbut-3-en-2-yl)-1H-indol-3-yl)propanoic acid (190):
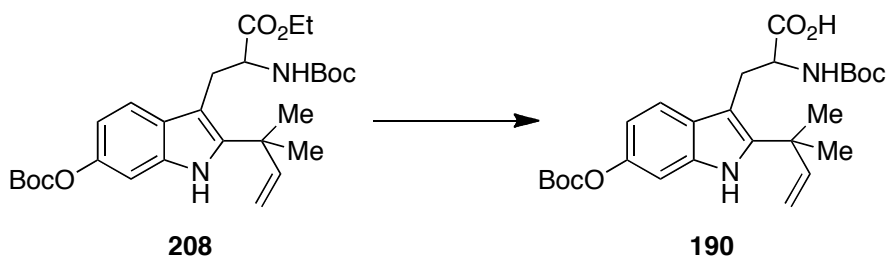
Crude ester **208** (1.85 g, 3.58 mmol) was dissolved in 2:1 H_2O/THF (36 mL) and LiOH (826 mg, 36.0 mmol) was added. The reaction stirred at room temperature overnight. The solvent was removed under reduced pressure and the resulting slurry was taken up in H_2O, acidified to pH 2 with 1M $KHSO_4$, and extracted with CH_2Cl_2 (2 x 50 mL) and EtOAc (2 x 50 mL). The combined organic layers were dried over Na_2SO_4 and concentrated under reduced pressure to afford **190** as a yellow amorphous solid that was used without further purification. Crude yield: 1.46 g, 2.98 mmol, 83%.

^{1}H-NMR (300 MHz, CDCl$_3$) δ 11.98 (bs, 1H) 9.70 (bs, 1H), 8.20 (d, J = 21.3 Hz, 1H), 7.51 (t, J = 9.6 Hz, 1H), 7.08 (s, 1H), 6.86 (d, J = 8.7 Hz, 1H), 6.07 (dd, J = 17.4, 10.2 Hz, 1H), 5.16-5.11 (m, 2H), 4.60-4.50 (m, 1H), 3.41-3.35 (m, 1H), 3.19-3.11 (m, 1H), 1.55 (s, 9H), 1.48 (s, 6H), 1.29-1.22 (m, 18H); ^{13}C NMR (75 MHz, CDCl$_3$) δ 177.2, 171.7, 155.6, 146.0, 134.1, 119.0, 113.6, 112.5, 103.6, 83.5, 80.2, 60.8, 39.3, 28.4, 28.0, 27.9, 21.3, 14.4. (jmf-02-604)

190
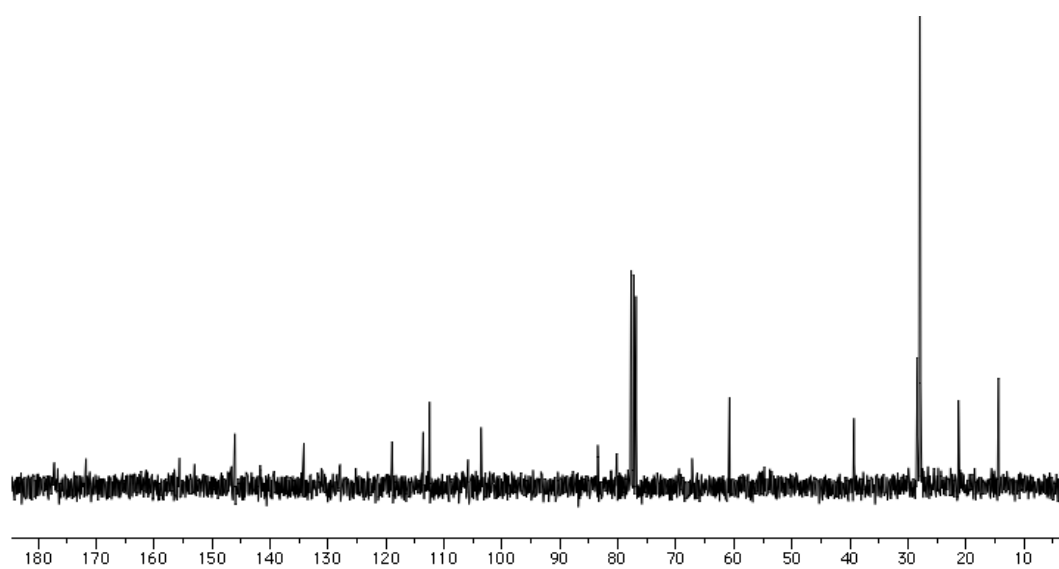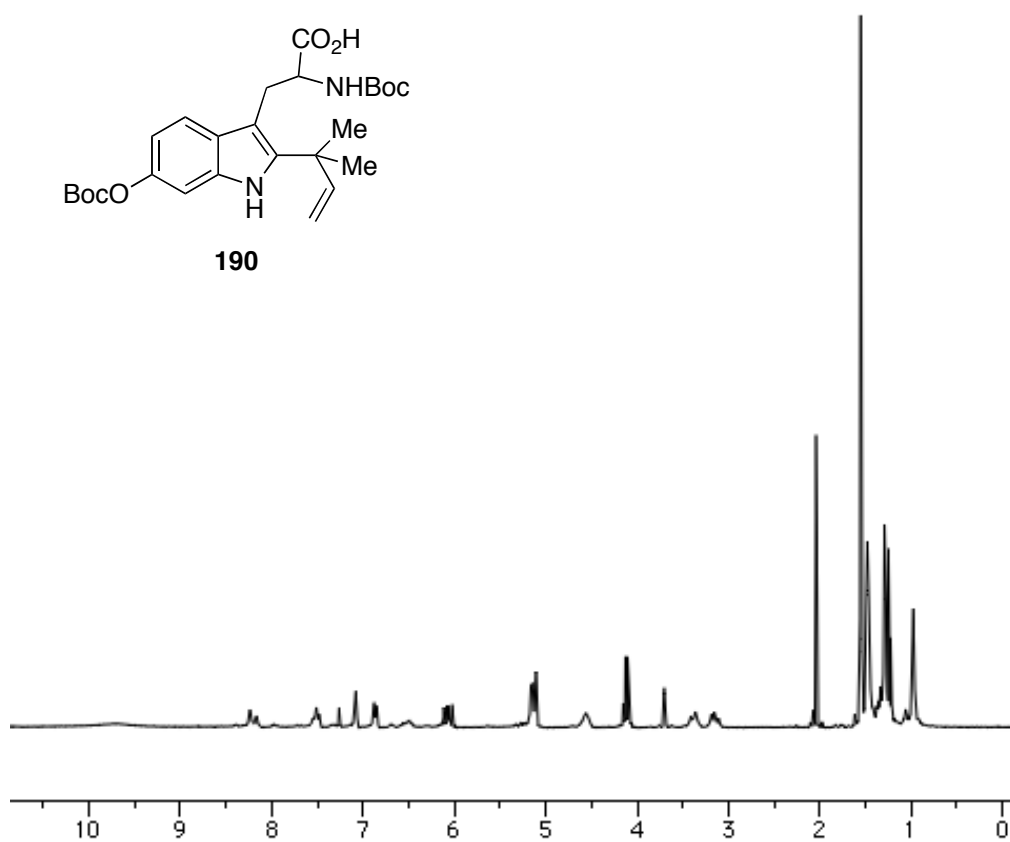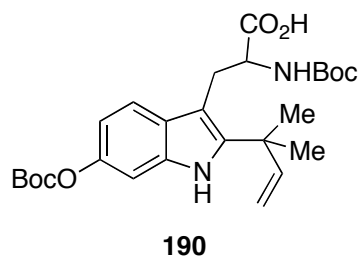
1-(benzyloxy)-3-methyl-2-nitrobenzene (212):
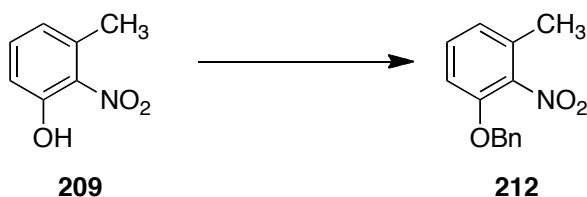
Commercially available nitrophenol (5.0 g, 32.7 mmol) was dissolved in 32.7 mL of DMF. Benzyl chloride (4.13 mL, 35.9 mmol) and potassium carbonate (4.51 g, 32.7 mmol) were added and the reaction mixture stirred for 4 hours at 100°C. The reaction mixture cooled to room temperature and was poured into 15 ml of water and extracted with ethyl acetate (3 x 70 mL). The organic layer was washed with 50 mL of each 1M sodium hydroxide, water, and brine, then dried over Na_2SO_4 and concentrated under vacuum. The residue was recrystalized from ethyl acetate and hexanes to afford the pure desired product. Yield: 7.16 g, 29.4 mmol, 90%.

^{1}H-NMR (300 MHz, CDCl$_3$) δ 7.38-7.25 (m, 5H), 7.35 (t, J = 7.8 Hz, 1H), 6.87 (dd, J = 12.0, 8.4 Hz, 2H), 5.16 (s, 2H), 2.31 (s, 3H). (jmf-01-205)
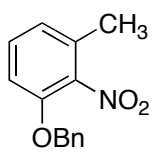
212
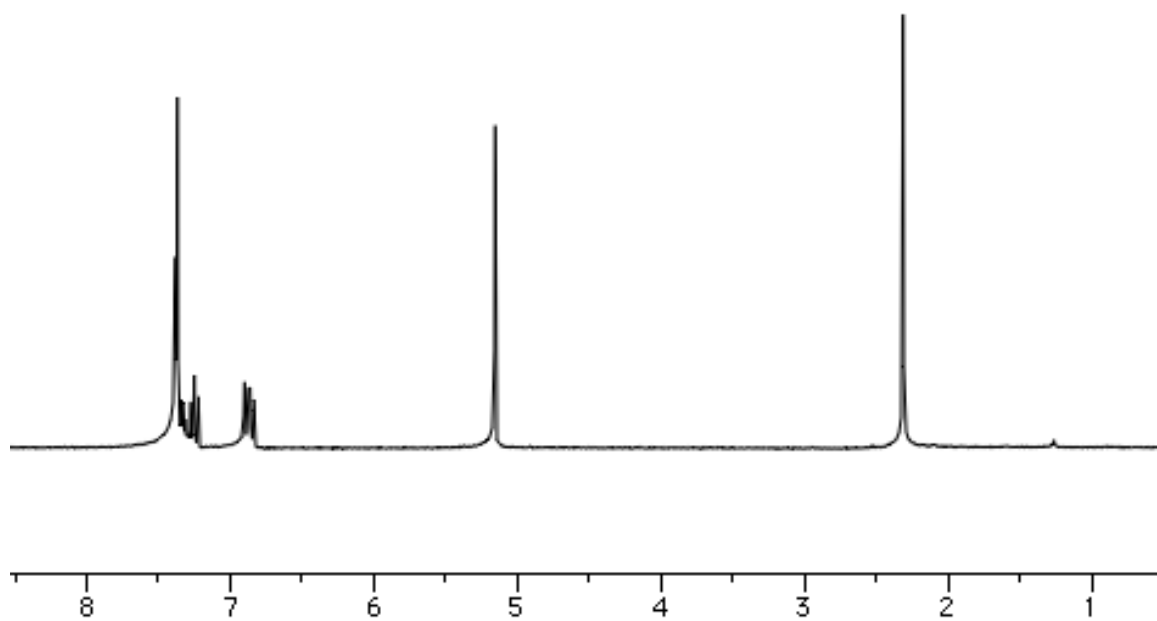
(*E*)-2-(2-(3-(benzyloxy)-2-nitrophenyl)ethylidene)hydrazinecarboxamide (213):
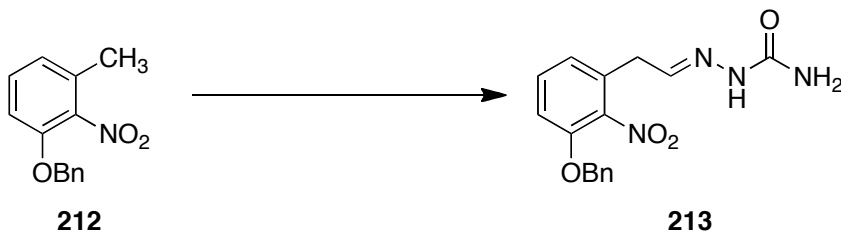
To a solution of nitrotoluene **212** (4.0 g, 16.44 mmol) in 16 mL of DMF, was added DMF-DMA (4.37 mL, 32.9 mmol) and pyrrolidine (2.75 mL, 32.9 mmol). The reaction was heated to 150°C and stirred for 6 hours. The mixture was cooled to 0°C and diluted with 16 mL of isopropyl ether. To the cooled solution, semicarbazine HCl (2.2 g, 19.7 mmol) in 1M HCl (19 mL) at 0°C was added and the reaction stirred for 10 minutes at room temperature. The precipitate was filtered and washed with water and isopropyl ether. Yield: 2.3 g, 7.0 mmol, 43%.

^{1}H-NMR (300 MHz, CDCl$_3$) δ 9.96 (bs, 1H), 7.48 (t, *J* = 7.8 Hz, 1H), 7.39-7.33 (m, 4H), 7.30 (d, *J* = 8.4 Hz, 1H), 7.14 (t, *J* = 5.4 Hz, 1H), 6.99 (d, *J* = 7.8 Hz, 1H), 6.13 (bs, 1H), 5.25 (s, 2H), 3.44 (d, *J* = 5.4 Hz, 2H), 3.32 (s, 2H). (jmf-01-272)
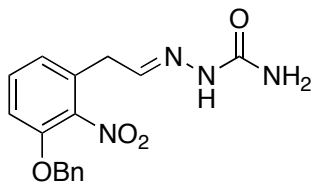
213
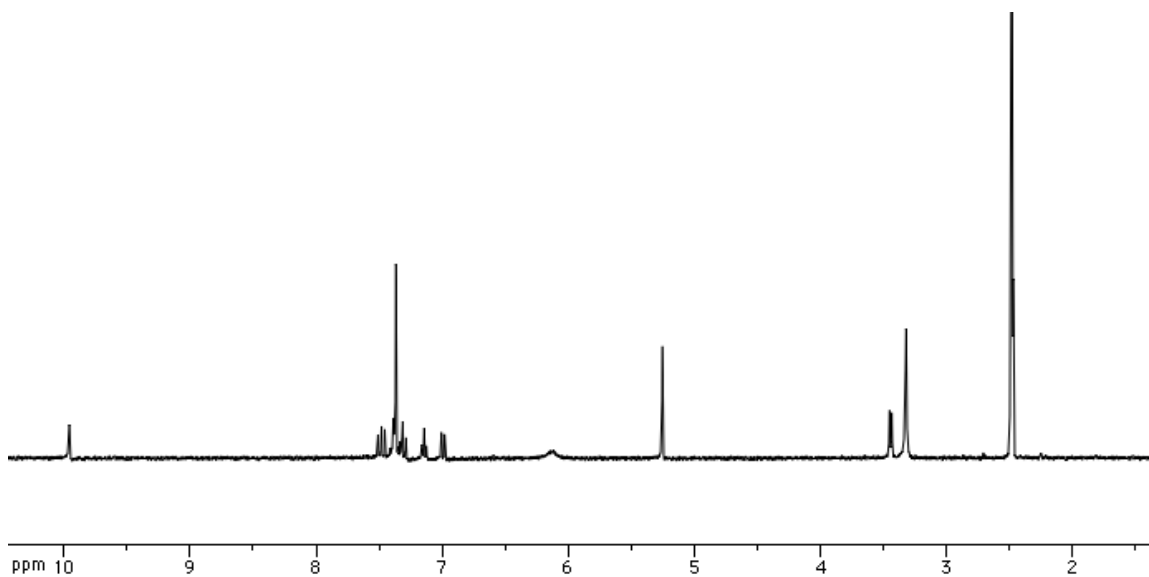
tert-butyl 1H-indol-7-yl carbonate (214):
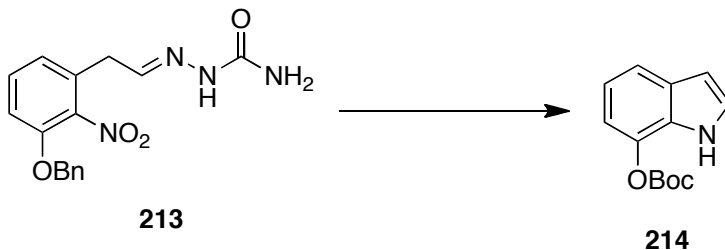
The semicarbazide (500 mg, 1.52 mmol), 5% Pd/C (10 mol%), and ethanol (5 mL) was stirred in a hydrogenation vessel under 42 psi of H_2 for 2 hours. The vessel was purged with Ar and the mixture was filtered through a pad of celite. The catalyst was washed with ethanol and the filtrate was concentrated. The residue was dissolved in $CHCl_3$ (20 mL) and washed with 10% aqueous citric acid (35 mL). The organic layer was separated and dried over $MgSO_4$ and concentrated. Crude yield: 147 mg, 1.10 mmol.

The crude 7-hydroxyindole (147 mg, 1.10 mmol) was dissolved in 2.2 mL of MeCN and the solution was cooled to 0°C. Di-*tert*-butyldicarbonate (216 mg, 0.99 mmol) and a catalytic amount of DMAP were added to the reaction mixture and the reaction stirred for 16 hours at room temperature. The reaction was concentrated and purified via flash column chromatography using 9:1 hexanes/ethyl acetate. Yield: 150 mg, 0.643 mmol, 58%.

^{1}H-NMR (300 MHz, $CDCl_3$) δ 8.45 (bs, 1H), 7.56-7.53 (m, 1H), 7.18-7.12 (m, 3H), 6.61-6.59 (m, 1H), 1.63 (s, 9H). (jmf-01-283)
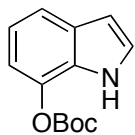
214
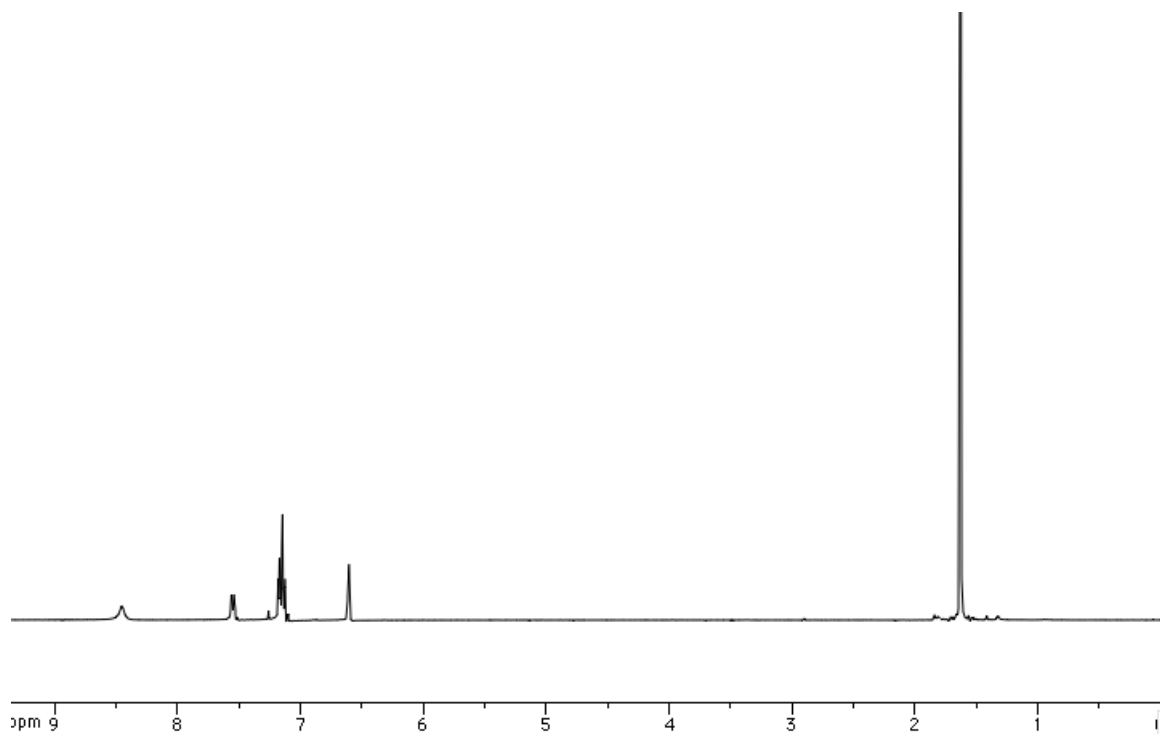
tert-butyl (3-chloro-1H-indol-7-yl) carbonate (215):

214   215
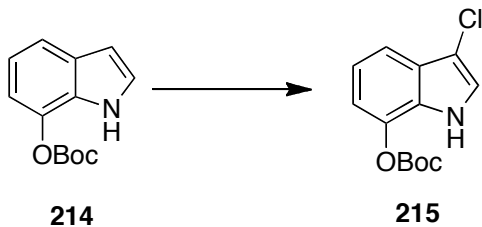
The 7-OBoc indole (593 mg, 2.54 mmol) was dissolved in 12 mL of MeOH and cooled to

0°C.   N-Chlorosuccinimide (393 mg, 2.54 mmol) was slowly added to the reaction

mixture in portions.   The solution stirred for 22 hours while warming to room

temperature. The reaction was quenched with brine (20 mL) and extracted with diethyl

ether (3 x 35 mL). The combined organic layer was washed with 35 mL of water, dried

over Na_2SO_4, and concentrated. The crude oil was purified via flash column

chromatography 85:15 hexanes/ethyl acetate. Yield: 500 mg, 1.87 mmol, 74%.

^{1}H-NMR (300 MHz, $CDCl_3$) δ 8.31 (bs, 1H), 7.50 (dd, J = 6.3, 3.0 Hz, 1H), 7.18-7.15

(m, 3H), 1.59 (s, 9H); (jmf-01-284)
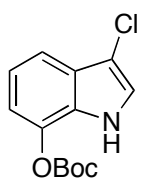
215
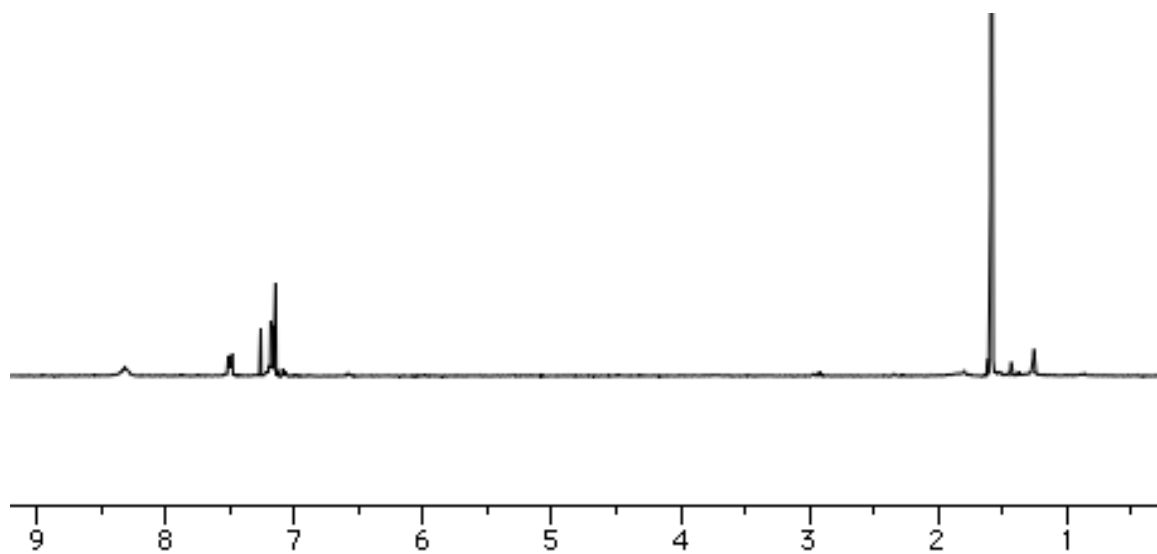
1*H*-indol-6-ol (188):
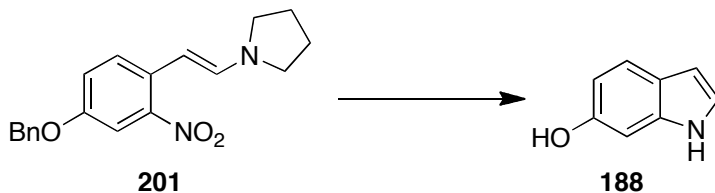
Enamine **201** (24.3 g, 74.9 mmol), and 10 wt.% Pd/C were dissolved in 250 mL of THF in a par shaker hydrogenation vessel. The vessel was purged with Ar and then filled with H_2 (40 psi) on the par shaker. The reaction mixture stirred for 3 hours. Following a quench with Ar, the mixture was filtered through a silica plug and rinsed with diethyl ether to provide pure **188** as a yellow foam. Yield: 9.97 g, 74.9 mmol, quantitative.

^{1}H-NMR (300 MHz, CDCl$_3$) δ 7.28 (d, J = 9.0 Hz, 1H), 6.92 (d, J = 3.3 Hz, 1H), 6.71 (m, 1H), 6.54 (dd, J = 8.4, 2.1 Hz, 1H), 6.26 (dd, J = 3.3, 0.9 Hz, 1H); ^{13}C NMR (75 MHz, CDCl$_3$) δ 152.8, 137.1, 131.0, 123.2, 121.1, 110.1, 101.9, 97.0; HRMS (ESI/APCI) calcd for C$_8$H$_6$NO (M–H) 1342.0455, found 132.0455. (jmf-02-700)

188
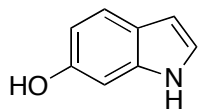
238
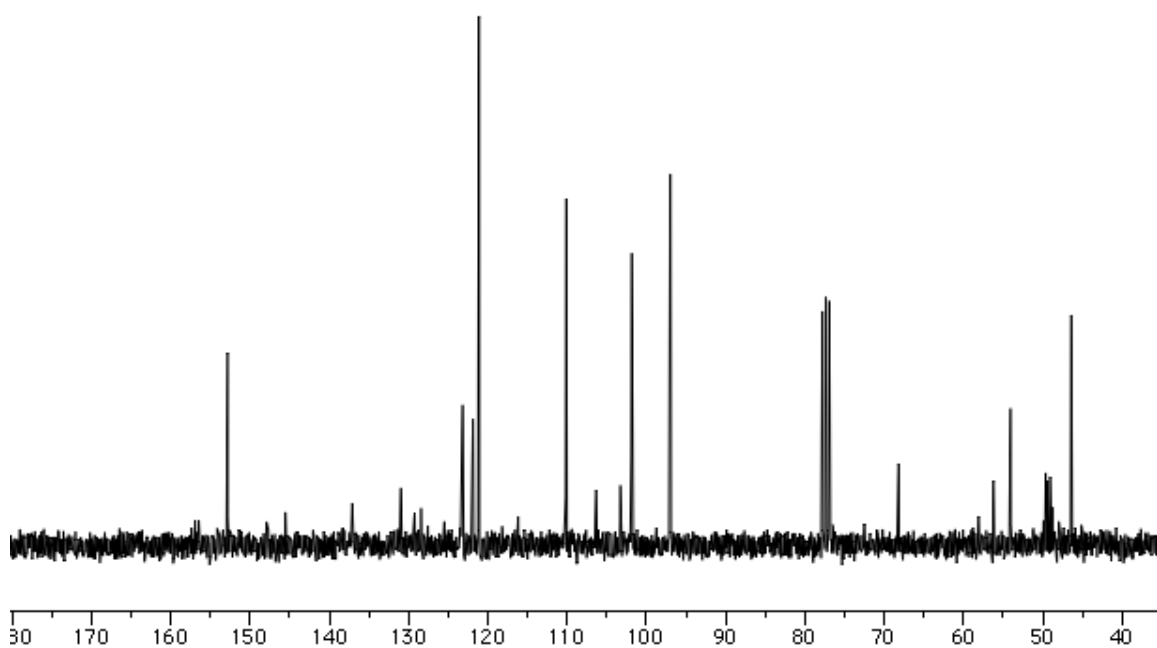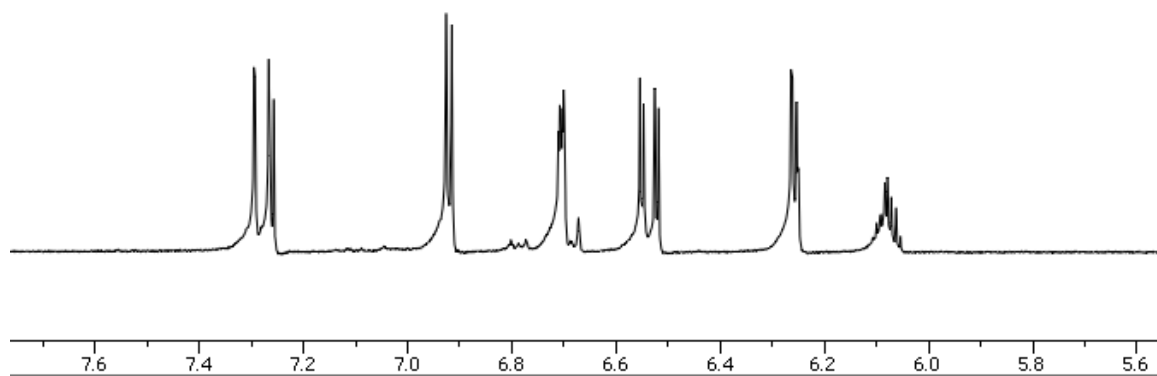
tert-butyl (3-methyl-2-nitrophenyl) carbonate (210):
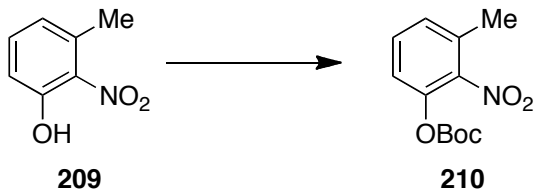
Commercially available nitrophenol **209** (500 mg, 3.27 mmol) was dissolved in 3.3 mL of MeCN and the solution was cooled to 0°C. Di-*tert*-butyldicarbonate (785 mg, 3.60 mmol) and a catalytic amount of DMAP were added to the cooled reaction mixture. The solution was allowed to warm to room temperature while stirring for 18 hours. The reaction was concentrated and purified via flash column chromatography using 9:1 hexanes/ethyl acetate. Yield: 800 mg, 3.14 mmol, 96%.

^{1}H-NMR (300 MHz, CDCl$_3$) δ 7.85 (d, *J* = 1.5 Hz, 1H), 7.34 (m, 2H), 2.59 (s, 3H), 1.56 (s, 9H); (jmf-01-211)
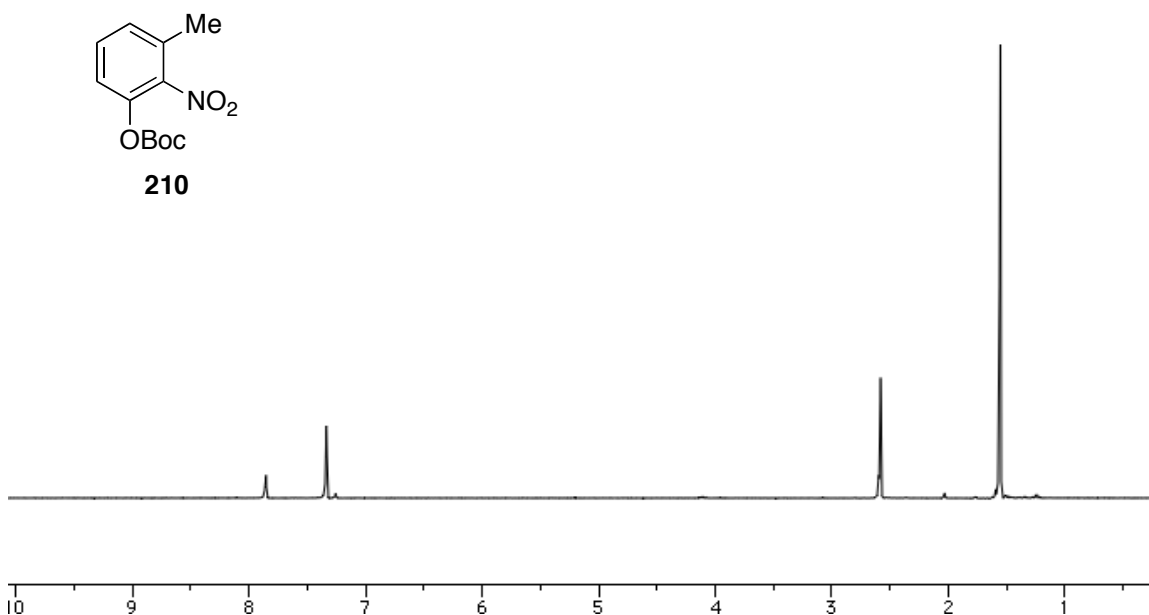
7.2.2 Chapter 4 Experimentals

(2S)-ethyl-1-(2-((tert-butoxycarbonyl)amino)-3-(6-((tert-butoxycarbonyl)oxy) -2-(2-methylbut-3-en-2-yl)-1H-indol-3-yl)propanoyl)pyrrolidine-2-carboxylate (218):
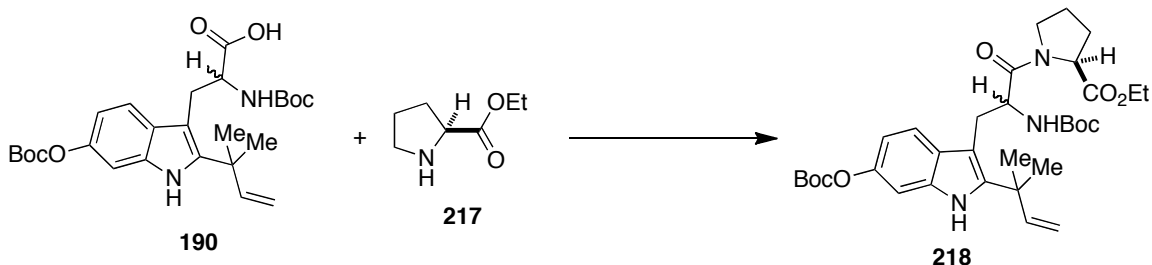
The crude acid was dissolved in acetonitrile (30 mL) and L-proline ethyl ester (426 mg, 2.98 mmol) was added. HATU (1.70 g, 4.47 mmol) and ^{i}Pr$_2$NEt (2.0 mL, 11.9 mmol) were added and the reaction stirred for 3 hours at room temperature. The reaction was quenched with 1M HCl (40 mL) and extracted with CH$_2$Cl$_2$ (3 x 75 mL). The combined organic layers were dried over Na$_2$SO$_4$ and concentrated under reduced pressure. The crude residue was purified by flash column chromatography and eluted with 3:1 hexanes/EtOAc to afford 1.08 g (59%) of **218** as a yellow amorphous solid.

^{1}H-NMR (300 MHz, CDCl$_3$) δ 8.35 (m, 1H), 7.48-6.74 (m, 3H), 6.04 (m, 1H), 5.52 (m, 1H), 5.15-5.06 (m, 2H), 4.62-1.98 (m, 9H), 1.51-1.12 (m, 3H); ^{13}C NMR (75 MHz, CDCl$_3$) δ 172.1, 171.3, 154.9, 152.7, 146.6, 145.3, 141.6, 133.6, 127.8, 119.2, 119.1, 113.4, 112.6, 106.0, 103.4, 83.2, 79.4, 61.1, 60.6, 59.3, 53.1, 46.6, 39.2, 28.5, 27.9, 27.4, 14.4, 14.3; IR (neat) 3351, 2979, 1753, 1634, 1497, 1450, 1143 cm^{-1}; HRMS (ESI/APCI) calcd for C$_{33}$H$_{48}$N$_3$O$_8$ (M+H) 614.3436, found 614.3434. (jmf-02-605)
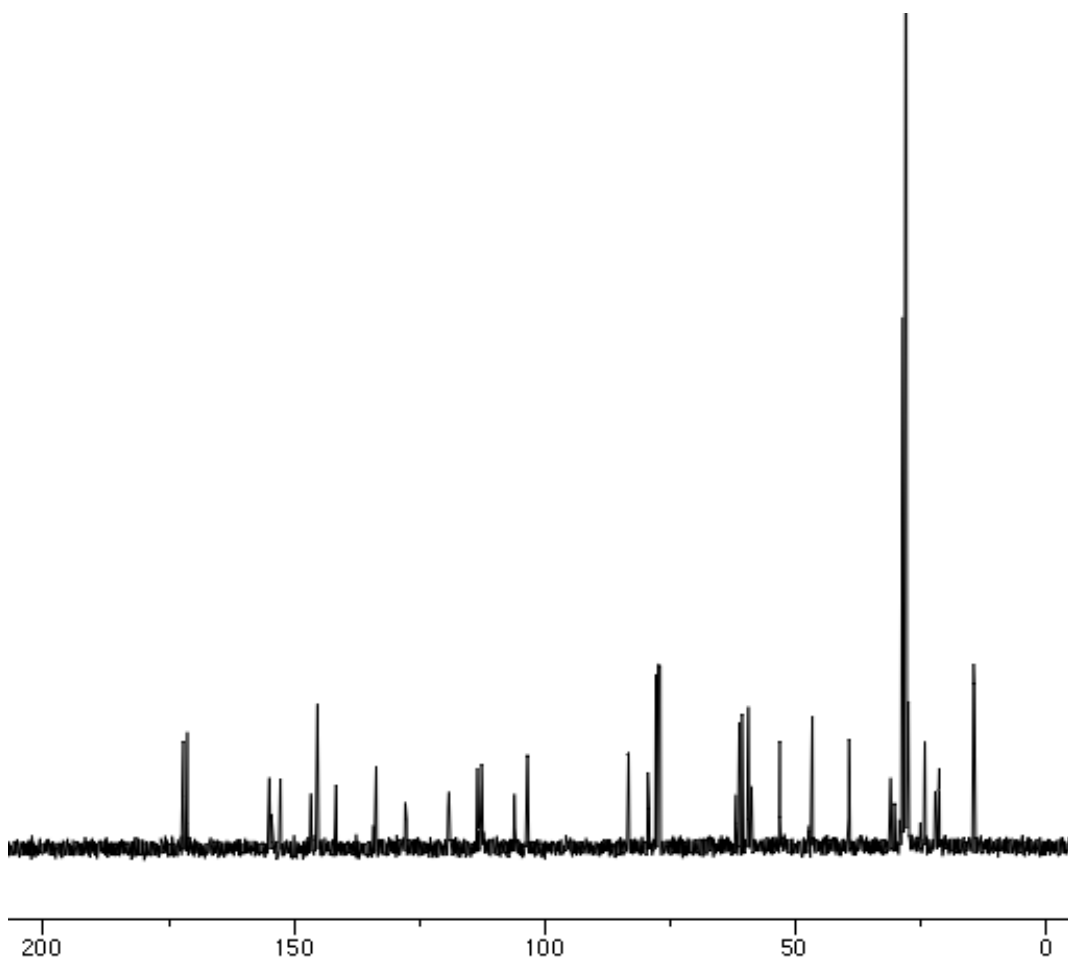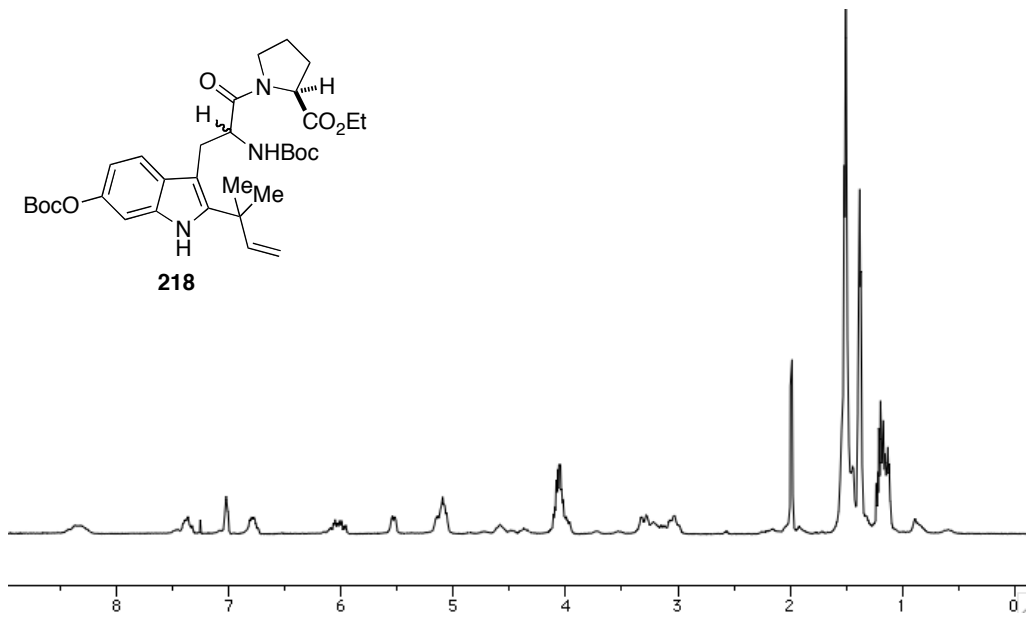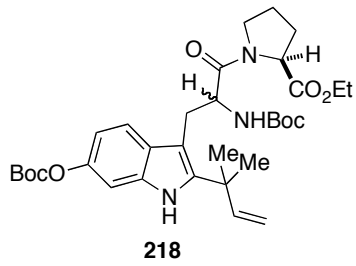
(3S,8aS)-3-((6-hydroxy-2-(2-methylbut-3-en-2-yl)-1H-indol-3-yl)methyl)-hexahydropyrrolo[1,2-a]pyrazine-1,4-dione (220).

218

220, 6-hydroxydeoxybrevianamide E
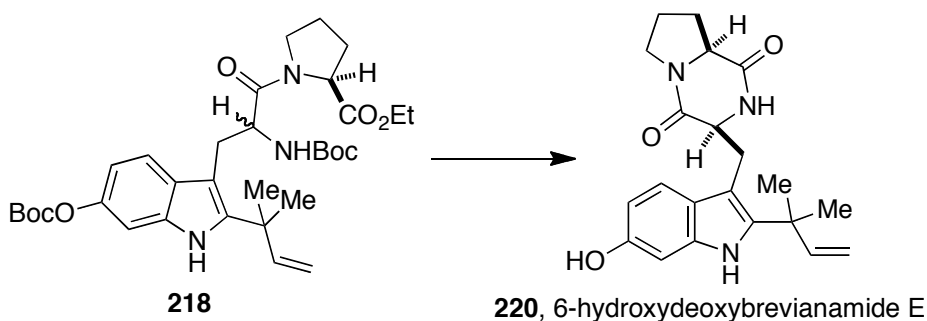
TFA (0.6 M) was added to a solution of **218** (1.08 g, 1.76 mmol) in CH₂Cl₂ (0.6 M) at 0°C. The reaction stirred for 3 hours at room temperature. The mixture was quenched with saturated NaHCO₃ to a pH 10 and extracted with EtOAc (3 x 20 mL). The combined organic layers were dried over Na₂SO₄ and concentrated under reduced pressure. The residue was dissolved in toluene (0.2 M) and 2-hydroxypyridine (31 mg, 0.328 mmol) was added. The reaction refluxed for 14 hours under Ar atmosphere, cooled to room temperature, and concentrated under reduced pressure. The residue was rediluted with CH₂Cl₂ (30 mL) and washed with 1M HCl (30 mL). The organic layer was dried over Na₂SO₄ and concentrated under reduced pressure. The crude residue was purified via flash column chromatography eluting with 5:95 MeOH/CH₂Cl₂ to afford 160 mg (27%) of the desired *cis* diastereomer as a cream foam. The *trans* diastereomer was isolated in 23% yield (140 mg) as yellow foam.

Cis: ^{1}H NMR (400 MHz, 20:1 CDCl$_3$/CD$_3$OD) δ 8.15 (m, 1H), 7.17 (d, *J* = 8.4 Hz, 1H), 6.71 (d, *J* = 2.4 Hz, 1H), 6.58 (dd, *J* = 8.4, 2.0 Hz, 1H), 6.04 (dd, *J* = 17.6, 10.4, 1H), 5.10-5.05 (m, 2H), 4.35 (dd, *J* = 11.2, 2.4 Hz, 1H), 4.00 (t, *J* = 7.6 Hz, 1H), 3.86-3.54 (m, 3H), 3.08 (dd, *J* = 14.8, 11.6 Hz, 1H), 2.30-1.82 (m, 6H), 1.45-1.38 (m, 6H); ^{13}C NMR (75 MHz, 20:1 CDCl$_3$/CD$_3$OD) δ 169.7, 166.3, 153.0, 146.1, 140.3, 135.9, 123.0, 118.3, 112.3, 110.0, 103.9, 96.9, 59.4, 55.1, 45.6, 39.1, 28.5, 28.0, 26.1, 25.9, 22.7; IR (neat) 3353, 2925, 1664, 1457 cm^{-1}; HRMS (ESI/APCI) calcd for C$_{21}$H$_{26}$N$_3$O$_3$ (M+H) 368.1969, found 368.1969. (jmf-02-608a)
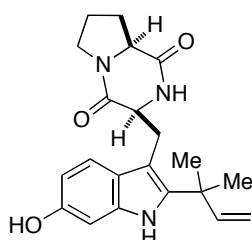
220, 6-hydroxydeoxybrevianamide E
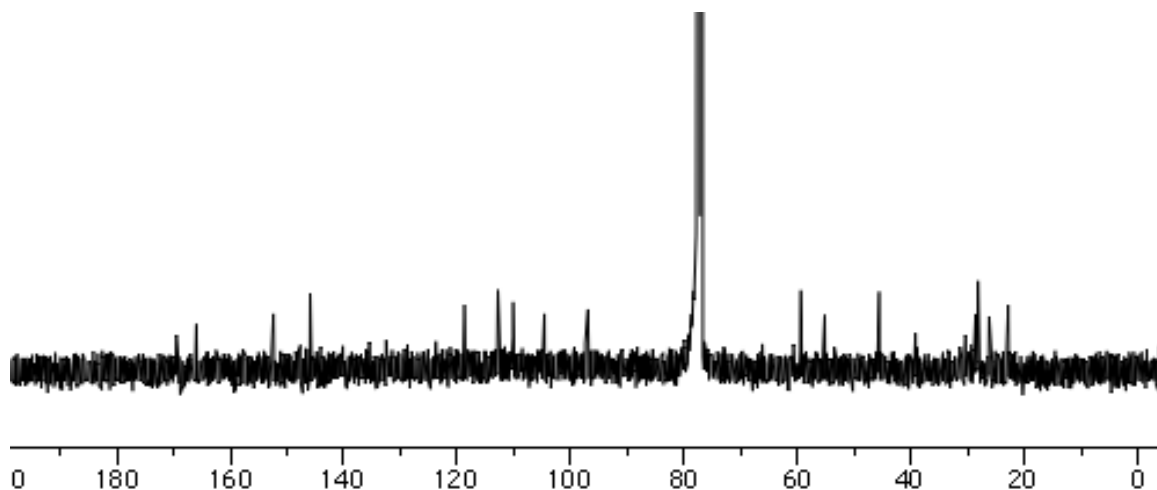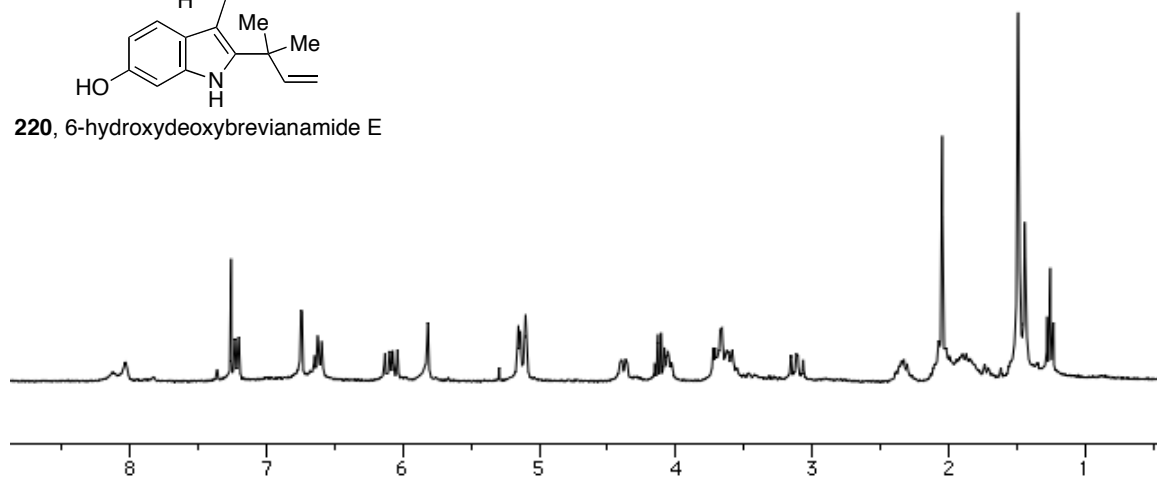
Trans: ^{1}H NMR (300 MHz, (CD$_3$)$_2$CO) δ 7.91 (bs, 1H), 7.32 (d, *J* = 8.4 Hz, 1H), 6.81 (d, *J* = 2.4 Hz, 1H), 6.64 (dd, *J* = 8.4, 2.1 Hz, 1H), 6.22 (dd, *J* = 17.4, 10.5 Hz, 1H), 5.67-5.63 (m, 1H), 5.14-5.03 (m, 2H), 4.42-4.38 (m, 1H), 4.20-4.17 (m, 1H), 3.64-3.42 (m, 3H), 3.07-2.98 (m, 1H), 2.00-1.82 (m, 3H), 1.56 (s, 3H), 1.54 (s, 3H); IR (neat) 3358, 2920, 1662, 1456 cm^{-1}; HRMS (ESI/APCI) calcd for C$_{21}$H$_{25}$N$_3$O$_3$Na (M+Na) 390.1788, found 390.179. (jmf-02-608b)

221

Notoamide J (43).

220, 6-hydroxydeoxybrevianamide E
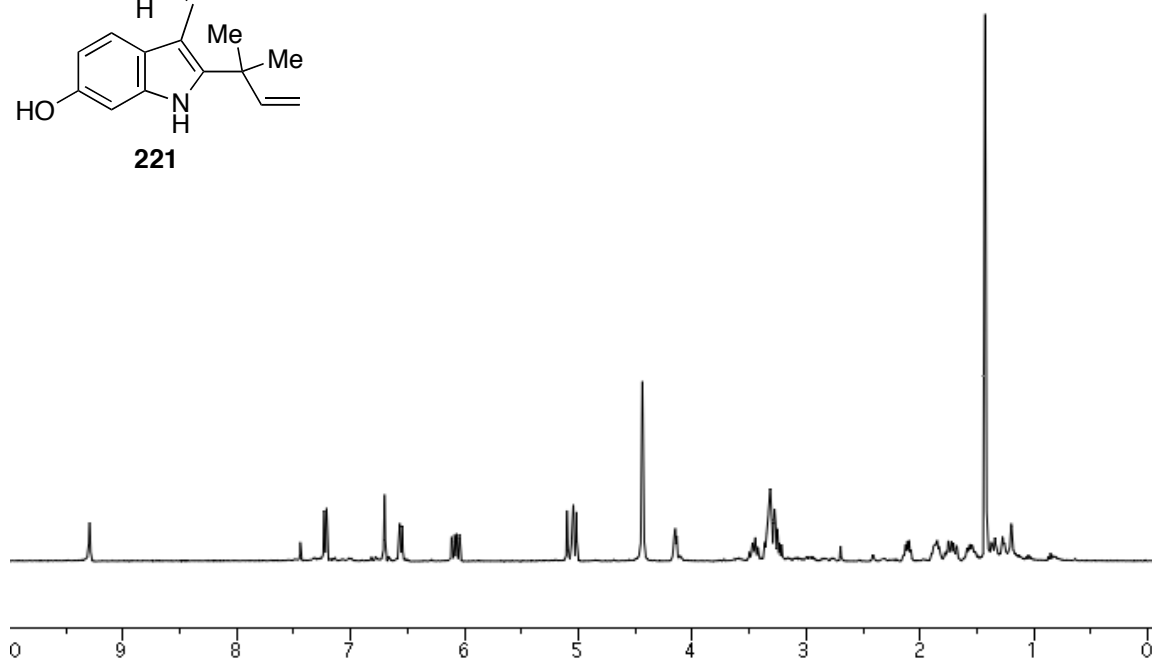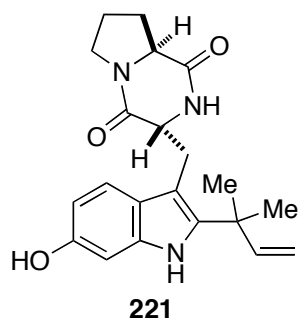
43, notoamide J
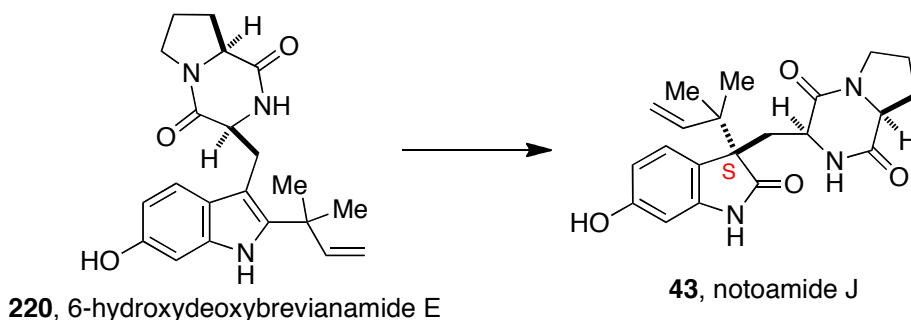
Davis oxaziridine (208 mg, 0.871 mmol) was added to a solution of **220** (160 mg, 0.436 mmol) in CH$_2$Cl$_2$ (9 mL). The reaction mixture was stirred 13 hours at room temperature and concentrated under reduced pressure. The residue was purified via flash column chromatography eluting with MeOH/CH$_2$Cl$_2$ (5:95) to give 52 mg (31%) of **43** as a white amorphous solid and 26 mg (15%) of **15** as a white amorphous solid.

^{1}H-NMR (300 MHz, acetone-d_6) δ 9.68 (bs, 1H), 8.59 (bs, 1H), 7.02 (d, J = 8.7 Hz, 1H), 6.49 (dd, J = 8.1, 5.7 Hz, 2H), 6.33 (bs, 1H), 6.12 (dd, J = 17.4, 10.8 Hz, 1H), 5.05 (dd, J = 16.8, 10.8 Hz, 1H), 5.04 (dd, J = 16.8, 10.8 Hz, 1H), 4.00 (t, J = 6.9 Hz, 1H), 3.49-3.34 (m, 2H), 3.28 (d, J = 9.6 Hz, 1H), 3.10 (d, J = 14.7 Hz, 1H), 2.18-2.11 (m, 1H), 2.10 (d, J = 6.6 Hz, 1H), 1.98-1.80 (m, 3H), 1.11 (s, 3H), 1.06 (s, 3H); ^{13}C NMR (75 MHz, CDCl$_3$) δ 183.2, 170.4, 165.7, 157.7, 143.3, 142.9, 126.8, 120.3, 114.5, 109.2, 98.6, 59.0, 57.8, 53.0, 45.9, 42.5, 31.7, 29.9, 28.2, 22.7, 21.8; IR (neat) 3265, 2971, 1670, 1429, 1155 cm^{-1}; HRMS (ESI/APCI) calcd for C$_{21}$H$_{25}$N$_3$O$_4$Na (M+Na) 406.1737, found 406.1739. (jmf-02-609)

notoamide J
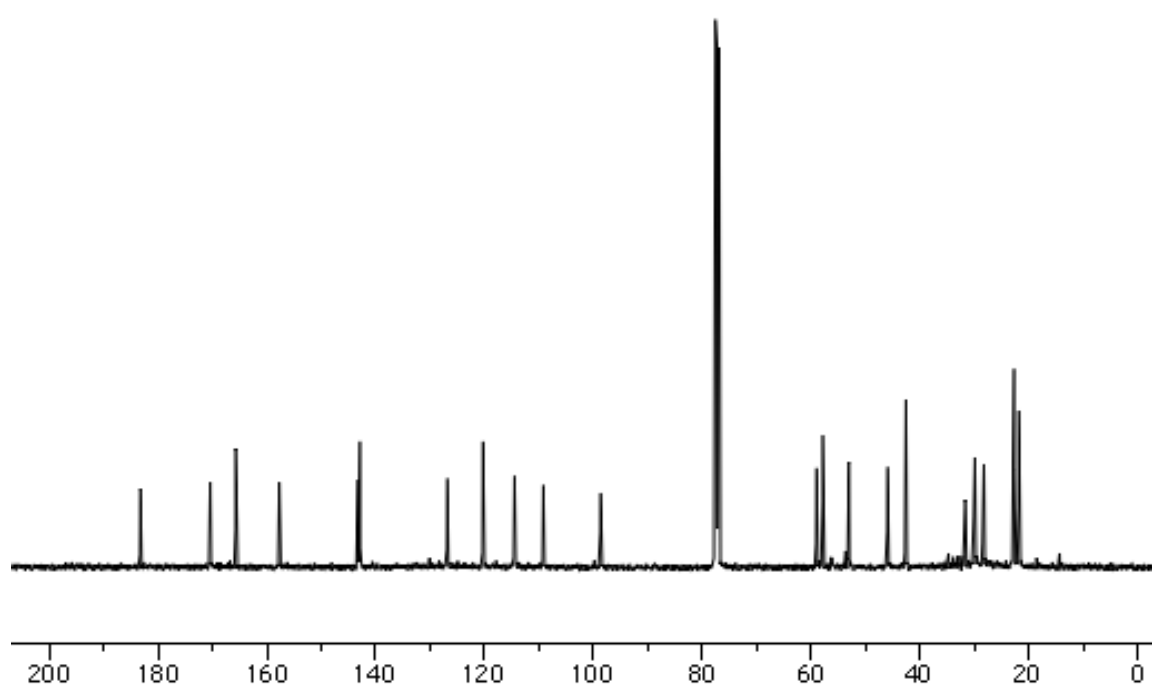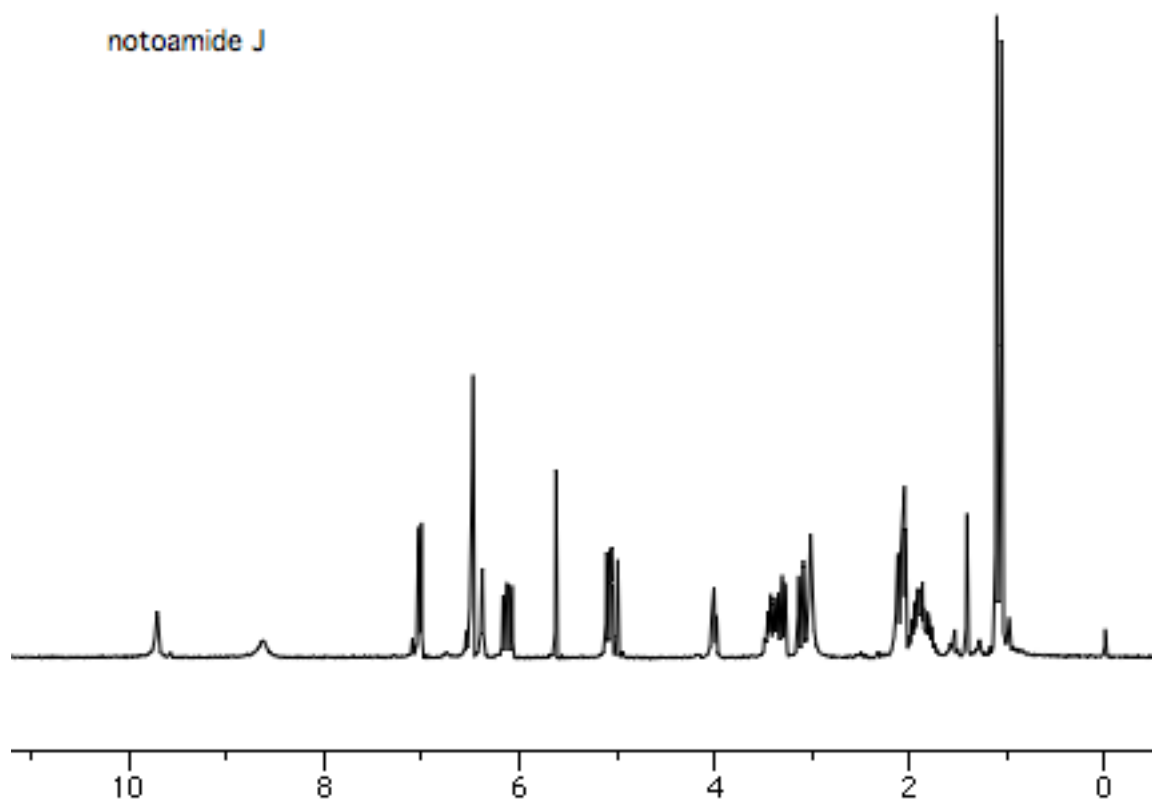
(2S)-ethyl 1-(2-((tert-butoxycarbonyl)amino)-3-(2-(2-methylbut-3-en-2-yl)-1H-indol-3-yl)propanoyl)pyrrolidine-2-carboxylate (243):
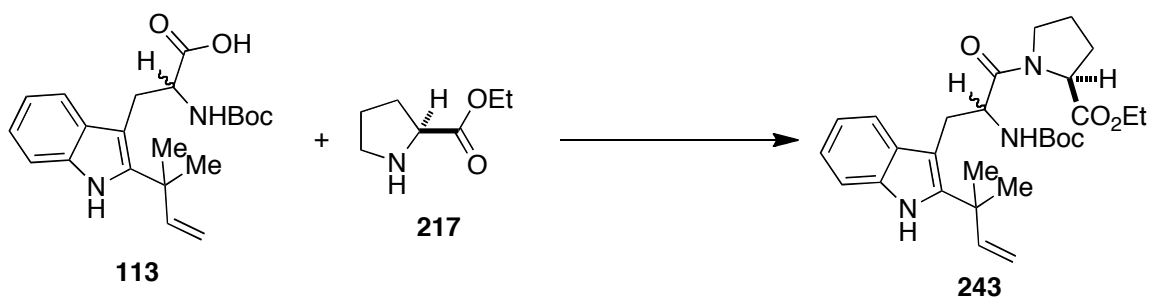
To a solution of acid **113** (500 mg, 1.34 mmol) in 13.4 mL MeCN was added L-proline ethyl ester (192 mg, 1.34 mmol). HATU (764 mg, 2.01 mmol) and ^{i}Pr$_2$NEt (0.93 mL, 5.36 mmol) were added to the solution and the reaction stirred at room temperature for 4 hours. The reaction was quenched with 20 mL 1M HCl and extracted with CH$_2$Cl$_2$ (3 x 30 mL). The combined organic layer was dried over Na$_2$SO$_4$ and concentrated under vacuum. The crude material was purified via flash column chromatography using 3:1 hexanes/ethyl acetate. Yield: 400.1 mg, 0.804 mmol, 60%

^{1}H-NMR (300 MHz, CDCl$_3$) δ 7.98-7.93 (m, 1H), 7.54-7.46 (m, 1H), 7.11-7.02 (m, 2H), 6.12 (dd, J = 10.5, 9.9 Hz, 1H), 5.60 (d, J = 8.4 Hz, 1H), 5.26-5.17 (m, 2H), 4.76-4.42 (m, 2H), 4.16-4.02 (m, 3H), 3.42-3.10 (m, 4H), 1.63 (s, 9H), 1.43 (s, 6H), 1.28-1.17 (m, 6H); ^{13}C NMR (75 MHz, CDCl$_3$) δ 172.2, 171.8, 171.4, 155.0, 145.6, 140.8, 134.1, 129.8, 121.8, 121.7, 119.4, 118.7, 112.5, 110.7, 106.0, 79.4, 61.8, 61.2, 60.6, 59.4, 53.1, 46.6, 39.3, 31.1, 28.7, 28.6, 28.0, 27.6, 24.1, 22.1, 21.3, 14.4, 14.3, 14.2; HRMS (ESI/APCI) calcd for C$_{28}$H$_{40}$N$_3$O$_5$ (M+H) 498.2962, found 498.2972. (jmf-02-698)

243

Deoxybrevianamide E (7)
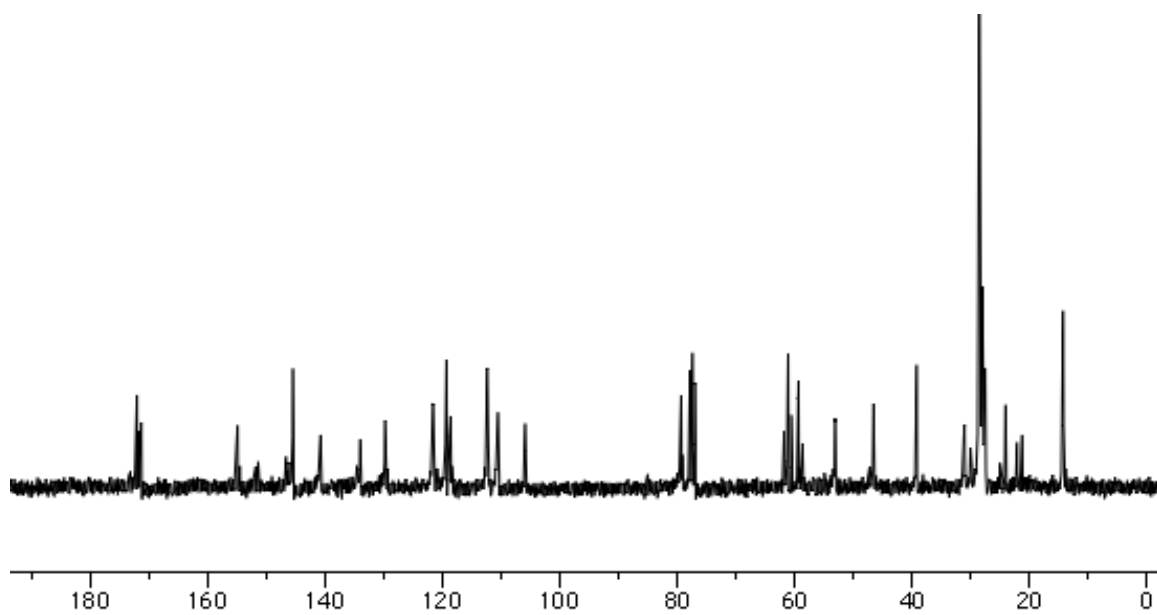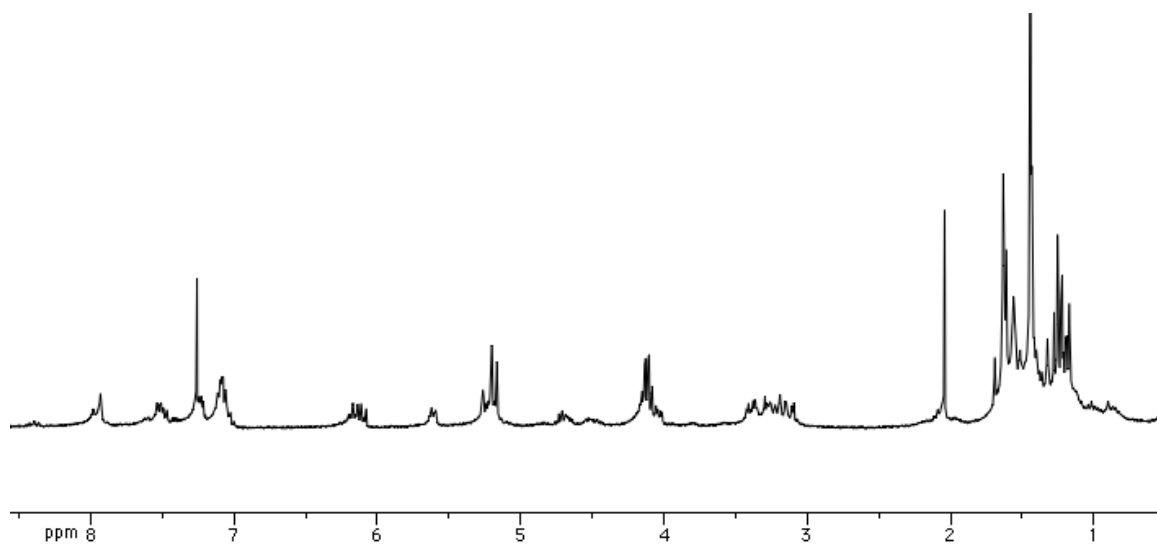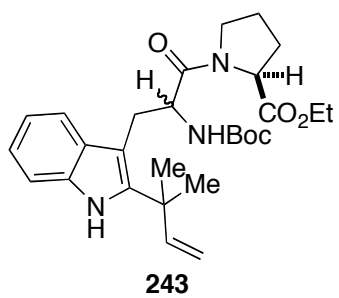
243   **7**, deoxybrevianamide E
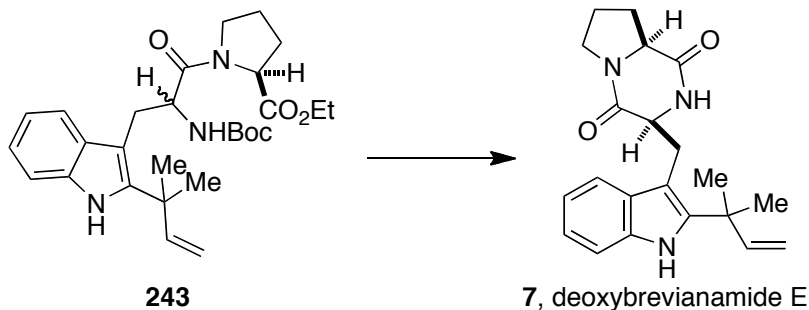
Peptide **243** (400 mg, 0.803 mmol) was dissolved in 2 mL CH_2Cl_2 and cooled to 0°C . TFA (2 mL) was added and the ice bath was removed. The reaction stirred at room temperature for 3 hours. The reaction was quenched with saturated aqueous $NaHCO_3$ to pH 10, extracted with ethyl acetate (3 x 50 mL), and dried over Na_2SO_4. The organic layer was concentrated under vacuum. The crude amine (320 mg, 0.805 mmol) was dissolved in toluene (8 mL) and 2-hydroxypyridine (15.3 mg, 0.161 mmol) was added to the solution. The reaction was heated to reflux and stirred for 15 hours. The mixture was concentrated and the residue was diluted with 10 mL CH_2Cl_2. The organic layer was washed with 15 mL 1M HCl, dried over Na_2SO_4, and concentrated. The crude material was purified via flash column chromatography with 3% MeOH in CH_2Cl_2 to afford a 1:1 mixture of *cis*:*trans* diastereomers (79% overall yield).

Cis: ^{1}H-NMR (300 MHz, CDCl$_3$) δ 8.08 (bs, 1H), 7.49 (d, J = 9.0 Hz, 1H), 7.32 (d, J = 8.1 Hz, 1H), 7.20-7.08 (m, 2H), 6.13 (dd, J = 17.7, 10.5 Hz, 1H), 5.69 (bs, 1H), 5.21 (s, 1H), 5.16 (d, J = 4.8 Hz, 1H), 4.44 (d, J = 10.5 Hz, 1H), 4.10-4.04 (m, 1H), 3.78-3.55 (m, 3H), 3.19 (dd, J = 15.5, 12.0 Hz, 1H), 2.39-2.31 (m, 1H), 2.10-1.86 (m, 4H), 1.56 (s, 6H); ^{13}C NMR (100 MHz, CDCl$_3$) δ 169.4, 166.0, 145.8, 141.6, 134.5, 129.2, 122.4, 120.3,

118.0, 113.0, 111.1, 104.8, 59.4, 55.1, 45.6, 39.2, 29.9, 28.6, 28.1, 28.0, 26.2, 22.8;

HRMS (ESI/APCI) calcd for $C_{21}H_{26}N_3O_2$ (M+H) 352.202, found 352.2022. (jmf-02-704)

7, deoxybrevianamide E

Oxindole (235 and 236)

7, deoxybrevianamide E

235
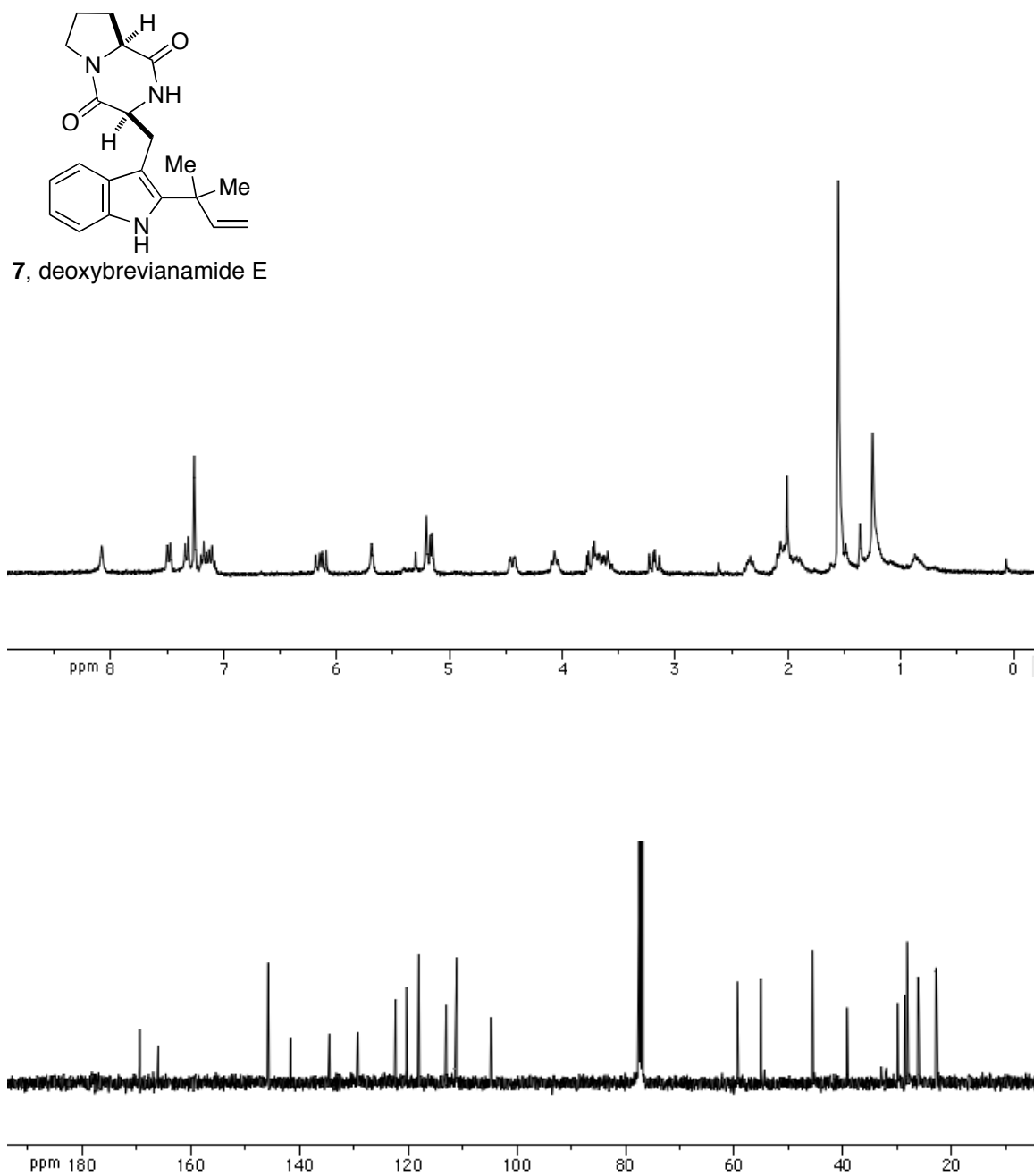
236
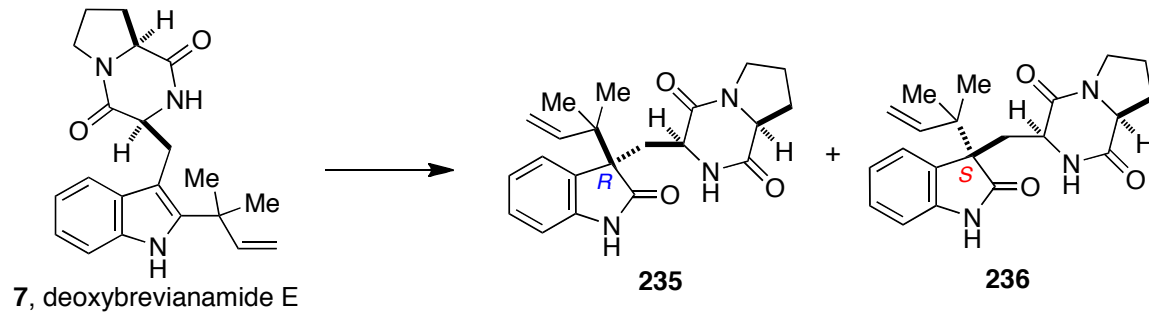
Deoxybrevianamide E **7** (220 mg, 1.25 mmol) was dissolved in CH_2Cl_2 (12.5 mL) and Davis oxaziridine (300 mg, 2.5 mmol) was added to the solution. The reaction stirred at room temperature for 18 hours. The mixture was concentrated and purified via flash column chromatography in 3% MeOH in DCM. The combined oxindoles were isolated and purified a second time via reverse phase prep-TLC (10% acetone in H_2O). The plate was run 4 times and the *R* and *S* isomers were isolated separately.

235: ^{1}H-NMR (300 MHz, CDCl$_3$) δ 7.29, (d, J = 1.5 Hz, 1H), 7.22-7.17 (m, 1H), 6.89-6.73 (m, 2H), 6.32 (dd, J = 17.7, 10.8 Hz, 1H), 5.14-5.04 (m, 2H), 3.93 (t, J = 8.1 Hz, 1H), 3.72 (dd, J = 11.4, 7.8 Hz, 1H), 3.60-3.47 (m, 2H), 2.89 (dd, J = 13.2, 11.4 Hz, 1H), 2.68-2.62 (m, 1H), 2.33-2.24 (m, 1H), 2.15-1.77 (m, 4H), 1.28 (s, 3H), 1.24 (s, 3H); (jmf-01-463)

235
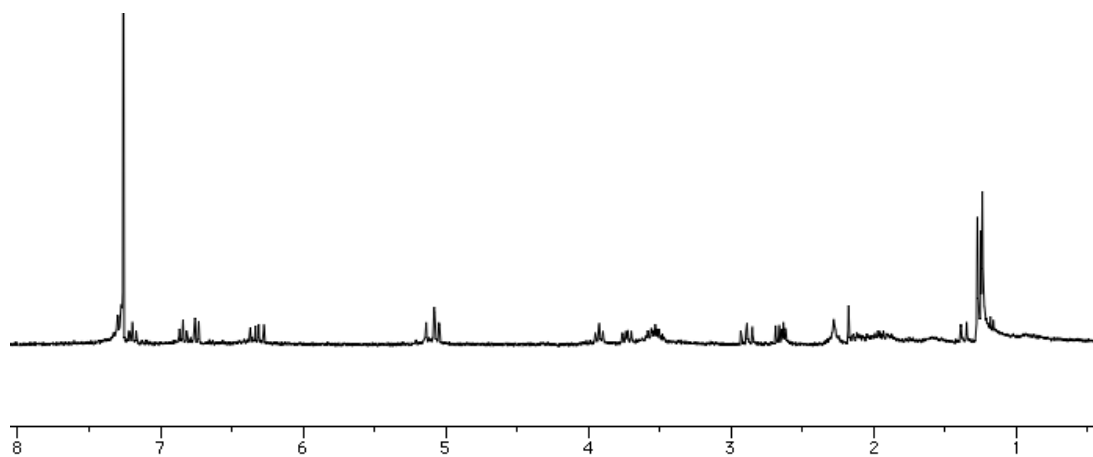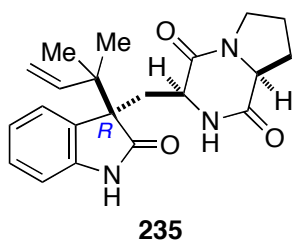
236: ^{1}H-NMR (300 MHz, CDCl$_3$) δ 7.32, (d, J = 8.4 Hz, 1H), 7.10 (t, J = 7.5 Hz, 1H), 6.79 (t, J = 8.1 Hz, 1H), 6.65 (d, J = 8.1 Hz, 1H), 6.40 (dd, J = 17.7, 10.8 Hz, 1H), 5.15 (dd, J = 27.0, 17.7 Hz, 2H), 4.30 (d, J = 14.1 Hz, 1H), 4.01 (t, J = 8.7 Hz, 1H), 3.52-3.47 (m, 1H), 3.37-3.29 (m, 1H), 3.16-3.07 (m, 1H), 2.71 (dd, J = 13.8, 10.8 Hz, 1H), 2.19-1.99 (m, 3H), 1.80-1.70 (m, 2H), 1.39 (s, 3H), 1.35 (s, 3H); ^{13}C NMR (100 MHz, d$_6$-acetone) δ 169.12, 164.7, 149.0, 145.5, 1311.9, 129.5, 125.0, 119.2, 111.7, 110.4, 94.8, 87.6, 59.6, 59.3, 45.0, 35.7, 27.1, 24.7, 24.1, 23.0; HRMS (ESI/APCI) calcd for C$_{21}$H$_{26}$N$_3$O$_3$ (M+H) 368.1969, found 368.1972. (jmf-01-464)

236
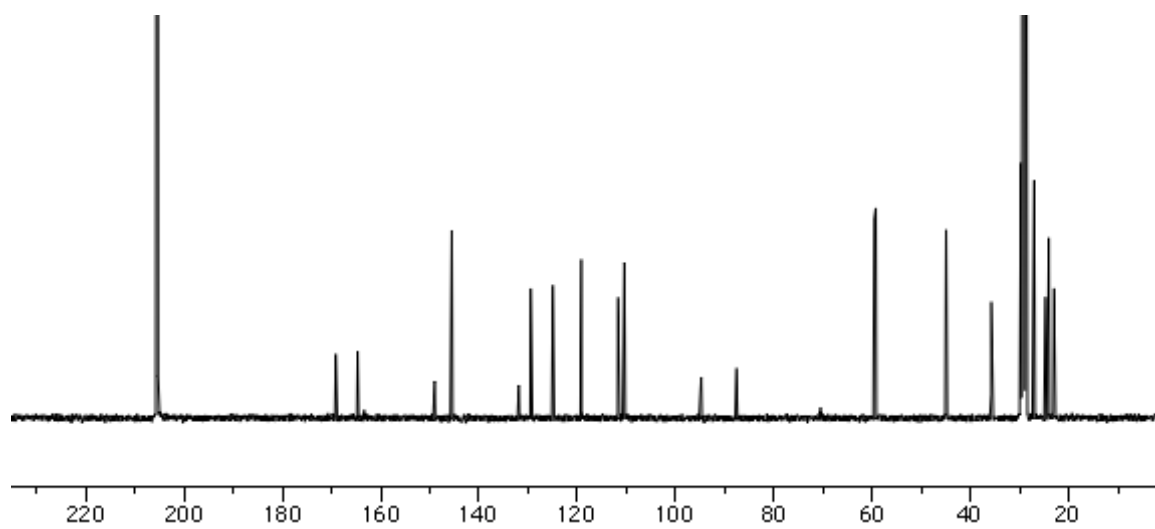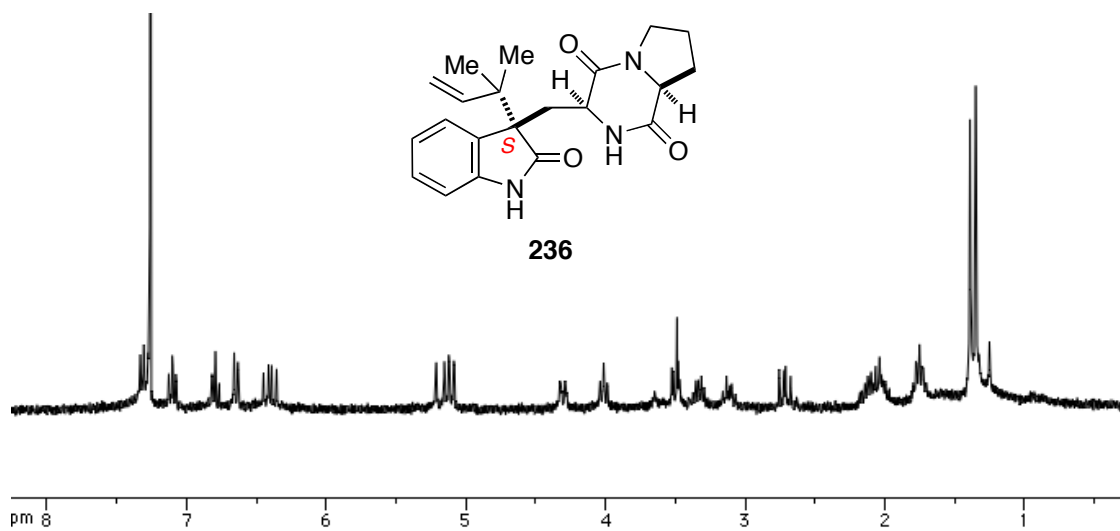
[^{13}C]$_2$-[^{15}N]-(2S)-ethyl 1-(2-((tert-butoxycarbonyl)amino)-3-(2-(2-methylbut-3-en-2-yl)-1H-indol-3-yl)propanoyl)pyrrolidine-2-carboxylate (248)
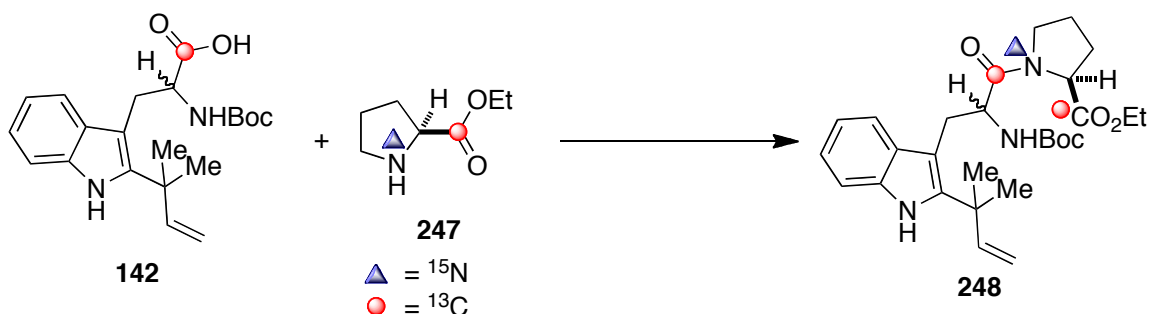
To a solution of ^{13}C labeled acid **142** (820 mg, 2.19 mmol) in 22 mL MeCN was added [^{13}C]$_2$-[^{15}N]-L-proline ethyl ester (317 mg, 2.19 mmol). HATU (1.25 g, 3.29 mmol) and ^{i}Pr$_2$NEt (1.53 mL, 8.76 mmol) were added to the solution and the reaction stirred at room temperature for 4 hours. The reaction was quenched with 30 mL 1M HCl and extracted with CH$_2$Cl$_2$ (3 x 40 mL). The combined organic layer was dried over Na$_2$SO$_4$ and concentrated under vacuum. The crude material was purified via flash column chromatography using 3:1 hexanes/ethyl acetate. Yield: 920 mg, 1.84 mmol, 84%

^{1}H-NMR (300 MHz, CDCl$_3$) δ 8.16 (bs, 1H),7.51-7.45 (m, 1H), 7.25-7.21 (m, 1H), 7.09-7.00 (m, 2H), 6.12 (dd, J = 17.4, 10.5 Hz, 1H), 5.62 (d, J = 8.4 Hz, 1H), 5.24-5.14 (m, 2H), 4.13-4.06 (m, 2H), 3.43-3.06 (m, 4H), 1.62 (s, 3H), 1.59 (s, 3H), 1.43 (s, 9H), 1.22-1.17 (m, 3H); ^{13}C NMR (100 MHz, CDCl$_3$) δ 172.1, 171.8, 171.4, 171.2, 145.6, 140.7, 133.9, 129.9, 121.9, 121.8, 119.5, 119.0, 118.8, 112.6, 112.5, 110.4, 106.2, 106.1, 79.4, 61.2, 60.6, 46.6, 46.5, 39.3, 31.2, 31.1, 30.1, 28.6, 28.3, 28.0, 27.5, 24.1, 22.1, 21.3, 14.4, 14.3. ^{13}C-enriched peaks: 172.1, 171.8, 171.4, 171.2 (jmf-01-498)

248

[^{13}C]$_2$-[^{15}N]-deoxybrevianamide E (4.48):

248

246, [^{13}C]$_2$-[^{15}N]-deoxybrevianamide E

[^{13}C]$_2$-[^{15}N]-Peptide **248** (920 mg, 1.84 mmol) was dissolved in 3 mL CH$_2$Cl$_2$ and cooled to 0°C . TFA (3 mL) was added and the ice bath was removed. The reaction stirred at room temperature for 3 hours. The reaction was quenched with saturated aqueous NaHCO$_3$ to pH 10, extracted with ethyl acetate (3 x 50 mL), and dried over Na$_2$SO$_4$. The organic layer was concentrated under vacuum. The crude amine (500 mg, 1.25 mmol) was dissolved in toluene (6.25 mL) and 2-hydroxypyridine (23 mg, 0.25 mmol) was added to the solution. The reaction was heated to reflux and stirred for 15 hours. The mixture was concentrated and the residue was diluted with 15 mL CH$_2$Cl$_2$. The organic layer was washed with 20 mL 1M HCl, dried over Na$_2$SO$_4$, and concentrated. The crude material was purified via flash column chromatography with 3% MeOH in CH$_2$Cl$_2$ to afford 156.4 mg (35%) of the *cis* diastereomer.

Cis: ^{1}H-NMR (300 MHz, CDCl$_3$) δ 8.27 (bs, 1H), 7.48 (d, *J* = 7.8 Hz, 1H), 7.31 (d, *J* = 8.1 Hz, 1H), 7.19-7.07 (m, 2H), 6.12 (dd, *J* = 17.4, 10.5 Hz, 1H), 5.70 (d, *J* = 4.8 Hz, 1H), 5.18 (d, *J* = 3.0 Hz, 1H), 5.13 (d, *J* = 3.9 Hz, 1H), 4.44 (d, *J* = 12.0 Hz, 1H), 4.06-4.04 (m, 1H), 3.77-3.55 (m, 3H), 3.23-3.13 (m, 1H), 2.37-2.30 (m, 1H), 2.18-1.85 (m, 3H), 1.54 (s, 6H); ^{13}C NMR (100 MHz, CDCl$_3$) δ 169.5, 166.2, 166.0, 145.8, 141.7,

134.6, 129.2, 122.3, 120.3, 118.0, 112.9, 111.1, 104.6, 60.6, 59.7, 59.1, 59.0, 55.5, 55.4, 54.8, 54.7, 45.7, 45.5, 45.4, 39.2, 28.6, 28.1, 26.1, 22.8, 21.3, 14.4. ^{13}C-enriched peaks: 169.5, 166.2, 166.0. (jmf-01-492)
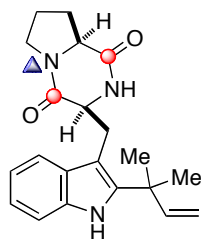
246, [^{13}C]$_2$-[^{15}N]-deoxybrevianamide E
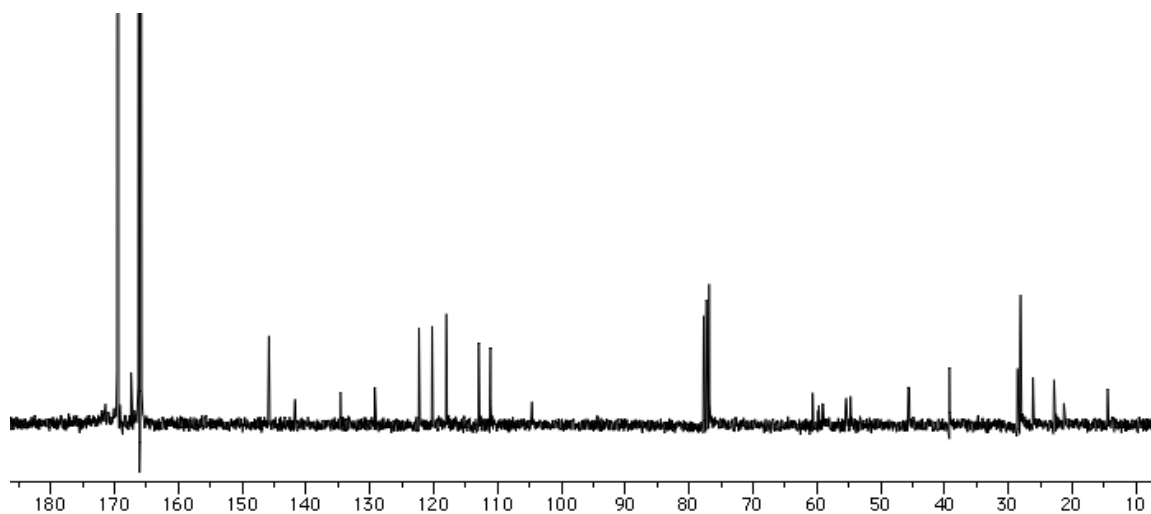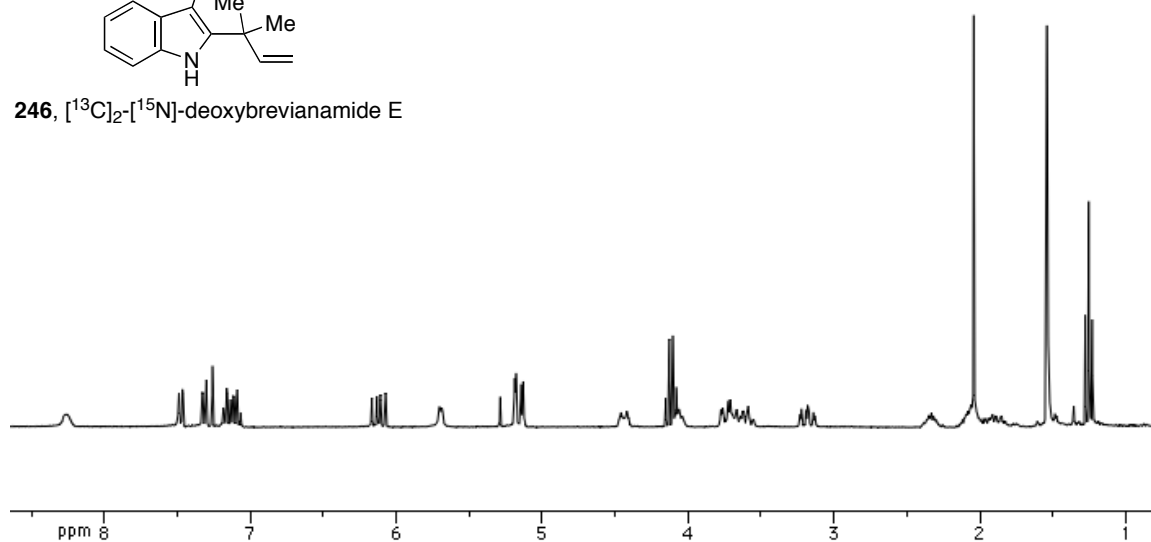
(2S,3R)-1-(tert-butoxycarbonyl)-3-hydroxypyrrolidine-2-carboxylic acid (251):

To a solution of 3-*cis*-β-hydroxyproline **80** (500 mg, 3.81 mmol) in THF (19 mL) was added di-*tert*-butyldicarbonate (873 mg, 4.00 mmol) and 1M NaOH (3.81 mL). The reaction mixture stirred at room temperature for 30 hours and the THF was removed under vacuum. Water (10 mL) was added to the residue and the slurry was acidified to pH 2 with saturated $KHSO_4$. The crude product was extracted with EtOAc (3x 35 mL), dried over Na_2SO_4 and concentrated. The crude material was a white foam that was recrystallized from hot EtOAc and hexanes. Yield: 872 mg, 3.77 mmol, 99%.

^{1}H-NMR (300 MHz, $CDCl_3$) δ 4.64-4.61 (m, 1H), 4.39-4.31 (m, 1H), 3.65-3.42 (m, 2H), 2.02 (m, 2H), 1.41 (d, *J* = 13.2 Hz, 9H); ^{13}C NMR (75 MHz, $CDCl_3$) δ 174.3, 155.7, 81.3, 72.7, 64.6, 44.4, 32.3, 28.6, 28.4. (jmf-02-763)

251

(2S,3R)-tert-butyl 2-((1-ethoxy-3-(2-(2-methylbut-3-en-2-yl)-1H-indol-3-yl)-1-oxopropan-2-yl)carbamoyl)-3-hydroxypyrrolidine-1-carboxylate (254):
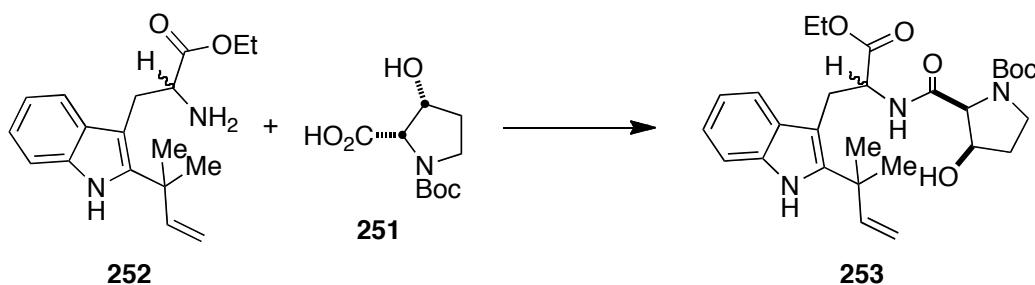
Amine **252** (182 mg, 0.606 mmol) and proline **251** (140 mg, 0.606 mmol) were stirred together in MeCN (6 mL) at room temperature. HATU (345 mg, 0.909 mmol) and DIPEA (0.422 mL, 2.42 mmol) were added to the reaction mixture and the reaction stirred at room temperature for 5 hours. The reaction was quenched with 1M HCl until acidic and extracted with CH_2Cl_2 (3x 15 mL). The combined organic layers were dried over Na_2SO_4 and concentrated. The crude product was purified via flash column chromatography via 50:50 hexanes-EtOAc. Yield: 308 mg, 0.600 mmol, 99%

^{1}H-NMR (300 MHz, CDCl$_3$) δ 7.99 (bs, 1H), 7.54 (d, J = 8.17 Hz, 1H), 7.47 (d, J = 7.2 Hz, 1H), 7.17-7.09 (m, 2H), 6.15 (dd, J = 17.7, 11.1 Hz, 1H), 5.28 (bs, 1H), 5.24-5.19 (m, 2H), 4.86-4.73 (m, 1H), 4.35-4.28 (m, 2H), 4.08-3.98 (m, 2H), 3.38-3.17 (m, 4H), 2.01-2.81 (m, 2H), 1.56 (s, 9H), 1.42 (m, 6H), 1.25 (t, J = 8.4 Hz, 3H); ^{13}C NMR (75 MHz, CDCl$_3$) δ 174.0, 172.9, 171.5, 166.0, 145.9, 141.1, 134.6, 129.8, 121.8, 119.8, 117.7, 112.4, 111.0, 104.9, 80.8, 73.1, 67.5, 61.7, 60.6, 54.5, 38.8, 28.3, 27.9, 27.8, 27.6, 21.3, 14.4, 13.9; HRMS (ESI/APCI) calcd for $C_{28}H_{39}N_3O_6Na$ (M+Na) 536.2731, found 536.2728. (jmf-02-762)

253
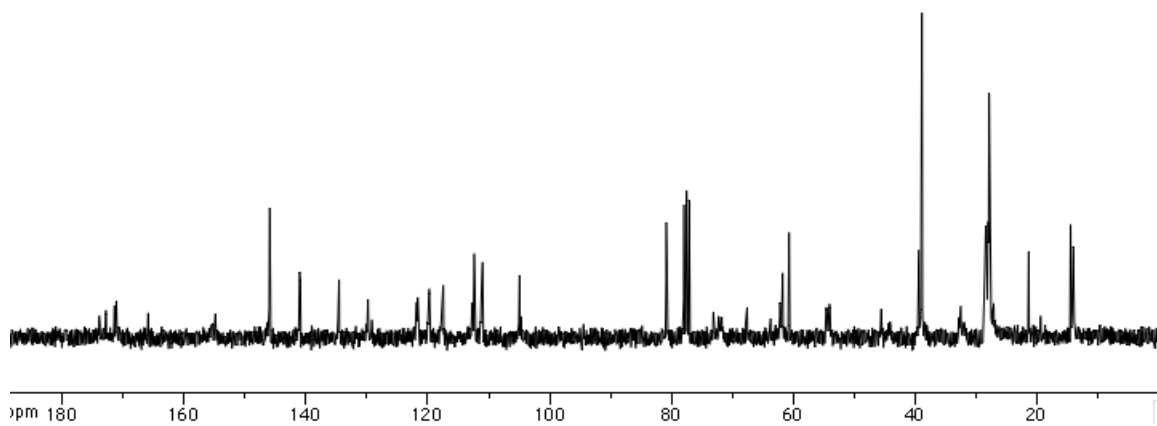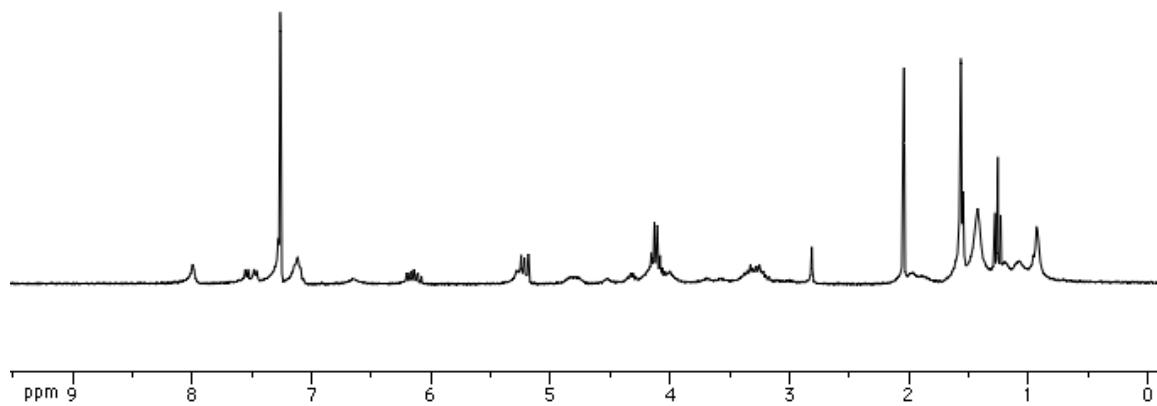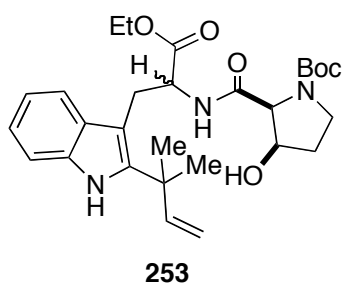
(8R,8aS)-8-hydroxy-3-((2-(2-methylbut-3-en-2-yl)-1H-indol-3-yl)methyl) hexahydropyrrolo[1,2-a]pyrazine-1,4-dione (254):

253   **254**
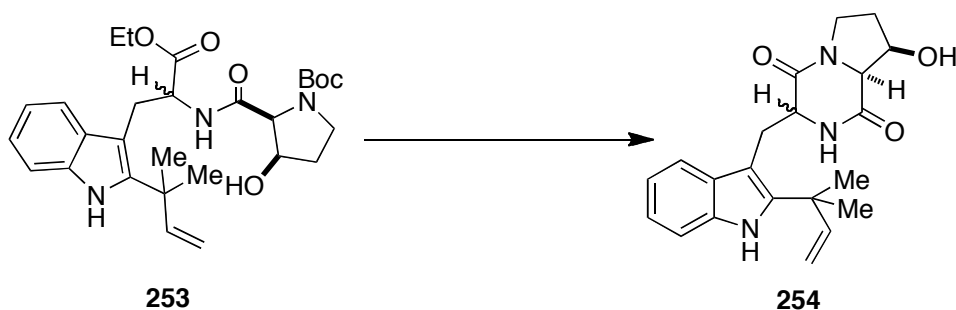
To a stirred solution of indole **253** (308 mg, 0.600 mmol) in CH_2Cl_2 (2 mL) at 0°C was slowly added TFA (2 mL). The reaction mixture stirred for 3 hours while warming to room temperature. The reaction was concentrated under vacuum and the residue was basified with aqueous saturated $NaHCO_3$ to pH 10. The crude material was extracted with EtOAc (3x 50 mL), the combined organic layers were dried over Na_2SO_4 and concentrated. The crude free amine (248 mg, 0.600 mmol) was dissolved in toluene (6 mL) and to the solution was added 2-hydroxy-pyridine (11 mg, 0.121 mmol). The reaction stirred at reflux for 15 hours. The mixture was concentrated under vacuum, diluted with CH_2Cl_2 and washed with 1M HCl (2x 20 mL). The organic layer was dried over Na_2SO_4 and concentrated. The crude material was purified via flash column chromatography with 3% MeOH in CH_2Cl_2 to afford a 1:1 ratio of *cis*:*trans* diketopiperazines, which were taken on as a mixture of diastereomers. Yield: 191 mg, 0.522 mmol, 87%.

Cis: ^{1}H-NMR (300 MHz, CDCl$_3$) δ 8.57 (bs, 1H), 7.45 (d, *J* = 7.5 Hz, 1H), 7.29 (d, *J* = 7.8 Hz, 1H), 7.15-7.03 (m, 2H), 6.08 (dd, *J* = 17.7, 10.5 Hz, 1H), 5.93 (bs, 1H), 5.13 (d, *J* = 2.7 Hz, 1H), 5.08 (d, *J* = 2.4 Hz, 1H), 4.60 (bs, 1H), 4.41 (d, *J* = 11.4 Hz, 1H), 3.99-3.52 (m, 4H), 3.17 (dd, *J* = 15, 11.7 Hz, 1H), 2.13-1.94 (m, 3H), 1.49 (d, *J* = 3.3 Hz, 6H); ^{13}C NMR (75 MHz, CDCl$_3$) δ 167.6, 166.0, 145.8, 142.0, 134.8, 129.3, 122.2, 120.1, 118.0, 112.8, 111.2, 104.5, 71.0, 64.8, 55.2, 44.2, 39.2, 30.6, 28.2, 28.0, 26.6 ; HRMS (ESI/APCI) calcd for C$_{21}$H$_{25}$N$_3$O$_3$Na (M+Na) 390.1788, found 390.1799. (jmf-02-706)

254
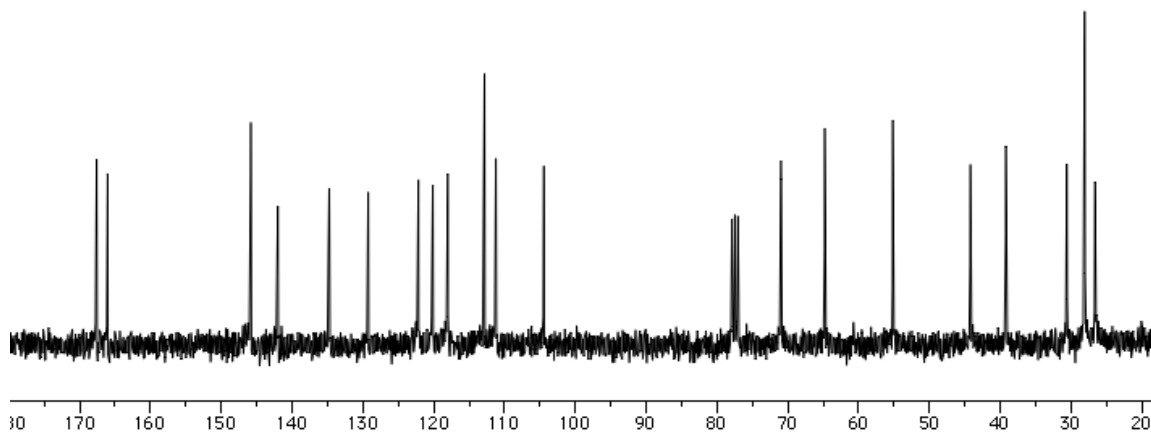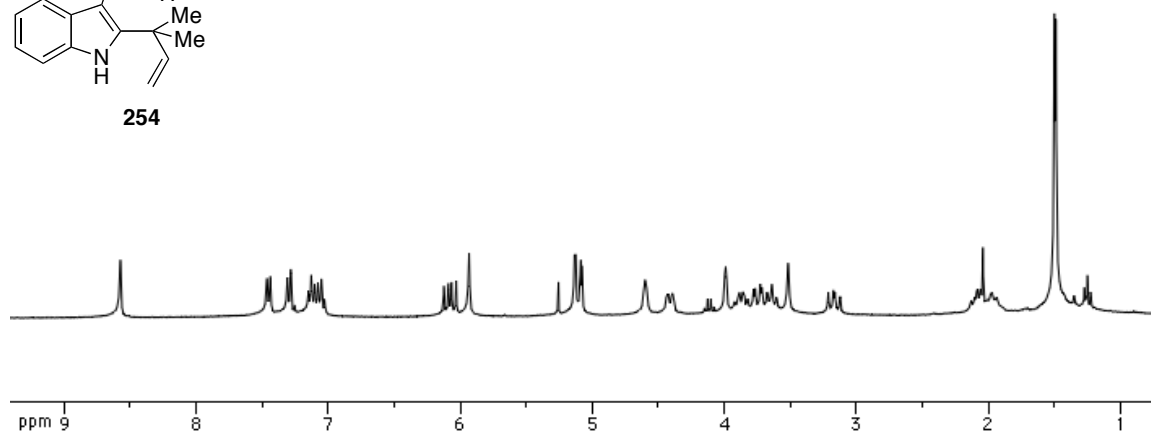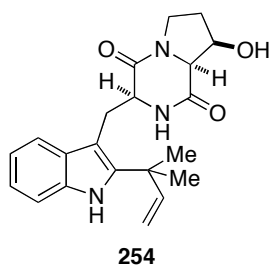
Trans: ^{1}H-NMR (300 MHz, CDCl$_3$) δ 8.35 (bs, 1H), 7.45 (m, 1H), 7.12 (m, 1H), 7.01-6.98 (m, 2H), 6.28 (m, 1H), 6.05 (dd, *J* = 17.4, 10.5 Hz, 1H), 5.27 (s, 1H) 5.14-5.07 (m, 2H), 4.49 (bs, 1H), 4.22-4.19 (m, 1H), 3.83-3.15 (m, 6H), 2.00-1.94 (m, 1H), 1.78-1.67 (m, 1H), 1.46 (s, 6H); ^{13}C NMR (75 MHz, CDCl$_3$) δ 167.5, 166.6, 146.2, 141.8, 134.4, 129.2, 121.9, 119.8, 118.7, 112.1, 110.7, 105.1, 70.9, 64.1, 58.5, 44.4, 39.3, 30.3, 30.1, 28.2, 28.0; HRMS (ESI/APCI) calcd for C$_{21}$H$_{26}$N$_3$O$_3$ (M+H) 368.1969, found 368.1965. (jmf-02-706)
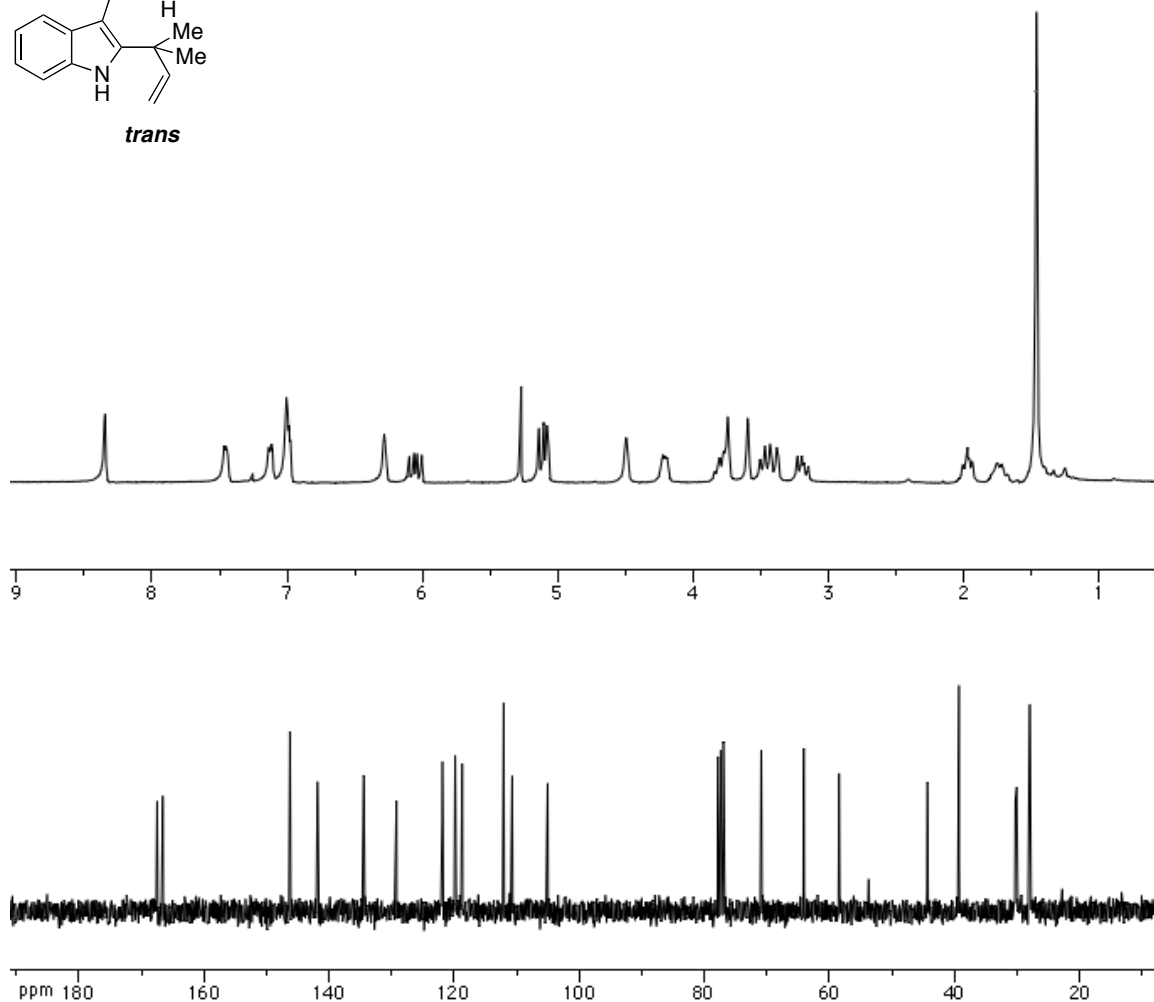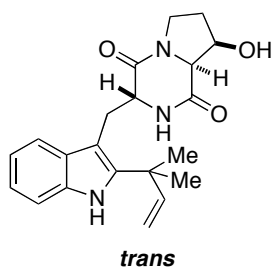
3-((2-(2-methylbut-3-en-2-yl)-1H-indol-3-yl)methyl)-2,3,6,7-tetrahydropyrrolo[1,2-a]pyrazine-1,4-dione (255):
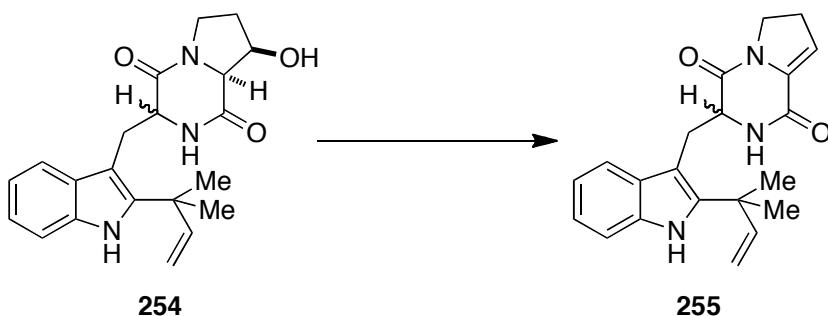
Alcohol **254** (113 mg, 0.308 mmol) was dissolved in MeCN (6 mL). To the solution, 40% DEAD in toluene (0.401 mL, 0.923 mmol) was added and the reaction stirred for 10 minutes at room temperature. Freshly distilled tributylphosphine (0.227, 0.923 mmol) was added and the reaction mixture stirred for 2 hours at room temperature. The solution was concentrated and purified via flash column chromatography in 3% MeOH in CH$_2$Cl$_2$ to afford a yellow oil. Yield: 101 mg, 0.290 mmol, 94%.

^{1}H-NMR (300 MHz, CDCl$_3$) δ 8.65 (bs, 1H), 7.49 (d, J = 7.5 Hz, 1H), 7.28 (d, J = 7.5 Hz, 1H), 7.13-7.03 (m, 2H), 6.13-6.03 (m, 2H), 5.79 (bs, 1H), 5.13-5.07 (m, 2H), 4.49 (d, J = 10.5 Hz, 1H), 4.08-4.00 (m, 2H), 3.70 (dd, J = 14.4, 3.6 Hz, 1H), 3.22 (dd, J = 14.4, 11.1 Hz, 1H), 2.77-2.70 (m, 2H), 1.51 (d, J = 3.0 Hz, 6H); ^{13}C NMR (75 MHz, CDCl$_3$) δ 162.8, 156.7, 146.0, 142.1, 134.7, 133.2, 129.0, 122.1, 120.0, 119.3, 118.3, 112.3, 111.1, 104.4, 57.7, 45.8, 39.3, 31.1, 28.2, 28.1, 28.0; HRMS (ESI/APCI) calcd for C$_{21}$H$_{24}$N$_3$O$_2$ (M+H) 350.1863, found 350.1872. (jmf-02-716)
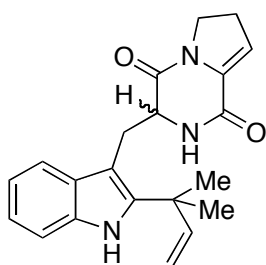
255
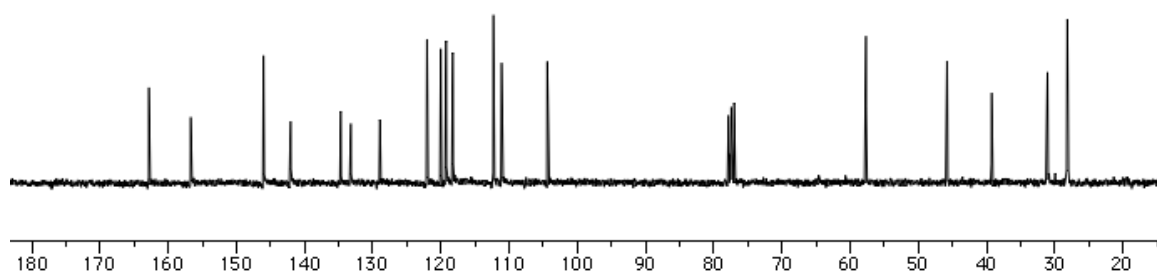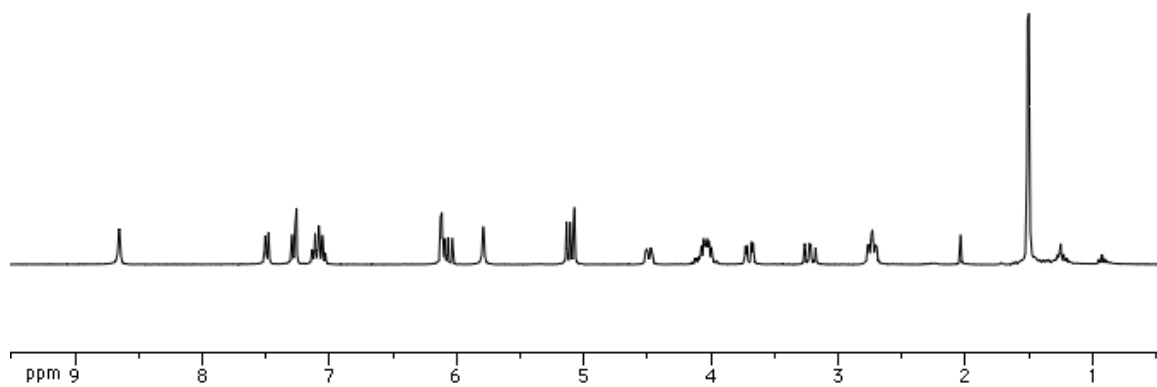
Diels-Alder Cycloadducts (257 and 258):

255 → **257**, *syn*
keto-pre-malbrancheamide

\+ **258**, *anti*
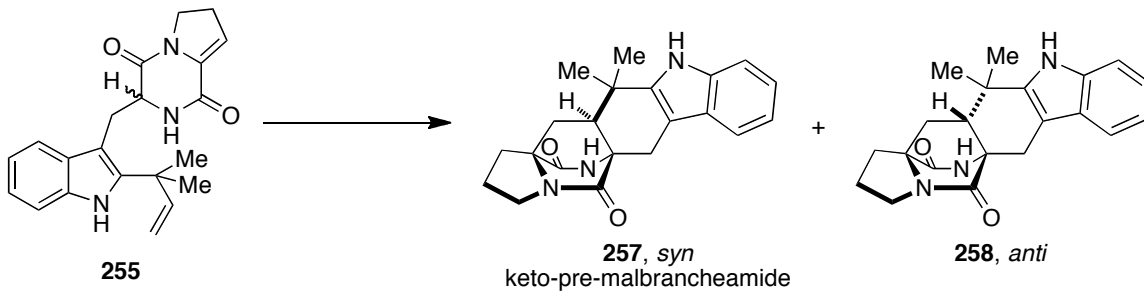
To a cooled solution (0°) of enamide **255** (101 mg, 0.290 mmol) in 25 mL MeOH was added 20% aqueous KOH (5 mL) and the reaction stirred for 16 hours at room temperature. The mixture was quenched with saturated aqueous NH$_4$Cl (30 mL) and extracted with CH$_2$Cl$_2$ (3x 30 mL). The combined organic layers were dried over Na$_2$SO$_4$ and concentrated under vacuum. The *syn*-isomer was collected by crashing the *anti*-diastereomer out of the solution. Using EtOAc and MeOH, the *anti*- product precipitated out as a white solid, leaving the *syn*-isomer in solution. Total combined yield: 79 mg, 0.226 mmol, 78%. *syn*: 55.8 mg *anti*: 23.2 mg

257: ^{1}H-NMR (400 MHz, 10:1 CDCl$_3$/CD$_3$OD) δ 7.43-7.40 (m, 1H), 7.24-7.22 (m, 1H), 7.05-6.95 (m, 2H), 3.66 (d, J = 15.6 Hz, 1H), 3.50-3.41 (m, 2H), 3.36-3.27 (m, 2H), 2.73-2.60 (m, 2H), 2.53-2.50 (m, 1H), 2.16-2.10 (m, 1H), 2.02-1.82 (m, 4H), 1.27 (s, 3H), 1.02 (s, 3H); ^{13}C NMR (100 MHz, 1:2 CDCl$_3$/CD$_3$OD) δ 174.5, 170.0, 140.2, 137.0, 126.8, 121.3, 118.7, 117.9, 110.8, 103.6, 66.9, 60.6, 44.2, 34.9, 30.9, 29.3, 28.2, 24.5, 23.3, 21.9, 14.0; HRMS (ESI/APCI) calcd for C$_{21}$H$_{23}$N$_3$O$_2$Na (M+Na) 372.1682, found 372.168. (jmf-02-718)
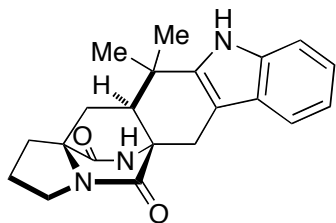
257, *syn*
keto-pre-malbrancheamide
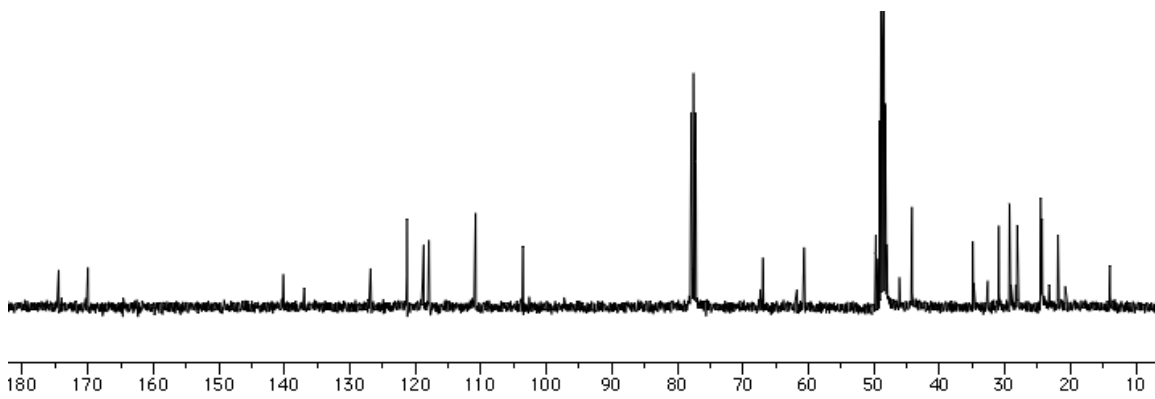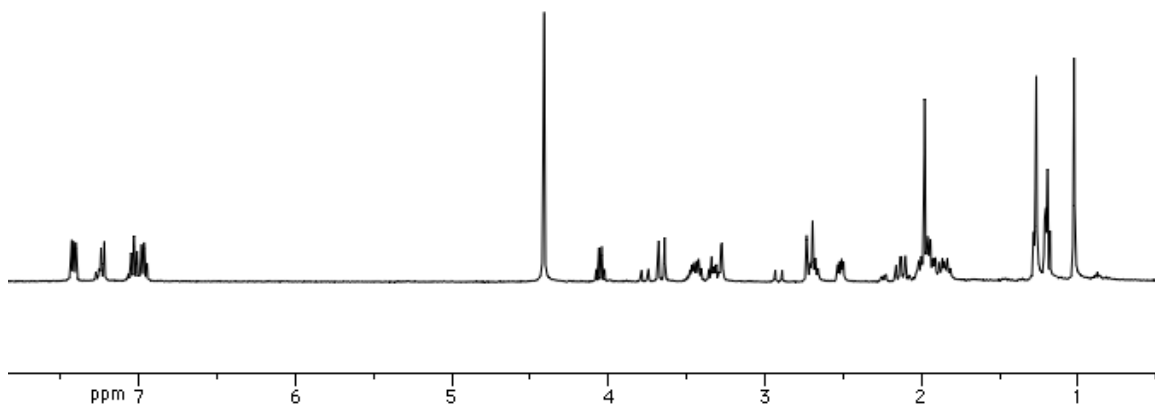
258: ^{1}H-NMR (400 MHz, 10:1 CDCl$_3$/CD$_3$OD) δ 7.43 (d, J = 7.6 Hz, 1H), 7.26 (d, J = 8.0 Hz, 1H), 7.07-6.96 (m, 2H), 3.76 (d, J = 16.4 Hz, 1H), 3.49-3.41 (m, 3H), 3.34-3.27 (m, 1H), 2.90 (d, J = 17.6 Hz, 1H), 2.72-2.65 (m, 2H), 2.24-2.21 (m, 1H), 2.10-1.78 (m, 4H), 1.27 (s, 3H), 1.17 (s, 3H); ^{13}C NMR (100 MHz, 1:21 CDCl$_3$/CD$_3$OD) δ 174.0, 170.2, 140.5, 137.0, 127.2, 121.5, 119.0, 118.0, 110.9, 102.7, 67.3, 61.7, 46.0, 44.3, 34.8, 32.6, 29.3, 24.5, 23.3, 21.9; HRMS (ESI/APCI) calcd for C$_{21}$H$_{24}$N$_3$O$_2$ (M+H) 350.1863, found 350.1864. (jmf-02-830)

258, *anti*

spiro-oxindole (238 and 259):

257, *syn*
keto-pre-malbrancheamide
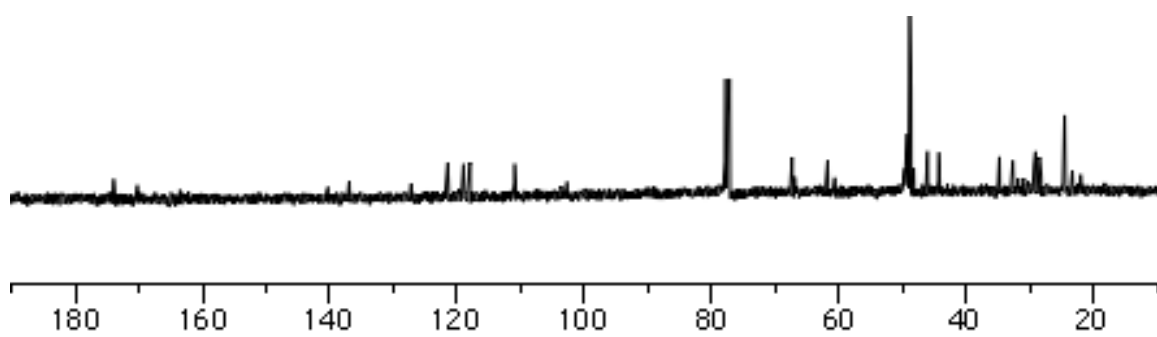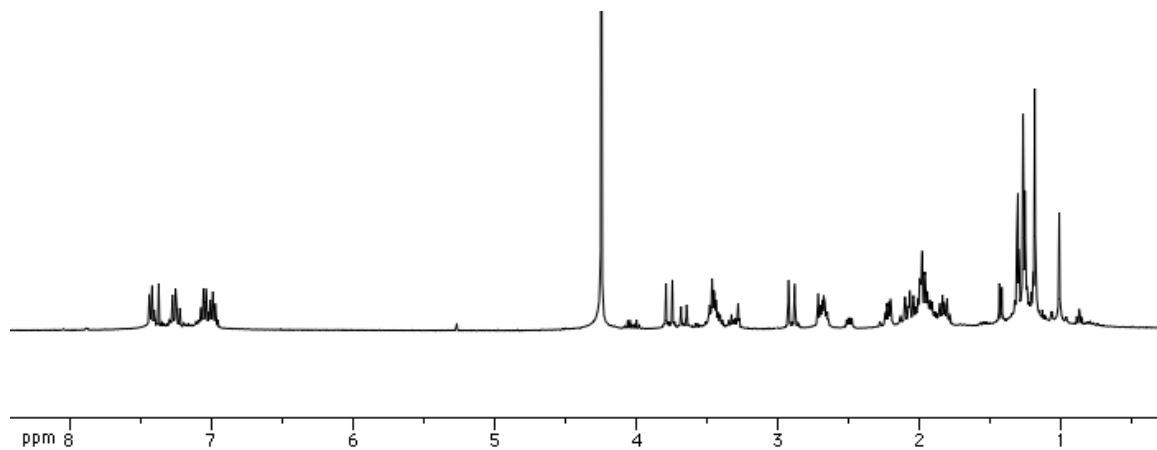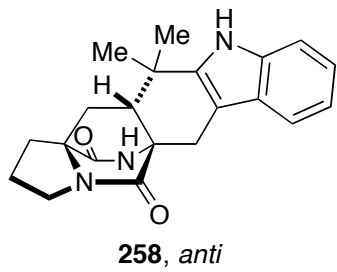
238   **259**
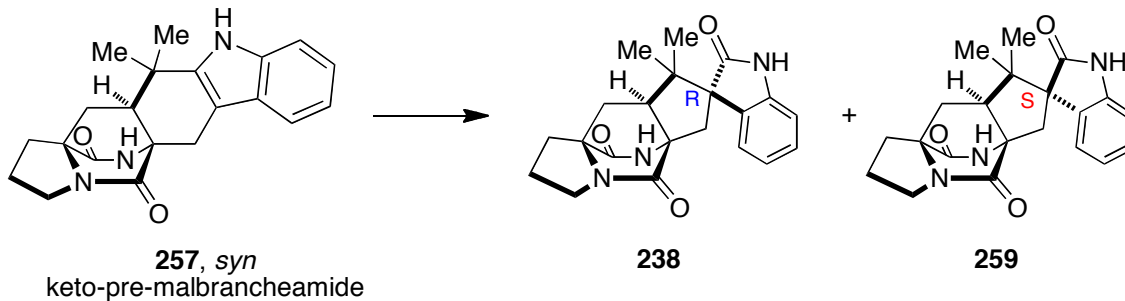
The *syn*-isomer **238** (56 mg, 0.160 mmol) was dissolved in CH$_2$Cl$_2$ (3.2 mL) and Davis oxaziridine (76 mg, 0.321 mmol) was added to the reaction mixture. The solution stirred at room temperature for 18 hours. The mixture was concentrated and purified via silica gel flash column chromatography using 50:1 CH$_2$Cl$_2$-MeOH to furnish a 1:1 mixture of diastereomers.

238: ^{1}H-NMR (400 MHz, CDCl$_3$) δ 7.36 (d, *J* = 7.6 Hz, 1H), 7.26-7.22 (m, 1H), 7.14-7.08 (m, 2H), 3.99 (bs, 1H), 3.66-3.61 (m, 1H), 3.37-3.29 (m, 3H), 2.75 (d, *J* = 16 Hz, 1H), 2.66-2.59 (m, 1H), 2.29 (d, *J* = 16 Hz, 1H), 2.10-2.02 (m, 1H), 1.95-1.85 (m, 3H), 1.77-1.70 (m, 2H), 1.23 (s, 3H), 1.03 (s, 3H); ^{13}C NMR (100 MHz, CDCl$_3$) δ 189.8, 173.5, 167.9, 153.3, 139.6, 129.9, 126.3, 122.0, 120.7, 83.0, 66.9, 60.0, 48.1, 44.3, 38.5, 33.9, 31.2, 29.3, 28.6, 24.4, 21.0; HRMS (ESI/APCI) calcd for C$_{21}$H$_{23}$N$_3$O$_3$Na (M+Na) 388.1632, found 388.1635. (jmf-02-721b)

238

259: ^{1}H-NMR (300 MHz, CDCl$_3$) δ 7.52 (d, J = 7.8 Hz, 1H), 7.43-7.33 (m, 2H), 7.24-7.16 (m, 1H), 3.96 (s, 1H), 3.40 (t, J = 6.6 Hz, 1H), 2.80 (d, J = 15.6 Hz, 1H), 2.76-2.67 (m, 1H), 2.01-1.93 (m, 6H), 1.86-1.73 (m, 3H), 1.43 (s, 3H), 1.30 (s, 3H); ^{13}C NMR (100 MHz, CDCl$_3$) δ 188.1, 172.4, 168.2, 151.9, 140.5, 130.0, 126.4, 122.2, 121.0, 82.3, 67.1, 61.9, 50.3, 44.0, 40.4, 37.9, 32.5, 28.9, 27.3, 24.3, 20.0; HRMS (ESI/APCI) calcd for C$_{21}$H$_{24}$N$_3$O$_3$ (M+H) 366.1812, found 366.1817. (jmf-02-721a)
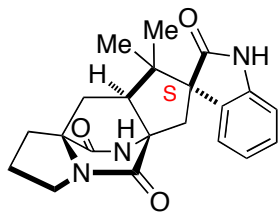
259
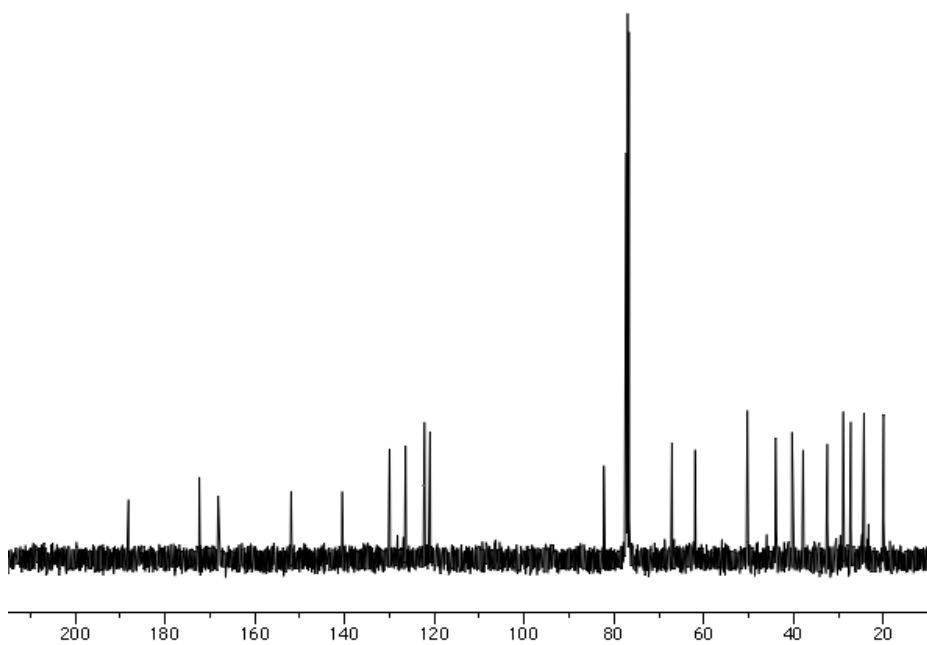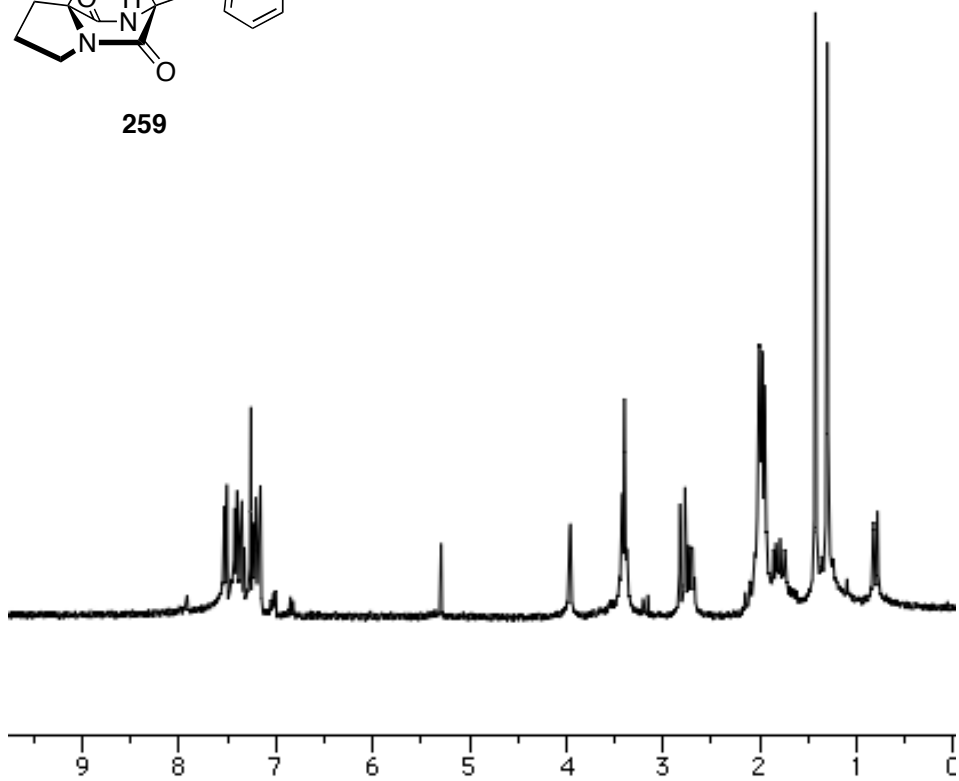
Oxindole (260 and 261):
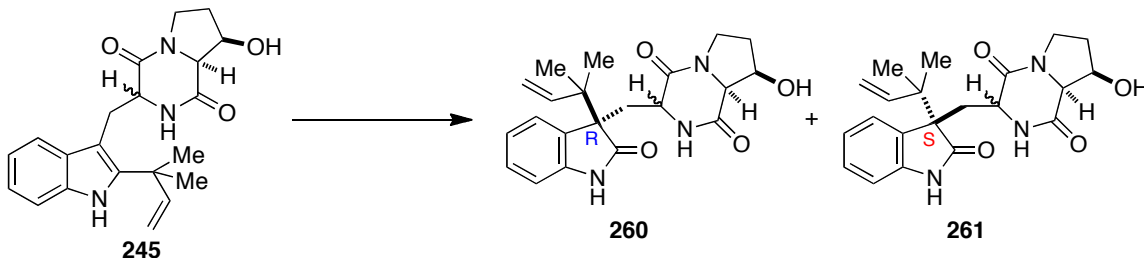
To a solution of a mixture of diketopiperazine diastereomers **4.63** (228 mg, 0.621 mmol) in CH$_2$Cl$_2$ (12 mL), was added Davis oxaziridine (296 mg, 1.24 mmol). The reaction mixture stirred for 15 hours at room temperature. The solution was concentrated and purified via flash column chromatography in 5% MeOH in CH$_2$Cl$_2$. Combined yield: 209 mg, 0.503 mmol, 81%.

260: ^{1}H-NMR (300 MHz, CDCl$_3$) δ 8.56 (bs, 1H), 7.25 (d, J = 7.5 Hz, 1H), 7.03 (t, J = 7.8 Hz, 1H), 6.90 (d, J = 7.8 Hz, 1H), 6.77 (s, 1H), 6.04 (dd, J = 17.1, 10.8 Hz, 1H), 5.06 (dd, J = 29.1, 11.1 Hz, 2H), 4.57 (t, J = 3.0 Hz, 1H), 3.88 (s, 1H), 3.75-3.52 (m, 3H), 3.26-3.14 (m, 3H), 2.30-2.22 (m, 1H), 2.12-2.05 (m, 1H), 1.93-1.72 (m, 3H), 1.13 (s, 3H), 1.08 (s, 3H); ^{13}C NMR (100 MHz, CDCl$_3$) δ 182.0, 168.6, 165.1, 142.5, 141.6, 129.6, 128.8, 126.3, 122.7, 114.8, 109.8, 70.8, 64.2, 58.1, 52.9, 44.4, 42.6, 31.5, 30.4, 22.6, 21.7; HRMS (ESI/APCI) calcd for C$_{21}$H$_{26}$N$_3$O$_4$ (M+H) 384.1918, found 384.1916. (jmf-02-720b)

260

279
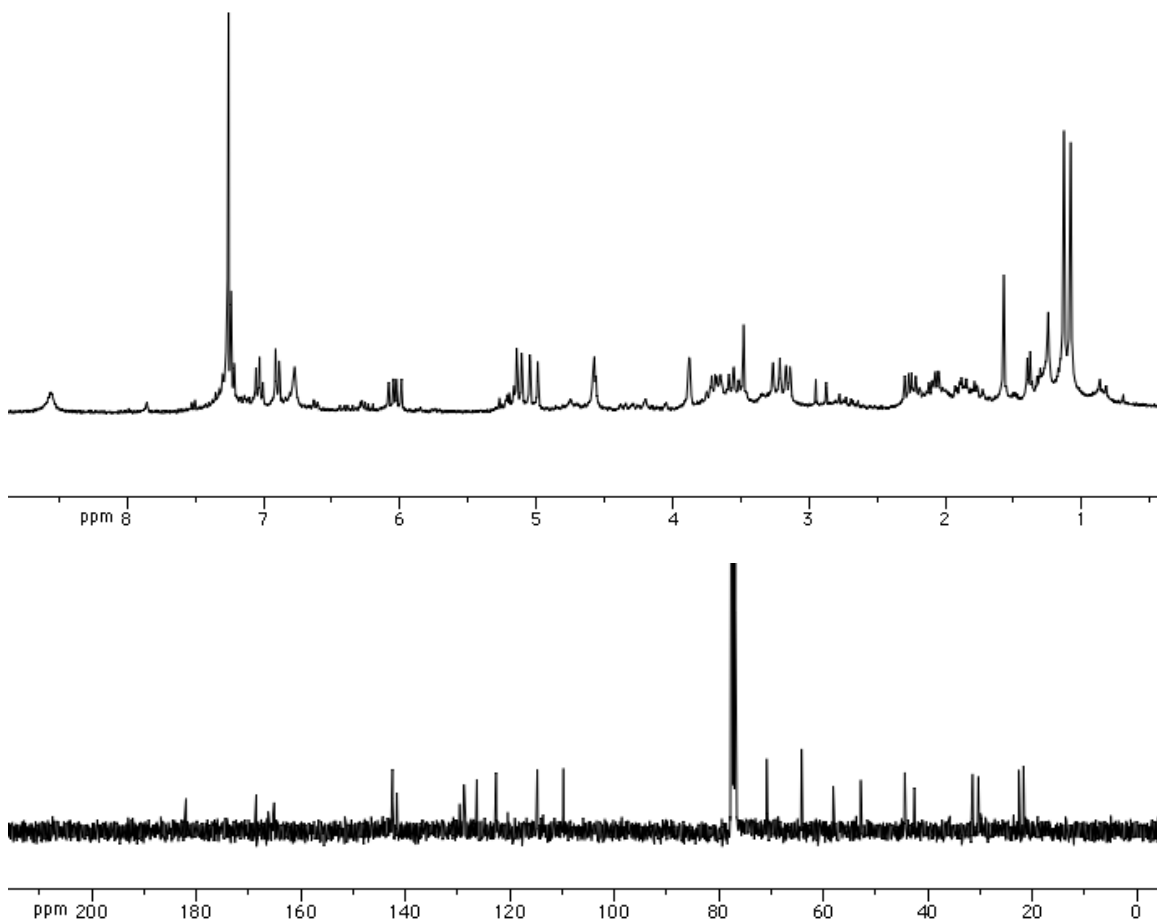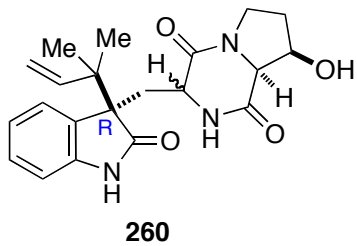
261: ^{1}H-NMR (300 MHz, CDCl$_3$) δ 7.27 (d, J = 8.7 Hz, 1H), 7.10 (t, J = 7.5 Hz, 1H), 6.78 (t, J = 7.2 Hz, 1H), 6.61 (d, J = 7.8 Hz, 1H), 6.38 (dd, J = 17.7, 10.8 Hz, 1H), 6.25 (s, 1H), 5.16 (dd, J = 23.7, 17.4 Hz, 2H), 4.53 (t, J = 3.3 Hz, 1H), 4.23 (d, J = 10.2 Hz, 1H), 4.01 (s, 1H), 3.48-3.40 (m, 3H), 3.34-3.24 (m, 2H), 2.71 (dd, J = 13.8, 11.1 Hz, 1H), 2.02-1.95 (m, 1H), 1.87-1.74 (m, 1H), 1.39 (s, 3H), 1.37 (s, 3H); ^{13}C NMR (75 MHz, CDCl$_3$) δ 168.2, 164.6, 147.8, 144.4, 130.8, 124.9, 120.6, 113.6, 110.6, 95.9, 87.8, 70.6, 64.1, 59.8, 45.0, 43.9, 35.8, 30.6, 25.9, 23.6; HRMS (ESI/APCI) calcd for C$_{21}$H$_{26}$N$_3$O$_4$ (M+H) 384.1918, found 384.1916. (jmf-02-720a)
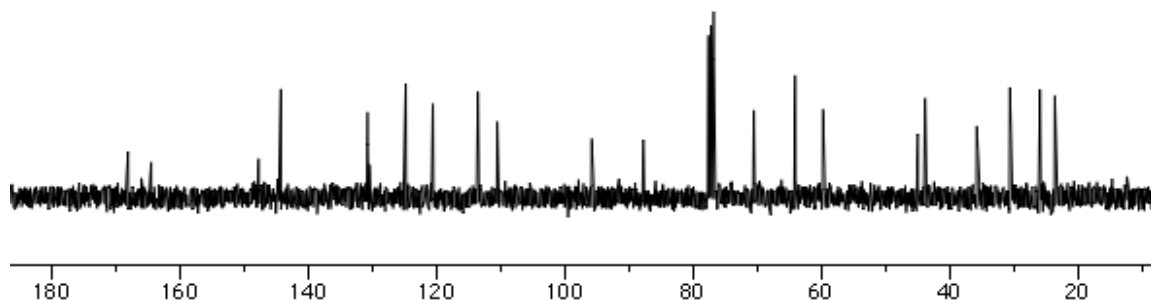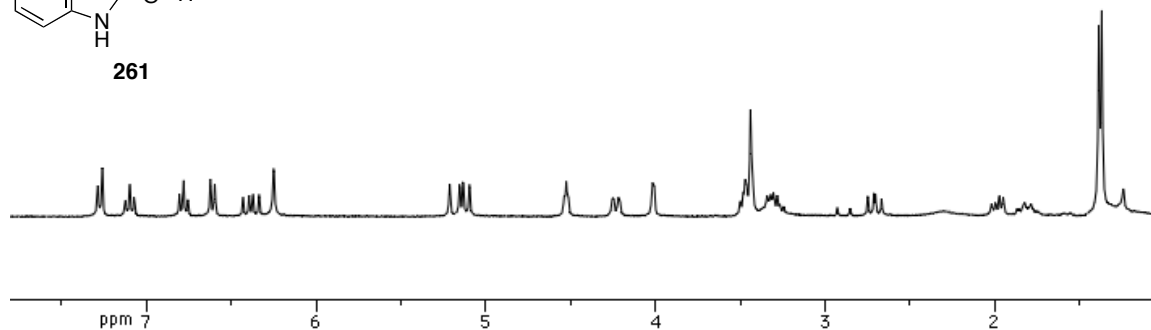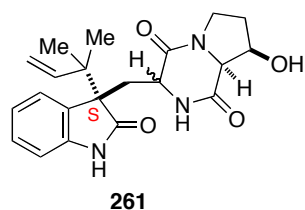
Enamide (262):

260 → **262**
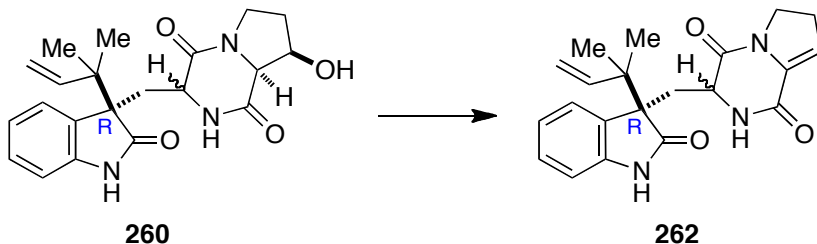
The *R*-oxindole **260** (114 mg, 0.297 mmol) was dissolved in CH₂Cl₂ (6 mL) and 40% DEAD in toluene (0.388 mL, 0.892 mmol) was added. The mixture stirred for 10 minutes at room temperature, and tributylphosphine (0.220 mL, 0.892 mmol) was added. The reaction stirred at room temperature for 4 hours, was concentrated under vacuum, and purified vial flash column chromatography using a gradient elution (70:30 hexanes-ethyl acetate to 30:70 hexanes-ethyl acetate). Yield: 72.7 mg, 0.199 mmol, 67%.

^{1}H-NMR (300 MHz, CDCl₃) δ 7.22 (d, J = 7.8 Hz, 1H), 7.18-7.10 (m, 1H), 6.84-6.72 (m, 1H), 6.62 (d, J = 7.8 Hz, 1H), 6.46 (s, 1H), 6.42-6.29 (m, 1H), 6.06 (t, J = 3.0 Hz, 1H), 5.25-5.05 (m, 2H), 4.15-3.95 (m, 1H), 3.92-3.76 (m, 1H), 2.90-2.82 (m, 1H), 2.79-2.65 (m, 3H), 1.44 (s, 3H), 1.34 (s, 3H), 1.26 (m, 2H). HRMS (ESI/APCI) calcd for C₂₁H₂₄N₃O₃ (M+H) 366.1812, found 366.1815. (jmf-02-528)
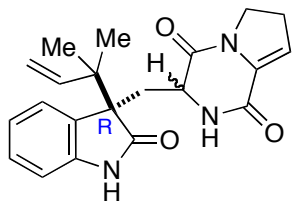
262
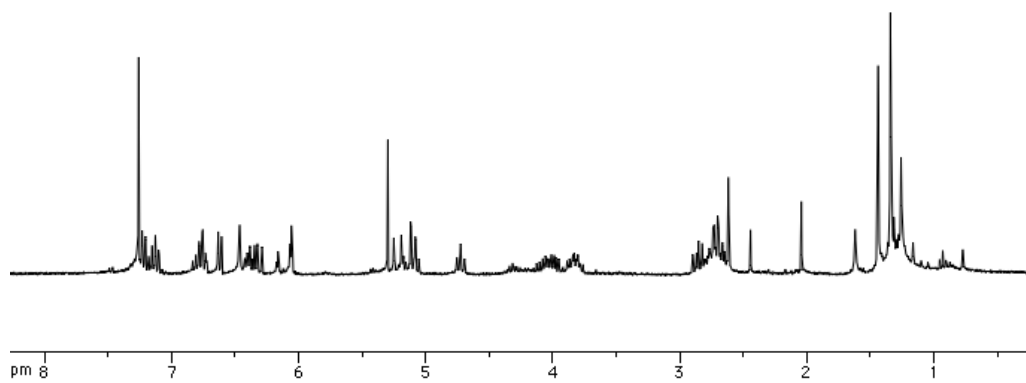
***Spiro*-oxindole (239 and 265):**
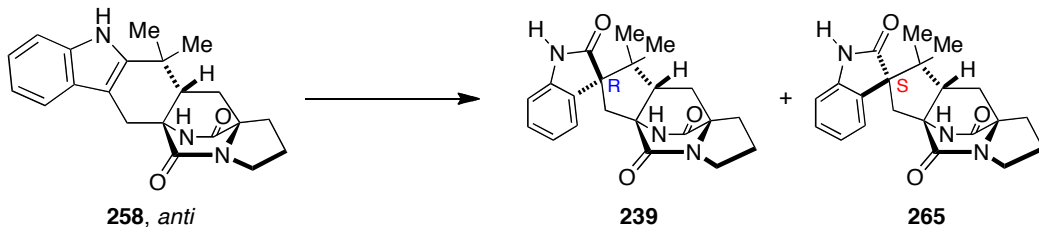
The *anti*-cycloadduct **258** (20 mg, 0.057 mmol) was dissolved in CH$_2$Cl$_2$ (2.2 mL) and Davis oxaziridine (41 mg, 0.172 mmol) was added. The reaction stirred at room temperature for 6 hours, was concentrated under vacuum, and purified via prep-TLC in 3% MeOH in DCM (x3).

R and *S* mixture: ^{1}H-NMR (300 MHz, CDCl$_3$) δ 7.55 (d, *J* = 7.5 Hz, 1H), 7.44 (d, *J* = 7.5 Hz, 1H), 7.40-7.35 (m, 1H), 7.12 (s, 1H), 3.45-3.32 (m, 4H), 2.87-2.71 (m, 3H), 2.07-1.98 (m, 6H), 1.88-1.79 (m, 3H), 1.68-1.59 (m, 2H), 1.46 (s, 3H), 1.34 (s, 3H), 1.30 (s, 3H), 1.24 (s, 3H). HRMS (ESI/APCI) calcd for C$_{21}$H$_{23}$N$_3$NaO$_3$ (M+Na) 388.1632, found 388.1635. (jmf-02-843)
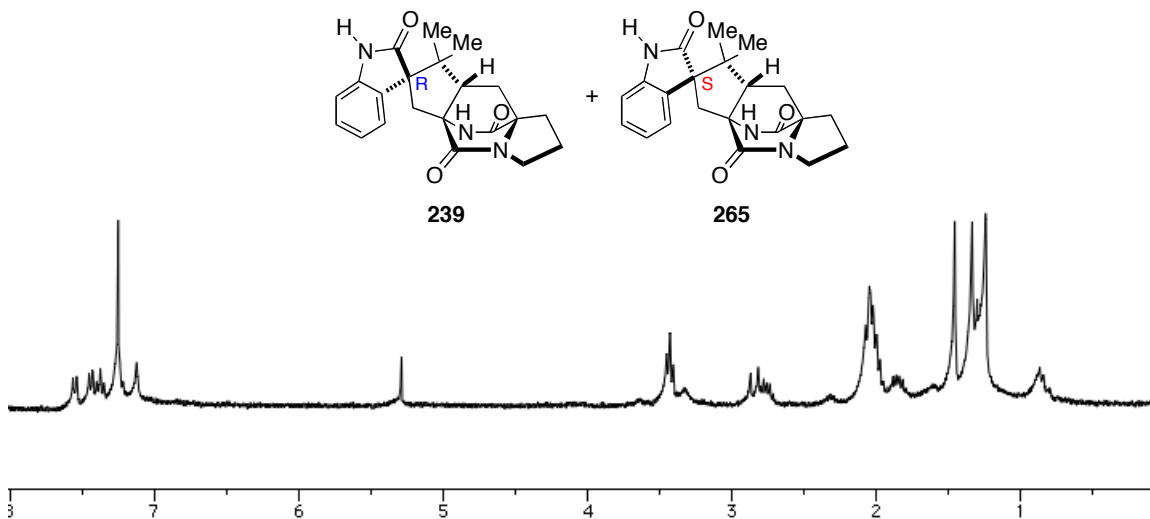
[^{13}C]$_2$-[^{15}N]-(2S)-tert-butyl 2-((3-(6-((tert-butoxycarbonyl)oxy)-2-(2-methylbut-3-en-2-yl)-1H-indol-3-yl)-1-ethoxy-1-oxopropan-2-yl)carbamoyl)pyrrolidine-1-carboxylate (269):
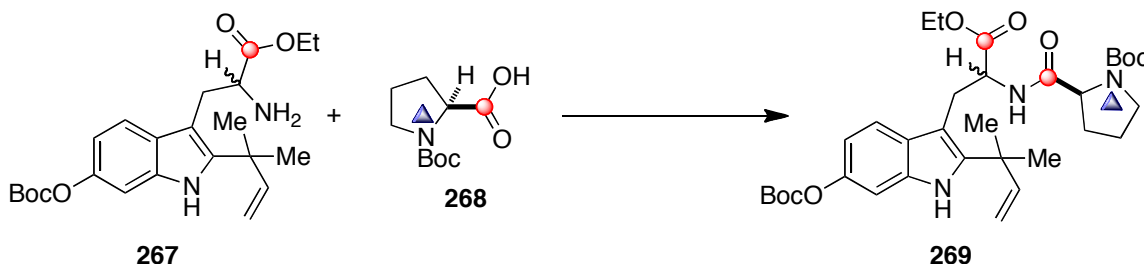
^{13}C-Amine **267** (610 mg, 1.46 mmol) and [^{13}C]-[^{15}N]-*N*-Boc-L-proline (317 mg, 1.46 mmol) were stirred in acetonitrile (15 mL) at 0ºC. HATU (832 mg, 2.19 mmol) and ^{i}Pr$_2$NEt (1.0 mL, 5.84 mmol) were added and the reaction stirred for 3 hours at room temperature. The reaction was quenched with 1M HCl (30 mL) and extracted with CH$_2$Cl$_2$ (3 x 50 mL). The combined organic layer was washed with brine (50 mL), dried over Na$_2$SO$_4$, and concentrated under reduced pressure. The crude residue was purified by flash column chromatography and eluted with 1:1 hexanes/EtOAc to afford 860 mg (95%) of **269** as a yellow amorphous solid.

^{1}H-NMR (300 MHz, CDCl$_3$) δ 8.40 (bs, 1H), 7.42-7.34 (m, 1H), 7.02 (d, *J* = 1.2 Hz, 1H) 6.83-6.81 (m, 1H), 6.09-5.98 (m, 1H), 5.13-5.06 (m, 2H), 4.80-4.69 (m, 1H), 4.22-3.74 (m, 3H), 3.47-2.95 (m, 4H), 2.00-1.67 (m, 2H) 1.66-1.16 (m, 28H), 1.12-0.92 (m, 2H); ^{13}C NMR (75 MHz, CDCl$_3$) δ 172.6, 172.4, 171.9, 170.7, 169.5, 169.2, 154.9, 152.8, 146.6, 145.7, 141.6, 134.1, 128.1, 118.5, 118.2, 113.5, 112.4, 105.4, 105.2, 103.7, 83.3, 80.6, 77.0, 61.4, 53.8, 53.0, 47.3, 39.3, 28.4, 27.9, 27.6, 14.1, 13.8; IR (neat) 3342, 2984,

1750, 1644, 1481, 1447, 1140 cm^{-1}; HRMS (ESI/APCI) calcd for C$_{31}$[^{13}C]$_2$H$_{47}$N$_2$[^{15}N] NaO$_8$ (M+Na) 639.3293, found 639.3293. (jmf-02-807)

269
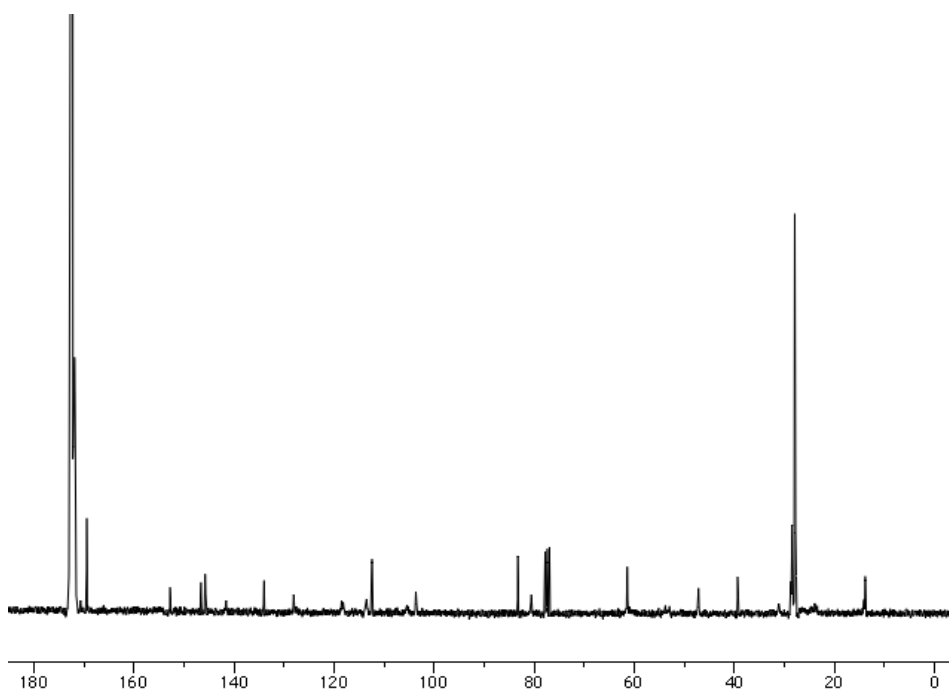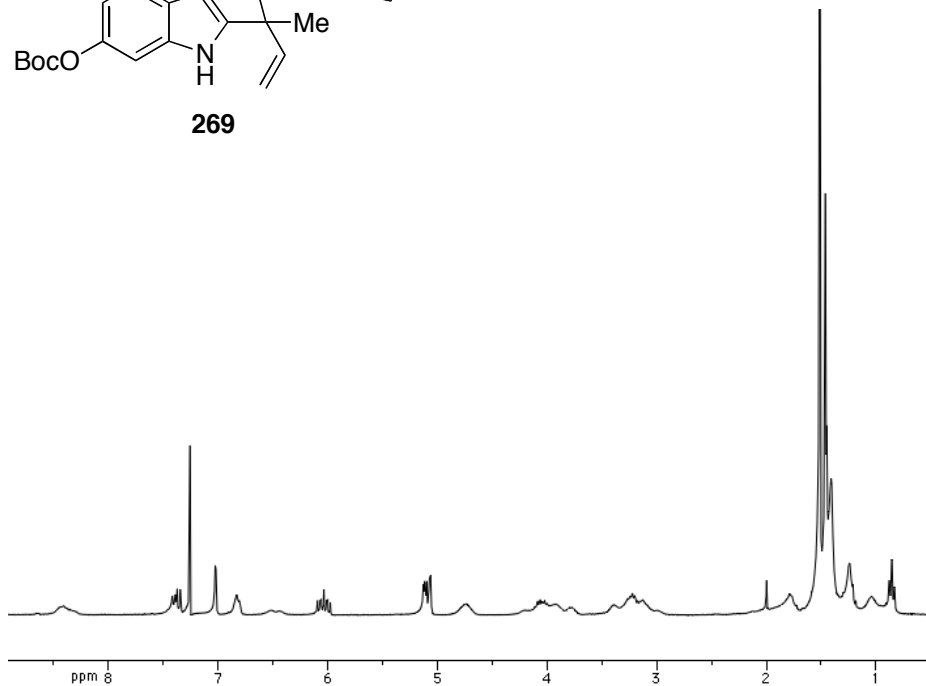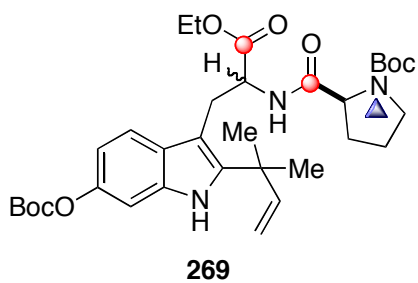
[¹³C]₂-[¹⁵N]- (3S,8aS)-3-((6-hydroxy-2-(2-methylbut-3-en-2-yl)-1H-indol-3-yl)methyl) hexahydropyrrolo[1,2-a]pyrazine-1,4-dione (266 and 271):

266, [¹³C]₂-[¹⁵N]-6-hydroxy-deoxybrevianamide E

271
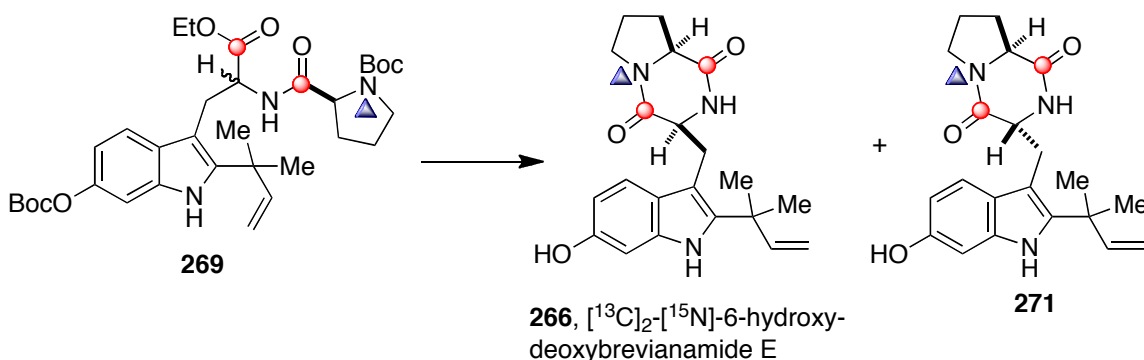
TFA (0.3 M) was slowly added to a solution of **269** (400 mg, 0.65 mmol) in CH₂Cl₂ (0.3 M) at 0°C. The reaction stirred for 3 hours at room temperature. The mixture was quenched with saturated NaHCO₃ to a pH 9 and extracted with EtOAc (3 x 20 mL). The combined organic layers were dried over Na₂SO₄ and concentrated under reduced pressure. The residue was dissolved in toluene (0.2 M) and 2-hydroxypyridine (8.6 mg, 0.09 mmol) was added. The reaction refluxed for 14 hours under Ar atmosphere, cooled to room temperature, and concentrated under reduced pressure. The residue was rediluted with CH₂Cl₂ (10 mL) and washed with 1M HCl (20 mL). The organic layer was dried over Na₂SO₄ and concentrated under reduced pressure. The crude residue was purified via flash column chromatography eluting with 3:97 MeOH/CH₂Cl₂ to afford 68 mg (40%) of the desired *cis*-diastereomer as cream foam. The *trans*-diastereomer was isolated in 38% yield (64 mg) as yellow foam (overall: 52% for two steps).

266, *Cis*: ¹H NMR (300 MHz, 20:1 CDCl₃/CD₃OD) δ 8.05 (bs, 1H), 7.22 (d, *J* = 8.7 Hz, 1H), 6.74 (d, *J* = 2.1 Hz, 1H), 6.61 (dd, *J* = 8.4, 2.1 Hz, 1H), 6.08 (dd, *J* = 17.4, 10.5, 1H), 5.15-5.09 (m, 2H), 4.38 (d, *J* = 11.4 Hz, 1H), 4.09-4.01 (m, 1H), 3.72-3.54 (m, 3H),

3.16-3.06 (m, 1H), 2.38-1.81 (m, 6H), 1.49-1.44 (m, 6H); ^{13}C NMR (75 MHz, CDCl$_3$) δ 169.7, 166.3, 153.0, 146.1, 140.3, 135.7, 123.2, 118.5, 112.5, 110.2, 104.1, 97.1, 60.7, 45.6, 39.1, 28.5, 28.1, 28.0, 26.2, 26.1, 22.7; enriched ^{13}C = 169.7 and 166.3; IR (neat) 3353, 2925, 1664, 1457 cm^{-1}; HRMS (ESI/APCI) calcd for C$_{19}$[^{13}C]$_2$H$_{26}$N$_2$[^{15}N]O$_3$ (M+H) 371.2006, found 371.2004. (jmf-02-813)

6-Hydroxydeoxybrevianamide E, 8

266, [^{13}C]$_2$-[^{15}N]-6-hydroxy-deoxybrevianamide E

6-Hydroxydeoxybrevianamide E, 8
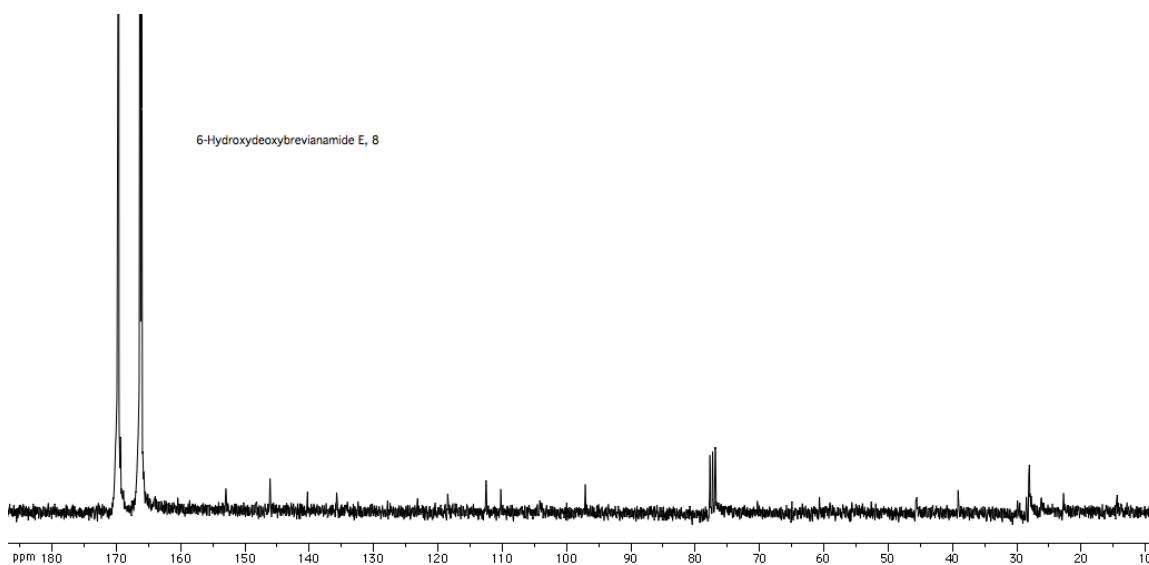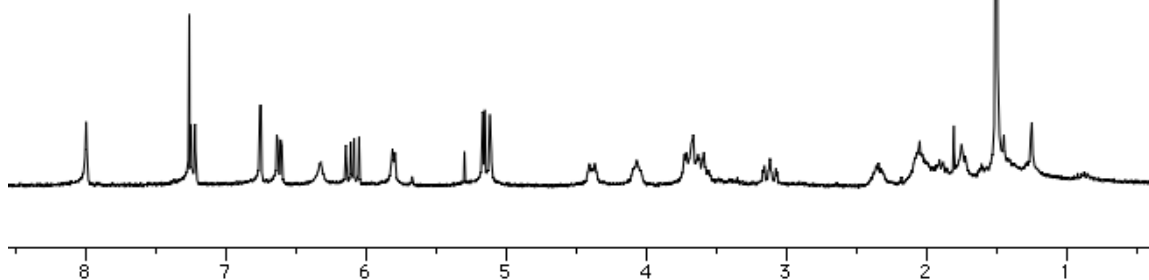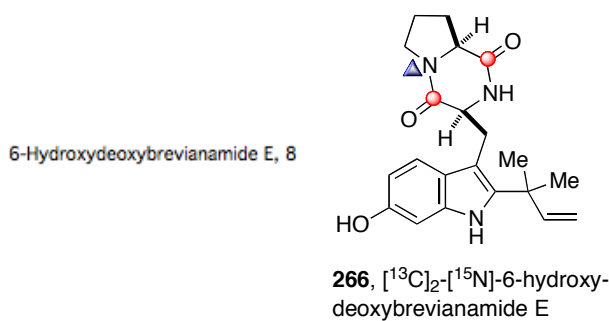
271, *Trans*: ^{1}H NMR (300 MHz, (CD$_3$)$_2$CO) δ 7.91 (bs, 1H), 7.32 (d, J = 8.4 Hz, 1H), 6.81 (d, J = 2.4 Hz, 1H), 6.64 (dd, J = 8.4, 2.1 Hz, 1H), 6.22 (dd, J = 17.4, 10.5 Hz, 1H), 5.67-5.63 (m, 1H), 5.14-5.03 (m, 2H), 4.42-4.38 (m, 1H), 4.20-4.17 (m, 1H), 3.64-3.42 (m, 4H), 3.07-2.98 (m, 1H), 2.00-1.82 (m, 3H), 1.56 (s, 3H), 1.54 (s, 3H); ^{13}C NMR (75 MHz, CDCl$_3$) δ 169.7, 166.3, 166.1, 152.8, 146.0, 140.2, 135.7, 123.2, 118.4, 112.3, 110.2, 104.1, 97.1, 65.1, 64.9, 60.5, 45.7, 39.1, 29.9, 28.1, 26.2, 22.7, 14.4; enriched ^{13}C = 169.7, 166.3, 166.1; IR (neat) 3358, 2920, 1662, 1456 cm^{-1}; HRMS (ESI/APCI) calcd for C$_{19}$[^{13}C]$_2$H$_{25}$N$_2$[^{15}N]O$_3$Na (M+Na) 393.1826, found 393.1826. (jmf-02-813)

trans-6-hydroxydeoxybrevianamide E

271

trans-6-hydroxydeoxybrevianamide E
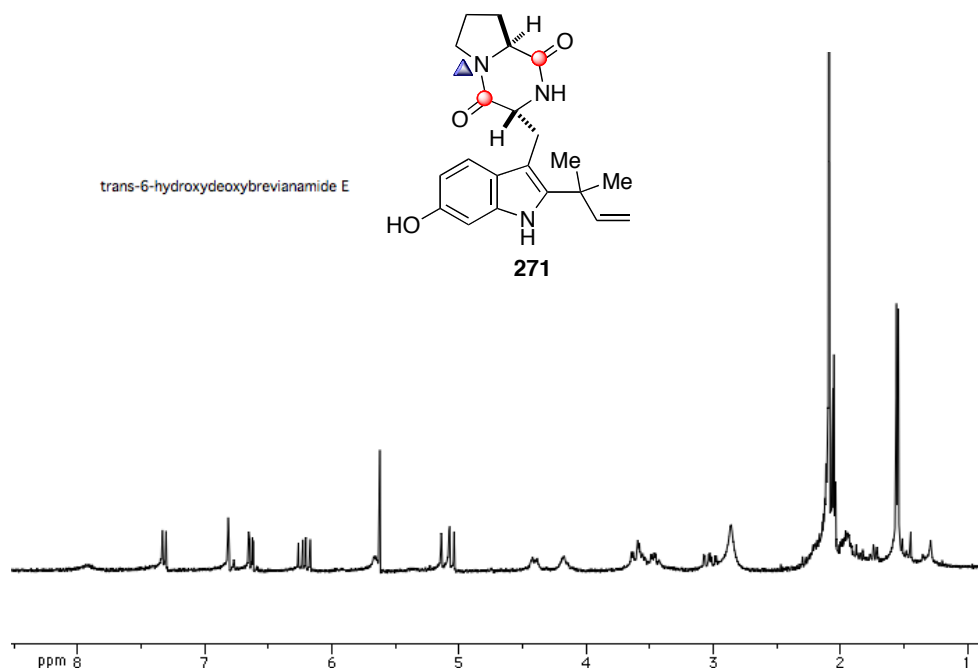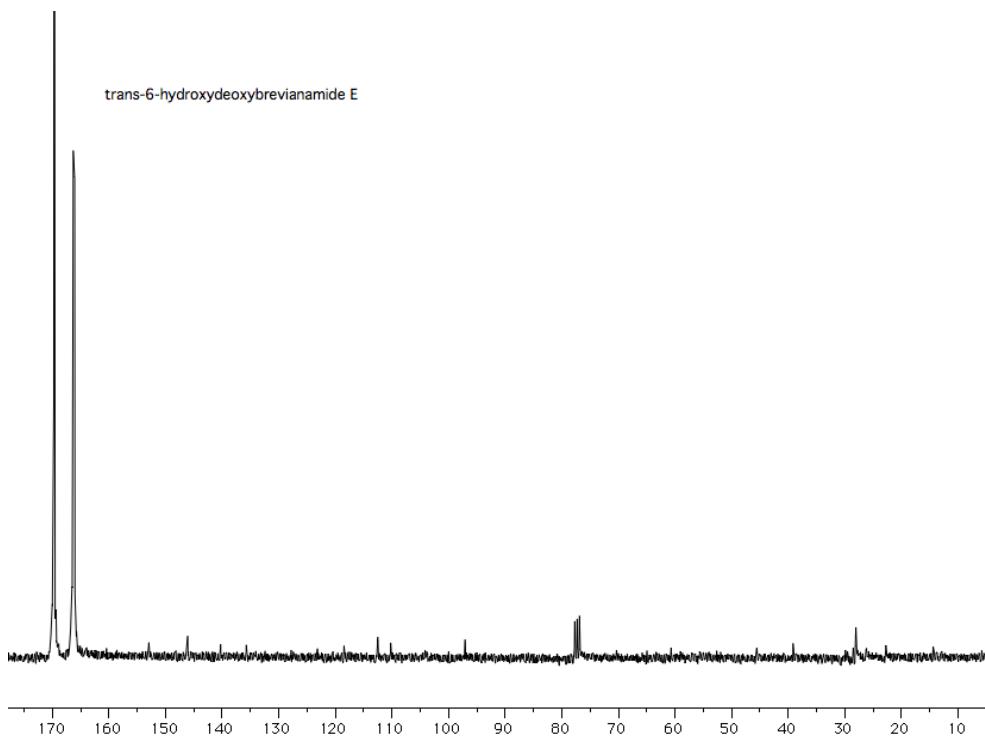
tert-butyl (3-((dimethylamino)methyl)-1H-indol-6-yl) carbonate (282):
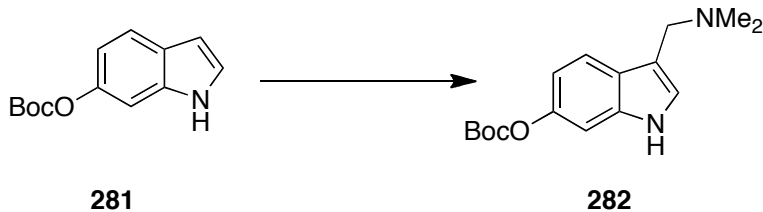
Acetic acid (60 mL) and 37% aqueous formaldehyde (2.08 mL 25.6 mmol) were stirred together at room temperature. To this solution 40% aqueous dimethylamine (11 mL, 96.5 mmol) was added and the reaction stirred for 7 minutes. A solution of 6-OBoc indole **281** (5.29 g, 22.7 mmol) in 10 mL of acetic acid was slowly added to the above solution and the reaction stirred for 15 hours at room temperature. The reaction mixture was basified to pH 10 with 2M NaOH and extracted with diethyl ether (3 x 100 mL). The combined organic layer was dried over Na_2SO_4 and concentrated under vacuum. Crude yield: 6.59 g, 22.7 mmol.

^{1}H NMR (300 MHz, CDCl$_3$) δ 9.21 (bs, 1H), 7.58 (d, J = 8.4 Hz, 1H), 7.08 (d, J = 2.1 Hz, 1H), 6.92-6.88 (m, 2H), 2.23 (s, 6H), 1.56 (s, 9H); ^{13}C NMR (75 MHz, CDCl$_3$) δ 153.1, 146.8, 136.1, 126.2, 125.3, 119.5, 113.6, 112.2, 104.2, 83.5, 66.1, 58.2, 54.4, 45.2, 28.0, 18.6, 15.5; HRMS (ESI/APCI) calcd for $C_{16}H_{23}N_2O_3$ (M+H) 291.1703, found 291.1706 (jmf-02-644).
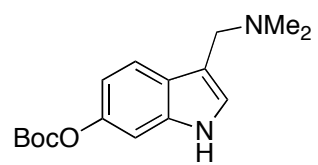
282
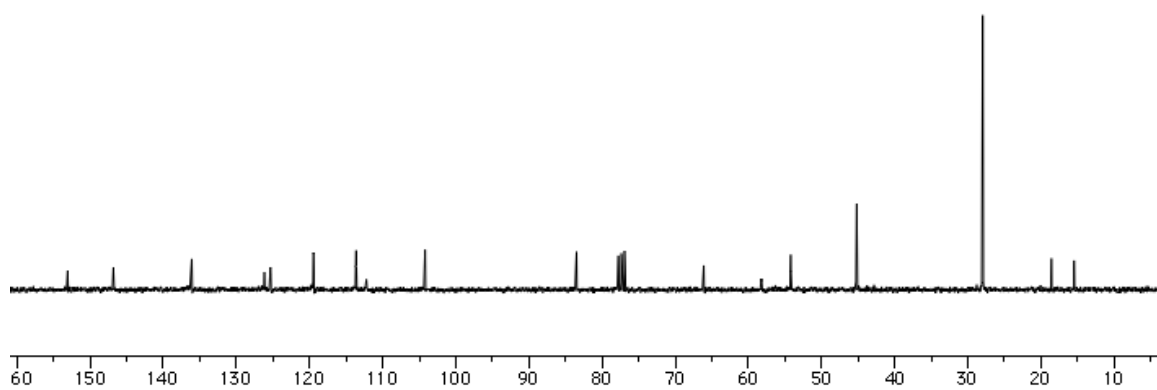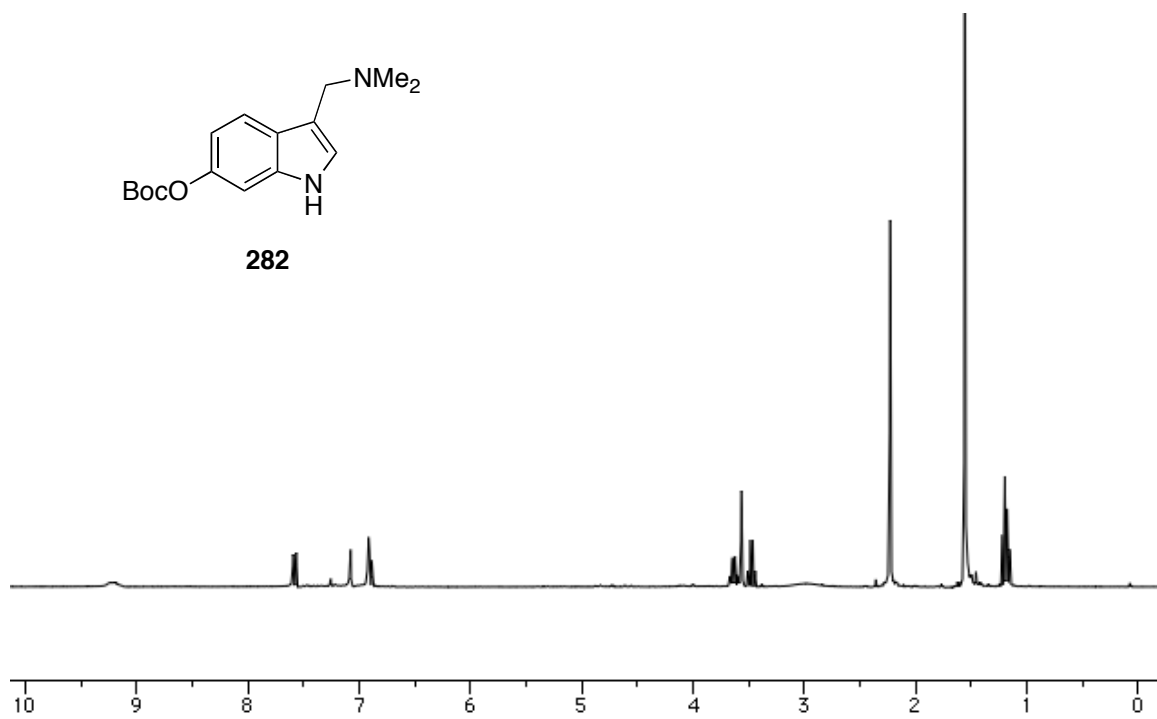
ethyl 3-(6-((tert-butoxycarbonyl)oxy)-1H-indol-3-yl)-2-((diphenylmethylene)amino)propanoate (283):
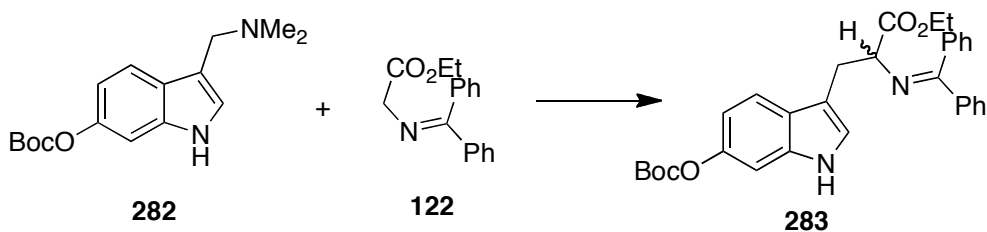
Gramine **282** (230 mg, 0.792 mmol), glycine **122** (211 mg, 0.792 mmol) and DABCO (88 mg, 0.792 mmol) were stirred together in MeCN (4 mL) at reflux for 18 hours. The reaction mixture was concentrated under vacuum and purified via flash column chromatography. The desired product eluted in 3:1 hexanes-ethyl acetate as a white amorphous solid. Yield: 353 mg, 0.689 mmol, 87%.

^{1}H NMR (300 MHz, CDCl$_3$) δ 8.26 (bs, 1H), 7.59-6.59 (m, 14H), 4.37 (dd, J = 8.7, 13.5 Hz, 1H) 4.20-4.12 (m, 2H), 3.42 (dd, J = 14.4, 5.1 Hz, 1H), 3.20 (dd, J = 14.1, 8.7 Hz, 1H), 1.58 (s, 9H), 1.22 (t, 3H); ^{13}C NMR (75 MHz, CDCl$_3$) δ 172.5, 171.0, 152.8, 147.0, 139.6, 136.0, 135.9, 130.5, 129.0, 128.5, 128.4, 128.2, 127.7, 125.9, 124.3, 119.3, 113.4, 111.9, 104.0, 83.4, 66.1, 61.2, 29.5, 28.0, 14.4; HRMS (ESI/APCI) calcd for C$_{31}$H$_{33}$N$_2$O$_5$ (M+H) 513.2384, found 513.238. (jmf-02-669)

283
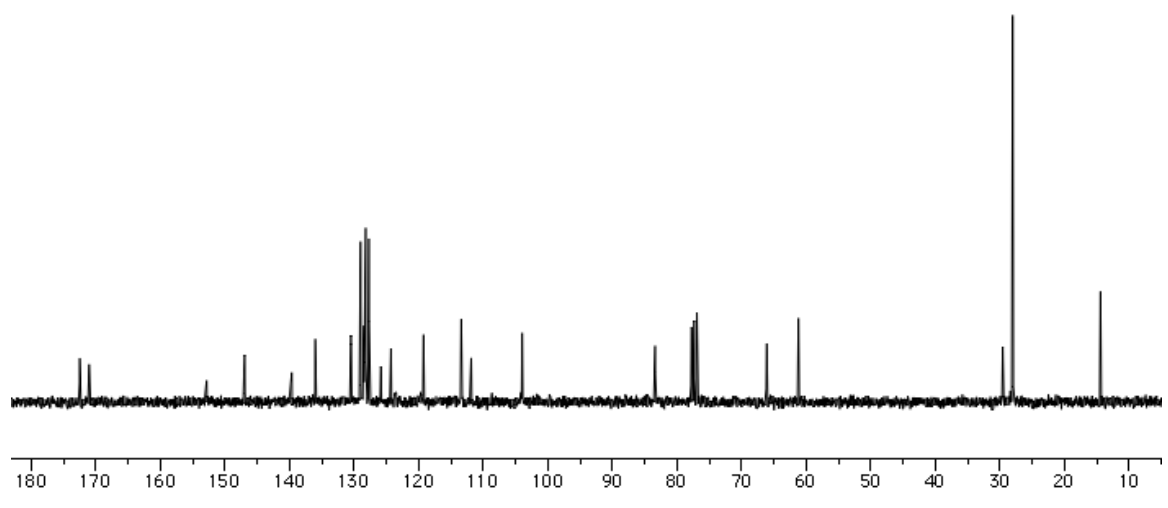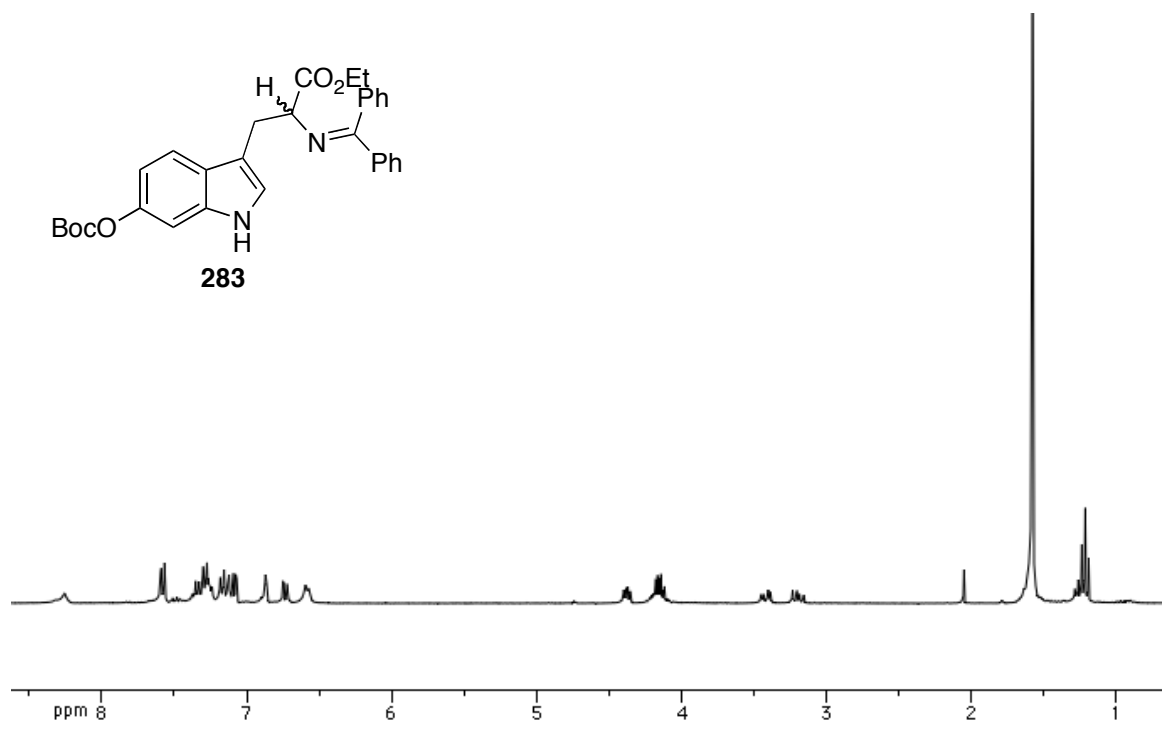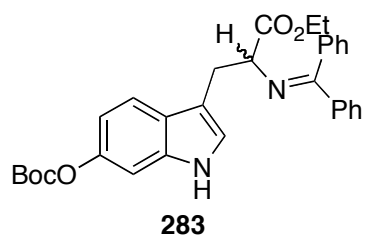
ethyl 2-((tert-butoxycarbonyl)amino)-3-(6-((tert-butoxycarbonyl)oxy)-1H-indol-3-yl)propanoate (284):
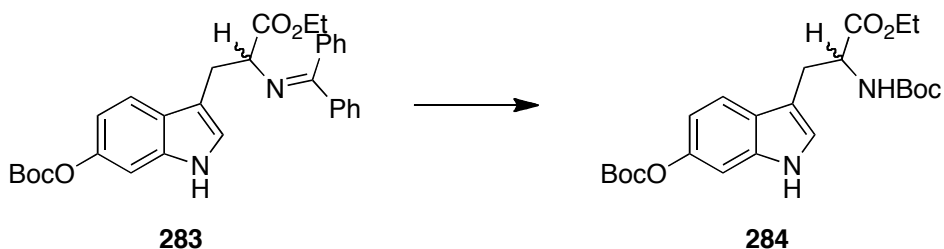
To a solution of imine **283** (340 mg, 0.663 mmol) in THF (5 mL) was added 1M HCl (1.65 mL). The reaction mixture stirred for 20 minutes at room temperature and the THF was removed under vacuum. The resulting slurry was basified with saturated aqueous NaHCO$_3$ (20 mL) and extracted with CH$_2$Cl$_2$ (3 x 30 mL). The combined organic layer was dried over Na$_2$SO$_4$ and concentrated under vacuum. The crude material was purified via flash column chromatography in 3:1 hexanes-ethyl acetate with the desired product eluting with a 5% MeOH in CH$_2$Cl$_2$ flush of the column. Yield: 228 mg, 0.656 mmol, 99%. The free amine (212 mg, 0.473 mmol) was dissolved in dioxane (2.36 mL) and cooled to 0ºC. Di-*tert*-butyl dicarbonate (108 mg, 0.496 mmol) and 1M NaOH (0.4 mL) were added to the stirring reaction mixture. The reaction was allowed to warm to room temperature over 18 hours, after which the reaction was concentrated and the residue was dissolved in water (5 mL). The slurry was acidified to pH 2 with saturated aqueous KHSO$_4$ and extracted with ethyl acetate. The combined organic layer was dried over Na$_2$SO$_4$ and concentrated under vacuum. Yield: 167 mg, 0.374 mmol, 79%.

^{1}H NMR (300 MHz, CDCl$_3$) δ 8.42 (bs, 1H), 7.49 (d, *J* = 8.4 Hz, 1H), 7.14 (s, 1H), 6.92-6.90 (m, 2H), 5.08 (d, *J* = 8.1 Hz, 1H), 4.61-4.56 (m, 1H), 4.14-4.09 (m, 2H), 3.70 (s, 2H), 3.24-3.22 (m, 2H), 1.57 (s, 9H), 1.41 (s, 9H), 1.18 (t, 3H); ^{13}C NMR (75 MHz,

CDCl$_3$) δ 172.5, 155.5, 152.8, 147.1, 136.0, 126.0, 123.8, 119.3, 113.8, 110.4, 104.2, 83.5, 80.1, 67.3, 61.6, 54.5, 28.5, 28.0, 14.3; HRMS (ESI/APCI) calcd for C$_{23}$H$_{32}$N$_2$O$_7$Na (M+Na) 471.2102, found 471.2105. (jmf-02-674)
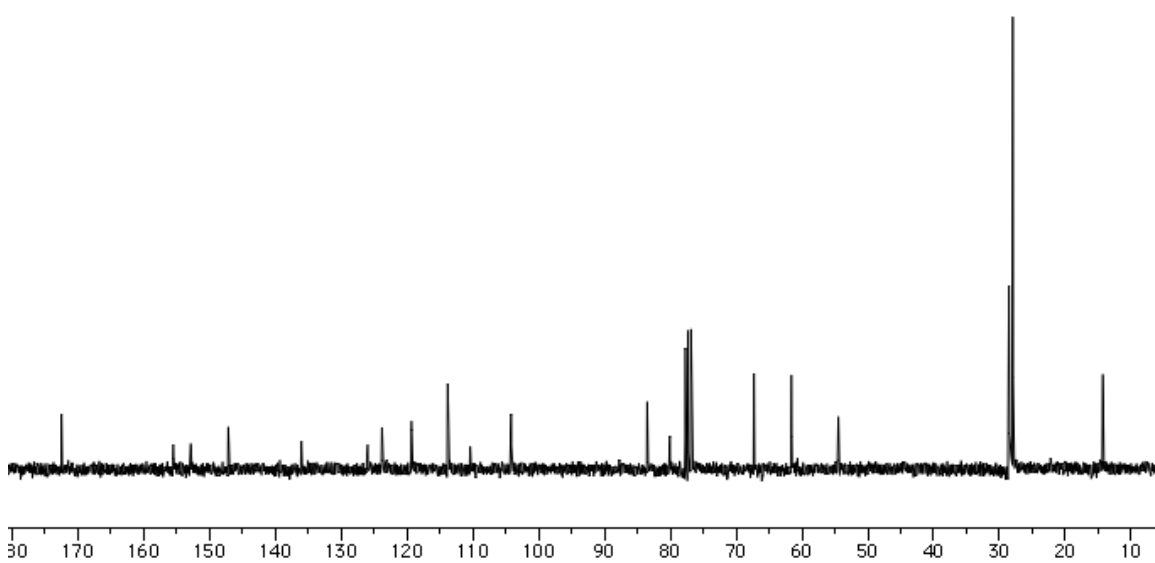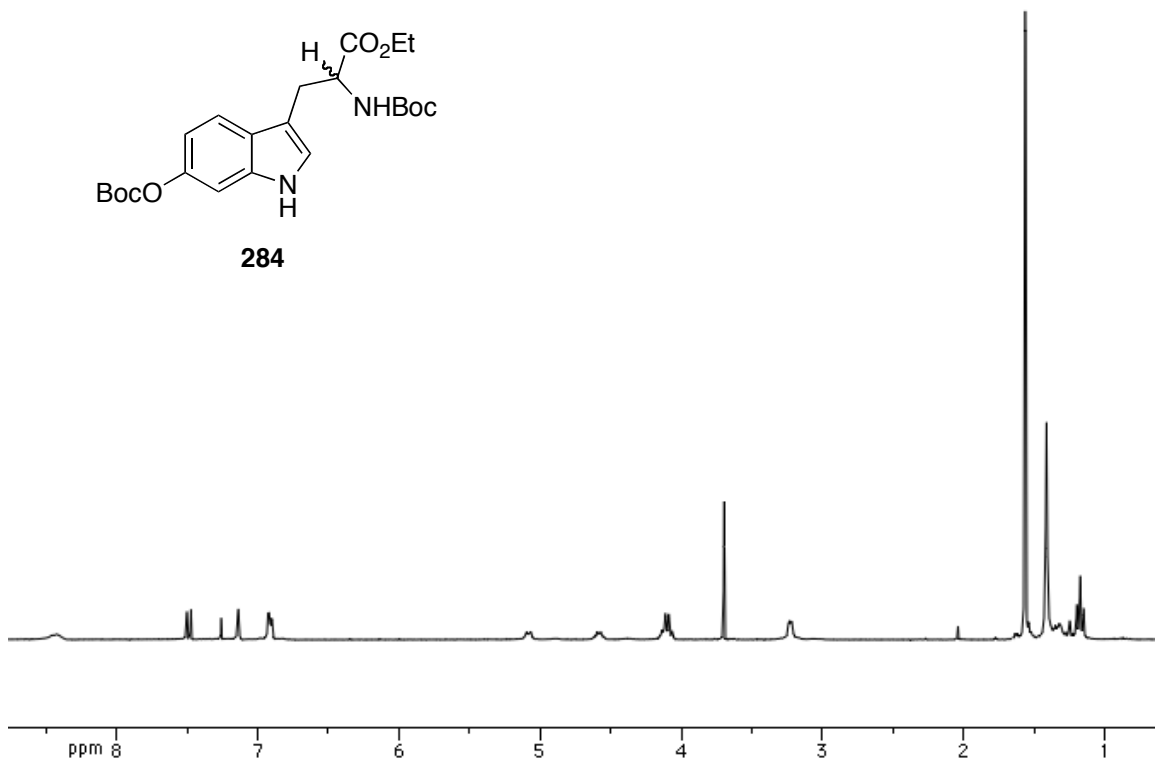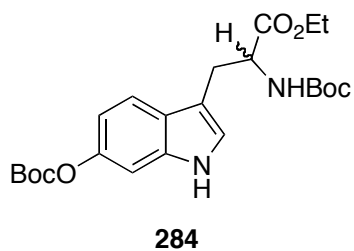
(2*S*)-ethyl   1-(2-((*tert*-butoxycarbonyl)amino)-3-(6-((*tert*-butoxycarbonyl)oxy)-1*H*-indol-3-yl)propanoyl)pyrrolidine-2-carboxylate (285):
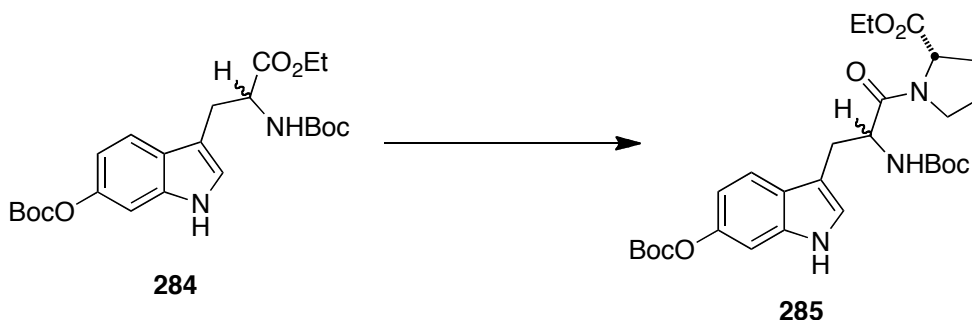
Indole **284** (240 mg, 0.535 mmol) was dissolved in THF (1.78 mL) and water (3.57 mL). To the solution, LiOH (128.2 mg, 5.35 mmol) was added and the reaction stirred at room temperature for 16 hours. The mixture was concentrated under vacuum and the residue was diluted with water (10 mL) and acidified to pH 2 with 1M KHSO$_4$. The crude material was extracted with ethyl acetate (2 x 20 mL) and CH$_2$Cl$_2$ (2 x 20 mL). The combined organic layer was dried over Na$_2$SO$_4$ and concentrated under vacuum. The crude acid (129 mg, 0.307 mmol) was dissolved in MeCN (3.1 mL) and L-proline ethyl ester (43 mg, 0.307 mmol) was added to the solution. HATU (175 mg, 0.461 mmol) and DIPEA (0.213 mL, 1.23 mmol) were added to the reaction mixture, and the solution stirred for 17 hours at room temperature. The reaction was quenched with 1M HCl (20 mL) and extracted with CH$_2$Cl$_2$ (3 x 30 mL). The combined organic layer was dried over Na$_2$SO$_4$ and concentrated.   The crude material was purified via flash column chromatography using 1:1 hexanes-ethyl acetate. Yield: 251 mg, 0.46 mmol, 86%.

Mixture of rotamers: ^{1}H NMR (400 MHz, CDCl$_3$) δ 7.58 (d, *J* = 8.8 Hz, 1H), 7.51-7.47 (m, 1H), 7.13-7.11 (m, 3H), 6.97 (s, 2H), 6.89-6.85 (m, 3H), 5.46 (d, *J* = 8.4 Hz, 1H) 5.27 (d, *J* = 8.4 Hz, 1H), 4.72-4.58 (m, 3H),4.46-4.43 (m, 1H), 4.15-4.07 (m, 6H), 3.65-

3.32 (m, 6H), 3.19-3.03 (m, 4H), 2.43-2.38 (m, 2H), 1.88-1.79 (m, 6H), 1.52 (s, 18H)1.23-1.17 (m, 6H); ^{13}C NMR (75 MHz, CDCl$_3$) δ 172.3, 172.1, 171.2, 170.9, 155.3, 152.8, 152.7, 147.2, 147.1, 135.9, 125.8, 124.8, 124.1, 119.4, 119.2, 113.8, 113.7, 111.1, 110.2, 104.1, 83.4, 83.3, 79.8, 61.3, 61.2, 59.3, 59.2, 53.6, 47.1, 46.9, 30.2, 29.2, 28.9, 28.7, 28.6, 28.5, 27.9, 25.1, 24.3, 14.3; HRMS (ESI/APCI) calcd for C$_{28}$H$_{40}$N$_3$O$_8$ (M+H) 546.281, found 546.2809. (jmf-02-676)

285

6-hydroxy-brevianamide F (276):
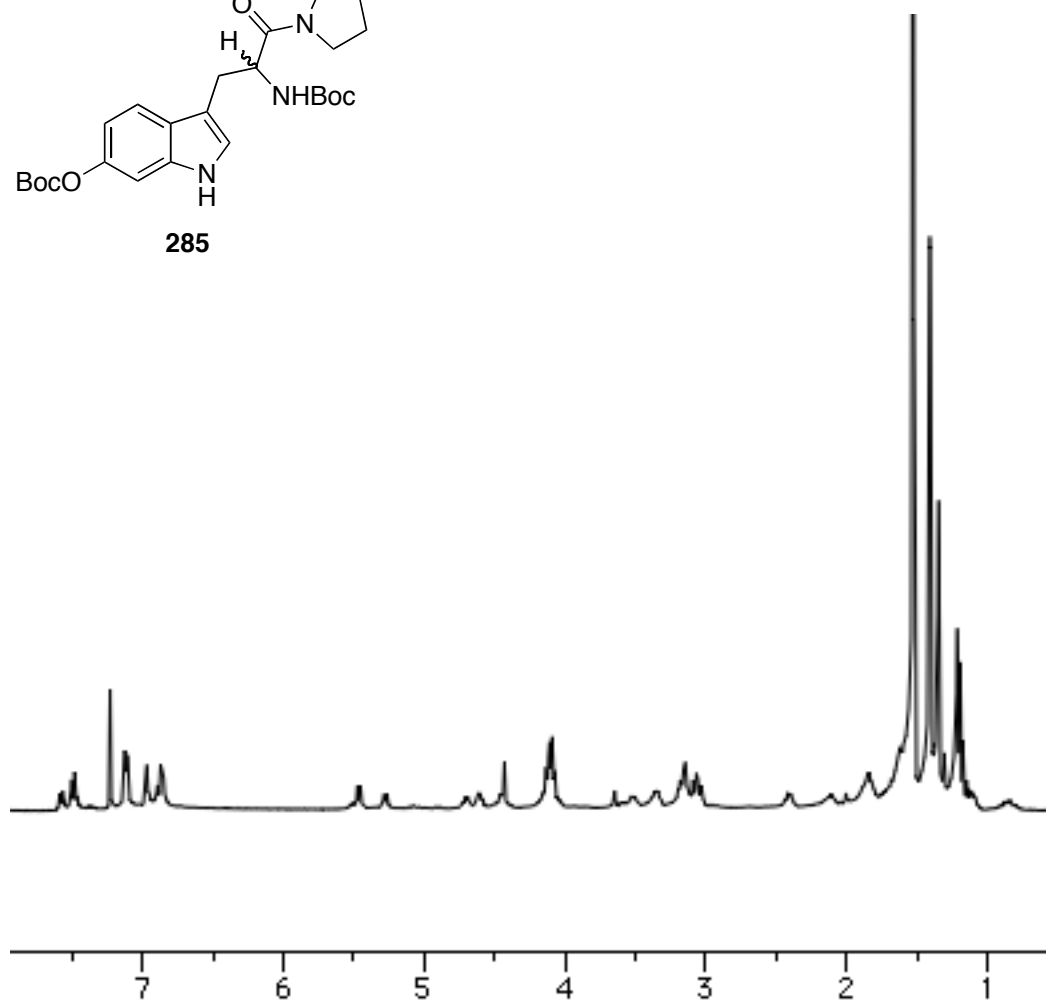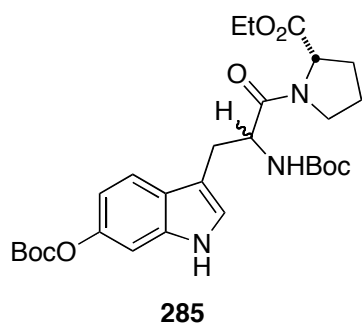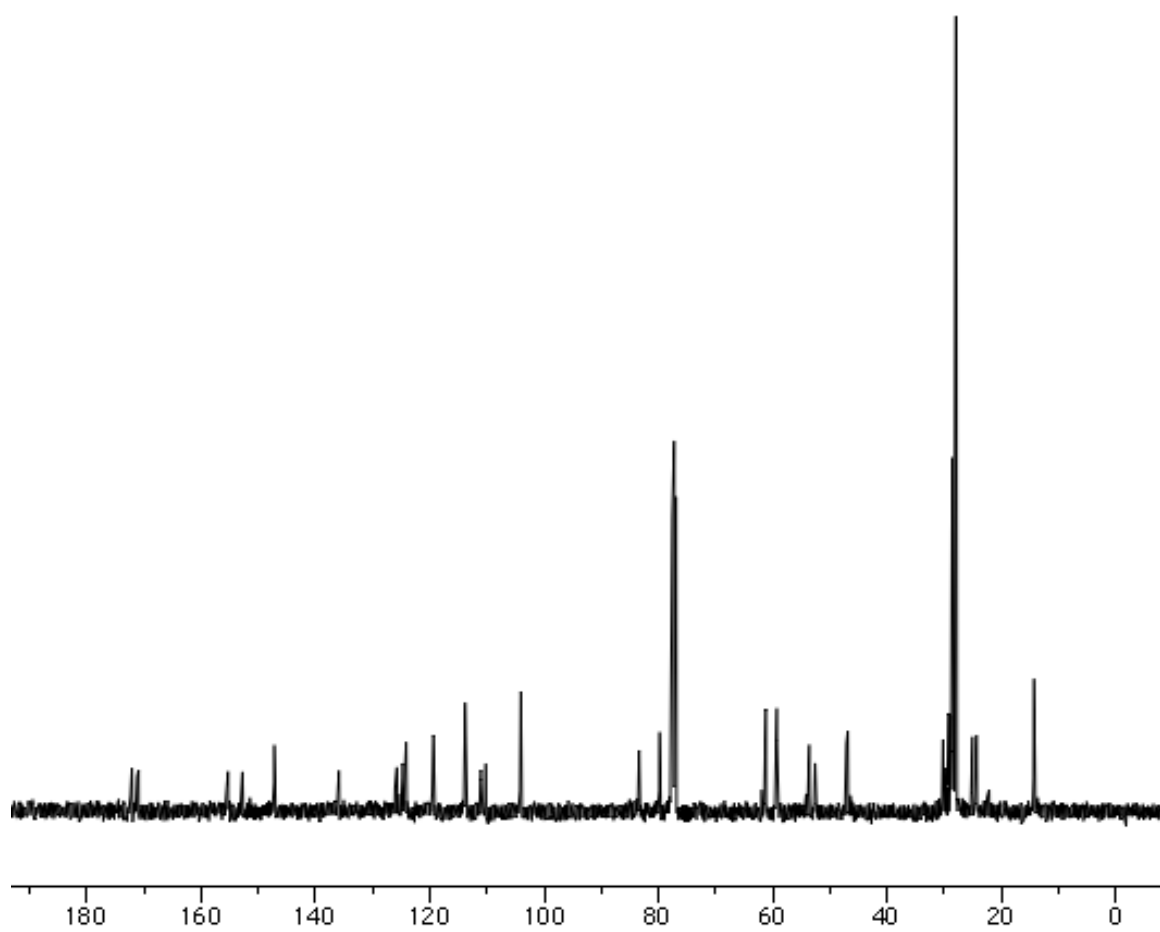
285   **276**, 6-hydroxybrevianamide F
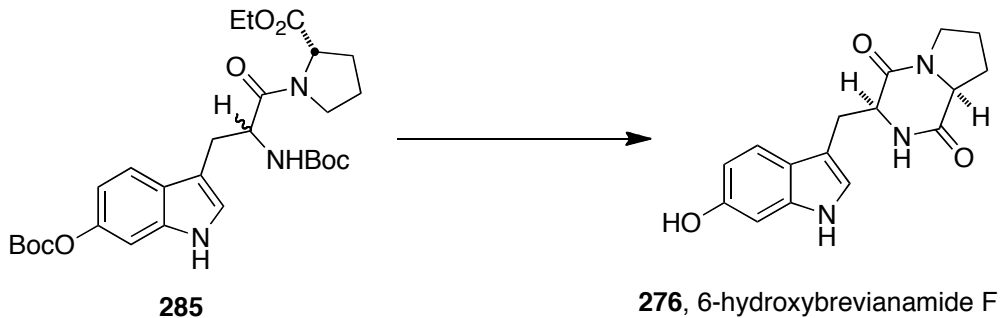
Peptide **285** (58.4 mg, 0.107 mmol) was dissolved in 1 mL CH_2Cl_2 and cooled to 0°C. TFA (1 mL) was slowly added to the solution and the ice bath was removed. The reaction mixture stirred for 2 hours, and was quenched with saturated aqueous $NaHCO_3$ to pH 10. The material was extracted with ethyl acetate (2 x 50 mL) and the combined organic layer was dried over Na_2SO_4 and concentrated. The crude amine (33 mg, 0.095) was dissolved in MeCN (1 mL) and NEt_3 (9.7 μL, 0.095 mmol) was added. The reaction mixture stirred at reflux for 6 hours. The solution cooled to room temperature, 1M HCl (5 mL) was added, and extracted with ethyl acetate (1 x 15 mL) and CH_2Cl_2 (1 x 15 mL). The organic layer was dried over Na_2SO_4 and concentrated under vacuum. The mixture of diketopiperazine diastereomers was purified via flash column chromatography with a gradient elution of 5-7% MeOH in DCM.

276, *Cis:* ^{1}H NMR (300 MHz, $CO(CD_3)_2$) δ 7.94 (bs, 1H), 7.41 (d, J = 8.7 Hz, 1H), 7.13 (s, 1H), 6.84 (s, 1H), 6.66-6.63 (m, 1H), 6.28 (bs, 1H), 5.63 (s, 1H), 4.37-4.33 (m, 1H), 4.17-4.11 (m, 1H), 3.58-3.35 (m, 4H), 3.01-2.93 (m, 4H) 2.32 (s, 3H), 1.82 (s, 3H), 1.78-1.71 (m, 3H), 1.66 (s, 3H); ^{13}C NMR (75 MHz, 20:1-$CDCl_3$/CD_3OD) δ 170.4, 153.0,

137.4, 123.3, 121.1, 119.2, 109.8, 96.7, 58.2, 57.9, 45.0, 30.6, 29.7, 28.7, 21.4; HRMS

(ESI/APCI) calcd for $C_{16}H_{18}N_3O_3$ (M+H) 300.1343, found 300.1338. (jmf-02-678)
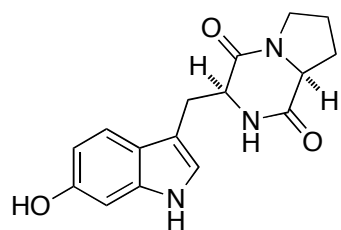
276, 6-hydroxybrevianamide F
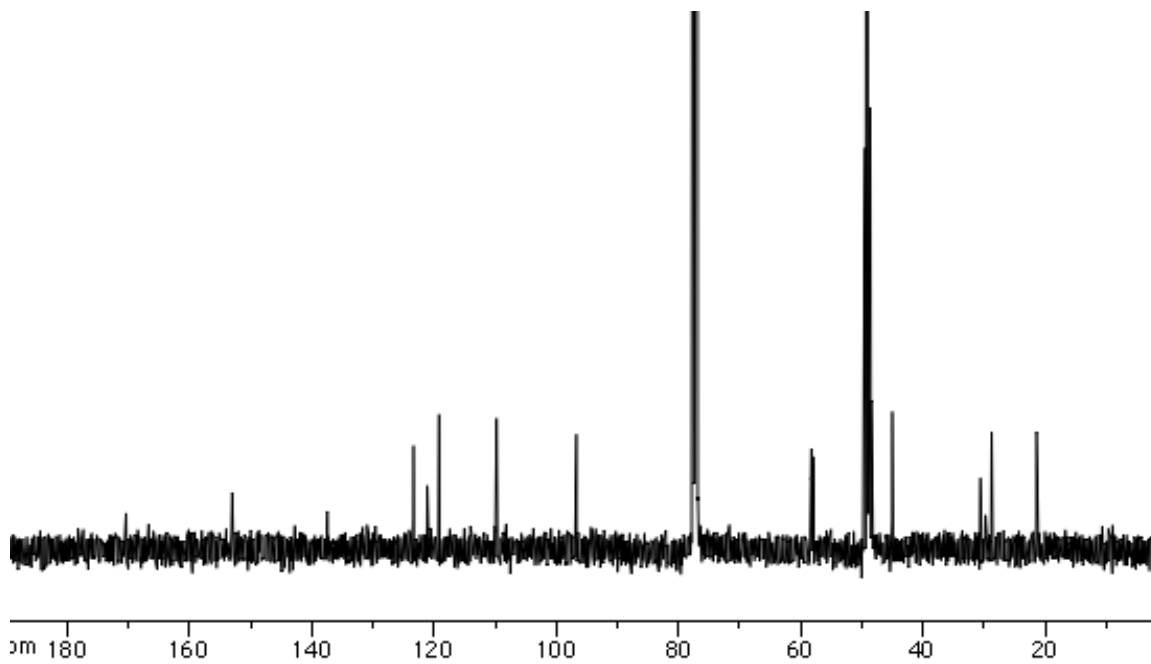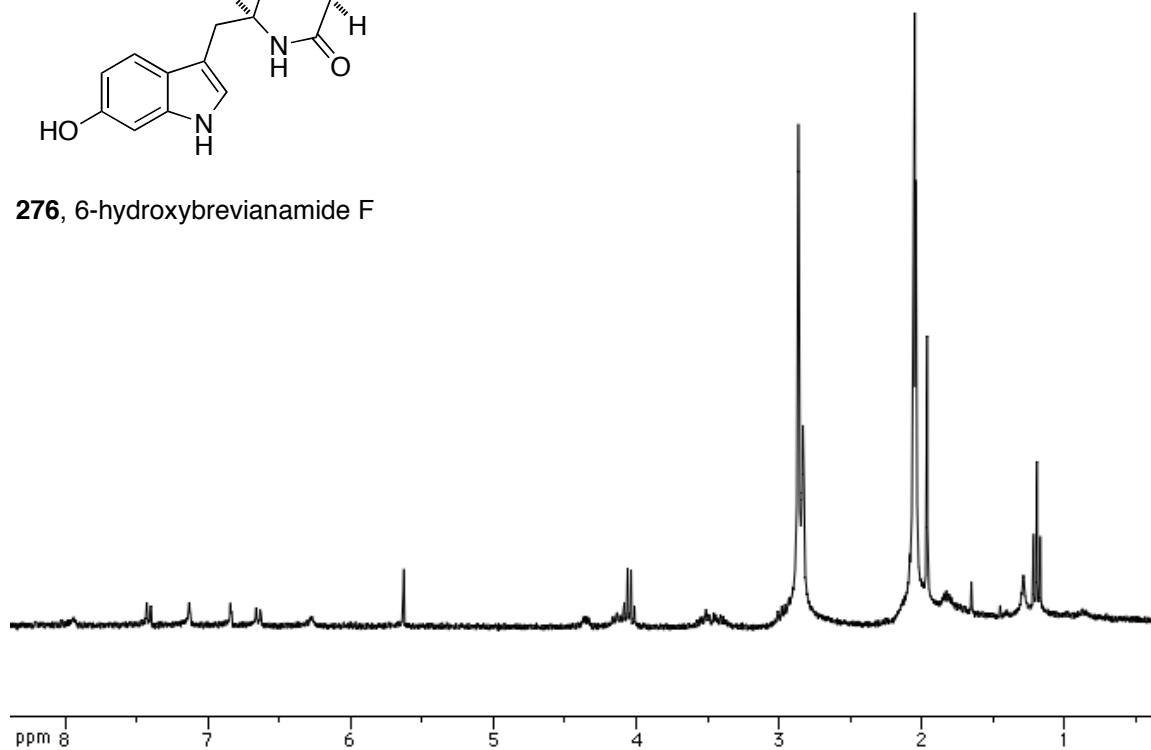
Trans: ^{1}H NMR (300 MHz, CDCl$_3$) δ 7.26 (d, *J* = 8.7 Hz, 1H), 6.77 (s, 1H), 6.69 (d, *J* = 2.1 Hz, 1H), 6.58 (dd, *J* = 8.7, 2.7 Hz, 1H), 4.13-4.10 (m, 1H), 3.31-3.29 (m, 3H), 3.02-2.93 (m, 3H) 2.39-2.34 (m, 2H), 1.94-1.85 (m, 2H), 1.76-1.66 (m, 2H), 1.56-1.48 (m, 2H); HRMS (ESI/APCI) calcd for C$_{16}$H$_{18}$N$_3$O$_3$ (M+H) 300.1343, found 300.1343. (jmf-02-667)

trans-6-hydroxybrevianamide F
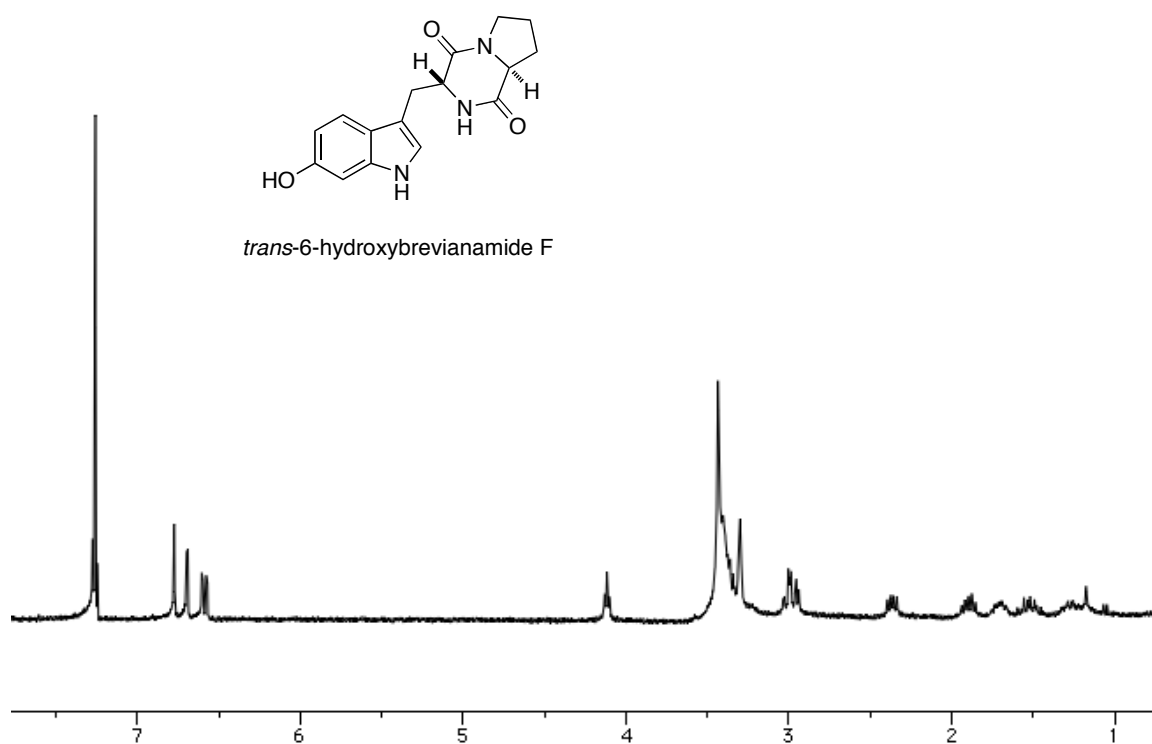
2-(3-methylbut-2-en-1-yl)-1-tosyl-1H-indole (286):
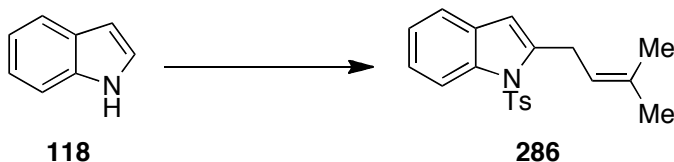
Indole **118** (2.34 g, 20.0 mmol) was dissolved in 100 mL THF and powdered KOH (5.61 g, 100.0 mmol) was added. The reaction stirred at room temperature for 10 minutes. To the solution, TsCl (4.20 g, 22.0 mmol) was added and the reaction stirred for 20 hours at room temperature. The solid was filtered and washed with CH$_2$Cl$_2$ (100 mL). The filtrate was concentrated and taken on to the next reaction. The Ts-protected indole (1.0 g, 3.68 mmol) was dissolved in 7.3 mL THF and cooled to -78°C. To the mixture, a 1.6M solution of *n*-BuLi in hexanes (2.76 mL, 4.42 mmol) was slowly added and the reaction stirred for 45 minutes at -78°C. Prenyl bromide (1.27 mL, 11.0 mmol) was quickly added and the reaction mixture stirred for 15 minutes at -78°C. The reaction was then allowed to warm to room temperature while stirring for 17 hours. The mixture was quenched with saturated aqueous NH$_4$Cl (25 mL) and extracted with CH$_2$Cl$_2$ (3 x 25 mL). The organic layer was washed with brine (2 x 50 mL), dried over Na$_2$SO$_4$, and concentrated under vacuum. The crude mixture was placed under high pressure vacuum in a 45°C oil bath to remove volatiles (4 hours). Yield: 850 mg, 2.50 mmol, 68%.

^{1}H NMR (300 MHz, CDCl$_3$) δ 8.22 (d, *J* = 9.0 Hz, 1H), 7.68 (d, *J* = 8.4 Hz, 2H), 7.42 (d, *J* = 8.1 Hz, 1H), 7.30-7.16 (m, 4H), 6.39 (s, 1H), 3.61 (s, 2H), 3.42 (m, 1H), 3.72 (d, *J* = 7.2 Hz, 2H), 2.32 (s, 3H), 1.82 (s, 3H), 1.78-1.71 (m, 3H), 1.66 (s, 3H); ^{13}C NMR (75 MHz, CDCl$_3$) δ 144.9, 141.4, 137.6, 136.5, 135.1, 130.1, 130.0, 126.5, 124.0, 123.7,

120.4, 120.0, 114.9, 109.2, 28.2, 26.0, 21.8, 18.0; HRMS (ESI/APCI) calcd for

$C_{20}H_{21}NO_2S$ (M+H) 340.1366, found 340.1375. (jmf-02-776)

286
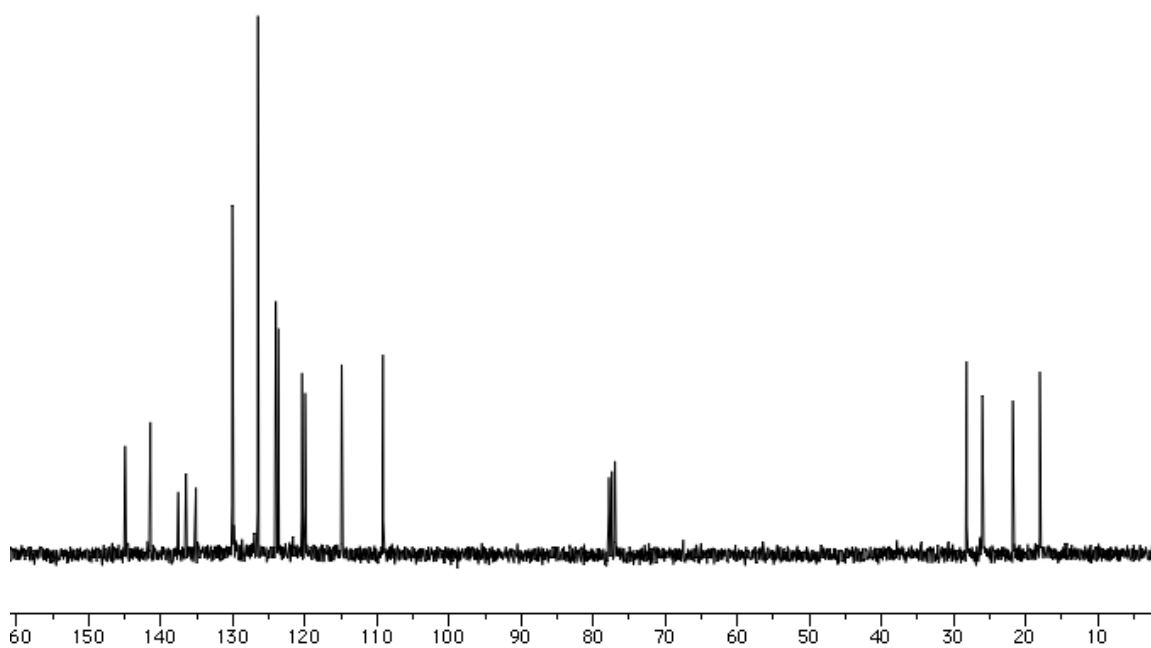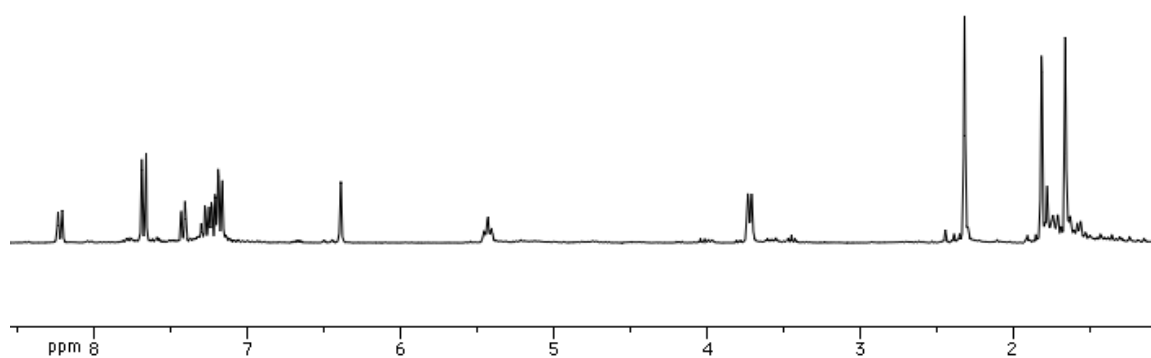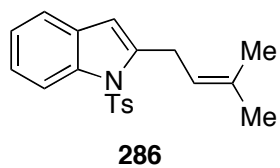
2-(3-methylbut-2-en-1-yl)-1H-indole (287):

286 **287**

To a solution of indole **286** (850 mg, 2.50 mmol) in MeOH (17 mL) was added Mg powder (243 mg, 10.0 mmol). The mixture was sonicated for 15 minutes at room temperature. The reaction was quenched with saturated aqueous NH$_4$Cl (30 mL), concentrated, and extracted with CH$_2$Cl$_2$ (3 x 25 mL). The organic layer was washed with saturated aqueous NaHCO$_3$ (50 mL) and brine (50 mL). The organic layer was dried over Na$_2$SO$_4$ and concentrated under vacuum. The crude material was purified via flash column chromatography in 40:1 Pet ether-ethyl acetate. Yield: 200 mg, 1.08 mmol, 43%.

^{1}H NMR (300 MHz, CDCl$_3$) δ 7.83 (bs, 1H), 7.60 (d, J = 8.4 Hz, 1H), 7.32 (d, J = 8.7 Hz, 1H), 7.21-7.14 (m, 2H), 6.31 (s, 1H), 3.61 (s, 2H), 5.45 (m, 1H), 3.52 (d, J = 7.2 Hz, 2H), 1.87 (s, 3H), 1.81 (s, 3H); ^{13}C NMR (75 MHz, CDCl$_3$) δ 139.0, 136.2, 134.8, 129.2, 121.2, 120.5, 120.1, 119.9, 110.7, 99.7, 27.4, 26.1, 18.2; HRMS (ESI/APCI) calcd for C$_{13}$H$_{16}$N (M+H) 186.1277, found 186.1279. (jmf-02-778)

287
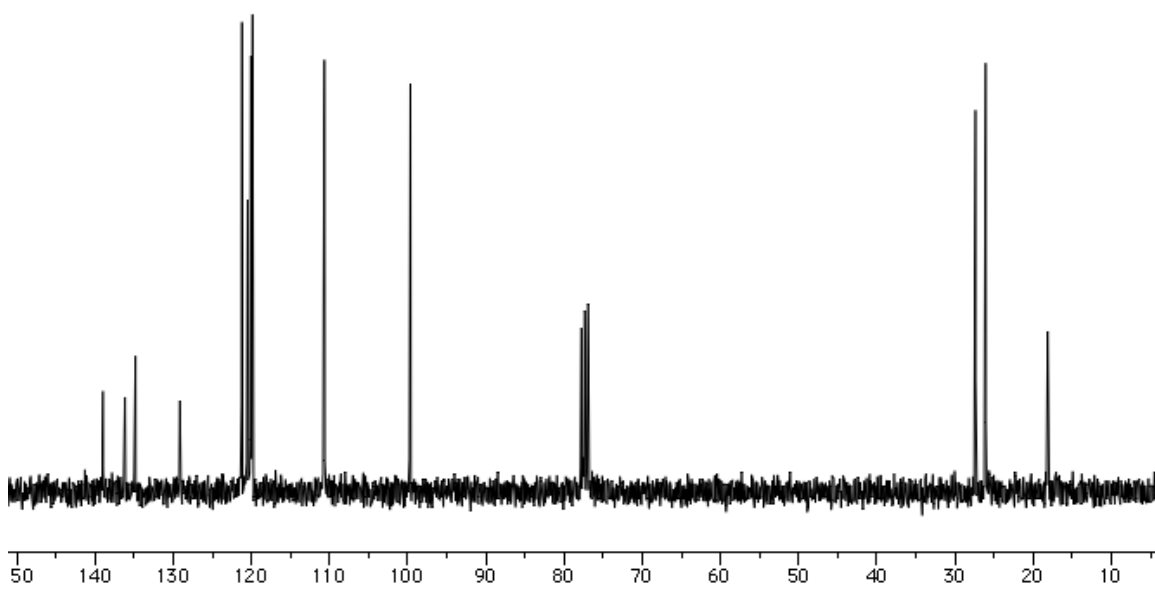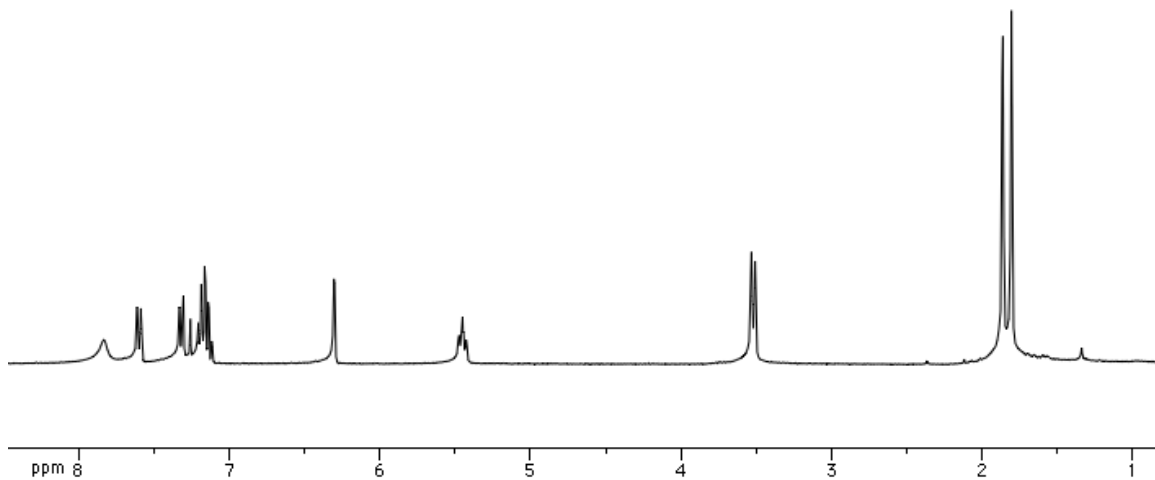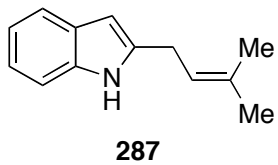
N,N-dimethyl-1-(2-(3-methylbut-2-en-1-yl)-1H-indol-3-yl)methanamine (288):
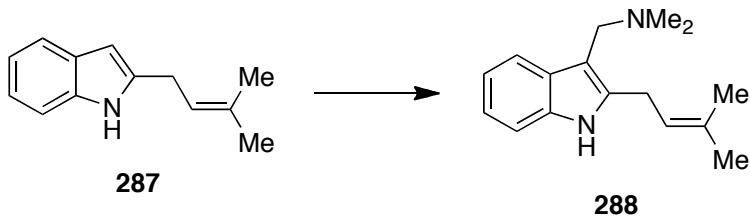
Acetic acid (2 mL) and 37% aqueous formaldehyde (0.100 mL 1.22 mmol) were stirred together at room temperature. To this solution 40% aqueous dimethylamine (0.517 mL, 4.59 mmol) was added and the reaction stirred for 7 minutes. A solution of indole **287** (200 mg, 1.08 mmol) in 1.27 mL of acetic acid was slowly added to the above solution and the reaction stirred for 15 hours at room temperature. The reaction mixture was basified to pH 10 with 2M NaOH and extracted with diethyl ether (3 x 25 mL). The combined organic layer was dried over Na_2SO_4 and concentrated under vacuum. Crude yield: 261 mg, 1.08 mmol

^{1}H NMR (300 MHz, CDCl$_3$) δ 8.06 (bs, 1H), 7.68-7.65 (m, 1H), 7.29-7.26 (m, 1H), 7.14-7.11 (m, 2H), 3.61 (s, 2H), 3.54 (d, *J* = 7.2 Hz, 2H), 2.31 (s, 6H), 1.81 (s, 3H), 1.78 (s, 3H); ^{13}C NMR (75 MHz, CDCl$_3$) δ 136.8, 135.3, 134.8, 129.7, 121.2, 120.6, 119.6, 118.9, 110.5, 108.4, 53.6, 45.7, 26.1, 25.4, 18.2; HRMS (ESI/APCI) calcd for $C_{14}H_{16}N$ (M-NMe$_2$ +H) 198.1277, found 198.128. (jmf-02-779)

288

307
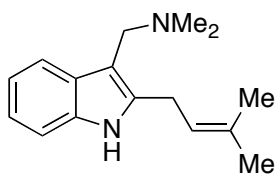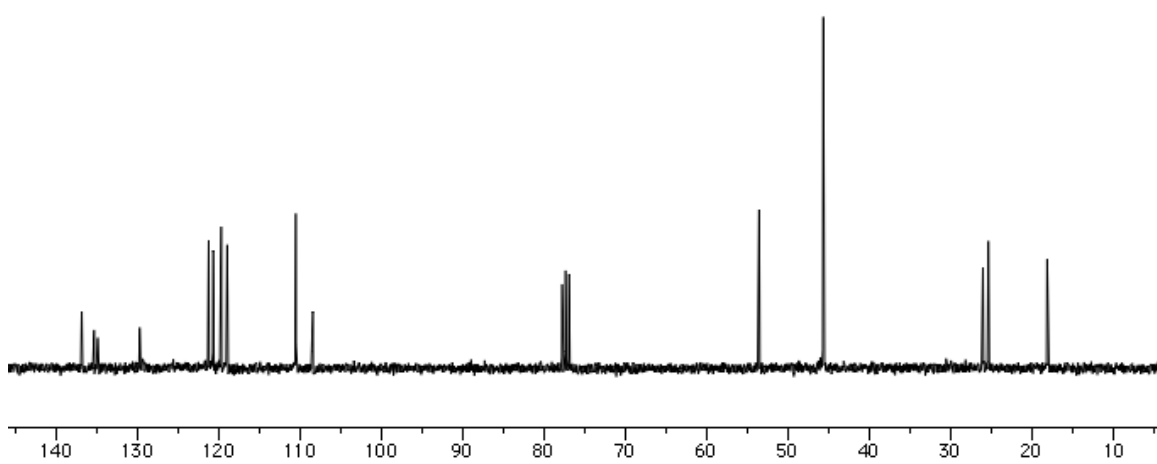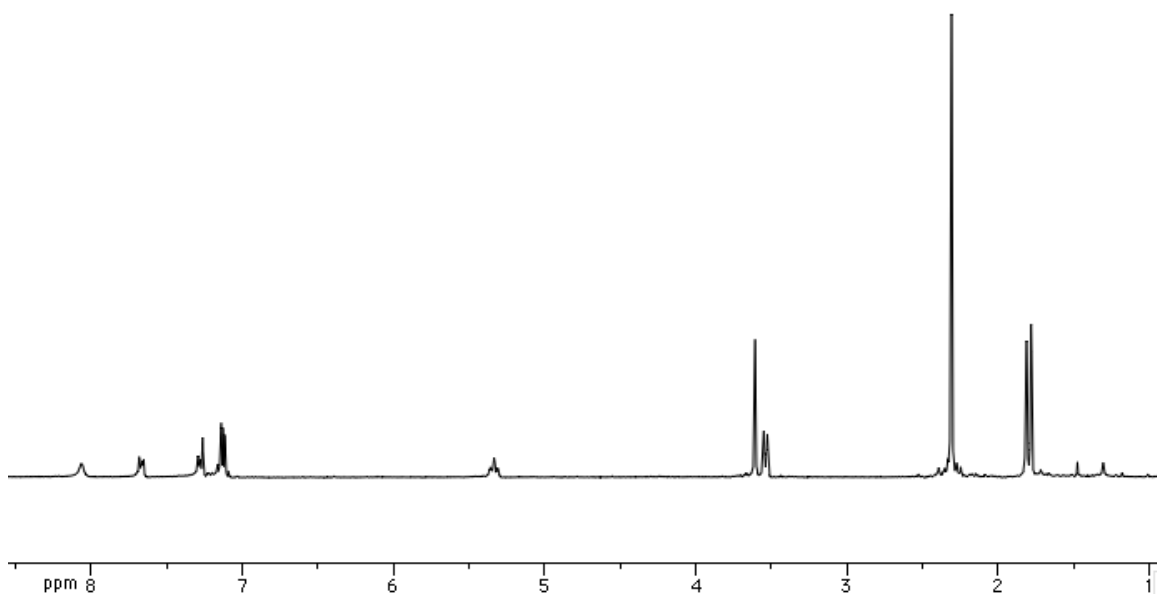
ethyl 2-((diphenylmethylene)amino)-3-(2-(3-methylbut-2-en-1-yl)-1H-indol-3-yl)propanoate (289):
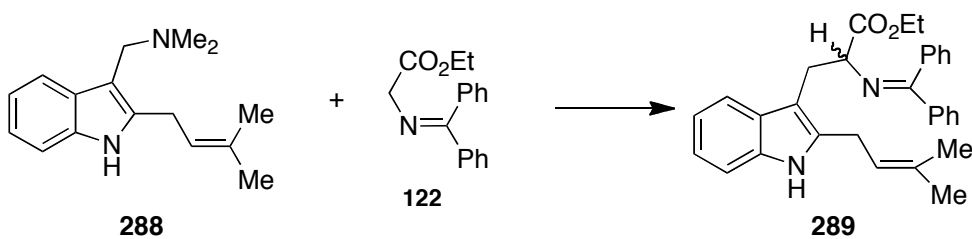
Gramine **288** (260 mg, 1.08 mmol), glycine **122** (317 mg, 1.18 mmol) and tributylphosphine (0.159 mL, 0.648 mmol) were stirred together in MeCN (5.4 mL) at 110ºC for 18 hours. The reaction mixture was cooled to room temperature, concentrated under vacuum and purified via flash column chromatography. The desired product eluted in 9:1 hexanes-ethyl acetate as an orange amorphous solid. Yield: 361 mg, 0.778 mmol, 72%.

^{1}H NMR (300 MHz, CDCl$_3$) δ 7.61-7.05 (m, 14H), 6.91-6.86 (m, 1H), 5.08 (bs, 1H), 4.37 (dd, J = 9.3, 4.2 Hz, 1H) 4.24-4.13 (m, 2H), 3.46-3.21 (m, 4H), 1.68 (s, 3H), 1.64 (s, 3H), 1.25 (t, 3H); ^{13}C NMR (75 MHz, CDCl$_3$) δ172.6, 170.3, 139.5, 136.0, 135.1, 134.7, 130.3, 129.3, 129.1, 128.1, 127.8, 121.0, 120.7, 119.3, 118.5, 110.2, 107.1, 66.2, 61.1, 28.3, 25.9, 25.3, 18.0, 14.4; HRMS (ESI/APCI) calcd for C$_{31}$H$_{33}$N$_2$O$_2$ (M+H) 465.2537, found 465.2544. (jmf-02-781)

289
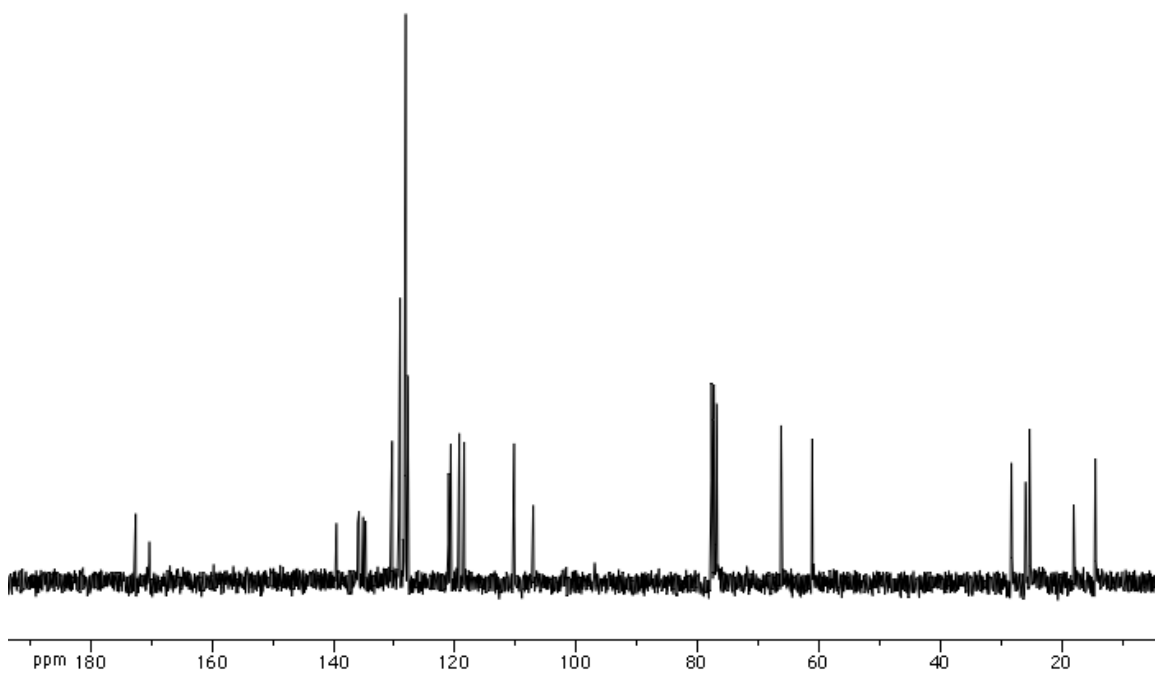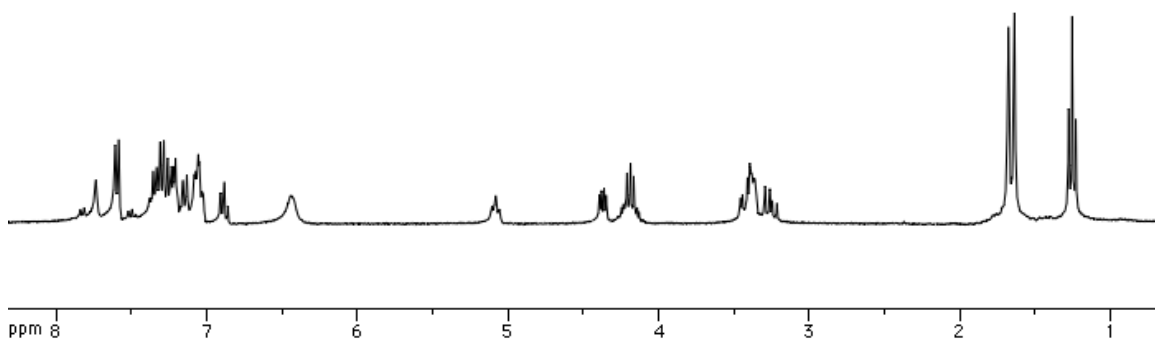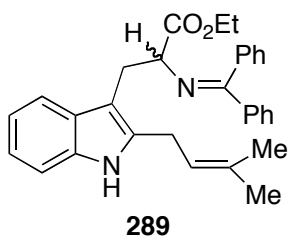
(2S)-tert-butyl 2-((1-ethoxy-3-(2-(3-methylbut-2-en-1-yl)-1H-indol-3-yl)-1-oxopropan-2-yl)carbamoyl)pyrrolidine-1-carboxylate (291):
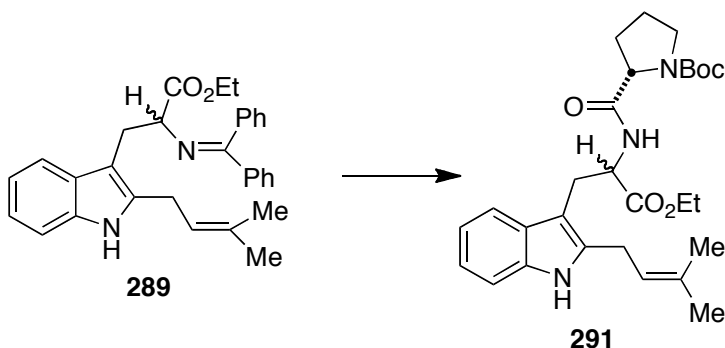
Imine **289** (501 mg, 1.08 mmol) was dissolved in 8 mL THF and 2.7 mL 1M HCl. The reaction stirred for 30 minutes at room temperature. The THF was removed in vacuo and the resulting slurry was basified with saturated aqueous NaHCO$_3$. The crude product was extracted with CH$_2$Cl$_2$ (3 x 30 mL), dried over Na$_2$SO$_4$ and concentrated under vacuum. The crude material was purified via flash column chromatography using 3:1 hexanes-ethyl acetate and the product eluted with a 10% MeOH in DCM flush of the column as an orange oil. The free amine (165 mg, 0.550 mmol) and N-Boc-L-proline (118 mg, 0.550 mmol) were stirred together in 5.5 mL MeCN. To the solution was added HATU (313 mg, 0.825 mmol) and DIPEA (0.383 mL, 2.2 mmol) and the reaction stirred at room temperature for 3 hours. The reaction mixture was quenched with 1M HCl (15 mL) and extracted with CH$_2$Cl$_2$ (3 x 30 mL). The combined organic layer was dried over Na$_2$SO$_4$ and concentrated. The crude material was purified via flash column chromatography in 1:1 hexanes-ethyl acetate. Yield: 240 mg, 0.482 mmol, 88%.

^{1}H NMR (300 MHz, CDCl$_3$) δ 7.48-7.39 (m, 2H), 7.08-7.04 (m, 2H), 5.27 (bs, 1H), 4.73 (dd, *J* = 8.4, 4.5 Hz, 2H) 4.13-3.93 (m, 3H), 3.69-3.52 (m, 2H), 3.48 (d, *J* = 6.9, 3H),

3.21-3.19 (m, 3H), 2.56-2.43 (m, 2H), 2.17-1.98 (m, 4H), 1.75 (s, 3H), 1.73 (s, 3H), 1.54 (s, 9H); ^{13}C NMR (100 MHz, CDCl$_3$) δ 172.3, 136.1, 135.3, 135.1, 121.5, 121.4, 120.3, 118.1, 117.8, 110.7, 80.8, 80.6, 61.5, 53.7, 53.6, 53.5, 47.2, 31.0, 28.5, 27.4, 26.0, 25.3, 25.2, 18.2, 14.0; HRMS (ESI/APCI) calcd for C$_{28}$H$_{40}$N$_3$O$_5$ (M+H) 498.2962, found 498.2963. (jmf-02-783)
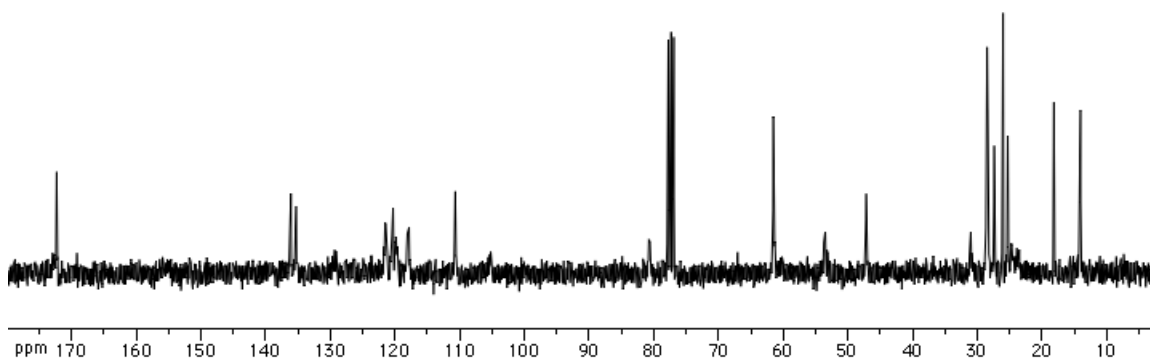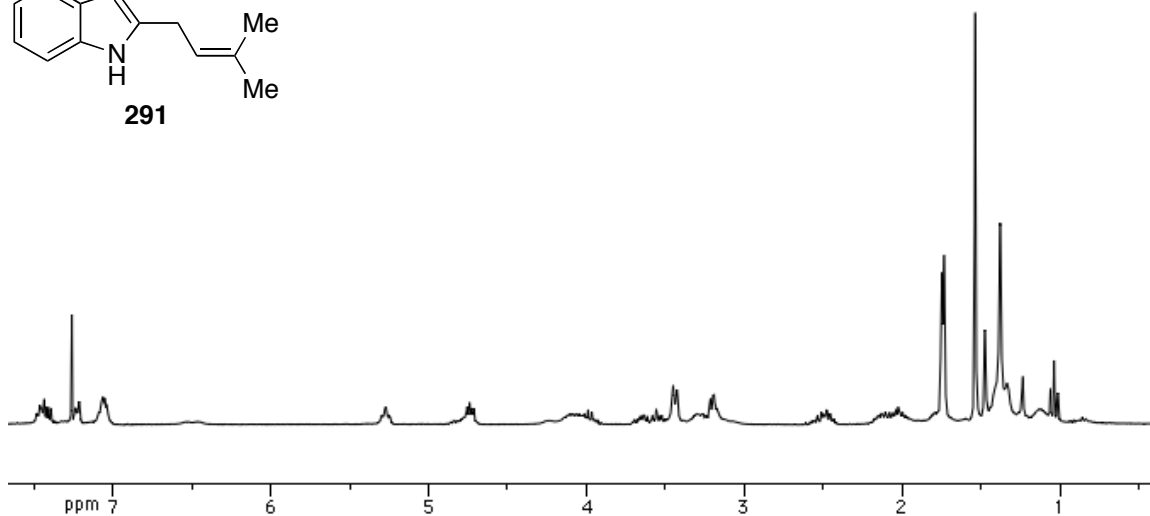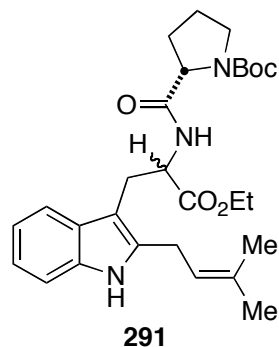
Tryprostatin B (278):

291   **278**
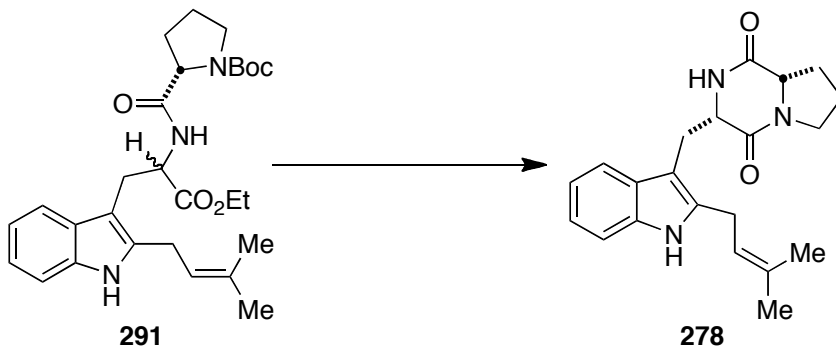
Peptide **291** (240 mg, 0.482 mmol) was dissolved in CH_2Cl_2 (1.6 mL) and cooled to 0°C.

TFA (1.6 mL) was slowly added to the cooled solution, and the reaction stirred at room

temperature for 3 hours. The reaction was quenched with saturated aqueous $NaHCO_3$ to

pH 10 and extracted with ethyl acetate (5 x 100 mL). The organic layer was dried over

Na_2SO_4 and concentrated. The crude free amine (169 mg, 0.459 mmol) was dissolved in

4.5 mL toluene and 2-hydroxypyridine (8.75 mg, 0.092 mmol) was added. The reaction

mixture stirred at reflux for 16 hours, which was then cooled to room temperature and

concentrated. The residue was diluted with CH_2Cl_2 (10 mL) and washed with 10 mL 1M

HCl. The organic layer was dried over Na_2SO_4 and concentrated. The crude material

was purified via flash column chromatography with 3% MeOH in DCM to afford a 1:1

mixture of tryprostatin B (**278**) and *trans*-tryprostatin B in 59% yield (**278**: 50 mg, 0.142

mmol)

^{1}H NMR (300 MHz, CDCl₃) δ 8.08 (bs, 1H), 7.47 (d, $J = 7.5$ Hz, 1H), 7.31 (d, $J = 8.1$

Hz, 1H), 7.18-7.06 (m, 2H), 5.64 (bs, 1H), 5.33-5.28 (m, 1H), 4.42-4.34 (m, 1H), 4.08-

4.03 (m, 1H), 3.71-3.59 (m, 3H), 3.48-3.44 (m, 1H), 2.99-2.83 (m, 1H), 2.39-2.29 (m,

1H), 2.03-1.88 (m, 3H), 1.77 (s, 3H), 1.74 (s, 3H); ^{13}C NMR (100 MHz, CDCl₃) δ 169.6,

166.7, 136.7, 135.7, 135.6, 128.2, 122.0, 120.1, 119.9, 117.9, 111.0, 104.8, 59.5, 54.8, 45.6, 28.5, 25.9, 25.8, 25.3, 22.8, 18.2; IR (neat) 3303, 2969, 1672, 1664 cm^{-1}; HRMS (ESI/APCI) calcd for $C_{21}H_{26}N_3O_2$ (M+H) 352.202, found 352.2024. (jmf-02-785)

tryprostatin B
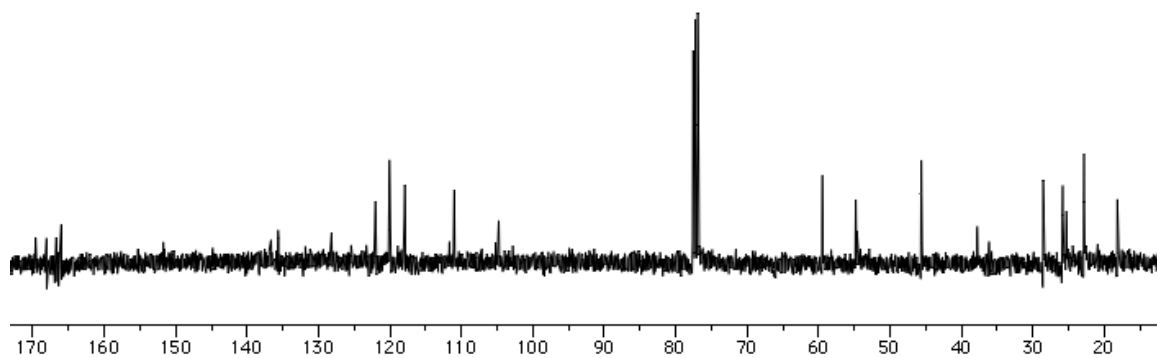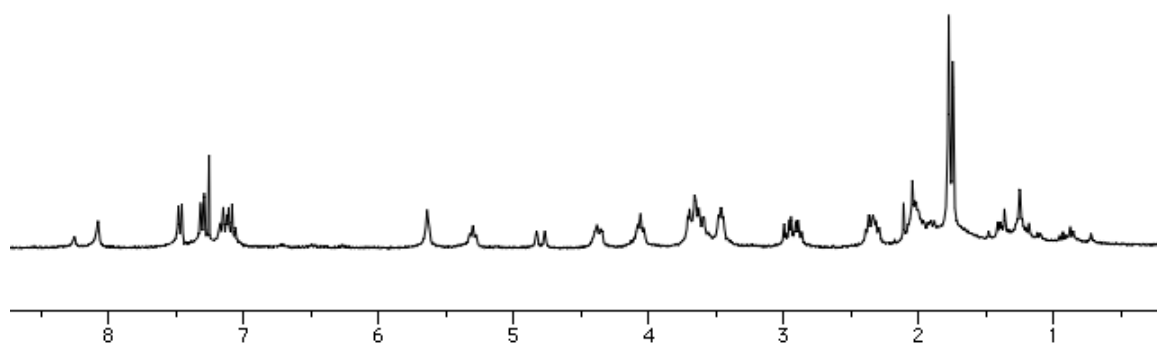
Trans: ^{1}H NMR (300 MHz, CDCl$_3$) δ 8.02 (bs, 1H), 7.51 (d, *J* = 7.2 Hz, 1H), 7.25 (d, *J* =

8.7 Hz, 1H), 7.13-7.04 (m, 2H), 6.40-6.35 (m, 1H), 5.31-5.26 (m, 1H), 4.78 (d, *J* = 8.7

Hz, 1H) 4.27-4.21 (m, 1H), 3.56-3.35 (m, 4H), 3.16-3.09 (m, 1H), 2.42-2.26 (m, 1H),

2.05-1.91 (m, 3H), 1.64 (s, 3H), 1.55 (s, 3H); HRMS (ESI/APCI) calcd for

C$_{21}$H$_{25}$N$_3$O$_2$Na (M+Na) 374.1839, found 374.1841.

trans-tryprostatin B
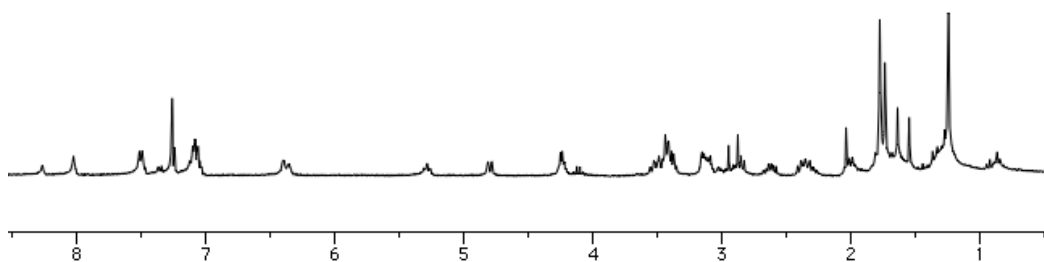
7.2.3 Chapter 6 Experimentals

2-Methyl-7-amino-1,8-naphthyridine (293):
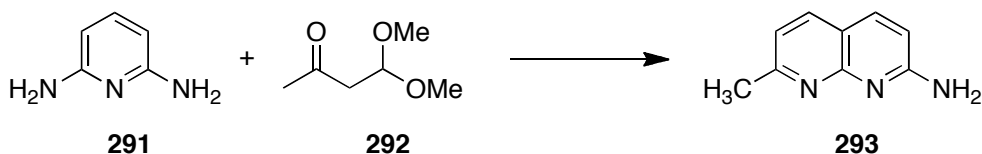
Concentrated phosphoric acid (18 mL) was cooled to 0°C. Commercially available 2,6-diaminopyridine **291** (2.0 g, 18.3 mmol) was added and the reaction was heated to 60°C. Commercially available 3-ketobutanal dimethyl acetal **292** (2.38 mL, 17.9 mmol) was added to the reaction mixture dropwise via a syringe pump over 30 minutes. The reaction was heated to 115°C for 3.5 hours. The reaction mixture was cooled to 0°C and ice cold 15% NH_4OH was quickly added in portions until pH 12. The product was extracted 5 times with $CHCl_3$, dried over Na_2SO_4 and concentrated. Yield: 2.53 g, 15.9 mmol, 89%.

^{1}H NMR (300 MHz, $CDCl_3$) δ 7.72 (d, J = 7.8 Hz, 1H), 7.66 (d, J = 8.7 Hz, 1H), 6.94 (d, J = 8.1 Hz, 1H), 6.63 (d, J = 9.0 Hz, 1H), 4.00 (bs, 2H), 2.53 (s, 3H). ^{13}C NMR (75 MHz, $CDCl_3$) δ 162.2, 159.9, 156.4, 138.1, 136.4, 119.0, 115.5, 111.8, 25.6; HRMS (ESI/APCI) calcd for $C_9H_{10}N_3$ (M+H) 160.0869, found 160.0871. (jmf-02-543)
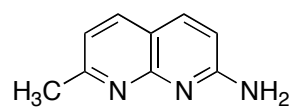
293
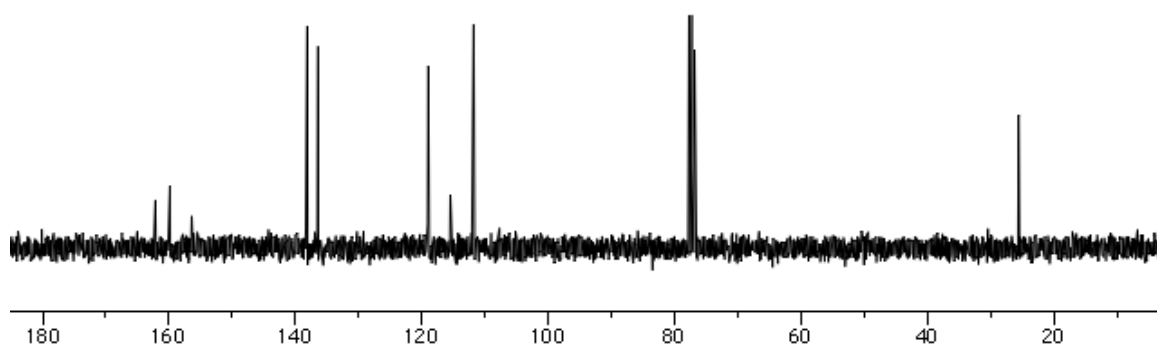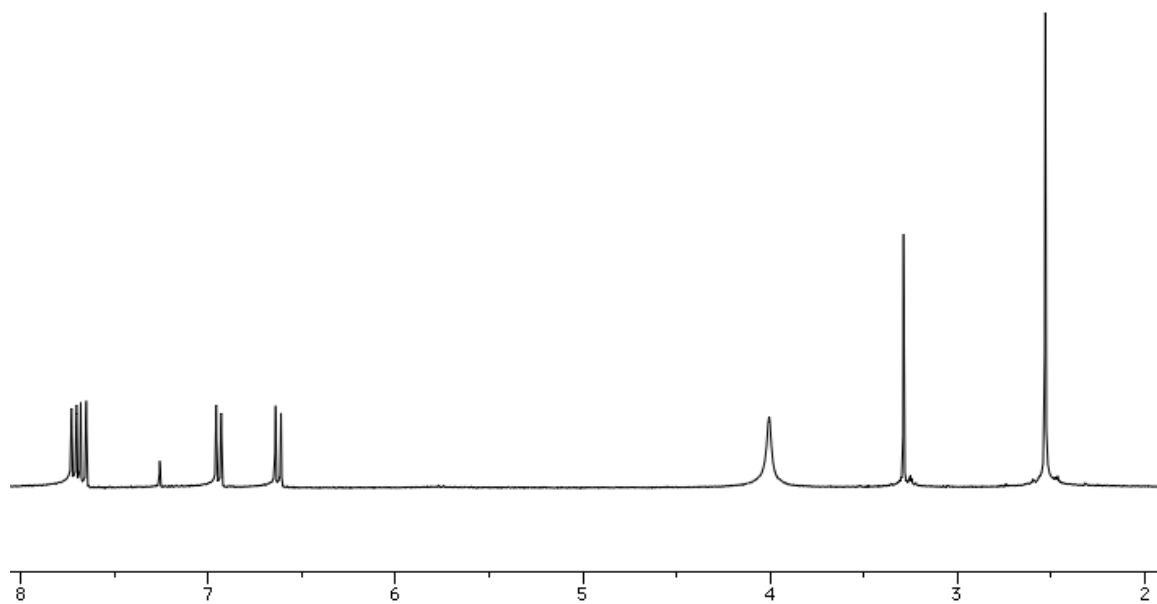
Suberoyl anhydride (299):

294 → **299**
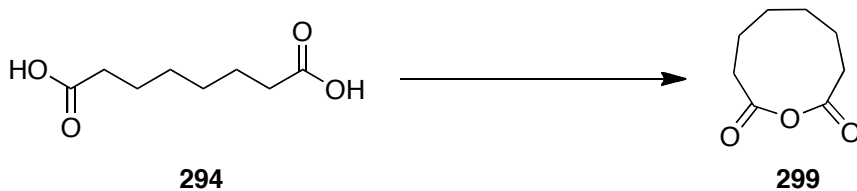
Commercially available suberic acid **294** (5.0 g, 28.7 mmol) was dissolved in acetic anhydride (10 mL) and heated to reflux for one hour. The reaction cooled to room temperature and the solvent was removed in vaccuo.   The resulting solid was recrystallized from acetonitrile. Yield: 4.39 g, 28.1 mmol, 98%.

^{1}H NMR (300 MHz, CDCl$_3$) δ 2.45 (t, J = 7.2 Hz, 4H), 1.72-1.62 (m, 4H), 1.41-1.37 (m, 4H). ^{13}C NMR (75 MHz, CDCl$_3$) δ 169.6, 35.2, 28.5, 24.1. (jmf-02-546)
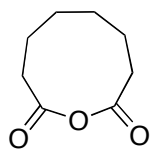
299
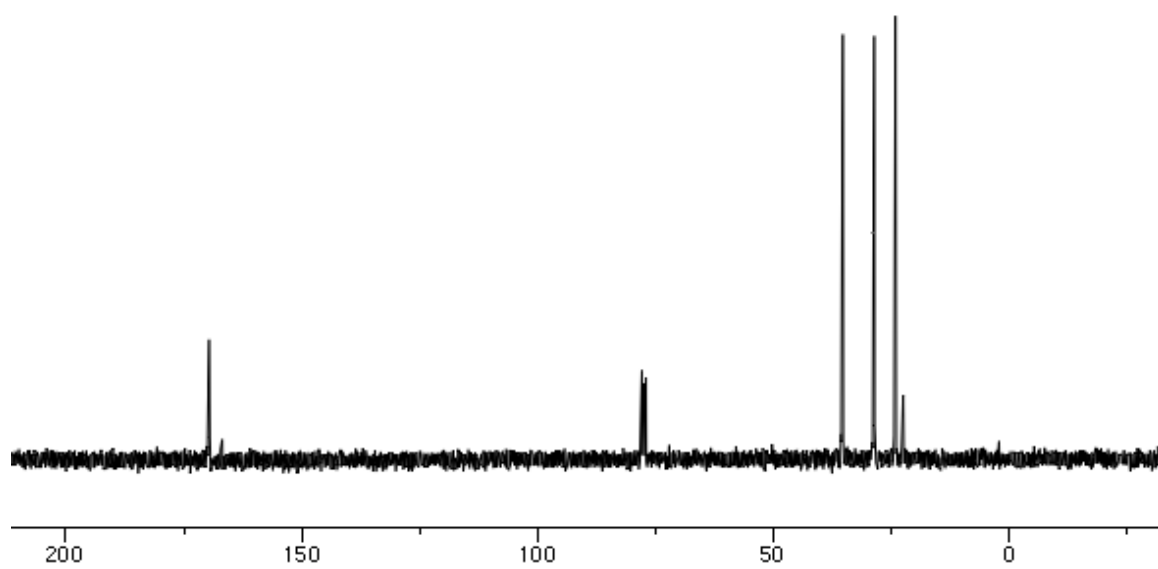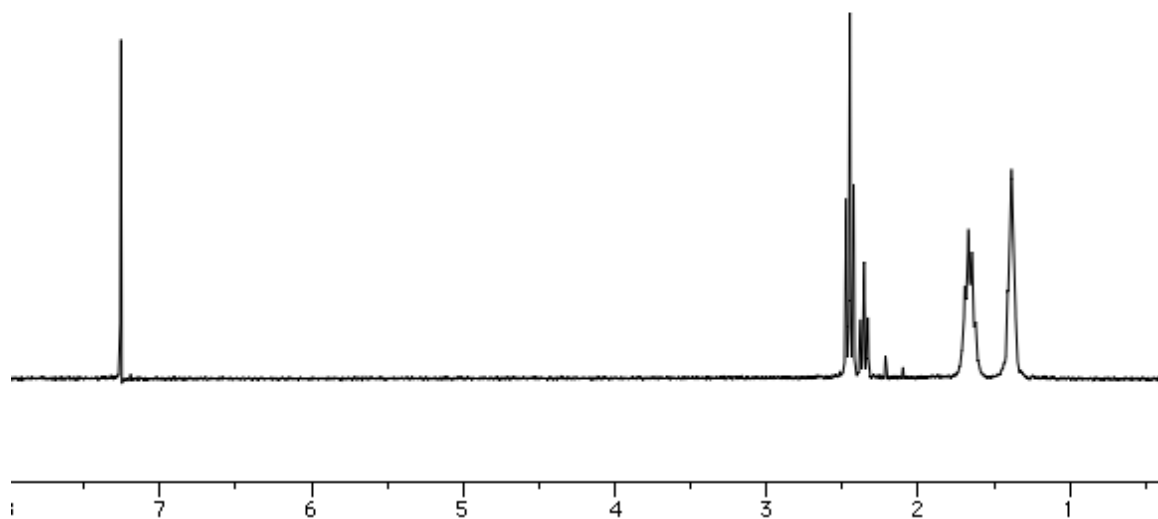
Naphthyrdine suberic acid (300):
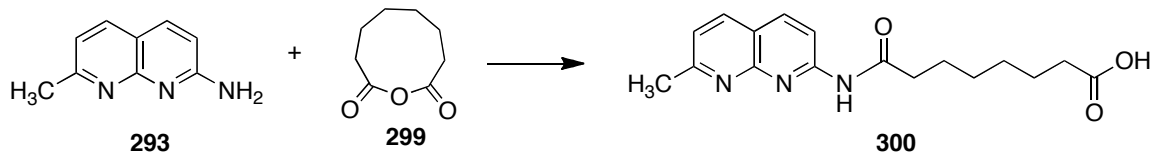
Suberoyl anhydride **299** (294 mg, 1.88 mmol) was dissolved in THF (9 mL). 2-Methyl-7-amino-1,8-naphthyridine **293** (300 mg, 1.88 mmol) was added to the reaction mixture and the reaction was heated to reflux for 1.5 hours. The reaction cooled to room temperature and water (40 mL) was added. The solid was filtered and the crude mixture was purified via flash column chromatography (5% MeOH in DCM). Yield: 320 mg, 1.02 mmol, 54%

^{1}H NMR (300 MHz, CDCl$_3$) δ 8.45 (d, J = 8.7 Hz, 1H), 8.09 (d, J = 8.7 Hz, 1H), 7.98 (d, J = 8.1 Hz, 1H), 7.24 (d, J = 11.1 Hz, 1H), 2.70 (s, 3H), 2.46 (t, J = 7.2 Hz, 2H), 2.32 (t, J = 7.2 Hz, 2H), 1.75-1.61 (m, 4H), 1.40-1.38 (m, 4H). ^{13}C NMR (75 MHz, 20:1 CDCl$_3$/CD$_3$OD) δ 173.8, 162.6, 154.2, 138.9, 137.3, 121.6, 118.5, 114.7, 37.5, 29.1, 25.2, 25.0. (jmf-02-549)

300
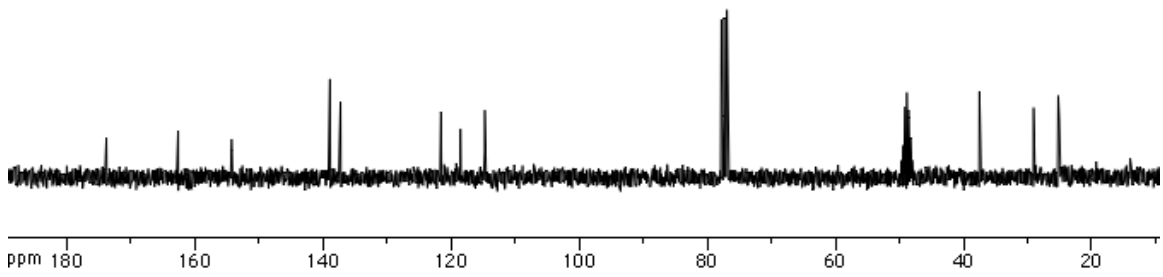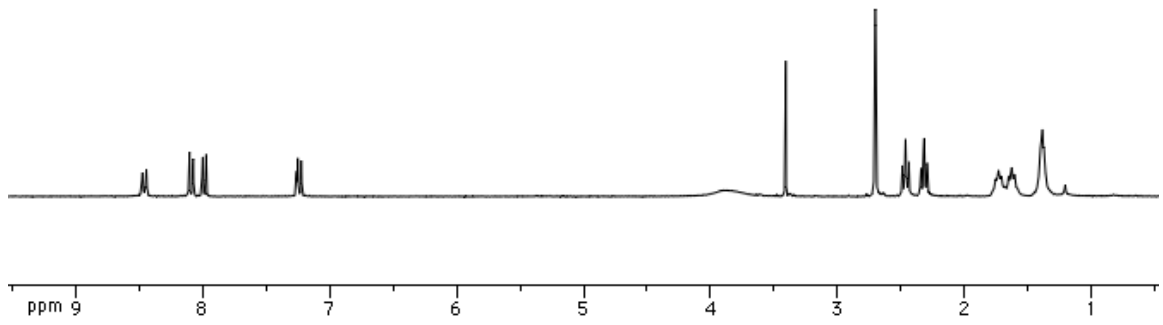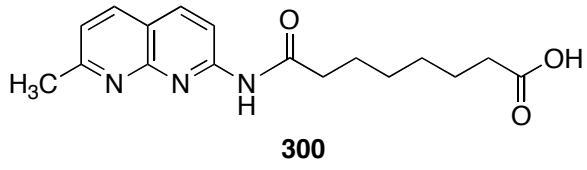
Vorinostat-naphthyridine analogue (289):
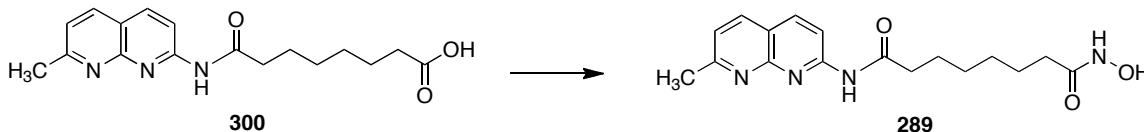
Naphthyridine suberic acid **300** (200 mg, 0.634 mmol) was dissolved in THF (3 mL) and cooled to 0°C. Ethyl chloroformate (0.078 mL, 0.824 mmol) and triethylamine (0.123 mL, 0.888 mmol) were added and the reaction mixture was stirred at room temperature of 10 minutes. The solid was filtered and the filtrate was added to hydroxylamine in water (2.10 mL, 1.05 mmol). The reaction stirred at room temperature for 45 minutes. The reaction was separated and extracted with ethyl acetate (3 x 20 mL). The organic layer was dried over Na$_2$SO$_4$ and concentrated. The crude mixture was purified via flash column chromatography (5% MeOH in DCM to 15% MeOH in DCM). Yield: 79.6 mg, 0.241 mmol, 38%.

^{1}H NMR (300 MHz, CDCl$_3$) δ 8.24 (d, J = 9.3 Hz, 1H), 7.96 (d, J = 8.7 Hz, 1H), 7.89 (d, J = 8.1 Hz, 1H), 7.12 (d, J = 8.1 Hz, 1H), 4.21 (s, 6H), 3.14 (s, 3H), 2.55 (s, 3H). ^{13}C NMR (75 MHz, 20:1 CDCl$_3$/CD$_3$OD) δ 173.6, 162.7, 154.3, 138.9, 137.2, 121.5, 118.5, 114.8, 37.6, 32.8, 29.1, 28.5, 25.3, 25.2, 25.1; HRMS (ESI/APCI) calcd for C$_{17}$H$_{23}$N$_4$O$_3$ (M+H) 331.1765, found 331.1759. (jmf-02-572)

289

N-Boc-β-alanine (304):

303 → **304**
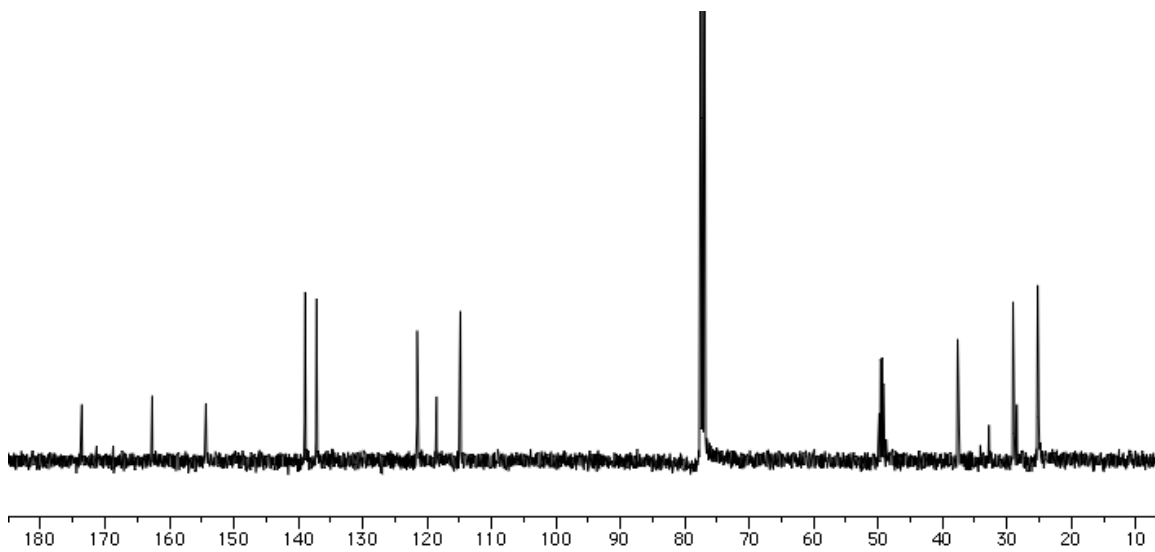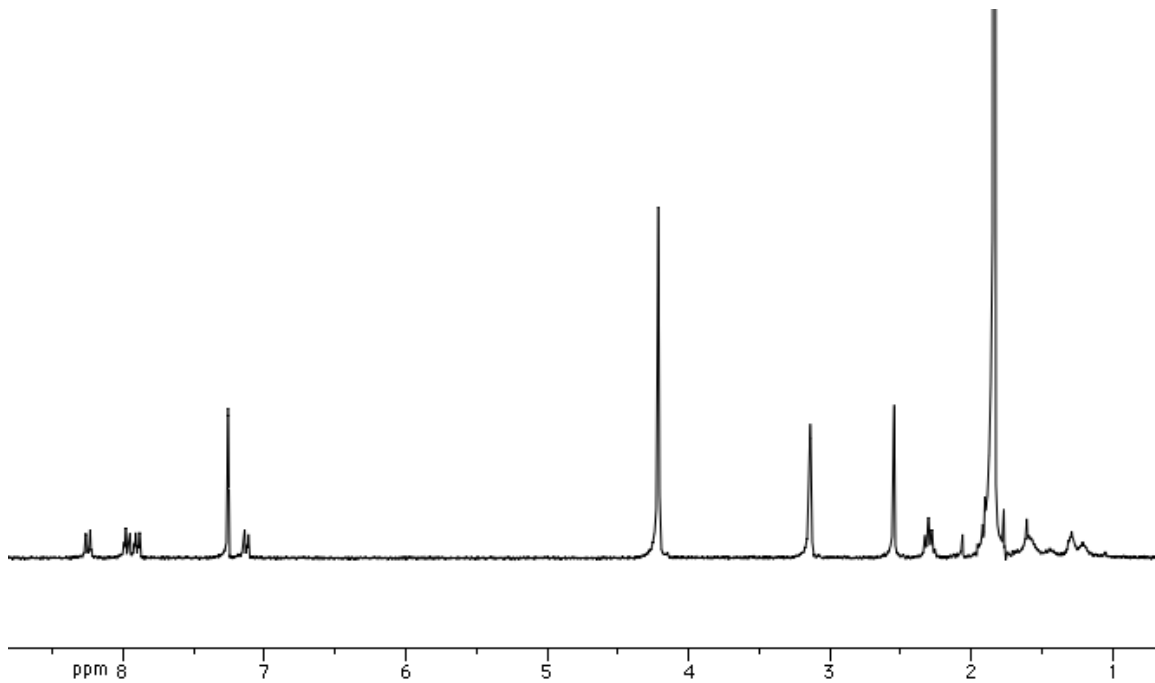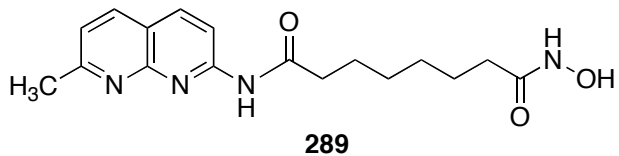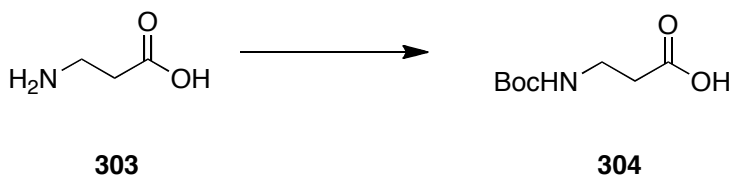
A solution of β-alanine **303** (2.67 g, 30 mmol) in a mixture of dioxane (60 mL), water (30 mL) and 1N NaOH (30 mL) was stirred and cooled in an ice-water bath. Ditert-butylpyrocarbonate (7.2 g, 33 mmol) was added, and stirring was continued at room temperature for 6 hours. The solution was then concentrated in a vacuum to about 30 mL, cooled in an ice-water bath and acidified to pH 2 with 1 M KHSO$_4$. The aqueous layer was extracted with ethyl acetate (2 x 50 mL) and the combined organic layers were dried over Na$_2$SO$_4$ and concentrated. Yield: 5.22 g, 27.6 mmol, 92%

^{1}H NMR (300 MHz, CDCl$_3$) δ 10.56 (bs, 1H), 3.37 (m, 2H), 2.56 (m, 2H), 1.42 (s, 9H).

^{13}C NMR (75 MHz, CDCl$_3$) δ 177.8, 156.3, 79.9, 36.1, 34.7, 28.6. (jmf-02-571)
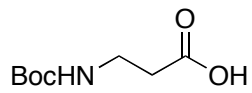
304
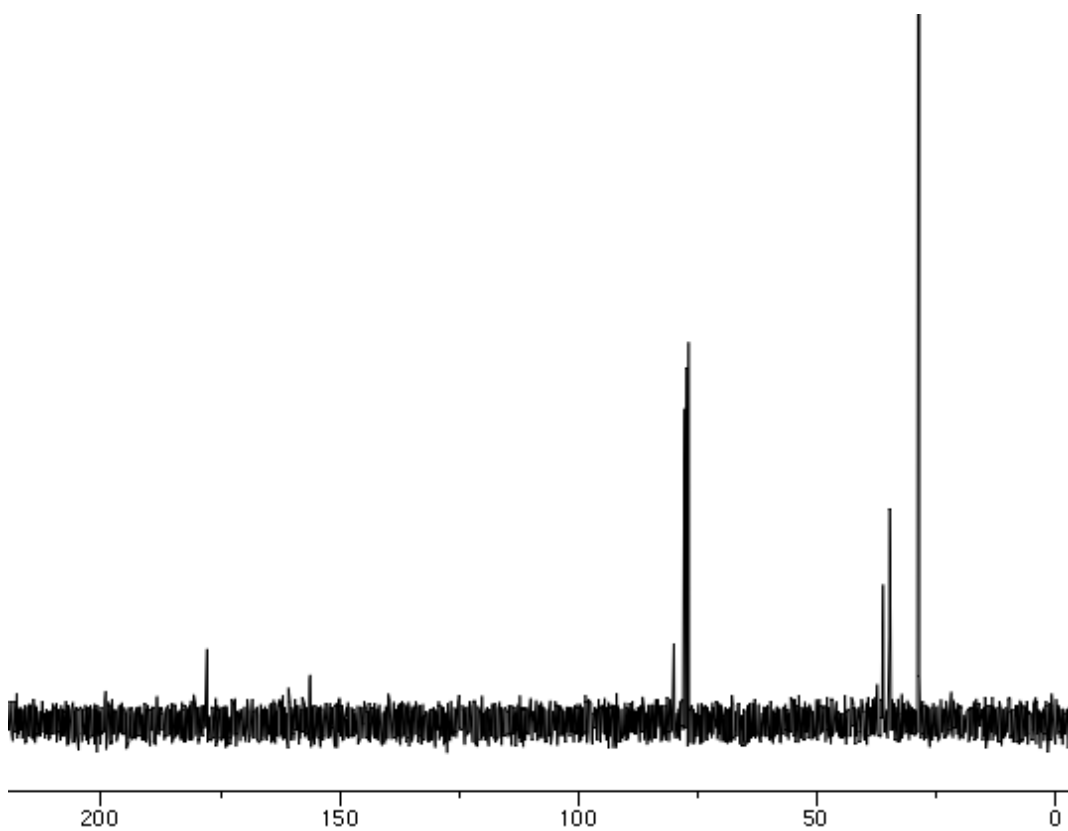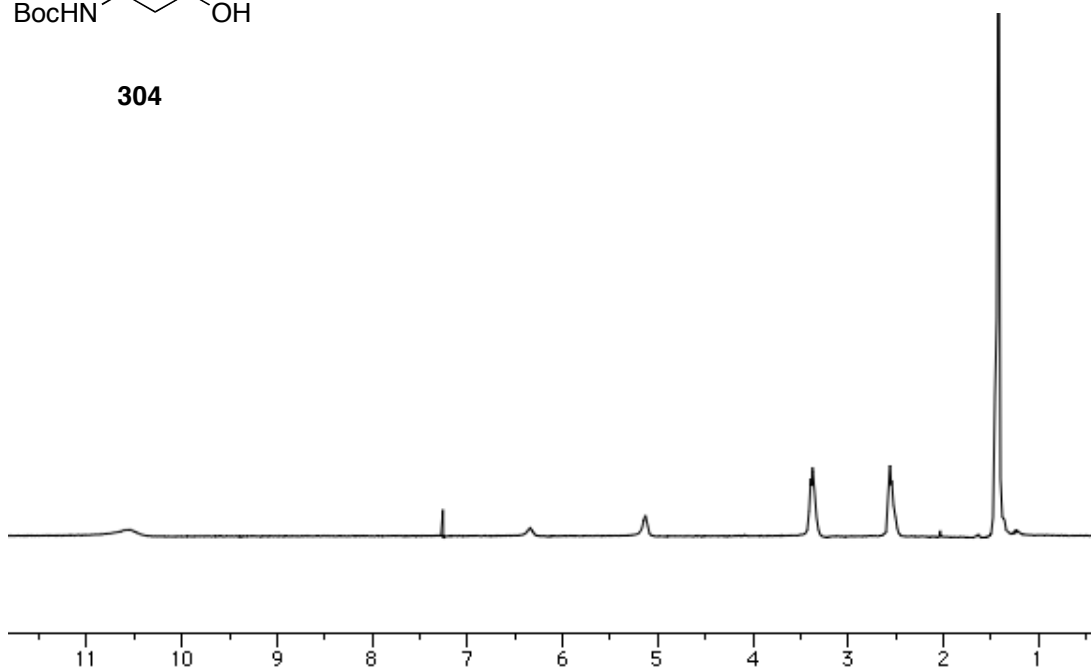
N-Boc-O-pentafluorophenyl-β-alanine (305):
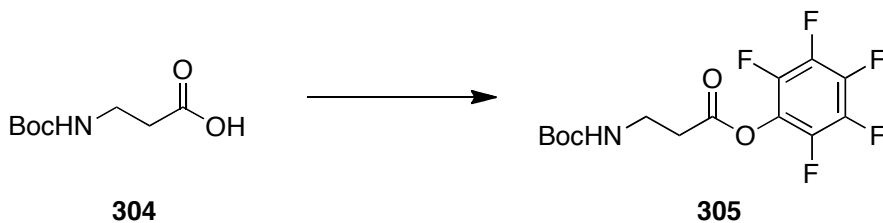
304   **305**

To a solution of N-Boc-β-alanine **304** (3.0 g, 15.7 mmol) in DMF (10 mL) was added

pentafluorophenol (2.2 g, 12.0 mmol) and EDCI (2.8 g, 14.6 mmol) The mixture was

stirred at room temperature for 24 hours. The solvent was evaporated and the crude

product was taken up in $CHCl_3$ (30 mL). The organic layer was washed with H_2O and

dried over $MgSO_4$. The solvent was evaporated in vacuo and the crude residue was

purified via silica gel flash column chromatography (1:1 $CHCl_3$/hexanes) to afford **17** as

a white solid. Yield: 2.95 g, 8.32 mmol, 53%

^{1}H NMR (300 MHz, $CDCl_3$) δ 5.02 (bs, 1H), 3.50 (q, J = 6.0, 6.3 Hz, 2H), 2.91 (t, J = 6.0

Hz, 2H), 1.43 (s, 9H). ^{13}C NMR (75 MHz, $CDCl_3$) δ 168.6, 156.0, 80.0, 36.2, 34.1, 28.5.

(jmf-02-572)

305
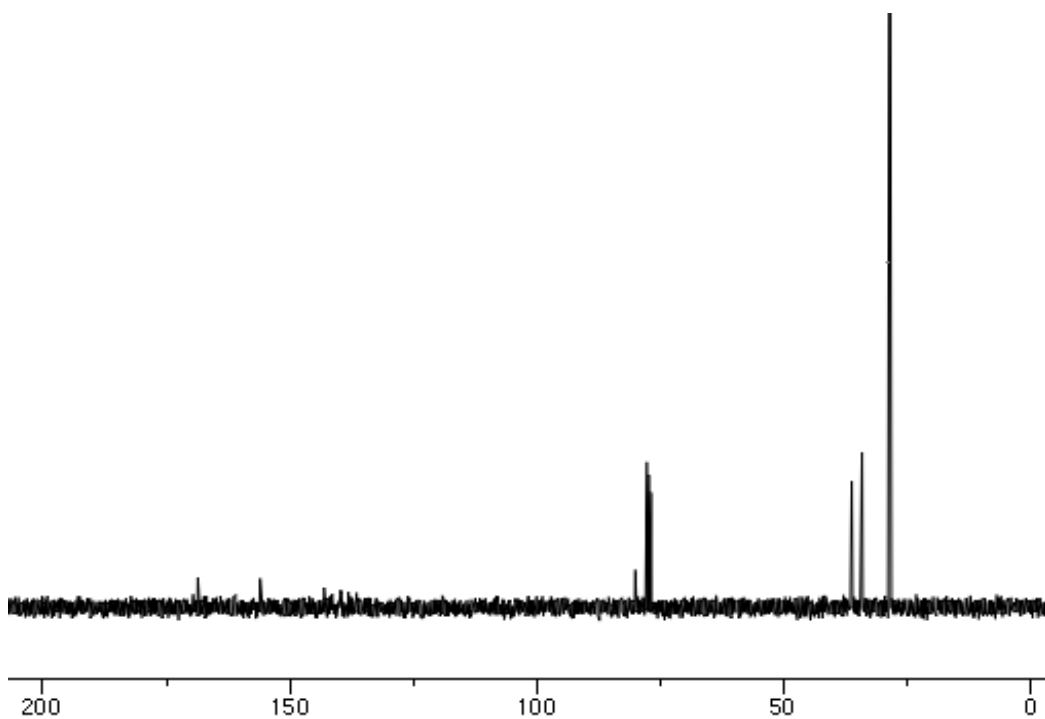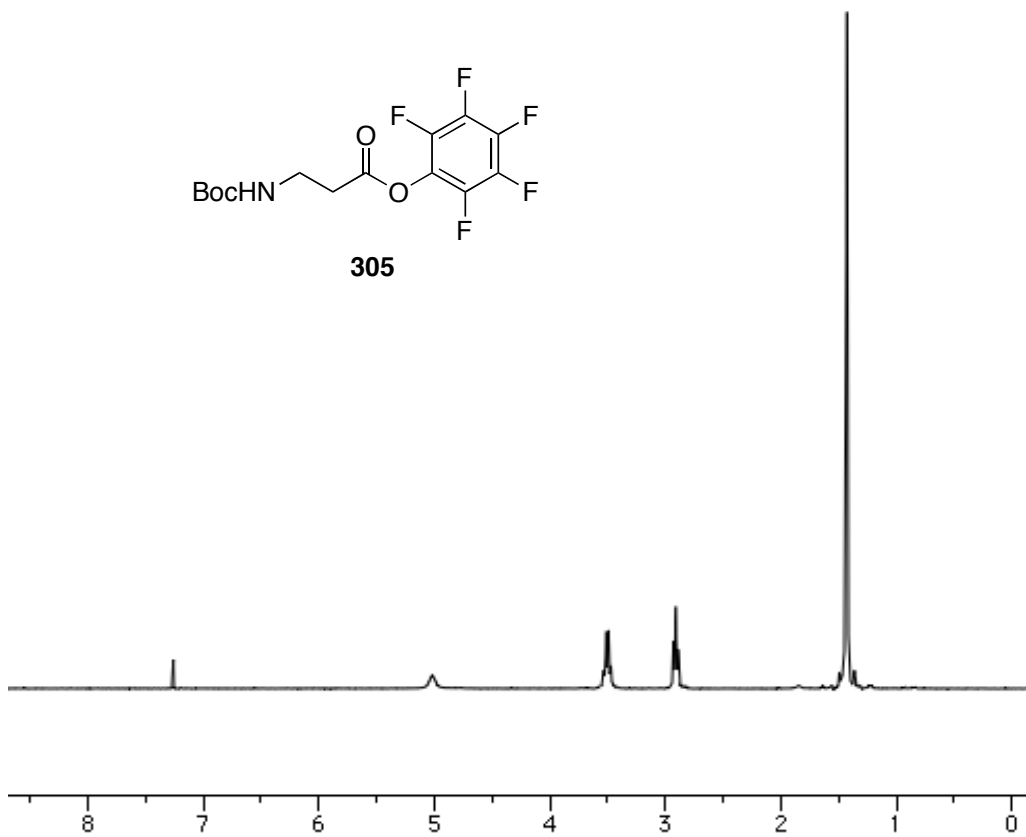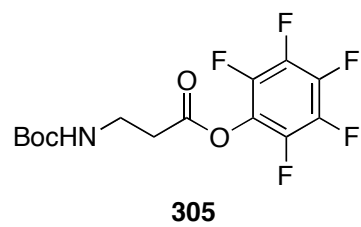
N-Boc-β-alanine-naphthyridine (306):
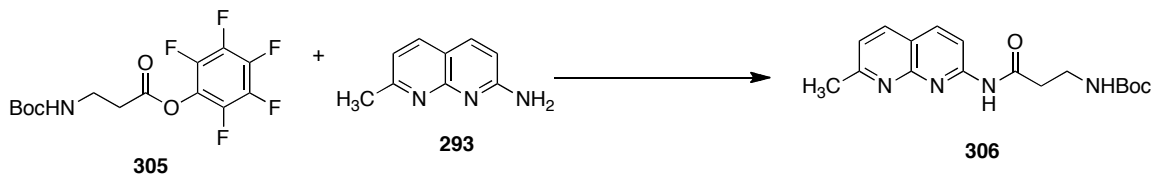
To a solution of the activated ester **305** (449 mg, 1.26 mmol) in dry DMF (4 mL) was added 2-amino-7-methyl-1,8-naphthyridine **293** (200 mg, 1.26 mmol) and DIPEA (162 mg, 1.26 mmol). The mixture was stirred at 40°C for 24 hours. The solvent was evaporated to dryness and the crude residue was purified via silica gel flash column chromatography (50:1 CHCl$_3$/MeOH). Yield: 400 mg, 1.21 mmol, 96%.

^{1}H NMR (300 MHz, CDCl$_3$) δ 9.82 (bs, 1H), 8.43 (d, J = 8.7 Hz, 1H), 8.11 (d, J = 8.7 Hz, 1H), 7.98 (d, J = 8.1 Hz, 1H), 7.25 (d, J = 8.1 Hz, 1H), 5.36 (bs, 1H), 2.94 (d, J = 1.2 Hz, 2H), 2.86 (d, J = 1.5 Hz, 2H), 2.71 (s, 3H), 1.39 (s, 9H). ^{13}C NMR (75 MHz, CDCl$_3$) δ 163.4, 162.3, 154.3, 154.0, 139.3, 136.9, 121.9, 118.7, 114.9, 79.5, 37.5, 36.8, 36.4, 31.7, 29.9, 28.6, 25.4. (jmf-02-575)

306
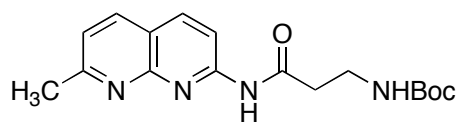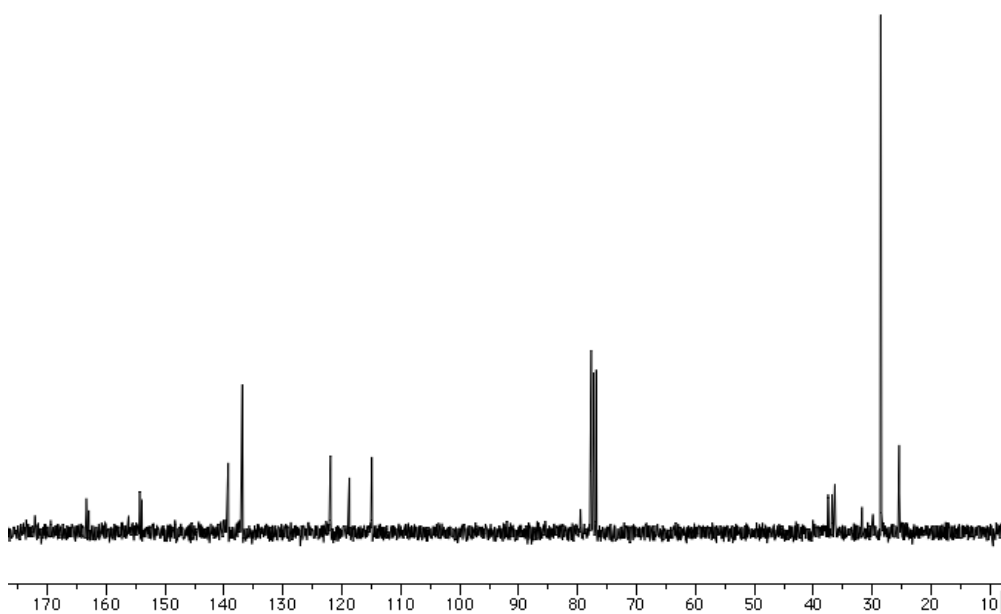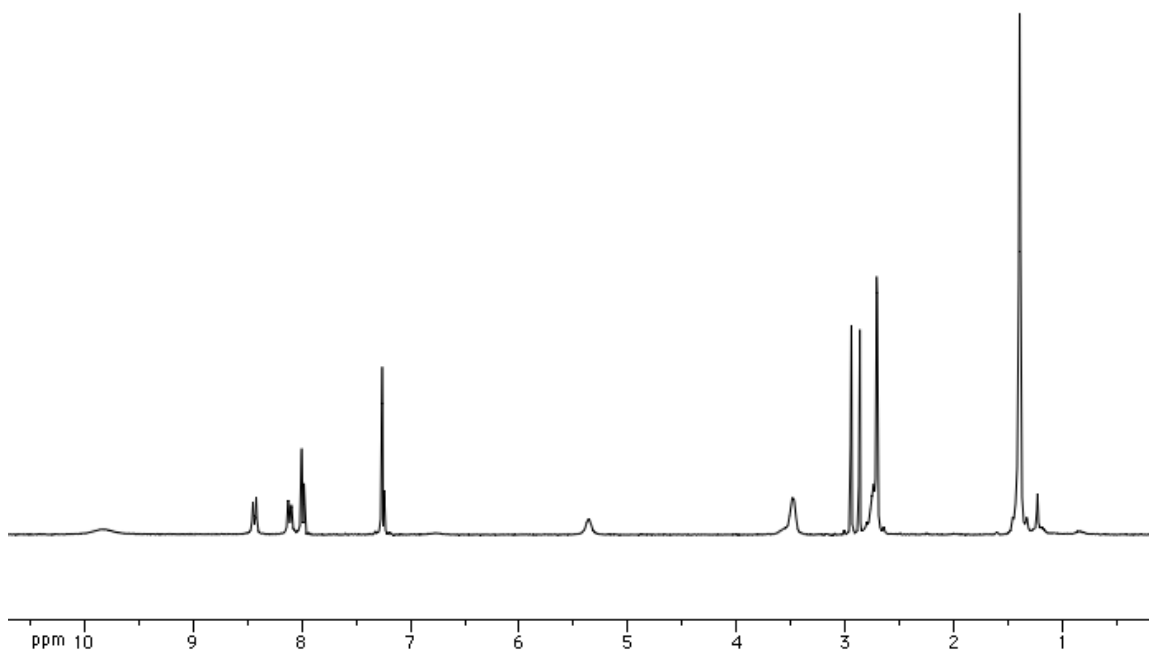
β-alanine-naphthyridine (307):

306 → **307**
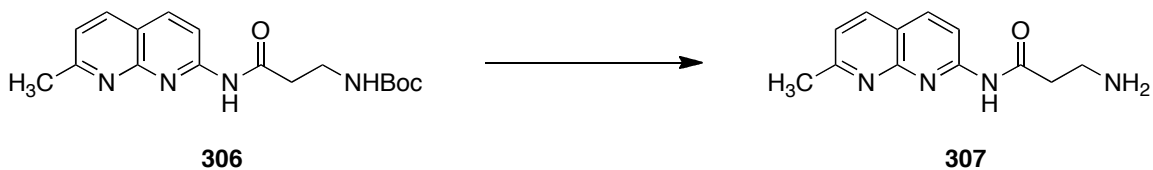
To a solution of **306** (191 mg, 0.58 mmol) in dry CHCl$_3$ (3 mL) at 0°C was added ethyl acetate containing 4M HCl (1.5 mL) and the mixture was stirred at room temperature for 30 minutes. The solvent was evaporated to dryness to give the hydrochloride salt of **19**. The hydrochloride salt of **307** was dissolved in H$_2$O (10 mL) and extracted into CHCl$_3$ by the addition of 28% aqueous ammonia solution. The organic layer was dried over MgSO$_4$ and the solvent was evaporated in vacuo to give **307**. Yield: 42.7 mg, 0.186 mmol, 32%.

^{1}H NMR (300 MHz, CDCl$_3$) δ 8.39 (d, J = 8.7 Hz, 1H), 8.05 (d, J = 9.0 Hz, 1H), 7.97 (d, J = 8.4 Hz, 1H), 7.25 (d, J = 8.4 Hz, 1H), 3.24-3.21 (m, 2H), 2.74 (s, 3H), 2.68-2.64 (m, 2H). (jmf-02-578)

307
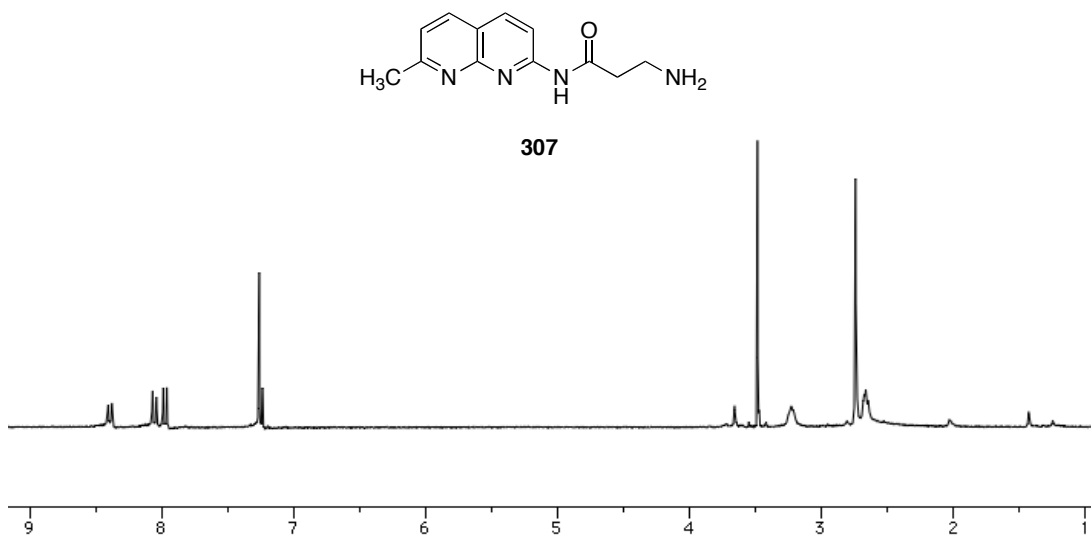
Naphthyridine-Melphalan (21):
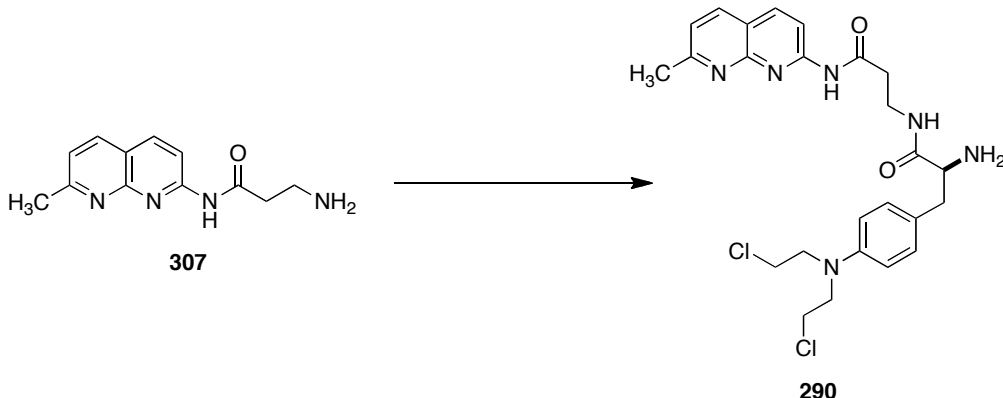
N-Boc-melphalan (90 mg, 0.22 mmol) and naphthyridine **307** (51 mg, 0.22 mmol) were dissolved in DCM (3.7 mL) followed by the addition of NMM (0.082 mL, 0.75 mmol). The reaction mixture stirred for 40 minutes at 0°C. EDCI (34 mg, 0.22 mmol) was added and the reaction mixture stirred for another 40 minutes at 0°C and then was allowed to warm to room temperature over 18 hours. The reaction mixture was diluted with DCM (15 mL) and washed with 10% aqueous citric acid (15 mL). The organic layer was dried over Na_2SO_4 and concentrated. The crude material was purified via silica gel flash column chromatography (50:1 $CHCl_3$/MeOH). Yield: 23 mg, 0.037 mmol, 17%. The Boc-protected N-melphalan (26 mg, 0.042 mmol) was dissolved in HCl saturated ethyl acetate (4.2 mL) and stirred for 2 hours at room temperature. The reaction was concentrated and purified via recrystallization (EtOH and diethyl ether). Yield: 9.13 mg, 0.176 mmol, 42%.

^{1}H NMR (300 MHz, $CDCl_3$) δ 8.60 (d, J = 7.8 Hz, 1H), 8.53 (d, J = 9.0 Hz, 1H), 8.33 (d, J = 9.3 Hz, 1H), 7.55 (d, J = 8.4 Hz, 1H), 6.99 (d, J = 7.8 Hz, 2H), 6.51 (d, J = 7.8 Hz, 2H), 3.58-3.53 (m, 4H), 3.49-3.44 (m, 4H), 3.40-3.31 (m, 1H), 3.21-3.20 (m, 6H), 2.66

(s, 3H); HRMS (ESI/APCI) calcd for $C_{25}H_{31}Cl_2N_6O_2$ (M+H) 517.188, found 517.1876.

(jmf-02-583)

290
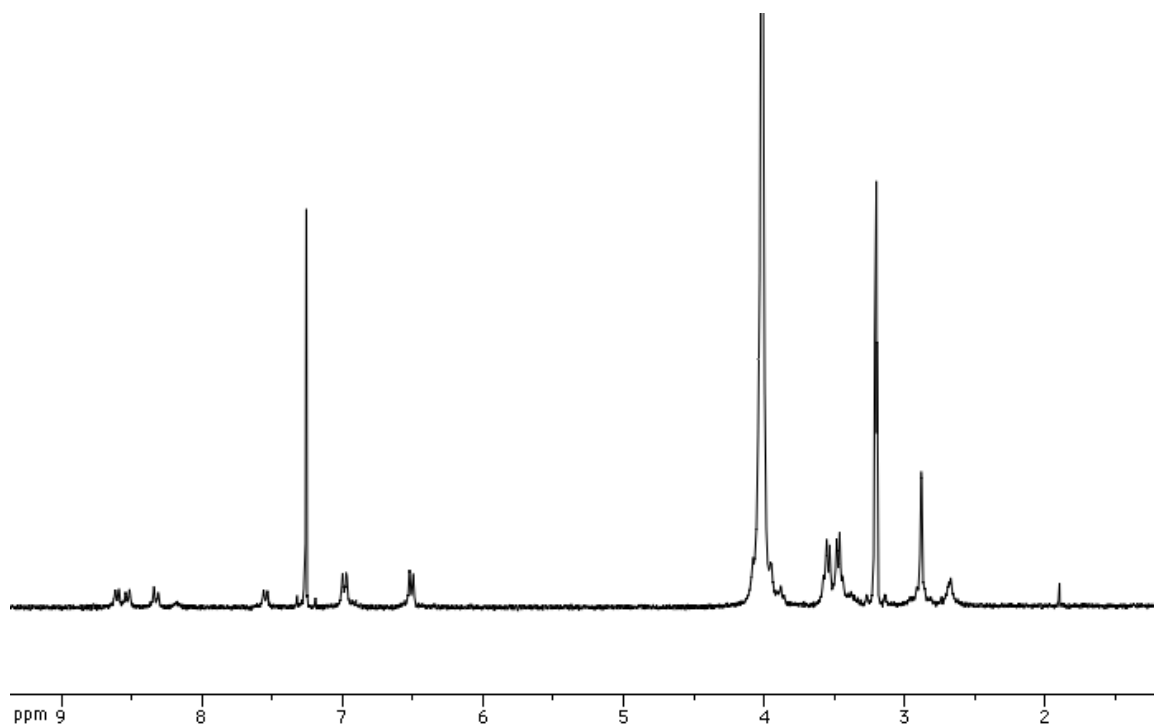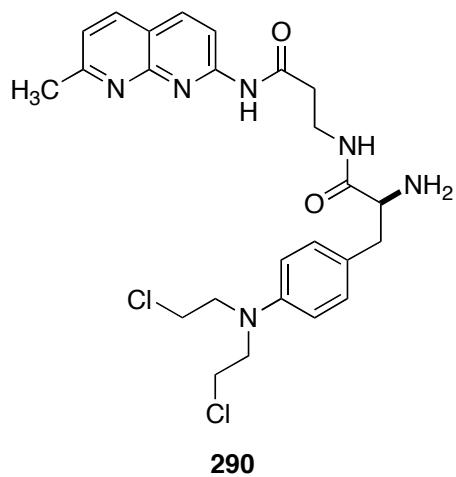
7.3 General Biosynthetic Considerations

$[^{13}C]_2$-$[^{15}N]_2$-L-Proline and $[^{13}C]$- L-glycine were obtained from the NIH Stable Isotopes Resource at Los Alamos National Laboratory. Cultures of *Aspergillus versicolor* NRRL 35600 were obtained from the Department of Agriculture in Peoria, Illinois. ^{1}H-NMR spectra and ^{13}C-NMR spectra were obtained on Varian 300, 400, 400 MR or 500 MHz NMR spectrometers. NMR spectra were taken in CDCl$_3$ (^{1}H, 7.26 ppm; ^{13}C, 77.0 ppm), CD$_3$OD (^{1}H, 3.31 ppm, 49.15 ppm), d$_6$-DMSO (^{1}H, 2.50 ppm, ^{13}C, 39.51 ppm) and D$_2$O (^{1}H, 4.79 ppm) obtained from Cambridge Isotope Labs. Mass spectra were obtained on Fisions VG Autospec using a high/low resolution magnetic sector.

7.4 Biosynthesis Experimentals

7.4.1 Procedure for Completing Feeding Studies

Terrestrial-derived *Aspergillus versicolor* NRRL 35600 was suspended in a sterile 10% glycerol solution. Spores from this culture were transferred to sterile malt extract agar slants (prepared from 25 g malt agar and 500 mL distilled H$_2$O); 20 μL of the suspension was used per slant. The slants were placed in an incubator at 25 ºC for 14 days. Potato Dextrose Broth (PDB) was prepared by dissolving 48 g of the medium and 6 g tryptose in 2L of doubly distilled H$_2$O (DDH$_2$O). The solution was heated to aid in dissolving the medium, which was then transferred to fernbach flasks (4 x 500 mL) and autoclaved.

Spores of *A. versicolor* from eight slants were shaken into the four fernbach flasks containing sterile PDB. The fernbach flasks were covered and gently placed in the incubator for 14 days at 25 ºC for the notoamide E, 6-hydroxydeoxybrevianamide E, and stephacidin A incorporation studies. The inoculated flasks used for the notoamide S

feeding study were allowed to incubate for 9 days. The PDB was removed leaving a disk of the fungus. The undersides of the disks, the mycelia cells, were rinsed with 100 mL of sterile water.

Sterile trace element solution (35 mM $NaNO_3$, 5.7 mM K_2HPO_4, 4.2 mM $MgSO_4 \cdot 7H_2O$, 1.3 mM KCl, 36 mM $FeSO_4 \cdot 7H_2O$, 25 mM $MnSO_4 \cdot H_2O$, 7 mM $ZnSO_4 \cdot 7H_2O$, and 1.5 mM $CuCl_2 \cdot 2H_2O$) containing the labeled precursor was placed into each of the flasks using a syringe and needle (Table 10). The fungal cells were incubated at 25°C for 14-21 days and each flask was swirled daily to ensure even distribution of the labeled compound.

Table 10. Details of each precursor incorporation experiment with *A. versicolor*.

Proposed Precursor	Mmol Precursor	Additive Used	Days Incubated
Notoamide E	0.096	N/A	14 days
6-OH-deoxybrevianamide E	0.159	DMSO	14 days
Stephacidin A	0.140	DMSO	21 days
Notoamide S	0.068	N/A	14 days

A detergent had to be used to dissolve the water-insoluble proposed precursors. The water-insoluble compounds were dissolved in 0.5 mL DMSO. TWEEN 80 (1% solution) was added to the dissolved precursor. Sterile trace element solution was added to each precursor/TWEEN 80 solution and the mixture was sonicated for 15 minutes to aid in micelle formation.

The aqueous solution was decanted and stored at 4°C with 1-2 mL of chloroform. The mycelia cells from each flask were harvested, combined with the cells from duplicate experiments and pureed in an Oster blender with 1:1 $MeOH$-$CHCl_3$. The puree was transferred to a 2 L Erlenmeyer flask, diluted to 1.2 L with 1:1 $MeOH$-$CHCl_3$, and placed

in the shaker for 24 hours. Celite (30 g) was added to the flask and allowed to shake for an extra 10 minutes. The suspension was filtered through Whatman #2 paper and the filtrate was stored at 4°C. The mycelia "cake" was diluted with 600 mL 1:1 MeOH-CHCl$_3$ and placed on the shaker for an additional 48 hours. The suspension was filtered through Whatman #2 paper, and the combined filtrates were concentrated under vacuum. The residue was dissolved in 250 mL H$_2$O and extracted with EtOAc (3 x 300 mL). The organic layer was concentrated and partitioned between MeCN and hexanes. The layers were separated, and the MeCN layer was concentrated under vacuum.

The crude material was purified via silica gel flash column chromatography (1% MeOH in DCM – 3% MeOH in DCM) to afford three fractions that were each analyzed by ^{13}C NMR spectroscopy. Fractions containing enrichment of ^{13}C were further purified via preparative thin layer chromatography (1000 mm, 3% MeOH in DCM x5).

7.4.2 Calculations of the Percentage of ^{13}C-incorporation

The percentage of ^{13}C-enrichment in the fungal metabolites from isotopically labeled biosynthetic precursors was calculated according to the method Lambert et al.[7.3] These calculations are based on the comparison of the mass spectrum of the labeled material to the mass spectrum of the unlabeled material. For these experiments, electrospray mass spectroscopy was used, thus the base peak in the mass spectrum was the M+H peak. For feeding studies using ^{15}N-labels, the additional ^{15}N was fixed. For these experiments the base peak was the M(^{15}N)+H for 6-hydroxydeoxybrevianamide E or M(^{15}N)$_2$+H for notoamide S.

Percent Incorporation of notoamide E into notoamide D:

Native Notoamide D ($C_{26}H_{31}N_3O_3$)
[M+H] (450.23): 73.78%
[M+H+1] (451.24): 21.94%
[M+H+2] (452.25): 3.76%
[M+H+3] (453.25): 0.47%
[M+H+4] (454.25): 0.05%

^{13}C Notoamide D from incorporation experiments:
[M+H] (450.23): 2.4%
[M+H+1] (451.24): 9.9%
[M+H+2] (452.25): 85.9%

[M+H+3] (453.25): 1.5%
[M+H+4] (454.25): 0.3%

Calculation of Native Notoamide D: (assume 100 molecules)
[M+H]: ^{12}C: 26 x 73.78 = 1918.28
[M+H+1]: ^{12}C: 25 x 21.94 = 548.5 ^{13}C: 1 x 21.94 = 21.94
[M+H+2]: ^{12}C: 24 x 3.76 = 90.24 ^{13}C: 2 x 3.76 = 7.52
[M+H+3]: ^{12}C: 23 x 0.47 = 10.81 ^{13}C: 3 x 0.47 = 1.41
[M+H+4]: ^{12}C: 22 x 0.05 = 1.1 ^{13}C: 4 x 0.05 = 0.2

total ^{12}C: 2568.93   total ^{13}C: 31.07

Native Notoamide D ^{13}C content: 31.07/(2568.93 +31.07) x 100% = 1.2%

Calculation for ^{13}C Notoamide D from incorporation experiments: (assume 100 molecules)

[M+H]: ^{12}C: 26 x 2.4 = 62.7
[M+H+1]: ^{12}C: 25 x 9.9 = 247.5 ^{13}C: 1 x 9.9 = 9.9
[M+H+2]: ^{12}C: 24 x 85.9 = 2061.6 ^{13}C: 2 x 85.9 = 171.8
[M+H+3]: ^{12}C: 23 x 1.5 = 34.5 ^{13}C: 3 x 1.5 = 4.5
[M+H+4]: ^{12}C: 22 x 0.3 = 6.6 ^{13}C: 4 x 0.3 = 1.2

total ^{12}C: 2412.9   total ^{13}C: 187.4

Notoamide D from incorporation experiments ^{13}C content: 187.4/(2412.9 + 187.4) x 100% = 7.2%

Percent incorporation of intact doubly ^{13}C-labeled Notoamide E = 7.2% - 1.2% = 6.0%

Percent Incorporation of notoamide E into notoamide C:
Native Notoamide C ($C_{26}H_{31}N_3O_3$)
[M+H] (450.23): 73.78%
[M+H+1] (451.24): 21.94%
[M+H+2] (452.25): 3.76%
[M+H+3] (453.25): 0.47%
[M+H+4] (454.25): 0.05%

^{13}C Notoamide C from incorporation experiments:
[M+H] (450.23): 0.0%
[M+H+1] (451.24): 10.8%
[M+H+2] (452.25): 87.4%
[M+H+3] (453.25): 1.7%
[M+H+4] (454.25): 0.1%

Calculation of Native Notoamide C: (assume 100 molecules)
[M+H]: ^{12}C: 26 x 73.78 = 1918.28
[M+H+1]: ^{12}C: 25 x 21.94 = 548.5 ^{13}C: 1 x 21.94 = 21.94
[M+H+2]: ^{12}C: 24 x 3.76 = 90.24 ^{13}C: 2 x 3.76 = 7.52
[M+H+3]: ^{12}C: 23 x 0.47 = 10.81 ^{13}C: 3 x 0.47 = 1.41
[M+H+4]: ^{12}C: 22 x 0.05 = 1.1 ^{13}C: 4 x 0.05 = 0.2

total ^{12}C: 2568.93   total ^{13}C: 31.07

Native Notoamide C ^{13}C content: 31.07/(2568.93 + 31.07) x 100% = 1.2%

Calculation for ^{13}C Notoamide C from incorporation experiments: (assume 100 molecules)

[M+H]: ^{12}C: 26 x 0.0 = 0.0
[M+H+1]: ^{12}C: 25 x 10.8 = 270 ^{13}C: 1 x 10.8 = 10.8
[M+H+2]: ^{12}C: 24 x 87.4 = 2097.6 ^{13}C: 2 x 87.4 = 174.8
[M+H+3]: ^{12}C: 23 x 1.7 = 39.1 ^{13}C: 3 x 1.7 = 5.1
[M+H+4]: ^{12}C: 22 x 0.1 = 2.2 ^{13}C: 4 x 0.1 = 0.4

total ^{12}C: 2408.9   total ^{13}C: 191.1

Notoamide C from incorporation experiments ^{13}C content: 191.1/(2408.9 + 191.1) x 100% = 7.4%

Percent incorporation of intact doubly ^{13}C-labeled Notoamide E = 7.4%- 1.2% = 6.2%

Percent Incorporation of 6-hydroxydeoxybrevianamide E into notoamide J:
Native Notoamide J ($C_{21}H_{25}N_3O_4$)
[M+H] (384.18): 77.9%
[M+H+1] (385.19): 18.9%
[M+H+2] (386.20): 2.84%
[M+H+3] (387.20): 0.32%
[M+H+4] (388.21): 0.03%

^{13}C Notoamide J from incorporation experiments:
[M+H] (384.18): 0%
[M+H+1] (385.19): 0%
[M+H+2] (386.20): 99.5%
[M+H+3] (387.20): 0%
[M+H+4] (388.20): 0.5%

Calculation of Native Notoamide J: (assume 100 molecules)
[M+H]: ^{12}C: 21 x 77.9 = 1635.9
[M+H+1]: ^{12}C: 20 x 18.9 = 378 ^{13}C: 1 x 18.9 = 18.9
[M+H+2]: ^{12}C: 19 x 2.84 = 53.96 ^{13}C: 2 x 2.84 = 5.68
[M+H+3]: ^{12}C: 18 x 0.32 = 5.76 ^{13}C: 3 x 0.32 = 0.96
[M+H+4]: ^{12}C: 17 x 0.03 = 0.51 ^{13}C: 4 x 0.03 = 0.12

total ^{12}C: 2074.13   total ^{13}C: 25.66
Native Notoamide J ^{13}C content: 25.66/(2074.13 +25.66) x 100% = 1.2%

Calculation for ^{13}C Notoamide J from incorporation experiments: (assume 100 molecules) ^{15}N-fixed at 1
 [M+H]: ^{12}C: 21 x 0 = 0
[M+H+1]: ^{12}C: 20 x 0 = 0 ^{13}C: 1 x 0.0 = 0.0
[M+H+2]: ^{12}C: 19 x 99.5 = 1890.5 ^{13}C: 2 x 99.5 = 199
[M+H+3]: ^{12}C: 18 x 0.0 = 0 ^{13}C: 3 x 0.0 = 0
[M+H+4]: ^{12}C: 17 x 0.5 = 8.5 ^{13}C: 4 x 0.5 = 2

total ^{12}C: 1899   total ^{13}C: 201
Notoamide J from incorporation experiments ^{13}C content: 201/(1899 + 201) x 100% = 9.6%

Percent incorporation of intact doubly ^{13}C-labeled 6-OH-DBE = 9.6% - 1.2% = 8.4%

Percent Incorporation of stephacidin A into notoamide B:
Native Notoamide B ($C_{26}H_{31}N_3O_3$)
[M+H] (448.22.): 73.8%
[M+H+1] (449.22): 21.93%
[M+H+2] (450.21): 3.75%
[M+H+3] (451.21): 0.47%
[M+H+4] (452.20): 0.05%

^{13}C Notoamide B from incorporation experiments:
[M+H] (450.20): 49.2%
[M+H+1] (451.20): 0.1%
[M+H+2] (452.19): 50.5%
[M+H+3] (453.19): 0.0%
[M+H+4] (454.18): 0.0%

Calculation of Native Notoamide B: (assume 100 molecules)
[M+H]: ^{12}C: 26 x 73.8 = 1918.8
[M+H+1]: ^{12}C: 25 x 21.93 = 548.25 ^{13}C: 1 x 21.93 = 21.93
[M+H+2]: ^{12}C: 24 x 3.75 = 90.0 ^{13}C: 2 x 3.75 = 7.5
[M+H+3]: ^{12}C: 23 x 0.47 = 10.81 ^{13}C: 3 x 0.47 = 1.41
[M+H+4]: ^{12}C: 22 x 0.05 = 1.1 ^{13}C: 4 x 0.05 = 0.2

total ^{12}C: 2568.96   total ^{13}C: 31.04

Native Notoamide B ^{13}C content: 31.04/(2568.96 +31.04) x 100% = 1.2%

Calculation for ^{13}C Notoamide B from incorporation experiments: (assume 100 molecules)

[M+H]: ^{12}C: 26 x 49.2 = 1279.2
[M+H+1]: ^{12}C: 25 x 0.1 = 2.5 ^{13}C: 1 x 0.1 = 0.1
[M+H+2]: ^{12}C: 24 x 50.5 = 1212 ^{13}C: 2 x 50.5 = 101
[M+H+3]: ^{12}C: 23 x 0.0 = 0 ^{13}C: 3 x 0.0 = 0
[M+H+4]: ^{12}C: 22 x 0.0 = 0 ^{13}C: 4 x 0.0 = 0

total ^{12}C: 2493.7   total ^{13}C: 101.1

Notoamide B from incorporation experiments ^{13}C content: 101.1/(2493.7 + 101.1) x 100% = 3.9%

Percent incorporation of intact doubly ^{13}C-labeled Stephacidin A = 3.9% - 1.2% = 2.7%

Percent Incorporation of notoamide S into notoamide D:
Native Notoamide D ($C_{26}H_{31}N_3O_3$)
[M+H] (450.23): 73.78%
[M+H+1] (451.23): 21.94%
[M+H+2] (452.24): 3.76%
[M+H+3] (453.25): 0.47%
[M+H+4] (454.25): 0.05%

^{13}C Notoamide D from incorporation experiments:
[M+H] (450.23): 1.3%
[M+H+1] (451.23): 3.9%
[M+H+2] (452.24): 94.8%
[M+H+3] (453.25): 0.0%
[M+H+4] (454.25): 0.0%

Calculation of Native Notoamide D: (assume 100 molecules)
[M+H]: ^{12}C: 26 x 73.78 = 1918.28
[M+H+1]: ^{12}C: 25 x 21.94 = 548.5 ^{13}C: 1 x 21.94 = 21.94
[M+H+2]: ^{12}C: 24 x 3.76 = 90.24 ^{13}C: 2 x 3.76 = 7.52
[M+H+3]: ^{12}C: 23 x 0.47 = 10.81 ^{13}C: 3 x 0.47 = 1.41
[M+H+4]: ^{12}C: 22 x 0.05 = 1.1 ^{13}C: 4 x 0.05 = 0.2

total ^{12}C: 2568.93   total ^{13}C: 31.07

Native Notoamide D ^{13}C content: 31.07/(2568.93 +31.07) x 100% = 1.2%

Calculation for ^{13}C Notoamide D from incorporation experiments: (assume 100 molecules)

[M+H]: ^{12}C: 26 x 1.3 = 33.8
[M+H+1]: ^{12}C: 25 x 3.9 = 97.5 ^{13}C: 1 x 3.9 = 3.9
[M+H+2]: ^{12}C: 24 x 94.8 = 2275.2 ^{13}C: 2 x 94.8 = 189.6
[M+H+3]: ^{12}C: 23 x 0.0 = 0 ^{13}C: 3 x 0.0 = 0
[M+H+4]: ^{12}C: 22 x 0.0 = 0 ^{13}C: 4 x 0.0 = 0

total ^{12}C: 2406.5   total ^{13}C: 193.5

Notoamide D from incorporation experiments ^{13}C content: 194.4/(2413.4 + 194.4) x 100% = 7.4%

Percent incorporation of intact doubly ^{13}C-labeled Notoamide S = 7.4% - 1.2% = 6.2%

Percent Incorporation of notoamide S into notoamide C:
Native Notoamide C ($C_{26}H_{31}N_3O_3$)
[M+H] (450.23): 73.78%
[M+H+1] (451.23): 21.94%
[M+H+2] (452.24): 3.76%
[M+H+3] (453.25): 0.47%
[M+H+4] (454.25): 0.05%

^{13}C Notoamide C from incorporation experiments:
[M+H] (450.25): 0.0%
[M+H+1] (451.): 4.7%
[M+H+2] (452.25): 94.5%
[M+H+3] (453.): 0.0%
[M+H+4] (454.): 0.8%

Calculation of Native Notoamide C: (assume 100 molecules)
[M+H]: ^{12}C: 26 x 73.78 = 1918.28
[M+H+1]: ^{12}C: 25 x 21.94 = 548.5 ^{13}C: 1 x 21.94 = 21.94
[M+H+2]: ^{12}C: 24 x 3.76 = 90.24 ^{13}C: 2 x 3.76 = 7.52
[M+H+3]: ^{12}C: 23 x 0.47 = 10.81 ^{13}C: 3 x 0.47 = 1.41
[M+H+4]: ^{12}C: 22 x 0.05 = 1.1 ^{13}C: 4 x 0.05 = 0.2

total ^{12}C: 2568.93   total ^{13}C: 31.07

Native Notoamide C ^{13}C content: 31.07/(2568.93 + 31.07) x 100% = 1.2%

Calculation for ^{13}C Notoamide C from incorporation experiments: (assume 100 molecules)

[M+H]: ^{12}C: 26 x 0.0 = 0.0
[M+H+1]: ^{12}C: 25 x 4.7 =117.5 ^{13}C: 1 x 4.7 = 4.7
[M+H+2]: ^{12}C: 24 x 94.5 = 2268.0 ^{13}C: 2 x 94.5 = 189.0
[M+H+3]: ^{12}C: 23 x 0.0 = 0.0 ^{13}C: 3 x 0.0 = 0.0
[M+H+4]: ^{12}C: 22 x 0.8 = 17.6 ^{13}C: 4 x 0.8 = 3.2

total ^{12}C: 2403.1   total ^{13}C: 196.9

Notoamide C from incorporation experiments ^{13}C content: 196.9/(2403.1 + 196.9) x 100% = 7.6%

Percent incorporation of intact doubly ^{13}C-labeled Notoamide S = 7.6%- 1.2% = 6.4

Percent Incorporation of notoamide S into notoamide B:
Native Notoamide B ($C_{26}H_{29}N_3O_4$)
[M+H] (448.22.): 73.8%
[M+H+1] (449.22): 21.93%
[M+H+2] (450.21): 3.75%
[M+H+3] (451.21): 0.47%
[M+H+4] (452.20): 0.05%

^{13}C Notoamide B from incorporation experiments:
[M+H] (450.20): 0.0%
[M+H+1] (451.20): 3.4%
[M+H+2] (452.19): 96.9%
[M+H+3] (453.19): 0.0%
[M+H+4] (454.18): 0.0%

Calculation of Native Notoamide B: (assume 100 molecules)
[M+H]: ^{12}C: 26 x 73.8 = 1918.8
[M+H+1]: ^{12}C: 25 x 21.93 = 548.25 ^{13}C: 1 x 21.93 = 21.93
[M+H+2]: ^{12}C: 24 x 3.75 = 90.0 ^{13}C: 2 x 3.75 = 7.5
[M+H+3]: ^{12}C: 23 x 0.47 = 10.81 ^{13}C: 3 x 0.47 = 1.41
[M+H+4]: ^{12}C: 22 x 0.05 = 1.1 ^{13}C: 4 x 0.05 = 0.2

total ^{12}C: 2568.96   total ^{13}C: 31.04

Native Notoamide B ^{13}C content: 31.04/(2568.96 +31.04) x 100% = 1.2%

Calculation for ^{13}C Notoamide B from incorporation experiments: (assume 100 molecules)

[M+H]: ^{12}C: 26 x 0.0 = 0.0
[M+H+1]: ^{12}C: 25 x 3.4 = 85.0 ^{13}C: 1 x 3.4 = 3.4
[M+H+2]: ^{12}C: 24 x 96.9 = 2325.6 ^{13}C: 2 x 96.9 = 193.8
[M+H+3]: ^{12}C: 23 x 0.0 = 0 ^{13}C: 3 x 0.0 = 0
[M+H+4]: ^{12}C: 22 x 0.0 = 0 ^{13}C: 4 x 0.0 = 0

total ^{12}C: 2410.6   total ^{13}C: 197.2

Notoamide B from incorporation experiments ^{13}C content: 197.2/(2410.6 + 197.2) x 100% = 7.6%

Percent incorporation of intact doubly ^{13}C-labeled Notoamide S = 7.6% - 1.2% = 6.4%

Percent Incorporation of notoamide S into stephacidin A:
Native Stephacidin A ($C_{26}H_{29}N_3O_3$)
[M+H] (432.22): 73.8%
[M+H+1] (433.22): 21.93%
[M+H+2] (434.23): 3.75%
[M+H+3] (435.23): 0.47%
[M+H+4] (436.24): 0.05%

^{13}C Stephacidin A from incorporation experiments:
[M+H] (432.22): 0.0%
[M+H+1] (433.22): 10.0%
[M+H+2] (434.23): 88.3%
[M+H+3] (435.23): 0.0%
[M+H+4] (436.24): 1.7%

Calculation of Native Stephacidin A: (assume 100 molecules)
[M+H]: ^{12}C: 26 x 73.8 = 1918.8
[M+H+1]: ^{12}C: 25 x 21.93 = 548.25 ^{13}C: 1 x 21.93 = 21.93
[M+H+2]: ^{12}C: 24 x 3.75 = 90.0 ^{13}C: 2 x 3.75 = 7.5
[M+H+3]: ^{12}C: 23 x 0.47 = 10.81 ^{13}C: 3 x 0.47 = 1.41
[M+H+4]: ^{12}C: 22 x 0.05 = 1.1 ^{13}C: 4 x 0.05 = 0.2

total ^{12}C: 2568.96   total ^{13}C: 31.04

Native Stephacidin A ^{13}C content: 31.04/(2568.96 +31.04) x 100% = 1.2%

Calculation for ^{13}C Stephacidin A from incorporation experiments: (assume 100 molecules)

[M+H]: ^{12}C: 26 x 0.0 = 0.0
[M+H+1]: ^{12}C: 25 x 10.0 = 250 ^{13}C: 1 x 10.0 = 10.0
[M+H+2]: ^{12}C: 24 x 88.3 = 2119.2 ^{13}C: 2 x 88.3 = 176.6
[M+H+3]: ^{12}C: 23 x 0.0 = 0 ^{13}C: 3 x 0.0 = 0
[M+H+4]: ^{12}C: 22 x 1.7 = 37.4 ^{13}C: 4 x 1.7 = 6.8

total ^{12}C: 2406.6   total ^{13}C: 193.4

Stephacidin A from incorporation experiments ^{13}C content: 193.4/(2406.6 + 193.4) x 100% = 7.4%

Percent incorporation of intact doubly ^{13}C-labeled Notoamide S = 7.4% - 1.2% = 6.2%

Percent Incorporation of notoamide S into versicolamide B:
Native Versicolamide B ($C_{26}H_{29}N_3O_4$)
[M+H] (448.22.): 73.8%
[M+H+1] (449.22): 21.93%
[M+H+2] (450.21): 3.75%
[M+H+3] (451.21): 0.47%
[M+H+4] (452.20): 0.05%

^{13}C Versicolamide B from incorporation experiments:
[M+H] (450.20): 0.0%
[M+H+1] (451.20): 0.0%
[M+H+2] (452.19): 99.7%
[M+H+3] (453.19): 0.0%
[M+H+4] (454.18): 0.3%

Calculation of Native Versicolamide B: (assume 100 molecules)
[M+H]: ^{12}C: 26 x 73.8 = 1918.8
[M+H+1]: ^{12}C: 25 x 21.93 = 548.25 ^{13}C: 1 x 21.93 = 21.93
[M+H+2]: ^{12}C: 24 x 3.75 = 90.0 ^{13}C: 2 x 3.75 = 7.5
[M+H+3]: ^{12}C: 23 x 0.47 = 10.81 ^{13}C: 3 x 0.47 = 1.41
[M+H+4]: ^{12}C: 22 x 0.05 = 1.1 ^{13}C: 4 x 0.05 = 0.2

total ^{12}C: 2568.96   total ^{13}C: 31.04

Native Versicolamide B ^{13}C content: 31.04/(2568.96 +31.04) x 100% = 1.2%

Calculation for ^{13}C Versicolamide B from incorporation experiments: (assume 100 molecules)

[M+H]: ^{12}C: 26 x 0.0 = 0.0
[M+H+1]: ^{12}C: 25 x 0.0 = 0.0 ^{13}C: 1 x 0.0 = 0.0
[M+H+2]: ^{12}C: 24 x 99.7 = 2392.8 ^{13}C: 2 x 99.7 = 199.4
[M+H+3]: ^{12}C: 23 x 0.0 = 0 ^{13}C: 3 x 0.0 = 0
[M+H+4]: ^{12}C: 22 x 0.3 = 6.6 ^{13}C: 4 x 0.3 = 1.2

total ^{12}C: 2399.4   total ^{13}C: 200.6

Versicolamide B from incorporation experiments ^{13}C content: 200.6/(2399.4 + 200.6) x 100% = 7.7%

Percent incorporation of intact doubly ^{13}C-labeled Notoamide S = 7.7% - 1.2% = 6.5%

References and Footnotes

1. Birch, A. J.; Wright, J. J., The Brevianamides: a New Class of Fungal Alkaloid. *J. Chem. Soc., Chem. Commun.* **1969**, 644-645.

2. Birch, A. J.; Wright, J. J., Studies in Relation to Biosynthesis-42. Structural Elucidation and Some Aspects of Biosynthesis of Brevianamide-A and Brevianamide-E. *Tetrahedron* **1970**, *26*, 2329-2344.

3. Birch, A. J.; Russel, R. A., Studies in Relation to Biosynthesis-44. Structural Elucidations of Brevianamide-B, Brevianamide-C, Brevianamide-D, and Brevianamide-F. *Tetrahedron* **1972**, *28*, 2999-3008.

4. Steyn, P. S., Austamide, A New Toxic Metabolite from *Aspergillus ustus*. *Tetrahedron Lett.* **1971**, *36*, 3331-3334.

5. Robbers, J. E.; Straus, J. W.; Tuite, J., The Isolation of Brevianamide A from *Penicillium ochraceum*. *J. Nat. Prod.* **1975**, *38*, 355-356.

6. Yamazaki, M.; Okuyama, E.; Kobayashi, M.; Inoue, H., The Structure of Paraherquamide, a Toxic Metabolite from *Penicillium paraherquei. Tetrahedron Lett.* **1981**, *22*, 135-136.

7. (a) Ondeyka, J. G.; Goegelman, R. T.; Schaeffer, J. M.; Kelemen, L.; Zitano, L., Novel Antinematodal and Antiparasitic Agents from *Penicillium charlesii. J. Antibiot.* **1990**, *43*, 1375-1379. (b) Goegelman, R.; Ondeyka, J. U.S. Patent 4,873,247.

8. Lopez-Gresa, M. P.; Gonzalez, M. C.; Ciavatta, L.; Ayala, I.; Moya, P.; Primo, J., Insecticidal Activity of Paraherquamides, Including Paraherquamide H and Paraherquamide I, Two New Alkaloids Isolated from *Penicillium cluniae*. *J. Agric. Food Chem.* **2006**, *54*, 2921-2925.

9. Blanchflower, S. E.; Bank, R. M.; Everett, J. R.; Reading, C., Further Novel Metabolites of the Paraherquamide Family. *J. Antibiot.* **1993**, *46*, 1355-1363.

10. Banks, R. M.; Blanchflower, S. E.; Everett, J. R.; Manger, B. R.; Reading, C., Novel Anthelmintic Metabolites from an *Aspergillus* Species; the Aspergillimides. *J. Antibiot.* **1997**, *50*, 840-846.

11. Blanchflower, S. E.; Banks, R. M.; Everett, J. R.; Manger, B. R.; Reading, C., New Paraherquamide Antibiotics with Anthelmintic Activity. *J. Antibiot.* **1991**, *44*, 492-497.

12. Liesch, J. M.; Wichmann, C. F., Novel Antinematodal and Antiparasitic Agents from *Penicillium charlesii*. II. Structure Determination of Paraherquamides B, C, D, E, F, and G. *J. Antibiot.* **1990**, *43*, 1380-1386.

13. Nielsen, K. F.; Sumarah, M. W.; Frisvad, J. C.; Miller, J. D., Production of Metabolites from the *Penicillium roqueforti* Complex. *J. Agric. Food Chem.* **2006**, *54*, 3756-3763.

14. Ding, Y.; Gruschow, S.; Greshock, T. J.; Finefield, J. M.; Sherman, D. H.; Williams, R. M., Detection of VM55599 and Preparaherquamide from *Aspergillus japonicus* and *Penicillium fellutanum*: Biosynthetic Implications. *J. Nat. Prod.* **2008**, *71*, 1574-1578.

15. Whyte, A. C.; Gloer, J. B.; Wicklow, D. T.; Dowd, P. F., Sclerotiamide: A New Member of the Paraherquamide Class with Potent Antiinsectan Activity from the Sclerotia of *Aspergillus sclerotiorum*. *J. Nat. Prod.* **1996**, *59*, 1093-1095.

16. (a) Qian-Cutrone, J.; Krampitz, K. D.; Shu, Y.-Z.; Chang, L.-P.; Lowe, S. E., US Patent 6,291,461. (b) Qian-Cutrone, J.; Huang, S.; Shu, Y.-Z.; Vydas, D.; Fairchild, C.; Menendez, A.; Krampitz, K.; Dalterio, R.; Klohr, S. E.; Gao, Q., Stephacidin A and B: Two Structurally Novel, Selective Inhibitors of the Testosterone-Dependent Prostate LNCaP Cells. *J. Am. Chem. Soc.* **2002**, *124*, 14556-14557.

17. Fenical, W.; Jensen, P. R.; Cheng, X. C., US Patent 6,066,635.

18. Sugie, Y.; Hirai, H.; Inagaki, T.; Ishiguro, M.; Kim, Y.-J.; Kojima, Y.; Sakakibara, T.; Sakemi, s.; Sugiura, A.; Suzuki, Y.; Brennan, L.; Duignan, J.; Huang, L. H.; Sutcliffe, J.; Kojima, N. J., A New Antibiotic CJ-17,665 from *Aspergillus ochraceus*. *J. Antibiot.* **2001**, *54*, 911-916.

19. Kato, H.; Yoshida, T.; Tokue, T.; Nojiri, Y.; Hirota, H.; Ohta, T.; Williams, R. M.; Tsukamoto, S., Notoamides A-D: Prenylated Indole Alkaloids Isolated from a Marine-Derived Fungus, *Aspergillus* sp. MF297-2 *Angew. Chem. Int. Ed.* **2007**, *46*, 2254-2256.

20. The structures of the norgeamides were published via the internet detailing the research performed by the Hans-Knöll Institute. www.hki-jena.de

21. Tsukamoto, S.; Kato, H.; Greshock, T. J.; Hirota, H.; Ohta, T.; Williams, R. M., Isolation of Notoamide E, a Key Precursor in the Biosynthesis of Prenylated

Indole Alkaloids in Marine-Derived Fungus, *Aspergillus* sp. MF297-2 *J. Am. Chem. Soc.* **2009**, *131*, 3834-3835.

22. Tsukamoto, S.; Kato, H.; Samizo, M.; Nojiri, Y.; Onuki, H.; Hirota, H.; Ohta, T., Notoamides F-K, Prenylated Indole Alkaloids Isolated from a Marine-Derived *Aspergillus* sp. MF297-2 *J. Nat. Prod.* **2008**, *71*, 2064-2067.

23. Tsukamoto, S.; Kawabata, T.; Kato, H.; Greshock, T. J.; Hirota, H.; Ohta, T.; Williams, R. M., Isolation of Antipodal (−)-Versicolamide B and Notoamides L-N from a Marine-Derived *Aspergillus* sp. MF297-2 *Org. Lett.* **2009**, *11*, 1297-1300.

24. Tsukamoto, S.; Umaoka, H.; Yoshikawa, K.; Ikeda, T.; Hirota, H., Notoamide O, a Structurally Unprecedented Prenylated Indole Alkaloid, and Notoamides P-R from a Marine-Derived Fungus, *Aspergillus* sp. MF297-2 *J. Nat. Prod.* **2010**, *73*, 1438-1440.

25. Greshock, T. J.; Grubbs, A. W.; Jiao, P.; Wicklow, D. T.; Gloer, J. B.; Williams, R. M., Isolation, Structure Elucidation, and Biomimetic Total Synthesis of Versicolamide B, and the Isolation of Antipodal (−)-Stephacidin A and (+)-Notoamide B from *Aspergillus versicolor* NRRL 35600. *Angew. Chem. Int. Ed.* **2008**, *47*, 3573-3577.

26. Williams, R. M.; Sanz-Cervera, J. F.; Stocking, E. M., Biosynthesis of Prenylated Indole Alkaloids Derived from Tryptophan. In *Topics in Current Chemistry, Volume on Biosynthesis-Terpenes and Alkaloids*; Lepper, F. Vederas, J. C., Eds.; Springer: Berlin, 2000; Vol. 209, pp 97-173.

27. (a) Stocking, E. M.; Sanz-Cervera, J. F.; Unkefer, C. J.; Williams, R. M., Studies on the Biosynthesis of Paraherquamide. Construction of the Amino Acid Framework. *Tetrahedron* **2001**, *57*, 5303. (b) Holmes, D. Post-doctoral report ETH **1990** (Argoni) and Kellenberger, J. L. Ph.D. Thesis, ETH **1997** (Arigoni). (c) Stocking, E. M.; Sanz-Cervera, J. F.; Williams, R. M.; Unkefer, C. J., Studies on the Biosynthesis of Paraherquamide: Origin of the β-Methyl Proline Ring. *J. Am. Chem. Soc.* **1996**, *118*, 7008-7009. (d) Stocking, E. M.; Martinez, R. A.; Silks, L. A.; Sanz-Cervera, J. F.; Williams, R. M., Studies on the Biosynthesis of Paraherquamide: Concerning the Mechanism of the Oxidative Cyclization of L-Isoleucine to β-Methyl Proline. *J. Am. Chem. Soc.* **2001**, *123*, 3391-3392.

28. Grubbs, A. W.; Artman (III), G. D.; Williams, R. M., Concise Syntheses of the 1,7-Dihydropyrano[2,3-*g*]indole Ring System of the Stephacidins, Aspergamides and Norgeamides. *Tetrahedron Lett.* **2005**, *46*, 9013-9016.

29. Grubbs, A. W.; Artman (III), G. D.; Tsukamoto, S.; Williams, R. M., A Concise Total Synthesis of the Notoamides C and D. *Angew. Chem. Int. Ed.* **2007**, *46*, 2257-2261.

30. Stocking, E. M.; Sanz-Cervera, J. F.; Williams, R. M., Studies on the Biosynthesis of Paraherquamide: Synthesis and Incorporation of a Hexacyclic Indole Derivative as an Advanced Metabolite. *Angew. Chem. Int. Ed.* **2001**, *40*, 1296-1298.

31. Stocking, E. M.; Sanz-Cervera, J. F.; Williams, R. M., Reverse versus Normal Prenyl Transferases in Paraherquamide Biosynthesis Exhibit Distinct Facial Selectivities. *Angew. Chem. Int. Ed.* **1999**, *38*, 786-789.

32. Stocking, E. M.; Williams, R. M.; Sanz-Cervera, J. F., Reverse Prenyl Transferases Exhibit Poor Facial Discrimination in the Biosynthesis of Paraherquamide A, Brevianamide A, and Austamide. *J. Am. Chem. Soc.* **2000**, *122*, 9089-9098.

33. Ding, Y.; de Wet, J. R.; Cavalcoli, J.; Li, S.; Greshock, T. J.; Miller, K. A.; Finefield, J. M.; Sunderhaus, J. D.; McAfoos, T. J.; Tsukamoto, S.; Williams, R. M.; Sherman, D. H., Genome-Based Characterization of Two Prenylation Steps in the Assembly of the Stephacidin and Notoamide Anticancer Agents in a Marine-Derived *Aspergillus* sp. MF297-2 *J. Am. Chem. Soc.* **2010**, *132*, 12733-12740.

34. Kumar, S. Multiple Myeloma-Current Issues and Controversies. *Cancer Treat. Rev.* **2010**, *36S2*, S3-S11.

35. Alexanian, R.; Dimopoulos, M. The Treatment of Multiple Myeloma. *New Engl. J. Med.* **1994**, *330*, 484-489.

36. Mahindra, A.; Hideshima, T.; Anderson, K. C., Multiple Myeloma: Biology of the Disease. *Blood Rev.* **2010**, *24 (Suppl. 1)*, S5-S11.

37. Rajkumar, S. V.; Dispenzieri, A.; Kyle, R. A., Monoclonal Gammopathy of Undertermined Significance, Waldenström Macroglobulinemia, AL Amyloidosis, and Related Plasma Cell Disorders: Diagnosis and Treatment. *Mayo Clin. Proc.* **2006**, *81*, 693-703.

38. Campbell, R. A.; Sanchez, E.; Steinberg, J.; Shalitin, D.; Li, Z.-W., Chen, H.; Berenson, J. R., Vorinostat Enhances the Antimyeloma Effects of Melphalan and Bortezomib. *Eur. J. Haematol.* **2009**, *84*, 201-211.

39. Barlogie, B.; Shaughnessy, J.; Tricot, G.; Jacobson, J.; Zangari, M.; Anaissie, E.; Walker, R.; Crowley, J., Treatment of Multiple Myeloma. *Blood* **2004**, *103*, 20-32 (and references therein).

40. Barlogie, B.; Epstein, J.; Selvanayagam, P.; Alexanian, R., Plasma Cell Myeloma—New Biological Insights and Advances in Therapy. *Blood* **1989**, *73*, 865-879.

41. Vescio, R. A.; Hong, C. H.; Cao, J.; Kim, A.; Schiller, G. J.; Lichtenstein, A. K.; Berenson, R. J.; Berenson, J. R., The Hematopoietic Stem Cell Antige, CD34, Is Not Expressed on the Malignant Cells in Multiple Myeloma. *Blood* **1994**, *84*, 3283-3290.

42. Berenson, J. R.; Li, Z.-W.; Shalitin D.; Leung, C.; Hu, C. M.; Shen, J.; Li, M.; Wang, C. S.; Steinberg, J.; Sanchez, E.; Chen, H.; Bonavida, B. Unpublished results.

43. Nakatani, K.; Sando, S.; Saito, I., Recognition of a Single Guanine Bulge by 2-Acylamino-1,8-naphthyridine. *J. Am. Chem. Soc.* **2000**, *122*, 2172-2177.

44. www.clinicaltrials.gov

45. Wilson, B. J.; Yang, D. T. C.; Harris, T. M., Production, Isolation, and Preliminary Toxicity Studies of Brevianamide A from Cultures of *Penicillium viridicatum*. *Appl. Microbiol.* **1973**, *26*, 633-635.

46. Wang, F.; Fang, Y.; Zhu, T.; Zhang, M.; Lin, A.; Gu, Q.; Zhu, W., Seven New Prenylated Indol Diketopiperazine Alkaloids from Holothurian-Derived Fungus *Aspergillus fumigatus*. *Tetrahedron* **2008**, *64*, 7986-7991.

47. Zhang, D.; Noviendri, D.; Nursid, M.; Yang, X.; Son, B. W., 12,13-Dihydroxyfumitremorgin C, Fumitremorgin C, and Brevianamide F, Antibacterial Diketopiperazine Alkaloids from the Marine-Derived Fungus *Pseudallescheria* sp. *Nat. Prod. Sci.* **2007**, *13*, 251-254.

48. Williams, R. M.; Cox, R. J., Paraherquamides, Brevianamides, and Asperparalines: Laboratory Synthesis and Biosynthesis. An Interim Report. *Acc. Chem. Res.* **2003**, *36*, 127-139.

49. Sanz-Cervera, J. F.; Glinka, T.; Williams, R. M., Biosynthesis of Brevianamides A and B: In Search of the Biosynthetic Diels-Alder Construction. *Tetrahedron* **1993**, *49*, 8471-8482 (and references therein).

50. Byung, H. L.; Clothier, M. F.; Dutton, F. E.; Nelson, S. J.; Johnson, S. S.; Thompson, D. P.; Geary, T. G.; Whaley, H. D.; Haber, C. L.; Marshall, V. P.; Kornis, G. I.; McNally, P. L.; Ciadella, J. I.; Martin, D. G.; Bowman, J. W.; Baker, C. A.; Coscarelli, E. M.; Alexander-Bowman, S. J.; Davis, J. P.; Zinser, E. W.; Wiley, V.; Lipton, M. F.; Mauragis, M. A., Marcfortine and Paraherquamide Class of Anthelmintics: Discovery of PNU-141962. *Curr. Top. Med. Chem.* **2002,** *2*, 779-793.

51. Ostlind, D. A.; Mickle, W. G.; Ewanciw, D. V.; Andriuli, F. J.; Campbell, W. C.; Hernandez, S.; Mochales, S.; Munguira, E., Efficacy of Paraherquamide Against Immature *Trichostrongylus colubriformis* in the Gerbil (*Meriones unguiculatus*). *Res. Vet. Sci.* **1990**, *48*, 260-261.

52. Zinser, E. W.; Wolfe, M. L.; Alexander-Bowman, S. J.; Thomas, E. M.; Davis, J. P.; Groppi, V. E.; Lee, B. H.; Thomphson, D. P.; Geary, T. G., Anthelmintic

Paraherquamides Are Cholinergic Antagonists in Gastrointestinal Nematodes and Mammals. *J. Vet. Pharmacol. Therap.* **2002**, *25*, 241-250.

53. Shoop, W. L.; Haines, H. W.; Eary, C. H.; Michael, B. F., Acute Toxicity of Paraherquamide as an Anthelmintic. *Am. J. Vet. Res.* **1992**, *53*, 2032-2034.

54. McKellar, Q. A.; Jackson, F., Veterinary Anthelmintics: Old and New. *Trends Parasitol.* **2004**, *20*, 456-461.

55. Herzon, S. B.; Myers, A. G., Enantioselective Synthesis of Stephacidin B. *J. Am. Chem. Soc.* **2005**, *127*, 5342-5344.

56. Baran, P. S.; Hafensteiner, B. D.; Ambhaikar, N. B.; Guerrero, C. A.; Gallagher, J. D., Enantioselective Total Synthesis of Avrainvillamide and the Stephacidins. *J. Am. Chem. Soc.* **2006**, *128*, 8678-8693.

57. Artman, G. D.; Grubbs, A. W.; Williams, R. M., Concise, Asymmetric, Stereocontrolled Total Synthesis of Stephacidins A, B and Notoamide B. *J. Am. Chem. Soc.* **2007**, *129*, 6336-6342.

58. McAfoos, T. J.; Li, S.; Tsukamoto, S.; Sherman, D. H.; Williams, R. M., Studies on the Biosynthesis of the Stephacidins and Notoamides. Total Synthesis of Notoamide S. *Heterocycles* **2010**, *82*, 461-472.

59. McAfoos, T. J.; Sunderhaus, J. D., Finefield, J. M.; Williams, R. M., unpublished results.

60. Hayashi, H.; Nishimoto, Y.; Nozaki, H., Asperparaline A, a New Paralytic Alkaloid from *Aspergillus japonicus* JV-23. *Tetrahedron Lett.* **1997**, *38*, 5655-5658.

61. Hayashi, H.; Nishimoto, Y.; Akiyama, K.; Nozaki, H., New Paralytic Alkaloids, Asperparaline A, B and C, from *Aspergillus japonicus* JV-23. *Biosci. Biotechnol. Biochem.* **2000**, *64*, 111-115.

62. Banks, R. M.; Blanchflower, S. E.; Everett, J. R.; Manger, B. R.; Reading, C. Novel Anthelmintic Metabolites from an *Aspergillus* Species; the Aspergillimides. *J. Antibiot.* **1997**, *50*, 840-846.

63. Williams, R. M.; Cox, R. J., Paraherquamides, Brevianamides, and Asperparalines: Laboratory Synthesis and Biosynthesis. An Interim Report. *Acc. Chem. Res.* **2003**, *36*, 127-139.

64. (a) Steyn, P. S., The Structures of Five Diketopiperazines from *Aspergillus ustus*. *Tetrahedron*, **1973**, *29*, 107-120. (b) Steyn, P. S.; Vleggaar, R., 12,13-Dihydro-12-hydroxyaustamide, a New Dioxopiperazine from *Aspergillus ustus*. *Phytochemistry* **1976**, *15*, 355-356.

65. Marínez-Luis, S.; Rodrígues, R.; Acevedo, L.; Gonzáles, M. C.; Lira-Rocha, A.; Mata, R., Malbrancheamide, a New Calmodulin Inhibitor from the Fungus *Malbranchea aurantiaca*. *Tetrahedron* **2006**, *62*, 1817-1822.

66. Capon, R. J.; Skene, C.; Stewart, M.; Ford, J.; O'Hair, R. A. J.; Williams, L.; Lacey, E.; Gill, J. H.; Heiland, K., Aspergillicins A-E: Five Novel Depsipeptides from the Marine-Derived Fungus *Aspergillus carneus*. *Org. Biomol. Chem.* **2003**, *1*, 1856-1862.

67. (a) Nielsen, K. F.; Sumarah, M. W.; Frisvad, J. C.; Miller, J. D., Production of Metabolites from the *Penicillium roqueforti* Complex. *J. Agric. Food Chem.* **2006**, *54*, 3756-3763. (b) O'Brien, M.; Nielsen, K. F.; O'Kiely, P.; Forristal, P.

D.; Fuller, H. T.; Frisvad, J. C., Mycotoxins and Other Secondary Metabolites Produced in Vitro by *Penicillium paneum* Frisvad and *Penicillium roqueforti* Thom Isolated from Baled Grass Silage in Ireland. *J. Agric. Food Chem.* **2006**, *54*, 9268-9276.

68. (a) Polonsky, J. Merrien, M.-A.; Prangé, T.; Pascard, C.; Moreau, S., Isolation and Structure (X-Ray Analysis) of Marcfortine A, a New Alkaloid from *Penicillium roqueforti*. *J. Chem. Soc., Chem. Commun.* **1980**, 601-602. (b) Prangé, T.; Billion, M.-A.; Vuilhorgen, M.; Pascard, C.; Polonsky, J., Structures of Marcfortine B and C (X-Ray Analysis), Alkaloids from *Penicillium roqueforti*. *Tetrahedron Lett.*, **1981**, *22*, 1977-1980.

69. Lin, Z.; Wen, J.; Zhu, T.; Fang, Y.; Gu, Q.; Zhu, W., Chrysogenamide A from an Endophytic Fungus Associated with *Cistanche deserticola* and Its Neuroprotective Effect on SH-SY5Y Cells. *J. Antibiot.* **2008**, *61*, 81-85.

70. Baldas, J.; Birch, A. J.; Russell, R. A., Studies in Relation to Biosynthesis. Part XLVI. Incorporation of Cyclo-L-Tryptophyl-L-Proline. *J. Chem. Soc. Perkin Trans I* **1974**, 50-52.

71. Sanz-Cervera, J. F.; Glinka, T.; Williams, R. M., Biosynthesis of Brevianamides A and B: In Search of the Biosynthetic Diels-Alder Construction. *Tetrahedron* **1993**, *49*, 8471-8482.

72. Stocking, E. M; Williams, R. M., Chemistry and Biology of Biosynthetic Diels-Alder Reactions. *Angew. Chem. Int. Ed.* **2003**, *42*, 3078-3115.

73. Gray, C. R.; Sanz-Cervera, J. F.; Silks, L. A.; Williams, R. M., Studies on the Biosynthesis of Asperparaline A: Origin of the Spirosuccinimide Ring System. *J. Am. Chem. Soc.* **2003**, *125*, 14692-14693.

74. Kuo, M. S.; Wiley, V. H.; Cialdella, J. I.; Yurek, D. A.; Whaley, H. A.; Marshall, V. P., Biosynthesis of Marcfortine A. *J. Antibiot.* **1990**, *49*, 1006-1013.

75. Miller, K. A.; Williams, R. M., Synthetic Approaches to the Bicyclo[2.2.2]diazaoctane Ring System Common to the Paraherquamides, Stephacidins, and Related Prenylated Indole Alkaloids. *Chem. Soc. Rev.* **2009**, *38*, 3160-3174.

76. (a) Porter, A. E. A.; Sammes, P. G., A Diels-Alder Reaction of Possible Biosynthetic Importance. *Chem. Commun.* **1970**, 1103. (b) Williams, R. M., Total Synthesis and Biosynthesis of the Paraherquamides: An Intriguing Story of the Biological Diels-Alder Construction. *Chem. Pharm. Bull*. **2002**, *50*, 711-740.

77. (a) Williams, R. M.; Sanz-Cervera, J. F.; Sancenón, F.; Marco, J. A.; Halligan, K., Biomimetic Diels-Alder Cyclizations for the Construction of the Brevianamide, Paraherquamide Sclerotamide, and VM55599 Ring Systems. *J. Am. Chem. Soc.* **1998**, *120*, 1090-1091. (b) Williams, R. M.; Sanz-Cervera, J. F.; Sancenón, F.; Marco, J. A.; Halligan, K., Biomimetic Diels-Alder Cyclizations for the Construction of the Brevianamide, Paraherquamide, Sclerotamide, and VM55599 Ring Systems. *Bioorg. Med. Chem.* **1998**, *6*, 1233-1241.

78. Greshock, T. J.; Grubbs, A. W.; Tsukamoto, S.; Williams, R. M., A Concise Biomimetic Total Synthesis of Stephacidin A and Notoamide B. *Angew. Chem. Int. Ed.* **2007**, *46*, 2262-2265.

79. Greshock, T.J.; Williams, R. M., Improved Biomimetic Total Synthesis of *d,l*-Stephacidin A. *Org. Lett.* **2007**, *9*, 4255-4258.

80. This transformation was previously employed in the biomimetic total synthesis of marcfortine C, which contains a pipecolic acid moiety as opposed to the proline ring. Greshock, T. J.; Grubbs, A. W.; Williams, R. M., Concise, Biomimetic Total Synthesis of *d,l*-Marcfortine C. *Tetrahedron* **2007**, *63*, 6124-6130.

81. Miller, K. A.; Tsukamoto, S.; Williams, R. M., Asymmetric Total Syntheses of (+)- and (−)-Versicolamide B and Biosynthetic Implications. *Nature Chem*. **2009**, *1*, 63-68.

82. Domingo, L. R.; Zaragoza, R. J.; Williams, R. M., Studies on the Biosynthesis of Paraherquamide A and VM99955. A Theoretical Study of Intramolecular Diels-Alder Cycloaddition. *J. Org. Chem.* **2003**, *68*, 2895-2902.

83. Williams, R. M.; Glinka, T.; Kwast, E., Facial Selectivity of the Intramolecular S_N2' Cyclization: Stereocontrolled Total Synthesis of Brevianamide B. *J. Am. Chem. Soc.* **1988**, *110*, 5927-5929.

84. Stocking, E. M.; Sanz-Cervera, J. F.; Williams, R. M., Total Synthesis of VM55599. Utilization of an Intramolecular Diels-Alder Cycloaddition of Potential Biogenetic Relevance. *J. Am. Chem. Soc.* **2000**, *122*, 1675-1683.

85. Schkeryantz, J. M.; Woo, J. C. G.; Siliphaivanh, P.; Depew, K. M.; Danishefsky, S. J., Total Synthesis of Gypsetin, Deoxybrevianamide E, Brevianamide E, and Tryprostatin B: Novel Constructions of 2,3-Disubstituted Indoles. *J. Am. Chem. Soc.* **1999**, *121*, 11964-11975.

86. (a) Somei, M.; Karasawa, Y.; Kaneko, C., Selective Monoalkylation of Carbon Nucleophiles with Gramine. *Heterocycles* **1981**, *16*, 941-949. (b) Kametani, T.; Kanaya, N.; Ihara, M. *J. Chem. Soc., Perkin Trans. 1* **1981**, 959.

87. Haddad, M.; Larcheveque, M., Chemoenzymatic Synthesis of *N*-Boc Protected (2*S*,3*R*)-3-Hydroxy-3-Methylproline. *Tetrahedron: Asymmetry* **2005**, *16*, 2243-2247.

88. K. Sommer, unpublished results.

89. Sommer, K.; Williams, R. M., Synthetic Studies Toward Paraherquamides E and F and Related ^{13}C-labeled Putative Biosynthetic Intermediates: Stereocontrolled Synthesis of the α-Alkyl-β-Methylproline Ring System. *Tetrahedron* **2008**, *64*, 7106-7111.

90. Denes, F.; Perez-Luna, A.; Chemla, F., Diastereocontrolled Synthesis of Enantioenriched 3,4-Disubstituted β-Proline. *J. Org. Chem.* **2007**, *72*, 398.

91. Batcho, A. D.; Leimgruber, W. *Org. Synth.* **1985**, *63*, 214.

92. Akao, A.; Nonoyama, N.; Mase, T.; Yasuda, N., Development of Large-Scale Preparations of Indole Derivatives: Evaluation of Potential Thermal Hazards and Studies of Reaction Kinetics and Mechanisms. *Org. Process Res. Dev.* **2006**, *10*, 1178-1183.

93. Ohkubo, M.; Nishimura, T.; Jona, H.; Honma, T.; Morishima, H., Practical Synthesis of Indolopyrralocarbazoles. *Tetrahedron* **1996**, *52*, 8099-8112.

94. Harada, H.; Fujii, A.; Kato, S., An Efficient and Practical Synthesis of *N,N*-Diethyl-7-indolyloxyacetamide via 7-Hydroxyindole. *Synth. Commun.* **2003**, *33*, 507-514.

95. Finefield, J. M.; Williams, R. M., Synthesis of Notoamide J: A Potentially Pivotal Intermediate in the Biosynthesis of Several Prenylated Indole Alkaloids. *J. Org. Chem.* **2010**, *75*, 2785-2789.

96. Finefield, J. M.; Greshock, T. J.; Sherman, D. H.; Tsukamoto, S.; Williams, R. M., Notoamide E: Biosynthetic Incorporation into Notoamides C and D in Cultures of *Aspergillus versicolor* NRRL 35600. *Tetrahedron Lett.* **2011**, *52*, 1987-1989.

97. Maiya, S.; Grundmann, A.; Li, S. M.; Turner, G., The Fumitremorgin Gene Cluster of *Aspergillus fumigatus*: Identification of a Gene Encoding Brevianamide F Synthetase. *ChemBioChem* **2006**, *7*, 1062-1069.

98. Meyers, D. M.; Obrian, G.; Du, W. L.; Bhatnagar, D.; Payne, G. A., Characterizaiton of *aflJ*, a Gene Required for Conversion of Pathway Intermediates to Aflatoxin. *Appl. Environ. Microbiol.* **1998**, *64*, 3713-3717.

99. Woloshuk, C. P.; Foutz, K. R.; Brewer, J. F.; Bhatnagar, D.; Cleveland, T. E.; Payne, G. A., Molecular Characterization of *aflR*, a Regulatory Locus for Aflatoxin Biosynthesis. *Appl. Environ. Microbiol.* **1994**, *60*, 2408-2414.

100. Grundmann, A.; Li, S.-M., Overproduction, Purification and Characterization of FtmPT1, a Brevianamide F Prenyltransferase from *Aspergillus fumigatus. Microbiology* **2005**, *151*, 2199-2207.

101. Grundmann, A.; Kuznetsova, T.; Afiyatullov, S.; Li, S. M., FtmPT2, an N-Prenyltransferase from *Aspergillus fumigatus*, Catalyzes the Last Step in the Biosynthesis of Fumitremorgin B. *ChemBioChem* **2008**, *9*, 2059-2063.

102. Ding, Y.; Greshock, T. J.; Miller, K. A.; Sherman, D. H.; Williams, R. M., Premalbrancheamide: Synthesis, Isotopic Labeling, Biosynthetic Incorporation, and Detection in Cultures of *Malbranchea aurantiaca*. *Org. Lett.* **2008**, *10*, 4863-4866.

103. Calculated according to the method outlined in: Lambert, J. B.; Shurvell, H. B.; Lightner, D. A.; Cooks, R. G. *Organic Structural Spectroscopy*; Prentice Hall: Upper Saddle River, NJ, 1998; pp 447-448.

104. Li, S.; Sherman, D. H., Unpublished Results.

105. Zazopoulos, E.; Lalli, E.; Stocco, D. M.; Sassone-Corsi, P., DNA Binding and Transcriptional Repression by DAX-1 Blocks Steroidogenesis. *Nature* **1997**, *390*, 311-315.

106. Froelich-Ammon, S. J.; Gale, K. C.; Osheroff, N., Site-Specific Cleavage of a DNA Hairpin by Topoisomerase II. *J. Biol. Chem.* **1994**, *269*, 7719-7725.

107. Trinh, T. Q.; Sinden, R. R., The Influence of Primary and Secondary DNA Structure in Deletion and Duplication Between Direct Repeats in *Escherichia coli*. *Genetics* **1993**, *134*, 409-422.

108. Bonnet, G.; Krichevsky, O.; Libchaber, A., Kinetics of Conformational Fluctuations in DNA Hairpin-Loops. *Proc. Natl. Acad. Sci. USA* **1998**, *95*, 8602-8606.

109. Tyagi, S.; Kramer, F. R., Beacons of Light, *Nature Biotechnology* **1996**, *14*, 303-308.

110. Barlogie, B.; Epstein, J.; Selvanayagam, P.; Alexanian, R., Plasma Cell Myeloma—New Biological Insights and Advances in Therapy. *Blood* **1989**, *73*, 865-879.

111. Vescio, R. A.; Hong, C. H.; Cao, J.; Kim, A.; Schiller, G. J.; Lichtenstein, A. K.; Berenson, R. J.; Berenson, J. R. The Hematopoietic Stem Cell Antigen, CD34, is not Expressed on the Malignant Cells in Multiple Myeloma. *Blood* **1994**, *84*, 3283-3290.

112. Brown, E. V., 1,8-Naphthyridines. I. Derivatives of 2- and 4-Methyl-1,8-naphthyridines. *J. Org. Chem.* **1965**, *30,* 1607-1610.

113. Gediya, L. K.; Chopra, P.; Purushottamachar, P.; Maheshwari, N.; Njar, V. C. O., A New Simple and High-Yield Synthesis of Suberoylanilide Hydroxamic Acid and Its Inhibitory Effect Alone or in Combination with Retinoids on Proliferation of Human Prostate Cancer Cells. *J. Med. Chem.* **2005**, *48*, 5047-5051.

114. (a) Chen, Y.; Lopez-Sanchez, M.; Savoy, D. N.; Billadeau, D. D.; Dow, G. S.; Kozikowski, A. P., A Series of Potent and Selective, Triazolylphenyl-Based Histone Deacetylases Inhibitors with Activity against Pancreatic Cancer Cells and *Plasmodium falciparum. J. Med. Chem.* **2008**, *51*, 3437-3448. (b) Charrier, C.; Roche, J.; Gesson, J.-P.; Bertrand, P., Antiproliferative Activities of a Library of Hybrids Between Indanones and HDAC Inhibitor SAHA and MS-275 Analogues. *Bioorg. Med. Chem. Lett.* **2007**, *17,* 6124-6146.

115. Berenson, J. R.; Li, Z.-W.; Finefield, J. M.; Williams, R. M.; Shalitin D.; Leung, C.; Hu, C. M.; Shen, J.; Li, M.; Wang, C. S.; Steinberg, J.; Sanchez, E.; Chen, H.; Bonavida, B., Unpublished results.

Appendix 1: Publications

Detection of VM55599 and Preparaherquamide from *Aspergillus japonicus* and *Penicillium fellutanum*: Biosynthetic Implications

Yousong Ding,[†] Sabine Gruschow,[†] Thomas J. Greshock,[‡] Jennifer M. Finefield,[‡] David H. Sherman,*[,†] and Robert M. Williams*[,‡,§]

Life Sciences Institute and Department of Medicinal Chemistry, The University of Michigan, 210 Washtenaw Avenue, Ann Arbor, Michigan 48109-2216, Department of Chemistry, Colorado State University, Fort Collins, Colorado 80523, and University of Colorado Cancer Center, Aurora, Colorado 80045

The secondary metabolites VM55599 (**4**) and preparaherquamide (**5**) have been identified by LC-MS[n] analysis as natural metabolites in cultures of *Penicillium fellutanum*, whereas preparaherquamide has been identified only in cultures of *Aspergillus japonicus*. In accord with a previous proposal, the identification of both metabolites, which have a diastereomeric relationship, provides indirect support for a unified biosynthetic scheme.

The paraherquamides (**6**),[1] together with the asperparalines (**7**),[2] stephacidins,[3] brevianamides,[4] marcfortines,[5] notoamides,[6] sclerotamide,[7] and malbrancheamides,[8] are secondary metabolites derived from fungi that feature a common bicyclo[2.2.2]diazaoctane core. It has been postulated that this ring system is generated through an intramolecular Diels−Alder cycloaddition of the C_5 moiety across the α-carbons of the amino acid subunits, as depicted in Scheme 1.[9]

Members of this unique family of metabolites are all derived from tryptophan, isoprene units of mevalonate origin, and a cyclic amino acid residue consisting of either proline, β-methylproline (and derivatives), or pipecolic acid. In 1993, Everett and co-workers described the isolation of VM55599 (**4**), a minor metabolite from culture extracts of a *Penicillium* spp. (IMI332995) that also produces paraherquamide A (**6**), among other paraherquamides.[10] Taking into account the structural similarities between these co-occurring metabolites, these authors proposed that **4** might indeed be a biosynthetic precursor of paraherquamide A.[10] The relative stereochemistry of **4** was assigned by Everett and co-workers through extensive ^{1}H NMR NOE experiments, but the small quantity of this compound isolated precluded the determination of its absolute configuration.[10] Our laboratory has previously determined the absolute configuration of VM55599 produced by *Penicillium* spp. IMI332995 by an asymmetric, biomimetic total synthesis.[11] We further demonstrated that **4** is not a biosynthetic precursor to paraherquamide A through the synthesis of double ^{13}C-labeled, racemic VM55599 (**4**), for which the lack of incorporation into **6** in cultures of *P. fellutanum* cast doubt on the intermediacy of this species in paraherquamide biosynthesis.[12]

Asperparalines A (**7**) and C and several members of the paraherquamide family, including VM55599, have been identified as being biosynthesized from β-methylproline.[13] Previous studies from our laboratories have revealed that (*S*)-isoleucine (L-Ile) serves as the biosynthetic precursor of the β-methyl-β-hydroxyproline residue in paraherquamide A as well as the β-methylproline residue of **7**.[13] This mandates that the L-Ile side chain stereochemistry is retained at C-14 in paraherquamide A and that hydroxylation occurs with *net retention* at C-14. Accordingly, these results brought into question the capacity of VM55599 (**4**) to serve as a biosynthetic precursor to the paraherquamides. If, as one could reasonably

speculate, L-Ile is a biosynthetic precursor not only to the paraherquamides but also to VM55599, the absolute stereochemistry of this compound must be that depicted in Scheme 2; we have rigorously confirmed the relative and absolute stereochemistry of **4** as mentioned above.[11] Thus, the absolute configuration of the bicyclo[2.2.2]diazaoctane core of VM55599 (**4**) is enantiomorphic to that of virtually all of the other members of the paraherquamide family.[14]

These experimental observations led us to propose a unified biosynthesis of the paraherquamides and VM55599 (**4**), as shown in Scheme 2. In this proposal, the biosynthetic precursors of the paraherquamides and that of **4** would arise as diastereomeric products of the putative intramolecular Diels−Alder cycloaddition of a common azadiene through two of four possible diastereomeric transition states (**24** and **25**). The major pathway (via **24**) produces species **5** (named "pre-paraherquamide"), which is further processed in the respective organisms to produce the paraherquamides and asperparalines. In support of this hypothesis, we have synthesized double ^{13}C-labeled species **5** and have demonstrated that this compound incorporates into paraherquamide A (**6**) in cultures of *P. fellutanum*.[12] Despite the incorporation of **5** into the biosynthesis of paraherquamide A, this putative intermediate has heretofore not been detected as a secondary metabolite in either paraherquamide- or asperparaline-producing fungi. Herein, we demonstrate that (i) paraherquamides A (**6**) and B are produced in both *P. fellutanum* and *Aspergillus japonicus*; (ii) both VM55599 (**4**) and preparaherquamide (**5**) are natural metabolites of the paraherquamide-producing organism *P. fellutanum*; and (iii) preparaherquamide (**5**) is also observed as a natural metabolite from *A. japonicus* cultures. The observation of VM55599 (**4**) and preparaherquamide (**5**) provides additional, indirect support for the unified biogenesis outlined in Scheme 2.

Results and Discussion

P. fellutanum and *A. japonicus* JV-23 were cultured and first examined for viable production of paraherquamide A (**6**), asperparaline A (**7**), and their derivatives, respectively. Authentic paraherquamide A was first analyzed by LC-MS[n], and its MS, MS[2], MS[3], and MS[4] spectra were informative in identifying this alkaloid, establishing the successful application of LC-MS[n] analysis in this study (Figure S1, Supporting Information). Next, paraherquamide A (**6**) in the *P. fellutanum* isolation was eluted at 14.47 min in the selected-ion monitoring (SIM) chromatograph and exhibited an ion at *m/z* 494.36 (calculated $[M + H]^+$: 494.26) by MS analysis (Figures 1C and 2A). Further MS[2], MS[3], and MS[4] analyses produced identical spectra to those of authentic paraherquamide A (Figures 2A and S1). Along with paraherquamide A, paraherqua-

* To whom correspondence should be addressed. Tel: (970) 491-6747 (R.M.W.) and (734) 615-9907 (D.H.S.). Fax: (970) 491-3944 (R.M.W.) and (734) 615-3641 (D.H.S.). E-mail: rmw@lamar.colostate.edu (R.M.W.) and davidhs@umich.edu (D.H.S.).
    † The University of Michigan.
    ‡ Colorado State University.
    § University of Colorado Cancer Center.

4, VM55599

5, pre-paraherquamide

6, paraherquamide A

7, asperparaline A (aspergillimide)

8, stephacidin A

9, stephacidin B

10, brevianamide A

11, brevianamide B

12, marcfortine A (R₁ = Me)
13, marcfortine B (R₁ = H)

14, marcfortine C

15, notoamide A (R₁ = OH, R₂ = H)
16, notoamide B (R₁ = H, R₂ = H)
17, sclerotiamide (R₁= H, R₂ = OH)

18, malbrancheamide (X = Y = Cl)
19, malbrancheamide B (X = H, Y = Cl)
20, pre-malbrancheamide (X = Y = H)
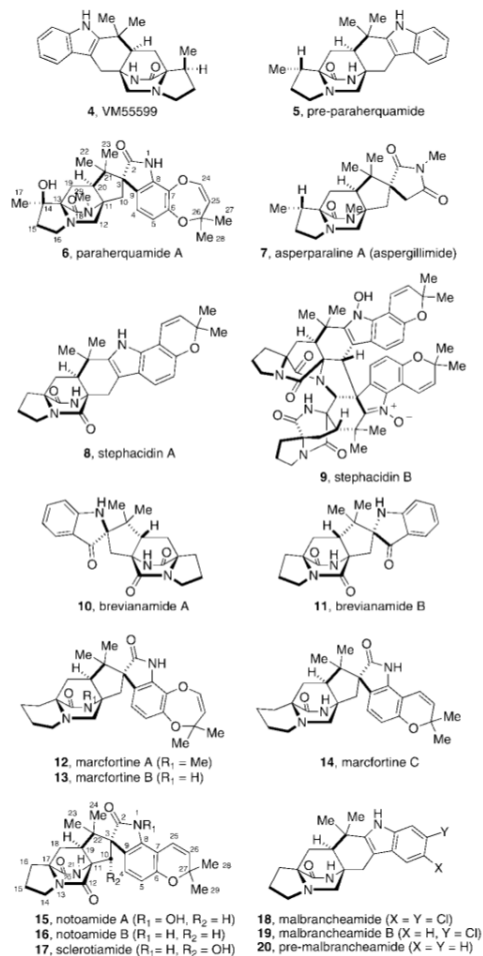
mides B−G have previously been isolated from *P. fellutanum* (previously named *P. charlesii*).[1] In this study, one compound at m/z 464.29 was detected in the fungal isolation and had a retention time of 14.95 min (Figures 1C and 2B). This compound was identified as paraherquamide B (calcd $[M + H]^+$: 464.25) by comparing its retention time and MS² spectrum to those of an authentic specimen (Figures 1 and S1).

In extracts from *A. japonicus* JV-23 cultures, asperparaline A (**7**) had a retention time of 7.58 min and exhibited an ion at m/z 360.29 (calcd $[M + H]^+$: 360.22) (Figures 1D and 2C). This metabolite was further analyzed by MS² analysis. In previous reports, *Aspergillus* species IMI 337664[2] and *A. sclerotiorum*[7] represented the first organisms outside of *Penicillium* spp. to produce paraherquamide congeners. In this study, we investigated paraherquamide production in *A. japonicus* JV-23. By comparing their retention times and MS^n spectra to those of authentic compounds, both paraherquamide A (14.45 min) and paraherquamide B (14.88 min) were identified in this *Aspergillus* spp. isolation, further indicating that both *Penicillium* spp. and *Aspergillus* spp. are able to produce these anthelmintic alkaloid metabolites (Figures 1 and S2). Moreover, this result strongly suggested one common

Scheme 1. Proposed Intramolecular Diels−Alder Construction of the Bicyclo[2.2.2]diazaoctane Core
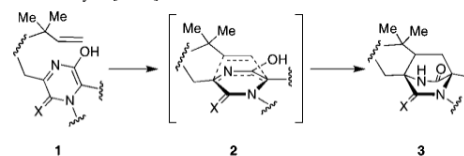
biosynthetic pathway shared by both asperparalines and paraherquamides in this fungus.

The *A. japonicus* JV-23 strain produced more paraherquamide B than paraherquamide A (**6**) in PDB medium under the growth conditions given. *A. japonicus* JV-23 is the first reported *Aspergillus* spp. to produce paraherquamide A itself, to the best of our knowledge, although Everett and co-workers isolated the paraherquamide congeners VM54159, SB203105, and SB200437 from *Aspergillus* strain IMI 337664.[2c] In extracts from *P. fellutanum*, two metabolites with m/z of 350 were separated and identified by LC-MS/MS analysis (Figure 3). The first peak had a retention time of 12.15 min, while the second metabolite was eluted at 12.64 min. These peaks were initially proposed to be VM55599 (**4**) and preparaherquamide (**5**), considering their theoretical molecular weights ($C_{22}H_{27}N_3O$, 349.22) and the previous isolation of **4** as the minor metabolite from *Penicillium* spp. IMI337664.[10]

To further identify these metabolites, synthetic and authentic (racemic) samples of **4** and **5** were used to secure standard MS and MS² fragmentation data (Figure S3). Interestingly, these two compounds, which are diastereomers, exhibited different fragmentation patterns in their MS² spectra. The ratio of the peak at m/z 322.26 to the peak at m/z 305.25 in the VM55599 MS² spectrum was larger than 1.0, while this ratio was significantly smaller than 1.0 in the preparaherquamide (**5**) MS² spectrum with the fragment at m/z 305.24 as the most intense peak, which likely serves as the distinctive feature of the MS² spectra of these two compounds (Figure S3). CO was lost from the peptide bond of parent ions to produce the first fragment at m/z 322.26, which was further fragmented to give a signal at m/z 305.25 by losing NH_3 (Figures 4 and S3). The same fragmentation pathway was observed for **5**. The fragmentation discrepancy observed in the MS² spectra of **4** and **5** was apparently affected by the single relative stereochemical difference at C-14 (paraherquamide numbering) between these two compounds. Comparing their MS² spectra with those of authentic compounds, VM55599 (**4**) ($t_R = 12.15$ min) and preparaherquamide (**5**) ($t_R = 12.64$ min) were identified in the extract from *P. fellutanum* cultures (Figures 3A−C and 4A, B). Preparaherquamide was thus observed as one natural metabolite, further strongly validating the putative pathway in Scheme 2.

In extracts from *A. japonicus* JV-23 cultures, only one metabolite at m/z 350 was identified by LC-MS/MS analysis (Figure 3D). When compared to the MS and MS² spectra of authentic standards, the metabolite with the retention time of 12.62 min was validated as preparaherquamide (Figure 4C). This represents the first identification of this putative precursor in an asperparaline-producing organism. Preparaherquamide (**5**) has been proposed by this laboratory as the key, common biosynthetic precursor to both the paraherquamides and the asperparalines.[9,13c] The identification of this substance in the paraherquamide- and asperparaline-producing *A. japonicus* JV-23 strain further supports the unified biogenetic hypothesis detailed in Scheme 2. Curiously, VM55599 was not detected as a natural metabolite from the *A. japonicus* JV-23 cultures.

Numerous alkaloids that display a wide spectrum of biological activities have been isolated from various fungi. An important and growing family of prenylated indole alkaloids is constituted by a common bicyclo[2.2.2]diazaoctane core derived mainly from tryptophan, proline, substituted proline derivatives, and isoprene units.

Scheme 2. Proposed Unified Biogenesis of Paraherquamides and Asperparalines
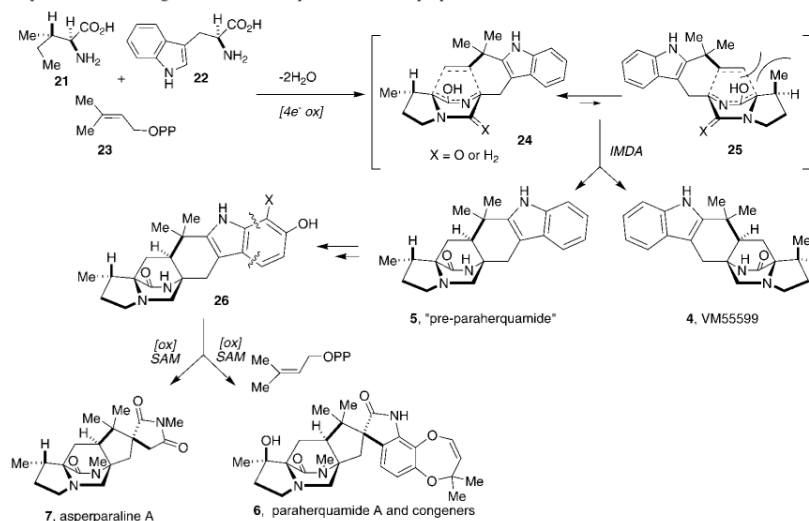
This family includes the paraherquamides,[1] asperparalines,[2] stephacidins,[3] brevianamides,[4] marcfortines,[5] notoamides,[6] sclerotiamide,[7] and the malbrancheamides.[8] Among these alkaloids, malbrancheamide is further distinguished by the presence of two chlorine atoms in the indole aromatic nucleus. Premalbrancheamide, which lacks the C-14 methyl group found in preparaherquamide, was recently isolated and identified as the precursor in malbrancheamide B biosynthesis.[15] By LC-MS/MS analysis, this natural metabolite exhibited a similar fragmentation pattern to VM55599 (**4**) and preparaherquamide (**5**). Similar to the results we obtained in precursor feeding experiments with **5**, synthetic doubly ^{13}C-labeled premalbrancheamide was also successfully incorporated into malbrancheamide B in *Malbranchea aurantiaca*.[12,15] The identification of both preparaherquamide and premalbrancheamide as natural, trace metabolites suggests that structurally related common precursors may be involved in the biosynthesis of other subgroups of alkaloids within this family and that the structural diversity of these alkaloids are likely introduced by downstream tailoring enzymes following the construction of the bicyclo[2.2.2]diazaoctane core.
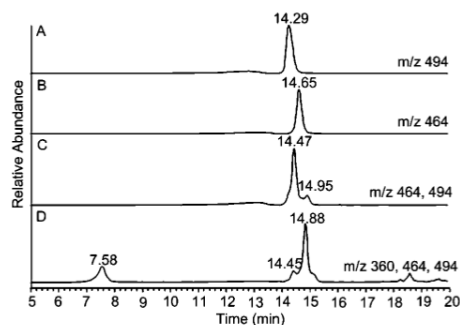
Figure 1. Selected-ion monitoring (SIM) chromatographs corresponding to authentic paraherquamide A (**6**) (*m/z* 494) (A), authentic paraherquamide B (*m/z* 464) (B), isolation from *P. fellutanum* culture (*m/z* 464 and 494) (C), and isolation from *A. japonicus* JV-23 (*m/z* 360, 464, and 494) (D).
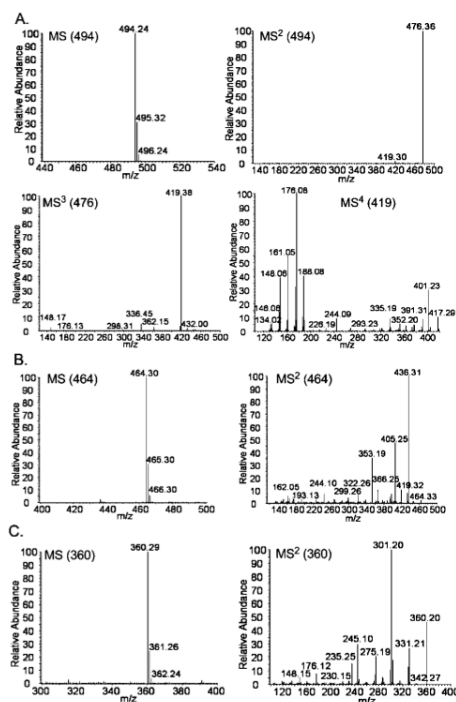
Figure 2. MS[n] spectra of paraherquamide A (**6**) (A) and paraherquamide B (B) from the isolation of *P. fellutanum* cultures, and asperparaline A (**7**) (C) from the extracts of *A. japonicus* JV-23. The integral *m/z* values of ions for each MS[n] analysis are included in the corresponding graphs.
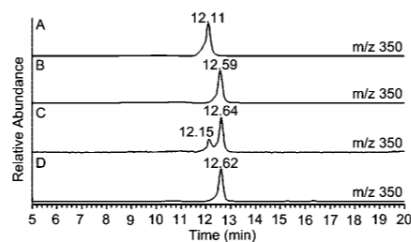
Figure 3. Selected-ion monitoring (SIM) chromatographs corresponding to the LC-MS[n] analysis of authentic VM55599 (**4**) (*m/z* 350) (A), authentic preparaherquamide (**5**) (*m/z* 350) (B), isolation from *P. fellutanum* cultures (*m/z* 350) (C), and isolation from *A. japonicus* JV-23 (*m/z* 350) (D).
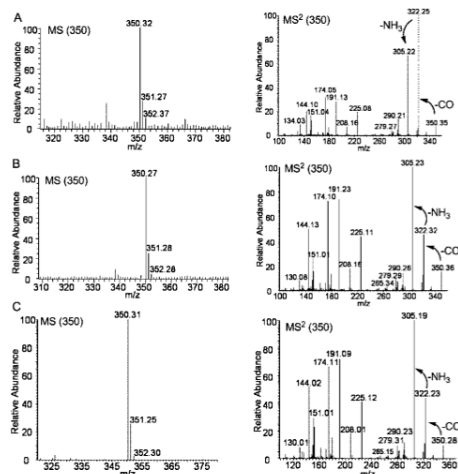
Figure 4. MS and MS[2] spectra of VM55599 (**4**) (A) and preparaherquamide (**5**) from the isolation from *P. fellutanum* culture (B), and preparaherquamide (**5**) from the extracts of *A. japonicus* JV-23 cultures (C). The integral *m/z* values of ions for each analysis are included in the corresponding graphs.

LC-MS/MS analysis has several important advantages with respect to sensitivity and selectivity in the detection of trace natural metabolites. In natural products identification, NMR techniques are widely used to directly provide structural information when sufficient amounts of purified substances are available. However, in the case of biosynthetic intermediates, there is often a paucity of material that is thus insufficient for NMR structural studies. This is a manifestation of biosynthetic intermediates being largely consumed by downstream tailoring enzymes, and thus these substrates do not accumulate. LC-MS/MS is an effective and powerful alternative in these cases and has been successfully used to identify many natural products in crude extracts by comparison with the respective reference compounds.[16] Herein, we were able to successfully deploy LC-MS/MS analysis to identify the presence of paraherquamide A (**6**), paraherquamide B, asperparaline A (**7**), VM55599 (**4**), and preparaherquamide (**5**) in crude fungal extracts using this technique.

In conclusion, we have demonstrated for the first time that preparaherquamide (**5**) is a natural secondary metabolite of the paraherquamide-producing organism *P. fellutanum* and the paraherquamide- and asperparaline-producing organism *A. japonicus*

JV-23. This report constitutes the first confirmatory evidence for the natural existence of preparaherquamide, albeit at low concentration levels. This provides additional support for the unified biogenesis we have proffered.[9,11–13] VM55599 (**4**) is also produced by *P. fellutanum* and is consistent with the initial identification of this substance from the related paraherquamide-producing organism *Penicillium* spp. IMI332995 described by Everett and co-workers.[10] As the identification of new paraherquamide-producing fungi are discovered in various environments around the world, we speculate here that VM55599 can be expected to be detected as a co-metabolite. It should be further noted that Miller and co-workers recently described the detection of VM55599 as a metabolite in several strains of *Penicillium paneum* on the basis of mass spectrometric data.[17] It is entirely possible that these workers might have instead detected preparaherquamide (or both), which has the same mass as VM55599. As in the previously established case of *P. fellutanum*, we conclude that VM55599 is a shunt (dead-end) metabolite, as it possesses the incorrect absolute (and relative) stereochemistry to be processed further to a paraherquamide-like structure. Likewise, we speculate that in *A. japonicus* the major pathway metabolite **5** is largely consumed by the downstream biosynthetic machinery responsible for the substantial oxidative elaboration of **5** into the asperparalines and paraherquamides. We are currently pursuing the synthesis and labeling of several plausible metabolites downstream of preparaherquamide to gain insight into the sequence of events following the construction of this early pathway metabolite in both paraherquamide- and asperparaline-producing fungi. Efforts to clone the biosynthetic gene clusters for the biosynthesis of these structurally unique and biologically important natural products are also currently under investigation in our laboratories.

Experimental Section

Chemicals and Strains. Ethyl acetate and methanol were HPLC grade from Sigma Aldrich (St. Louis, MO), while acetonitrile used in LC-MS[n] analysis was LC-MS grade from J. T. Baker (Phillipsburg, NJ). A MilliQ H_2O purification system (Millipore Ltd., Bedford, MA) generated water for LC-MS[n] analysis. Trifluoroacetic acid (99%, reagent plus) and formic acid (>98%, ACS reagent) were also purchased from Sigma Aldrich. Authentic paraherquamide A (**6**),[18] VM55599 (**4**),[11,12] and preparaherquamide (**5**)[12] were synthesized following previously published procedures. Paraherquamide B (as the unnatural enantiomer) was obtained by total synthesis.[18b] *P. fellutanum* (ATCC20841) was purchased from American Type Culture Collection (Manassas, VA), while *A. japonicus* JV-23 was provided by Dr. Hideo Hayashi of Osaka Prefecture University.

Cultures of *P. fellutanum* and *A. japonicus* JV-23. *P. fellutanum* and *A. japonicus* JV-23 were initially grown in two different solid media (20 g of malt extract, 20 g of glucose, 1 g of peptone, and 20 g of agar in 1 L of deionized water) and (20 g of potato-dextrose broth and 20 g of agar in 1 L of deionized water), respectively, at 25 °C in the dark for 2 weeks. Fungal mycelia and spores were then transferred into 300 mL of sterile corn steep liquor medium (22 g of corn steep liquor and 40 g of glucose per liter of deionized water) for *P. fellutanum* or 300 mL of sterile potato-dextrose broth (PDB) (24 g of potato-dextrose broth per liter of deionized water) for *A. japonicus* JV-23, in 2 L Erlenmeyer flasks. Both fungal strains were then grown at 25 °C in the dark for 4 weeks.

Sample Extraction. The cultures with fungal mycelium were adjusted to pH 10–12 by 10 M KOH. The cultures were then extracted with an equal volume of ethyl acetate twice. The combined organic layer from each culture was washed with water, dried over anhydrous magnesium sulfate, and evaporated to dryness. The residues were redissolved in methanol prior to LC-MS[n] analysis.

LC-MS[n] Analysis. LC-MS[n] analysis was performed using a ThermoFinnigan LTQ linear ion-trap instrument equipped with electrospray source and Surveyor HPLC system at room temperature. Separations were carried out with a Waters XBridge C_{18} (3.5 μm, 2.1 × 150 mm) column at a flow rate of 210 μL/min with solvent A (water with 0.1% formic acid) and solvent B (acetonitrile with 0.1% formic acid). Solvent B was kept at 15% in solvent A for 2.5 min and then was gradually

increased to 40% over 12.5 min and 80% over 2 min and then maintained at 80% for 6 min to elute fungal metabolites. The column was further re-equilibrated with 15% solvent B for 25 min. For mass spectrometry, the capillary temperature was set to 275 °C with the source voltage at 3.6 kV, the source current at 3.5 μA, the capillary voltage at 30 V, and the tube lens at 119 V. Sheath gas flow was set to 28 psi, and auxiliary gas flow was 5 arbitrary units. The normalized collision energy for ion fragmentation was 30%. The injection volume was 5−10 μL, and spectra were recorded in the positive-ion mode. Selected-ion monitoring (SIM) chromatographs were obtained at the selected *m/z* values.

Supporting Information Available: MS^n spectra of authentic paraherquamide A (**6**) and authentic paraherquamide B; MS^n spectra of two metabolites at 14.45 and 14.88 min from the extract from *A. japonicus* JV-23; MS and MS^2 spectra of authentic VM55599 (**4**) and authentic preparaherquamide (**5**). This material is available free of charge via the Internet at http://pubs.acs.org.

References and Notes

(1) (a) Yamazaki, M.; Okuyama, E.; Kobayashi, M.; Inoue, H. *Tetrahedron Lett.* **1981**, *22*, 135–136. (b) Ondeyka, J. G.; Goegelman, R. T.; Schaeffer, J. M.; Kelemen, L.; Zitano, L. *J. Antibiot.* **1990**, *43*, 1375–1379. (c) Liesch, J. M.; Wichmann, C. F. *J. Antibiot.* **1990**, *43*, 1380–1386. (d) Blanchflower, S. E.; Banks, R. M.; Everett, J. R.; Manger, B. R.; Reading, C. *J. Antibiot.* **1991**, *44*, 492–497.
(2) (a) Hayashi, H.; Nishimoto, Y.; Nozaki, H. *Tetrahedron Lett.* **1997**, *38*, 5655–5658. (b) Hayashi, H.; Nishimoto, Y.; Akiyama, K.; Nozaki, H. *Biosci. Biotechnol. Biochem.* **2000**, *64*, 111–115. (c) Banks, R. M.; Blanchflower, S. E.; Everett, J. R.; Manger, B. R.; Reading, C. *J. Antibiot.* **1997**, *50*, 840–846.
(3) (a) Qian-Cutrone, J.; Huang, S.; Shu, Y.-Z.; Vyas, D.; Fairchild, C.; Menendez, A.; Krampitz, K.; Dalterio, R.; Klohr, S. E.; Gao, Q. *J. Am. Chem. Soc.* **2002**, *124*, 14556–14557. (b) Qian-Cutrone, J.; Krampitz, K.; Shu, Y.-Z. Chang, L. P. U.S. Patent 6,291,461, 2001.
(4) (a) Birch, A. J.; Wright, J. J. *J. Chem. Soc., Chem. Commun.* **1969**, 644–645. (b) Birch, A. J.; Wright, J. J. *Tetrahedron* **1970**, *26*, 2329–2344. (c) Birch, A. J.; Russell, R. A. *Tetrahedron* **1972**, *28*, 2999–3008. (d) Bird, B. A.; Remaley, A. T.; Campbell, I. M. *Appl. Environ. Microbiol.* **1981**, *42*, 521–525. (e) Bird, B. A.; Campbell, I. M. *Appl. Environ. Microbiol.* **1982**, *43*, 345–348. (f) Robbers, J. E.; Straus, J. W. *Lloydia* **1975**, *38*, 355–356. (g) Paterson, R. R. M.; Hawksworth, D. L. *Trans. Br. Mycol. Soc.* **1985**, *85*, 95–100. (h) Wilson, B. J.; Yang, D. T. C.; Harris, T. M. *Appl. Microbiol.* **1973**, *26*, 633–635. (i) Coetzer, J. *Acta Crystallogr.* **1974**, *B30*, 2254–2256.
(5) (a) Polonsky, J.; Merrien, M.-A.; Prange, T.; Pascard, C. *J. Chem. Soc., Chem. Comm.* **1980**, 601–602. (b) Prange, T.; Buillion, M-A.; Vuilhorgne, M.; Pascard, C.; Polonsky, J. *Tetrahedron Lett.* **1980**, *22*, 1977–1980.
(6) (a) Kato, H.; Yoshida, T.; Tokue, T.; Nojiri, Y.; Hirota, H.; Ohta, T.; Williams, R. M.; Tsukamoto, S. *Angew. Chem., Int. Ed.* **2007**, *46*, 2254–2256.
(7) Whyte, A. C.; Gloer, J. B. *J. Nat. Prod.* **1996**, *59*, 1093–1095.
(8) (a) Martinez-Luis, S.; Rodriguez, R.; Acevedo, L.; Gonzalez, M. C.; Lira-Rocha, A.; Mata, R. *Tetrahedron* **2006**, *62*, 1817–1822. (b) Figueroa, M.; del Carmen González, M.; Mata, R. *Nat. Prod. Res.* **2008**, *22*, 709–714. (c) Miller, K. A.; Welch, T. R.; Greshock, T. J.; Ding, Y.; Sherman, D. H.; Williams, R. M. *J. Org. Chem.* **2008**, *73*, 3116–3119.
(9) (a) Stocking, E.; Williams, R. M. *Angew. Chem., Int. Ed.* **2003**, *42*, 3078–3115. (b) Cox, R. J.; Williams, R. M. *Acc. Chem. Res.* **2003**, *36*, 127–139. (c) Williams, R. M. *Chem. Pharm. Bull.* **2002**, *50*, 711–740. (d) Williams, R. M.; Sanz-Cervera, J. F.; Stocking, E. In *Topics in Current Chemistry, Volume on Biosynthesis-Terpenes and Alkaloids*; Leeper, F., Vederas, J. C., Eds.; Springer-Verlag: Berlin, 2000; Vol. 209, pp 97−173.
(10) Blanchflower, S. E.; Banks, R. M.; Everett, J. R.; Reading, C. *J. Antibiot.* **1993**, *46*, 1355–1363.
(11) Sanz-Cervera, J. F.; Williams, R. M. *J. Am. Chem. Soc.* **2002**, *124*, 2556–2559.
(12) (a) Stocking, E. M.; Sanz-Cervera, J. F.; Williams, R. M. *J. Am. Chem. Soc.* **2000**, *122*, 1675–1683. (b) Stocking, E. M.; Sanz-Cervera, J. F.; Williams, R. M. *Angew. Chem., Int. Ed.* **2001**, *40*, 1296–1298.
(13) (a) Stocking, E.; Sanz-Cervera, J. F.; Williams, R. M.; Unkefer, C. J. *J. Am. Chem. Soc.* **1996**, *118*, 7008–7009. (b) Stocking, E. M.; Martinez, R. A.; Silks, L. A.; Sanz-Cervera, J. F.; Williams, R. M. *J. Am. Chem. Soc.* **2001**, *123*, 3391–3392. (c) Gray, C.; Sanz-Cervera, J. F.; Williams, R. M. *J. Am. Chem. Soc.* **2003**, *125*, 14692–14693. (d) Stocking, E.; Sanz-Cervera, J. F.; Unkefer, C. J.; Williams, R. M. *Tetrahedron* **2001**, *57*, 5303–5320.
(14) Both enantiomers of stephacidin A and notoamide B have recently been isolated from distinct *Aspergillus* spp.; see:Greshock, T. J.; Grubbs, A. W.; Jiao, P.; Wicklow, D. T.; Gloer, J. B.; Williams, R. M. *Angew. Chem., Int. Ed.* **2008**, *47*, 3573–3577.
(15) Ding, Y.; Miller, K. A.; Greshock, T. J.; Sherman, D. H.; Williams, R. M. (unpublished results).
(16) (a) Hayasaka, Y.; Wilkinson, K. L.; Elsey, G. M.; Raunkjaer, M.; Sefton, M. A. *J. Agric. Food Chem.* **2007**, *55*, 9195–9201. (b) Koh, H. L.; Wang, H.; Zhou, S.; Chan, E.; Woo, S. O. *J. Pharm. Biomed. Anal.* **2006**, *40*, 653–661. (c) Ding, B.; Zhou, T.; Fan, G.; Hong, Z.; Wu, Y. *J. Pharm. Biomed. Anal.* **2007**, *45*, 219–226.
(17) Nielsen, K. F.; Sumarah, M. W.; Frisvad, J. C.; Miller, J. D. *J. Agric. Food Chem.* **2006**, *54*, 3756–3763.
(18) (a) Williams, R. M.; Cao, J.; Tsujishima, H.; Cox, R. J. *J. Am. Chem. Soc.* **2003**, *125*, 12172–12178. (b) Cushing, T. D.; Sanz-Cervera, J. F.; Williams, R. M. *J. Am. Chem. Soc.* **1993**, *115*, 9323–9324. (c) Domingo, L. R.; Zaragozá, R. J.; Williams, R. M. *J. Org. Chem.* **2003**, *68*, 2895–2902.

NP800292N

J|A|C|S
ARTICLES

Genome-Based Characterization of Two Prenylation Steps in the Assembly of the Stephacidin and Notoamide Anticancer Agents in a Marine-Derived *Aspergillus* sp.

Yousong Ding,[†] Jeffrey R. de Wet,[‡] James Cavalcoli,[‡] Shengying Li,[†]
Thomas J. Greshock,[§] Kenneth A. Miller,[§] Jennifer M. Finefield,[§]
James D. Sunderhaus,[§] Timothy J. McAfoos,[§] Sachiko Tsukamoto,[ǁ]
Robert M. Williams,*,[§] and David H. Sherman*,[†]

*Life Sciences Institute and Departments of Medicinal Chemistry, Microbiology & Immunology,
and Chemistry, University of Michigan, Ann Arbor, Michigan 48109, Center for Computational
Medicine and Bioinformatics, University of Michigan, Ann Arbor, Michigan 48109, Department
of Chemistry, Colorado State University, Fort Collins, Colorado 80523, USA and University of
Colorado Cancer Center, Aurora, Colorado 80045, Graduate School of Pharmaceutical
Sciences, Kumamoto University, 5-1 Oe-honmachi, Kumamoto 862-0973, Japan*

Received June 6, 2010; E-mail: davidhs@umich.edu; rmw@lamar.colostate.edu

Abstract: Stephacidin and notoamide natural products belong to a group of prenylated indole alkaloids containing a core bicyclo[2.2.2]diazaoctane ring system. These bioactive fungal secondary metabolites have a range of unusual structural and stereochemical features but their biosynthesis has remained uncharacterized. Herein, we report the first biosynthetic gene cluster for this class of fungal alkaloids based on whole genome sequencing of a marine-derived *Aspergillus* sp. Two central pathway enzymes catalyzing both normal and reverse prenyltransfer reactions were characterized in detail. Our results establish the early steps for creation of the prenylated indole alkaloid structure and suggest a scheme for the biosynthesis of stephacidin and notoamide metabolites. The work provides the first genetic and biochemical insights for understanding the structural diversity of this important family of fungal alkaloids.

Introduction

Structurally complex fungal-derived natural products account for a significant number of clinical therapeutics for treatment of human and animal diseases.[1] Due to emerging appreciation for the high level of biodiversity within this group of eukaryotes, an increasing number of natural products have been isolated from fungal sources and screened for bioactive secondary metabolites.[2] Recently, a family of fungal-derived prenylated alkaloids has attracted increasing interest for its remarkably diverse bioactivities including insecticidal, antitumor, anthelmintic, calmodulin inhibitory, and antibacterial properties, and intriguing structural features. These natural products are comprised of L-tryptophan, a second cyclic amino acid residue, and one or two isoprene units (Scheme 1).[3] The isolation and characterization of two key biosynthetic intermediates, preparaherquamide (**1**) and premalbrancheamide (**2**), in the biosynthesis

of the paraherquamides (**3**) and malbrancheamides (**4**),[4,5] respectively, suggest that two amino acid residues are condensed to generate the *cyclo*-L-tryptophan-L-proline analog **5** or **6**. The tryptophanyl subunit of the dipeptide is subsequently prenylated in a reverse manner to generate compound **7** or **8** (Scheme 1). The bicyclo[2.2.2]diazaoctane core in **1** and **2** possibly arises from an intramolecular Diels−Alder (IMDA) reaction after oxidizing **7** or **8** to form a putative pyrazine-derived azadienophile. However, the detailed understanding of assembly and modification of these biosynthetic building blocks remain highly obscure.

Recently, a group of new prenylated indole alkaloids, the notoamides (A−E, **9**−**13**), were isolated from a marine-derived *Aspergillus* sp. (Figure 1a).[6,7] Interestingly, stephacidin A (**14**) and deoxybrevianamide E (**15**) were purified from the same fungal strain, indicating the possible role of **15** as a common biosynthetic intermediate.[7] In 2006, a bimodular nonribosomal peptide synthetase (NRPS) gene (*ftmA*) was mined from an *A. fumigatus* genome sequence, and its heterologous expression led to accumulation of the *cyclo*-L-tryptophan-L-proline product

[†] Life Sciences Institute and Departments of Medicinal Chemistry, Microbiology & Immunology, and Chemistry, University of Michigan.
[‡] Center for Computational Medicine and Bioinformatics, University of Michigan.
[§] Colorado State University.
[ǁ] Kumamoto University.
(1) Keller, N. P.; Turner, G.; Bennett, J. W. *Nat. Rev. Microbiol.* **2005**, *3* (12), 937–47.
(2) Pelaez, F. Biological activities of fungal metabolites. In *Handbook of Industrial Mycology*; An, Z., Ed.; Marcel Dekker: New York, 2005; pp 49−922.
(3) Williams, R. M.; Cox, R. J. *Acc. Chem. Res.* **2003**, *36* (2), 127–39.

(4) Ding, Y.; Greshock, T. J.; Miller, K. A.; Sherman, D. H.; Williams, R. M. *Org. Lett.* **2008**, *10* (21), 4863–6.
(5) Stocking, E. M.; Sanz-Cervera, J. F.; Williams, R. M. *Angew. Chem., Int. Ed.* **2001**, *40* (7), 1296–8.
(6) Tsukamoto, S.; Kato, H.; Greshock, T. J.; Hirota, H.; Ohta, T.; Williams, R. M. *J. Am. Chem. Soc.* **2009**, *131* (11), 3834–5.
(7) Kato, H.; Yoshida, T.; Tokue, T.; Nojiri, Y.; Hirota, H.; Ohta, T.; Williams, R. M.; Tsukamoto, S. *Angew. Chem., Int. Ed.* **2007**, *46* (13), 2254–6.

Scheme 1. Biosynthetic Subunits and Putative Route to Paraherquamide (**3**) and Malbrancheamide (**4**)*[a]*
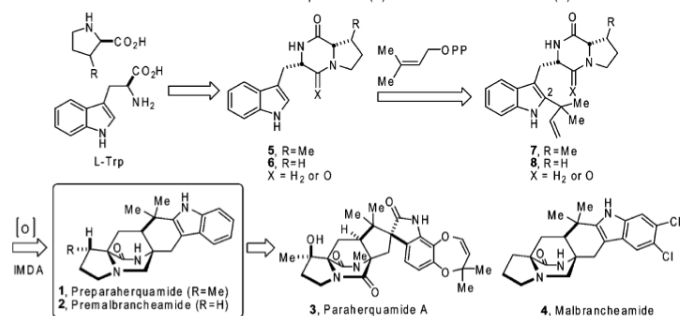
[a] Molecules in the boxes have been validated as the building blocks or biosynthetic intermediates based on precursor incorporation studies.
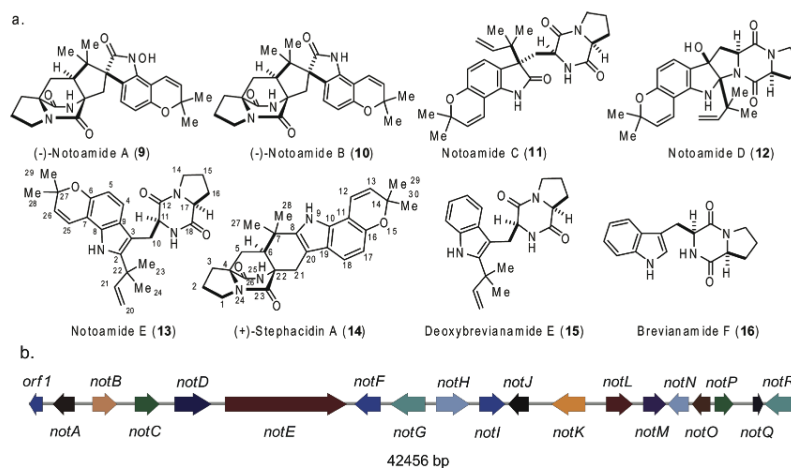
Figure 1. Genetic studies of fungal alkaloids produced in the marine-derived fungus *Aspergillus* sp. (a) Selected fungal alkaloids isolated from the marine-derived *Aspergillus* sp. Compound **16** was not reported in the fungal strain but was expected as the direct precursor of compound **15**. (b) The notoamide (*not*) biosynthetic gene cluster derived from complete sequencing and bioinformatic mining of *Aspergillus* sp. MF297-2 genome.

brevianamide F (**16**).[8] We reasoned that an NRPS with a function coincident with FtmA would be expected for the notoamide biosynthetic pathway, where **16** in this marine-derived *Aspergillus* sp. is elaborated in an alternative manner compared to *A. fumigatus*[9] that mediates biosynthesis of one ergot alkaloid, fumitremorgin. Herein, we report the identification of the first gene cluster for the biosynthesis of the stephacidin and notoamide family of prenylated alkaloids based on genome mining and biochemical analysis. These studies include a detailed characterization of the elusive deoxybrevianamide E synthase (e.g., reverse prenyl-transferase) as well as a second normal prenyltransferase that provide new insights into the assembly of the structurally and biologically diverse class of bicyclo[2.2.2]diazaoctane-derived natural products.

(8) Maiya, S.; Grundmann, A.; Li, S. M.; Turner, G. *ChemBioChem* **2006**, *7* (7), 1062–9.
(9) Grundmann, A.; Li, S. M. *Microbiology* **2005**, *151* (7), 2199–207.

Results

Localization and Analysis of the Notoamide (*Not*) Gene Cluster from a Marine-Derived *Aspergillus* sp. through Genome Mining. The genome of the stephacidin- and notoamide-producing marine-derived *Aspergillus* sp. MF297−2 was sequenced to ∼15 times coverage of the average published *Aspergillus* genome size (32.5 Mb) using Roche 454FLX technology (unpublished data). An open reading frame (*orf*) named *notE* (Figure 1b) was identified from the genome sequence using *ftmA* to probe for homologous genes.[8] NotE is a presumed bimodular NRPS (Table 1) with adenylation (A)-thiolation (T)-condensation (C)-A-T-C domain organization and shares 47% amino acid sequence identity with FtmA (Table 1). In addition to *notE*, eighteen other genes were identified in a 42456-bp region of the chromosome encompassed by four overlapping genome assembly nodes (Figure 1b). At the left end of the gene cluster, the product of *orf1* was predicted to be the *N*-terminus of a capsule polysaccharide biosynthesis protein

Table 1. Features of the *Not* Gene Products

Protein	Size bp/aa	Exon	Function	Relative (identity/similarity [%])	Accession number
Orf1	731/224	1−113, 173−731	partial polysaccharide synthase	capsule polysaccharide biosynthesis protein from *Aspergillus fumigatus* (43/63)	XP_748327
NotA	1199/339	1293−1568, 1643−1971, 2023−2179, 2234−2491	negative regulator	NmrA family protein from *Ajellomyces capsulatus* (45/64)	EEH03447
NotB	1344/401	3486−4079, 4141−4487, 4568−4829	FAD binding domain protein	FAD binding domain protein from *A. clavatus* (44/63)	XP_001268514
NotC	1350/427	5819−6996, 7066−7168	prenyltransferase	FtmH from *A. fumigatus* (50/66)	BAH24002
NotD	2025/621	8012−8294, 8389−8927, 8996−10036	oxidoreductase	oxidoreductase from *Microsporum canis* (40/59)	EEQ33235
NotE	6723/2241	10787−17509	NRPS	FtmA from *A. fumigatus* (47/67)	XP_747187
NotF	1431/453	17924−18053, 18126−19354	prenyltransferase	tryptophan dimethylallyltransferase from *Coccidioides posadasii* (40/62)	EER24759
NotG	1901/544	19899−20086, 20171−20272, 20337−20635, 20689−20810, 20879−21799	P450	cytochrome P450 from *A. fumigatus* (62/75)	XP_747185
NotH	1836/502	22422−22668, 22734−22822, 22897−22996, 23060−23128, 23187−23765, 23836−24257	P450	cytochrome P450 from *Neosartorya fischeri* (47/65)	XP_001261652
NotI	1423/434	24803−24962, 25021−25939, 26003−26225	FAD binding domain protein	FAD binding domain protein from *A. clavatus* (44/63)	XP_001268514
NotJ	1113/371	26390−27502	unknown	hypothetical protein from *Salinispora arenicola* (52/65)	YP_001537335
NotK	1851/564	28771−29141, 29196−29569, 29620−30389, 30445−30621	efflux pump	MFS transporter from *N. fischeri* (87/93)	XP_001265322
NotL	1455/484	31789−33243	transcriptional activator	C6 zinc finger domain protein from *N. fischeri* (53/62)	XP_001265321
NotM	1266/402	33816−34597, 34654−35080	unknown	hypothetical protein from *Talaromyces stipitatus* (74/82)	XP_002482929
NotN	1126/340	35192−35244, 35299−35895, 35948−36317	dehydrogenase	alcohol dehydrogenase from *Penicillium marneffei* (60/76)	XP_002147947
NotO	993/331	36520−37512	short-chain dehydrogenases/ reductase	hypothetical protein from *Nectria hematococca* (66/80)	EEU36425
NotP	1020/322	37770−37930, 37985−38789	unknown	metallo-β-lactamase domain protein from *T. stipitatus* (80/88)	XP_002482927
NotQ	569/152	39871−40059, 40120−40316, 40370−40439	unknown	hypothetical protein from *T. stipitatus* (88/94)	XP_002482928
NotR	1517/461	40514−41140, 41212−41727, 41791−42030	transcriptional coactivator	hypothetical protein from *P. marneffei* (45/61)	XP_002144868

involved in a primary metabolic pathway. At the right end of the gene cluster, a protein encoded by *notR* showed 38% sequence identity to the AflJ aflatoxin pathway transcriptional coactivator.[10] Bioinformatic analysis indicated that NotB and NotI show high similarity to FAD-dependent monooxygenases while NotD is a presumed flavin-dependent oxidoreductase. NotG and NotH show high sequence similarity to fungal CYP450s, both of which might be involved in the formation of the isoprene-derived pyran ring (Scheme 2). Furthermore, NotN and NotO are predicted to function as a dehydrogenase and a short-chain dehydrogenase/reductase, respectively. The *notK* gene encodes a putative efflux pump, which might specify excretion of alkaloid products from the cell. As with NotR, NotL shares high protein sequence similarity to AflR while NotA is a predicted biosynthetic pathway transcriptional repressor.[11] These regulators offer opportunities to understand the notoamide pathway gene expression, and the potential to manipulate fungal

alkaloid production in this unique marine-derived *Aspergillus* sp.[12] NotC and NotF, two predicted aromatic prenyltransferases, presumably catalyze the two key prenylation reactions including a first reverse prenyltransfer step leading to **15**. NotC shows a 50% sequence identity to FtmH (also called FtmPT2) in *A. fumigatus* while NotF shows the highest identity (40%) to a putative dimethylallyl tryptophan synthase (EER24759) in *Coccidioides posadasii*.[13] However, the putative functions of products encoded by *notJ*, *notM*, *notP*, and *notQ* remain unknown based on bioinformatics analysis.

Determination of NotF as the Deoxybrevianamide E Synthase. We first examined the role of NotF in notoamide biosynthesis. Its cDNA was prepared by removing the 72-bp intron using an overlapping PCR strategy (Supplementary Table 1). The recombinant enzyme was purified with Ni-NTA resin to about 90% purity, and its native protein status was determined as an oligomer with an observed molecular weight of 292 kDa

(10) Meyers, D. M.; Obrian, G.; Du, W. L.; Bhatnagar, D.; Payne, G. A. *Appl. Environ. Microbiol.* **1998**, *64* (10), 3713−7.
(11) Woloshuk, C. P.; Foutz, K. R.; Brewer, J. F.; Bhatnagar, D.; Cleveland, T. E.; Payne, G. A. *Appl. Environ. Microbiol.* **1994**, *60* (7), 2408−14.
(12) Flaherty, J. E.; Payne, G. A. *Appl. Environ. Microbiol.* **1997**, *63* (10), 3995–4000.
(13) Grundmann, A.; Kuznetsova, T.; Afiyatullov, S.; Li, S. M. *ChemBioChem* **2008**, *9* (13), 2059−63.

369

Scheme 2. The Putative Biosynthetic Pathway for Stephacidin A (**14**) and the Notoamide Natural Products[a]
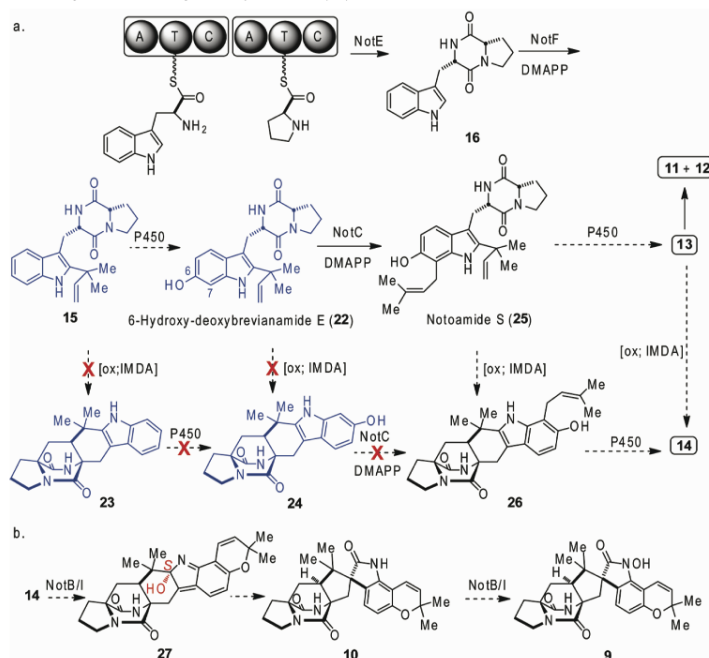
[a] (a) The early stages in the stephacidin and notoamide biosynthesis. **25** serves as the common precursor to **13** and **14**. **13** is then converted into **11** and **12**. Substrates used in NotC studies were labeled in blue. (b) Notoamide A (**9**) and B (**10**) are possibly derived from **14**. The solid arrows represent reactions that have been confirmed with bioinformatic analysis, biochemical analysis, or precursor incorporation experiments, while the dashed arrows indicate proposed biosynthetic steps. The red symbol X indicates the reaction is not supported by the current study.

(53.6 kDa as the calculated monomeric size) by gel filtration (Supplementary Figure 1).

Next, the function of NotF was tested with doubly ^{13}C-labeled brevianamide F (**17**, Supplementary Figure 2). The product **18** exhibited the same retention time (17.38 min) as authentic **15** but its [M+H]+ ion was 354.19, bearing the expected 2.00-Da shift from [**15**+H]+ (352.19) (Figure 2a). In MS² analysis, **18** was fragmented in the same manner as **15** and the m/z differences (1 or 2 Da) of three major fragments (m/z values at 199.14, 286.17, and 298.14 for **18**) in two MS² spectra originated from the two ^{13}C atoms in **17** (Supplementary Figure 3). These results demonstrate that NotF is the deoxybrevianamide E (**15**) synthase and catalyzes the key reverse prenylation at C-2 of the indole ring leading to the bicyclo[2.2.2]diazaoctane core during biosynthesis of many fungal alkaloids within this family. In contrast, **16** in *A. fumigatus* is ultimately converted to fumitremorgin following normal prenylation at C-2 by FtmB.[9]

As a next step, the substrate selectivity of NotF was investigated with L-Trp, **17**, cyclo-(L-Phe-L-Pro) **19**, cyclo-(L-Trp-L-Trp) **20**, and cyclo-(L-Trp-L-Tyr) **21** (Supplementary Figure 2). No prenylated products for any of these unnatural substrates were detected by LC-MS analysis. This result provides strong evidence for the early timing and high selectivity of the NotF-catalyzed reaction in the alkaloid biosynthetic pathway (Scheme 2a). Moreover, the structural similarities among **16**, **19**, **20**, and **21** suggested that both amino acid residues in **16**

are critical for selective interactions between the substrate and the NotF reverse prenyltransferase.

Determination of NotC as the 6-Hydroxy-7-prenyl-deoxybrevianamide E Synthase. The role of NotC, the second predicted prenyltransferase from the marine-derived *Aspergillus* sp. MF297−2, was also investigated. Its cDNA was similarly generated by an overlapping PCR strategy and was expressed in *E. coli* (Supplementary Table 1). The recombinant protein was purified with a single Ni-NTA affinity column, and its native protein status was determined as a monomer with an observed molecular weight of 61 kDa (51.1 kDa as the calculated monomeric size) by gel filtration (Supplementary Figure 1).

Stephacidin A (**14**) is a central advanced intermediate featuring a pyran ring but lacking a spiroxindole implicating the mode of assembly and timing of the bicyclo[2.2.2]diazaoctane family of fungal alkaloids.[7,14] We propose that **14** is produced from deoxybrevianamide E (**15**) in a series of reactions, including hydroxylation at C-6 (following **13** numbering system), followed by normal prenylation at C-7, oxidation of the dioxopiperazine ring, IMDA and ring closure to the pyran (Scheme 2a). This hypothesis and the order of these reactions were examined by the determination of NotC activity with four

(14) Qian-Cutrone, J.; Huang, S.; Shu, Y. Z.; Vyas, D.; Fairchild, C.; Menendez, A.; Krampitz, K.; Dalterio, R.; Klohr, S. E.; Gao, Q. *J. Am. Chem. Soc.* **2002**, *124* (49), 14556–7.
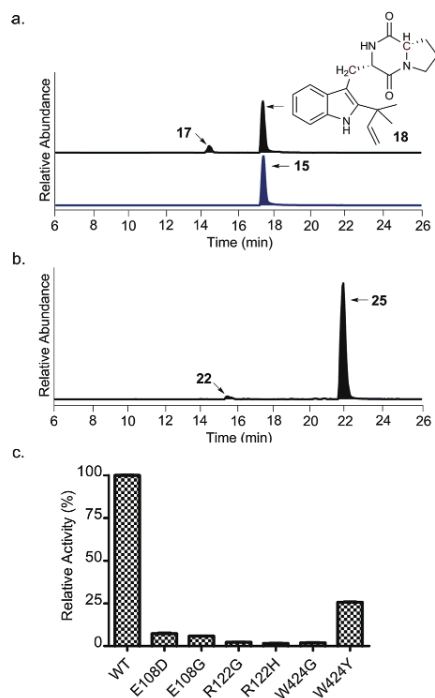
Figure 2. Determination of NotF and NotC prenyltransferase activities. (a) Identification of NotF product (**18**) by LC-MS/MS analysis as described in Methods. (b) Identification of NotC reaction product (**25**) by LC-MS/MS analysis as described in Methods. The product (**25**) was further characterized by ^{1}H and ^{13}C NMR analysis. (c) Investigation of key residues in the reaction of the reverse prenyltransferase NotF by site-directed mutagenesis. Data shown are means ± s.d. from two independent experiments.

structurally related putative substrates, **15**, **22**, **23**, and **24** (Scheme 2a). Compounds **22** and **24** were synthesized according to Supplementary Schemes 1 and Scheme 2, respectively. NotC showed high selectivity toward 6-hydroxy-deoxybrevianamide E (**22**) with three additional substrates failing to be converted to products by the enzyme (Figure 2b). The *m/z* value of the product was 436.17, the same as that of the singly prenylated **22** (calculated MW of 435.25), in MS analysis. Also, three major fragment ions in the MS^2 spectrum of the enzyme product exhibited *m/z* values at 280.20, 368.17, and 380.22 (Supplementary Figure 4). The difference between these and the major ions in MS^2 spectrum of **15** is 84-Da, which is consistent with the MW sum of one oxygen atom and one isoprene unit linked to the indole ring of **15**. We also chemically synthesized notoamide S (6-hydroxy-7-prenyl-deoxybrevianamide E, **25**)[15] as the authentic standard and compared the authentic substance with the NotC product by LC and ^{1}H NMR analyses. Both compounds exhibit the same LC retention time (Supplementary Figure 5) and displayed identical ^{1}H NMR spectra (Supplementary Figure 6). The NotC product was further confirmed to

be notoamide S (**25**)[15] by comparison with **13** (Supplementary Table 2). Chemical shifts of ^{1}H and ^{13}C NMR spectra between the product and **13** were essentially identical with the exception of C-25 and C-27.[6] The significant differences at these two positions reflect the double bond position in the attached isoprene unit and also indicate that the pyran is not formed in **25**. These results demonstrated that NotC catalyzes a normal prenyltransfer reaction at C-7 of the indole aromatic ring system in **22**. Moreover, analysis of NotC substrate selectivity suggests that the biosynthetic pathway of **13** and **14** might not proceed through substrates **23** or **24** (Scheme 2a). Instead, **15** is first hydroxylated at C-6 of the indole ring, and the product **22** is subsequently prenylated at C-7 by NotC to generate **25**, a biosynthetic precursor of both **13** and **14**. Accordingly, notoamide J was isolated from the culture of this marine-derive fungus, and contains only one C-6 (following **13** numbering system) hydroxy group.[16] The precise path from **25** to **14** requires further investigation, although we have demonstrated that stephacidin A (**14**) does not arise directly from notoamide E (**13**), suggesting that generation of the pyran follows formation of the bicyclo[2.2.2]diazaoctane core[6].

Biochemical Characterization of NotF and NotC. Both NotF and NotC tolerated a broad range of temperature (4 to 42 °C for NotF while 16 to 42 °C for NotC) and pH (6.0 to 9.0) (Supplementary Figure 7). Enzyme activity was independent of divalent cation, although addition of 5 mM Mg^{2+}, Ca^{2+} or Mn^{2+} slightly enhanced catalysis (about 100−120%) (Supplementary Figure 8). Significant reduction of enzyme activity (2% − 35%) was observed with Cu^{2+}, Zn^{2+}, Fe^{2+}, or Sn^{2+} (5 mM). Unlike previous observations with a normal aromatic prenyltransferase (MaPT)[17] and CloQ,[18] EDTA caused only minor effects on NotF and NotC activity (remaining 90−95%), possibly indicating that the active-site pocket of both prenyltransferases might be less exposed to solvent. However, the exact mechanism for nonchelating inhibition of this group of metal-independent enzymes by EDTA remains unclear.

The reactions of both NotF and NotC followed Michaelis−Menten kinetics (Supplementary Figure 9). The K_m and V_{max} values for doubly ^{13}C-labeled brevianamide F (**17**) in the NotF reactions were 4.33 ± 0.43 μM and 0.89 ± 0.02 μM/min, respectively, giving a maximal turnover value of 19.1 ± 0.4 min^{-1}. Similarly, the enzyme K_m and V_{max} values for dimethylallyl diphosphate (DMAPP) were 1.31 ± 0.22 μM and 1.18 ± 0.03 μM/min, respectively. Its maximal turnover value (25.3 ± 0.6 min^{-1}) and enzyme catalytic efficiency value (19.31 μM$^{-1}\cdot$min^{-1}) were slightly higher than those of **17** (k_{cat}/K_m = 4.41 μM$^{-1}\cdot$min^{-1}). Compared to FtmB using **16** as a substrate in a normal prenylation step (K_m = 55 μM, k_{cat}/K_m = 6.08 μM$^{-1}\cdot$min^{-1}), NotF showed more restricted substrate selectivity and higher substrate binding affinity with a similar enzyme catalytic efficiency.[19] In addition, we also determined the kinetic parameters for the NotC normal prenyltransferase. The K_m and V_{max} values for **22** in the NotC reactions were 2.64 ± 0.33 μM and 1.30 ± 0.04 μM/min, respectively, while for DMAPP these values were determined to be 1.89 ± 0.20 μM and 1.45 ± 0.03 μM/min, respectively. Similar to NotF, the maximal turnover

(15) McAfoos, T. J.; Li, S.; Tsukamoto, S.; Sherman, D. H.; Williams, R. M. *Heterocycles* **2010**, *82* (1), DOI: 10.3987/COM-10-S(E)19.

(16) Tsukamoto, S.; Kato, H.; Samizo, M.; Nojiri, Y.; Onuki, H.; Hirota, H.; Ohta, T. *J. Nat. Prod.* **2008**, *71* (12), 2064–7.

(17) Ding, Y.; Williams, R. M.; Sherman, D. H. *J. Biol. Chem.* **2008**, *283* (23), 16068–76.

(18) Pojer, F.; Wemakor, E.; Kammerer, B.; Chen, H.; Walsh, C. T.; Li, S. M.; Heide, L. *Proc. Natl. Acad. Sci. U.S.A.* **2003**, *100* (5), 2316–21.

(19) Zou, H.; Zheng, X.; Li, S. M. *J. Nat. Prod.* **2009**, *72* (1), 44–52.

value (67.4 ± 1.4 min^{-1}) and enzyme catalytic efficiency value (35.66 μM$^{-1}\cdot$min^{-1}) of NotC were also slightly higher than those of **22** (60.5 ± 1.9 min^{-1}, 22.92 μM$^{-1}\cdot$min^{-1}, respectively).

In this study, three key amino acid residues located in the predicted NotF reaction pocket were mutated to probe the reaction mechanism of this reverse aromatic prenyltransferase (Supplementary Figure 10). R108 was predicted to be a substitute for the divalent metal ion and to interact with the DMAPP pyrophosphate group. Generation of the R108H and R108G mutants (Supplementary Figure 1a) resulted in proteins with less than 2% catalytic activity, confirming the vital role of R108 for effective catalytic function (Figure 2c). Another highly conserved key residue for substrate binding in NotF is E108, which may form a H-bond with N−H in the **16** indole ring system.[20] Both E108D and E108G mutants lost at least 92% of their activity (Figure 2c). This result suggests that a specific side chain length in this acidic amino acid residue is important for H-bond formation. Recently, the crystal structure of FgaPT2, a normal fungal aromatic prenyltransferase, revealed the presence of a defined network consisting of five Tyr residues to prevent the DMAPP-derived carbocation from reacting adventitiously with nucleophiles.[20] All of these residues are conserved in NotF except Y413, which is replaced with W424 (Supplementary Figure 10). Although W424Y still retained about 25% of its activity for production of **18**, the corresponding W424G lesion resulted in >98% loss of catalytic activity, validating the importance of this analogous aromatic network in the notoamide reverse prenyltransferase reaction (Figure 2c).

Proposed Biosynthetic Pathway for the Stephacidin and Notoamide Biosynthesis in Marine-Derived *Aspergillus* sp. MF297-2. Based on the biochemical characterization of two prenyltransferases and the predicted biochemical function of related gene products in the isolated gene cluster, a putative notoamide biosynthetic pathway is proposed (Scheme 2). Briefly, we presume that **16** is produced from L-Trp and L-Pro by the NotE NRPS and is subsequently reverse prenylated at C-2 by NotF to produce **15**. In the next step, the indole ring is hydroxylated at C-6, which is likely catalyzed by one of the two *not* pathway-encoded P450s. NotC is then responsible for normal prenylation at C-7 position of **22** to produce **25**. From this intermediate, notoamide E (**13**) is generated following ring closure to the pyran, a process possibly controlled by the second P450, and then may be converted into notoamide C (**11**) and notoamide D (**12**).[6] The direct connection from **13** to **14** was not observed in double ^{13}C-labeled precursor incorporation experiments, whereby **13** was previously envisioned to be converted by an oxidase to the pyrazine-derived dienophile followed by IMDA to directly produce stephacidin A (**14**) (Scheme 2a).[6] The enzyme(s) that promote bicyclo[2.2.2]diazaoctane formation remain unknown. Recently, a flavin-dependent oxidase in solanapyrone biosynthesis was shown to catalyze both oxidation and subsequent Diels−Alder cycloaddition reactions,[21] indicating that the predicted oxidoreductases (e.g., NotB, NotD, and NotI) are possible candidates for catalyzing the IMDA reaction in the notoamide biosynthesis. Alternative to the pathway through **13**, **14** may be produced from **25** after the stepwise oxidation, IMDA, and ring closure (Scheme 2a). We propose that **14** is

regiospecifically hydroxylated by a monooxygenase, possibly NotB or NotI, to give **27** for subsequent pinacol-like rearrangement to produce notoamide B (**10**). Such an intriguing rearrangement reaction has not been previously observed in a natural product biosynthetic pathway, and a putative mechanism is proposed (Supplementary Figure 11). A rare *N*-hydroxylation reaction is required to generate the final notoamide A product (**9**) (Scheme 2b). The biosynthetic scheme proposed here provides an initial understanding of the assembly and modification of biosynthetic building blocks for this important group of bioactive prenylated fungal alkaloids.

Discussion

The advent of next-generation sequencing has provided tremendous opportunities to identify novel natural products and their biosynthetic pathways through genome mining of bacterial, fungal,[22] and plant[23] genomes. This approach has proved increasingly important in current natural product biosynthesis studies with the availability of increasing numbers of microbial genome sequences. For example, many orphan biosynthetic gene clusters were identified from the genome sequence of well-studied *Streptomyces coelicolor* A3(2), and novel natural products such as 2-alkyl-4-hydroxymethylfuran-3-carboxylic acids were uncovered with the guidance of genome mining.[24,25] In this study, we employed an allied approach to study the biosynthesis of prenylated indole alkaloids and also to initiate an understanding of fungal genetic evolution and adaptation to different environmental niches. The entire genome of the notoamide-producing marine-derived *Aspergillus* sp. was sequenced at ∼15X coverage, enabling the *not* gene cluster identification through sequence file database comparison to *ftmA* (Figure 1). With this gene cluster it is now possible to pursue studies toward a complete understanding of the assembly, tailoring, and regulation of this family of bioactive fungal alkaloids and to further develop them as medicinal agents.

Fungal aromatic prenyltransferases have attracted increasing interest because of their important roles in the biosynthesis of natural products and potential applications in drug development. Currently, more than 100 putative indole prenyltransferases have been revealed by BLAST searches in the public genome database.[26] Biochemical investigations of over 10 recombinant enzymes in this group finds that catalytic functions are independent of divalent metal ions.[26,27] In these reactions, an isoprene unit can be transferred onto different positions of the indole ring system.[27] Moreover, in a normal prenylation reaction, DMAPP alkylates an aromatic substrate through its C1′ atom via an S_N2 displacement, while the C3′ position is involved in the reverse prenyltransfer reaction via an $S_N2′$ displacement. Remarkably, these enzymes can utilize a series of structurally similar analogs as their aromatic substrates.[17,27,28] In contrast to other characterized enzymes in this group, NotF (reverse) and NotC (normal) prenyltransferases showed highly restricted substrate specificities. NotF specifically prenylates **16** (at C-2),

(20) Metzger, U.; Schall, C.; Zocher, G.; Unsold, I.; Stec, E.; Li, S. M.; Heide, L.; Stehle, T. *Proc. Natl. Acad. Sci. U.S.A.* **2009**, *106* (34), 14309–14.

(21) Kasahara, K.; Miyamoto, T.; Fujimoto, T.; Oguri, H.; Tokiwano, T.; Oikawa, H.; Ebizuka, Y.; Fujii, I. *ChemBioChem* **2010**, *11* (9), 1245–52.

(22) Corre, C.; Challis, G. L. *Nat. Prod. Rep.* **2009**, *26* (8), 977–86.

(23) Lodeiro, S.; Xiong, Q.; Wilson, W. K.; Kolesnikova, M. D.; Onak, C. S.; Matsuda, S. P. *J. Am. Chem. Soc.* **2007**, *129* (36), 11213–22.

(24) Corre, C.; Song, L.; O'Rourke, S.; Chater, K. F.; Challis, G. L. *Proc. Natl. Acad. Sci. U.S.A.* **2008**, *105* (45), 17510–5.

(25) Bentley, S. D.; et al. *Nature* **2002**, *417* (6885), 141–7.

(26) Li, S. M. *Appl. Microbiol. Biotechnol.* **2009**, *84* (4), 631–9.

(27) Steffan, N.; Grundmann, A.; Yin, W. B.; Kremer, A.; Li, S. M. *Curr. Med. Chem.* **2009**, *16* (2), 218–31.

(28) Balibar, C. J.; Howard-Jones, A. R.; Walsh, C. T. *Nat. Chem. Biol.* **2007**, *3* (9), 584–92.

confirming its role as the elusive deoxybrevianamide E synthase, while only **22** is utilized by NotC (C-7 alkylation) in the biosynthesis of the stephacidin and notoamides (Figure 2). The mechanism of the reverse prenyltransferase was also probed by site-directed mutagenesis to understand the reaction of this group of enzymes.[17,20] Future structural studies of NotF and the comparison to FgaPT2[20] are expected to contribute further information about the regio- and stereospecificity of the reverse and normal prenyltransfer reactions. We expect this analysis will likely illuminate the lack of facial selectivity previously observed for the reverse prenylation step[29] and facilitate expansion of the enzyme substrate range and efficiency. More importantly, the combined studies of NotF and NotC provide direct evidence to establish a biosynthetic scheme for this family of bioactive prenylated fungal alkaloids. Finally, the high *in vitro* catalytic efficiencies of recombinant NotF and NotC suggest their potential value as biocatalysts for chemoenzymatic production of bioactive fungal alkaloid analogs in drug development.

Identification and characterization of the notoamide gene cluster also provides the initial basis to understand the formation of three pairs of antipodal natural products derived from a marine-derived and a terrestrial *Aspergillus* sp.[30,31] In the marine-derived fungal strain, (−)-notoamide B (**10**), (−)-versicolamide B (**38**), and (+)-stephacidin A (**14**) are produced,[7,30] while their antipodal counterparts, **39**, **40**, and **41**, respectively, are isolated from the terrestrial *A. versicolor* NRRL 25660 strain (Supplementary Figure 12).[31] Based on the putative notoamide biosynthetic pathway, we propose that formation of **14** and **41** might be controlled by the IMDA reaction. Subsequently, **10** and **39** are possibly derived from **14** and **41**, respectively, in these two distinct fungal strains. It remains unclear whether generation of (−)- and (+)-versicolamide B (**38** and **40**) occurs in the pathway through stephacidin A due to their opposite stereogenic centers at C-6 (Supplementary Figure 12).[30] Instead, **13** might be converted into **11**, subsequently producing **38** in the following IMDA reaction in the marine-derived fungus.[30] The detailed biochemical characterization of biosynthetic enzymes from both fungal strains is in progress and will shed more light on the biosynthesis of these unique antipodal natural products.

Identification of biocatalysts from fungal alkaloid biosynthetic pathways may also enable production of natural products and their analogs through heterologous expression and metabolic engineering.[32−34] It is estimated that >99% of microorganisms in the environment fail to grow in the laboratory, and the potential to find pharmaceutically important natural products from fungal sources remains vastly underexplored. Introducing natural product gene clusters into more technically and industrially amenable microorganisms such as *E. coli* and yeast represents an attractive way to obtain suitable quantities of natural products and to identity novel leads in drug discovery and development programs.[34] Moreover, a microorganism can

be further optimized for the efficient production of a target metabolite using traditional mutation and selection methods, as well as new tools from systems biology and synthetic biology.[35] Identification of the notoamide gene cluster provides such an opportunity to produce bioactive fungal alkaloids and analogs thereof through pathway engineering and heterologous expression.

Methods

Materials and Strains. Authentic deoxybrevianamide E (**15**), doubly ^{13}C-labeled brevianamide F (**17**), and keto-premalbranchea-mide (**23**) were synthesized following previously published procedures.[4,36] Standard methods for DNA isolation and manipulation were performed as described by Sambrook et al.[37] Genomic DNA from *Aspergillus* MF297-2 was isolated with a MasterPure Yeast DNA Purification kit (Epicenter Biotechnologies) as described in the manual. The GenBank accession numbers for *notC*, *notF*, and the complete assembled *not* gene cluster are GU564534, GU564535, and HM622670, respectively. *E. coli* DH5α was used for cloning and plasmid harvesting while *E. coli* BL21 CodonPlus-(DE3)-RIPL was used for protein overexpression.

Expression and Purification of NotC and NotF. Details about the preparation of *notC* and *notF* cDNAs and of *notF* mutant DNAs are included in the Supporting Information and Supplementary Table 1. The expressed enzymes were purified with a single Ni-NTA column (Supporting Information). As determined by SDS-PAGE analysis, the purity of proteins was more than 90%. The native status of proteins was determined by gel filtration (Supplementary Figure 1).

Determination of Enzyme Activities. Compounds **22** and **24** were chemically synthesized to examine NotC activity (Supporting Information). The 100-μL reaction mixture contained 0.5 μg of NotF, its mutants, or NotC; 5 mM MgCl$_2$; 0.1 mM **17** (NotF or its mutants) or **22** (NotC); and 0.15 mM DMAPP in the reaction buffer (50 mM Tris-Cl, pH 7.5, 10% glycerol, and 3 mM β-mercapto-ethanol). The reaction was initiated by adding enzyme after prewarming the other components at room temperature for 1 min. After mixing well and briefly centrifuging, the reactions were further incubated at room temperature for 45−60 min and stopped with 10 μL of 1.5 M trichloroacetic acid. The mixtures were mixed and centrifuged at 13 000*g* for 5 min. An aliquot of the 100-μL solution was subjected to HPLC coupled with an XBridge C18 column (5 μm, 4.6 mm × 250 mm), at a wavelength of 222 nm. Solvent B (acetonitrile in 0.1% TFA) was increased from 30% to 40% for 5 min and then increased to 80% over 20 min for the detection of products. LC-MS[2] analysis was performed by using a ThermoFinni-gan LTQ linear ion-trap instrument equipped with an electrospray source and a Surveyor HPLC system at room temperature. Separations were performed with an XBridge C18 (3.5 μm, 2.1 mm × 150 mm) column at a flow rate of 200 μL/min with solvent A (water with 0.1% formic acid) and solvent B (acetonitrile with 0.1% formic acid). Solvent B was kept at 2% in solvent A for 4 min and then was gradually increased to 90% over 16 min. After being washed with 90% solvent B for 2 min, the column was further re-equilibrated with 2% solvent B for 10 min. The spectra were recorded in positive ion mode. Product **25** was further characterized with ^{1}H and ^{13}C NMR analysis (Supporting Information).

Kinetics Analysis. The 100-μL reaction mixture contained 0.25 μg of NotF or 0.11 μg of NotC and 5 mM MgCl$_2$ in the reaction buffer. Details about the experiment procedures were included in the Supporting Information. All experiments were performed in duplicate. The data were fit to the Michaelis−Menten equation in Prism 4.0 (GraphPad Software).

(29) Stocking, E. M.; Sanz-Cervera, J. F.; Williams, R. M. *Angew. Chem., Int. Ed.* **1999**, *38* (6), 786–9.
(30) Tsukamoto, S.; Kawabata, T.; Kato, H.; Greshock, T. J.; Hirota, H.; Ohta, T.; Williams, R. M. *Org. Lett.* **2009**, *11* (6), 1297–300.
(31) Greshock, T. J.; Grubbs, A. W.; Jiao, P.; Wicklow, D. T.; Gloer, J. B.; Williams, R. M. *Angew. Chem., Int. Ed.* **2008**, *47* (19), 3573–7.
(32) Chemler, J. A.; Koffas, M. A. *Curr. Opin. Biotechnol.* **2008**, *19* (6), 597–605.
(33) Wenzel, S. C.; Muller, R. *Curr. Opin. Biotechnol.* **2005**, *16* (6), 594–606.
(34) Zhang, H.; Wang, Y.; Pfeifer, B. A. *Mol. Pharm.* **2008**, *5* (2), 212–25.

(35) Lee, S. Y.; Kim, H. U.; Park, J. H.; Park, J. M.; Kim, T. Y. *Drug Discovery Today* **2009**, *14* (1−2), 78–88.
(36) Miller, K. A.; Welch, T. R.; Greshock, T. J.; Ding, Y.; Sherman, D. H.; Williams, R. M. *J. Org. Chem.* **2008**, *73* (8), 3116–9.
(37) Sambrook, J.; Russel, D. W. *Molecular Cloning - A Laboratory Manual*, 3rd ed.; Cold Spring Harbor Laboratory Press: New York, 2001.

373

Supporting Information Available: Remaining methods, including genome sequencing and assembly, assay for enzyme metal independence, detailed synthetic procedures of **22** and **24**, determination of enzyme optimal conditions, characterization of **25**, antipodal fungal prenylated alkaloids, and the complete list of authors in ref 25. This material is available free of charge via the Internet at http://pubs.acs.org.

JA1049302

Synthesis of Notoamide J: A Potentially Pivotal Intermediate in the Biosynthesis of Several Prenylated Indole Alkaloids

Jennifer M. Finefield and Robert M. Williams*

Department of Chemistry, Colorado State University, Fort Collins, Colorado 80523

rmw@lamar.colostate.edu
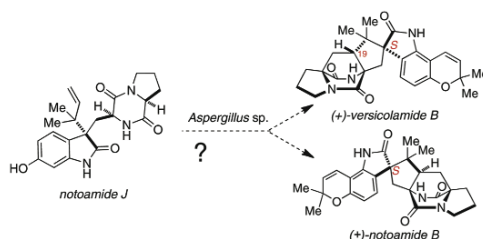
An efficient total synthesis of notoamide J, a new prenylated indole alkaloid and potential biosynthetic precursor, is described herein. Starting from L-proline and a substituted tryptophan derivative, this synthesis also employs an oxidation and pinacol rearrangement for the formation of the oxindole in the final step.

Introduction

Over the past decade, our laboratory has extensively studied the biosynthesis of naturally occurring prenylated indole alkaloids,[1] specifically the paraherquamides,[2] brevianamides,[3] notoamides,[4] and stephacidins,[5] among others. These families of secondary metabolites have been isolated from various fungi of the genera *Aspergillus* and *Penicillium* and have exhibited a wide range of biological activity, including insecticidal, antitumor, anthelmintic, and antibacterial activity.[6] Their desirable biological activity, as well as the complex amino acid skeleton[7] and bicyclo[2.2.2]diazaoctane ring, makes these prenylated indole alkaloids attractive targets for total synthesis.[8]

Over the past several years, the number of new prenylated indole alkaloids isolated from fungi of both marine and terrestrial origin has greatly increased. Recently, Tsukamoto and co-workers isolated notoamide J (1),[4b] one of six novel secondary metabolites, from a marine-derived *Aspergillus*

(1) (a) Williams, R. M. *Chem. Pharm. Bull.* **2002**, *50*, 711–740. (b) Williams, R. M.; Cox, R. J. *Acc. Chem. Res.* **2003**, *36*, 127–139. (c) Stocking, E. M.;Sanz-Cervera, J. F.; Williams, R. M. *Angew. Chem.* **2001**, *113*, 1336–1338; *Angew. Chem., Int. Ed.* **2001**, *40*, 1296–1298.

(2) (a) Yamazaki, M.; Okuyama, E.; Kobayashi, M.; Inoue, H. *Tetrahedron Lett.* **1981**, *22*, 135–136. (b) Ondeyka, J. G.; Goegelman, R. T.; Schaeffer, J. M.; Kelemen, L.; Zitano, L. *J. Antibiot.* **1990**, *43*, 1375–1379. (c) Liesch, J. M.; Wichmann, C. F. *J. Antibiot.* **1990**, *43*, 1380–1386. (d) Banks, R. M.; Blanchflower, S. E.; Everett, J. R.; Manger, B. R.; Reading, C. *J. Antibiot.* **1997**, *50*, 840–846.

(3) (a) Birch, A. J.; Wright, J. J. *Tetrahedron* **1970**, *26*, 2329. (b) Birch, A. J.; Wright, J. J. S. *J. Chem. Soc., Chem. Commun.* **1969**, 644–645. (c) Birch, A. J.; Russell, R. A. *Tetrahedron* **1972**, *28*, 2999.

(4) (a) Kato, H.; Yoshida, T.; Tokue, T.; Nojiri, Y.; Hirota, H.; Ohta, T.; Williams, R. M.; Tsukamoto, S. *Angew. Chem., Int. Ed.* **2007**, *46*, 2254–2256. (b) Tsukamoto, S.; Kato, H.; Samizo, M.; Nojiri, Y.; Onuki, H.; Hirota, H.; Ohta, T. *J. Nat. Prod.* **2008**, *71*, 2064–2067. (c) Greshock, T. J.; Grubbs, A. W.; Jiao, P.; Wicklow, D. T.; Gloer, J. B.; Williams, R. M. *Angew. Chem., Int. Ed.* **2008**, *47*, 3573–3577. (d) Tsukamoto, S.; Kato, H.; Greshock, T. J.; Hirota, H.; Ohta, T.; Williams, R. M. *J. Am. Chem. Soc.* **2009**, *131*, 3834–3835. (e) Tsukamoto, S.; Kawabata, T.; Kato, H.; Greshock, T. J.; Hirota, H.; Ohta, T.; Williams, R. M. *Org. Lett.* **2009**, *11*, 1297–1300.

(5) (a) Qian-Cutrong, J.; Huang, S.; Shu, Y.-Z.; Vyas, D.; Fairchild, C.; Menendez, A.; Krampitz, K.; Dalterio, R.; Klohr, S. E.; Gao, Q. *J. Am. Chem. Soc.* **2002**, *124*, 14556–14557. (b) Kato, H.; Yoshida, T.; Tokue, T.; Nojiri, Y.; Hirota, H.; Ohta, T.; Williams, R. M.; Tsukamoto, S. *Angew. Chem., Int. Ed.* **2007**, *46*, 2254–2256.

(6) (a) Qian-Cutrong, J.; Krampitz, K. D.; Shu, Y.-Z.; Chang, L.-P.; Lowe, S. E. U.S. Patent 6,291,461. (b) Blanchflower, S. E.; Banks, R. M.; Everett, J. R.; Manger, B. R.; Reading, C. *J. Antibiot.* **1991**, *44*, 492–497. (c) Whyte, A. C.; Gloer, J. B.; Wicklow, D. T.; Dowd, P. F. *J. Nat. Prod.* **1996**, *59*, 1093–1095.

(7) (a) Williams, R. M.; Stocking, E. M.; Sanz-Cervera, J. F. *Top. Curr. Chem.* **2000**, *209*, 98–173. (b) Stocking, E. M.; Sanz-Cervera, J. F.; Unkefer, C. J.; Williams, R. M. *Tetrahedron* **2001**, *57*, 5303.

(8) (a) Grubbs, A. W.; Artman, G. D., III; Williams, R. M. *Tetrahedron Lett.* **2005**, *46*, 9013–9016. (b) Grubbs, A. W.; Artman, G. D., III; Tsukamoto, S.; Williams, R. M. *Angew. Chem., Int. Ed.* **2007**, *46*, 2257–2261. (c) Miller, K. A.; Welch, T. R.; Greshock, T. J.; Ding, Y.; Sherman, D. H.; Williams, R. M. *J. Org. Chem.* **2008**, *73*, 3116–3119.

SCHEME 1. **Possible Biogenetic Relationships via Notoamide J**
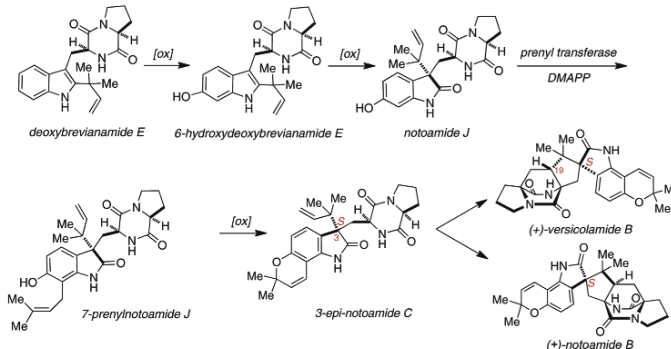
SCHEME 2. **Retrosynthetic Plan**
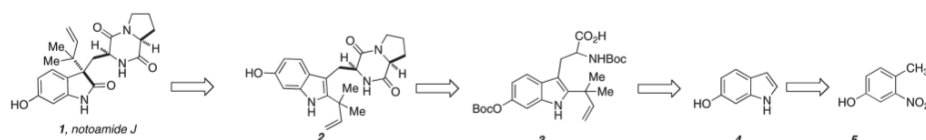
sp. that was collected in the Sea of Japan off the Noto Peninsula. Like the rest of the notoamides, **1** contains both tryptophan and proline, as well as an isoprene unit; however, this natural product lacks the bridged bicyclo[2.2.2]diazaoctane ring system, a distinguishing characteristic observed in many of the prenylated indole alkaloids such as the paraherquamides and brevianamides. Notoamide J also lacks the pyranoindole ring system often found in the notoamides, norgeamides,[9] and stephacidins. However, notoamide J does contain two notable structural features, both of which may allow **1** to serve as an advanced intermediate along the biosynthetic pathway to other notoamides. First, notoamide J is only one of a handful of metabolites to contain an oxindole ring system, in which one could envision the oxindole moiety to serve as a biosynthetic precursor to the numerous natural products containing the spiro-oxindole ring system. Notoamide J is unique among the alkaloids in these families of natural products as it displays substitution only at the C-6 position of the indole. This feature allows one to envisage that the unsubstituted hydroxy group at this position could lead to the biosynthetic formation of the pyranoindole ring system. These two structural characteristics provide provocative hints that notoamide J could be a biosynthetic precursor to notoamide B and/or versicolamide B. A possible series of biogenetic relationships between notoamide J and the more advanced metabolites (+)-versicolamide B and (+)-notoamide B are illustrated in

Scheme 1. It is reasonably assumed that notoamide J is fashioned from the common biosynthetic precursor, deoxybrevianamide E by aromatic hydroxylation at the 6-position of the indole ring. A subsequent oxidation and pinacol-type rearrangement furnishes the oxindole notoamide J. Subsequent prenylation of notoamide J at the C-7 position yields 7-prenylnotoamide J that would serve as the key precursor for biosynthetic construction of the pyran ring system, yielding 3-*epi*-notoamide C, a natural metabolite identified by Tsukamoto and co-workers. Final oxidation of 3-*epi*-notoamide C to an azadiene and intramolecular Diels−Alder cycloaddition could, in principle, lead to (+)-versicolamide B and/or (+)-notoamide B. The former conversion has recently been experimentally verified by this laboratory.[10]

As part of our program aimed at the elucidation of the entire notoamide/stephacidin biosynthetic pathway, we desired a synthesis of notoamide J that was readily amenable to the incorporation of stable isotopes from which probe substrates could be interrogated. We report here the first synthesis of notoamide J which also serves to corroborate the structural assignment recently published by Tsukamoto and co-workers.

Following established chemistry deployed in our laboratory,[8] we planned notoamide J arising from an oxidation and pinacol rearrangement of **2** (Scheme 2). The dioxopiperazine **2** could be obtained by coupling and cyclizing L-proline ethyl ester with the reverse prenylated tryptophan derivative **3**, which we could easily obtain from 6-hydroxyindole **4**.

(9) The structures of the norgeamides were published via the internet detailing the research performed by the Hans-Knöll Institute. See: http://www.hki-jena.de/index.php.

(10) Miller, K. A.; Tsukamoto, S.; Williams, R. M. *Nat. Chem.* **2009**, *1*, 63–68.

SCHEME 3.   Leimgruber−Batcho Synthesis of Indole 4
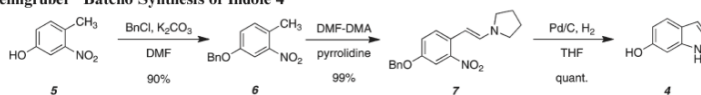
SCHEME 4.   Synthesis of the Reverse Prenylated Tryptophan Derivative 13
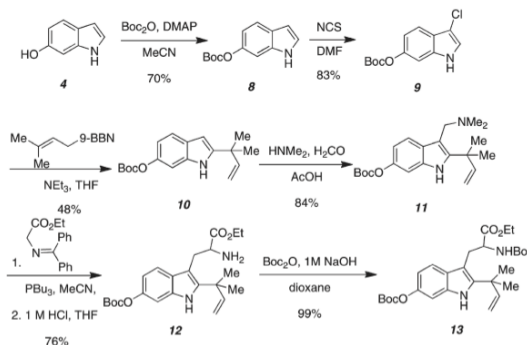
SCHEME 5.   Assembly of Notoamide J
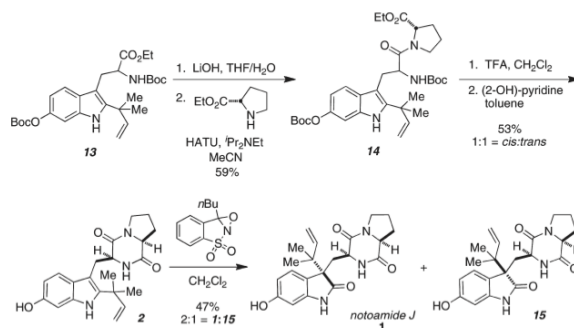
Formation of **4** could be achieved from **5** following the Leimgruber−Batcho protocol.[11]

Results and Discussion

Following a modified Leimgruber−Batcho indole synthesis (Scheme 3), commercially available nitrophenol was readily converted to the desired 6-hydroxyindole. 4-Methyl-3-nitrophenol (**5**) was first protected as benzyl ether **6**, followed by condensation of the nitrotoluene with *N,N*-dimethylformamide dimethyl acetal and pyrrolidine to afford **7**. Reductive cyclization and benzyl deprotection using hydrogenation were achieved in one step to yield the desired 6-hydroxyindole (**4**).

Following Boc protection of the 6-hydroxyindole (Scheme 4), formation of the C-2 reverse prenylated indole was carried out following the excellent procedure established by Danishefsky and co-workers.[12] The C-3 indole position of **8** was chlorinated using NCS in DMF to afford **9**, which was treated with prenyl-9-BBN in the presence of NEt$_3$ to yield the reverse prenylated indole **10**. Pure **10** was obtained in 48% yield due to the complication of removing excess 9-BBN from the reaction mixture. The gramine **11** was formed by treatment of **10** with dimethylamine and formaldehyde, which was coupled with the benzophenone imine of glycine by a modified Somei−Kametani coupling protocol.[13] Imine

(11) Batcho, A. D.; Leimgruber, W. *Org. Synth.* **1985**, *63*, 214.

(12) Schkeryantz, J. M.; Woo, J. C. G.; Siliphaivanh, P.; Depew, K. M.; Danishefsky, S. J. *J. Am. Chem. Soc.* **1999**, *121*, 11964.

377

hydrolysis afforded the tryptophan derivative **12**, which was readily converted to the corresponding N-Boc carbamate **13**.

Following standard saponification conditions of **13**, the N-Boc acid was achieved in good yield, which was subsequently coupled with L-proline ethyl ester in the presence of HATU and DIPEA to provide the amide **14** (Scheme 5). Treatment of **14** with TFA removed both Boc protecting groups to afford the free amine, which was subsequently cyclized with 2-hydroxypyridine to provide both the _cis-_ and _trans-_dioxopiperazines **2** as a 1:1 ratio, which were readily separated by column chromatography.

Completion of the synthesis required the treatment of the _cis_-dioxopiperazine **2** with excess Davis oxaziridine[14] to afford a 2:1 ratio of notoamide J and 3-_epi_-notoamide J, which were readily separable by chromatography. Synthetic **1** was identical to the natural product in all respects (¹H, ¹³C, HRMS, CD).[4b]

In summary, the first total synthesis of notoamide J was completed in 15 steps and 0.78% overall yield. Research is currently underway to establish both the biosynthesis of notoamide J and its role in the biosynthetic pathway of notoamide B and versicolamide B. The synthesis recorded here allows for easy access to isotopomers of notoamide J, which allow us to interrogate the potential role of this species as a potential biosynthetic precursor to more complex natural congeners. Work along these lines is in progress and will be reported on in due course.

Experimental Section

¹H and ¹³C spectra were obtained using 300 or 400 MHz spectrometers. The chemical shifts are given in parts per million (ppm) relative to TMS at δ 0.00 ppm or to residual CDCl₃ δ 7.26 ppm for proton spectra and relative to CDCl₃ at δ 77.23 ppm for carbon spectra. IR spectra were recorded on an FT-IR spectrometer as thin films. Mass spectra were obtained using a high/low-resolution magnetic sector mass spectrometer. Flash column chromatography was performed with silica gel grade 60 (230−400 mesh). Unless otherwise noted, materials were obtained from commercially available sources and used without further purification. Dichloromethane (CH₂Cl₂), tetrahydrofuran (THF), toluene (PhMe), _N,N_-dimethylformamide (DMF), acetonitrile (CH₃CN), triethylamine (Et₃N), and methanol (MeOH) were all degassed with argon and passed through a solvent purification system containing alumina or molecular sieves.

(_E_)-4-Benzyloxy-2-nitro-β-pyrrolidinostyrene **7** was synthesized by a known method established within the literature.[11] Compounds **9** and **10** were synthesized via literature methods.[8a]

tert-**Butyl 1_H_-indol-6-yl carbonate (8):** Enamine **7** (24.3 g, 74.9 mmol) was combined with 10% Pd/C (2.43 g) and dissolved in THF (250 mL). The reaction mixture was stirred under H₂ at 40 psi for 2 h. The reaction mixture was filtered through a pad of silica gel, and the catalyst was washed with diethyl ether. The filtrate was concentrated, and crude **4** was immediately taken up in acetonitrile (150 mL) and cooled to 0 °C. Di-_tert_-butyl dicarbonate (14.7 g, 67.4 mmol) and a catalytic amount of DMAP were added, and the reaction mixture was stirred for 2 h at room temperature. The reaction was concentrated and purified via flash column chromatography in 95:5 hexanes/ethyl acetate. The product was collected as a white solid in 70% yield

(12.2 g): white crystalline solid (mp 141−143 °C); ¹H NMR (300 MHz, CDCl₃) δ 8.16 (br s, 1H), 7.60 (d, _J_ = 8.4 Hz, 1H), 7.21 (m, 1H), 7.18 (t, _J_ = 5.7 Hz, 1H), 6.93 (dd, _J_ = 8.7, 2.1 1H), 6.52 (m, 1H), 1.58 (s, 9H); ¹³C NMR (75 MHz, CDCl₃) δ 153.0, 147.0, 135.7, 126.0, 125.2, 121.2, 114.2, 104.0, 102.7, 83.5, 28.0; IR (neat) 3413, 2981, 1738, 1457, 1395, 883, 722 cm⁻¹; HRMS (ESI/APCI) calcd for C₁₃H₁₅NO₃Na (M + Na) 256.0944, found 256.0944.

tert-**Butyl-3-((dimethylamino)methyl)-2-(2-methylbut-3-en-2-yl)-1_H_-indol-6-yl carbonate (11):** Aqueous formaldehyde (1.26 mL, 15.5 mmol) was diluted with glacial acetic acid (35 mL). Aqueous dimethylamine (6.5 mL, 58.5 mmol) was added, followed by addition of indole **10** (4.15 g, 13.7 mmol) diluted in glacial acetic acid (10 mL). The reaction mixture was stirred at room temperature for 14 h. The reaction mixture was diluted with 1 M NaOH to a pH > 10. The aqueous layer was extracted with diethyl ether, and the combined organic layer was dried over Na₂SO₄ and concentrated to afford 4.14 g (84%) of an amber oil that was taken on to the next reaction without further purification: ¹H NMR (300 MHz, CDCl₃) δ 7.99 (br s, 1H), 7.62 (d, _J_ = 8.7 Hz, 1H), 7.08 (d, _J_ = 2.1 Hz, 1H), 6.87 (dd, _J_ = 8.4, 2.1 Hz, 1H), 6.12 (dd, _J_ = 17.7, 11.1 Hz, 1H), 5.16 (dd, _J_ = 6.0, 0.9 Hz, 1H), 5.12 (d, _J_ = 0.3 Hz, 1H), 3.55 (s, 2H), 2.19 (s, 6H), 1.56 (s, 9H), 1.53 (s, 6H); ¹³C NMR (100 MHz, CDCl₃) δ 152.9, 146.5, 146.3, 142.0, 133.7, 128.6, 119.7, 113.4, 112.32, 109.0, 103.1, 83.3, 54.1, 45.5, 39.6, 28.0, 27.3; IR (neat) 3385, 2933, 1734, 1466, 1142, 1013, 886 cm⁻¹; HRMS (ESI/APCI) calcd for C₂₁H₃₁N₂O₃ (M + H) 359.2329, found 359.2324.

Ethyl 2-amino-3-(6-((_tert_-butoxycarbonyl)oxy)-2-(2-methyl-but-3-en-2-yl)-1_H_-indol-3-yl)propanoate (12): Gramine **11** (4.14 g, 11.5 mmol), _N_-(diphenylmethylene)glycine ethyl ester (2.80 g, 10.5 mmol), tributylphosphine (850 μL, 4.2 mmol), and acetonitrile (53 mL) were combined and stirred for 20 h at reflux under Ar. The reaction was concentrated and purified via flash column chromatography in 10% ethyl acetate in hexanes to afford 2.76 g of a yellow amorphous solid, which was dissolved in THF (36 mL). Then, 1 M HCl (12.0 mL) was added, and the reaction mixture was stirred for 30 min at room temperature. The solvent was removed under reduced pressure, and the residue was rediluted with saturated aqueous NaHCO₃ until basic. The mixture was extracted with CH₂Cl₂ (2 times), dried over Na₂SO₄, and concentrated. The crude residue was purified by flash column chromatography (3:1 hexanes/ethyl acetate; 5:95 MeOH/CH₂Cl₂) to give 1.51 g (76%) of **12** as a yellow oil: ¹H NMR (300 MHz, CDCl₃) δ 8.44 (br s, 1H), 7.43 (d, _J_ = 8.7 Hz, 1H), 7.05 (d, _J_ = 1.8 Hz, 1H), 6.83 (dd, _J_ = 8.7, 2.1 Hz, 1H), 6.00 (dd, _J_ = 17.7, 10.2 Hz, 1H), 5.07−5.01 (m, 2H), 4.12−4.00 (m, 2H), 3.75 (dd, _J_ = 9.6, 5.1 Hz, 1H), 3.22 (dd, _J_ = 14.4, 4.8 Hz, 1H), 2.95 (dd, _J_ = 14.4, 9.6 Hz, 1H), 1.53 (s, 9H), 1.42 (s, 6H), 1.12 (t, _J_ = 6.9 Hz, 3H); ¹³C NMR (75 MHz, CDCl₃) δ 175.6, 153.1, 146.5, 146.1, 141.6, 134.2, 127.9, 119.0, 113.3, 112.0, 106.8, 103.7, 83.4, 61.0, 56.1, 39.3, 31.3, 27.9, 27.8, 14.4, 14.2; IR (neat) 3389, 2977, 1734, 1465, 1243, 1143, 885 cm⁻¹; HRMS (ESI/APCI) calcd for C₂₃H₃₃N₂O₅ (M + H) 417.2384, found 417.2388.

Ethyl 2-((_tert_-butoxycarbonyl)amino)-3-(6-((_tert_-butoxycarbonyl)-oxy)-2-(2-methylbut-3-en-2-yl)-1_H_-indol-3-yl)propanoate (13): Boc₂O (824 mg, 3.78 mmol) and 1 M NaOH (3.60 mL, 3.60 mmol) were added to a solution of amine **12** (1.50 g, 3.60 mmol) in dioxane (18 mL). The reaction mixture stirred at room temperature for 1 h and then concentrated under reduced pressure to remove the dioxane. The resulting slurry was taken up in H₂O, acidified to pH 2 with 1 M KHSO₄, and extracted with EtOAc (3 × 50 mL). The combined organic layers were dried over Na₂SO₄ and concentrated under reduced pressure to afford 1.85 g of **13** as a yellow amorphous solid that was used without further purification: ¹H NMR (300 MHz, CDCl₃) δ 8.11 (br s, 1H), 7.42 (d, _J_ = 8.7 Hz, 1H), 7.06 (s, 1H), 6.86 (d, _J_ = 8.4 Hz, 1H), 6.07 (dd, _J_ = 17.7, 10.5 Hz, 1H), 5.17−5.06 (m, 3H), 4.49 (m, 1H), 4.05−3.90 (m, 2H), 3.28−3.12 (m, 2H), 1.55

(13) (a) Somei, M.; Karasawa, Y.; Kaneko, C. _Heterocycles_ **1981**, _16_, 941. (b) Kametani, T.; Kanaya, N.; Ihara, M. _J. Chem. Soc., Perkin Trans. 1_ **1981**, 959.

(14) (a) Davis, F. A.; Townson, J. C.; Vashi, D. B.; Thimma Reddy, R.; McCauley, J. P.; Harakal, M. E.; Gosciniak, D. _J. Org. Chem._ **1990**, _55_, 1254−1261. (b) Snider, B. B.; Zeng, H. _J. Org. Chem._ **2003**, _68_, 545−563.

(s, 9H), 1.52 (s, 9H), 1.32 (s, 6H), 1.02 (t, J = 6.9 Hz, 3H); ^{13}C NMR (75 MHz, CDCl$_3$) δ 173.1, 152.8, 146.7, 146.0, 141.4, 134.0, 128.0, 119.0, 113.5, 112.4, 106.1, 103.4, 83.3, 79.8, 61.4, 54.8, 39.4, 28.4, 28.0, 27.8, 27.6, 14.4, 14.0; IR (neat) 3388, 2979, 1755, 1464, 1369, 1143 cm^{-1}; HRMS (ESI/APCI) calcd for C$_{28}$H$_{40}$N$_2$O$_7$Na (M + Na) 539.2728, found 539.2727.

(2*S*)-Ethyl-1-(2-((*tert*-butoxycarbonyl)amino)-3-(6-((*tert*-butoxycarbonyl)oxy)-2-(2-methylbut-3-en-2-yl)-1*H*-indol-3-yl)propanoyl)-pyrrolidine-2-carboxylate (14): The ethyl ester tryptophan derivative **13** (1.85 g, 3.60 mmol) was dissolved in 2:1 H$_2$O/THF (36 mL), and LiOH (826 mg, 36.0 mmol) was added. The reaction mixture was stirred at room temperature for 20 h. The solvent was removed under reduced pressure, and the resulting slurry was taken up in H$_2$O, acidified to pH 2 with 1 M KHSO$_4$, and extracted with CH$_2$Cl$_2$ (2 × 50 mL) and EtOAc (2 × 50 mL). The combined organic layers were dried over Na$_2$SO$_4$ and concentrated under reduced pressure. The resulting crude residue was dissolved in acetonitrile (30 mL), and L-proline ethyl ester (426 mg, 2.98 mmol) was added. HATU (1.70 g, 4.47 mmol) and ^{i}Pr$_2$NEt (2.0 mL, 11.9 mmol) were added, and the reaction mixture was stirred for 3 h at room temperature. The reaction was quenched with 1 M HCl (40 mL) and extracted with CH$_2$Cl$_2$ (3 × 75 mL). The combined organic layers were dried over Na$_2$SO$_4$ and concentrated under reduced pressure. The crude residue was purified by flash column chromatography and eluted with 3:1 hexanes/EtOAc to afford 1.08 g (59%) of **14** as a yellow amorphous solid: ^{1}H NMR (300 MHz, CDCl$_3$) δ 8.35 (m, 1H), 7.48−6.74 (m, 3H), 6.04 (m, 1H), 5.52 (m, 1H), 5.15−5.06 (m, 2H), 4.62−1.98 (m, 9H), 1.51−1.12 (m, 30H); ^{13}C NMR (75 MHz, CDCl$_3$) δ 172.1, 171.3, 154.9, 152.7, 146.6, 145.3, 141.6, 133.6, 127.8, 119.2, 119.1, 113.4, 112.6, 106.0, 103.4, 83.2, 79.4, 61.1, 60.6, 59.3, 53.1, 46.6, 39.2, 28.5, 27.9, 27.4, 14.4, 14.3; IR (neat) 3351, 2979, 1753, 1634, 1497, 1450, 1143 cm^{-1}; HRMS (ESI/APCI) calcd for C$_{33}$H$_{48}$N$_3$O$_8$ (M + H) 614.3436, found 614.3434.

(3*S*,8a*S*)-3-((6-Hydroxy-2-(2-methylbut-3-en-2-yl)-1*H*-indol-3-yl)methyl)-hexahydropyrrolo[1,2-*a*]pyrazine-1,4-dione (2): TFA (0.6 M) was added to a solution of **14** (1.08 g, 1.76 mmol) in CH$_2$Cl$_2$ (0.6 M) at 0 °C. The reaction stirred for 3 h at room temperature. The mixture was quenched with saturated NaHCO$_3$ to pH 10 and extracted with EtOAc (3 × 20 mL). The combined organic layers were dried over Na$_2$SO$_4$ and concentrated under reduced pressure. The residue was dissolved in toluene (0.2 M), and 2-hydroxypyridine (31 mg, 0.328 mmol) was added. The reaction refluxed for 14 h under Ar atmosphere, cooled to room temperature, and concentrated under reduced pressure. The residue was rediluted with CH$_2$Cl$_2$ (30 mL) and washed with 1 M HCl (30 mL).

The organic layer was dried over Na$_2$SO$_4$ and concentrated under reduced pressure. The crude residue was purified via flash column chromatography eluting with 5:95 MeOH/CH$_2$Cl$_2$ to afford 160 mg (27%) of the desired *cis* diastereomer as a cream foam. The *trans* diastereomer was isolated in 23% yield (140 mg) as yellow foam: ^{1}H NMR (400 MHz, 20:1 CDCl$_3$/CD$_3$OD) δ 8.15 (m, 1H), 7.17 (d, J = 8.4 Hz, 1H), 6.71 (d, J = 2.4 Hz, 1H), 6.58 (dd, J = 8.4, 2.0 Hz, 1H), 6.04 (dd, J = 17.6, 10.4, 1H), 5.10−5.05 (m, 2H), 4.35 (dd, J = 11.2, 2.4 Hz, 1H), 4.00 (t, J = 7.6 Hz, 1H), 3.86−3.54 (m, 3H), 3.08 (dd, J = 14.8, 11.6 Hz, 1H), 2.30−1.82 (m, 6H), 1.45−1.38 (m, 6H); ^{13}C NMR (75 MHz, 20:1 CDCl$_3$/CD$_3$OD) δ 169.7, 166.3, 153.0, 146.1, 140.3, 135.9, 123.0, 118.3, 112.3, 110.0, 103.9, 96.9, 59.4, 55.1, 45.6, 39.1, 28.5, 28.0, 26.1, 25.9, 22.7; IR (neat) 3353, 2925, 1664, 1457 cm^{-1}; HRMS (ESI/APCI) calcd for C$_{21}$H$_{26}$N$_3$O$_3$ (M + H) 368.1969, found 368.1969.

Notoamide J (1). Davis oxaziridine (208 mg, 0.871 mmol) was added to a solution of **2** (160 mg, 0.436 mmol) in CH$_2$Cl$_2$ (9 mL). The reaction mixture was stirred 13 h at room temperature and concentrated under reduced pressure. The residue was purified via flash column chromatography eluting with MeOH/CH$_2$Cl$_2$ (5:95) to give 52 mg (31%) of **1** as a white amorphous solid and 26 mg (15%) of **15** as a white amorphous solid: ^{1}H NMR (300 MHz, acetone-d_6) δ 9.68 (br s, 1H), 8.59 (bs, 1H), 7.02 (d, J = 8.7 Hz, 1H), 6.49 (dd, J = 8.1, 5.7 Hz, 2H), 6.33 (br s, 1H), 6.12 (dd, J = 17.4, 10.8 Hz, 1H), 5.05 (dd, J = 16.8, 10.8 Hz, 1H), 5.04 (dd, J = 16.8, 10.8 Hz, 1H), 4.00 (t, J = 6.9 Hz, 1H), 3.49−3.34 (m, 2H), 3.28 (d, J = 9.6 Hz, 1H), 3.10 (d, J = 14.7 Hz, 1H), 2.18−2.11 (m, 1H), 2.10 (d, J = 6.6 Hz, 1H), 1.98−1.80 (m, 3H), 1.11 (s, 3H), 1.06 (s, 3H); ^{13}C NMR (75 MHz, CDCl$_3$) δ 183.2, 170.4, 165.7, 157.7, 143.3, 142.9, 126.8, 120.3, 114.5, 109.2, 98.6, 59.0, 57.8, 53.0, 45.9, 42.5, 31.7, 29.9, 28.2, 22.7, 21.8; IR (neat) 3265, 2971, 1670, 1429, 1155 cm^{-1}; HRMS (ESI/APCI) calcd for C$_{21}$H$_{25}$N$_3$O$_4$Na (M + Na) 406.1737, found 406.1739.

Supporting Information Available: Full spectral characterization of notoamide J including comparison spectra to natural material. This material is available free of charge via the Internet at http://pubs.acs.org.

J. Org. Chem. Vol. 75, No. 9, 2010 **2789**

379

Notoamide E: biosynthetic incorporation into notoamides C and D in cultures of *Aspergillus versicolor* NRRL 35600

Jennifer M. Finefield [a], Thomas J. Greshock [a], David H. Sherman [b], Sachiko Tsukamoto [c], Robert M. Williams [a,d,*]

[a] *Department of Chemistry, Colorado State University, 1301 Center Avenue, Fort Collins, CO 80523, USA*
[b] *Life Sciences Institute and Department of Medicinal Chemistry, The University of Michigan, 210 Washtenaw Avenue, Ann Arbor, MI 48109-2216, USA*
[c] *Graduate School of Pharmaceutical Sciences, Kumamoto University, 5-1 Oe-honmachi, Kumamoto, 862-0973, Japan*
[d] *University of Colorado Cancer Center, Aurora, CO 80045, USA*

ABSTRACT

Notoamide E, a short-lived secondary metabolite, has been proposed as a biosynthetic intermediate to several advanced metabolites isolated from *Aspergillus versicolor*. In order to verify the role of this indole alkaloid along the biosynthetic pathway, synthetic doubly ^{13}C-labeled notoamide E was fed to *Aspergillus versicolor*. Analysis of the metabolites showed significant incorporation of notoamide E into the natural products notoamides C and D.

© 2011 Elsevier Ltd. All rights reserved.

1. Introduction

Prenylated indole alkaloids containing either a diketopiperazine ring or a core bicyclo[2.2.2]diazaoctane ring system constitute a unique and well-known family of natural products. These secondary metabolites, specifically the brevianamides,[1] paraherquamides,[2] stephacidins,[3] and notoamides,[4,5] are produced by various genera of fungi, mainly *Aspergillus* and *Penicillium* spp., and exhibit a wide range of biological activity. Biosynthetically, these structurally complex molecules are derived from tryptophan, a cyclic amino acid such as proline, β-methyl-proline, or pipecolic acid, and one or two isoprene residues. These structural features have made this family of natural products attractive from not only a synthetic perspective,[6] but also a biosynthetic standpoint.[7] Recently, Tsukamoto and co-workers isolated several secondary metabolites from a marine-derived *Aspergillus* sp. that hinted at a possible biosynthetic pathway leading from deoxybrevianamide E to (+)-stephacidin A (**1**), and eventually to (−)-notoamide B (**2**). Among these metabolites was a new alkaloid, notoamide E (**3**), which is a short-lived natural metabolite. Notoamide E was found to appear in the culture on day five and completely consumed by day six. It was postulated that the rapid disappearance of **3** was due to the conversion of this metabolite into other downstream metabolites, such as **1**, **2**, **4**, and **5**, among others.[5,6] (Fig. 1).

We immediately directed our attention to determining the exact role **3** played in the biosynthetic pathway of these unique secondary metabolites. Initially, we were expecting to see the conversion of **3** into (+)-**1**, (−)-**2** and other notoamides.

In order to address these questions, notoamide E was synthesized in doubly ^{13}C-labeled form and fed to the marine *Aspergillus* sp. Unexpectedly, formation of labeled or unlabeled (+)-**1** and (−)-**2**, as well as all other bridged bicyclo[2.2.2]diazaoctane-containing compounds, were not observed or detected although they are typically the major metabolites produced by this fungus. Furthermore, notoamide C (**4**) and notoamide D (**5**) were isolated and found to contain ^{13}C-enrichment at the expected C-12 and C-17 positions. Tsukamoto also reported the isolation of 3-*epi*-notoamide C (**6**), a diastereomer to **4** that is not produced by the culture under normal growth conditions. While **6** has not been isolated in the normal medium of either *Aspergillus* sp. or *Aspergillus versicolor*, Tsukamoto observed that the yield of **6** (1.26 mg) was nearly four times that of **4** (0.33 mg) in the feeding experiment of notoamide E with *Aspergillus* sp.[5] Three new structurally unique minor metabolites displaying ^{13}C-enrichment were also isolated. These new alkaloids, notoamides E2, E3, and E4,[5] are not present in the normal culture of *Aspergillus* sp. when cultivated on the standard nutrient-rich medium. The lack of formation of (+)-**1** and (−)-**2**, as well as the production of new metabolites, suggests that the presence of excess **3** in the growth medium alters the metabolite profile of this marine-derived *Aspergillus* sp., and may interrupt the biosynthesis of the major metabolites.[5]

* Corresponding author.
  E-mail address: rmw@lamar.colostate.edu (R.M. Williams).
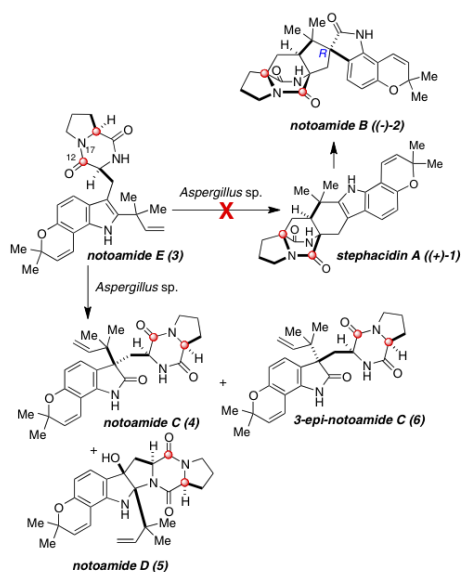
Figure 1. Result of marine *Aspergillus* sp. feeding experiment with ^{13}C-labeled **3**.

In a separate work, Gloer and co-workers isolated (−)-stephacidin A (**1**), (+)-notoamide B (**2**) and (+)-versicolamide B from a terrestrial fungus, *Aspergillus versicolor*.[4c] These samples possess the opposite absolute configuration to those metabolites previously isolated from both *Aspergillus ochraceus* WC76466 and the marine-derived *Aspergillus* sp., and they also represent the isolation of the first set of antipodal stereoisomers within the paraherquamide—stephacidin family (Fig. 2).[3,4] The isolation of these enantiomeric natural metabolites from an *Aspergillus* fungus has sparked further interest into elucidating the biosynthetic pathway for the formation of the bicyclo[2.2.2]diazaoctane ring system, which has been strongly implicated as being responsible for the enantio-diverging event.

With the discovery of these antipodal metabolites from different *Aspergillus* species, questions arose as to whether these unique
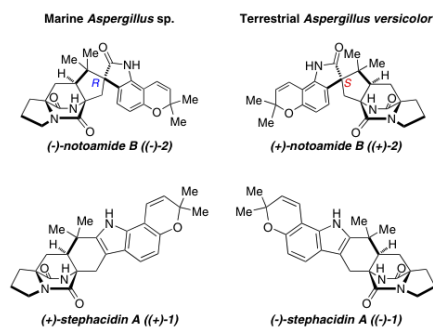
Figure 2. Structures of antipodal natural metabolites isolated from marine-derived *Aspergillus* sp. and terrestrial-derived *Aspergillus versicolor*.

natural products are biosynthesized along a similar, if not identical, biosynthetic pathway. Although **3** has not yet been isolated from the natural *A. versicolor* culture, we reasoned that if the biosynthetic pathways were substantially the same in both species, then *A. versicolor* would also incorporate labeled **3** into **4**, **5**, and **6**. Furthermore, based on Tsukamoto's results,[4d] we also expected to see the lack of incorporation of **3** into any compounds containing the bridged bicyclo[2.2.2]diazaoctane core, such as (−)-**1** and (+)-**2**.

2. Materials and methods

A culture of *A. versicolor* NRRL 35600 was obtained from the Department of Agriculture in Peoria, IL. This culture was transferred to malt extract agar slants and allowed to incubate for 14 days. Potato Dextrose Broth was prepared by dissolving 48 g of the medium and 6 g tryptose in 2 L of doubly distilled H_2O (DDH$_2$O). The solution was heated to aid in dissolving the medium, which was then transferred to fernbach flasks (4 × 500 mL) and autoclaved. Spores of *A. versicolor* were added to the broth from the agar slants. The fernbach flasks were covered and gently placed in the incubator for 14 days. Doubly ^{13}C-labeled notoamide E (42 mg, 0.096 mmol), the synthesis of which we have recently reported,[5,6] was dissolved in 1 mL acetone with 0.2 mL TWEEN 80. The solvent was dried and the residue was dissolved in 300 mL of a sterile trace element solution (35 mM NaNO$_3$, 5.7 mM K$_2$HPO$_4$, 4.2 mM MgSO$_4$·7H$_2$O, 1.3 mM KCl, 36 mM FeSO$_4$·7H$_2$O, 25 mM MnSO$_4$·H$_2$O, 7 mM ZnSO$_4$·7H$_2$O, and 1.5 mM CuCl$_2$·2H$_2$O). The fungal broth was decanted and the fungal cells were washed with 100 mL sterile DDH$_2$O. The precursor/trace element solution (150 mL) was added to each flask using a syringe and needle. The fungal cells were incubated at 25 °C for 14 days and each flask was swirled daily to ensure even distribution of the labeled compound. The trace element solution was decanted, and the fungus was pureed in a blender with 1:1 MeOH–CHCl$_3$. The puree was transferred to a 2 L Erlenmeyer flask, diluted to 1.2 L with 1:1 MeOH-CHCl$_3$, and placed in the shaker for 24 h. Celite (30 g) was added to the flask and allowed to shake for an extra 10 min. The suspension was filtered through Whatman #2 paper and the filtrate was stored at 4 °C. The mycelia 'cake' was diluted with 600 mL 1:1 MeOH–CHCl$_3$ and placed on the shaker for an additional 48 h. The suspension was filtered through Whatman #2 paper, and the combined filtrates were concentrated under vacuum. The residue was dissolved in 250 mL H$_2$O and extracted with EtOAc (3 × 300 mL). The organic layer was concentrated and partitioned between MeCN and hexanes. The layers were separated, and the MeCN layer was concentrated under vacuum.[4c,5,8] The crude material was purified via silica gel flash column chromatography (1% MeOH in DCM–3% MeOH in DCM) to afford three fractions that were each analyzed by ^{13}C NMR spectroscopy. Enrichment of ^{13}C was found in the latter two fractions, which were further purified via preparative thin layer chromatography (1000 mm, 3% MeOH in DCM × 5) to yield ^{13}C-labeled notoamide C (8.1 mg) and notoamide D (11.2 mg).

3. Results and discussion

Significant ^{13}C incorporation was observed by ^{13}C NMR spectroscopy at C-12 and C-17 of notoamides C and D. From analysis of the electrospray mass spectra, incorporation of intact doubly ^{13}C-labeled **3** into **4** was determined to be 6.2%, while incorporation into **5** was 6.0%.[9,10] Interestingly, upon closer inspection, trace amounts of doubly ^{13}C-labeled 3-*epi*-notoamide C (**6**), unlabeled (−)-**1**, and unlabeled (+)-**2** were also detected by LC–MS (Table 1). In contrast to the metabolite profile observed by Tsukamoto and co-workers, only trace amounts of **6** were detected and there-

Table 1
Intact incorporation of double ^{13}C-labeled notoamide E (**3**) into isolated metabolites.

Metabolite	% Specific incorporation	Notes
Notoamide C	6.2%	8.1 mg
3-*epi*-Notoamide C	ND[a]	Trace isolated
Notoamide D	6.0%	11.2 mg
Stephacidin A	0%	Trace isolated
Notoamide B	0%	Trace isolated

[a] Not enough material to adequately calculate the % incorporation.

fore we were unable to reliably calculate the percentage of intact incorporation. As mentioned above, Tsukamoto observed a complete lack of production of any compounds containing the bicyclo[2.2.2]diazaoctane core, and while (−)-**1** and (+)-**2** are usually the major metabolites in the normal medium of *A. versicolor*, we did isolate trace amounts of these unlabeled compounds (Table 1).[4c,5]

In summary, we have shown that the proposed precursor, notoamide E, incorporates into three minor secondary metabolites, **4**, **5**, and **6** in *A. versicolor*. We observed that excess **3** in cultures of *A. versicolor* resulted in the production of only trace amounts of the metabolites, (−)-stephacidin A and (+)-notoamide B. The results observed from the feeding experiments of double ^{13}C-labeled **3** with both the Tsukamoto marine-derived *Aspergillus* sp. and *A. versicolor* pose some interesting questions about the biosynthetic pathway of the major metabolites produced by these organisms. During the feeding experiment of **3** with *A. versicolor*, we observed that **6** was only produced in trace amounts, unlike the incorporation study with *Aspergillus* sp. where the yield of **6** was more than **4**. This could be a distinguishing difference between the two *Aspergillus* species. We have also observed an inversion in the amounts of the major and minor metabolites that are normally produced by *A. versicolor* when notoamide E was provided to the culture medium. When grown on normal media, notoamides C and D are produced in trace amounts by *A. versicolor*. In contrast, when labeled notoamide E was added to the culture media, these substances were isolated as the major metabolites. These results suggest that the addition of excess **3** does not abrogate the oxidative transformations of notoamide E into notoamides C, D and *epi*-notoamide C. On the other hand, the suppression of the formation of stephacidin A and notoamide B observed in the presence of added notoamide E, suggests that these compounds inhibit or divert the enzymatic machinery responsible for the production of the bicyclo[2.2.2]diazaoctane-containing metabolites, especially stephacidin A and notoamide B. Furthermore, results from both sets of feeding studies establish that notoamide E is not a biosynthetic substrate for the putative oxidase that is postulated to mediate the intramolecular Diels–Alder cycloaddition, as evidenced by the lack of incorporation of **3** into any bicyclo[2.2.2]diazaoctane-containing natural products. Notoamide E is, on the other hand, firmly established as a biosynthetic precursor to notoamides C and D.

These findings therefore suggest the presence of a branch point in the biosynthetic pathway, just prior to the formation of notoamide E. The details of this putative inhibitory process are currently under investigation as well as efforts to identify the key branch point that diverts to the biosynthetic precursor to stephacidin A, and metabolites derived from stephacidin A (such as notoamide B, stephacidin B, among others) which currently remain enigmatic.

Supplementary data

Supplementary data (calculations of percent incorporations reported in this study.) associated with this Letter can be found, in the online version, at doi:10.1016/j.tetlet.2011.02.078.

References and notes

1. (a) Birch, A. J.; Wright, J. J. *Tetrahedron* **1970**, *26*, 2329; (b) Birch, A. J.; Wright, J. S. *J. Chem. Soc., Chem. Commun.* **1969**, 644–645; (c) Birch, A. J.; Russell, R. A. *Tetrahedron* **1972**, *28*, 2999.
2. (a) Yamazaki, M.; Okuyama, E.; Kobayashi, M.; Inoue, H. *Tetrahedron Lett.* **1981**, *22*, 135–136; (b) Ondeyka, J. G.; Goegelman, R. T.; Schaeffer, J. M.; Kelemen, L.; Zitano, L. *J. Antibiot.* **1990**, *43*, 1375–1379; (c) Liesch, J. M.; Wichmann, C. F. *J. Antibiot.* **1990**, *43*, 1380–1386; (d) Banks, R. M.; Blanchflower, S. E.; Everett, J. R.; Manger, B. R.; Reading, C. *J. Antibiot* **1997**, *50*, 840–846.
3. Qian-Cutrone, J.; Huang, S.; Shu, Y-Z.; Vyas, D.; Fairchild, C.; Menendez, A.; Krampitz, K.; Dalterio, R.; Klohr, S. E.; Gao, Q. *J. Am. Chem. Soc.* **2002**, *124*, 14556–14557.
4. (a) Kato, H.; Yoshida, T.; Tokue, T.; Nojiri, Y.; Hirota, H.; Ohta, T.; Williams, R. M.; Tsukamoto, S. *Angew. Chem., Int. Ed.* **2007**, *46*, 2254–2256; (b) Tsukamoto, S.; Kato, H.; Samizo, M.; Nojiri, Y.; Onuki, H.; Hirota, H.; Ohta, T. *J. Nat. Prod.* **2008**, *71*, 2064–2067; (c) Greshock, T. J.; Grubbs, A. W.; Jiao, P.; Wicklow, D. T.; Gloer, J. B.; Williams, R. M. *Angew. Chem., Int. Ed.* **2008**, *47*, 3573–3577; (d) Tsukamoto, S.; Kawabata, T.; Kato, H.; Greshock, T. J.; Hirota, H.; Ohta, T.; Williams, R. M. *Org. Lett.* **2009**, *11*, 1297–1300; (e) Tsukamoto, S.; Umaoka, H.; Yoshikawa, K.; Ikeda, T.; Hirota, H. *J. Nat. Prod.* **2010**, *73*, 1438–1440.
5. Tsukamoto, S.; Kato, H.; Greshock, T. J.; Hirota, H.; Ohta, T.; Williams, R. M. *J. Am. Chem. Soc.* **2009**, *131*, 3834–3835.
6. (a) Grubbs, A. W.; Artman, G. D., (III); Tsukamoto, S.; Williams, R. M. *Angew. Chem., Int. Ed.* **2007**, *46*, 2257–2261; (b) Greshock, T. J.; Grubbs, A. W.; Tsukamoto, S.; Williams, R. M. *Angew. Chem., Int. Ed.* **2007**, *46*, 2262–2265.
7. (a) Williams, R. M. *Chem. Pharm. Bull.* **2002**, *50*, 711–740; (b) Williams, R. M.; Cox, R. J. *Acc. Chem. Res.* **2003**, *36*, 127–139; (c) Stocking, E. M.; Sanz-Cervera, J. F.; Williams, R. M. *Angew. Chem.* **2001**, *113*, 1336–1338. *Angew. Chem., Int. Ed.* **2001**, *40*, 1296-1298..
8. (a) Stocking, E. M.; Williams, R. M.; Sanz-Cervera, J. F. *J. Am. Chem. Soc.* **2000**, *122*, 9089–9098; (b) Stocking, E. M.; Sanz-Cervera, J. F.; Unkefer, C. J.; Williams, R. M. *Tetrahedron* **2001**, *57*, 5302–5303.
9. (a) Stocking, E. M.; Sanz-Cervera, J. F.; Williams, R. M. *Angew. Chem., Int. Ed.* **2001**, *40*, 1296–1298; (b) Ding, Y.; Greshock, T. J.; Miller, K. A.; Sherman, D. H.; Williams, R. M. *Org. Lett.* **2008**, *10*, 4863–4866.
10. Calculated according to the method outlined in: Lambert, J. B.; Shurvell, H. B.; Lightner, D. A.; Cooks, R. G. *Organic Structural Spectroscopy*; Prentice Hall: Upper Saddle River, NJ, 1998. pp. 447–448.

Drug Delivery: Design and Synthesis of a Novel Prodrug for the Targeted Treatment of Brain Tumors

Abstract/Specific Aims:

The aim of this proposal is to develop a novel method of drug delivery targeted toward the treatment of brain tumors. Several important factors need to be considered when developing treatments for brain tumors, such as how to effectively transport the therapeutic agent across the blood brain barrier (BBB) and how to actively target the tumor. Glucose is an essential nutrient for both the brain and tumors, and as such, glucose crosses the BBB and enters tumor cells via a specific transporter protein, GLUT-1. By utilizing the glucose transporter protein, several prodrugs (**1-4**, Figure 1) could be synthesized that employ a glucose derivative (2-deoxy-glucose) acting as a carrier across the BBB and into the tumor. Through an acid-labile linker, the glucose derivative could be cleaved from the active chemotherapeutic agent once in the acidic microenvironment of the tumor. Given that prodrugs **1-4** contain 2-deoxy-glucose (2-DG) as the carrier, as opposed to D-glucose, once the ester bond is hydrolyzed, 2-DG could also act as a chemotherapeutic agent.
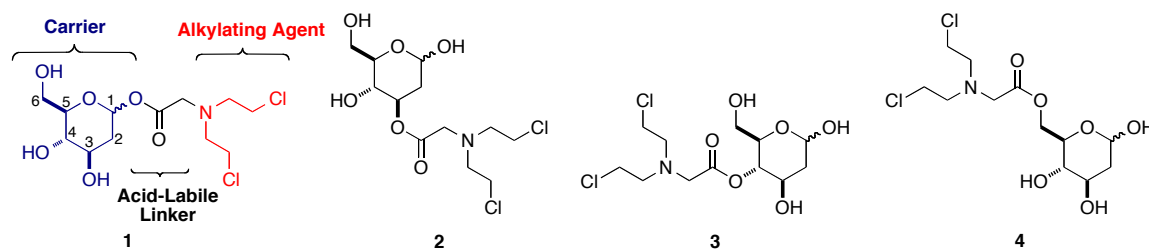
Figure 1. Proposed prodrug compounds.

Specific Aims for this Proposal:

1. To develop a method of drug delivery that will allow the drug to cross the blood brain barrier (BBB).
2. To develop a strategy that allows the drug to specifically target the brain tumor while minimizing the effect of the drug on normal healthy cells.
3. To form an efficient prodrug that is only activated within the brain tumor.

Background and Significance:

The efficiency of currently available chemotherapeutics used in the treatment of cancer is greatly limited by the inability of these drugs to differentiate between cancer cells and normal healthy cells.[1] The poor biodistribution (BD) of conventional treatments

limits the amount of the anti-cancer drug that can be administered safely, thereby reducing their efficacy in eliminating malignant cells.[2] The use of a drug delivery system can aid in the BD of traditional drugs by selectively targeting tumors and treating the cancerous cells, while minimizing exposure of healthy cells to the drug. Thus, targeted drug delivery can not only lower the dose of the drug, but also reduce the side effects. Several methods of targeted drug delivery have been explored over the years, but only a few of these therapeutic agents have been approved for treatment.

The treatment of central nervous system (CNS) disorders are often complicated by the presence of protective barriers that restricts the passage of foreign particles into the brain.[3] As shown in Figure 2, there are two vascular barriers in the brain, the endothelial blood-brain barrier (BBB) and the epithelial blood-cerebrospinal fluid barrier (BCSFB). In order for any therapeutic agents to reach the brain, they must cross one of these two physiological barriers. In terms of drug delivery, the BBB is the most relevant barrier since the area of the BBB is about 1000 times larger than that of the BSDFB.[4] Unfortunately, many neurotherapeutics are unsuccessful in treating CNS disorders because they cannot be effectively delivered to the brain.[5]
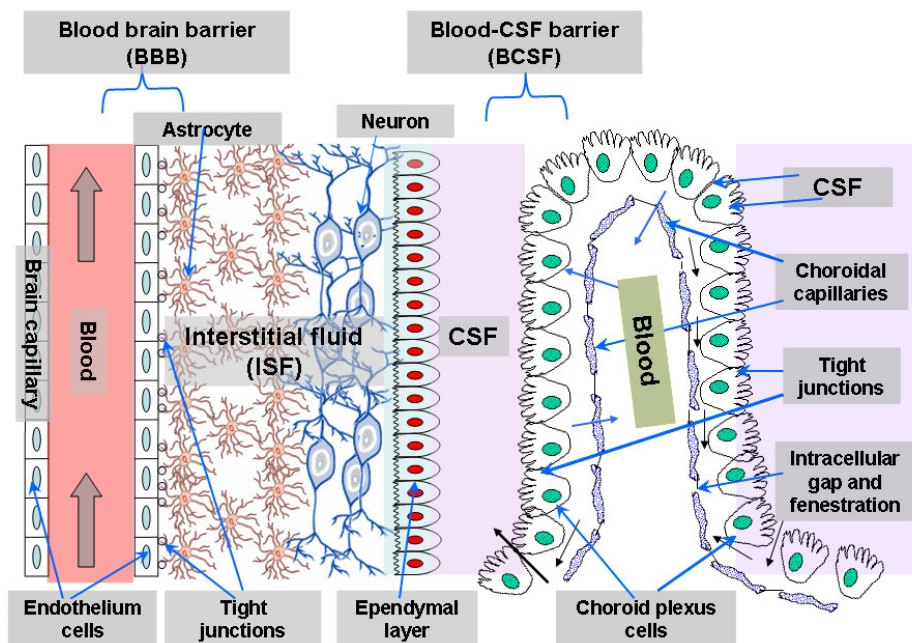
Figure 2. Overview of the two main barriers in the CNS.[3]

Due to the presence of tight junctions between adjacent cells, molecules are inhibited from penetrating the BBB between gaps of cells within the plane of the membrane. However, there are four main transport systems for the passage of substances across the BBB (Figure 3).[6,8] First, there is passive diffusion, which allows for fat-soluble substances to dissolve in the cell membrane and cross the barrier. Examples of substances that pass the BBB through passive diffusion are alcohol, nicotine, and caffeine. The second method is active transport, which works by carrying essential substances that the brain needs, such as glucose or amino acids, by way of special transport proteins embedded in the membrane of the barrier. The third method of passage

is receptor-mediated transport. Specific molecules, such as insulin, can link to receptors on the surface of the brain and be escorted through the barrier. Finally, native plasma proteins such as albumin, which are poorly transported, can be cationized to increase their uptake by adsorptive-mediated endocytosis and transcytosis.[8] These transport systems have become increasingly important in the development of drug delivery across the BBB.[7] By linking the desired therapeutic agent to molecules such as glucose or insulin, the drug can be transported into the brain.
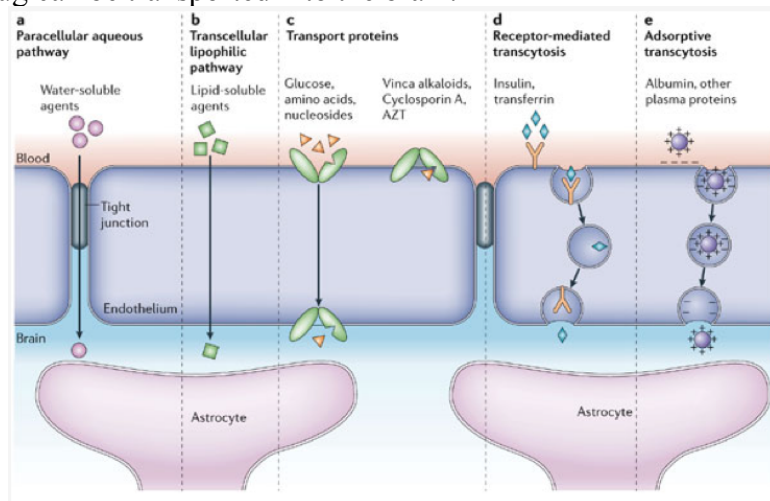
Figure 3. Pathways across the blood brain barrier.[8]

Glucose transport is one of the most essential and well-studied transport systems across the BBB.[9] Glucose is the main nutrient of the brain, and about 20% of glucose in the bloodstream is metabolized in the brain. Thus, glucose is actively transported across the BBB by the passive glucose transporter, GLUT-1.[10] The conjugation of glucose to a desired therapeutic agent could allow for transportation of the drug across the BBB. In fact, this method was recently attempted in the treatment of Parkinson's disease (Figure 4).[11] L-Dopa is the most widely used treatment for Parkinson's disease; however, only a small percentage of L-dopa actually makes it into the brain since L-dopa is also converted to dopamine in peripheral tissues. This premature conversion of L-dopa also causes unwanted side effects in patients, and unfortunately, once dopamine is formed outside the brain it cannot cross the BBB. One way to direct treatment to the brain, while reducing the side effects from dopamine, is by conjugating dopamine to glucose. Preliminary results showed that the drug-glucose system was transported across the BBB via the GLUT-1 transporter and induced therapeutic effects against Parkinson's disease.
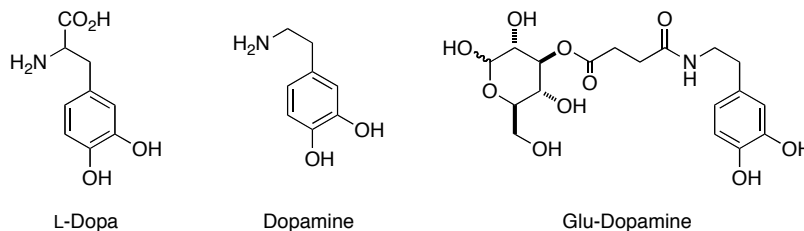
Figure 4. Structures of dopamine precursor (L-dopa), dopamine, and the glucose-dopamine prodrug (glu-dopamine).

It has been known for some time that glucose serves as an energy source for both healthy and cancerous cells.[10,12] As shown in Figure 5, glycolysis is responsible for the conversion of glucose to pyruvate, which results in the net production of two molecules of ATP per glucose molecule.[13] However, cancer cells contain a higher number of glucose transporters (GLUT-1) than healthy cells, which results in a faster rate of glucose metabolism in cancer cells.[10] This increased uptake of glucose contributes to the rapid growth of malignant cells and tumors. Furthermore, the elevated rates of glucose uptake, in conjunction with the reduced rates of oxidative phosphorylation, result in the accumulation of lactic acid and an overall acidic pH state of the tumor.[14] The acidic microenvironment of the tumor is also brought about by insufficient blood supply and poor lymphatic drainage.
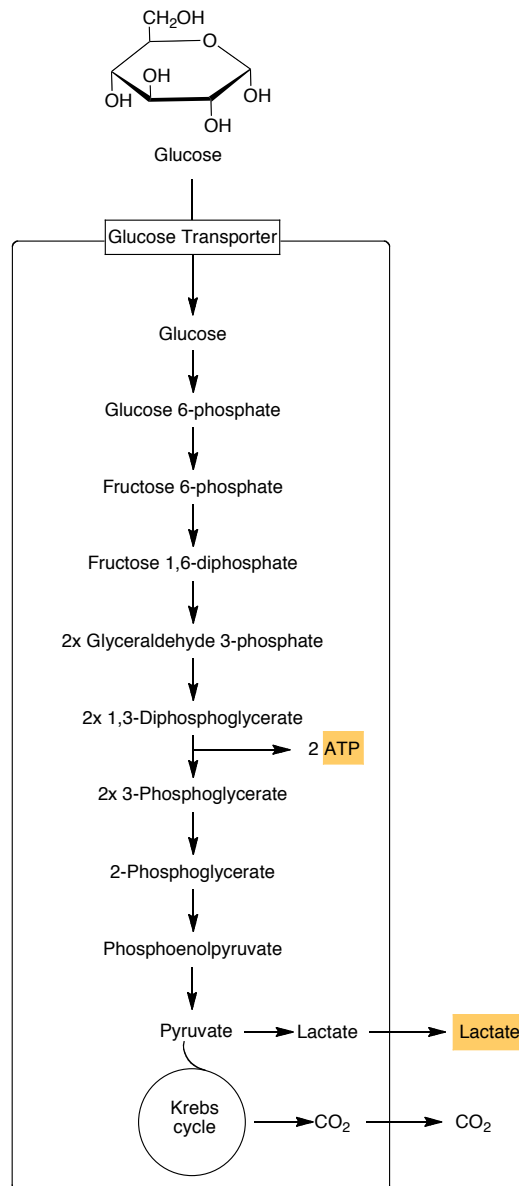
Figure 5. Metabolism of glucose.

It has been well established that glucose is a necessary nutrient for the brain, and as such, the capacity of the glucose transporter at the BBB is significantly higher than those of other nutrient transporters.[7] Likewise, glucose is also a necessary nutrient for brain tumors to survive. As a result, cancer cells have increased rates of glucose metabolism when compared with healthy cells, due to an increased expression of GLUT-1. However, the use of glucose as a targeted delivery system for the treatment of brain tumors has not been deeply explored.

In 1996, the known antitumor agent chlorambucil was conjugated to several glucose derivatives (Figure 6, **5-8**), and research showed that these conjugates recognized the human GLUT-1 glucose transporter.[15] Inhibition studies determined that all four compounds reacted with the GLUT-1 transporter, albeit with varying degrees of affinity. Unfortunately, further investigations revealed that the glu-chlorambucil derivatives reacted with the glucose transporters in a non-penetrating way, which was attributed to the presence of the bulky, hydrophobic chlorambucil moiety.

5, X = O, R = CH$_3$
6, X = O, R = H
7, X = N, R = CH$_3$
8, X = N, R = H
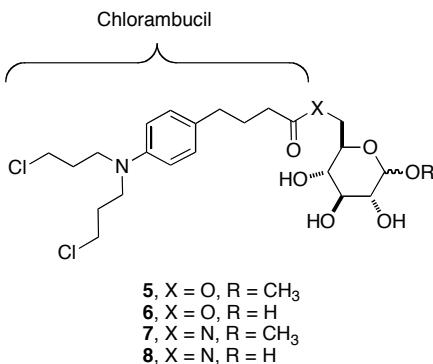
Figure 6. Glucose-chlorambucil derivatives **5-8**.

In order to restrict the bulkiness of the alkylating moiety, research was directed toward the synthesis of glucose-busulfan derivatives. To mimic the mode of action of busulfan, mesylated glucose derivatives (**9-12**) were synthesized (Figure 7) and tested with the human GLUT-1 transporter.[16] Results showed that mesylation of OH-4 and OH-6 displayed a slightly diminished affinity for the GLUT-1 glucose transporter, while mesylation of OH-3 led to complete loss of affinity. These findings suggest that certain structural requirements are necessary for binding of D-glucose derivatives to the GLUT-1 transporter protein. Additionally, involvement of the OH-1, OH-3, and OH-6 in binding to the transporter has also been demonstrated.[16] Thus, small structural changes in the sugar-carrier can either increase or decrease the affinity for the carrier.

Busulfan

9, R^1 = H, R^2 = H, R^3 = Ms
10, R^1 = Ms, R^2 = H, R^3 = H
11, R^1 = Ms, R^2 = H, R^3 = Ms
12, R^1 = H, R^2 = Ms, R^3 = H
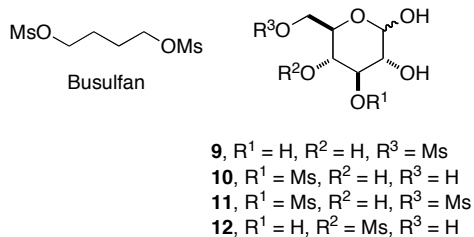
Figure 7. Methylsulfonyl derivatives.

It may seem counterintuitive to conjugate a drug to glucose, since this sugar essentially feeds the brain tumor. It should also be remembered, however, that glycolysis is enhanced in transformed cells and provides at least some, if not all, of the energy for cell proliferation. Thus, antiglycolytic strategies stand as promising new leads for anti-cancer therapeutics.[17] One way to achieve inhibition of glycolysis is through the use of 2-deoxy-D-glucose (2-DG), a glucose analogue that is preferentially captured by cancer cells. As shown in Figure 8, 2-DG is taken up by the cancer cell, where it undergoes phosphorylation, similar to D-glucose. However, phosporylated-2-DG cannot be metabolized or diffused outside the cells.
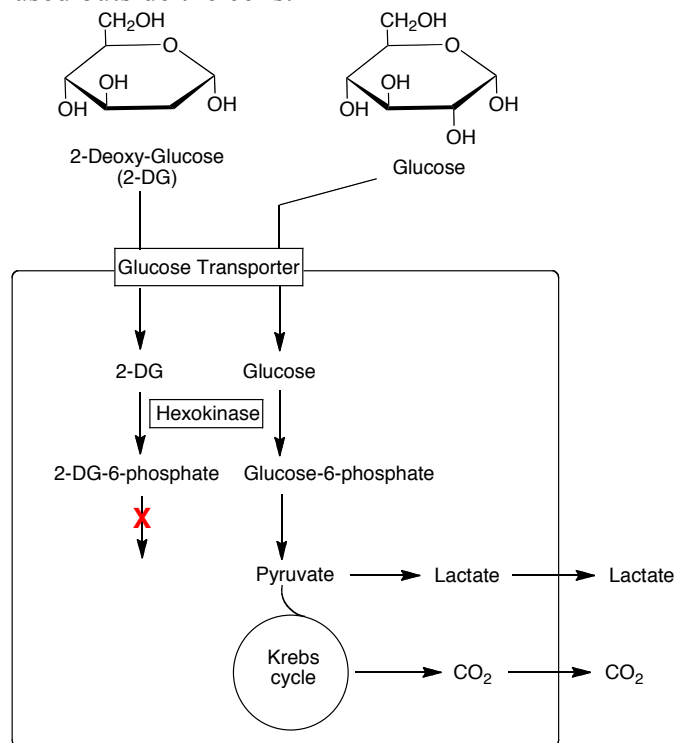
Figure 8. Metabolism of 2-DG.[13]

Previous studies have shown that when cancer cells are treated with 2-DG, four different responses have been observed: (1) proliferation slow down; (2) proliferation arrest without signs of apoptosis; (3) strong cell cycle arrest accompanied by moderate apoptosis induction; and (4) massive apoptosis.[17] In addition, the GLUT-1 transporter cannot differentiate between D-glucose and 2-deoxy- D-glucose, so 2-DG is efficiently transported across the BBB. In the past few years, 2-DG has entered clinical trials for the treatment of patients with malignant glioma, the most common and lethal form of brain cancer.[18] Preliminary results have shown that patients display excellent tolerance to a combined treatment of orally administered 2-DG and hypofractionated radiotherapy. Phase III efficacy trials are currently at an advanced stage, and results have shown that patients display extensive tumor necrosis with well-preserved normal brain tissue adjoining the tumor. These promising results indicate that 2-DG treatment differentiates between tumor and normal tissue.

Described herein is the synthesis of a novel prodrug utilizing 2-DG as a carrier to transport a modified alkylating agent across the BBB. Once inside the acidic

microenvironment of the tumor, the drug will be cleaved from the carrier, allowing for two methods of chemotherapeutic treatment to work individually. The alkylating drug will work by cross-linking DNA, thereby blocking fundamental metabolic processes such as replication and transcription, while the 2-DG carrier inhibits glycolysis within cancerous cells.

Research Design and Methods:

We envision the development of a carrier-linker-drug system that will accomplish three things: (1) transportation of the drug across the blood brain barrier; (2) targeted drug delivery to the brain tumor; and (3) activation of the drug specifically within the tumor. To achieve these goals, four 2-DG derivatives (**1-4**, Figure 9) will be synthesized and tested, in order to evaluate the positions of the sugar molecule that can be substituted without altering the affinity to the GLUT-1 transporter protein. Additionally, each derivative will be equipped with an acid-labile linker for pH-responsive drug release within the tumor.
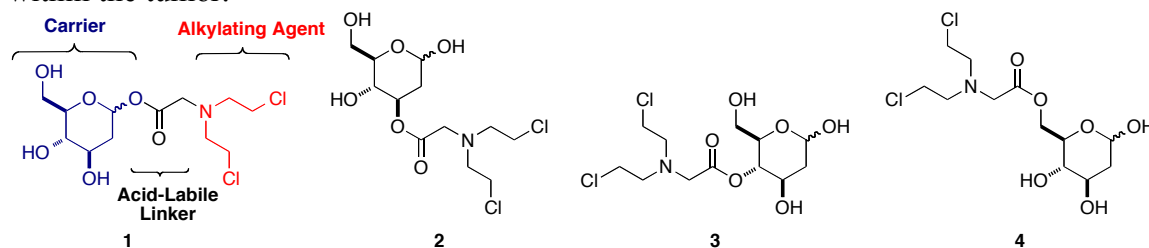
Figure 9. 2-deoxy-glucose derivatives

Retrosynthetically, the 2-DG derivatives (**1-4**) could arise from the benzyl deprotection of **13-16** (Scheme 1). Coupling of **21**, which is derived from glycine **22** and ethylene oxide **23**, with the 2-DG free hydroxyl moiety (**17-20**) affords the carrier-linker-drug skeleton (**13-16**).
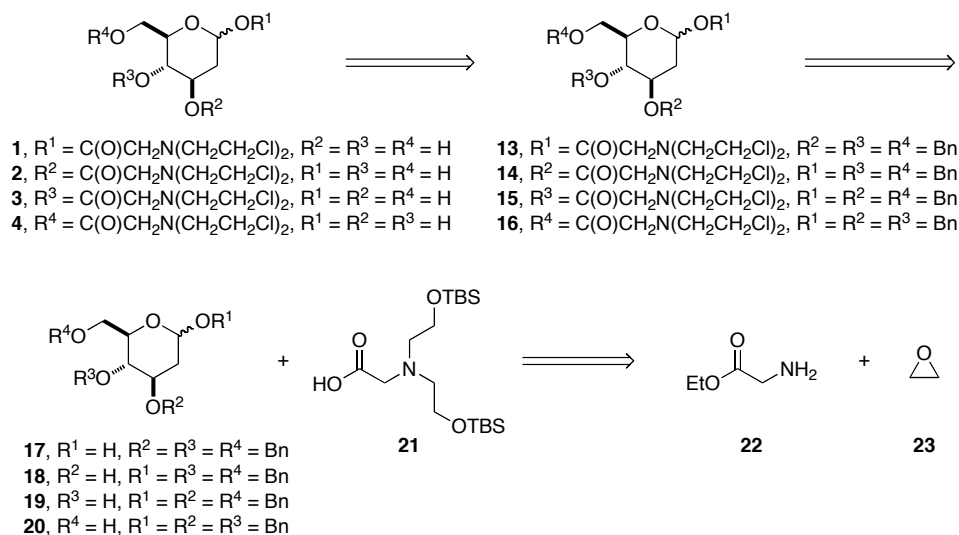
Scheme 1. Retrosynthetic analysis of the carrier-linker-drug skeleton.

The formation of the 2-DG carriers (**17-20**) would require individual syntheses in order to ensure that one of the hydroxyl groups remains unprotected. As shown in Scheme 2, the synthesis of **17** would begin by treating commercially available **24** with 48% HBr and PPh$_3$ in CH$_2$Cl$_2$ to yield the corresponding 2-deoxysugar in a one-pot procedure.[19]
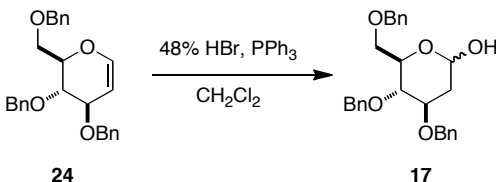
Scheme 2. One-pot synthesis of **17**.

As shown in Scheme 3, compound **18** is envisioned from commercially available **25**, which upon treatment with benzyl alcohol in the presence of toluenesulfonic acid will afford the 2-benzyloxy protected 2-DG derivative **26**. According to literature precedence, the reaction of **26** in the presence of dibutyltin oxide in benzene, tetrabutylammonium iodide, and allyl bromide (**27**) should afford OH-3 allylated product **28**.[20] Bis-benzyl protection of **28** using standard conditions would yield **29**, and subsequent deallylation by treatment with Pd(PPh$_3$)$_4$, acetic acid, and *p*-toluenesulfinate would provide the desired 2-DG derivative **18**.[20,21]
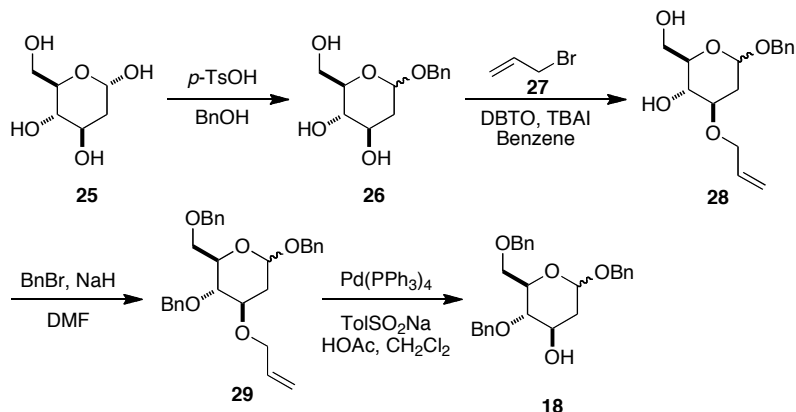
Scheme 3. Synthesis of **18**.

Compound **19** is devised from commercially available 2-deoxy-glucose (Scheme 4). Condensation of **25** with benzyl alcohol in the presence of toluenesulfonic acid should afford the benzyl glycoside of 2-deoxy-glucose (**26**, shown above). In situ diol protection under standard conditions will then afford 4,6-*O*-benzylidene derivative **30**.[22] Protection of the free alcohol moiety with benzyl chloride and potassium hydroxide in DMF should furnish **31**, which will undergo subsequent reductive ring opening with sodium cyanoborohydride to give **19**.[23]
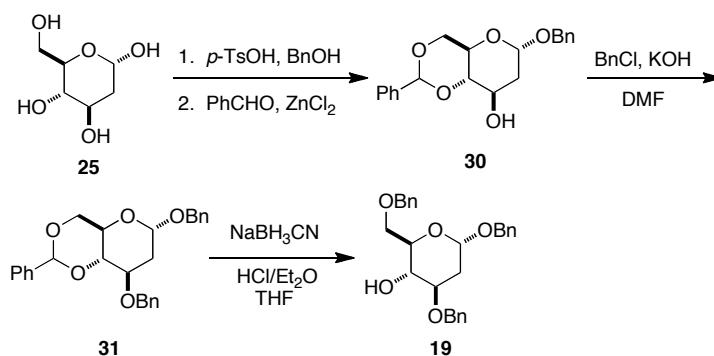
Scheme 4. Synthesis of 2-DG derivative **19**.

The final 2-DG derivative **20** is planned from **25** via selective tritylation of the 6-hydroxyl moiety to afford **32**. Global benzyl protection will yield **33**, which will then be subjected to selective detritylation to yield the desired primary alcohol **20**.[24]
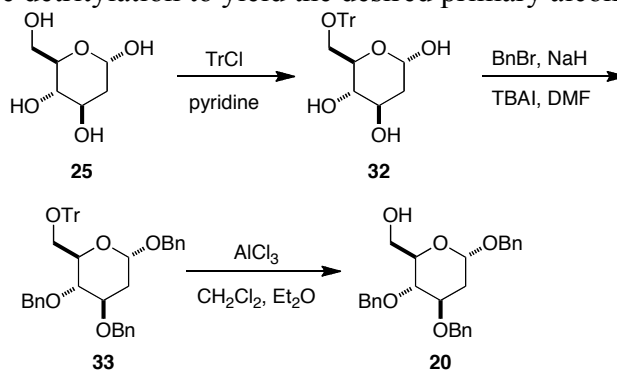
Scheme 5. Synthesis of derivative **20**.

As Scheme 6 shows, the linker-drug portions of targets **1-4** are envisioned from initial condensation of commercially available glycine ethyl ester **22** with ethylene oxide **23** to give **34**. Protection of the primary alcohols using TBSCl, followed by saponification of the ethyl ester under standard conditions should then afford **21**.
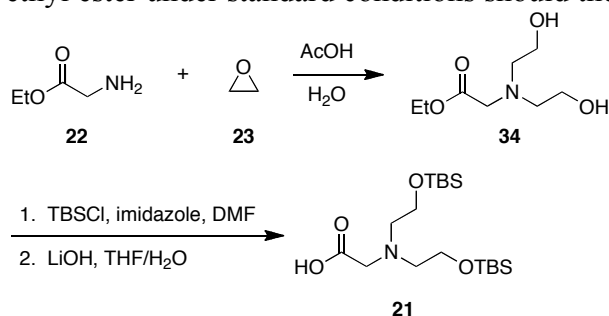
Scheme 6. Formation of the linker-drug derivative **21**.

At this stage, the linker-drug side chains will be appended to the 2-DG derivatives via treatment with DCC and DMAP, thereby affording esters **35-38** (Scheme 7).[25] Cleavage of the TBS protecting groups, followed by conversion of the primary alcohols to the corresponding chlorides will yield the benzyl-protected derivatives **13-16**. Global

deprotection using standard hydrogenation conditions should then give the desired carrier-linker-drug compounds **1-4**.

17, R^1 = H, R^2 = R^3 = R^4 = Bn
18, R^2 = H, R^1 = R^3 = R^4 = Bn
19, R^3 = H, R^1 = R^2 = R^4 = Bn
20, R^4 = H, R^1 = R^2 = R^3 = Bn

35, R^1 = C(O)CH$_2$N(CH$_2$CH$_2$OTBS)$_2$, R^2 = R^3 = R^4 = Bn
36, R^2 = C(O)CH$_2$N(CH$_2$CH$_2$OTBS)$_2$, R^1 = R^3 = R^4 = Bn
37, R^3 = C(O)CH$_2$N(CH$_2$CH$_2$OTBS)$_2$, R^1 = R^2 = R^4 = Bn
38, R^4 = C(O)CH$_2$N(CH$_2$CH$_2$OTBS)$_2$, R^1 = R^2 = R^3 = Bn

13, R^1 = C(O)CH$_2$N(CH$_2$CH$_2$Cl)$_2$, R^2 = R^3 = R^4 = Bn
14, R^2 = C(O)CH$_2$N(CH$_2$CH$_2$Cl)$_2$, R^1 = R^3 = R^4 = Bn
15, R^3 = C(O)CH$_2$N(CH$_2$CH$_2$Cl)$_2$, R^1 = R^2 = R^4 = Bn
16, R^4 = C(O)CH$_2$N(CH$_2$CH$_2$Cl)$_2$, R^1 = R^2 = R^3 = Bn

1, R^1 = C(O)CH$_2$N(CH$_2$CH$_2$Cl)$_2$, R^2 = R^3 = R^4 = H
2, R^2 = C(O)CH$_2$N(CH$_2$CH$_2$Cl)$_2$, R^1 = R^3 = R^4 = H
3, R^3 = C(O)CH$_2$N(CH$_2$CH$_2$Cl)$_2$, R^1 = R^2 = R^4 = H
4, R^4 = C(O)CH$_2$N(CH$_2$CH$_2$Cl)$_2$, R^1 = R^2 = R^3 = H

Scheme 7. Synthesis of the carrier-linker-drug derivatives **1-4**.

With prodrugs **1-4** prepared, several tests will be necessary to evaluate their therapeutic effects. Initially, the two most important aspects to study will be uptake of the prodrugs by the GLUT-1 transporter protein, as well as their cytotoxicity. An additional experiment will include testing the rate of hydrolysis of the ester bond.

In vitro models of the BBB have been developed to better understand the underlying cell biology, to predict drug permeability prior to animal studies, and to overcome the inherent difficulty in performing BBB molecular level studies in vivo.[26] One established method that evaluates the ability of glucose-drug derivatives to interact with the glucose transporter GLUT-1 is the use of human erythrocytes, since these cells express the same GLUT-1 transporter as that of the BBB.[10] The interaction of prodrugs **1-4** with GLUT-1 can be determined via literature methods previously established to measure the efficiency of these compounds to prevent the uptake of ^{14}C-glucose (IC$_{50}$) in human erythrocytes.[15,16] A more recently established in vitro model utilizes murine brain microvascular endothelial cells co-cultured with rat primary astrocytes in the presence of biochemical inducing agents.[26] This model expresses functional GLUT-1 transporter proteins and could serve as an excellent experiment to test the binding and uptake of compounds **1-4**.

Once it has been established which prodrugs react with the GLUT-1 transporter, additional studies will be carried out. In order to test the cytotoxicity of the prodrug derivatives, various brain tumor cell lines will be inoculated with the derivatives, and cell viability will be evaluated at regular time intervals.

Another important aspect to study is hydrolysis of the prodrugs' ester bond. Since the alkylating agent needs to be delivered to the brain tumor, it is important that the ester bond does not cleave prior to passing the BBB and entering the tumor. Since tumors exhibit a slightly acidic environment, the stability of the prodrug ester bond will be tested with phosphate buffer solutions of varying pH levels in parallel experiments. The

392

prodrug will be tested further in human plasma to ensure that the ester linkage does not cleave under normal physiological conditions.

Pending the results of the above experiments, additional in vitro and in vivo testing of the prodrugs will be required. It will be important to determine if the prodrug is actually delivered to the brain tumor, which can be accomplished through in vivo studies using mice (or rats) implanted with specific brain tumors. Radiolabeled ^{18}F-DG prodrug derivatives will be synthesized and injected into the mouse.[17] Positron emission tomography (PET scans) will then enable visualization of the tagged prodrug compound in order to check for its presence within the malignant tumor.

Potential Difficulties and Limitations:

While not all of the difficulties or limitations can be anticipated, a few of the potential shortcomings of this proposal are listed here, along with how these issues might be addressed.

1. It is possible that the 2-DG prodrugs are too bulky or hydrophobic to cross the BBB via the GLUT-1 transporter. If this is the case, there are a number of other carrier-mediated transport systems that could allow passage of a prodrug across the BBB. One such method would be to couple the alkylating agent to an amino acid, such as phenylalanine, or to a nucleoside such as adenosine.[27]

2. There is a possibility that the ester bond could be cleaved prematurely by an esterase, thus releasing the alkylating agent prior to passage across the BBB. One way to address this issue is to slightly alter the synthesis of the prodrug in order to include different pH-labile cross-linkers, such as a hydrazone moiety or a phosphoramidate.[14]

3. Another dimension of the BBB that has not been discussed is the presence of efflux proteins. These proteins are responsible for pushing unwanted substances from the brain into the blood. There is a possibility that once the prodrug enters the brain, the active efflux transport (AET) protein will expel the drug from the central nervous system. One way to counteract the AET system is to develop a co-drug that could inhibit the AET protein.[27]

References

1. Sarin, H., Recent Progress Towards Development of Effective Systemic Chemotherapy for the Treatment of Malignant Brain Tumors. *J. Transl. Med.* **2009**, *7*, 77-90.
2. Allen, T. M.; Cullis, P. R., Drug Delivery Systems: Entering the Mainstream. *Science* **2004**, *303*, 1818-1822.
3. Bhaskar, S.; Tian, F.; Stoeger, T.; Kreyling, W.; de la Fuente, J. M.; Grazu, V.; Borm, P.; Estrada, G.; Ntziachristos, V.; Razansky, D., Multifunctional Nanocarriers for Diagnostics, Drug Delivery and Targeted Treatment Across Blood-Brain Barrier: Perspectives on Tracking and Neuroimaging. *Part. Fibre. Toxicol.* **2010**, *7*, 3-27.
4. Lichota, J.; Skjorringe, T.; Thomsen, L. B.; Moos, T. Macromolecular Drug Transport into the Brain Using Targeted Therapy. *J. Neurochem.* **2010**, *113*, 1-13.
5. Alam, M. I.; Beg, S.; Samad, A.; Baboota, S.; Kohli, K.; Ali, J.; Ahuja, A.; Akbar, M., Strategy for Effective Brain Drug Delivery. *Eur. J. Pharm. Sci.* **2010**, *40*, 385-403.
6. Jain, K. K. (ed.), *Drug Delivery to the Central Nervous System*, Neuromethods, *45*.
7. Tsuji, A. Small Molecular Drug Transfer across the Blood-Brain Barrier via Carrier-Mediated Transport Systems. *NeuroRx*, **2005**, *2*, 54-62.
8. Abbott, N. J.; Ronnback, L.; Hansson, E., Astrocyte-Endothelial Interactions at the Blood-Brain Barrier. *Nature Rev. Neurosci.* **2006**, *7*, 41-53.
9. Qutub, A. A.; Hunt, C. A., Glucose Transport to the Brain: A Systems Model. *Brain Res. Rev.* **2005**, *49*, 595-617.
10. Uriel, C.; Egron, M.-J.; Santarromana, M.; Scherman, D.; Antonakis, K.; Herscovici, J., Hexose Keto-C-Glycoside Conjugates: Design, Synthesis, Cytotoxicity, and Evaluation of Their Affinity for the Glucose Transporter Glut-1. *Bioorg. Med. Chem.* **1996**, *4*, 2081-2090.
11. Dalpiaz, A.; Filosa, R.; de Caprariis, P.; Conte, G.; Bortolotti, F.; Biondi, C.; Scatturin, A.; Prasad, P. D.; Pavan, B., Molecular Mechanism Involved in the Transport of a Prodrug Dopamine Glycosyl Conjugate. *Int. J. Pharm.* **2007**, *336*, 133-139.
12. Hatanaka, M., Transport of Sugars in Tumor Cell Membranes. *Biochim. Biophys. Acta* **1974**, *355*, 77-104.
13. Squire, L.; Robers, J. L.; Spitzer, N. C.; Zigmond, M. J. *Fundamental Neuroscience 2nd ed.*; Elsevier: New York, NY, 2002; pp 334-346.
14. Gao, W.; Chan, J. M.; Farokhzad, O. C., pH-Responsive Nanoparticles for Drug Delivery. *Mol. Pharmaceutics* **2010**, *7*, 1913-1920.
15. Halmos, T.; Santarromana, M.; Antonakis, K.; Scherman, D., Synthesis of Glucose-Chlorambucil Derivatives and their Recognition by the Human GLUT1 Glucose Transporter. *Eur. J. Pharm. Sci.* **1996**, *318*, 477-484.
16. Halmos, T.; Santarromana, M.; Antonakis, K.; Scherman, D., Synthesis of *O*-Methylsulfonyl Derivatives of D-Glucose as Potential Alkylating Agents for Targeted Drug Delivery to the Brain. Evaluation of their Interaction with the Human Erythrocyte GLUT1 Hexose Transporter. *Carbohydr. Res.* **1997**, *299*, 15-21.

17. Zhang, X. D.; Deslandes, E.; Villedieu, M.; Poulain, L.; Duval, M.; Gauduchon, P.; Schwartz, L.; Icard, P., Effect of 2-Deoxy-D-Glucose on Various Malignant Cell Line *In Vitro*. *Anticancer Res.* **2006**, *26*, 3561-3566.

18. Prasanna, V. K.; Venkataramana, N. K.; Dwarakanath, B. S.; Santhosh, V., Differential Responses of Tumors and Normal Brain to the Combined Treatment of 2-DG and Radiation in Gliomablastoma. *J. Cancer Res. Ther.* **2009**, *S1*, S44-S47.

19. Niu, Y.; Cao, X.; Ye, X.-S., Improved Synthesis of Phytosphingosine and Dihydrosphingosine from 3,4,6-Tri-*O*-benzyl-D-galactal. *Helv. Chim. Acta* **2008**, *91*, 746-752.

20. David, S.; Thieffry, A.; Veyrieres, A., A Mild Procedure for the Regiospecific Benzylation and Allylation of Polyhydroxy-Compounds via their Stannylene Derivatives in Non-polar Solvents. *J. Chem. Soc., Perkin Trans. 1* **1981**, 1796-1801.

21. Notz, W.; Hartel, C.; Waldscheck, B.; Schmidt, R. R., De Novo Synthesis of a Methylene-Bridged Neu5Ac-α-(2,3)-Gal *C*-Disaccharide. *J. Org. Chem.* **2001**, *66*, 4250-4260.

22. Chiu, T. M. K.; Sigillo, K.; Gross, P. H.; Franz, A. H., Synthesis of Anomerically Pure, Furanose-Free α-Benzyl-2-amino-2-deoxy-D-altro- and D-manno-pyranosides and Some of their Derivatives. *Synthetic Commun.* **2007**, *37*, 2355-2381.

23. Tai, V. W.-F.; Imperiali, B., Substrate Specificity of the Glycosyl Donor for Oligosaccharyl Transferase. *J. Org. Chem.* **2001**, *66*, 6217-6228.

24. Amigues, E. J.; Greenberg, M. L.; Ju, S.; Chen, Y.; Migaud, M. E., Synthesis of Cyclophospho-glucoses and Glucitols. *Tetrahedron* **2007**, *63*, 10042-10053.

25. Schramm, S.; Dettner, K.; Unverzagt, C., Chemical and Enzymatic Synthesis of Buprestin A and B—Bitter Acylglucosides from Australian Jewel Beetles (Coleoptera: Buprestidae). *Tetrahedron Lett.* **2006**, *47*, 7741-7743.

26. Shayan, G.; Choi, Y. S.; Shusta, E. V.; Shuler, M. L.; Lee, K. H., Murine *In Vitro* Model of the Blood-Brain Barrier for Evaluating Drug Transport. *Eur. J. Pharm. Sci.* **2011**, *42*, 148-155.

27. Pavan, B.; Dalpiaz, A.; Ciliberti, N.; Biondi, C.; Manfredini, S.; Vertuani, S., Progress in Drug Delivery to the Central Nervous System by the Prodrug Approach. *Molecules* **2008**, *13*, 1035-1065.